GEOLOGICAL SURVEY OF CANADA
PAPER 90-8

MINERAL DEPOSIT STUDIES IN NOVA SCOTIA

VOLUME 1

edited by
A.L. Sangster

1990

Energy, Mines and Resources Canada
Énergie, Mines et Ressources Canada

Canada

Nova Scotia

Department of Mines and Energy

Contribution to Canada-Nova Scotia Mineral Development Agreement 1984-89, a subsidiary agreement under the Economic and Regional Development Agreement. Project funded by the Geological Survey of Canada.

Contribution à l'Entente auxiliaire Canada/Nouvelle-Écosse sur l'exploitation minérale 1984-89 faisant partie de l'Entente de développement économique et régional. Ce projet a été financé par la Commission géologique du Canada.

Energy, Mines and Resources Canada
Énergie, Mines et Ressources Canada

91-04645/

GEOLOGICAL SURVEY OF CANADA
PAPER 90-8

MINERAL DEPOSIT STUDIES IN NOVA SCOTIA

VOLUME 1

edited by
A.L. Sangster

1990

© Minister of Supply and Services Canada 1990

Available in Canada through authorized bookstore agents and
other bookstores

or by mail from

Canadian Government Publishing Centre
Supply and Services Canada
Ottawa, Canada K1A 0S9

and from

Geological Survey of Canada offices:

601 Booth Street
Ottawa, Canada K1A 0E8

3303-33rd Street N.W.,
Calgary, Alberta T2L 2A7

A deposit copy of this publication is also available for
reference in public libraries across Canada

Cat. No. M44-90/8E
ISBN 0-660-13620-1

Price subject to change without notice

Technical Editor
S. Elliott-Meadows

Editorial and drafting assistance
R. Bretzlaff, R.D. Knight

Cover description
Sulphide-filled cells in noncompacted
woody material, Yava. See Figure 20,
page 224 for further details.

Contents

1 Introduction

3 J.R. HILL
A geological and geochemical study of metacarbonate rocks and contained mineral deposits, Cape Breton Island, Nova Scotia

31 A.L. SANGSTER, M.F. JUSTINO, and R.I. THORPE
Metallogeny of the Proterozoic marble-hosted zinc occurrences at Lime Hill and Meat Cove, Cape Breton Island, Nova Scotia

67 R.P. RAESIDE
Low-pressure metamorphism of the Lime Hill gneissic complex, Bras d'Or Terrane, Cape Breton Island, Nova Scotia

77 R.A. JAMIESON, P.C. TALLMAN, H.E. PLINT, and K.A. CONNORS
Regional geological setting of pre-Carboniferous mineral deposits in the western Cape Breton Highlands, Nova Scotia

101 A.L. SANGSTER, R.I. THORPE, and A.K. CHATTERJEE
A reconnaissance lead isotopic study of mineral occurrences in pre-Carboniferous basement rocks of northern and central Cape Breton Island, Nova Scotia

115 A.L. SANGSTER
Metallogeny of the Meguma Terrane, Nova Scotia

163 J.R. HENDERSON and M.N. HENDERSON
Crack-seal texture in bedding-parallel, gold-bearing, columnar-quartz veins: evidence of fossil water sills

169 P.F. WILLIAMS and C. HY
Origin and deformational and metamorphic history of gold-bearing quartz veins on the Eastern Shore of Nova Scotia

195 C.J. MWENIFUMBO, P.G. KILLEEN, and M.C. GRAVES
Borehole geophysical logging at the Lake Charlotte manganese prospect, Meguma Group, Nova Scotia

203 D.F. SANGSTER and P.D. VAILLANCOURT
Geology of the Yava sandstone-lead deposit, Cape Breton Island, Nova Scotia, Canada

245 C.E. RAVENHURST, P.H. REYNOLDS, M. ZENTILLI, H.W. KRUEGER, and J. BLENKINSOP
Strontium isotopic geochemistry of lead-zinc/barite deposits and host rocks of the Carboniferous Minas Sub-basin, Nova Scotia

257 D. BIRK and J.C. WHITE
Trace elements in bituminous coals, roof clays, and underclays of the Sydney Basin, Nova Scotia: ash chemistry, element sites, and mineralogy

INTRODUCTION

This volume contains 12 reports on research carried out under the Canada-Nova Scotia Mineral Development Agreement, 1984-1989. Ten papers result from projects supervised by the Mineral Deposits Subdivision, Mineral Resources Division, Geological Survey of Canada. Two papers are invited contributions resulting from work carried out elsewhere but that is compatible with the objectives of this volume. The papers report on a wide range of activities related to mineral deposit geology, including mineral deposit modelling, geochemistry, structural geology, isotope geology, borehole geophysics, and regional mapping. The volume is a truly co-operative product in that it contains papers authored or co-authored by university-based geologists (Acadia University, Dalhousie University, University of New Brunswick, Carleton University), consultants and contractors (Northwood Geoscience, Cuesta Research, Krueger Enterprises, Inc., Atlantic Coal Institute), as well as by geologists from the Nova Scotia Department of Mines and Energy and the Geological Survey of Canada. Many of the projects reported on in this volume interfaced with mineral exploration activities in Nova Scotia and thus the results reported here have benefitted from the co-operation of personnel of numerous mineral exploration companies. Their participation is individually acknowledged throughout the volume.

Mineral deposit studies in Nova Scotia under the Mineral Development Agreement were grouped in three different project categories: one dealing with mineral occurrences in the highland basement complexes; a second with occurrences within the metasedimentary rocks of the Meguma Terrane; and a third directed at mineral occurrences hosted by sedimentary rocks of Carboniferous age. The papers in this volume reflect this distribution of activities with five devoted to the geology and mineral deposits of basement rocks on Cape Breton Island, four on the geology and mineral occurrences of the Meguma Terrane, and three on mineral occurrences hosted by Carboniferous rocks.

The papers presented in this volume represent the culmination of four years of geological investigations under the Canada-Nova Scotia Mineral Development Agreement. The results reported here contribute significantly to the knowledge of certain mineral environments in Nova Scotia and it is anticipated that they will help foster further mineral exploration and development in the province.

The editor thanks those who assisted in any way with the realization of project results reported herein. Gratitude is expressed to P.S. Giles, D.A. Murray, and the geological staff of the Nova Scotia Department of Mines and Energy, many of whom discussed aspects of most GSC projects, both formally in annual planning meetings, and more informally during the course of project work. The Nova Scotia Department of Mines and Energy also provided logistical support for some projects from their Stellarton Office. In this regard I particularly thank John McMullin and Dennis Murphy. The projects also benefitted from comment by members of the Nova Scotia Chamber of Mineral Resources via annual meetings of the Industrial Review Committee. Contributors to these meetings included D.W. Black, W.B. Burton, T. Day,

INTRODUCTION

Le présent recueil comprend douze articles où sont présentés les résultats de recherches menées dans le cadre de l'Entente Canada - Nouvelle-Écosse sur l'exploitation minérale (1984-1989). Dix de ces articles portent sur des projets supervisés par la Sousdivision des gîtes minéraux de la Division des ressources minérales de la Commission géologique du Canada. Les deux autres articles sont des contributions sollicitées dans lesquelles les auteurs décrivent des travaux effectués dans d'autres régions, mais dont la nature s'harmonise bien aux objectifs du présent ouvrage. Les rapports traitent d'une vaste gamme de domaines reliés à l'étude de la géologie des gîtes minéraux: modélisation des gîtes minéraux, géochimie, géologie structurale, méthodes isotopiques, géophysique dans les trous de forage et cartographie à l'échelle régionale. Le présent recueil résulte d'une véritable entreprise de coopération puisque les articles qui s'y retrouvent ont été rédigés, de façon individuelle ou en collaboration, par des géologues affiliés à des universités (Université Acadia, Université Dalhousie, Université du Nouveau-Brunswick, Université Carleton), par des experts-conseils et des entrepreneurs (Northwood Geoscience, Cuesta Research, Krueger Enterprises Inc., Atlantic Coal Institute) ainsi que par des géologues à l'emploi du ministère des Mines et de l'Énergie de la Nouvelle-Écosse et de la Commission géologique du Canada. De plus, bon nombre des projets décrits dans le présent volume étaient liés, de près ou de loin, à des programmes d'exploration minière se déroulant en Nouvelle-Écosse et, de ce fait, les auteurs ont pu bénéficier de la coopération d'employés de nombreuses sociétés d'exploration minière. La participation de chacune de ces personnes est soulignée dans les différents articles.

Les études de gîtes minéraux exécutées en Nouvelle-Écosse aux termes de l'Entente sur l'exploitation minérale ont été divisées en trois groupes, selon qu'elles se rapportaient: 1) aux indices minéralisés situés dans les complexes de socle des hautes terres, 2) aux indices minéralisés contenus dans les roches métasédimentaires du terrane de Meguma ou 3) aux indices minéralisés encaissés dans des roches sédimentaires du Carbonifère. Les articles présentés dans les pages qui suivent reflètent cette division; en effet, on dénombre cinq articles portant sur la géologie et les gîtes minéraux des roches de socle de l'île du CapBreton, quatre sur la géologie et les indices minéralisés du terrane de Meguma et trois sur les indices minéralisés encaissés dans des roches carbonifères.

Cette collection d'articles est le fruit des études de géologie entreprises sur une période de quatre ans en vertu de l'Entente Canada - Nouvelle-Écosse sur l'exploitation minérale. Les résultats présentés dans ces articles constituent un apport considérable à l'ensemble des connaissances de certains environnements hôtes de minéralisations de la Nouvelle-Écosse et devraient contribuer à stimuler les activités d'exploration et d'exploitation minérales dans la province.

Le rédacteur en chef remercie tous ceux qui ont participé, d'une façon ou d'une autre, au succès des projets faisant l'objet de ce rapport. Il convient de souligner particulièrement la collaboration de P.S. Giles et de D.A. Murray, ainsi que des nombreux spécialistes en géologie

D. Duncan, C.B. MacKenzie, B.E. MacNabb, A.J. O'Donnell, and D.W. Pollock. J. Colwell contributed to the Industrial Review Committee as university representative.

The editor also thanks those scientists who assisted in the production of this volume by reviewing the papers presented here. They are as follows:

Reviewers from institutions outside the Geological Survey of Canada

S.M. Barr, Acadia University, Wolfville, Nova Scotia
R.C. Boehner, Nova Scotia Department of Mines and Energy, Halifax, Nova Scotia
J. Bourne, Université de Québec à Montréal, Montréal, Québec
R. Doig, McGill University, Montreal, Quebec
H.V. Donohoe, Nova Scotia Department of Mines and Energy, Halifax, Nova Scotia
W.K. Fyson, University of Ottawa, Ottawa, Ontario
M. Gauthier, Université de Québec à Montréal, Montréal, Québec
Y. Héroux, Institut national de la recherche scientifique, Québec, Québec
D.J. Kontak, Nova Scotia Department of Mines and Energy, Halifax, Nova Scotia
R.P. Raeside, Acadia University, Wolfville, Nova Scotia
B.R. Rust, University of Ottawa, Ottawa, Ontario
H.S. Swinden, Newfoundland Department of Mines and Energy, St. John's, Newfoundland
M. Zentilli, Dalhousie University, Halifax, Nova Scotia
One reviewer who chose to remain anonymous.

Reviewers from the Geological Survey of Canada

G.R. Bernius, Mineral Resources Division, Ottawa
K.L. Currie, Continental Geoscience Division, Ottawa
J.R. Henderson(2), Continental Geoscience Division, Ottawa
K.H. Poulsen(2), Mineral Resources Division, Ottawa
D.F. Sangster, Mineral Resources Division, Ottawa
W.D. Sinclair, Mineral Resources Division, Ottawa
R.I. Thorpe, Mineral Resources Division, Ottawa
G. Goodarzi, Institute of Sedimentary and Petroleum Geology, Calgary
O. van Breemen, Continental Geoscience Division, Ottawa
G.P. Watson, Mineral Resources Division, Ottawa

Alan L. Sangster

du ministère des Mines et de l'Énergie de la Nouvelle-Écosse qui ont contribué à la majorité des projets de la CGC en discutant de différents aspects des travaux avec les chercheurs, que ce soit de façon officielle lors des réunions annuelles de planification, ou de façon amicale, au cours des travaux en tant que tels. Certains projets ont aussi profité d'une aide logistique fournie par le bureau de Stellarton du ministère des Mines et de l'Énergie de la Nouvelle-Écosse. À cet égard, on remercie de façon particulière MM. John McMullin et Dennis Murphy. Les différentes études ont également bénéficié des commentaires émis par les membres de la Nova Scotia Chamber of Mineral Resources à l'occasion des réunions annuelles du Comité d'examen de l'industrie. Les participants à ces rencontres comprenaient D.W. Black, W.B. Burton, T. Day, D. Duncan, C.B. MacKenzie, B.E. MacNabb, A.J. O'Donnell et D.W. Pollock. J. Colwell a aussi pris part aux activités du Comité d'examen de l'industrie à titre de représentant des universités.

Enfin, le rédacteur en chef remercie tous les scientifiques qui ont participé à la publication du présent recueil en évaluant les articles qui le composent. Le nom de ces personnes est donné ci-après.

Réviseurs pour la Commission géologique du Canada provenant d'autres organismes

S.M. Barr, Université Acadia, Wolfville, Nouvelle-Écosse
R.C. Boehner, ministère des Mines et de l'Énergie de la Nouvelle-Écosse, Halifax, Nouvelle-Écosse
J. Bourne, Université du Québec à Montréal, Montréal, Québec
R. Doig, Université McGill, Montréal, Québec
H.V. Donohoe, ministère des Mines et de l'Énergie de la Nouvelle-Écosse, Halifax, Nouvelle-Écosse
W.K. Fyson, Université d'Ottawa, Ottawa, Ontario
M. Gauthier, Université de Québec à Montréal, Montréal, Québec
Y. Héroux, Institut national de la recherche scientifique, Québec, Québec
D.J. Kontak, ministère des Mines et de l'Énergie de la Nouvelle-Écosse, Halifax, Nouvelle-Écosse
R.P. Raeside, Université Acadia, Wolfville, Nouvelle-Écosse
B.R. Rust, Université d'Ottawa, Ottawa, Ontario
H.S. Swinden, ministère des Mines et de l'Énergie, St. John's, Terre-Neuve
M. Zentilli, Université Dalhousie, Halifax, Nouvelle-Écosse
Un des reviseur a tenu à l'anonymat

Réviseurs pour la Commission géologique du Canada

G.R. Bernius, Division des ressources minérales, Ottawa
K.L. Currie, Division géoscientifique du continent
R. Henderson(2), Division géoscientifique du continent
K.H. Poulsen(2), Division des ressources minérales, Ottawa
D.F. Sangster, Division des ressources minérales, Ottawa
W.D. Sinclair, Division des ressources minérales, Ottawa
R.I. Thorpe, Division des ressources minérales, Ottawa
G. Goodarzi, Institut de géologie sédimentaire et pétrolière, Calgary
O. van Breemen, Division géoscientifique du continent
G.P. Watson, Division des ressources minérales, Ottawa

Alan L. Sangster

A geological and geochemical study of metacarbonate rocks and contained mineral deposits, Cape Breton Island, Nova Scotia[1]

J.R. Hill[2]

Hill, J.R., A geological and geochemical study of metacarbonate rocks and contained mineral deposits, Cape Breton Island, Nova Scotia; in Mineral Deposit Studies in Nova Scotia, Volume 1, edited by A.L. Sangster, Geological Survey of Canada, Paper 90-8, p. 3-29, 1990.

Abstract

Carbonate and calc-silicate lithologies are a major component of late Precambrian to early Paleozoic metasedimentary rocks in Cape Breton Island. Metacarbonate rocks can be distinguished on a regional basis by lithological, metamorphic, geochemical, metallogenic, and to limited extent, age criteria. In central Cape Breton Island, thick sequences of calcite and dolomite marble and calc-silicate marble are interbedded with clastic metasedimentary rocks that have traditionally been included with the George River Group. Major compositional and metamorphic variations are evident in George River Group marble, especially between the low-grade, pure calcite and dolomite marble of the Creignish Hills-North Mountain area, and the higher grade, impure, siliceous, and predominantly dolomitic marble of the Boisdale Hills area. Major and trace element patterns suggest that compositional variability between marble units within these two areas is controlled by variations in the clastic content of the carbonate rocks. Metallic mineralization, consisting of iron oxide, base metal sulphide, tungsten-, tin-, and precious metal-bearing minerals, is predominantly skarn-associated and related to discrete contact metasomatic environments.

Within the Cape Breton Highlands crystalline terrane, carbonate units within medium-grade paragneiss sequences, including the McMillan Flowage Formation, the Cape North Group and others, are of much more limited distribution. Marble lithologies are richer in silica, alumina, and related major elements contributed by clastic impurities in the original depositional environment. The Cape Breton Highlands carbonate units are also enriched in copper and zinc but sulphide mineralization is not common.

Siliceous dolomite marble and calc-silicate units, associated with high metamorphic grade migmatite, represent another distinct class of metacarbonate rock in Cape Breton Island. The Lime Hill gneissic complex in central Cape Breton Island, and the Blair River Complex in northwestern Cape Breton Island appear to represent remnants of crystalline basement rocks which are older than George River Group and other metasedimentary rocks of uncertain age in the Cape Breton Highlands. Marble units found at Lime Hill and within the Blair River Complex at Meat Cove, are host to zinc deposits metallogenically comparable to carbonate-hosted zinc + / – lead deposits of the Grenville Supergroup in the Canadian Shield.

---

[1] Contribution to the Canada – Nova Scotia Mineral Development Agreement, 1984-1989. Project carried by the Mineral Resources Division, Geological Survey of Canada, Project 860008.

[2] Northwood Geoscience, 357 Preston St., Suite 201, Ottawa, Ontario, K1S 4M8.

Résumé

Les roches carbonatées et calcosilicatées représentent une importante composante des roches métasédimentaires, dont l'âge varie du Précambrien supérieur au Paléozoïque inférieur, de l'Île du Cap-Breton. À l'échelle régionale, les roches métacarbonatées se distinguent à leur lithologie, leur caractère métamorphique et géochimique, leur métallogénie, et dans une certaine mesure, leur âge. Dans la région centrale de l'Île du Cap-Breton, d'épaisses séquences de marbre calcitique et dolomitique et de marbre calco-silicaté sont interstratifiées avec des roches métasédimentaires clastiques qui traditionnellement étaient placées dans le groupe de George River. D'importantes variations de la composition et du métamorphisme sont apparentes dans le marbre du groupe de George River, en particulier entre le marbre pur, calcitique et dolomitique, faiblement métamorphisé, de la région des collines Creignish et du mont North, et le marbre siliceux et principalement dolomitique, impur, et fortement métamorphisé, de la région des collines Boisdale. Le schéma de la distribution des éléments principaux et éléments en traces semble indiquer que la variabilité de composition observée entre les unités à marbre de ces deux régions est régie par des variations du contenu clastique des roches carbonatées. La minéralisation métallifère, caractérisée par la présence d'oxydes de Fe, de sulfures de métaux communs, de minéraux renfermant des composants lithophiles et métaux précieux, est surtout associée à des skarns et liée à des milieux discrets caractérisés par une métasomatose de contact.

À l'intérieur du terrane cristallin des hautes terres du Cap-Breton, les unités carbonatées contenues dans les séquences à paragneiss, moyennement métamorphisées, en particulier la formation de McMillan Flowage, le groupe de Cape North ainsi que d'autres, ont une répartition beaucoup plus limitée. Les roches de type marbre sont enrichies en silice, en alumine et en éléments principaux connexes, introduits par les impuretés clastiques dans le milieu sédimentaire originel. Les unités carbonatées des hautes terres du Cap-Breton sont aussi enrichies en cuivre et en zinc, mais la minéralisation sulfurée n'est pas fréquente.

Les unités à marbre dolomitique siliceux et unités calco-silicatées, associées avec une migmatite caractéristique d'un degré de métamorphisme élevé, représentent une autre classe distincte de roches métacarbonatées de l'Île du Cap-Breton. Le complexe de Lime Hill situé dans la région centrale de l'Île du Cap-Breton et le complexe de Blair River situé dans la région nord-ouest de la même île, semblent représenter des vestiges de roches du socle cristallin qui sont plus ancienne que le groupe de George River et autres roches sédimentaires d'âge incertain présentes dans les hautes terres du Cap-Breton. Des unités à marbre rencontrées à l'emplacement de la colline Lime et à l'intérieur du complexe de Blair River dans la baie Meat, abritent des gîtes zincifères qui, métallogéniquement, s'apparentent aux gîtes zincifères ± plombifères contenus dans des roches carbonatées du supergroupe de Grenville dans le Bouclier canadien.

INTRODUCTION

A geological and geochemical study of metacarbonate rocks on Cape Breton Island, Nova Scotia was initiated in 1986. The project was designed primarily to evaluate the mineral resource potential of upper Precambrian to lower Paleozoic carbonate-bearing metasedimentary rocks. The work focused on systematic geological mapping and lithogeochemical sampling of carbonate rocks within the George River Group and similar metasedimentary sequences. Selected carbonate-hosted metallic and industrial mineral occurrences were also studied to improve the understanding of specific styles and environments of mineralization.

This paper summarizes the results of a statistical evaluation of geochemical analytical data for these carbonate rocks. Compositional variations in marble lithologies are interpreted with regard to regional geological and metallogenic criteria, and specific carbonate environments of potential economic interest are identified. A synthesis of the numerous classes of mineral deposits commonly hosted in metacarbonate terranes is presented in an attempt to formulate specific exploration guidelines.

STUDY AREAS

Five areas on Cape Breton Island underlain by carbonate-bearing metasedimentary rocks of late Precambrian to early Paleozoic age were examined during the study (Fig. 1), and include: 1) Creignish Hills; 2) North Mountain-Marble Mountain; 3) Boisdale Hills; 4) Cape Dauphin-Kellys Cove; and 5) Cape Breton Highlands. Four of the areas have been historically included within the George River Group (e.g. Fletcher, 1877; Guernsey, 1928): areas 1 to 4 are dominated by clastic metasedimentary rocks interbedded with lesser calcite and dolomite marble and minor metavolcanic rocks, whereas area 5 is underlain by carbonate-bearing metasedimentary assemblages of variable age and of contrasting metamorphic and sedimentological affinity to the George River lithologies. Marble and calc-silicate units examined here represent a very minor component of orthogneissic and paragneissic units and lower grade metasedimentary and metavolcanic rocks. Rare carbonate lithologies also occur within high-grade metamorphic rocks of the Blair River Complex in the northwestern Cape Breton Highlands.

METHODOLOGY

Previous regional mapping (Milligan, 1970) was used extensively to identify localities underlain by carbonate rock. Geological relationships were mapped at a scale of 1:10 000 using mineralogy, colour, and texture to distinguish discrete marble types. Associated plutonic rocks were mapped and sampled with emphasis on the recognition of contact metamorphic relationships with carbonate rocks. Representative samples of carbonate units were collected within each study area at a sample density of approximately five per square kilometre.

In total, 554 samples of carbonate rock and associated lithologies were collected. Features such as colour, grain size, texture, structure, alteration, type of mineralization, and dominant mineralogy were recorded for each rock sample in a form suitable for computer handling.

All chemical analyses were carried out by X-Ray Assay Laboratories Limited, Toronto, Ontario. A variety of geochemical techniques was used for analysis of major element oxides and minor and trace elements (Ba, Sr, Rb, Cr, Nb, Zr, and Y; see Table 1). A total of 68 reference and 45 blind duplicate standards were included in the sample sequence. Reference standard samples were inserted at a frequency of one in ten; blind duplicate samples were inserted at a frequency of one in fifteen. Results indicate a high degree of precision in reproducibility of geochemical values for all elements.

A complete listing of the geochemical data including lithological descriptions is presented elsewhere (Hill, 1987b, 1989).

GEOLOGY OF PRE-CARBONIFEROUS METACARBONATE ROCKS

Regional geology

On Cape Breton Island, carbonate-bearing metasedimentary rocks of inferred Precambrian to early Paleozoic age have historically been included within the George River Group. The term "George River" originally appeared in a description of pre-Carboniferous crystalline limestone and serpentine-bearing dolomite in the Georges River area of the Boisdale Hills (Honeyman, 1872). Fletcher (1877) adopted the nomenclature to describe these and similar marble units interbedded with clastic metasedimentary rocks and intruded by a varied suite of plutonic rocks in the Boisdale Hills and the Cape Dauphin-Kellys Cove area. The name continued to be applied throughout Cape Breton Island to describe the metasedimentary sequences underlying the Creignish Hills, North Mountain-Marble Mountain, the Cape Dauphin-Kellys Cove area, and even the higher metamorphic grade paragneiss underlying the Cape Breton Highlands (Guernsey, 1928; Bell and Goranson, 1938; Douglas, 1942; Weeks, 1954; Kelly, 1967; Milligan, 1970).

In reality, the George River Group is a loosely-defined lithostratigraphic unit containing interbedded carbonate and clastic metasedimentary and minor metavolcanic rocks of variable metamorphic grade and of probable late Precambrian age (Milligan, 1970). The carbonate units range in composition from relatively pure crystalline limestone and dolostone of very low metamorphic grade, as in the Creignish Hills and North Mountain areas, to more highly metamorphosed calcareous, dolomitic, or siliceous marble in the Boisdale Hills. Associated clastic sedimentary rocks vary in metamorphic grade and include quartzite, impure quartzite, and feldspathic sandstone which stratigraphically confine carbonate members. Argillaceous and volcanic rocks are of more limited distribution.

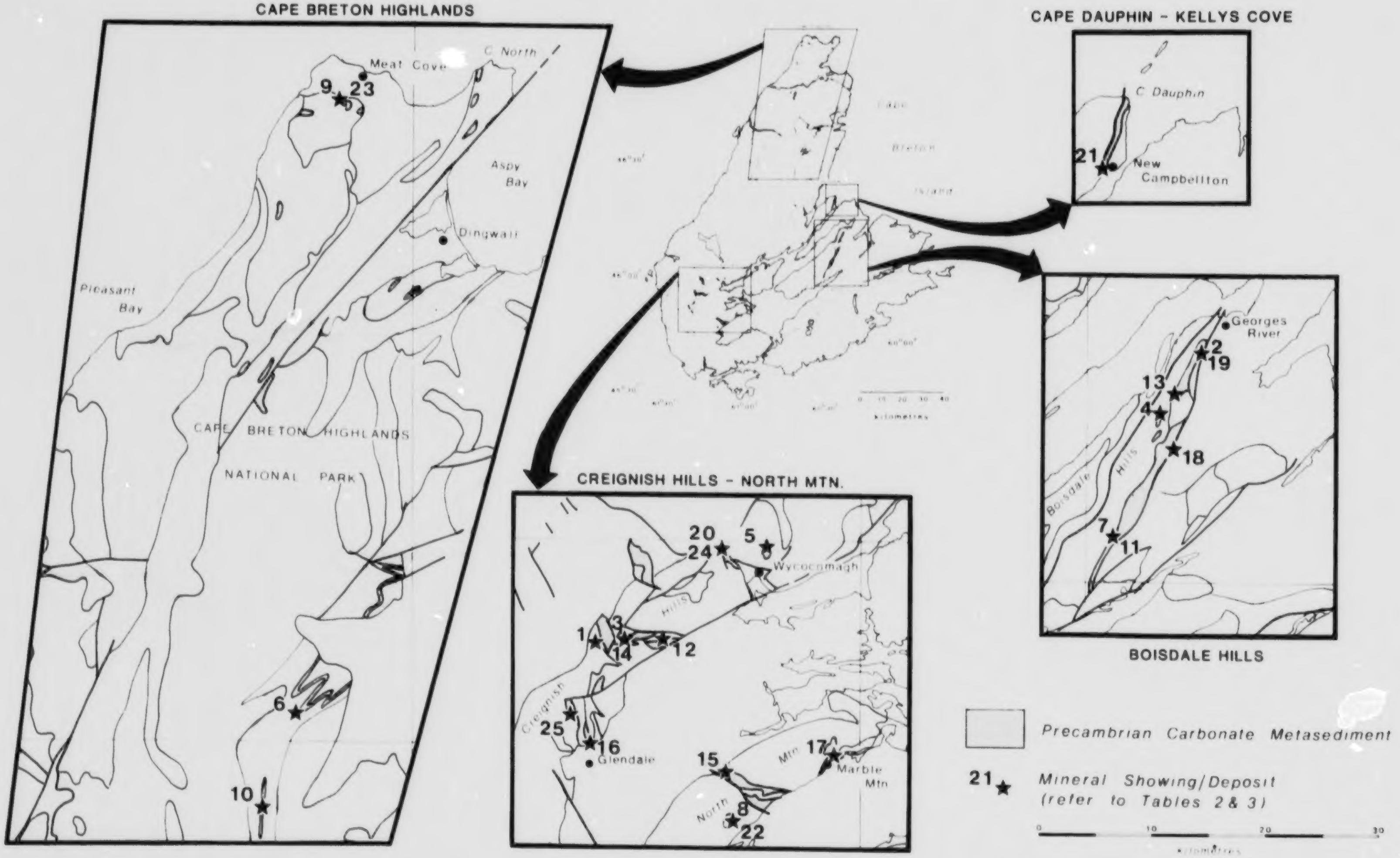
CAPE BRETON HIGHLANDS
Meat Cove
C North
9
23
Aspy Bay
Dingwall
Pleasant Bay
CAPE BRETON HIGHLANDS
NATIONAL PARK
6
10
Cape
Breton
Island
kilometres
CAPE DAUPHIN - KELLYS COVE
C Dauphin
21
New Campbellton
CREIGNISH HILLS - NORTH MTN.
20
24
5
Wycocomagh
Hills
1
3
14
12
Creignish
25
16
Glendale
15
North
8
22
Mtn
17
Marble Mtn
Georges River
2
19
13
4
18
Boisdale
Hills
7
11
BOISDALE HILLS
Precambrian Carbonate Metasediment
21
Mineral Showing/Deposit (refer to Tables 2 & 3)
0
10
20
30
kilometres

Figure 1. Location of study areas in Cape Breton Island. Shaded areas represent regions underlain by pre-Carboniferous carbonate metasedimentary formations (after Milligan, 1970; Keppie, 1979; Barr et al., 1987b). Metallic and industrial mineral occurrences are numbered according to Tables 2 and 3 respectively.

Table 1. Summary of laboratory analytical techniques, including detection limits.

Component	Method	Detection Limit
major element oxides	XRF[1]	0.01 %
whole rock minor elements	XRF	10 ppm
Cu	DCP[2]	0.05 ppm
Zn	DCP	0.05 ppm
Pb	DCP	2 ppm
Sn	XRF	3 ppm
W	NA[3]	1 ppm
Mo	DCP	1 ppm
As	FAA[4]	0.01 ppm
Sb	NA	0.20 ppm
Hg	CV[5]	5 ppb
Ag	DCP	0.05 ppm
Au	FADCP[6]	1 ppb

[1] X-ray Fluorescence
[2] Directly Coupled Plasma
[3] Neutron Activation
[4] Flame Atomic Absorption
[5] Cold Vapour
[6] Fire Assay, Directly Coupled Plasma

Throughout the Cape Breton Highlands, highly metamorphosed and deformed carbonate-clastic metasedimentary sequences are more difficult to correlate with George River Group rocks than has been implied by previous workers (e.g. Milligan, 1970; Wiebe, 1972; Murray, 1976; Keppie, 1979). Here, carbonate units form a very minor component of the clastic rock sequences. For example, in the northeastern Cape Breton Highlands, the Cape North Group (Macdonald and Smith, 1980) is dominated by semipelitic and pelitic gneiss with rare discontinuous marble and calc-silicate gneiss interlayers. Similarly, stratified units of the McMillan Flowage Formation, southeastern Cape Breton Highlands (Raeside and Barr, 1986) consist predominantly of metapelitic to metapsammitic and quartzite members with thin marble and calc-silicate interbeds. Isolated marble and calc-silicate horizons have also been recognized in gneissic terrane of the central Cape Breton Highlands (Neale, 1963a,b, 1964a,b; Barr et al., 1987c).

A new subdivision of Cape Breton Island pre-Carboniferous geology, based predominantly on intrusive age relationships, partially resolves some of these stratigraphic problems (Barr et al., 1988; Barr and Raeside, 1989). According to this reorganization, the crystalline rocks that underlie the Cape Breton Highlands and central Cape Breton Island are grouped into three major tectonostratigraphic zones. These are: 1) the Blair River Complex, which contains high-grade migmatitic gneiss intruded by plutonic rocks of Helikian age (1100 to 1500 Ma); 2) the Aspy Terrane, which contains most of the metamorphic rocks of the central and southern Cape Breton Highlands and intruded by post-Silurian plutonic rocks; and 3) the Bras d'Or Terrane, which covers much of central Cape Breton Island but which also includes the McMillan Flowage Formation of the eastern Cape Breton Highlands, characterized by latest Precambrian/Early Cambrian plutonic ages. George River Group metasedimentary and metavolcanic rocks dominate in the Bras d'Or zone.

Throughout the Bras d'Or zone, a series of distinctive high-temperature, low-pressure migmatitic gneisses are in fault contact with George River Group metasedimentary rocks (Raeside and Barr, 1988). The Lime Hill gneissic complex is typical, forming an isolated block of high-grade, marble-bearing paragneiss in fault contact with low metamorphic grade, George River Group sedimentary and volcanic rocks lying to the east (Justino and Sangster, 1987). In this regard, it bears tectonic and metamorphic similarity to a gneissic complex identified in the Kellys Mountain area which is believed to represent pre-George River basement (R.P. Raeside, pers. comm., 1988). Similar isolated carbonate-bearing gneissic units are intimately associated with George River Group metasedimentary rocks near Whycocomagh in the northeastern Creignish Hills (Milligan, 1970; J.R. Hill, unpublished data).

Description of carbonate lithologies

A complex variety of lithologies compose the George River Group and similar carbonate-bearing metasedimentary sequences throughout Cape Breton Island. The carbonate rocks can be grouped petrologically and metamorphically as follows:

1) cryptocrystalline limestone;
2) cryptocrystalline dolostone;
3) fine to coarse grained calcite marble;
4) fine to coarse grained dolomite marble;
5) siliceous (calcareous or dolomitic) marble which contains <40 percent silicate minerals;
6) (Ca,Mg,Fe)-silicate rocks of either regional or contact metamorphic origin which contain >40 percent silicate minerals.

During geological mapping, the ability to identify and trace individual carbonate units is severely hampered by the lack of exposure throughout most of Cape Breton Island. Interpretation of sedimentary relationships and of the postdepositional tectonic and intrusive history of the succession is therefore difficult. Differentiation of lithologies based on field relationships such as colour or texture is of little use in mapping intimately interbedded, laterally variable, structurally complex, and poorly exposed carbonate units. Instead, lithologies are differentiated according to mineralogy (especially the field determination of calcite to dolomite ratios), metamorphic grade, and degree of hydrothermal alteration. The work was supported by laboratory examination of thin sections and geochemical analyses.

Creignish Hills

Carbonate rocks of the George River Group underlying the Creignish Hills are dominated by calcite marble and crystalline to cryptocrystalline limestone. According to Milligan (1970), calcareous rocks lie in the middle of a

4500 m thick, clastic metasedimentary sequence which includes minor metavolcanic rocks. Major thicknesses of carbonate rock underlie the area between Whycocomagh and Glendale throughout the northern half of the Creignish Hills.

Regional metamorphic grade is within the biotite zone of the greenschist facies. Phlogopite is the dominant prograde metamorphic mineral in impure carbonate units. At a number of localities within the Glencoe area, metamorphic grade increases near intrusive contacts where calc-silicate minerals such as forsterite, tremolite, diopside, monticellite, and andradite are associated with minor base metal sulphides and iron oxides.

The most widely distributed carbonate lithology is a banded equigranular calcite marble which is light to dark grey, blue, or green, and medium to coarse grained. Light toned layers consist of almost pure, coarse grained calcite, whereas darker layers contain very fine grained argillaceous (micaceous) and/or carbonaceous material. The banding therefore appears to represent bedding. All marble and crystalline limestone units are very highly fractured, and calcite-filled veins pervasively cut compositional layering. Very narrow graphite or carbonaceous veinlets also cut massive calcite marble units. Some of the carbonaceous marbles are distinctly H_2S-bearing but sulphides are generally absent. Highly foliated, phlogopite-bearing siliceous calcite marble occurs as 1 to 10 m thick interbeds within cleaner massive marble and are particularly common in the carbonate sequence near upper and lower contacts with clastic rocks.

Cryptocrystalline limestone and dolostone horizons form relatively isolated units in the carbonate sequence but are most common near contacts with clastic sedimentary rocks. Limestones and dolostones tend to be black to dark grey, massive, competent, and generally siliceous (>5 weight percent SiO_2). Most are cut by calcite- and/or dolomite-filled fractures. The lack of low-grade metamorphic textures in most limestones and dolostones can be considered anomalous since they commonly occur in conformable contact with marble. Preservation of these apparently unmetamorphosed units may reflect contrasts in relative heat conductivity within carbonate rock types caused by variations in water content. Preservation may also be a function of ductility contrasts whereby pure carbonate units behave in a more ductile manner under the heat and stress conditions of low-grade thermal metamorphism thereby undergoing recrystallization more readily than the considerably more siliceous and brittle limestone and dolostone units.

Pure dolomite marbles are rare in the Creignish Hills. Varieties include a light grey to buff to white, medium to coarse grained, sugary-textured dolomite marble and a massive blue-grey, very fine grained, highly fractured (brecciated) dolomite marble. Discordant zones of dolomitization, located within massive calcareous marble, are recognized by their characteristic brecciated buff-coloured "lizard-skin" texture and by a resistance to weathering compared with the more crystalline, massive calcitic marble.

North Mountain

Precambrian carbonate metasedimentary rocks underlying North Mountain occur within three distinct geological settings. Serpentine-, calc-silicate-, and sulphide-bearing marble, including some relatively pure calcite and dolomite varieties, are located in the Lime Hill area (Occurrence 8, Fig. 1). The carbonate rocks are part of the Lime Hill gneissic complex which contains high-grade cordierite-andalusite/sillimanite gneiss intruded by a multiphase plutonic complex (Raeside, 1987). Carbonate units associated with the Lime Hill zinc deposit exhibit a mineral assemblage dominated by olivine, diopside, tremolite, and their alteration products talc and serpentine. Trace monticellite, chondrodite, and merwinite were identified by Chatterjee (1980) in the high-grade dolomitic rocks with minor occurrences of wollastonite in calcite marble.

Carbonate rock types similar to George River Group marbles underlying the Creignish Hills are located north and northeast of Lime Hill in the area of Kennedys Big Brook-Dallas Brook (Occurrence 15, Fig. 1). These low metamorphic grade rocks are characterized by massive hematitic calcite marble cut by a dense network of calcite- and hematite-filled veins. Numerous varieties of grey banded calcite marble, thinly foliated micaceous calcite marble, and massive blue-grey dolomite marble are interbedded with the massive hematitic calcite marble. In the same area, cryptocrystalline, dark grey to black, massive limestone and dolomite, similar to those found in the Creignish Hills, are interbedded in a tightly folded sequence of slate with minor quartzite.

In the Marble Mountain area, George River Group marbles exhibit a metamorphic grade intermediate between that at Lime Hill and at Kennedys Big Brook-Dallas Brook. Carbonate units examined in the Marble Mountain quarry and surrounding area form isolated blocks, perhaps representing xenoliths, within porphyrytic quartz monzonite. Metamorphic grade of the carbonate rock is higher than elsewhere in the North Mountain area, with the exception of Lime Hill. Impure siliceous carbonate units contain olivine, actinolite, minor diopside, talc, and serpentine. Pure carbonate lithologies, for which the Marble Mountain area is famous, are also present and include fine to coarse grained, white to buff calcite marble (which have been recovered in the past for use as building stone), varieties of light and dark grey, thickly banded calcite marble (Fig. 2), and, less commonly, units of relative high purity dolomite marble.

Boisdale Hills

Precambrian carbonate-bearing George River Group metasedimentary rocks form a continuous 25 km long belt extending from Georges River Inlet in the north to East Bay, Bras d'Or Lake, in the south (Fig. 1) (Bell and Goranson, 1938; Milligan, 1970). To the west, the sequence is bounded by the Boisdale Hills composite pluton which ranges in composition from diorite to granodiorite to syenite. The pluton is late Hadrynian to Cambrian in age (Barr and Setter, 1986). Varieties of grey banded calcite and dolomite marble dominate the carbonate sequence and are interstratified with more massive white to buff dolomite and locally persistent, very fine grained, massive dolomite marble breccia.

A majority of the marbles are siliceous and contain (Ca,Mg,Fe)-silicate minerals. Calc-silicate assemblages most commonly include fine grained, disseminated diopside, forsterite, and accessory sphene although some sections contain 20 to 30 percent tremolite megacrysts up to 15 mm long. Minor garnet occurs in metasedimentary rocks near intrusions. Low-temperature retrograde metamorphism, especially evident in the Scotch Lake area, has resulted in talc-serpentine-calcite alteration of the higher grade (Ca,Mg)-silicate minerals and the total destruction of the original higher temperature assemblage.

Marble units commonly contain a significant micaceous component of phlogopite and lesser biotite. In the central part of the belt, marbles grade into a thick clastic sequence dominated by quartzite and feldspathic arenite. The transition from carbonate to clastic sedimentary rock is best observed in a section on Frenchvale Brook in the central Boisdale Hills. Here, tightly folded siliceous carbonate, interbedded with feldspathic sandstone, contains a major (Ca,Mg)-silicate mineral component forming dark high-relief bands alternating with light-coloured, nonsiliceous dolomitic calcite marble (Fig. 3).

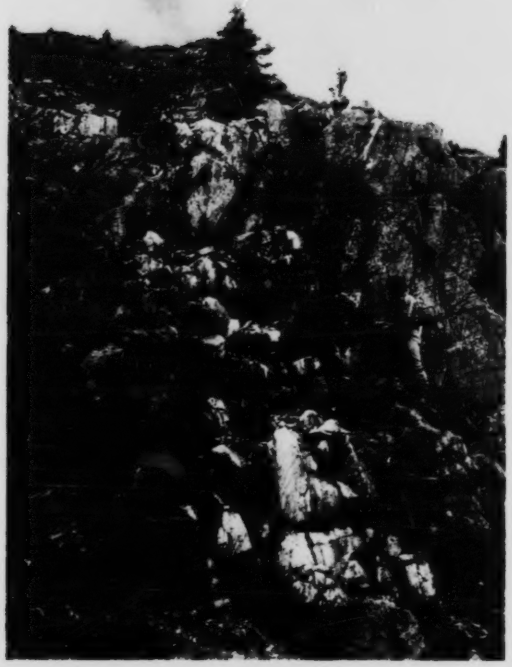

Figure 2. Light and dark grey, banded calcite marbles, north face, lower pit, Marble Mountain quarry (GSC 204624-F).

Cape Dauphin-Kellys Cove

Marble outcrops in a discontinuous belt 7 km long by 100 to 800 m wide from Cape Dauphin in the north to the dolomite quarry at Kellys Cove in the south. These

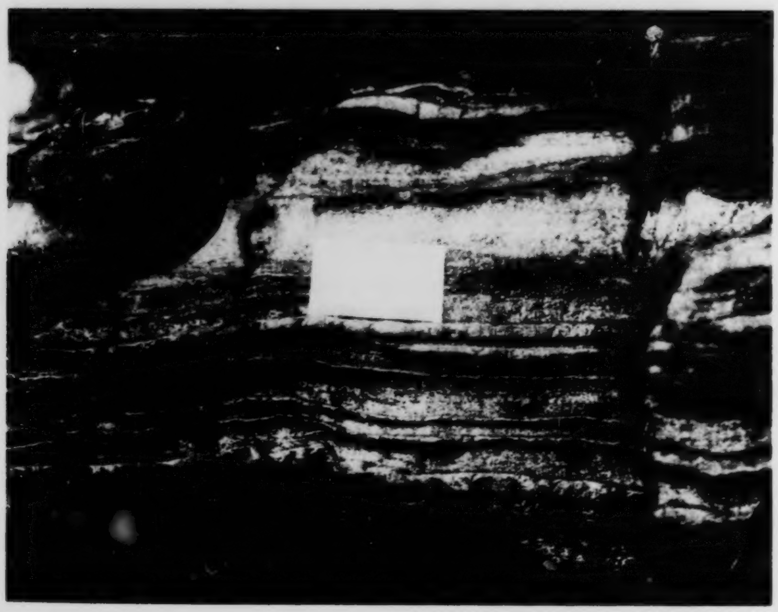

Figure 3. Interlayered pure and siliceous (calc-silicate-bearing) marbles at the carbonate-clastic sedimentary rock transition, Frenchvale Brook, central Boisdale Hills belt (GSC 204624-I).

rocks are lithologically similar to those underlying the Boisdale Hills and have traditionally been included in the George River Group (Fletcher, 1877; Bell and Goranson, 1938; Douglas, 1942). To the west, the sequence is fault-bounded and in intrusive contact with the Kellys Mountain granite and syenogranite pluton. To the east, George River Group metasedimentary rocks are unconformably overlain by Carboniferous sandstone, conglomerate, petroliferous limestone, and coal.

Carbonate lithologies include: 1) grey, banded to fissile calcite marble, which may be carbonaceous and micaceous; 2) green to pink, laminated siliceous calcite marble containing epidote + / – sphene-rich layers with hematite and chlorite alteration; 3) buff to white, massive, crystalline, very pure dolomite marble which varies in texture from medium to coarse grained in the Cape Dauphin area to very fine grained and weakly multicoloured in the Kellys Cove quarry; and 4) black to dark grey, thinly interbedded, cryptocrystalline limestone and calcareous argillite. The thickest section is exposed in the Cape Dauphin area where laminated siliceous calcite marble is overlain by a massive, coarse grained, pure dolomite marble and underlain by at least 200 m of thinly laminated and interstratified quartzite and argillite.

Mineral assemblages are indicative of upper greenschist to lower amphibolite facies regional metamorphism. Diagnostic minerals, including garnet, sphene, and epidote, occur in thin clastic interbeds within the siliceous calcite marble. Locally, evidence of higher grade contact metamorphism is indicated by the development of garnet-diopside skarn in xenoliths within the granitoid intrusion. Analyses of carbonate rocks from the area, to be discussed in a later section, suggest that contact metamorphism and/or metasomatism related to intrusion of the Kellys Mountain pluton dominated the postdepositional history of the Cape Dauphin-Kellys Cove sequence.

Cape Breton Highlands

The marble lithologies examined in the Cape Breton Highlands are a minor component of a heterogeneous, structurally complex sequence of orthogneiss, paragneiss, and lower metamorphic grade clastic units intruded by plutonic rocks of various ages and compositions. The carbonate-bearing rocks of the Cape Breton Highlands can be distinguished from similar late Precambrian carbonate-clastic rocks in central Cape Breton Island, predominantly by the relative scarcity of marble.

The McMillan Flowage Formation, examined in the north near McMillan Flowage (north of Occurrence 6, Fig. 1) and also farther south along the Barachois and North rivers (area of Occurrence 10, Fig. 1), contains a series of narrow siliceous marble units that vary in thickness from 50 to 100 m. These units consist of green to grey, calc-silicate and mica-bearing calcite marble with interbeds of relatively pure, buff to white, calcite or dolomite marble. Figure 4 shows light-coloured, calc-silicate-bearing calcite marble interbedded with amphibolite representing either mafic volcanic rocks or mafic sills. Minor foliated zones consisting of >50 percent calc-silicate minerals in a calcareous matrix also occur. Calc-silicate minerals include tremolite, pargasite, olivine, and diopside with accessory grossular, idocrase, epidote, and zoisite. The principal aluminosilicate mineral is phlogopite with lesser amounts of biotite, microcline, and muscovite. The prograde silicate minerals have been altered to talc, serpentine, and chlorite. Metamorphic grade of the enclosing clastic metasedimentary sequences which dominate the McMillan Flowage Formation varies from lower greenschist facies in the south to upper amphibolite facies (sillimanite zone) in the north (Barr et al., 1985).

To the southwest, thin (< 100 m) but persistent marble units have been recognized in the Middle River area of the southern Cape Breton Highlands within a major sequence of paragneiss. A carbonate unit examined in Middle River consists of white massive calcite and dolomite marble containing 1 to 3 percent calc-silicate minerals.

In the northern highlands, carbonate horizons in the Cape North Group form discontinuous beds and lenses, 0.3 to 100 m in width, of relatively pure, white to buff, coarse grained dolomite and calcite marble. Phlogopite, biotite, or graphite are common accessory minerals occurring as thin foliations. Variable thicknesses of calc-silicate gneiss may be associated with the marble units in contact with enclosing semipelitic and pelitic metasedimentary rocks. Calc-silicate units consist of variable amounts of calcite, dolomite, diopside, tremolite, biotite, phlogopite, and pyrite. Serpentine-talc alteration is common.

Six kilometres southwest of Dingwall (Fig. 1), phlogopite-bearing dolomite marble beds approximately 40 cm thick are interstratified with (< 10 cm thick) tremolitic calcite marble associated with amphibolite (Fig. 5). The carbonate units belong to the Money Point Group (Barr et al., 1987b). Fifteen kilometres farther southwest, thicker units of pure to slightly micaceous or graphitic, highly foliated calcite and dolomite marble, up to 50 m in thickness, were examined. Here, narrow calc-silicate-rich bands are interlayered with dolomite or calcite marble together forming 10 to 50 m thick units intercalated within quartzite and semipelite (Fig. 6). This sequence is part of the Cape North Group (Barr et al., 1987b).

Isolated exposures of Zn-rich, high-MgO, siliceous marble occur in a high-grade metamorphic complex in the Meat Cove area of northwestern Cape Breton Island. They are similar to the siliceous dolomite marble found at Lime Hill. Magnesian calc-silicate-rich marble, which hosts the Meat Cove zinc deposit, occurs with quartz-feldspar-biotite gneiss in xenoliths within the Lowland Brook syenite. The marble xenoliths are assumed to have been derived from a calcareous unit in the Polletts Cove Brook Group which is the oldest member of the Grenvillian Blair River Complex (Barr et al., 1987a).

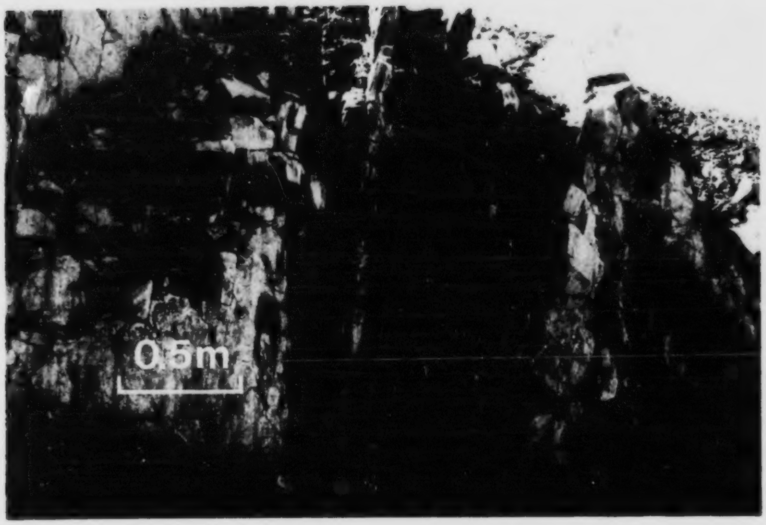

Figure 4. Calc-silicate-bearing calcite marble interlayered with mafic sills (or metavolcanic rocks), McMillan Flowage area (GSC 204624-J).

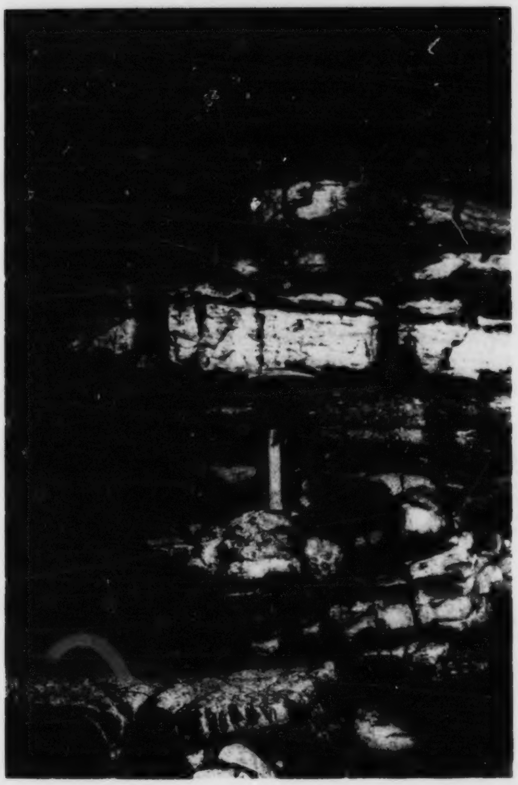

Figure 5. Narrow dolomite marble interbeds (light-toned layers) in a high-grade paragneissic sequence which also includes minor amphibolites (dark beds), South Aspy River, northern Cape Breton Highlands (GSC 204624-K).

Relationships between carbonate sequences

Clastic-carbonate metasedimentary rocks form a significant component of the pre-Carboniferous crystalline rocks on Cape Breton Island. Their stratigraphic equivalence is, however, less apparent than previous workers have suggested (e.g. Fletcher, 1877; Guernsey, 1928; Milligan, 1970). Detailed geological studies during the past five to ten years have led to a refinement of the original interpretation of Cape Breton Island geology. Results of the present study have shown that carbonate units within the George River Group and similar pre-Carboniferous supracrustal sequences can be discriminated on the basis of composition and style of metamorphism. Five sequences are recognized.

1) Marble and calc-silicate units associated with metasedimentary rocks in the Cape Breton Highlands are petrologically similar, with the exception of the Zn-bearing, high-grade siliceous dolomite marble at Meat Cove. These include carbonate units of the Cape North Group (Macdonald and Smith, 1980), McMillan Flowage Formation (Raeside and Barr, 1986), and Middle River metamorphic suite (Jamieson et al., 1984).

2) Marble and crystalline limestone/dolostone units that underlie the Creignish Hills and North Mountain (east of Lime Hill to Marble Mountain) form a uniform assemblage of predominantly calcareous marble associated with equal volumes of arenaceous and argillaceous metasedimentary rocks and minor metavolcanic rocks. Based on mineral assemblages in clastic metasedimentary rocks, regional metamorphic grade appears to be low, varying from subgreenschist to greenschist facies. Higher metamorphic grade carbonate rocks have been identified in isolated localities throughout the Glencoe area of Creignish Hills, associated with contact metamorphic environments. Calc-silicate-bearing marbles are also common throughout the Marble Mountain area where metamorphic grade is slightly higher.

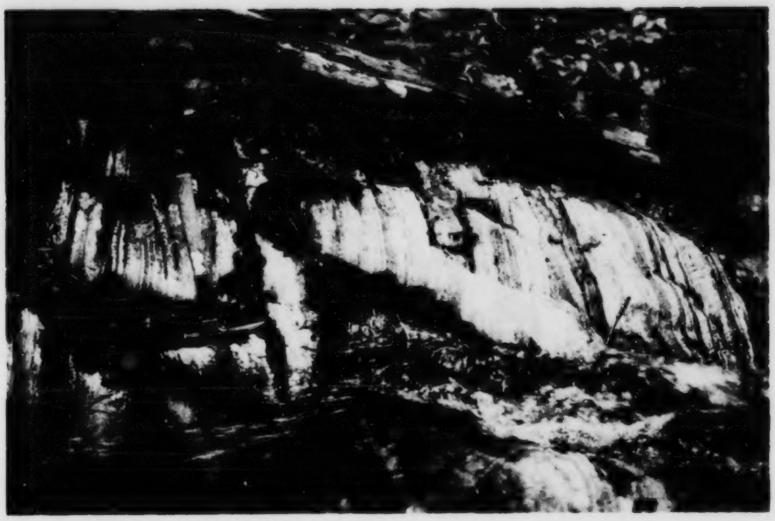

Figure 6. Thinly interlayered dolomite marble (light) and calc-silicate gneiss (dark) forming a 50 m thick carbonate layer in a high-grade metasedimentary sequence, North Aspy River area, northern Cape Breton Highlands (GSC 204624-L).

3) Boisdale Hills marble can be distinguished both chemically and geologically from Creignish Hills/North Mountain or Cape Breton Highland marble. The Boisdale Hills area is underlain by a sequence of siliceous dolomite marble and calcite marble which has been more highly metamorphosed than those in the Creignish Hills. The most commonly recognized (Ca,Mg)-silicate mineral assemblages are forsterite-diopside-tremolite +/− sphene in siliceous dolomite marble and diopside-wollastonite in calcite marbles. Associated clastic lithologies are predominantly arenaceous and only very rarely argillaceous. No metavolcanic rocks have been recognized in the sequence.

4) Carbonate units in the Cape Dauphin-Kellys Cove belt are similar in composition to marbles described previously from the Boisdale Hills but are of slightly lower metamorphic grade. The sequence contains high purity dolomite marble and siliceous varieties of calcite marble as well as a minor thickness of meta-argillite and quartzite. Garnet-epidote-sphene and, locally, garnet-diopside assemblages are common in rocks of suitable composition. Both the Cape Dauphin-Kellys Cove and the Boisdale Hills carbonate-bearing sequences are structurally and stratigraphically similar and form north-northeastward-trending, narrow linear belts composed of medium- to high-grade, carbonate-clastic metasedimentary rocks. They are bounded on the west by late Hadrynian to Early Cambrian, multiphased intrusive complexes and on the east by Carboniferous limestone, sandstone, and conglomerate.

5) Carbonate units are also associated with high-grade paragneiss complexes that are in fault contact with George River Group rocks in the Bras d'Or zone. The dolomite marbles that host the Lime Hill zinc deposit and the associated calcite marbles are of medium to high metamorphic grade, and form part of a high-temperature, low-pressure migmatitic gneiss complex which is inferred to represent a pre-George River basement complex (Justino and Sangster, 1987; Raeside and Barr, 1988; Raeside, 1990). Similarly, the calc-silicate-bearing marbles at the Meat Cove zinc deposit are part of the upper amphibolite to granulite facies Polletts Cove Brook Group. A metamorphic age of 1040 Ma and an igneous age of 1100 to 1500 Ma has been obtained from U-Pb (zircon) dating of the Lowland Brook syenite which intruded the carbonate-bearing metasedimentary rocks (Barr et al., 1987a). This is the only confirmed Grenville metamorphic age on Cape Breton Island.

GEOLOGY AND GEOCHEMISTRY OF CARBONATE-HOSTED MINERAL OCCURRENCES

Introduction

Metallic mineral production from marble-hosted ores has been limited to the recovery of iron from small deposits in the Boisdale Hills. Very minor quantities of magnetite and hematite ore were shipped from the Currie Mine and Glencoe Road deposit during the late 1800s and early 1900s (Wright, 1975). In the 1950s, increased exploration activity for base metals led to the discovery of the Meat Cove and Lime Hill zinc deposits, the largest marble-hosted base metal deposits in Nova Scotia.

Precambrian marbles in Cape Breton Island have been exploited more successfully as a source of carbonate products for industrial mineral markets. As early as the late 19th century, deposits of George River Group marble at Scotch Lake and Frenchvale in the Boisdale Hills produced metallurgical quality marble for the steel mills at Sydney. A large facility at Marble Mountain on the southwestern shore of Bras d'Or Lake produced a variety of marble products including cut stone, metallurgical flux, and agricultural lime. The only full-time quarrying operation currently active is located at Kellys Cove where agricultural and metallurgical-grade dolomite is produced. Considerable potential for the production of carbonate products has been defined in numerous large tonnage reserves of George River Group marble located throughout the Creignish Hills (Luke and MacDonald, 1988).

Metallic mineral deposits

Table 2 summarizes the lithological, mineralogical, and geochemical characteristics of 13 mineral occurrences examined during the study. The data were compiled during field examination and sampling of exposed workings and by the study of published geological reports and assessment files. Due to the vintage of many of the showings, little surface exposure exists and waste heaps provide the only source of samples. Data were also obtained from a study of calc-silicate mineral chemistry by Walker (1988) who examined the mineralogy of the Scotch Lake, Glencoe Cu, Upper Leitches Creek, and Whycocomagh skarn showings as well as the Glencoe Pb-Zn and Upper Georges River disseminated sulphide occurrences.

The metallic mineralization in Precambrian marble has been classified according to metal association, form, and distribution of mineralization and lithological association. Two major categories are defined:

1) Polymetallic Skarn. Mineralization appears to be related to a discrete contact metamorphic and metasomatic event and may be both carbonate-hosted and intrusive-hosted. Calc-silicate lithologies indicative of local metamorphic grades higher than the regional grade are intimately associated with this type of mineralization. Occurrences of this type are further subdivided according to metal association as follows:

a) Fe +/− Cu skarn
b) Fe + Cu +/− W, Mo, Sn skarn
c) Pb + Zn + Ag +/− Au, Cu skarn.

2) Stratabound. Mineralization is generally restricted to a discrete carbonate unit. It is neither related to a definable contact metamorphic event nor is it associated with calc-silicate-bearing marble lithologies of higher metamorphic grade than the regional grade. Occurrences of this type can be further subdivided according to morphology and metal association as follows:

a) stratiform Zn or Fe
b) irregular disseminated Cu-Pb-Zn.

In this classification, skarn deposits are defined as metallic mineral concentrations associated with (Ca, Mg, Fe, Al, Mn) silicate rocks that formed by metasomatic replacement of original carbonate-rich rocks through interaction with magmatic hydrothermal fluids. Whereas a majority of the metacarbonate-hosted metallic mineral occurrences examined during the study are associated with calc-silicate-bearing marble lithologies, a genetic distinction is made in the classification between skarn-hosted mineralization that appears to have been derived from magmatic hydrothermal processes related to a contact metasomatic event (polymetallic skarn deposits) and mineralization that shows no apparent relationship to contact metamorphism or metasomatism (stratabound deposits).

Polymetallic skarn deposits

Skarn occurrences are distinguished from stratabound mineralization by displaying at least three of the following relationships: 1) the spatial association of a post-depositional intrusive body; 2) the presence of a mineral assemblage that is representative of a higher metamorphic grade than is present in the regional rocks; 3) the presence of "massive" calc-silicate (skarn) rock which may cut inferred stratigraphic boundaries; and 4) metallic mineralization which replaces "massive" calc-silicate units. Skarn-associated metallic mineralization occurs in seven of the thirteen metallic mineral showings examined.

Iron (magnetite) skarns are represented by the Glencoe Road and Scotch Lake iron showings (Occurrences 1 and 2, respectively, Fig. 1). Mineralization at both localities is dominated by magnetite with lesser pyrite and minor chalcopyrite at Glencoe Road and sphalerite at Scotch Lake. The metallic minerals form massive, irregular to tabular replacement bodies associated with calcic skarn at Glencoe Road and magnesian skarn at Scotch Lake. The differentiation between calcic and magnesian magnetite skarn is recognized by Einaudi et al. (1981) in their classification of skarn deposits worldwide. The Glencoe Road magnetite showing, containing pyroxene-epidote skarn in contact with mafic monzodiorite, represents the calcic magnetite variety. In contrast, the pargasite-tremolite-phlogopite-serpentine assemblage, which replaces dolomite marble at the Scotch Lake showing, is typical of magnesian magnetite skarn deposits. In an Mg-dominated system, Fe is unable to be accommodated by the calc-silicate minerals and thus tends to form magnetite (Einaudi et al., 1981).

Fe-Cu skarns are represented by showings at Glencoe, Upper Leitches Creek, Whycocomagh, and McMillans Brook (Occurrences 3 to 6, respectively, Fig. 1). In addition to Fe and Cu, anomalous Sn and Mo are present. The Whycocomagh deposit also contains anomalous W, and trace wolframite has been reported at the Glencoe Cu skarn (Chatterjee, 1979b) and scheelite at the McMillans Brook Fe-Cu skarn (Chatterjee, 1977). Pyrite and chalcopyrite are the principal metallic minerals in addition to minor pyrrhotite. At Whycocomagh, magnetite is also common. Host lithologies include mixed calcite and dolomite marbles in contact with felsic granitoid (quartz monzonite to monzodiorite) intrusions. Prograde calc-silicate mineral assemblages include andradite-diopside-forsterite plus tremolite (Whycocomagh), andradite-salitic pyroxene (Glencoe), andradite-pargasite-actinolite plus wollastonite and diopside (Upper Leitches Creek), wollastonite-axinite-sphene and idocrase-chondrodite (McMillans Brook). The conditions under which mineralization occurred, particularly depth and CaO:MgO ratio of the host marble, appear to have been different at all four localities. In particular, the occurrence at McMillans Brook is quite complex in that four different types of mineralization have been recognized, only two of which are associated with contact metamorphism (Chatterjee, 1977). However, the metallic mineral association of pyrite, chalcopyrite, and magnetite associated with W +/− Mo-bearing minerals, the association with felsic granitoid intrusions, and the indication of oxidizing ore-forming conditions (andradite, salitic pyroxene, pyrite) show similarities to the copper skarn deposit classification of Einaudi et al. (1981).

Table 2. Geological and geochemical characteristics of metacarbonate-hosted metallic mineral occurrences on Cape Breton Island.

Occurrence	Classification	Distribution and Form of Mineralization	Economic Mineralogy	Gangue Mineralogy	Host Lithologies	Mineralization Geochemistry												n
						Cu (ppm)	Zn (ppm)	Pb (ppm)	Total Fe (%)	W (ppm)	Mo (ppm)	Sn (ppm)	As (ppm)	Sb (ppm)	Hg (ppb)	Ag (ppm)	Au (ppb)	
1. Glencoe Road	Fe Skarn	massive, replacement	magnetite pyrite chalcopyrite	epidote diopside calcite serpentine quartz	calcite marble xenolith in hornblende-biotite monzodiorite	457	85.0	30.0	56.8	3.3	1.2	1.5	5.5	2.6	5.2	0.6	2.0	3
2. Scotch Lake	Fe skarn	massive, tabular, stratiform	magnetite pyrite sphalerite	tremolite-pargasite- diopside-grossular serpentine-chlorite- phlogopite apatite epidote sphene dolomite	serpentinitic dolomite marble	35.1	0.29%	48.3	28.5	0.7	1.2	5.0	0.5	0.1	21.0	0.25	0.5	3
3. Glencoe Cu	Fe-Cu Skarn	irregular, lensoid, replacement	chalcopyrite pyrrhotite pyrite wolframite marcasite	andradite-salitic pyroxene olivine-monticellite tremolite phlogopite-calcite	massive, micaceous calcite marble + hornblende quartz monzonite	1900	50.0	4.0	10.9	0.5	24.0	15.0	58.0	1.0	21.0	0.5	6.0	1
4. Upper Leitches Creek	Fe-Cu Skarn	massive, tabular	pyrrhotite pyrite chalcopyrite marcasite	diopside-pargasite- garnet actinolite wollastonite serpentine- phlogopite-chlorite- calcite epidote sphene	pure calcite and dolomite marbles	0.13%	118	1.0	17.2	0.5*	4.0*	8.0*	29.0*	0.2*	13.0*	0.5*	31.0*	3 *n=1
5. Whycocomagh	Fe-Cu Skarn	disseminated replacement + fracture-controlled	magnetite chalcopyrite pyrite sphalerite molybdenite pyrrhotite	diopside-andradite- forsterite pargasite-tremolite talc calcite serpentine-chlorite- phlogopite sphene	calcite marble + granodiorite stock	0.12%	41.2	3.0	10.4	120	30.0	7.7	43.7	0.6	12.6	0.25	10.5	4
6. McMillans Brook	Fe-Cu Skarn	massive + fracture-controlled	pyrite chalcopyrite pyrrhotite bornite	REGIONAL forsterite monticellite diopside idocrase	siliceous calcite and dolomite marble	33	120	1.0	5.4	1.0	2.0	6.0	1.0	1.9	6.0	0.25	0.5	1
		disseminated	as above + cassiterite scheelite molybdenite	CONTACT wollastonite axinite chondrodite idocrase tremolite phlogopite sphene (Chatterjee, 1977)	as above + quartz monzonite													

Table 2. Continued

						Mineralization Geochemistry												
Occurrence	Classification	Distribution and Form of Mineralization	Economic Mineralogy	Gangue Mineralogy	Host Lithologies	Cu (ppm)	Zn (ppm)	Pb (ppm)	Total Fe (%)	W (ppm)	Mo (ppm)	Sn (ppm)	As (ppm)	Sb (ppm)	Hg (ppb)	Ag (ppm)	Au (ppb)	n
7. Rear Boisdale	Pb-Zn-Ag Skarn	irregular bands, masses, disseminations	pyrite sphalerite galena chalcopyrite magnetite pyrrhotite	ferrodolomite calcite quartz serpentine phlogopite sphene	graphitic calcite marble + minor dolomite marble	400	7.8%	3.0%	0.44	1.5	0.5	2.8	5890	58.8	27.3	82.3	1350	3
8. Lime Hill	Stratabound Zn	banded disseminated	sphalerite pyrite chalcopyrite arsenopyrite scheelite	olivine-monticellite-merwinite diopside wollastonite antigorite-talc-calcite-phlogopite (Chatterjee, 1980)	siliceous dolomite marble + serpentine marble minor calcite marble	20.2	0.86%	41	25.3*	4.3	4.4	4.0	4.0	2.2	7.1*	0.5	0.5*	60 *n=17
9. Meat Cove	Stratabound Zn	banded disseminated + massive replacement + vein-controlled	sphalerite galena pyrrhotite pyrite chalcopyrite	forsterite-periclase chondrodite-monticellite diopside-spinel talc-brucite-antigorite (Chatterjee, 1979a)	siliceous dolomite marble xenolith + hornblende syenite	15.1	4.59%	17.0	2.6	1.6	6.1	1.0	14.0	0.5	587	0.9	1.3	24
10. Barachois River	Stratabound Fe	massive, lensoid stratiform	magnetite pyrite	diopside tremolite serpentine	serpentinized, diopside-bearing dolomite marble	25.0	170	1.0	38.0	0.5	0.5	1.5	0.2	0.2	2.5	0.25	0.5	1
11. Currie Mine	Stratabound Fe	massive, lensoid stratiform	hematite trace pyrite, chalcopyrite	calcite chlorite phlogopite dolomite	serpentinized, calc-silicate-bearing calcite marble	210	31.0	1.0	14.4	28.0	3.0	1.5	4.0	0.3	2.5	0.25	2.0	1
12. Glencoe Pb-Zn	Disseminated Sulphides	irregular disseminated	galena sphalerite	calcite dolomite serpentine phlogopite quartz	massive calcite to dolomitic calcite marble	5.6	91.1	49.7	0.6	0.5*	0.5*	2.0*	0.9*	0.1*	26.7	0.25*	0.5*	10 *n=2
13. Upper Georges River	Disseminated Sulphides	irregular disseminated	chalcopyrite bornite pyrite sphalerite	dolomite calcite serpentine phlogopite trace forsterite	buff dolomite marble cut by felsic and diabase dykes	0.14%	0.22%	380	0.6	1.2	2.0	2.0	2.7	0.5	24.2	1.2	1.2	2

The Rear Boisdale showing is an example of Pb-Zn-Ag skarn-associated mineralization hosted in graphitic calcite marble (Occurrence 7, Fig. 1). Galena, sphalerite, and pyrite with accessory chalcopyrite are found in massive and disseminated sulphide samples collected from a waste heap adjacent to an early 1900s exploration shaft. The samples also contain anomalous silver (up to 180 ppm) and gold (up to 2.7 ppm). Although the showing does not outcrop, diamond-drill records from the area (Nova Scotia Department of Mines and Energy, Assessment Record AR 11K/01B 28-C-65) describe massive disseminated and stringer sulphide and iron oxide zones, associated with a "lime-silicate aureole", in contact with hornblende-biotite granite. Lead isotope analysis of galena from the Rear Boisdale occurrence also indicates an intrusive affiliation for sulphide mineralization (Sangster and Thorpe, 1987). The Rear Boisdale occurrence may be representative of the calcic lead-zinc class of skarn deposits described by Einaudi et al. (1981).

Stratabound/stratiform Zn-Fe deposits

The Lime Hill and Meat Cove stratabound deposits are similar to significant zinc +/− lead deposits and occurrences hosted in Helikian dolomite marble in Grenville Supergroup rocks. The largest deposits in the Grenville Supergroup are in the Balmat-Edwards district of northern New York (deLorraine and Dill, 1982). Similar smaller occurrences are also located in the Maniwaki-Gracefield area of southwestern Quebec (Gauthier and Brown, 1986) and throughout southeastern Ontario (e.g. Long Lake, Renprior, Spry, Slave Lake) (Sangster and Bourne, 1982). Sulphide mineralization is characteristically hosted in regionally metamorphosed dolomite and calc-silicate-bearing dolomite marble as coarse grained, massive to banded disseminated concentrations of sphalerite +/− galena, pyrrhotite, pyrite, and chalcopyrite. The stratiform and concordant nature of mineralization, its association with dolomite marble members of the stratigraphic sequence, and its age correlation to Grenville Supergroup host rocks suggest that ore deposition was synsedimentary (Fletcher and Farquhar, 1982) with only minor remobilization during regional metamorphism. In such a metallogenic environment, ore fluids are thought to be evolved basin brines chemically similar to the fluids responsible for Mississippi Valley-type deposits (Whelan et al., 1984), with sulphide minerals deposited in a submarine-exhalative environment (Gauthier and Brown, 1986).

Stratiform/stratabound zinc deposits occur at Lime Hill and Meat Cove on Cape Breton Island (Occurrences 8 and 9, respectively, Fig. 1). Both deposits are characterized by the presence of banded disseminated sphalerite contained almost entirely within a siliceous dolomite marble (Fig. 7). Magnesian and calcic calc-silicate mineral assemblages indicative of high metamorphic grade are present at both sites.

At Meat Cove, vein and stringer pyrite, chalcopyrite, and trace bornite have also been identified in a syenite intrusion at the carbonate contact (Chatterjee, 1979a). Chatterjee implied that the Meat Cove zinc deposit was formed in a contact metasomatic environment in which sphalerite replaced magnesian skarn (a forsterite-periclase-monticellite-diopside-tremolite-bearing unit). However, similarities in the style of mineralization and geological setting between the Meat Cove deposit and zinc mineralization at Lime Hill, suggest that both are similar to marble-hosted zinc deposits of the Grenville Supergroup.

A skarn association for Lime Hill mineralization is not indicated by clinopyroxene compositions. Analyses from a number of Lime Hill marble samples average 81 mole percent diopside and 0.1 to 1.5 mole percent johannsenite (Walker, 1988) compared with pyroxene analyses from zinc skarn deposits compiled by Einaudi et al. (1981) which typify base metal skarn-related pyroxenes as dominantly hedenbergite-johannsenite compositions. Taken in conjunction with isotope studies by Sangster and Thorpe (1988), who identified similar lead and sulphur isotopic compositions in sulphides from Lime Hill, Meat Cove, and a number of stratabound zinc deposits hosted in Grenville Supergroup dolomite marble, the pyroxene data tend to support the hypothesis that Lime Hill and, by inference Meat Cove, are not skarn deposits. Additionally, zinc-bearing marbles at the Meat Cove deposit are thought to belong to the carbonate-bearing Polletts Cove Brook Group which is Helikian or older in age (Barr et al., 1987a). The age of the Lime Hill deposit is somewhat more controversial. Sangster and Thorpe (1988) have suggested that the Grenville isotopic signature of Lime Hill galena supports a depositional age correlative to the Grenville Supergroup, although it is apparent that the Lime Hill area escaped medium- to high-pressure Grenvillian metamorphism (Raeside, 1987).

Iron-rich stratabound mineralization at the Barachois River showing occurs in a thin carbonate unit of the McMillan Flowage Formation, and similar mineralization at the Currie Mine is found in marbles of the George River Group (Occurrences 10 and 11, respectively, Fig. 1). Mineralized zones occur as narrow discontinuous lenses of massive iron oxides (magnetite at Barachois River and hematite after magnetite at the Currie showing), conformable to local compositional layering. A calc-silicate mineral assemblage of regional metamorphic grade is present in siliceous dolomite to dolomitic calcite marbles at both localities. Little geological data are available for either showing and a metallogenic model for ore deposition would be highly speculative. However, small magnetite-rich iron formations are associated with stratiform zinc mineralization in siliceous Mg-carbonate units of the Grenville Supergroup (discussed above). Both the iron formations and the stratiform zinc mineralization are thought to have formed from similar synsedimentary processes (Gauthier and Brown, 1986).

Irregular disseminated Cu-Pb-Zn mineralization

Disseminated sulphide mineralization of limited distribution can be observed at a number of localities within George River Group marble. The localities described in Table 2 represent two occurrences discovered during the

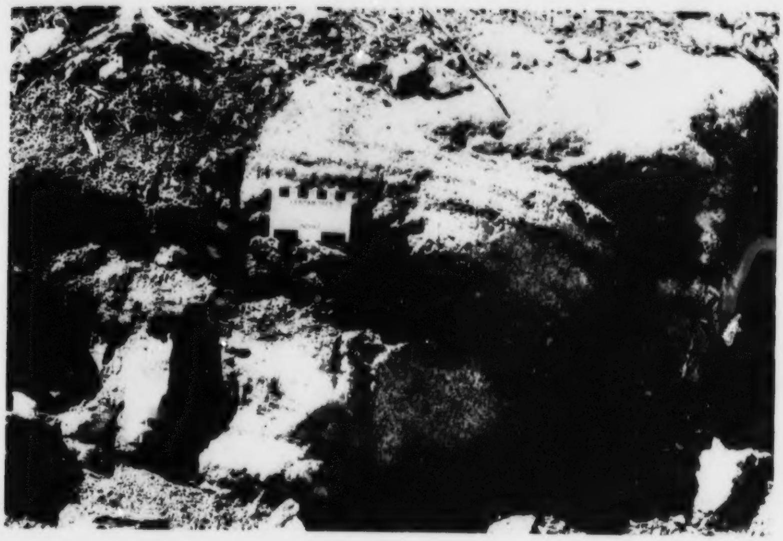

Figure 7. Banded disseminated sphalerite mineralization (dark layers) in siliceous dolomite marble cut by secondary gossanous iron mineralization (limonite after pyrite) which weathers recessively, Lime Hill zinc deposit (GSC 204624).

present study (Hill, 1987b). The Glencoe Pb-Zn and Upper Georges River showings (Occurrences 12 and 13, respectively, Fig. 1) consist of 1 to 2 percent combined disseminated galena, sphalerite, chalcopyrite, and pyrite hosted in relatively pure (SiO_2 <5.0 percent) calcite and dolomite marble. A calc-silicate mineral assemblage representative of regional metamorphic grade (forsterite-phlogopite-serpentine) is observed in marbles at both showings.

Similar styles of mineralization have been reported in George River Group carbonates at other localities including minor occurrences of disseminated galena in the Campbell Lakes and Frenchvale areas of the Boisdale Hills (Hill, 1987a, Table 56.1). Insufficient geological data is available, due mainly to poor exposure of mineralized units, to conclusively support any one metallogenic model for this type of mineralization. At the Upper Georges River showing, diabase and felsic porphyry dykes are spatially associated with mineralization as is a dioritic phase of the Boisdale Hills Pluton. Contact metamorphic relationships are slightly more obvious but no indication of widespread metasomatic activity is present. It is suggested that mineralization at each of the sites is probably syngenetic to diagenetic in origin and related to similar but more localized processes that resulted in the formation of the larger stratabound deposits such as Lime Hill.

Industrial mineral deposits

Industrial mineral deposits of carbonate rock and carbonate-associated minerals are grouped according to petrology and mineralogy as follows:
1) calcite marble deposits;
2) dolomite marble deposits;
3) (Ca,Mg,Fe,Al)-silicate mineral deposits;
4) marble-hosted, noncalc-silicate mineral deposits.

A total of 12 occurrences and deposits were examined during the study and summarized according to lithology, economic characteristics, and geochemistry (Table 3). Good surface exposure of some of the larger carbonate deposits (such as Glencoe and Glendale), as well as the exposure provided by numerous past and current quarrying operations, allowed for extensive and detailed data collection.

Calcite and dolomite marble deposits

Calcite and dolomite marble formations of the George River Group have been a significant source of mineral production on Cape Breton Island. Quarry operations at Marble Mountain, Scotch Lake, Frenchvale, and more recently, Kellys Cove, represent a mining history that goes back to 1865. Marbles are exploited because of specific chemical or physical properties that make them suitable for a variety of uses including filler/extender products, cement, metallurgical flux, agricultural and industrial lime, mine rock dust, aggregate, and building/architectural stone. Their potential for use in the manufacture of highly specialized products is dependent upon a series of industry-defined physical and chemical standards (Hill, 1987b).

The Glencoe deposit (Occurrence 14, Fig. 1) contains one of the largest volumes of pure calcite marble on Cape Breton Island. The deposit is composed of a structurally complex sequence of grey, banded to massive, calcite and siliceous calcite marbles with minor dolomite marble interlayers. Very high purity (>95 percent $CaCO_3$) white calcite marble, suitable for filler/extender products or as an ore of calcium metal, form laterally extensive units up to 100 m in thickness in the Glencoe succession. Marble units generally contain at least 95 percent carbonate minerals (calcite and dolomite) and are correspondingly low in silica, alumina, total iron, and alkalis. Sulphur and

Table 3. Geological and geochemical characteristics of metacarbonate industrial mineral occurrences on Cape Breton Island. (Note: LOI = Loss On Ignition, NCC = Noncarbonate Carbon, n.a. = not analyzed, Mt = Million tonnes).

Occurrence	Commodities	Description of Rock Types	Production/Reserces	Major Element Geochemistry (%)									
				SiO_2	CaO	MgO	CaO:MgO	Al_2O_3	$Fe_2O_3^T$	LOI	S	NCC	n
14. Glencoe	calcite and dolomite marble	1. varieties of grey, banded, fine- to medium-grained, micaceous/graphitic, calcite marble	no production 160 Mt metallurgical grade reserves 300+ Mt cement grade reserves (MacNeil, 1977)	3.84	50.4	2.18	64.8	0.87	0.31	41.5	0.008*	0.11*	21 *n=14
		2. white, massive, medium- to coarse-grained, calcite marble		1.80	53.1	2.05	74.7	0.28	0.13	42.5	0.005	0.03	3
		3. blue-grey to white, very fine grained, massive, dolomite marble		0.83	31.6	21.3	1.50	0.23	0.22	45.7	0.005	0.19	4
15. Campbell Brook	calcite marble	varieties of thinly laminated, pink to buff and grey to blue, hematitic calcite marble, occasionally micaceous	no production	2.14	46.8	6.37	66.1	0.56	0.43	42.8	n.a.	n.a.	5
16. Glendale	calcite marble	1. buff to white, massive, fine grained calcite marble	no production 77+ Mt cement grade reserves[1]	1.44	51.0	4.14	12.3	0.26	0.13	42.9	0.005	0.005	1
		2. grey, banded, fine grained, hematitic calcite marble		5.73	51.1	1.24	41.2	1.53	0.65	39.0	0.005	0.41	3
		3. thinly laminated, grey, micaceous calcite marble.		13.5	40.2	5.30	7.6	3.52	2.40	32.2	0.005	0.005	1
17. Marble Mountain	calcite and dolomite marble	1. grey-blue, banded, medium grained calcite marble	2.3 Mt metallurgical and agricultural grade marbles + dimension stone (1865 to 1921). current production = aggregate 5.0+ Mt cement grade reserves[1]	2.5	49.3	4.36	11.3	0.27	0.37	42.0	0.005*	0.21*	9 *n=6
		2. highly fractured, multicoloured, fine grained siliceous calcite marble		6.98	48.4	1.97	33.4	1.81	1.05	36.7	0.12	0.63	4
		3. massive, white to buff, coarse grained, pure calcite marble		1.6	53.5	1.28	61.5	0.49	0.08	42.6	0.005	0.005	8
		4. massive, grey, medium grained dolomite marble cut by serpentine-epidote-filled fractures		5.95	30.3	21.5	1.4	0.3	0.50	41.4	0.005	0.25	2
18. Frenchvale	dolomite marble	1. varieties of massive to banded, grey to green, medium to coarse grained dolomite marble often micaceous and serpentinitic	0.05 Mt metallurgical grade marble (1964) current production = aggregate	13.3	29.0	16.9	1.8	1.0	1.4	37.4	n.a.	n.a.	5
		2. biotite diorite											
		3. biotite granite											

Table 3. Continued

Occurrence	Commodities	Description of Rock Types	Production/Reserces	Major Element Geochemistry (%)									
				SiO_2	CaO	MgO	CaO:MgO	Al_2O_3	$Fe_2O_3^T$	LOI	S	NCC	n
19. Scotch Lake	dolomite marble	1. massive, light green-grey, medium grained dolomite marble with variable talc-serpentine alteration 2. lamprophyre dykes	metallurgical grade marble (1899 to 1954) no current production	4.2	36.9	16.3	3.8	0.058	0.68	39.9	0.17*	0.21*	11 *n=7
20. Churchview	dolomite marble	massive, white to buff, medium grained, pure dolomite marble	2000 t filler grade (1920s) 4.3 Mt reserves[1]	2.32	30.0	20.1	1.5	0.37	0.17	45.6	n.a.	n.a.	4
21. Kellys Cove	dolomite marble	massive, pink-grey and green-buff, fine to very fine grained, pure dolomite marble	current production = metallurgical and agricultural grade dolomite 3.5 Mt reserves[1]	1.24	30.1	22.0	1.4	0.24	0.32	46.0	n.a.	n.a.	2
22. Lime Hill	wollastonite	prograde metamorphism of calcite marble	no production	Not analysed									
23. Meat Cove	brucite	retrograde alteration of periclase, up to 15% disseminated brucite crystals	no production	Not analysed									
24. Whycocomagh	talc, soapstone	talc-serpentine alteration of narrow dolomite marble interbeds, <30 cm in thickness, in clastic metasediments	no production	Not analysed									
25. Glendale	graphite	black, sooty, flaky to amorphous graphite schist layers containing pyrite nodules, <100 m thick, in thinly laminated, black carbonaceous limestone and calc-argillite	no production						20.1	25.8	11.6	12.2	4

[1] Luke and Macdonald, 1988

noncarbonate carbon are also low. Ore reserve estimates in the Glencoe area have outlined significant tonnages of metallurgical grade marble, defined by a 2.5 percent SiO_2 cutoff, and industrial grade marble, defined by a 4.0 percent MgO cutoff (MacNeil, 1977).

A succession of calcite marble strata in the North Mountain area is of similar high purity (Occurrence 15, Fig. 1). The Campbell Brook (Kennedys Big Brook) area is underlain by a thick succession of banded to thinly laminated, pink and grey calcite marble composed of 96 percent carbonate minerals. The marble contains higher total iron than the Glencoe carbonates, but is lower in silica and alumina.

Another large tonnage calcite marble deposit has been delineated near Glendale (Occurrence 16, Fig. 1). The marble is similar in appearance and chemistry to marble occurring at Campbell Brook but is less consistent in purity. Thinly laminated zones, 5 mm in thickness, composed of phlogopite-rich and calcite-rich layers up to 10 m in thickness occur within the pure calcite marbles. These micaceous zones contribute an undesirable aluminosilicate component to the total volume of calcite marble available.

The Marble Mountain quarry (Occurrence 17, Fig. 1) was historically the only major producer of cut marble stone on Cape Breton Island. The lower quarry exposes a major thickness of grey banded calcite marble composed of potential cement-grade material (Fig. 8). Interstratified with this unit is a very high purity, white to buff, coarse grained marble composed of >98 percent carbonate minerals, with potential as a mineral filler/extender product (Luke and MacDonald, 1988).

The Frenchvale and Scotch Lake quarries (Occurrences 18 and 19, respectively, Fig. 1) are two former producers of metallurgical and agricultural grade marble. Currently, they contain no reserves of carbonate material suitable for modern industry requirements. Both quarries expose sections of the more dolomitic and siliceous marble formations characteristic of the George River Group exposed in the Boisdale Hills. The marbles also tend to be enriched in disseminated sulphide minerals compared to marbles exposed in the Creignish Hills. Marble at the Frenchvale and Scotch Lake quarries consists of massive, grey to green, highly fractured, calc-silicate-bearing dolomite which has been altered to a talc-serpentine-bearing marble. At Scotch Lake, closely spaced lamprophyre dykes have intruded the dolomite marble thereby complicating the recovery of a suitable commercial carbonate product from the area (Isenor, 1984) (Fig. 9).

High purity dolomite marble formations can be found at Churchview and Kellys Cove (Occurrences 20 and 21, respectively, Fig. 1). Filler grade material used in paint manufacture was recovered from a white to buff, coarse grained, massive dolomite marble quarried at Churchview during the 1920s. At New Campbellton, the Kellys Cove quarry recovers a very fine grained, massive dolomite marble which is processed for use as agricultural lime and metallurgical flux. Phases of the dolomite marble in both localities are of very high purity and are closely comparable in chemical composition to dolomite currently exploited by Chromasco at the Haley deposit, Renfrew County, Ontario, for magnesium (Hill, 1987b). Coarse grained, buff to white dolomite marble displaying the physical properties of a quality dimension stone occurs in the Cape Dauphin area.

(Ca,Mg,Fe,Al)-silicate mineral deposits

Calc-silicate mineral assemblages develop in the system $CaO\text{-}MgO\text{-}SiO_2\text{-}CO_2\text{-}H_2O$ under conditions of thermal metamorphism and/or hydrothermal alteration. The mineral assemblages may form in contact metamorphic/metasomatic environments, and thereby be related to skarn metallic deposits, or they may evolve during regional prograde or retrograde metamorphism of impure carbonate rock. A variety of calc-silicate minerals of potential economic value may form, including wollastonite, asbestiform tremolite, garnet, olivine, periclase, and magnesite, or their alteration products, including

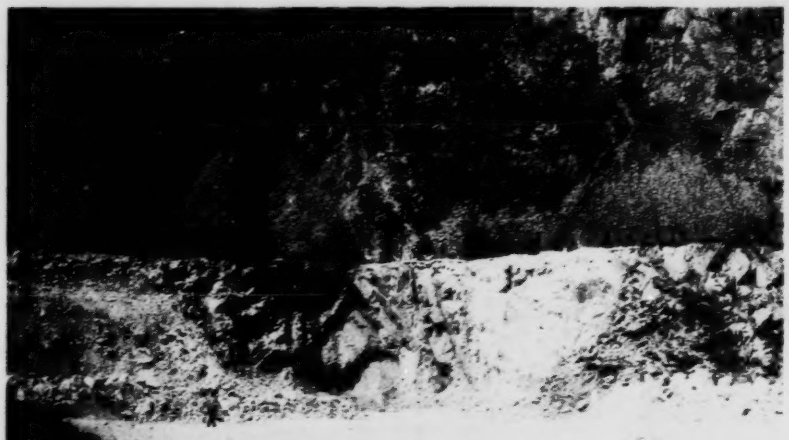

Figure 8. Marble Mountain quarry, north face lower pit, exposing a succession of isoclinally-folded, pure to impure, light buff to dark grey, calcite marble (GSC 204624-B).

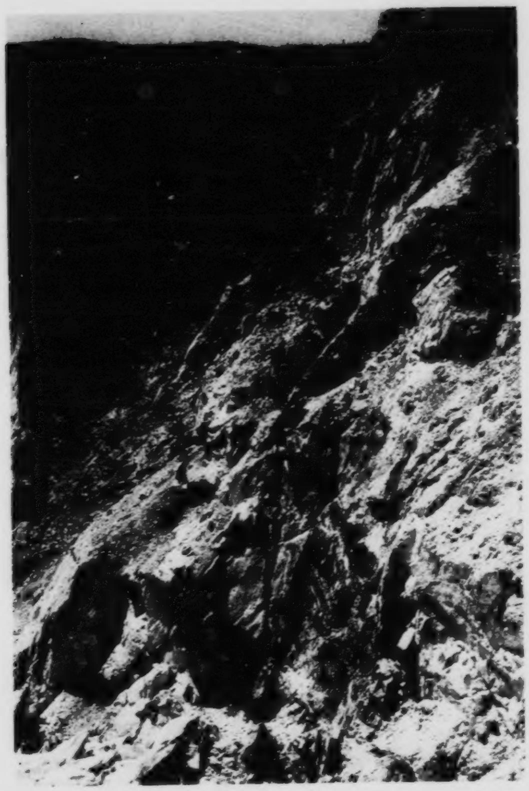

Figure 9. Scotch Lake quarry, exposing steeply dipping, highly fractured, serpentinized, siliceous dolomite cut by a lamprophyre dyke/sill (GSC 204624-A).

talc-serpentine (soapstone) and brucite. Of these, wollastonite at Lime Hill, brucite associated with the Meat Cove zinc deposit, and talc occurrences in the Whycocomagh area, are of interest on Cape Breton Island.

The calcite marble at Lime Hill contains minor amounts of wollastonite (Occurrence 22, Fig. 1). It occurs as acicular to blocky, fine grained aggregates with calcic diopside, in centimetre-scale bands. The wollastonite-diopside bands appear to be restricted to calcite marble adjacent to Cambrian granitoid dykes (A.L. Sangster, pers. comm., 1988). At Meat Cove (Occurrence 23, Fig. 1), up to 15 percent disseminated brucite has formed during the retrograde alteration of periclase in the Mg-rich calc-silicate assemblage associated with the zinc mineralization. In the Whycocomagh (Churchview) area, adjacent to the Churchview dolomite deposit (Occurrence 24, Fig. 1), minor talc has been reported since 1896. The showings are described as narrow bands of massive cream-coloured talc, <30 cm in thickness, hosted by grey quartzite. Narrow interbeds of talc-serpentine rock occur in isolated outcrops of clastic metasedimentary rocks. The talc formations described in the literature may thus represent very highly altered dolomite marble lenses interstratified with arenaceous metasedimentary rocks of the George River Group.

Marble-hosted, noncalc-silicate mineral deposits

This type of occurrence is singularly represented by the Glendale graphite showing which is located in the central Creignish Hills (Occurrence 25, Fig. 1). The deposit consists of highly deformed, carbonaceous to graphitic and pyritic schist, 100 m thick, in a black cryptocrystalline limestone (Fig. 10). It is unclear whether the graphite schists represent bedding-parallel layers in the carbonate sequence or whether they represent discordant shear zones. The carbonaceous layers are likely sedimentary in origin but have undergone some degree of remobilization and perhaps concentration during regional metamorphism. Pyrite nodules up to 5 cm in diameter have developed within the graphite schist. Samples of pyrite analyzed during this study contained as much as 28 ppb gold.

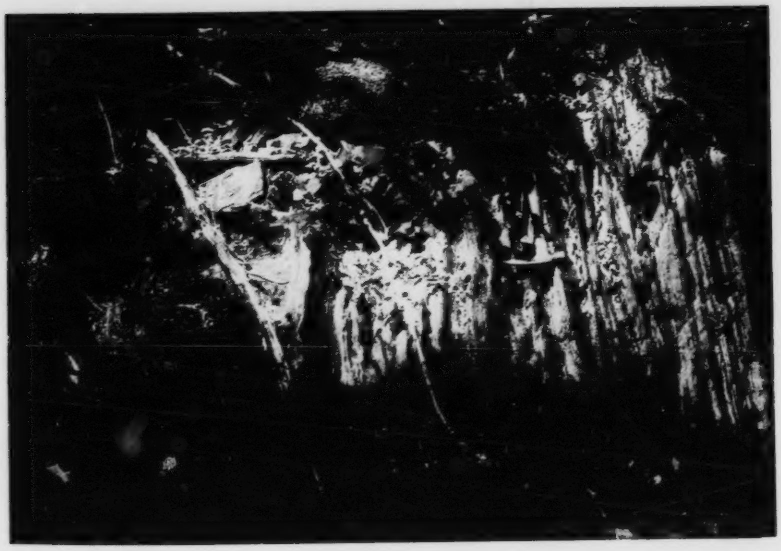

Figure 10. Deformation contrast between highly contorted, graphitic schist lenses (on the left) in contact with less highly deformed, banded crystalline limestone (on the right), Glendale graphite showing (GSC 204624-D).

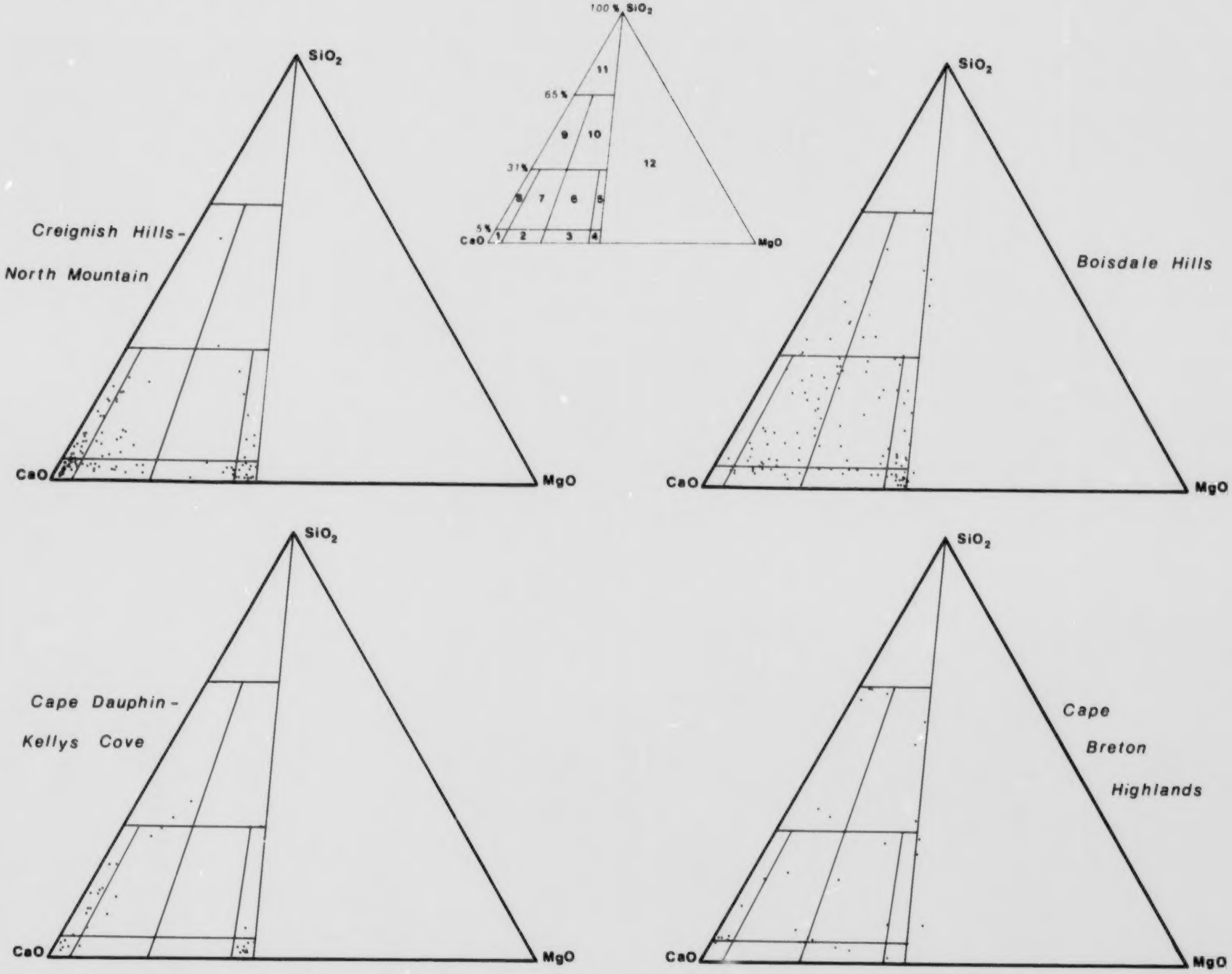

Figure 11. SiO_2-MgO-CaO weight percent ternary diagrams for carbonate analyses according to study area. Field boundaries adapted from Storey and Vos (1981, Fig. 8a). 1 = calcite marble, 2 = dolomitic calcite marble, 3 = calcitic dolomite marble, 4 = dolomite marble, 5 = siliceous dolomite marble, 6 = siliceous calcitic dolomite marble, 7 = siliceous dolomitic calcite marble, 8 = siliceous dolomite marble, 9 = calc-silicate calcite marble, 10 = calc-silicate dolomite marble, 11 = calc-silicate rock (skarn), 12 = MgO-enriched rock (including magnesite marble).

GEOCHEMISTRY OF PRE-CARBONIFEROUS METACARBONATE ROCKS

Chemical classification of carbonate rocks

Carbonate rocks are commonly classified according to relative proportions of calcite and dolomite determined by field tests using dilute HCl or Alizarin stain, by petrographic examination in thin section, or by analytical means. Most pure carbonate lithologies exhibit a well defined partition between pure dolomite rock and what Goudge (1938) referred to as magnesian limestone (Cao:MgO ratio of approximately 1.7 or 90 volume percent dolomite). The boundary between magnesian limestone and limestone is less distinct. Hewitt (1960) devised a similar threefold scheme which placed the dolomite break arbitrarily at 50 volume percent dolomite (CaO:MgO = 3.95). Pettijohn (1975) later developed a fourfold classification to include limestone, dolomitic limestone, calcareous dolostone, and dolostone.

Storey and Vos (1981) outlined a classification of carbonate rocks based on the relative proportions of CaO, MgO, and SiO_2 in a study of Grenville Supergroup marbles in the Renfrew area, Ontario. Their system was adapted for use in the chemical classification of Cape Breton Island marbles during this study (see Fig. 11). Compared with the field method of carbonate classification, using visual identification and diagnostic testing of mineral components, chemical analyses are obviously more accurate in classifying intermediate carbonate compositions. Pure carbonate end members are readily recognizable in the field. However, as grain size decreases, so does ease of identification (Hill, 1987b).

In this study, marble is defined as carbonate rock containing less than 50 weight percent SiO_2 and a CaO:MgO ratio which may vary from approximately 1.4 for pure dolomite to infinity for pure calcite. Low-silica marbles with CaO:MgO ratio less than 1.4 contain MgO-rich minerals such as magnesite, periclase, or brucite. Samples that contain concentrations greater than 50 weight percent SiO_2 are not considered carbonates under this classification but instead are referred to as calc-silicate or skarn units. In classifying siliceous marbles (SiO_2 = 5 to 50 percent) according to carbonate composition, it is assumed that the present composition of the sample is equivalent to the composition of the original carbonate sediment. This assumption is valid if regional isochemical metamorphism has been dominant in marble genesis (Perry, 1969; Einaudi et al., 1981; Guilbert and Park, 1986, p. 437).

All carbonate analyses of the current study, excluding those originating from areas of known metallic mineralization, are plotted on SiO_2-MgO-CaO ternary diagrams (Fig. 11). Compositional field boundaries correspond to the major chemical classes of marble (modified from Storey and Vos, 1981). The ternary plots demonstrate the wide range of compositions represented by metacarbonate sequences throughout Cape Breton Island.

Variations in carbonate rock chemistry are also evident between each area. The Creignish Hills-North Mountain marbles are dominated by relatively pure calcite marble with a small component of low-silica dolomite marble. In contrast, carbonate samples from the Boisdale Hills cover a broad range of impure dolomite to dolomitic calcite marble. Samples from the Cape Dauphin-Kellys Cove marble belt tend to occur within the pure calcite and pure dolomite marble fields, although a higher proportion of siliceous samples are present than in the Creignish Hills-North Mountain population. The distribution of carbonate samples from the Cape Breton Highlands defines a highly variable assemblage of pure to impure calcite and dolomite marble.

Regional implications of the geochemical data

A broad spectrum of sedimentary and metamorphic rock types is represented in the pre-Carboniferous metasedimentary terranes of Cape Breton Island. As implied in Figure 11, marble formations can also be distinguished on a chemical basis. Statistical evaluation of the major and trace element data further quantifies the chemical dissimilarities. Variation plots (Fig. 12), based on arithmetic averages of major and trace element data for the five study areas (Boisdale Hills, Creignish Hills, Cape Dauphin-Kellys Cove, Cape Breton Highlands, and North Mountain) define three chemically similar carbonate assemblages. They are:

1) carbonate rocks from the Creignish Hills and North Mountain areas (Areas 2 and 5), characterized by low levels of Si, Al, Na, K, Ti, Zr, Sr, Rb, Ba, Mn, and the base metals, and a highly calcitic carbonate composition (CaO:MgO ratio ranges from 37 to 47);
2) carbonate rocks of the Cape Breton Highlands (Area 4) characterized by elevated major and minor element contents (including Si, Al, Ti, Mn, Fe, Zr, Sr, Ba, Rb, Cu, and Zn);
3) carbonate rocks from the Boisdale Hills and the Cape Dauphin-Kellys Cove belt (Areas 1 and 3), containing major and minor element concentrations intermediate between the high purity Creignish Hills-North Mountain marbles and the impure Cape Breton Highlands marbles, as well as containing anomalous concentrations of Zn and Pb.

Chemical variation plots using notched box and whisker diagrams (Fig. 13) also illustrate compositional variations between carbonate populations. The diagrams summarize the following statistical parameters (from McGill et al., 1978; Kurzl, 1988): 1) the 75th, 25th, and 50th percentile levels of each population forming the top, bottom, and horizontal bisector of the box, respectively; 2) the range of values represented by the "whiskers" which cover sample values 1.5 times the interquartile range and thus define the threshold cutoffs; 3) anomalous data points (outliers) which lie beyond the whiskers and are marked as single points; and 4) the standard deviation at the 95th confidence interval represented by the width of the notch. The width of the box is proportional to the square root of the number of observations in the population. Data for SiO_2, Al_2O_3, CaO:MgO, TiO_2,

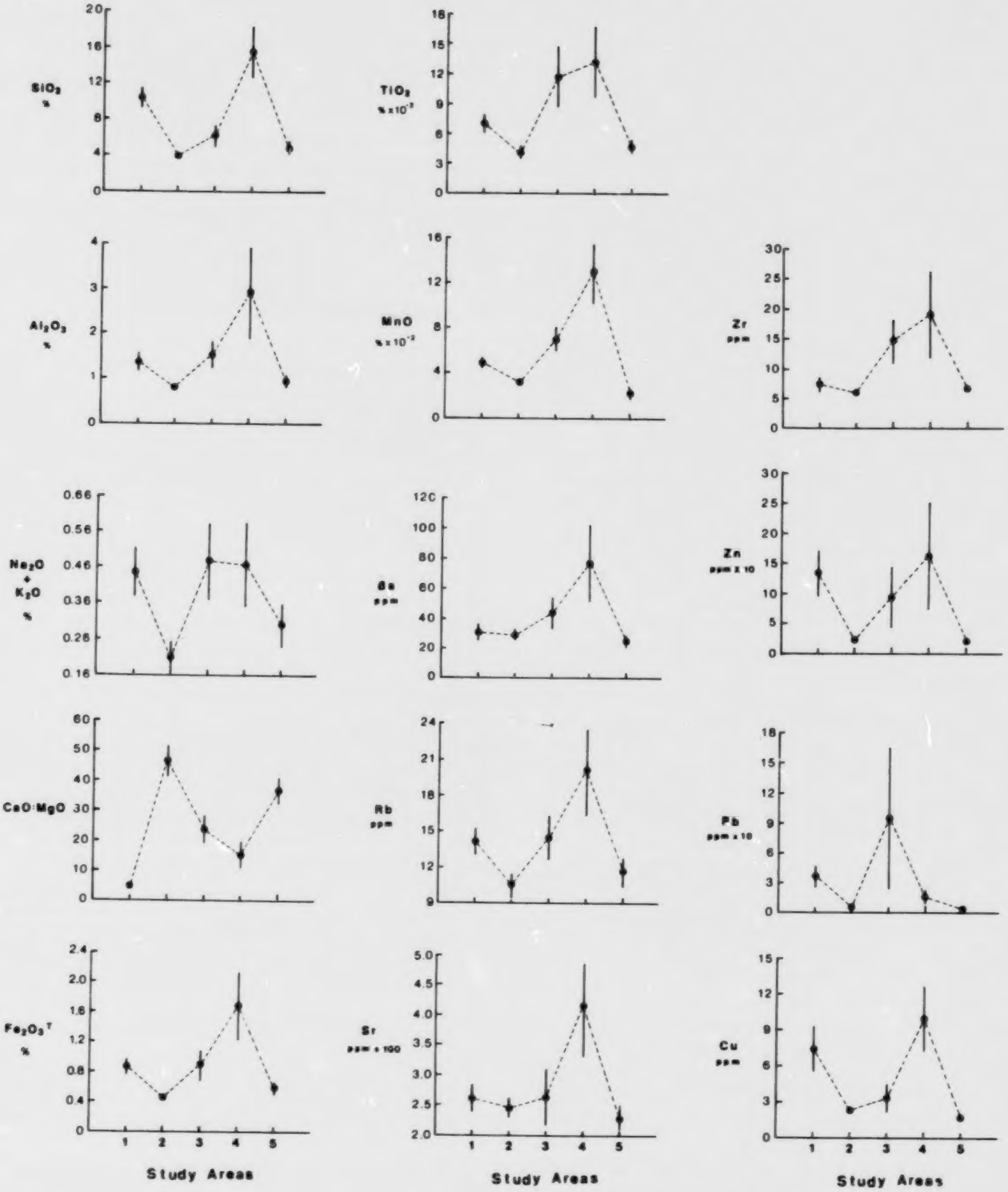

Figure 12. Mean value plots (with standard error bars) of major, minor, and trace elements for five areas of carbonate rock. Areas are: 1 = Boisdale Hills (n=123), 2 = Creignish Hills (n=138), 3 = Cape Dauphin-Kellys Cove (n=37), 4 = Cape Breton Highlands (n=27), 5 = North Mountain (n=69).

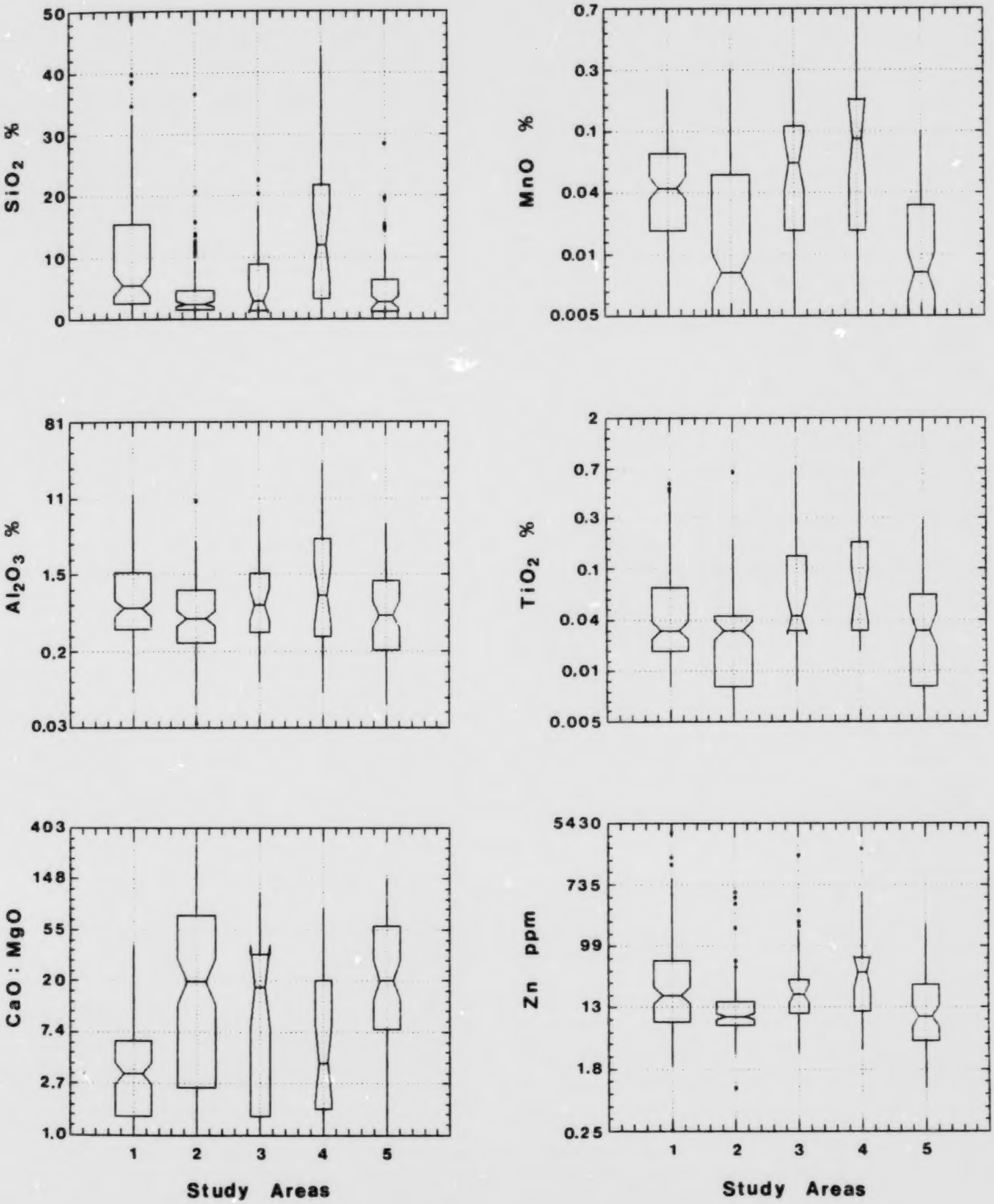

Figure 13. Notched box and whisker plots of selected major and trace element data for five areas of carbonate rock. Interpretation of these plots is dicussed in the text. Areas as in Figure 12.

MnO, and Zn support the same three compositional groupings of carbonate rock defined above.

Statistically, sample populations from the five study areas show a remarkable degree of chemical uniformity within each group in spite of their highly variable lithological composition and appearance. Detailed comparison between chemical and field data for individual marble samples demonstrates that variations in physical properties, such as colour, degree of fracturing, texture, or carbonaceous content, do not correlate with chemical variations. The Creignish Hills, North Mountain, and Boisdale Hills carbonates show little statistical variance for most elements. In contrast, the Cape Breton Highlands and Cape Dauphin-Kellys Cove populations demonstrate considerably more sample variance, particularly for the trace elements (Fig. 12). This may be related more to the limited size of these two populations than to inherent chemical diversity.

Metallogenic implications of the geochemical data

Marble formations, similar to those studied on Cape Breton Island, are thought to undergo little chemical change during regional metamorphism. A recent lithogeochemical study by Munyanyiwa and Hanson (1988) demonstrated that major and trace element compositions of amphibolite grade marble and calc-silicate units of the Proterozoic Zambezi belt are related to the aluminosilicate mineral content of the original carbonate rocks. They concluded that clays and detrital micas were the most important contributors of Al_2O_3, SiO_2, TiO_2, FeO, Na_2O, K_2O, Ba, Rb, Cr, Ni, and Zn to marble chemical signatures. Detrital zircon was assumed to have contributed Zr and Y.

Similar studies were completed by the author using geochemical data for Cape Breton Island marbles (Hill, 1988). Results of that study indicated a strong positive correlation, shown by discriminant analysis, between the basic rock-forming elements (including Si, Al, Na, K, Fe, P, Ba, Rb, Cr, Ti, Zr, and Y) in George River Group marbles of the Boisdale and Creignish hills. This relationship strongly suggests that their distribution is directly related to the composition of the original sedimentary rocks. In contrast, the geochemical signature of marble units within the Cape Dauphin-Kellys Cove belt points to postdepositional addition by metasomatic activity. A strong positive correlation between the rock-forming elements (here including Si, Al, K, Fe, Ti, P, Cr, Zr, and Ba) and the base metals (including Cu, Pb, and Zn) implies that mineralization is associated with the introduction of iron, silica, alumina, and other magmatic components into the carbonate rock by hydrothermal fluids during the preliminary stages of contact metasomatism. Intrusion of the Kellys Mountain leucogranite locally initiated contact metasomatic reactions which led to the development of skarn lithologies at the carbonate-intrusive contact. Similar, though less conclusive evidence of metasomatic alteration is present in the geochemical signature of Cape Breton Highlands marbles.

In addition to sedimentological, metamorphic, and primary compositional variations, it is apparent that carbonate metasedimentary sequences of Cape Breton Island demonstrate variable metallogenic characteristics. The Creignish Hills-North Mountain carbonate sequence (excluding Lime Hill) contains low background base metal values compared with limestones worldwide determined by Taylor (1964). Similarly, values defined by Hill (1987b) for the determination of anomalous base metal samples in the Creignish Hills-North Mountain population can be considered low. Threshold values (equivalent to the 95th percentile of the population) are 5 ppm Cu, 44 ppm Zn, and 7 ppm Pb. It is therefore apparent that no regional-scale metasomatic metal introduction was associated with low-temperature regional metamorphism of the area. Metallic mineralization is restricted to specific sites such as the Fe-Cu skarn occurrences at Whycocomagh and Glencoe or the Fe skarn occurrence at Glencoe Road. A number of mineralized sites were discovered during the present study, an example being the Glencoe Pb-Zn showing. They consist of disseminated base metal sulphide minerals in massive calcareous to siliceous marble of low metamorphic grade.

Marble in the Boisdale Hills is characterized by significantly higher background base metal values than Creignish marbles, i.e. 50 percent higher for Cu and Pb and 150 percent higher for Zn. Threshold values are correspondingly high at 40 ppm Cu, 660 ppm Zn, and 92 ppm Pb (Hill, 1987b). Higher regional grades of metamorphism appear to be related to intrusion of the multiphased Boisdale Hills pluton during the late Precambrian to earliest Cambrian (Barr and Setter, 1986). There is little evidence to suggest that elevated base metal values are related to regional-scale metasomatic (metalliferous) activity associated with plutonism. Instead, the characteristic chemical signature of the Boisdale marbles reflects the chemistry of the original sedimentary environment. Much of the metallic mineralization identified in the area is restricted to specific sites of contact metamorphism and metasomatism. Metallic occurrences such as the Upper Leitches Creek Fe-Cu skarn, Scotch Lake Fe skarn, or the Rear Boisdale Pb-Zn-Ag skarn, are associated with high metamorphic grade, massive calc-silicate lithologies which are replaced by sulphide and/or iron oxide mineralization. Other sites containing minor disseminated base metal sulphide mineralization, such as the Upper Georges River occurrence, show no obvious relationship to contact metamorphic and/or hydrothermal events.

Precambrian carbonate rocks from the Cape Dauphin-Kellys Cove area contain background zinc values comparable to those found in the Boisdale marbles and background lead and copper levels closer to those observed in the Creignish carbonate rocks. Base metal mineralization in the area is spatially associated with the granitoid-carbonate contact. One sample site was found to contain disseminated galena and sphalerite in a siliceous calcite marble at the intrusive contact (Hill, 1987b, Map 3-1). Another isolated outcrop of garnet-epidote skarn, with no sulphides, is located 3 km farther north in the Cape Dauphin area at the leucogranite contact zone.

Cape Breton Highlands carbonate rocks have the highest background values for Cu, Zn, and the rock-forming elements compared to marbles from the other areas. As discussed previously, element associations suggest that the chemical signature of highlands marbles is, in part, related to clastic components in the original sedimentary rocks. The McMillans Brook Fe-Cu (+/− Sn, W, Mo) skarn showing, hosted within carbonate rocks of the McMillan Flowage Formation, is the only known site of metallic mineralization associated with contact metamorphism. As described by Chatterjee (1977), one phase of mineralization at McMillans Brook, consisting of intrusive-hosted Fe-Cu-Mo and skarn-hosted Sn-W-Mo, postdates regional metamorphism and is associated with the intrusion of quartz monzonite stocks. At the same locality and farther north along strike (see Hill, 1987b, Maps 4-1 and 4-1a), gossanous Cu-Zn-As mineralization is hosted within tremolite-serpentine-bearing calc-silicate units related to regional sillimanite grade metamorphism (Chatterjee, 1977). The remaining nonferrous metallic showings examined throughout the Cape Breton Highlands consist of isolated occurrences of disseminated sphalerite and galena in calc-silicate-bearing calcite marbles. No other zinc occurrences similar to the Meat Cove deposit are recognized in the Cape Breton Highlands. It is concluded that only limited potential for skarn-associated metallic mineralization exists within marble formations of the high-grade Cape Breton Highlands metasedimentary rocks given the paucity of carbonate lithologies.

SUMMARY AND CONCLUSIONS

Marble-bearing metasedimentary assemblages representing pre-Carboniferous carbonate-detrital shelf sequences can be subdivided into four unique classes based on geological and geochemical criteria.

1) Thick carbonate units interstratified with clastic metasedimentary rocks and mafic to intermediate volcanic rocks of low to moderate metamorphic grade characterize the Creignish Hills and North Mountain areas. Both areas host thick sections of high purity, predominantly calcite marble suitable for industrial applications, including cement, agricultural and metallurgical products, and filler material. Metallic mineral potential in the area is restricted to isolated skarn occurrences containing variable amounts of Fe, Cu, Mo, and W.

2) George River Group rocks underlying the Boisdale Hills are composed of massive, medium to high metamorphic grade, calc-silicate-bearing marbles interbedded with arenaceous metasedimentary rocks. Although the type section is located here, carbonate lithologies are quite different in both appearance and composition when compared with George River marbles underlying the Creignish Hills. The high aluminum and calc-silicate mineral content of the marbles appears to be a product of regional metamorphism of impure limestones and dolostones rather than regional metasomatism. Retrograde alteration leading to the development of a talc-serpentine-calcite mineral assemblage is also widespread throughout the area.

Lithologically similar metasedimentary rocks have been preserved in the Cape Dauphin-Kellys Cove area. The metasedimentary belt is composed of low to medium metamorphic grade, thinly interbedded, high purity dolomite marble and pure to siliceous varieties of calcite marble with minor quartzite and argillite. The metacarbonate rocks are similar in lithological composition to marbles of the Boisdale Hills sequence but are of lower metamorphic grade. Most striking is the fact that both pre-Carboniferous sequences form structurally and stratigraphically similar north-northeastward-trending, narrow linear carbonate-clastic metasedimentary belts bounded on the west by late Hadrynian to Early Cambrian, multiphased intrusive complexes and on the east by Carboniferous limestone, sandstone, and conglomerate. Marble units from both regions also contain higher than average background base metal values, but only locally has metallic mineralization been recognized related to specific contact metamorphic events or to structurally-controlled hydrothermal processes.

3) Marble units associated with high metamorphic grade, pre-Carboniferous metasedimentary sequences of the Cape Breton Highlands are distinct from metacarbonates observed in central Cape Breton Island. Marble units form isolated and discontinuous units <100 m in thickness interstratified with detrital metasedimentary rocks. Both lithological and compositional evidence indicate that the Cape Breton Highlands carbonate-clastic sequence cannot be considered equivalent to George River Group metasedimentary rocks and metavolcanic rocks located in central Cape Breton Island. Geochemical data indicate that the posttectonic composition of marble and calc-silicate units is a function of original depositional or diagenetic environments. Only locally has magmatism led to metasomatic alteration of the original sedimentary chemistry.

4) The fourth class of Precambrian carbonate assemblage is characterized by the zinc-rich siliceous dolomite marbles that occur at Lime Hill and Meat Cove. They are contained within high-grade metasedimentary sequences which appear to represent older crystalline basement to George River Group metasedimentary rocks. In the Meat Cove area, this has been confirmed by radiometric dating, which indicates that carbonate members are part of a Helikian crystalline complex, whereas in the Lime Hill area, metallogenic evidence suggests an age correlation with the Grenville Supergroup.

ACKNOWLEDGMENTS

The author acknowledges the capable assistance of A.R. Misner and G.D.T. Walker during field studies on Cape Breton Island. A petrographic and mineral chemistry study of calc-silicate rocks by G.D.T. Walker, completed as part of an undergraduate thesis at Acadia University, is also acknowledged. Special thanks are extended to J.G.R. Peers, Peers Management Associates Limited, Sydney, for logistical support during field work.

Technical discussions with numerous individuals on recent developments in Cape Breton Island geology are appreciated. They include: A.L. Sangster, Geological Survey of Canada; S.M. Barr and R.P. Raeside, Acadia University; D.A. Murray, A.K. Chatterjee, and R.H. MacDonald, Nova Scotia Department of Mines and Energy; G.C. Milligan, Dartmouth, N.S.; and H.R. Oldale and F.M. Isenor, University College of Cape Breton. The manuscript benefitted considerably from critical review by D.F. Sangster, Geological Survey of Canada, and R.P. Raeside, Acadia University.

REFERENCES

Barr, S.M. and Raeside, R.P.
1989: Tectono-stratigraphic terranes in Cape Breton Island, Nova Scotia; Implications for the configuration of the northern Appalachian orogen: Geology, v. 17, p. 822-825.

Barr, S.M. and Setter, J.R.D.
1986: Petrology of the granitoid rocks of the Boisdale Peninsula, central Cape Breton Island, Nova Scotia; Nova Scotia Department of Mines and Energy, Paper 84-1, 75 p.

Barr, S.M., Jamieson, R.D., and Raeside, R.P.
1985: Igneous and metamorphic geology of the Cape Breton Highlands; Annual General Meeting, Geological Association of Canada-Mineralogical Association of Canada, Fredericton, New Brunswick, Excursion 10, 45 p.

Barr, S.M., Raeside, R.P., and van Breemen, O.
1987a: Grenvillian basement in the northern Cape Breton Highlands, Nova Scotia; Canadian Journal of Earth Sciences, v. 24, p. 992-997.

Barr, S.M., Raeside, R.P., and Jamieson, R.A.
1987b: Geological map of the igneous and metamorphic rocks of northern Cape Breton Island, Nova Scotia; Geological Survey of Canada, Open File 1594, 6 maps, scale 1:50 000.

Barr, S.M., Raeside, R.P., White, C.E., and Yaowanoiyothin, W.
1987c: Geology of the northeastern and central Cape Breton Highlands, Nova Scotia; *in* Current Research, Part A, Geological Survey of Canada, Paper 87-1A, p. 199-207.

Barr, S.M., Raeside, R.P., Dunning, G.R., and Jamieson, R.A.
1988: New U-Pb ages from the Cape Breton Highlands and correlations with southern Newfoundland: a Lithoprobe East contribution; Geological Association of Canada-Mineralogical Association of Canada, Joint Annual Meeting, 1988, Program with Abstracts, v. 13, p. A5.

Bell, W.A. and Goranson, E.A.
1938: Sydney and Glace Bay sheets; Geological Survey of Canada, Maps 360A, 361A, 362A with descriptive notes.

Chatterjee, A.K.
1977: Copper-zinc deposit at McMillans Brook, Victoria County, Cape Breton Island; Nova Scotia Department of Mines and Energy, Report of Activities 1976, Report 77-1, p. 55-66.
1979a: Geology of the Meat Cove zinc deposit, Cape Breton Island, Nova Scotia; Nova Scotia Department of Mines and Energy, Paper 79-3, 27 p.
1979b: Copper-tungsten mineralization at Glencoe, Inverness County, Cape Breton Island; Nova Scotia Department of Mines and Energy, Report of Activities for 1978, Report 79-1, p. 61-64.
1980: Mineralization and associated wall rock alteration in the George River Group, Cape Breton Island, Nova Scotia; Ph.D. thesis, Dalhousie University, Halifax, Nova Scotia, 197 p.

deLorraine, W.F. and Dill, D.B.
1982: Structures, stratigraphic controls and genesis of the Balmat zinc deposits, northwest Adirondacks, New York; Geological Association of Canada, Special Paper 25, p. 571-596.

Douglas, G.V.
1942: The New Campbellton dolomite deposit; Nova Scotia Department of Mines, Annual Report on Mines, 1941, p. 82-92.

Einaudi, M.T., Meinert, L.D., and Newberry, R.J.
1981: Skarn deposits; Economic Geology, 75th Anniversary Volume, p. 317-391.

Fletcher, I.R. and Farquhar, R.M.
1982: Lead isotope compositions of Balmat ores and their genetic implications; Economic Geology, v. 77, p. 464-473.

Fletcher, M.
1877: Explorations and surveys in Cape Breton, Nova Scotia; Geological Survey of Canada, Report of Progress, 1875-76, p. 369-418.

Gauthier, M. and Brown, A.C.
1986: Zinc and iron metallogeny in the Maniwaki-Gracefield district, southwestern Quebec; Economic Geology, v. 81, p. 89-112.

Goudge, M.F.
1938: Limestones of Canada: their occurrence and characteristics, Part 4; Canada Department of Mines and Resources, Mines and Geology Branch, Report 781, 362 p.

Guernsey, T.D.
1928: Geology of North Mountain, Nova Scotia; Geological Survey of Canada, Summary Report, 1927, Part C.

Guilbert, J.M. and Park, C.F.
1986: The Geology of Ore Deposits; W.H. Freeman and Company, New York, 985 p.

Hewitt, D.F.
1960: The limestone industries of Ontario; Ontario Department of Mines, Industrial Minerals Circular 5, 177 p.

Hill, J.R.
1987a: A preliminary report on geology and on mineral occurrences in Precambrian carbonate rocks, Cape Breton Island, Nova Scotia; *in* Current Research, Part A, Geological Survey of Canada, Paper 87-1A, p. 533-542.
1987b: Geology and geochemistry of Precambrian carbonate rocks, Cape Breton Island, Nova Scotia; Geological Survey of Canada, Open File 1597.
1988: Geochemical differentiation of Precambrian metacarbonate assemblages, Cape Breton Island, Nova Scotia; *in* Current Research, Part B, Geological Survey of Canada, Paper 88-1B, p. 173-185.
1989: Follow-up geology and geochemistry of metacarbonate formations and their contained mineral occurrences, Cape Breton Island, Nova Scotia; Geological Survey of Canada, Open File Report 2077, 43 p.

Honeyman, D.
1872: Notes on the geology of Nova Scotia and Cape Breton Island; Proceedings and Transactions of the Nova Scotia Institute of Natural Science, v. 3, p. 193-204.

Isenor, F.M.
1984: Results of diamond drilling on the MacDonald property, Scotch Lake area, Cape Breton County; Nova Scotia Department of Mines and Energy, Assessment Report.

Jamieson, R.A., Craw, D., and Doucet, P.
1984: Geology of the southwestern Cape Breton Highlands, Nova Scotia; Geological Survey of Canada, Open File 1041, 4 maps.

Justino, M. and Sangster, A.L.
1987: Geology in the vicinity of the Lime Hill occurrence, Cape Breton Island, Nova Scotia; *in* Current Research, Part A, Geological Survey of Canada, Paper 87-1A, p. 555-561.

Kelly, D.G.
1967: Baddeck and Whycocomagh map-areas with emphasis on Mississippian stratigraphy of central Cape Breton Island, Nova Scotia; Geological Survey of Canada, Memoir 351, 65 p. including Maps 1211A (NTS 11K/2) and 1212A (NTS 11F/14).

Keppie, D.J.
1979: Geological map of the Province of Nova Scotia; Nova Scotia Department of Mines and Energy, scale 1:500 000.

Kurzl, H.
1988: Exploratory data analysis: recent advances for the interpretation of geochemical data; Journal of Geochemical Exploration, v. 30, p. 309-322.

Luke, P. and MacDonald, R.H.
1988: Limestone and dolomite in Nova Scotia; Nova Scotia Department of Mines and Energy, Information Circular 13.

Macdonald, A.S. and Smith, D.K.
1980: Geology of Cape North area, northern Cape Breton Island, Nova Scotia; Nova Scotia Department of Mines and Energy, Paper 80-1, 60 p.

MacNeil, D.J.
1977: The Glencoe limestone and dolomite survey, Inverness County, Nova Scotia — preliminary reports; Nova Scotia Department of Mines and Energy, Open File Report 329, 63 p.

McGill, R., Tukey, J.W., and Larsen, W.A.
1978: Variations of box plots; American Statistician, v. 32, p. 12-16.

Milligan, G.C.
1970: Geology of the George River Series, Cape Breton; Nova Scotia Department of Mines and Energy, Memoir 7, 111 p.

Munyanyiwa, H. and Hanson, R.E.
1988: Geochemistry of marbles and calcsilicate rocks in the Pan-African Zambezi belt, Zambia; Precambrian Research, v. 38, p. 177-200.

Murray, D.L.
1976: The structural relationship between the Fourchu Group and the George River Group in the Clyburn Brook-Ingonish River area, Cape Breton, Nova Scotia; Nova Scotia Department of Mines and Energy, Open File Report 140, 20 p.

Neale, E.R.W.
1963a: Geology, Pleasant Bay, Cape Breton Island, Nova Scotia; Geological Survey of Canada, Map 1119A (NTS 11K/15), scale 1 inch to 1 mile.
1963b: Geology, Dingwall, Cape Breton Island, Nova Scotia; Geological Survey of Canada, Map 1124A (NTS 11K/16), scale 1 inch to 1 mile.
1964a: Geology, Cape St. Lawrence, Nova Scotia; Geological Survey of Canada, Map 1149A (NTS 11N/02), scale 1 inch to 1 mile.
1964b: Geology, Cape North, Nova Scotia; Geological Survey of Canada, Map 1150A (NTS 11N/01), scale 1 inch to 1 mile.

Perry, D.V.
1969: Skarn genesis at the Christmas Mine, Gila County, Arizona; Economic Geology, v. 64, p. 255-270.

Pettijohn, F.J.
1975: Sedimentary Rocks; 3rd edition, Harper and Row, New York, 628 p.

Raeside, R.P.
1987: Geology and metamorphism of the Lime Hill gneissic complex, Inverness County, Cape Breton Island; *in* Mines and Minerals Branch, Report of Activities, 1987, Part A, edited by J.L. Bates and D.R. MacDonald, Nova Scotia Department of Mines and Energy, Report 87-5, p. 193-196.
1990: Low-pressure metamorphism of the Lime Hill gneissic complex, Bras d'Or Terrane, Cape Breton Island, Nova Scotia; *in* Mineral Deposit Studies in Nova Scotia, Volume 1, edited by A.L. Sangster, Geological Survey of Canada, Paper 90-8, p. **-**.

Raeside, R.P. and Barr, S.M.
1986: Stratigraphy and structure of the southeastern Cape Breton Highlands, Nova Scotia; Maritime Sediments and Atlantic Geology, v. 22, p. 264-277.
1988: The Bras d'Or zone: a suspect terrane in Cape Breton Island, N.S.; Geological Association of Canada-Mineralogical Association of Canada, Joint Annual Meeting, 1988, Program With Abstracts, v. 13, p. A102.

Sangster, A.L. and Bourne, J.
1982: Geology of the Grenville Province and regional metallogenesis of the Grenville Supergroup; *in* Precambrian Sulphide Deposits, edited by R.M. Hutchinson, C.D. Spence, and J.M. Franklin, Geological Association of Canada, Special Paper 25, p. 91-125.

Sangster, A.L. and Thorpe, R.I.
1987: Lead isotope composition of galenas from metacarbonate-hosted zinc occurrences, Cape Breton Island, Nova Scotia; *in* Mines and Minerals Branch, Report of Activities, 1987, Part A, edited by J.L. Bates and D.R. MacDonald, Nova Scotia Department of Mines and Energy, Report 87-5, p. 225-227.
1988: Sulphur and lead isotope studies on two Grenville-type, marble-hosted zinc occurrences, Cape Breton, Nova Scotia; Geological Society of America, Northeastern Section, 23rd Annual Meeting, 1988, Abstracts with Programs, v. 20, p. 67.

Storey, C.C. and Vos, M.
1981: Industrial minerals of the Pembroke-Renfrew area, Part 1: Marble; Ontario Geological Survey, Mineral Deposits Circular 21.

Taylor, S.R.
1964: Abundance of chemical elements in the Earth's crust: a new table; Geochimica et Cosmochimica Acta, v. 28, p. 1273-1285.

Walker, G.D.T.
1988: Mineral chemistry of diopside, garnet and amphiboles from carbonate and calcsilicate rocks, Cape Breton Island, Nova Scotia; B.Sc. thesis, Acadia University, Wolfville, Nova Scotia, 137 p.

Weeks, L.J.
1954: Southeast Cape Breton Island, Nova Scotia; Geological Survey of Canada, Memoir 277, 112 p. (includes Map 1026A).

Whelan, J.F., Rye, R.O., and deLorraine, W.
1984: The Balmat-Edwards zinc-lead deposits — synsedimentary ore from Mississippi Valley-type fluids; Economic Geology, v. 79, p. 239-265.

Wiebe, R.A.
1972: Igneous and tectonic events in northeastern Cape Breton Island, Nova Scotia; Canadian Journal of Earth Sciences, v. 9, p. 1262-1277.

Wright, J.D.
1975: Iron deposits of Nova Scotia; Nova Scotia Department of Mines and Energy, Economic Geology Series 75-1, 154 p.

Metallogeny of the Proterozoic marble-hosted zinc occurrences at Lime Hill and Meat Cove, Cape Breton Island, Nova Scotia[1]

A.L. Sangster[2], M.F. Justino[3], and R.I. Thorpe[2]

Sangster, A.L., Justino, M.F., and Thorpe, R.I., Metallogeny of the Proterozoic marble-hosted zinc occurrences at Lime Hill and Meat Cove, Cape Breton Island, Nova Scotia; in Mineral Deposit Studies in Nova Scotia, Volume 1, edited by A.L. Sangster, Geological Survey of Canada, Paper 90-8, p. 31-66, 1990.

Abstract

Marble-hosted zinc occurrences at Lime Hill and Meat Cove on Cape Breton Island are geologically, geochemically, and isotopically (S and Pb) similar to a distinctive group of zinc occurrences hosted by Grenville Supergroup marble in Ontario, Quebec, and New York. The occurrences share a magnesian calc-silicate mineralogy, with serpentine, forsterite, talc, diopside, and tremolite present within mixed calcite-dolomite or dolomite marble terranes. Major element compositions indicate that the host rocks are dolomite and siliceous dolomite marble, containing negligible quantities of Al_2O_3, K_2O, Na_2O, and MnO. Sphalerite-bearing marble contains anomalous contents of Cd, Hg, and locally, minor Pb. Minor elements commonly associated with base metal sulphide deposits, including Ag, Au, As, Sb, Co, Ni, and Mo, are low.

Sulphur isotopic compositions of Meat Cove and Lime Hill sphalerite are heavy (12.4 to 17.5 ‰ and 9.5 to 12.6 ‰, respectively) and are similar to sulphide sulphur isotopic compositions at the heavy end of the range for Grenville Supergroup deposits. Values are also near or slightly below those for contemporaneous seawater.

Lead isotopic values for Meat Cove and Lime Hill galenas are near $^{206}Pb/^{204}Pb = 17.109$, $^{207}Pb/^{204}Pb = 15.496$, $^{208}Pb/^{204}Pb = 36.451$, and $^{206}Pb/^{204}Pb = 17.043$, $^{207}Pb/^{204}Pb = 15.565$, $^{208}Pb/^{204}Pb = 36.733$, respectively. These primitive compositions are similar to reported values for deposits in the Grenville Supergroup and are dissimilar to those for vein galenas genetically related to Cambrian intrusions, which are more radiogenic and near $^{206}Pb/^{204}Pb = 18.504$, $^{207}Pb/^{204}Pb = 15.680$, $^{208}Pb/^{204}Pb = 38.294$.

The genetic interpretations based on these data are that the deposits are not pyrometasomatic skarns, as previously believed, but rather, are probably metamorphosed variants of Mississippi Valley-type or sedimentary exhalative deposits. The heavy sulphur isotopic signature clearly suggests a sulphur source within the enclosing carbonate rocks. The lead isotopic compositions suggest that the lead was derived from sedimentary rocks that had evolved within the upper crust and that its mobilization to form galena occurred at about the time of formation of deposits in the Grenville Supergroup. The dolomitic nature of the host rocks, the monoelemental Zn-rich character of the mineralization, the low Mn content of both mineralization and calc-silicate minerals, and the overall low trace element contents are compatible with formation, either as sedimentary exhalative or Mississippi Valley-type deposits, from carbonate basin brines.

---

[1] Contribution to the Canada - Nova Scotia Mineral Development Agreement, 1984-1989. Project carried by the Mineral Resources Division, Geological Survey of Canada, Project 860008.

[2] Geological Survey of Canada, 601 Booth St., Ottawa, Ontario, K1A 0E8.

[3] Department of Geology, Acadia University, Wolfville, Nova Scotia, B0P 1X0.

Résumé

Dans les régions de Lime Hill et de Meat Cove, dans l'île du Cap-Breton, des venues de Zn logées par un marbre sont géologiquement, géochimiquement et isotopiquement (S et Pb) comparables à un groupe distinctif de venues de Zn trouvées dans le marbre du supergroupe de Grenville en Ontario, au Québec et dans l'État de New York. Les venues ont en commun une minéralogie de type calco-silicaté avec magnésium; de la serpentine, de la forstérite, du talc, de la diopside et de la trémolite se manifestent au sein de terranes à marbre de type mixte calcitique-dolomitique, ou dolomitique. Les compositions en éléments principaux indiquent que les roches hôtes sont un marbre dolomitique et un marbre dolomitique siliceux, contenant des quantités négligeables de Al_2O_3, K_2O, Na_2O et MnO. Le marbre contenant de la sphalérite se caractérise par des anomalies des teneurs en Cd, Hg et, par endroits, par des anomalies peu importantes en Pb. Les teneurs en éléments accessoires généralement associés aux gisements sulfurés de métaux communs, notamment les teneurs en Ag, Au, As, Sb, Co, Ni et Mo, sont faibles.

Les compositions isotopiques du soufre, dans la sphalérite de Meat Cove et Lime Hill, sont élevées (12,4 à 17,5 ‰ et 9,5 à 12,6 ‰ respectivement) et sont semblables aux compositions isotopiques du soufre contenu dans des sulfures, à l'extrémité «lourde» de la gamme typique des gisements du supergroupe de Grenville. Les valeurs se rapprochent aussi, ou se situent légèrement au-dessous, de celles de l'eau de mer contemporaine.

Les valeurs isotopiques du plomb dans le cas des galènes de Meat Cove et de Lime Hill sont proches de $^{206}Pb/^{204}Pb = 17,109$, $^{207}Pb/^{204}Pb = 15,496$, $^{208}Pb/^{204}Pb = 36,451$ et $^{206}Pb/^{204}Pb = 17,043$, $^{207}Pb/^{204}Pb = 15,565$, $^{208}Pb/^{204}Pb = 36,733$ respectivement. Ces compositions primitives sont semblables aux valeurs notées dans le cas des gisements du supergroupe de Grenville, et sont différentes de celles des galènes filoniennes génétiquement apparentées aux intrusions cambriennes, qui sont plus radiogéniques et se rapprochent de $^{206}Pb/^{204}Pb = 18,504$, $^{207}Pb/^{204}Pb = 15,680$, $^{206}Pb/^{204}Pb = 38,294$.

Les interprétations génétiques fondées sur ces données indiquent que les gisements ne sont pas des skarns pyrométasomatiques, comme on le croyait autrefois, mais qu'il s'agit plutôt probablement de variantes métamorphisées de gisements du type de la vallée du Mississippi ou de gisements exhalatifs sédimentaires. La signature isotopique lourde du soufre indique clairement une source sulfurée contenue dans les roches carbonatées encaissantes. La composition isotopique du plomb semble indiquer que ce plomb provenait de roches sédimentaires formées à l'intérieur de la croûte supérieure, et que la mobilisation de cet élément, aboutissant à la formation de galène, s'est produite à peu près à l'époque de la formation des gisements du supergroupe de Grenville. La nature dolomitique des roches hôtes, le caractère monoélémentaire de la minéralisation, avec enrichissement en Zn, la basse teneur en Mn à la fois de la minéralisation et des minéraux calco-silicatés, et la teneur en éléments en traces dans l'ensemble faible, s'accordent avec la formation des gisements, soit sous forme de gisements exhalatifs sédimentaires ou de gisements du type de la vallée du Mississippi, à partir de saumures de bassins carbonatées.

INTRODUCTION

The middle to late Precambrian basement rocks on Cape Breton Island contain two marble-hosted zinc occurrences which have similar field relationships and mineralogical character to metamorphosed zinc occurrences hosted by Grenville Supergroup marble in Ontario, Quebec, and New York. The Meat Cove and Lime Hill zinc occurrences (Fig. 1 and 2) were both discovered and initially explored during the mid-1950s. They have both been subjected to several programs of mineral exploration and, although no commercially viable reserves have been identified, they continue to be of sufficient interest to attract continued exploration. Currently estimated reserves (Energy, Mines and Resources, 1986) stand at 4 400 000 tons grading 4.0 percent Zn and 0.47 lb/t Cd for the Meat Cove deposit and 2 000 000 tons grading 2.5 percent Zn or 150 000 tons grading 9.0 percent Zn for the Lime Hill occurrence.

The Lime Hill and Meat Cove occurrences have historically been regarded as contact metasomatic skarns related to nearby intrusions (Keating, 1960; Chatterjee, 1977, 1979, 1980). In contrast, the deposits and occurrences hosted by Grenville Supergroup marble, although originally considered to be contact metasomatic replacements of limestone (Alcock, 1930), have more recently been attributed to processes that resulted in the formation of sedimentary exhalative or Mississippi Valley-type deposits (Uglow, 1916; Lea and Dill, 1968; Sangster, 1970; deLorraine and Dill, 1982; Sangster and Bourne, 1982; Whelan et al., 1984; Gauthier and Brown, 1986). This paper reports on the results of a program of geological, major and trace element, and lead and sulphur isotopic investigations which provide a basis for comparison of the Grenville and Nova Scotia mineralization and provide new evidence regarding the origin and age of the Nova Scotia occurrences.

REGIONAL GEOLOGICAL SETTING

Cape Breton Island contains a number of highly deformed metamorphic/plutonic terranes of pre-Middle Devonian age which are overlain by unmetamorphosed, but locally faulted and folded, post-Middle Devonian and Carboniferous clastic and chemical sedimentary rocks. Barr and Raeside (1986) have proposed a new tectonostratigraphic subdivision of the pre-Carboniferous rocks on Cape Breton Island (Fig. 1) which provides a rational basis for further discussion of the geology of these rocks. Their divisions, from northwest to southeast, include:
1) the "Grenvillian" Blair River Complex, which is composed of the Polletts Cove Brook gneiss and anorthosite, syenite, and gabbro to granodiorite intrusions. These rocks are at amphibolite or transitional to granulite facies metamorphic grade;
2) the Aspy Terrane, characterized by Silurian and older layered rocks and a mixed suite of Silurian and Devonian granitic intrusions;
3) the Bras d'Or Terrane, characterized by a low metamorphic grade assemblage of Late Proterozoic platformal clastic and carbonate sedimentary rocks (classical George River Group, Milligan, 1970) with small areas of high-grade gneiss (in black and "L" and "K" on Fig. 1) of uncertain age which may be basement to the lower grade rocks. The small gneissic bodies are distinct from gneiss that occurs in the Blair River Complex, having undergone low pressure-high temperature metamorphism (Jamieson, 1984; Raeside, 1990). Plutonism is mainly latest Proterozoic to Cambrian in age;
4) the Avalon Terrane, which contains a Late Proterozoic to Ordovician assemblage of volcanic and sedimentary rocks that have been intruded by Cambrian and Devonian granitoid plutons.

Precambrian carbonate rocks are widespread in three of the tectonostratigraphic subdivisions of Cape Breton Island: the Bras d'Or Terrane, the Aspy Terrane, and the Blair River Complex. Historically these have all been arbitrarily assigned to the George River Group (Milligan, 1970). Recent work (Barr and Raeside, 1986, 1989; Hill, 1987, 1988, 1989, 1990) has shown that the George River Group (sensu stricto) is restricted to the Bras d'Or Terrane and that areas of high metamorphic grade gneissic rocks and marble, traditionally assigned to the George River Group, are different. These include rocks of the Blair River Complex, basement gneiss of the Bras d'Or Terrane (e.g. Lime Hill and Kellys Mountain gneiss), and low to high metamorphic grade rocks of the Aspy Terrane.

The Meat Cove zinc deposit is hosted by dolomite marble of the Polletts Cove Brook Group of the Blair River Complex. The marble host rocks form a xenolith within the Lowland Brook syenite which has yielded a U-Pb (zircon) metamorphic age of 1040 +10/−40 Ma and an igneous age of 1100 to 1500 Ma (Barr et al., 1987b). Barr (pers. comm., 1989) considers the Blair River Complex to represent Grenvillian basement and correlates it with the Long Range Inlier-Indian Head Complex of western Newfoundland.

The Lime Hill zinc deposit is hosted by dolomite marble of the Lime Hill gneissic complex, part of the Bras d'Or Terrane. The Lime Hill gneiss is similar to, and can be correlated with, the Kellys Mountain gneiss (Raeside, 1989) which has yielded a metamorphic age of 701 +/−66 Ma (Rb-Sr biotite, Olszewski et al., 1981). The Bras d'Or Terrane gneissic rocks have been correlated with the Brookville gneiss of southern New Brunswick, the Great Village River Gneiss and Mount Thom Complex of the Cobequid Highlands of mainland Nova Scotia, and the Grey River gneiss of southwestern Newfoundland (Donohoe and Cullen, 1983; Donohoe and Wallace, 1983; O'Brien et al., 1983; Dunning and O'Brien, 1989).

GEOLOGY OF THE LIME HILL ZINC OCCURRENCE

Introduction

At Lime Hill, the mineralized marble has historically been assigned to the late Precambrian George River Group (Fletcher, 1881), which outcrops at much lower metamorphic grades a short distance northeast of the property (Fig. 2). The profound difference in metamorphic grade

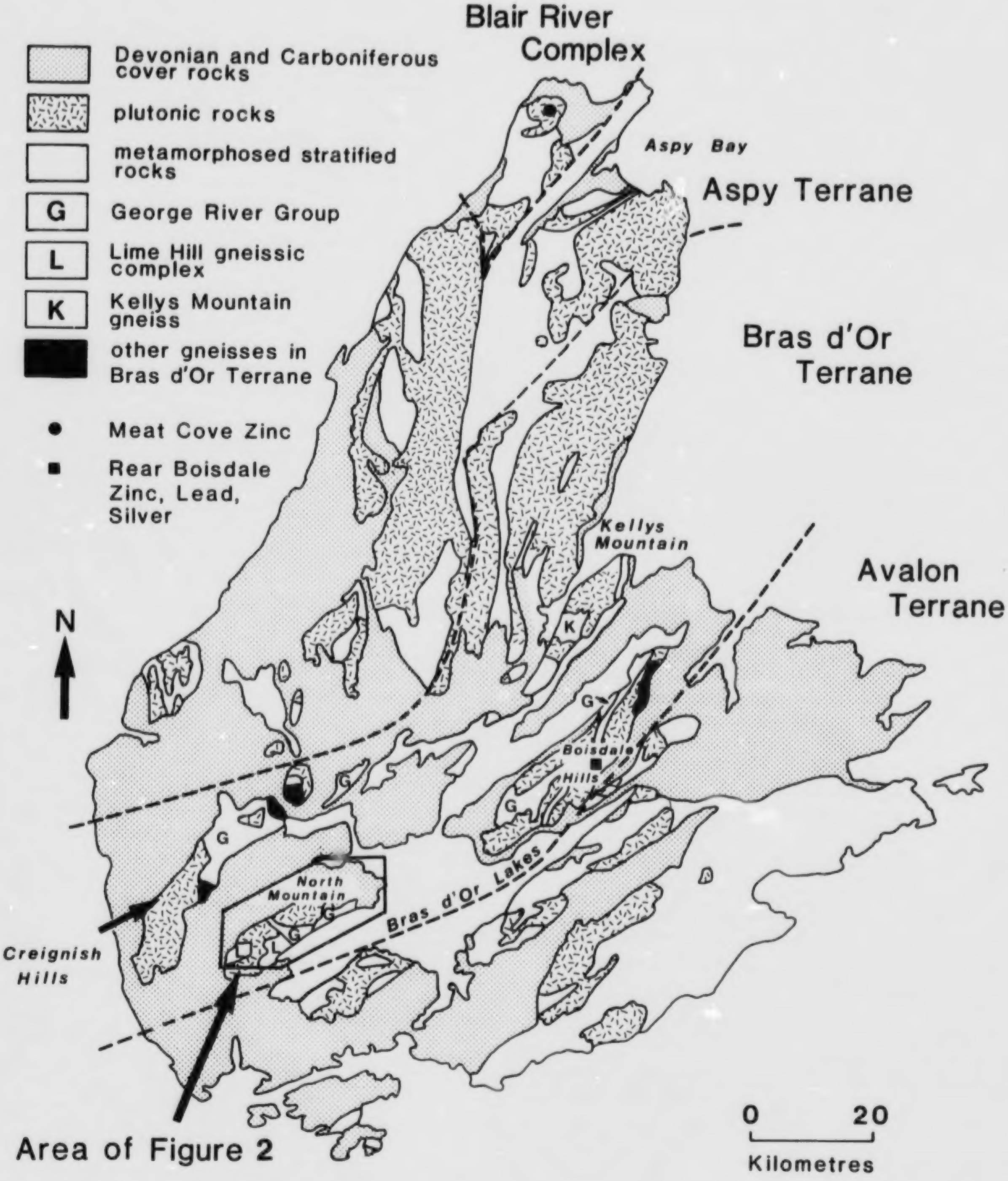
Devonian and Carboniferous cover rocks
plutonic rocks
metamorphosed stratified rocks
G George River Group
L Lime Hill gneissic complex
K Kellys Mountain gneiss
other gneisses in Bras d'Or Terrane
● Meat Cove Zinc
■ Rear Boisdale Zinc, Lead, Silver
Blair River Complex
Aspy Bay
Aspy Terrane
Bras d'Or Terrane
Kellys Mountain
K
Avalon Terrane
N
G
Boisdale Hills
G
G
G
North Mountain
G
G
L
Bras d'Or Lakes
Creignish Hills
Area of Figure 2
0
20
Kilometres

Figure 1. Tectonostratigraphic subdivisions of Cape Breton Island with locations of the Meat Cove Zn occurrence, Rear Boisdale Zn-Pb-Ag occurrence, the North Mountain (Lime Hill area), the Kellys Mountain gneiss (K), the Lime Hill gneissic complex (L), and other areas of "basement-like" gneiss (black)(modified after Barr and Raeside, 1986).

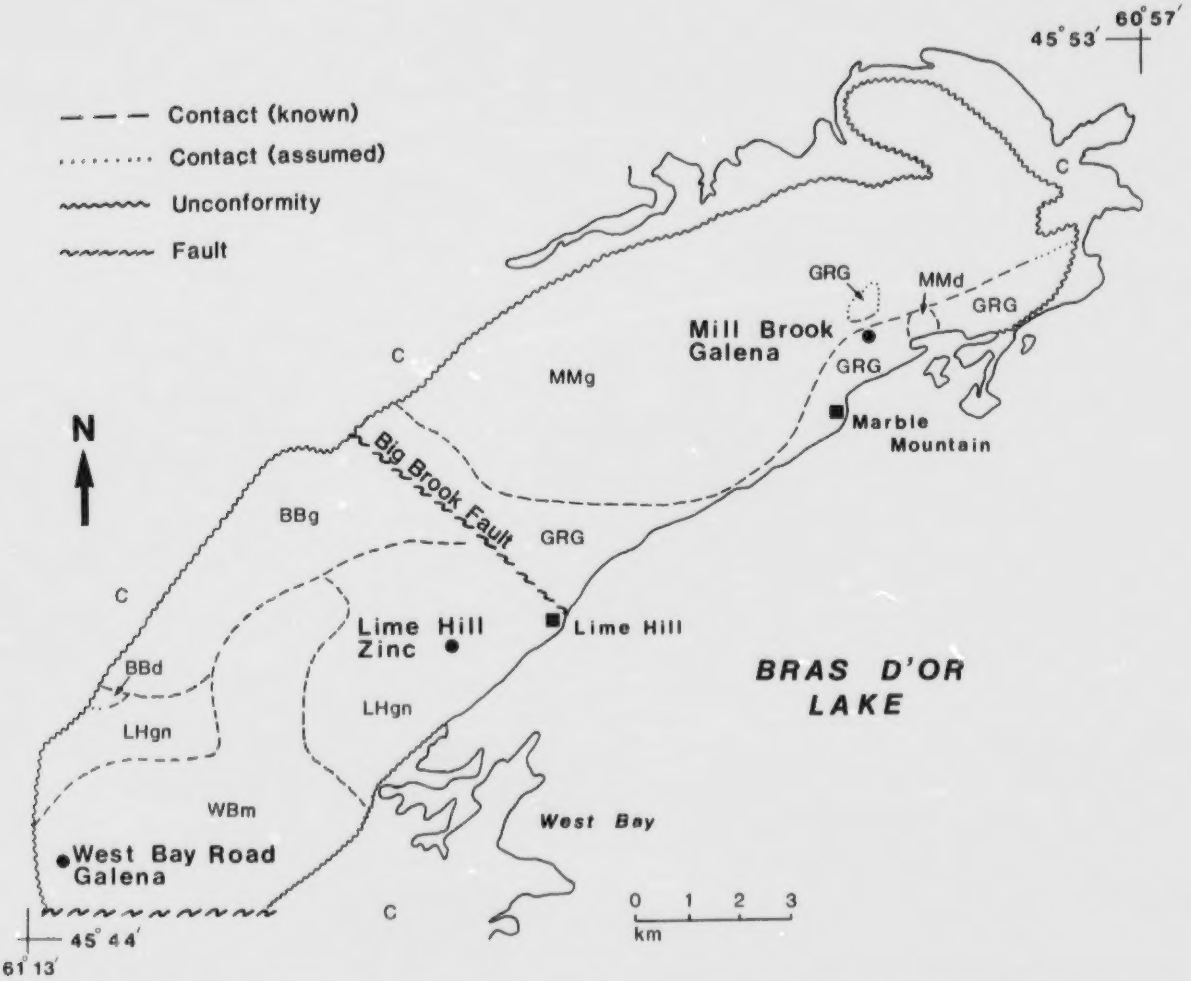

Figure 2. Geology of the North Mountain area with locations of the Lime Hill Zn occurrence and the West Bay Road and Mill Brook vein Pb occurrences. Symbols: LHgn=Lime Hill gneiss; GRG=George River Group; MMg=Marble Mountain tonalite, granodiorite; MMd=Marble Mountain quartz diorite; BBg=Big Brook tonalite, granodiorite; BBd=Big Brook diorite; WBm=West Bay monzogranite; C=Carboniferous cover rocks.

between rocks at Lime Hill and typical George River Group metasedimentary rocks was recognized by Guernsey (1928). The gneissic rocks with interlayered marble were mapped with granitic intrusions by Kelly (1967) and Milligan (1970). Chatterjee (1980) described the Lime Hill marble as roof pendants within granitoid rocks.

Recent mapping (Justino, 1985; Justino and Sangster, 1987) has defined the Lime Hill gneissic complex, including the mineralized carbonates, to be separate and distinct from, and possibly an upfaulted basement to, rocks of the George River Group. The Lime Hill gneissic complex is composed dominantly of polydeformed migmatitic paragneiss, dolomite and calcite marble, calc-silicate rocks, orthogneiss, and amphibolite. Marble accounts for less than 10 percent of the exposed area of the gneissic complex. Raeside (1990) studied the mineral phase relationships within the gneiss and found no evidence of thermal variation related to the extensive Cambrian granitic intrusions, and supported the thesis that the Lime Hill gneiss is part of a pre-George River Group gneissic complex. Raeside (1990) determined that its mineral assemblages reflect metamorphism under low-pressure (<400 MPa) and high-temperature (>650°C) conditions, and correlated the rocks with similar lithologies on Kellys Mountain defined by Jamieson (1984).

Geology of the Lime Hill area

At the Lime Hill zinc occurrence, the gneissic complex consists predominantly of a metacarbonate rock suite containing dolomite marble and siliceous dolomite marble with lesser calcite marble and calc-silicate rock (Fig. 3). The gneissic metasedimentary rocks that compose most of the complex are exposed mainly along the northern edge of the map area. The gneiss complex was intruded by a small tonalite body and a large number of granitic and mafic dykes.

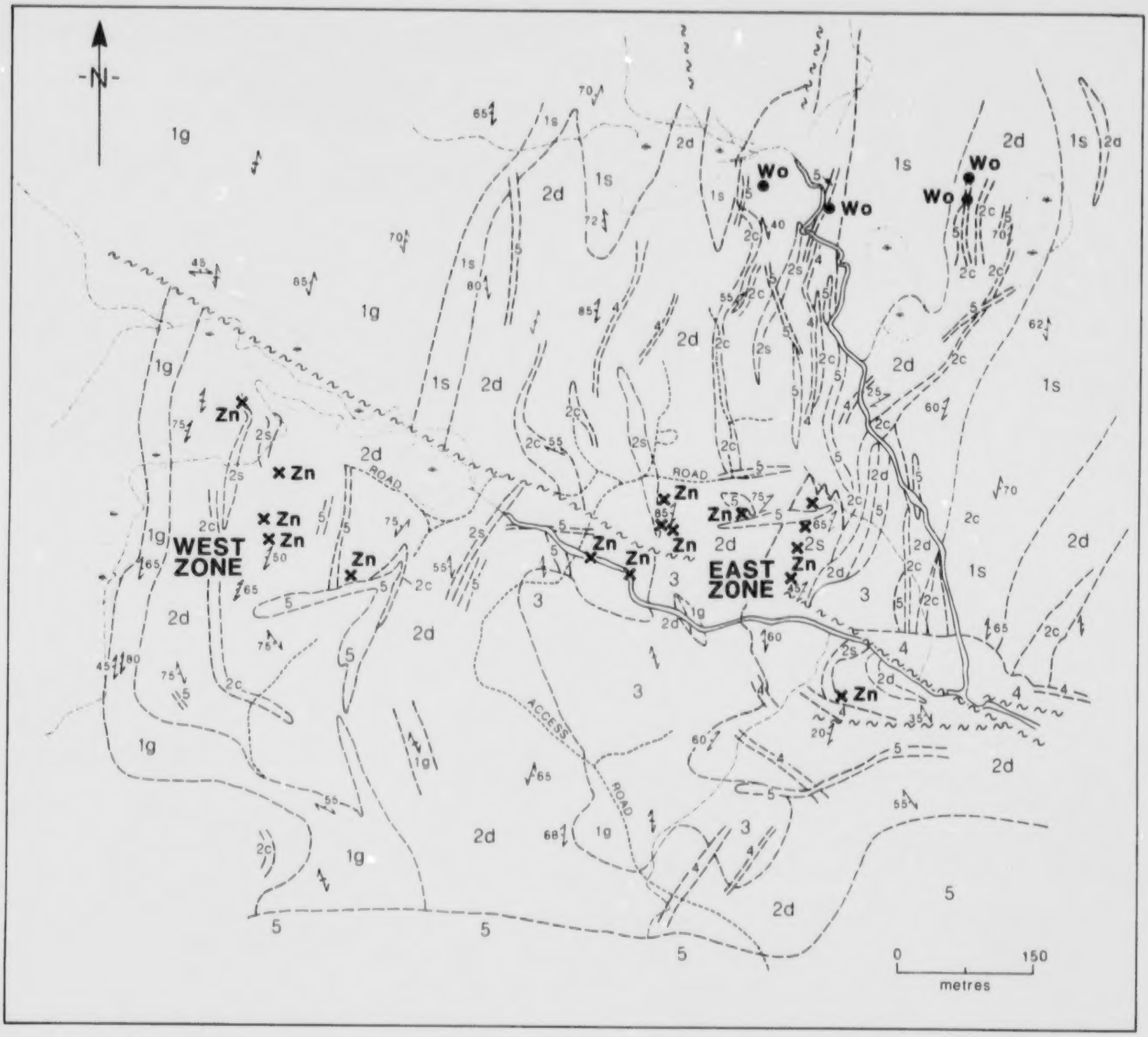

Figure 3. Geology of the Lime Hill Zn occurrence. Legend: 1. Biotite-quartz-feldspar gneiss, (1g) +/− cordierite +/− sillimanite +/− garnet, (1s) more mica-rich; 2. Marble, (2c) calcite marble, (2d) dolomite marble, (2s) serpentine marble (>15 percent serpentine); 3. Tonalitic orthogneiss; 4. Foliated amphibolite dykes; 5. Late granitic dykes of several ages; • Wo=wollastonite occurrence; x Zn=sphalerite occurrence; ↗70 =strike and dip of foliation; ∼∼ =fault.

The marble shows a continuous range in composition from calcite marble, wollastonite-calcite marble, and calc-silicate rock to the predominant lithologies, siliceous dolomite marble and dolomite marble (Fig. 4; Appendix I).

Dolomite marble

Dolomite marble constitutes the largest part of the Lime Hill metacarbonate suite. It is medium grained, white, buff and grey weathering, and contains a weak foliation which is best expressed by differential weathering of marble with slightly higher contents of calcite and minor contents of calc-silicate minerals. The dolomite contains minor but variable amounts of calcite and <10 percent silicate minerals. The silicate minerals include serpentine pseudomorphs after forsterite, relict forsterite, phlogopite, diopside, and tremolite.

Serpentine-dolomite marble

Serpentine marble is the second most abundant carbonate lithology, although it composes less than 10 percent of

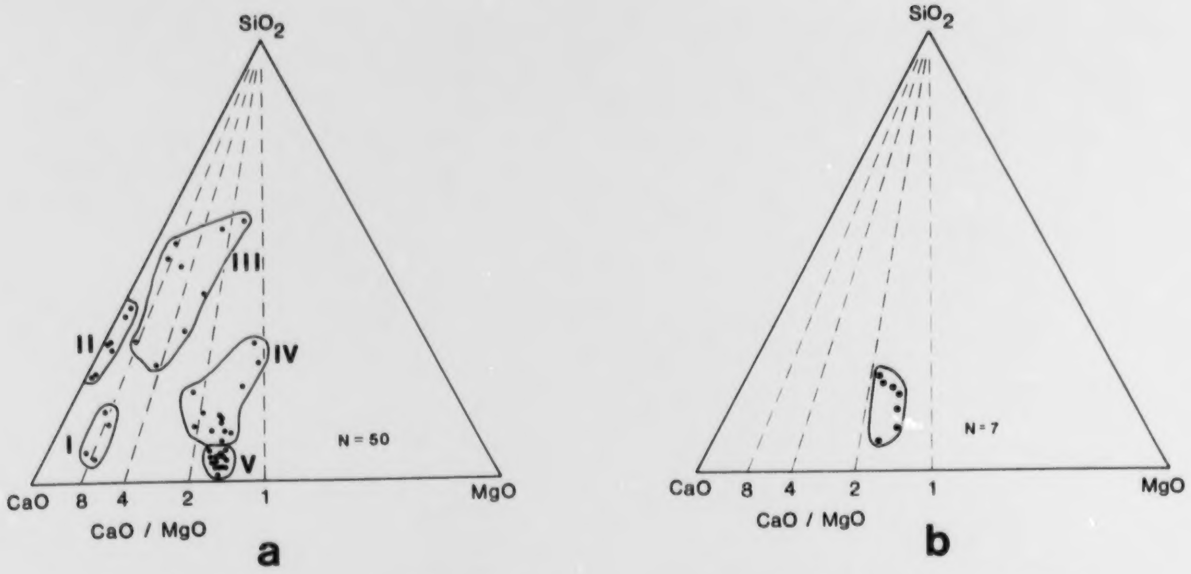

Figure 4. SiO_2-CaO-MgO variation diagrams illustrating the composition of marble and calc-silicate lithologies. CaO/MgO ratio of pure dolomite = 1.4. a) Lime Hill: I = calcite marble, II = wollastonite-diopside-calcite marble, III = diopside +/− quartz +/− plagioclase rock, IV = serpentine-dolomite marble, and V = dolomite marble. b) Meat Cove: serpentine-brucite marble.

the exposed marble. It occurs most commonly, but not exclusively, in zinc mineralized areas. It is medium grained and composed of calcite with lesser dolomite and 10 to 50 percent serpentine. Accessory minerals include talc, diopside, tremolite, and traces of chondrodite, brucite, and pyrite. Most of the serpentine is pseudomorphous after euhedral metamorphic forsterite (Fig. 5a,b), whereas a few percent serpentine occurs in some rocks filling late fractures cutting all minerals. Serpentine varies from waxy yellow-green to dark green-black, and normally occurs disseminated in bands which contain 10 to 25 percent serpentine and which are intercalated with clean dolomite marble, calcite marble, and calc-silicate layers. Diopside and tremolite are commonly fresh and unaltered. Chatterjee (1980) reported the presence of monticellite and merwinite which were not recognized in this study.

Calc-silicate rock

Two types of calc-silicate layers occur within the serpentine-dolomite marble. Most common are layers 5 to 50 cm thick which are composed of either massive, very fine grained diopside or variable proportions of diopside and plagioclase +/− quartz. These layers are commonly pale green to cream-white, and may either be massive or exhibit subtle millimetre-scale colour banding. The calc-silicate bands occur within the serpentine-forsterite marble and are fresh and unaltered. The second type of calc-silicate layer is composed of layers 10 to 50 cm thick consisting of thin bands of calcite plus serpentine psuedomorphs after euhedral forsterite that alternate with finely banded aggregates of massive serpentine, phlogopite, plagioclase, and calcite (Fig. 5c). Both types of alternating laminae may contain accessory pyrite and sphalerite.

Calcite marble

Calcite marble is medium grained and occurs as beds, 2 to 20 m thick, within both dolomite and serpentine-dolomite marble. It exhibits subtle light grey and blue-grey layering on a scale of 0.5 to 2 cm. Wollastonite-diopside assemblages are found in calcite marble near its contacts with granitic dykes.

Paragneiss

Several varieties of gneiss are present at Lime Hill. Two varieties of biotite-feldspar-quartz gneiss predominate; one whitish weathering variety that is quartz-feldspar-rich, and a second that is rusty weathering and biotite-rich. Cordierite, sillimanite, garnet, and hypersthene are present locally and have undergone retrograde metamorphism. An extensive description of the gneiss (Raeside, 1990) can be found elsewhere in this volume.

Intrusive rocks

The host rocks of the Lime Hill zinc prospect have been intruded by a small body of weakly to moderately foliated tonalite and numerous dykes of variable composition that may be related to the larger Big Brook granodiorite and West Bay granite plutons, which intrude the Lime Hill gneiss to the north and west. Seven varieties of dykes have been identified based on composition, texture, orientation, and crosscutting relationships. The dykes range in composition from leucogranite to syenite to diorite. They are highly irregular to tabular, massive to lineated, and equigranular to pegmatoidal. Some varieties of dykes were observed cutting the orthogneiss. Trench exposures indicate that the granitic dykes weather 1 to 4 m higher

a

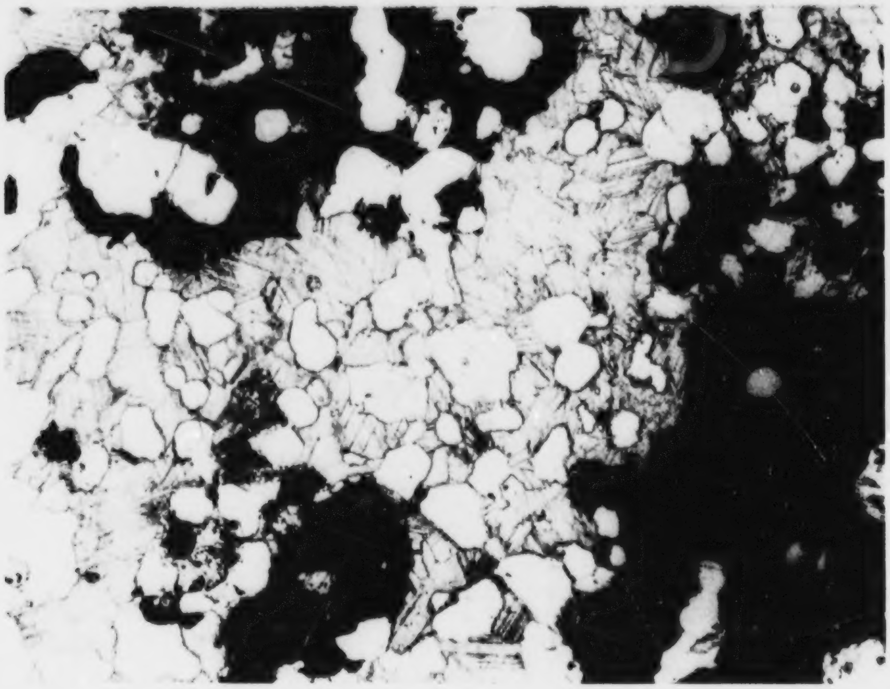

b

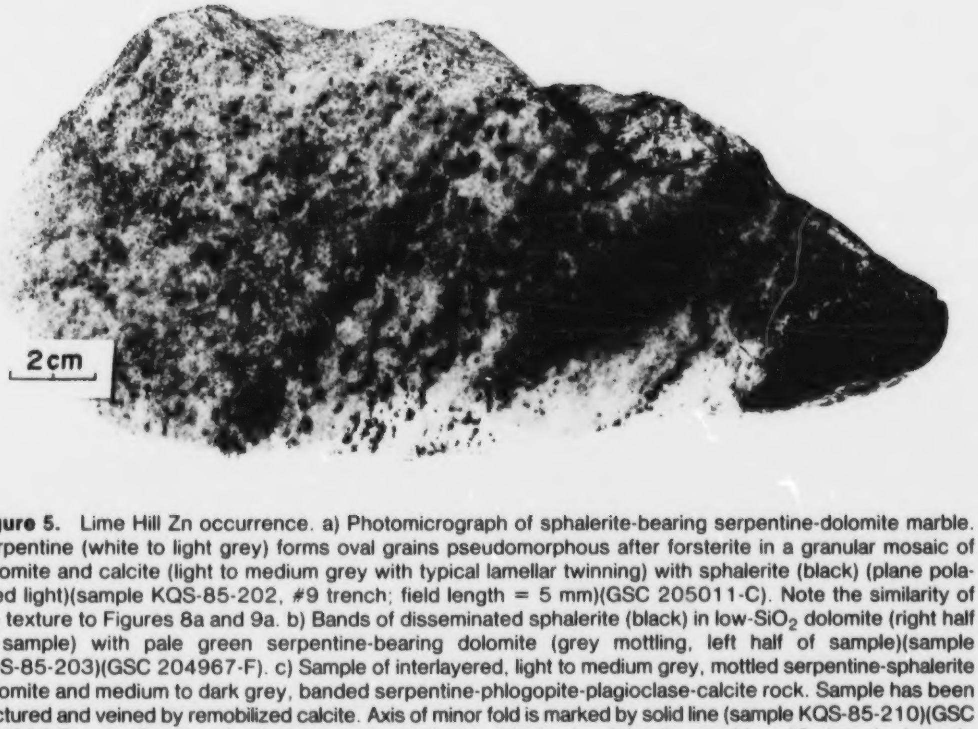

Figure 5. Lime Hill Zn occurrence. a) Photomicrograph of sphalerite-bearing serpentine-dolomite marble. Serpentine (white to light grey) forms oval grains pseudomorphous after forsterite in a granular mosaic of dolomite and calcite (light to medium grey with typical lamellar twinning) with sphalerite (black) (plane polarized light)(sample KQS-85-202, #9 trench; field length = 5 mm)(GSC 205011-C). Note the similarity of the texture to Figures 8a and 9a. b) Bands of disseminated sphalerite (black) in low-SiO_2 dolomite (right half of sample) with pale green serpentine-bearing dolomite (grey mottling, left half of sample)(sample KQS-85-203)(GSC 204967-F). c) Sample of interlayered, light to medium grey, mottled serpentine-sphalerite dolomite and medium to dark grey, banded serpentine-phlogopite-plagioclase-calcite rock. Sample has been fractured and veined by remobilized calcite. Axis of minor fold is marked by solid line (sample KQS-85-210)(GSC 204967-E). d) Bands of disseminated sphalerite (black) in dolomite marble, #9 trench (sample KQS-85-201)(GSC 204967-B).

c

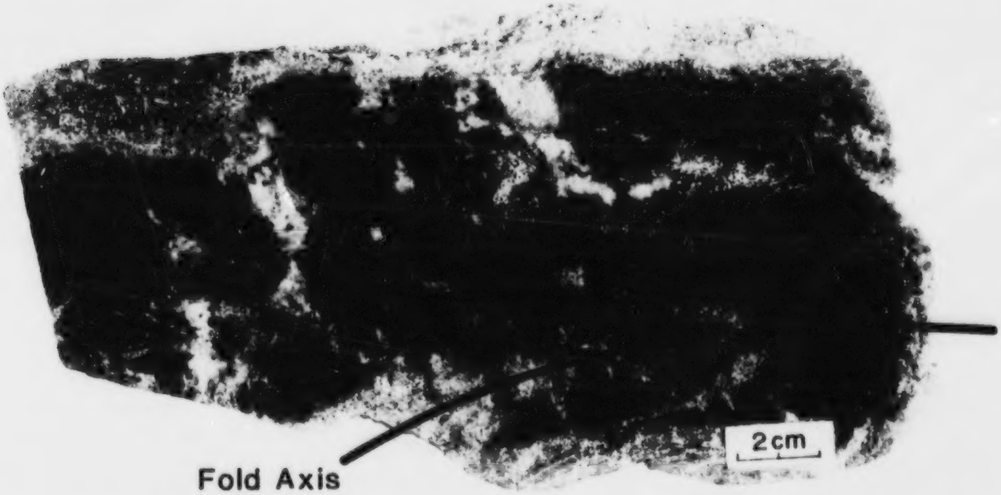
2cm
Fold Axis

d

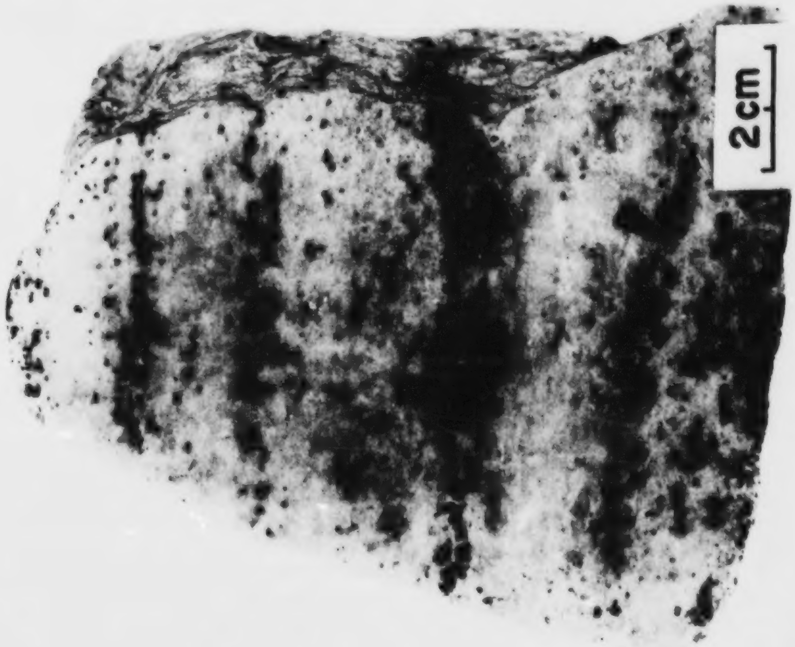

than the surrounding marble, resulting in preferential outcropping of granite and resulting in poor exposure of marble in the intervening recessively-weathered areas. Contact metamorphic effects around the dykes are minimal, consisting only of a zone a few centimetres wide containing a greater abundance of calc-silicate minerals which have been altered to serpentine. Chemical analyses of representative samples of each lithology are presented in Table 1.

Tonalitic orthogneiss is cut by unfoliated granitic dykes, suggesting that the tonalite is significantly older than the youngest granitic dykes which were presumed to be Cambrian (Cormier, 1972). However, U-Pb (zircon) ages on the two lithologies (P.A. Hunt and A.L. Sangster, unpublished data) indicate identical ages of 539 +/−1 Ma and 541 +14.5/−23.5 Ma for the tonalite and unfoliated granite dykes, respectively.

Structural geology

The structure of the rocks in the vicinity of the Lime Hill zinc occurrence is poorly known due to the overall lack of outcrop. Mapping of the occurrence on the exploration grid (Justino and Sangster, 1987) defined a prominent north-south structural fabric containing the regional foliation and both steeply plunging and subhorizontal minor fold axes. These trends are in marked contrast to the dominant northeast fabric documented in George River Group rocks both on North Mountain and elsewhere on Cape Breton Island (Milligan, 1970). The relative stratigraphic positions of the metacarbonate and metaclastic rocks are unknown. The interpreted distribution of lithologies as presented in Figure 3 suggests north-south isoclinal folding. Lineations and minor fold axes with a dominant shallow north plunge are coincident with the overall plunge of the east zone zinc mineralization (Nova Scotia Department of Mines, Assessment File 5-J-45), suggesting that the gneissic rocks structurally overlie the mineralized marble.

Table 1. Chemical analyses of representative samples of intrusions spatially associated with marble-hosted zinc occurrences, Cape Breton Island.

		SFB-86-IV GRANODIORITE DYKE LIME HILL	SFB-86-II TONALITE GNEISS LIME HILL	SFB-86-601 LOWLAND BROOK SYENITE MEAT COVE
SiO_2	%	74.40	65.40	56.90
Al_2O_3	%	13.90	16.70	17.80
CaO	%	2.32	4.96	3.73
MgO	%	0.68	1.89	1.74
Na_2O	%	3.76	3.58	5.34
K_2O	%	2.68	1.13	4.15
Fe_2O_3	%	1.45	4.21	6.93
MnO	%	0.05	0.13	0.20
TiO_2	%	0.21	0.50	1.53
P_2O_5	%	0.07	0.13	0.71
LOI	%	0.54	1.70	0.77
TOTAL	%	100.06	100.33	99.80
Sr	PPM	400	380	500
Ba	PPM	610	230	1900
Rb	PPM	110	50	60
Cr	PPM	10	20	10
Zr	PPM	70	150	460
Y	PPM	20	40	80
V	PPM	0.5	0.5	8
Nb	PPM	10	20	20

The map area (Fig. 3) is traversed by a major west-northwest-striking left-lateral fault which appears to have resulted in the observed offset between the east and west mineralized zones. Its orientation is similar to that of the Big Brook Fault which bounds the Lime Hill gneiss to the northeast. It is believed to be a young fault, but its relationship to the Carboniferous cover rocks is not known. Several small north-south faults were mapped in the area.

Geology of the zinc occurrences

The zinc mineralization at Lime Hill is exposed in two zones that parallel the lithological layering and foliation within the marble host rock. The east mineralized zone (Fig. 3) contains three mineralized structures, the Main, "C", and #2 areas, which have been exposed in trenches and by diamond drilling along a strike length of 300 m. The west zone has an indicated strike length of only 200 m. Diamond-drill logs (Nova Scotia Department of Mines and Energy, Assessment File 11F/14 58-J-33) indicate the presence of mineralized intersections ranging from 25 cm to as much as 10 m with grades ranging from a few percent Zn to 10 percent Zn over 8 m. Grades and thicknesses of mineralized intercepts differ widely between adjacent holes, perhaps suggesting extensive structural involvement in grade and thickness distribution.

The stratabound, carbonate-hosted mineralization occurs in both disseminated and massive form. Most of the mineralized rock contains medium to coarse grained sphalerite, disseminated in bands that vary from one centimetre to several metres in thickness and are parallel to lithological layering in dolomite, serpentine-dolomite, or serpentine rock (Fig. 5b,c,d). Other sulphide minerals are sparse and consist of minor disseminated pyrrhotite and/or pyrite and rare chalcopyrite. Multiply folded layers of disseminated sphalerite with flat to shallow north plunges can be seen locally in the #9 trench (see below) and the #39 trench at the northern end of the east zone. Sphalerite also occurs as massive layers that vary from 10 to 50 cm in thickness and are oriented parallel or subparallel to the disseminated sphalerite layers. Accessory minerals include minor pyrrhotite and pyrite, and in a few cases, pyrite was the dominant sulphide mineral. Grain size in some layers is exceptionally coarse, with individual sphalerite grains as much as 10 cm in diameter. In trench #35, at the southern end of the west zone, a massive sulphide band was observed that truncates bedding-parallel bands of disseminated sphalerite. Both the coarse grain size and crosscutting massive sulphide layers resemble "spangle ore" within the Balmat, New York deposits, where this type of mineralization has been interpreted as sulphides that have been remobilized into fault zones during metamorphism (deLorraine and Dill, 1982).

Chatterjee (1977) reported the presence of scheelite in association with wollastonite-bearing calcite marble and also in massive sphalerite. Scheelite was not observed during the current work and tungsten was below its detection limit in the analyses obtained.

Geology of the #9 trench

The extensive trenches at Lime Hill are badly caved and provide little useful structural information. The best available exposure is in the #9 trench which exposes mineralized bedrock at the southern end of the east zone mineralized area. The geology of this trench is described briefly here to provide some insight into the relationships between marble and granitic dykes and the types of structure that may control the distribution of mineralization on the property.

The rocks exposed in the #9 trench (Fig. 6) consist of dolomite marble and siliceous dolomite marble with lesser calcite marble and calc-silicate rock, all cut by unfoliated granitic dykes. The marble contains multiple generations of minor folds suggesting that folds may potentially constitute a structural control for sulphide lenses. A late, north-south shear zone is well exposed in the southern part of the trench. Layering in the marble strikes 000° to 020° with subvertical dips, except in the northwestern corner of the trench where dips flatten to about 60° east. Sphalerite occurs 1) disseminated in both the clean and serpentine-bearing dolomites, 2) as massive sheets and lenses in dolomite, and 3) as breccia fragments in sheared and crushed marble. Two dykes are parallel to the marble contacts (020° azimuth) but the eastern dyke dips much more flatly, at about 45° east. An east-west, semicontinuous exposure of granite at the northern end of the trench, which appears continuous with the north-south exposures, may indicate that the granitic intrusions form irregular sheets. The marble-granite contact is sharp with no visible metamorphic effect or addition of metasomatic components.

Both steeply plunging and shallowly plunging small folds can be seen in the trench. Folds that plunge steeply south (75°) occur in the south-central and southern part of the trench and are associated with thickened bedding-parallel layers of massive sphalerite. Shallowly plunging folds are exposed in the southeastern part of the trench (area of enlarged geology in Fig. 6) and in the north-central part of the trench. The northern structure is a simple fold of a massive sulphide band 15 cm thick and no sulphide concentration effect is observed. The apparent thickening illustrated in Figure 6 is a result of sphalerite exposure on an outcrop surface plunging parallel to the fold axis. The folding in the southern end of the trench is much more complex. Here, a band of disseminated sphalerite 2 to 3 cm thick can be traced through a system of refolded folds with subparallel axes that plunge 10° south. No structural concentration of sphalerite is evident in either generation of folds.

GEOLOGY OF THE MEAT COVE ZINC OCCURRENCE

At Meat Cove the sulphide-bearing marble is a large xenolith within the Lowland Brook hornblende syenite (Fig. 7; Table 1). This syenite body has intruded a suite of high-grade gneiss of the Blair River Complex. Petrographic studies of the gneiss (Barr et al., 1987b) indicate an early metamorphic event at upper amphibolite facies, transitional to granulite facies, with a later greenschist facies overprinting. These gneisses were previously included with rocks of the late Precambrian George River Group (Neale, 1964; Milligan, 1970; Chatterjee, 1979, 1980; Smith and Macdonald, 1981). Recent remapping of northern Cape Breton Island (Barr et al., 1987a) has resulted in the attribution of a Grenville age, based on a metamorphic age of 1040 + 30/ – 40 Ma (U-Pb zircon) from the Lowland Brook syenite (Barr et al., 1987b). The authors assigned an igneous age of 1100 to 1500 Ma to the intrusion, but the limited nature of scatter in the data suggests that this age may well be less than 1300 Ma (O. van Breemen, pers. comm., 1989).

Surface exposure of marble in the vicinity of the Meat Cove occurrence is poor, the only significant outcrop being at the northeast showing. Exploration trenches that previously exposed mineralization and an adit into the mineralized zone are badly caved and weathered and provided no information at the time this work was done. Reports on the geology of the adits and trenches can be found in Chatterjee (1979, 1980). Most samples on which this study is based were obtained from dump material.

The mineralization at Meat Cove forms a southeast-striking zone that is about 1200 m long and as much as 35 m wide, dipping moderately to the east (Keating, 1960). Drill records indicate that the mineralization forms large tabular zones of disseminated sphalerite within the marble, but provides little information on the variety and geometry of the marble host rocks. Keating (1960) reported the partial definition of a large syncline associated with the mineralized portion of the marble, and that sphalerite was "conspicuous in minor folds in the limestone" and had a tendency to be hosted by the more impure marble.

Dump material from an adit driven into the deposit consists almost exclusively of serpentine-dolomite marble (Fig. 8a,b; Appendix I) consisting of variable proportions of calcite, dolomite, serpentine, brucite, talc, minor phlogopite, and relict forsterite. The serpentine is pseudomorphous after euhedral metamorphic forsterite. Brucite occurs as medium grained aggregates of very fine grained needles which show the typical "thumb print" texture reflecting the hydration of periclase (Fig. 8c). Reconnaissance microprobe analyses of the minerals indicate that the phlogopite in some cases contains as much as 3 or 4 percent Ba (i.e. Appendix IIB, sample SFB-86-594). The marble exhibits well developed layering (Fig. 8b,d) which results from distinct and numerous changes in the relative proportions of carbonate, serpentine (5 to 30 percent), and brucite (0 to 15 percent). Compositions of the marble at Meat Cove are restricted to a range of values scattered along the dolomite-silica join

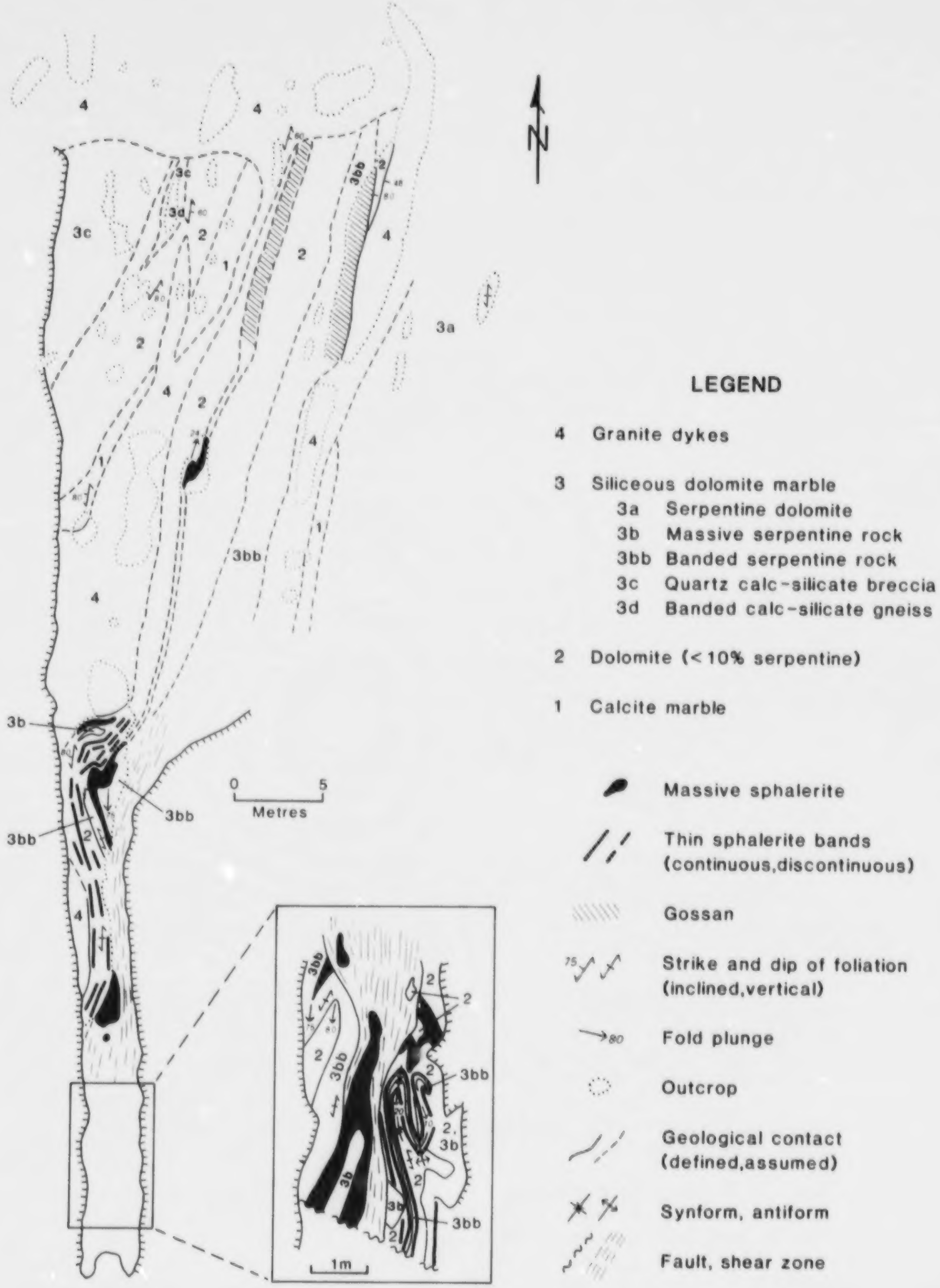
N
4
3c
3d
2
1
3bb
3a
3b
0 5
Metres
1m
LEGEND
4 Granite dykes
3 Siliceous dolomite marble
3a Serpentine dolomite
3b Massive serpentine rock
3bb Banded serpentine rock
3c Quartz calc-silicate breccia
3d Banded calc-silicate gneiss
2 Dolomite (< 10% serpentine)
1 Calcite marble
Massive sphalerite
Thin sphalerite bands (continuous, discontinuous)
Gossan
Strike and dip of foliation (inclined, vertical)
Fold plunge
Outcrop
Geological contact (defined, assumed)
Synform, antiform
Fault, shear zone

Figure 6. Geology of the #9 trench area, Lime Hill Zn occurrence.

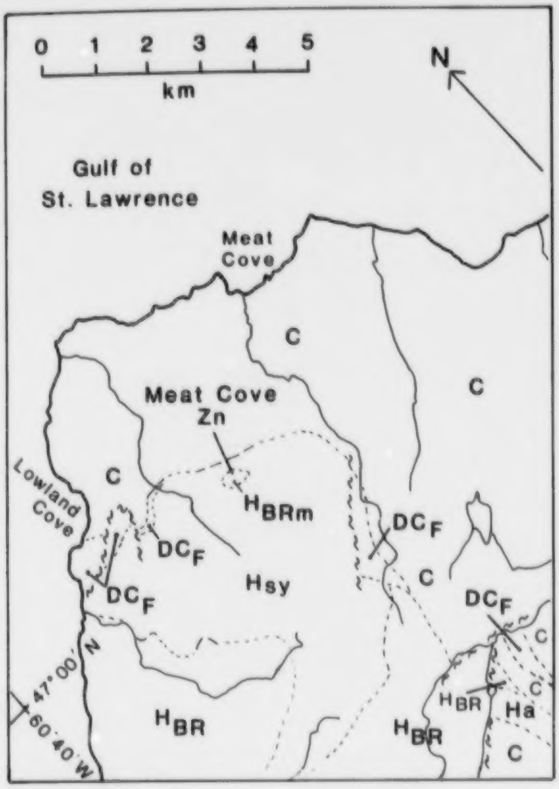

Figure 7. Geology of the Blair River Complex, Meat Cove area (modified after Raeside et al., 1986). Symbols: Middle Proterozoic — H_{BR}=Blair River Complex, H_{BRm}=Blair River Complex marble, Hsy=Lowland Brook syenite, Ha=anorthosite; Devono-Carboniferous — DC_F=Fisset Brook Formation (volcanic rocks); Carboniferous — C=clastic cover rocks.

(Fig. 4b) and are similar to those for the dolomitic lithologies from Lime Hill, with the exception that overall SiO_2 values are marginally lower. As at Lime Hill, the silica-rich dolomite at Meat Cove contains only low contents of Al_2O_3, Na_2O, and K_2O.

Sulphide mineralization consists mainly of sphalerite, although minor pyrite and pyrrhotite are present. Galena and chalcopyrite are rare. The galena samples obtained for lead isotopic analyses (see below) were not from sphalerite-bearing samples but from massive coarse grained diopside rock, possibly a true skarn. Chatterjee (1979) reported the presence of germanite and renierite, accounting for the presence of up to 160 ppm Ge in the sphalerite. Sphalerite is most commonly disseminated in layers parallel to the lithological layering in the serpentine-brucite marble (Fig. 8b,d). No evidence of significant folding was seen in the larger dump specimens, though in several dump samples, lithological geometries were noted that could indicate boudinage prior to the retrograde metamorphic event that produced the serpentine-brucite assemblage (Fig. 8b—upper right).

OVERVIEW OF GRENVILLE SUPERGROUP MARBLE-HOSTED ZINC OCCURRENCES

Much of the new data presented here on the Lime Hill and Meat Cove occurrences is directly compared to similar data for well documented occurrences hosted by marble in Grenville Supergroup rocks. In the following paragraphs the general character of the deposits and occurrences in Grenville Supergroup rocks is discussed to permit the reader to better appreciate the comparisons that are made with the Nova Scotia occurrences.

The Central Metasedimentary Belt of the Grenville Province of southeastern Ontario, southern Quebec, and northwestern New York State is composed of a basal suite of 1) mafic metavolcanic rocks, which occupy the axial zone of the fold belt, and 2) a major metasedimentary succession, which overlies this and flanks it to the northwest and southeast and consists of marble-dominated lithologies, including calcite and dolomite marble, varieties of calc-silicate and quartzofeldspathic paragneiss, quartzite, and minor amphibolite. Marble is also extensively intercalated with the metavolcanic rocks within the metavolcanic-dominated parts of the fold belt. Marble-hosted zinc occurrences are common throughout much of the area (deLorraine and Dill, 1982; Sangster and Bourne, 1982; Whelan et al., 1984; Gauthier and Brown, 1986). They are generally Zn-rich to the exclusion of other metals, and they are dominated by calc-silicate gangue mineral assemblages. The deposits and occurrences are stratiform, though highly overprinted by structures imposed during the Grenville metamorphic event, so that deposits are typically foliation- or fold-controlled with large down-plunge extensions. Four types of Zn-Pb occurrences have been distinguished on the basis of their host rock assemblages and general geological setting within the fold belt (Sangster, 1970; Sangster and Bourne, 1982).

Type 1 deposits

These include the polymetallic deposits at New Calumet (Sangster, 1967) and Montauban, Quebec (Bernier et al., 1987). They contain sphalerite, galena, pyrrhotite, pyrite, chalcopyrite, and Ag-bearing sulphosalt minerals in thin calc-silicate marble horizons in silicate gneiss interpreted to be of volcanic origin. Both deposits contain Au-rich zones that are distinct from, but spatially associated with, the calc-silicate-hosted mineralization. These two deposits have historically been included with the deposits outlined below, but they are geologically distinct in the low proportion of marble present in their host rocks and in their polymetallic, Ag-rich character.

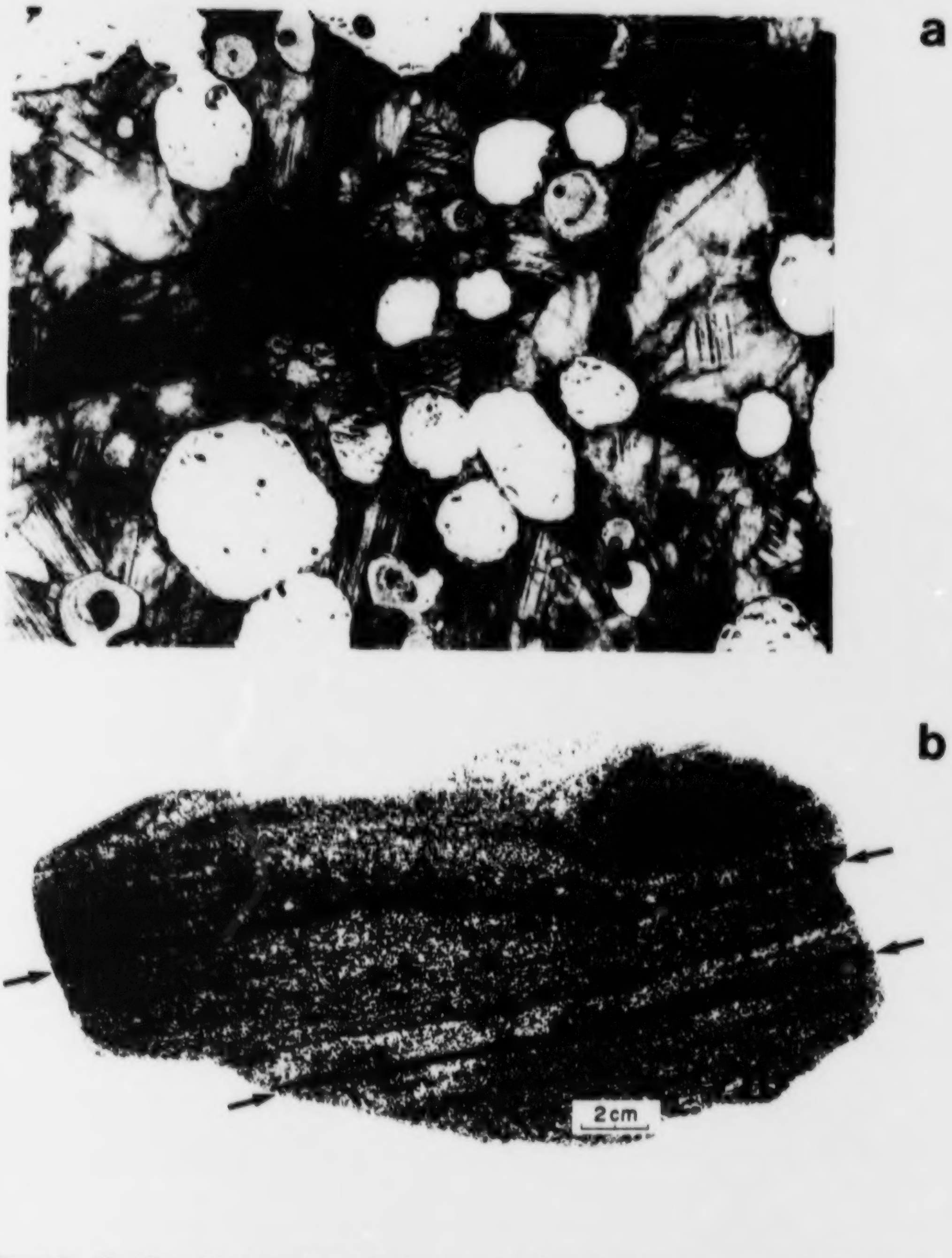

Figure 8. Meat Cove Zn occurrence. a) Photomicrograph of sphalerite-bearing serpentine-dolomite marble. Serpentine (white to light grey) forms oval grains pseudomorphous after forsterite, in a granular mosaic of dolomite and calcite (light to medium grey with typical lamellar twinning) with sphalerite (black)(plane polarized light)(sample SFB-86-589, main adit dump; field length = 5 mm)(GSC 205011). b) Serpentine-dolomite marble with well developed layering resulting from variations in colour index caused by the relative proportions of serpentine and sphalerite (dark) and calcite, dolomite, and brucite (light). Note boudin in upper right corner of specimen. Zn-rich layers are indicated by arrows (GSC 204967). c) Photomicrograph of brucite-serpentine (dark grey mottling)-sphalerite (black) marble. Brucite (Br) in centre of the photograph consists of bundles of fine needles that commonly exhibit a texture resembling a fingerprint (grain in right-centre). Brucite may compose up to 15 percent of some marbles (sample SFB-86-574; crossed nicols, field length = 5 mm)(GSC 205011-B). d) Meat Cove Zn occurrence (sample from adit dump). Bands of submassive sphalerite (arrows) in dolomite marble adjacent to serpentine-rich dolomite (dark grey mottling) forming right quarter of sample (GSC 204967-C).

c

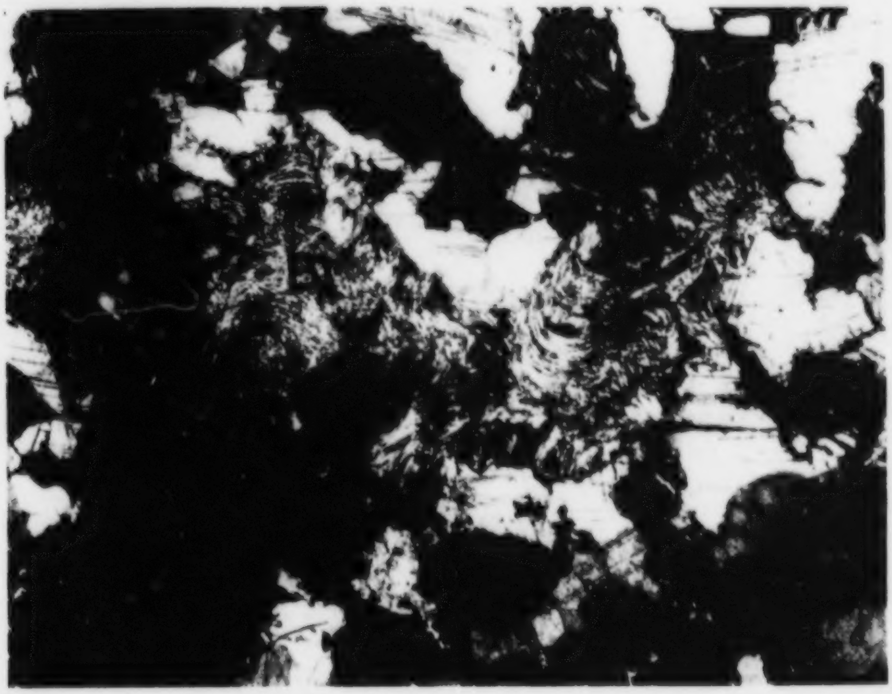

d

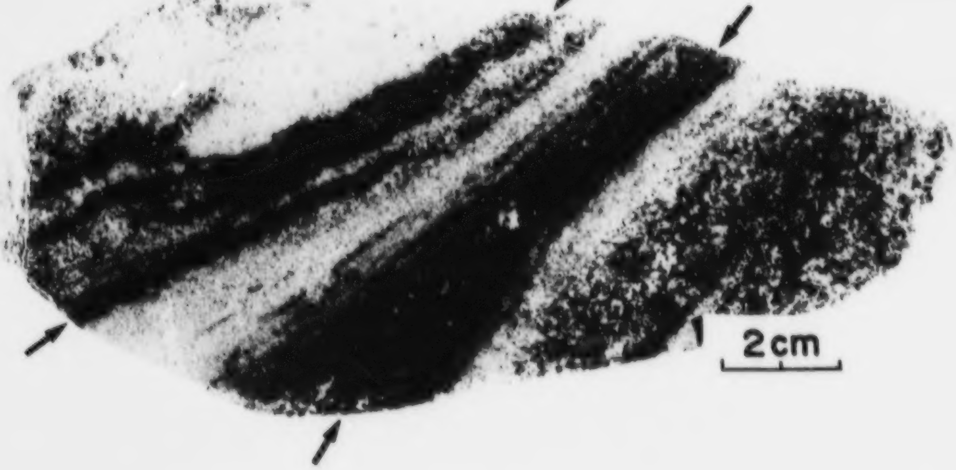

Type 2 deposits

These deposits are hosted by marble within the outcrop limits of the metavolcanic rocks (Cadieux and Spry occurrences) and are Zn-rich with minor accessory pyrite and pyrrhotite and only traces of galena. The host marble is dominated by intercalated silica-rich and silica-free dolomite units, which are the predominant local carbonate lithologies (Sangster, 1970; Carter et al., 1979; Carter, 1984; Malczak et al., 1985; Soever and Meusy, 1986).

Type 3 deposits

These deposits occur in marble adjacent to the metavolcanic terrane (e.g. Long Lake, Slave Lake, Thirty Island Lake, Pharaoh, Leitch, Lafontaine, and Bouchette) and are hosted by thin, weakly siliceous dolomite or calcareous dolomite units, within carbonate sequences dominated by calcite marble. They contain sphalerite, with minor iron sulphide, and rarely galena (Carter et al., 1979; Carter, 1984; Malczak et al., 1985; Gauthier and Brown, 1986). An example of sphalerite-mineralized serpentine-dolomite marble from the Lafontaine occurrence (Fig. 9a,b) is included for comparison to similar lithologies from Lime Hill (Fig. 5a,b) and Meat Cove (Fig. 8a,b).

Type 4 deposits

These deposits occur in marble distant from the main area in which metavolcanic rocks are exposed, and near the interpreted margins of the Central Metasedimentary Belt. Examples include the major producing Balmat, Edwards, and Pierrepont deposits, as well as a small noncommercial deposit at Salerno Lake. They occur within extensive areas of intercalated dolomite marble and siliceous dolomite marble strata. The deposits contain primarily sphalerite, accessory pyrite and pyrrhotite, and local traces of galena. The stratigraphic succession at Balmat contains abundant anhydrite of apparent sedimentary, evaporitic origin (Lea and Dill, 1968; deLorraine and Dill, 1982; Easton and Bartlett, 1984; Whelan et al., 1984).

GEOCHEMISTRY OF MINERALIZED MARBLE

A selection of samples of mineralized and unmineralized marble lithologies from the Lime Hill and Meat Cove occurrences were analyzed for their major and trace element compositions (Appendixes IA,B, IIA,B). Also, a suite of 41 mineralized samples collected from five zinc occurrences hosted by Grenville Supergroup marble in Ontario and Quebec are presented (Appendix IIA,B) for comparison with the analyses from the Nova Scotia occurrences. Analyses of the calcite marble, wollastonite marble, and calc-silicate rock from Lime Hill, although not discussed further, are included (Appendix IA,B) to chemically characterize these lithologies. The following discussion focuses on the dolomite marble and serpentine-dolomite marble that host the mineralization.

The major element compositions of mineralized marble from Lime Hill, Meat Cove, and the Grenville Supergroup occurrences are similar (Fig. 10A). These rocks are dolomite and contain variable amounts of SiO_2, Fe_2O_3, and Zn as the only major components other than volatiles (S, CO_2). The Al_2O_3, K_2O, and Na_2O contents are low and reflect the local occurrence of phlogopite. Ternary plots of SiO_2-CaO-MgO for the mineralized and unmineralized marble indicates that they are similar in chemical composition (Fig. 11). Occurrences from the Grenville Supergroup have a wider range of SiO_2 contents and Zn-bearing marble is dolomite (Appendix II). The three serpentine-rich samples from Lime Hill have CaO/MgO ratios well above that of pure dolomite.

The sphalerite-bearing marbles from Lime Hill and Meat Cove have distinctive suites of trace elements, which are similar to those in sphalerite-bearing marble from the Grenville Supergroup deposits (Fig. 10b). Hg and Cd are elevated in the Nova Scotia occurrences, but Hg levels are nevertheless about an order of magnitude less than in Grenville Supergroup occurrences (see Appendix IIB). Cd is enriched to similar levels. The Meat Cove occurrence contains elevated Ge. The amounts of most other trace elements are anomalously low and, for the most part, lower than found in the Grenville Supergroup occurrences. Whenever an elevated trace element value was recorded, this was commonly for a single anomalous sample and the value was, in many cases, several orders of magnitude higher than those for other samples in the population (e.g. Pb = 1566 ppm in sample KQS-85-234 from Lime Hill or Ba = 6130 ppm in sample SFB-86-594 from Meat Cove; see Appendix IIB). The elements considered to be anomalously low include Au, As, Cu, Pb, Ag, Bi, Sb, Ba, Ni, Co, and Mo. W, reported to occur as scheelite at Lime Hill with sphalerite (Chatterjee, 1977), and Sn, reported to occur as stannite at Meat Cove (Chatterjee, 1979), are not anomalous in the analyzed samples (Appendix IIB).

SULPHUR ISOTOPIC ANALYSES

Sulphur isotopic analyses were carried out on bulk sphalerite separates from 100 to 250 g hand specimens of sphalerite-bearing marble from the Lime Hill and Meat Cove occurrences (Appendix III). Samples from Lime Hill were selected to represent low- to high-grade mineralization and the widest possible geographic distribution, with some included from surface trenches and drillholes from both the east and west zones. Due to a lack of exposure, samples of mineralized marble from Meat Cove were selected to reflect the variation in mineralized rock on the main zone dump, with two samples from small exposures along the northwest zone.

Results of the analyses indicate a heavy isotopic signature and restricted range of values about the average for each of the Nova Scotia occurrences. The ranges of values obtained for both occurrences are almost identical to those for Type IV and the isotopically heavier Type III Grenville Supergroup-hosted occurrences (Appendix IV, Fig. 12).

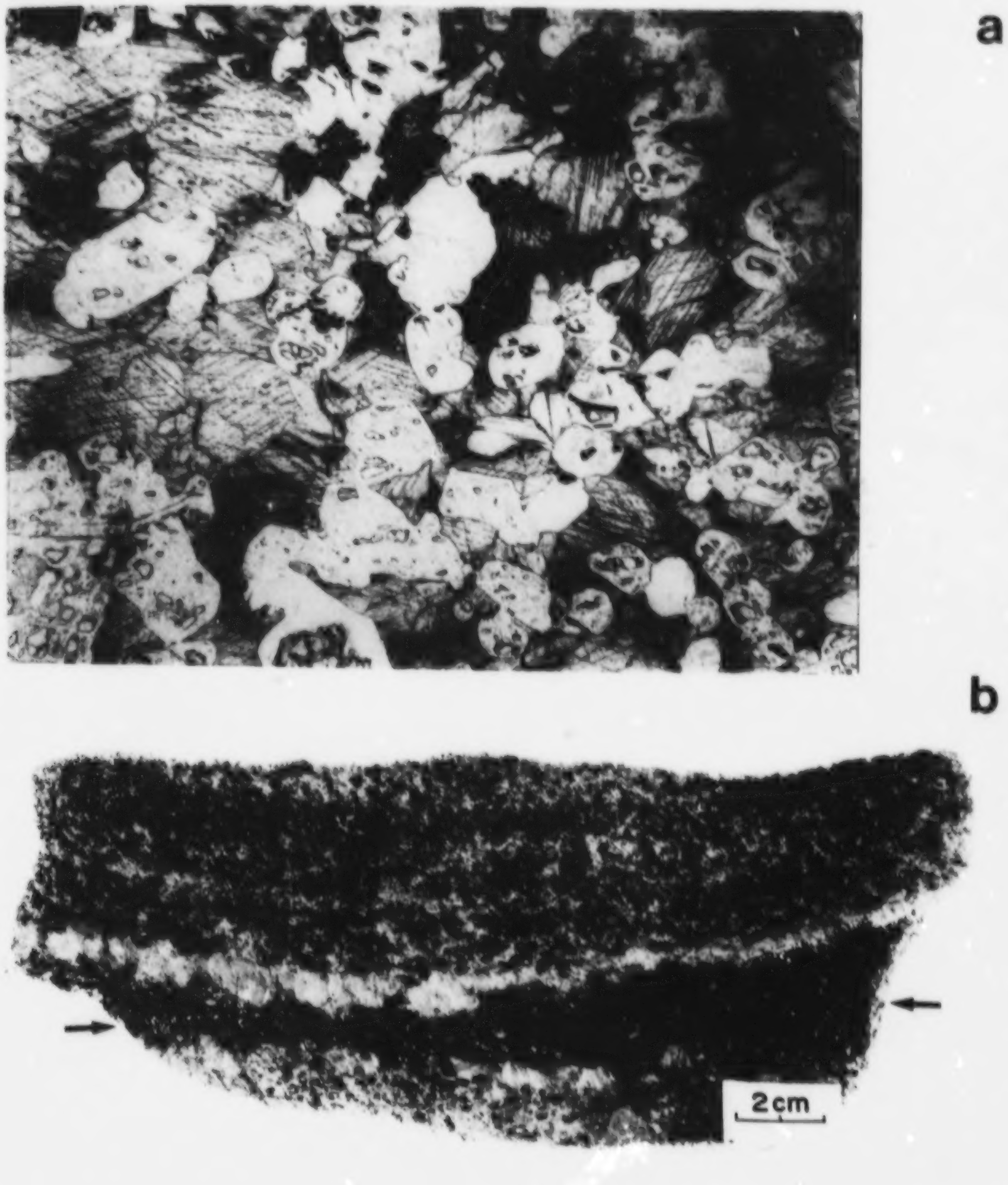

Figure 9. Lafontaine Zn occurrence, Quebec. a) Photomicrograph of sphalerite-bearing serpentine-dolomite marble. Note the similarity of this lithology to serpentine-dolomite marble from the Lime Hill (Fig. 5a) and Meat Cove (Fig. 8a) occurrences (GSC 205011-A). b) Sphalerite band (arrows) in serpentine-dolomite (dark grey) marble from the Grenville Supergroup is similar to mineralization at Lime Hill and Meat Cove (GSC 204967-A).

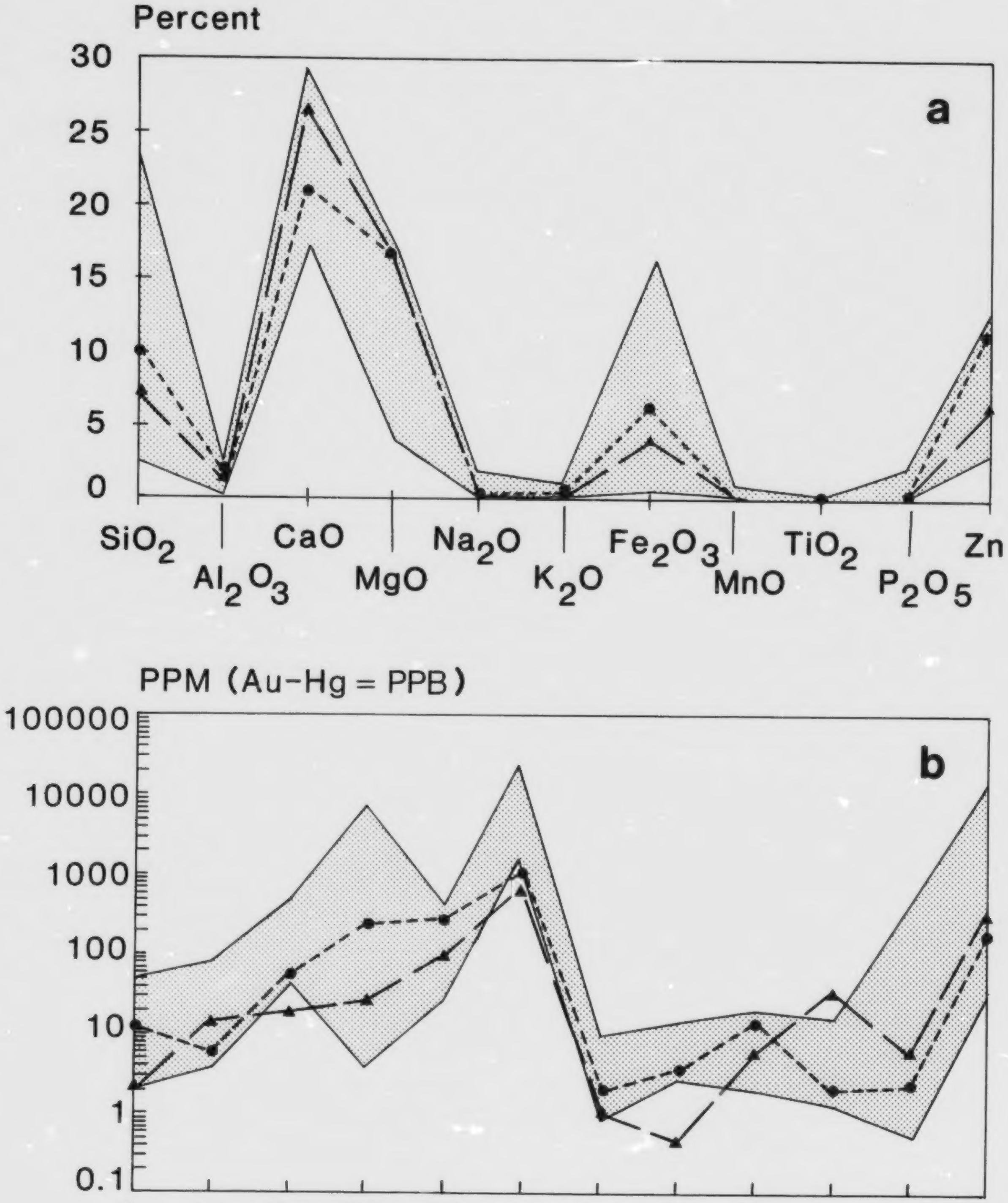

Figure 10. a) Major element comparison between range of compositions of 38 sphalerite-bearing marble samples from five occurrences in Grenville Supergroup rocks (shaded area) with sphalerite-bearing marble from the Lime Hill (shorter dashes with circles, average of 15 analyses) and Meat Cove (longer dashes with triangles, average of 20 analyses) occurrences. The slightly greater Mg content of the Cape Breton Island occurrences is reflected in the dominance of the serpentine-brucite-forsterite mineralogy in contrast to the dominant diopside-tremolite-serpentine +/− forsterite assemblage of the Grenville occurrences. b) Comparison of selected trace element compositions of 38 sphalerite-bearing marble samples from five occurrences in Grenville Supergroup marble (shaded area) and the Lime Hill (shorter dashes with circles, average of 8 analyses) and Meat Cove (longer dashes with triangles, average of 20 analyses) occurrences.

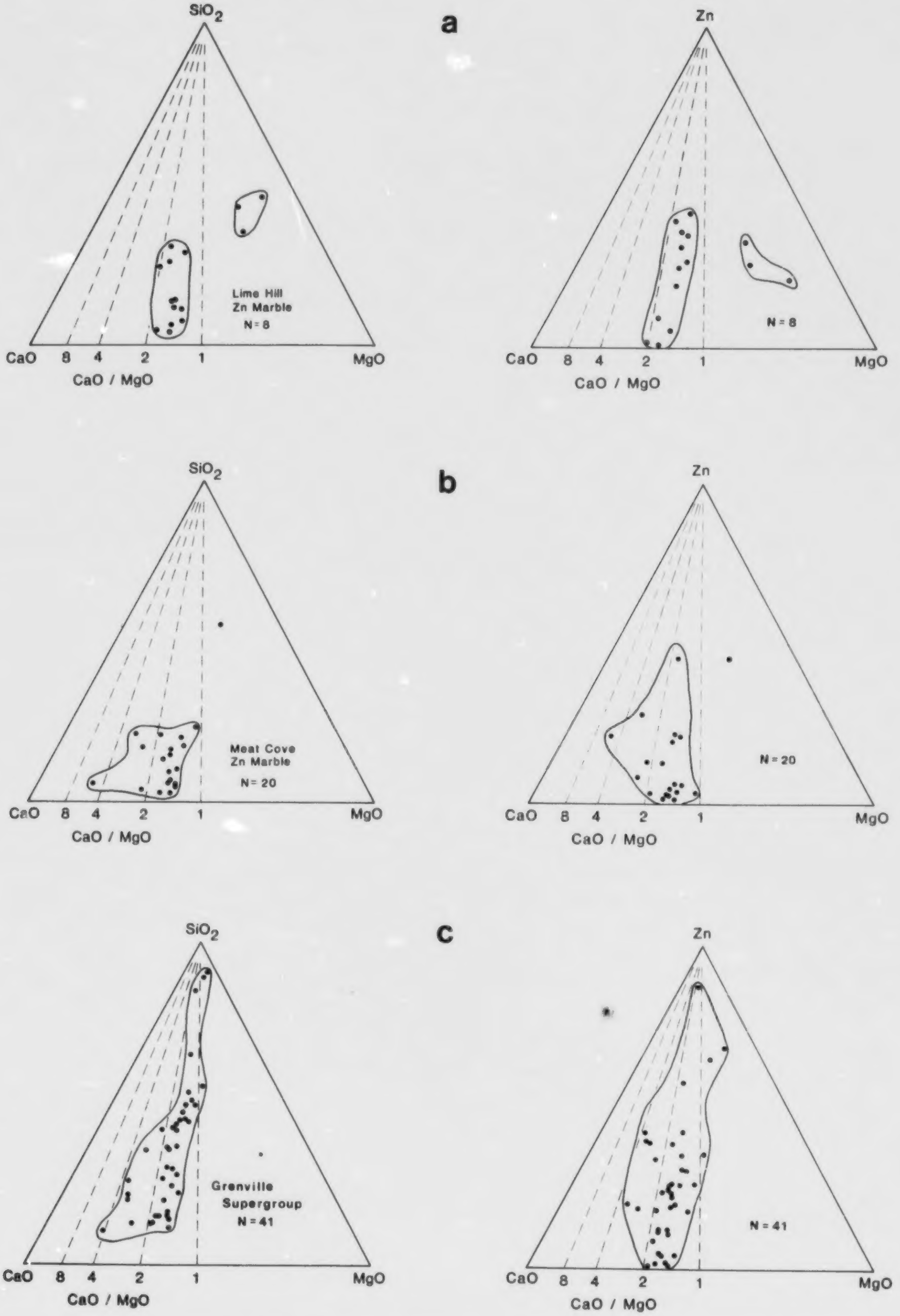

Figure 11. SiO_2-CaC-MgO and Zn-CaO-MgO variation diagrams illustrating the composition of sphalerite-bearing marble from the Lime Hill, Meat Cove, and five marble-hosted Zn occurrences from the Grenville Supergroup of Ontario and Quebec. The diagrams illustrate the common features of these occurrences with marble compositions near dolomite (CaO/MgO=1.4) and variable but elevated contents of SiO_2. Compositions with CaO/MgO < 1 at Lime Hill and Meat Cove are serpentine-rich lithologies which have probably undergone some local removal of $CaCO_3$ during retrograde regional metamorphism.

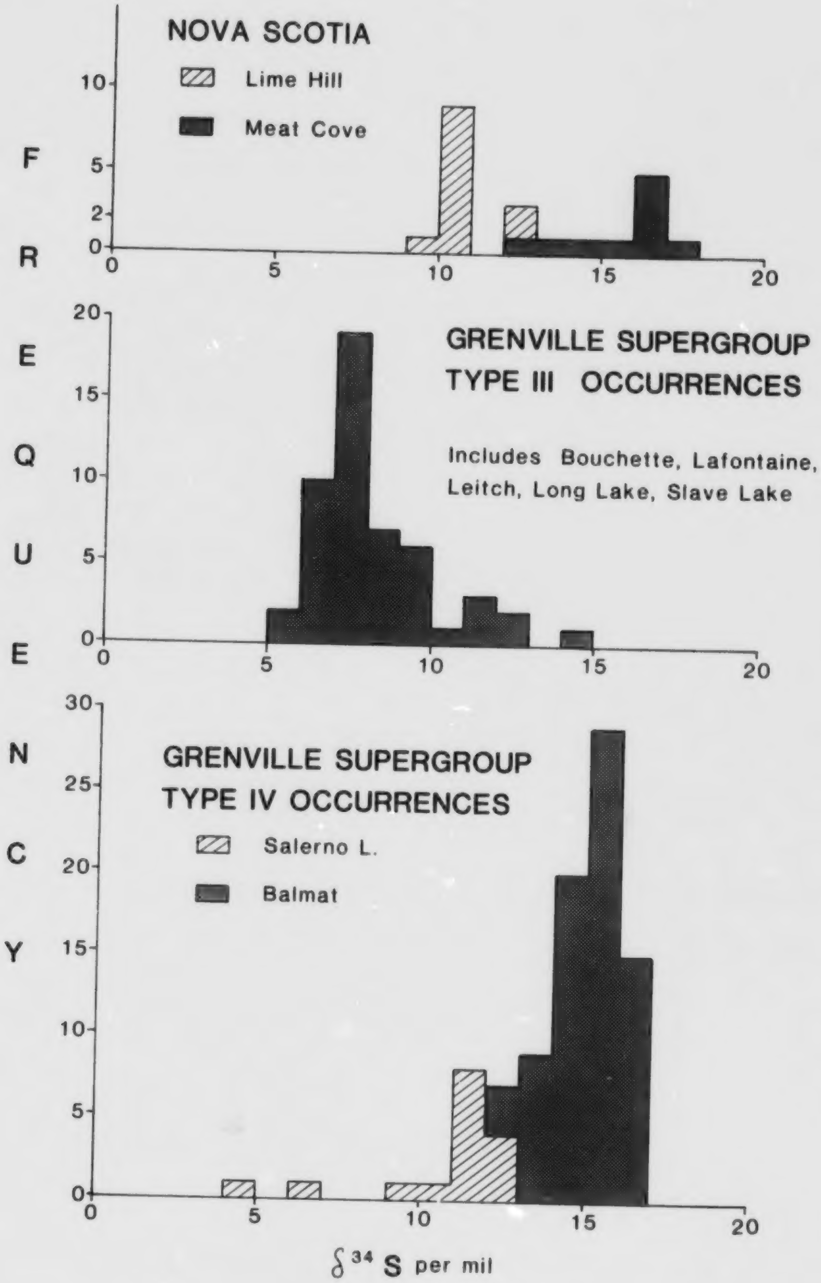

Figure 12. S isotopic compositions of sphalerite from the Lime Hill, Meat Cove, and Grenville Supergroup marble-hosted Zn occurrences. Balmat $\delta^{34}S$ data after Whelan et al., 1984.

LEAD ISOTOPIC ANALYSES

Lead isotopic analyses are reported here for galenas from the Lime Hill and Meat Cove zinc occurrences and for three small vein occurrences (Boisdale Hills, Mill Brook, West Bay Road; Fig. 1 and 2) that are associated with latest Precambrian to Early Cambrian granite (Barr and Setter, 1984; M. Justino in Raeside, 1990; P.A. Hunt and A.L. Sangster, unpublished data), which cuts the Middle to Late Proterozoic basement rocks (Appendix V). The lead isotopic compositions for the Lime Hill and Meat Cove galena samples are distinct but both are substantially less radiogenic than values obtained from other mineralization in Nova Scotia, including Late Proterozoic-Cambrian volcanogenic sulphides from the Stirling deposit (Miller, 1979) and mineralization interpreted as sedimentary exhalative within Cambro-Ordovician rocks of the Meguma Terrane at Eastville (Fig. 13). However, the Lime Hill and Meat Cove analyses resemble those obtained from Grenville Supergroup deposits of similar character. Galenas from base metal vein occurrences associated with Cambrian granite near West Bay Road and on Mill Brook (Fig. 2), near Lime Hill, and from the Rear Boisdale Pb-Zn-Ag occurrence (Ponsford and Lyttle, 1984) have a much more radiogenic signature and in this regard are isotopically dissimilar to lead from the Lime Hill and Meat Cove galenas.

DISCUSSION

The origin of the Nova Scotia deposits has been attributed to contact metasomatic processes (Keating, 1960; Chatterjee, 1977, 1979, 1980). On the other hand, deposits in Grenville Supergroup rocks that are similar geologically, geochemically, and isotopically (S, Pb) have been attributed to epigenetic and/or syngenetic processes (i.e. assigned to the Mississippi Valley-type or sedimentary exhalative classes) related to the development of large carbonate depositional basins (Uglow, 1916; Lea and Dill, 1968; Sangster, 1970; deLorraine and Dill, 1982; Sangster and Bourne, 1982; Whelan et al., 1984; Gauthier and Brown, 1986). The high-grade metamorphism that has affected the marble, and the contained mineralization, at Lime Hill and Meat Cove has eliminated the use of genetic criteria based largely on primary textures and structures. Skarn, sedimentary exhalative, and Mississippi Valley-type deposits are, however, significantly different in their major and trace element compositions, sulphur isotopic compositions of coexisting sulphides, and lead isotopic compositions of galenas.

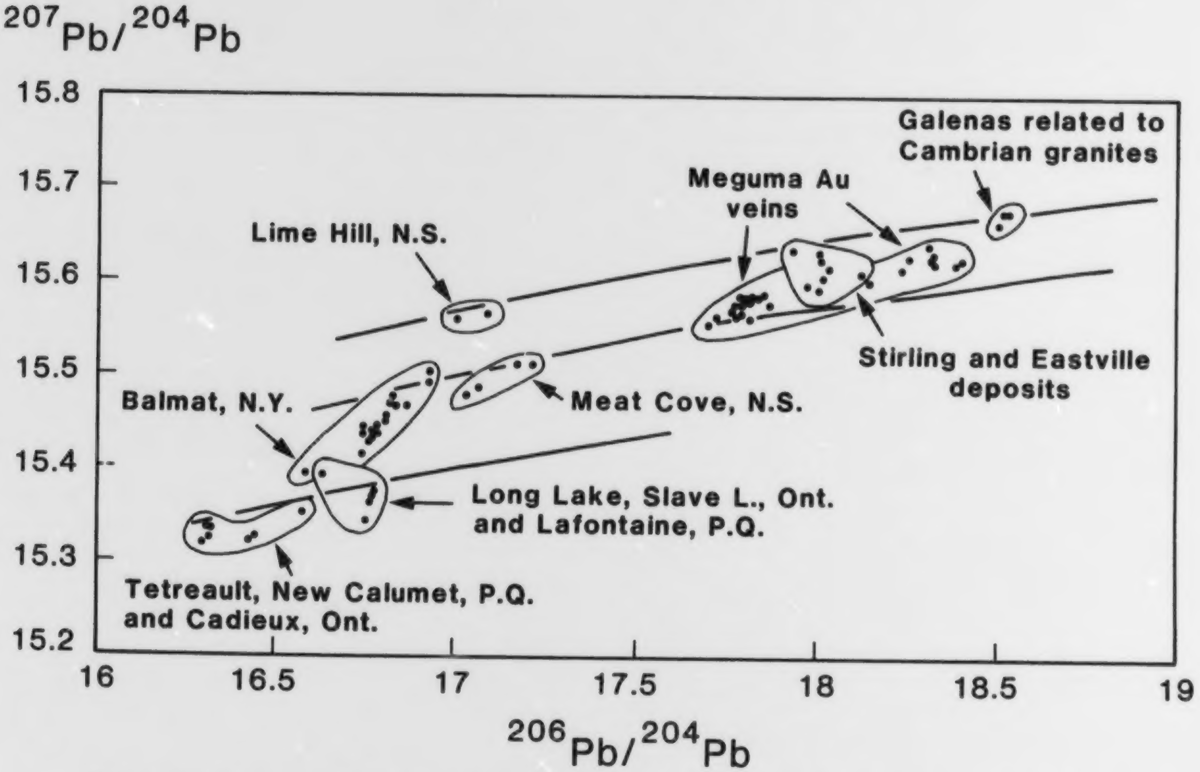

Figure 13. Pb isotopic compositions of galena from the Lime Hill and Meat Cove occurrences, Pb occurrences related to Cambrian intrusions, Grenville Supergroup marble-hosted Zn occurrences (after Fletcher, 1979; Fletcher and Farquhar, 1982a,b), and other selected Pb isotopic values (R. Thorpe, unpublished data) from Cambrian rocks elsewhere in Nova Scotia (Stirling massive sulphide, Bourinot Formation, southeast Cape Breton Island (Weeks, 1954; Miller, 1979); gold veins, Meguma Terrane (Malcolm, 1929; Sangster, 1990; some data from Farquhar and Haynes, 1986); and Eastville Zn-Pb occurrence (Binney et al., 1986)). Reference curves are, from bottom to top, the mantle, orogene, and upper crust growth curves of Zartman and Doe (1981).

Geochemistry

A consideration of the whole rock and trace element data provides an excellent basis for differentiation between various proposed genetic models for the highly metamorphosed Lime Hill and Meat Cove occurrences.

Skarn deposits are chemically distinct from sedimentary exhalative and Mississippi Valley-type deposits in two major characteristics:

1) First, Zn-Pb skarns are typically polymetallic deposits with Zn:Pb = 1:1 to 1:2 and Ag contents between 30 and 300 g/t (Einaudi et al., 1981). Einaudi et al. (1981) also indicated that the Ag-rich ores occur outside the zone of massive calc-silicate skarn and consequently low-grade calc-silicate rocks, such as are found at Lime Hill and Meat Cove, should be Ag- and Pb-rich with an essential sulphosalt mineralogy, i.e. with significant Cu, As, and Sb, and not depleted in these elements as is observed (Appendix I, II).

2) Zn-Pb skarn mineralization is characterized by the presence of hedenbergitic pyroxene with a significant (5 to 25 percent) mole percent content of johannsenite (Einaudi et al., 1981; Burton et al., 1982; Einaudi and Burt, 1982; Shimizu and Iiyama, 1982; Yun and Einaudi, 1982; Meinert, 1987). Whole rock analyses (Appendix I) and microprobe analyses of diopside, olivine, and serpentine in Table 2 indicate very low Mn contents in both rock and contained silicate minerals associated with the carbonate-hosted Zn mineralization. The low whole rock Mn contents and relatively pure diopside-forsterite compositions observed here are more appropriately explained as normal products of the regional metamorphism of siliceous dolomite (Deer et al., 1962; Winkler, 1979; Munyanyiwa and Hanson, 1988) than to contact-related metasomatic processes.

Table 2. Chemical analyses of silicate minerals associated with marble-hosted zinc mineralization, Lime Hill and Meat Cove, Nova Scotia. Lime Hill diopside analyses after Walker (1988), from Hill (1989).

	DIOPSIDE		OLIVINE		SERPENTINE	
	LIME HILL	MEAT COVE	LIME HILL	MEAT COVE	LIME HILL	MEAT COVE
n =	8	11	9	5	15	25
Na_2O	0.32	0.00	0.00	0.00	0.39	0.00
MgO	17.33	16.67	55.32	57.13	43.87	45.03
Al_2O_3	0.80	4.90	0.00	0.00	0.12	2.35
SiO_2	54.40	51.14	42.07	40.53	41.65	38.96
K_2O	0.01	0.08	0.00	0.00	0.00	0.01
CaO	25.90	25.96	0.00	0.00	0.02	0.04
TiO_2	0.13	0.19	0.00	0.00	0.05	0.07
Cr_2O_3	0.01	0.07	0.00	0.00	0.02	0.02
MnO	0.05	0.10	0.00	0.00	0.03	0.04
FeO	1.88	0.63	1.73	0.27	1.37	1.10
TOTAL	100.83	99.73	99.12	97.93	87.52	87.62
Hed/Fay	4.02	2.08	1.77	0.26	-	-
Joh/Kneb	0.15	0.33	0.00	0.00	-	-
Diop/For	95.83	97.59	98.23	99.74	-	-

Hed=hedenbergite; Joh=johannsenite; Diop=diopside; Fay=fayalite; Kneb=Knebelite; For=forsterite.

The distinction between sedimentary exhalative and Mississippi Valley-type deposits in unmetamorphosed rocks is based mainly on geological setting and gross form of the mineralization. Mississippi Valley-type deposits commonly occur in platform carbonate sequences peripheral to large sedimentary basins (Sangster, 1983, in press). Deposits occur preferentially in dolomitized limestone host rocks, with sphalerite and/or galena mineralization, controlled primarily by porosity developed during processes of dolomitization or brecciation, giving rise to submassive to broadly disseminated mineralized zones. Deposits, though commonly stratabound, are epigenetic and show well developed, crosscutting relationships both on local and deposit scales. Zn/Zn + Pb ratios in deposits are highly variable and average about 0.8. Deposits generally contain recoverable and elevated levels of Cd (Sangster, in press) and are variably enriched in Hg (Jolly and Heyl, 1968; Jonasson and Sangster, 1974), but are otherwise low in trace elements, such as As, Sb, Ag, Co, and Ni. Typical deposits or districts include Pine Point (Fritz and Jackson, 1972; Kyle, 1981), Gays River (Akande, 1982; Akande and Zentilli, 1983), Tri-state (Brockie et al., 1968; Hagni, 1976), and Cornwallis Island (Kerr, 1977). The Pb-rich end member districts are those containing the Old Lead Belt and New Lead Belt (Viburnum trend) (Snyder and Gerdemann, 1968). The pure Zn end member district is the East Tennessee district (Crawford and Hoagland, 1968; Hoagland, 1976).

Sedimentary exhalative deposits are polymetallic, syngenetic, and stratiform and are commonly composed of massive, well banded, or layered sulphides. These deposits occur in a variety of sedimentary lithologies in basinal sediments reflecting fault, rather than bedding-plane control on flow of the mineralizing fluid (Gustafson and Williams, 1981; Large, 1983; Sangster, in press). Examples of deposits in various host lithologies include Rammelsberg, Germany in black shale (Kraume et al., 1955; Sperling, 1980); Sullivan, British Columbia in quartzite and argillite (Freeze, 1966; Hamilton et al., 1983); Tynagh, Ireland in limestone and Silvermines, Ireland in dolomite and limestone (Evans, 1976); and Balmat, New York in dolomite with associated anhydrite (Whelan et al., 1984). The distribution of Zn/Zn + Pb values in sedimentary exhalative deposits in general is similar to that in Mississippi Valley-type deposits, but the pure Zn and Pb end member deposits are lacking (Sangster, in press). Sedimentary exhalative deposits are commonly Ag-rich (Gustafson and Williams, 1981; Lydon, 1983) and contain sufficient As, Sb, and Cu to support a sulphosalt mineralogy. Hg contents of sedimentary exhalative deposits are not well documented in the literature, but appear to be highly variable. Goodfellow et al. (1983) reported very low Hg, less than 150 ppb, in the Howards Pass deposit. Elevated Hg is reported in the Tom deposit (to 250 ppm — W. Goodfellow, pers. comm., 1989), and in the Balmat district (to 1190 ppm in sphalerite concentrates — Whelan et al., 1984). Hg is reported from many of the Irish deposits, including Gortdrum (Evans, 1976), Navan (Findlay et al., 1984), and Keel (Meyer and Evans, 1973).

Comparison of the Lime Hill and Meat Cove occurrences, on the basis of present knowledge, to sedimentary exhalative and Mississippi Valley-type deposits suggests that they may be more closely related to Mississippi Valley-type than to sedimentary exhalative deposits. The Nova Scotia occurrences contain mainly disseminated sulphides, not massive, banded sulphides as observed in most sedimentary exhalative deposits. Disaggregation of a massive sulphide body during metamorphism and deformation, to produce a disseminated deposit, is considered unlikely, suggesting that the disseminated character of the Lime Hill and Meat Cove mineralization reflects a disseminated protolith. Consequently, the Lime Hill and Meat Cove occurrences are probably most closely related to epigenetic Mississippi Valley-type deposits. This conclusion is dependent to some extent on the nature and character of the metamorphic deformation and recrystallization. Mineralization at both occurrences shows variations in grade parallel to lithological contacts. Unfortunately, there is not sufficient exposure at either occurrence to determine whether this apparent stratigraphic control is real or a product of transposition of various other mineralized structures into conformity with the foliation.

An accurate comparison of the compositions of the marble-hosted occurrences of Nova Scotia (analyses presented in Appendix I, II) and Mississippi Valley-type deposits is hampered by a lack of whole rock ore analyses for Mississippi Valley-type deposits in the literature. Abundant mineral analyses and lithological descriptions allow a general comparison. The marble-hosted zinc mineralization is characterized by dolomitic host rocks, which is characteristic of Mississippi Valley-type deposits. The SiO_2 enrichment and low contents of Al_2O_3, Na_2O, and K_2O is compatible with disseminated, hydrothermal silica enrichment which is documented to have occurred in some Mississippi Valley-type deposits (Grogan and Bradbury, 1968; Snyder and Gerdemann, 1968). The observed presence of Cd and Hg, with variable but low Pb contents and the presence of other minor trace elements such as Ag, As, Sb, Au, Bi, Mo, Co, and Ni are typical of many Mississippi Valley-type deposits and a few sedimentary exhalative deposits. From these data, it might be concluded that the Lime Hill and Meat Cove deposits were deposited from Mississippi Valley-type carbonate basin brines. The disseminated nature of most mineralization suggests that the protolith was most probably of the epigenetic Mississippi Valley-type. However, the presence of layer-parallel massive sulphides, particularly at Lime Hill, does not permit the elimination of the sedimentary exhalative model as a possible alternative until better quality exposure is available.

Sulphur isotope results

The isotopic composition of sulphide sulphur constrains models for the origin of sulphide mineral deposits and occurrences (Taylor, 1987). Intrusions with mantle-derived sulphur typically have isotopic compositions near 0 ‰ and associated deposits commonly contain sulphur ranging from +5 to -5 ‰, except where large quantities of sulphur have been assimilated from the wall rocks. Seawater sulphate is heavy and has varied in composition throughout post-Archean time from a high of +35 ‰ in the Cambrian to a low of +11 ‰ in the Permo-Triassic (Claypool et al., 1980). Proterozoic seawater sulphate may have been quite constant in composition at about +15 ‰ (Claypool et al., 1980; A.L. Sangster, unpublished data, Grenville Supergroup). Deposits hosted by sedimentary rocks and containing sulphur that is isotopically heavy, commonly ranging between +10 and +30 ‰, are generally believed to have obtained their sulphur from reduction of seawater sulphate either directly or via deposition from closed-system brines in which ^{34}S is enriched beyond levels encountered in normal seawater. A compilation by Sangster (in press) indicates that the isotopic composition of both sedimentary exhalative and Mississippi Valley-type deposits have averaged about 15 ‰ below the composition of contemporaneous seawater. Normal biogenic reduction of seawater sulphate in an organic-rich environment, such as commonly occurs diagenetically in black shales, results in sulphide sulphur with an isotopic composition of 40 +/−25 ‰ less than seawater sulphate (Ohmoto et al., in press).

The heavy sulphur isotopic signature of the Lime Hill and Meat Cove marble-hosted sphalerite is similar to that of sphalerite from Type IV marble-hosted deposits in the Grenville Supergroup (Fig. 12). The sulphur in Meat Cove sphalerite (12.4 to 17.5 ‰; avg. 15.6 ‰, Appendix IV) is isotopically similar to sulphur from the much larger Balmat, New York deposits. There, composite sphalerite samples representing most ore zones and mineralization types average 12.5 to 14.7 ‰, with an overall range from 11.3 to 17.5 ‰ for individual samples in the Fowler orebody (Whelan et al., 1984). The sulphur in Lime Hill sphalerite (9.5 to 12.2 ‰; avg. 10.8 ‰) is similar to that in most samples of Salerno Lake sphalerite (9.7 to 12.6 ‰; avg. 11.7 ‰; excluding two samples at 4.4 and 6.4 ‰).

This heavy isotopic signature is very different from $\delta^{34}S$ values for various types of skarn deposits. A compilation of skarn $\delta^{34}S$ values (Taylor, 1987) shows that the average isotopic composition of most skarn sulphur is between −5 and +10 ‰ and that average values for four Zn-Pb-Ag districts are in the range −5 to +4 ‰. In most cases these values reflect the composition of sulphur from a magmatic source, with variable additional contributions of sulphur from the host rocks at some sites.

Sparse data suggest that the isotopic composition of Middle to Late Proterozoic seawater sulphate was probably between +15 and +20 ‰ (Claypool et al., 1980; A.L. Sangster, unpublished data). The similarity of the Meat Cove and slightly lower Lime Hill $\delta^{34}S$ values to those roughly established for contemporaneous seawater sulphate suggests that the sphalerite was deposited from fluids exhaled into a closed-system brine pool where seawater sulphate was enriched in ^{34}S.

In a detailed study of the Balmat deposits, Whelan et al. (1984) interpreted similar values, in marble believed to be of similar age to those being considered here (Sangster and Thorpe, 1988), to be a product of deposition of the sphalerite from Mississippi Valley-type basin brines exhaled onto the seafloor. This is in contrast to the introduction of these brines into structural traps such as is responsible for Mississippi Valley, East Tennessee, Pine Point, and similar deposits.

Lead isotope results

A strong similarity between the array of lead isotopic compositions exhibited by base metal and marble-hosted zinc occurrences in the Grenville Supergroup and the Lime Hill and Meat Cove occurrences is evident in Figure 13. Analyses from the New Calumet and Tetreault volcanogenic deposits and the Cadieux marble-hosted deposit (Fletcher and Farquhar, 1982a) are the most primitive and lie on the mantle curve of Zartman and Doe (1981). This is compatible with a syndepositional origin for these deposits (Sangster, 1967, 1970) with lead being derived from material newly differentiated from the mantle at the time of sedimentation and ore formation (Fletcher and Farquhar, 1982a). The linear array of Balmat ratios is interpreted (Fletcher and Farquhar, 1982b) to reflect contributions of lead to the ore fluid from two sources, one of which is compositionally similar to that which supplied the lead with a mantle character in the stratabound deposits, and a second possibly derived from upper crustal terranes with more radiogenic lead. This model is in turn compatible with a sedimentary exhalative origin for the Balmat deposit from Mississippi Valley-type brines, as proposed by Whelan et al. (1984). The scatter along the mixing line is interpreted to reflect the continuously evolving basin-brine leaching system with associated variations in the contribution of mantle and crustally derived lead to the brine (Fletcher and Farquhar, 1982b).

The Meat Cove lead plots near the radiogenic end of the Balmat cluster but samples are slightly richer in ^{206}Pb. Replicate analyses of these galenas indicate significant inhomogeneity (Appendix V) and this could reflect a small lead contribution from the Lowland Brook syenite, which hosts the marble xenolith containing the zinc mineralization. Alternatively, the analyzed galena may have been formed from trace lead in the sedimentary rocks at the time of intrusion of the Lowland Brook syenite and therefore may be slightly younger than the zinc deposit. In either case, the Meat Cove lead isotopic compositions indicate a Grenville age and are compatible with a sedimentary exhalative origin for the deposit similar to that attributed to the deposits hosted by Grenville Supergroup marble. This age and origin can be accommodated by assigning the marble xenolith to Grenville Supergroup equivalent rocks, deposited after 1300 Ma, but younger than the 1040 Ma metamorphic age of the Lowland Brook syenite (Barr et al., 1987b). This interpretation requires a reassessment of the 1500 to 1100 Ma intrusive age attributed to the syenite (Barr et al., 1987b) to perhaps 1300 to 1100 Ga. This may, in fact, be implied from the limited scatter of analytical values presented by Barr et al. (1987b, Fig. 3). The lead isotopic ratios of the Lime Hill galenas also cluster with the Grenville Supergroup galenas. The Lime Hill galena has a more radiogenic composition, but this lies on the same mixing line as the Balmat galenas and closer to the crustal curve of Zartman and Doe (1981). This suggests that the Lime Hill galena formed at about the same time as the Balmat galena from a lead source with a composition approximating that of the radiogenic end member of the Balmat trend.

The lead isotopic analyses presented here are in agreement with proposed origins for the Grenville deposits from sedimentary exhalative brines (Lea and Dill, 1968; Sangster, 1970; deLorraine and Dill, 1982; Sangster and Bourne, 1982) which derived most of their metal content from sedimentary components within the basins in which they were deposited (Whelan et al., 1984). The attribution of a contact metasomatic origin to the Lime Hill deposit (Chatterjee, 1980) is discounted on the basis of the much more radiogenic composition of lead from vein galenas from occurrences at Rear Boisdale, West Bay Road, and Mill Brook that are known to be associated with late Precambrian-Cambrian intrusions.

SUMMARY AND CONCLUSIONS

The new data presented here on the Lime Hill and Meat Cove deposits suggests that they are metamorphosed Mississippi Valley-type or sedimentary exhalative deposits formed from Mississippi Valley-type basin brines. The evidence for this is as follows:

1) The presence of thin beds of disseminated and massive sulphides paralleling lithological layering in the marble suggests that a sedimentary exhalative model may be applicable to these deposits. However, the widespread occurrence of disseminated mineralization at Meat Cove, and to a lesser extent at Lime Hill, may reflect metamorphosed disseminated epigenetic mineralization in carbonate rocks with structurally transposed layering.

2) The moderate concentrations of SiO_2 and low concentrations of Al_2O_3, Na_2O, K_2O, and MnO within the host rock, the sphalerite-rich character of the mineralization, and the generally low levels of most trace elements in the mineralization, are all similar to chemical patterns attributed to Mississippi Valley-type deposits formed from brines generated within carbonate basins. These characteristics differ from those typical of contact metasomatic skarn deposits. The Cape Breton Island occurrences are close geological and geochemical analogues of the Grenville Supergroup occurrences, but contain much less massive mineralization than is seen in the Grenville occurrences.

3) The sulphur isotopic compositions of sphalerite are similar to those recorded for sedimentary exhalative/Mississippi Valley-type deposits and also similar to those for Grenville Supergroup deposits of similar age that have been described as sedimentary exhalative, possibly deposited from basinal brines (Whelan et al., 1984; Gauthier and Brown, 1986).

4) The similarity of the galena compositions at Lime Hill and Meat Cove, adjacent to intrusions of vastly different age, and the much more radiogenic nature of the lead in galenas from veins in the region that are believed to be associated with Cambrian intrusions, a) indicate that, contrary to previous suggestions, the Cambrian intrusions were not the source of the mineralizing fluids, and b) confirms the genetic importance of the association of the deposits with carbonate basins and brines derived from these basins.

SIGNIFICANCE FOR MINERAL EXPLORATION

Carbonate rocks and marble are widespread in the Precambrian rocks on Cape Breton Island, commonly referred to as the George River Group (Hill, 1990). It has been recognized recently that these rocks are of several different ages (Hill, 1990) from Grenville (Barr et al., 1987b) to possibly Silurian (Jamieson et al., 1990; Dunning et al., in press). The mineralized dolomite marble at Meat Cove is the oldest of these and may correlate with rocks of different metamorphic character at Lime Hill (Sangster and Thorpe, 1988) and possibly Kellys Mountain (Jamieson, 1984). They probably do not correlate with carbonate rocks of very different character in the Creignish Hills, at North Mountain, and in the Boisdale Hills(?), with the exception that they could be age equivalent to marble in small areas of higher grade gneiss recently documented to constitute basement to those rocks (black in Fig. 1). Exploration for deposits similar to Lime Hill and Meat Cove, following the model presented here, should be restricted to these limited areas of gneiss interpreted as basement to the George River Group.

The revised mineral deposit model proposed here has important implications for exploration within the known mineralized areas and elsewhere. The intensity of metamorphism and deformation suggests that better grade mineralization will be structurally controlled, probably occurring within the hinges of folds and healing syndeformation faults, as has been described at Balmat (deLorraine and Dill, 1982). Structural mapping and drilling for "pencil-shaped" sulphide lenses in folds parallel to the regional lineation will probably be the most effective method of exploration.

ACKNOWLEDGMENTS

This paper is a product of a complex division of effort carried out over the last several years. The Lime Hill property was mapped by Mario Justino as part of an M.Sc. thesis project at Acadia University on the plutonic history of North Mountain. Evelyn Inglis completed an excellent compilation of previous work, documented the sources of information and available drill core, and assisted the senior author in the detailed mapping of trenches. Able field assistance was also provided by Kevin Jones and 'Sandy' Sears during the summers of 1985 and 1986. We gratefully acknowledge continuing constructive dialogue with Sandra Barr and Rob Raeside of Acadia University and Jim Patterson and Ken Northcote of the Nova Scotia Department of Mines and Energy. We also thank Michel Gauthier of the Université de Québec à Montréal, Marcos Zentilli of Dalhousie University, and Jim Franklin of the Geological Survey of Canada for reviewing the manuscript. We acknowledge the contribution of Richard C.J. Edwards and Charlie Pegg of Bluestack Resources for their interest in the Lime Hill part of the project, expressed in their recutting of an old exploration survey grid to allow more controlled mapping of the property than would otherwise have been possible. Also, we express our deepest thanks to Mr. and Mrs. Robert Campbell of Malagawatch for their hospitality during our work at Lime Hill and to Mr. and Mrs. MacDonald of Lime Hill who kindly allowed us to use their front lawn as a parking lot during the course of the work.

REFERENCES

Akande, S.O.
1982: Genesis of the lead-zinc mineralization at Gays River, Nova Scotia, Canada: a geologic, fluid inclusion, and stable isotopic study; Ph.D. thesis, Dalhousie University, Halifax, Nova Scotia, 348 p.

Akande S.O. and Zentilli, M.
1983: Genesis of lead-zinc mineralization at Gays River, Nova Scotia, Canada; *in* International Conference on Mississippi-Valley type lead-zinc deposits (Proceedings Volume), edited by G. Kisvarsanyi, S.K. Grant, W.P. Pratt, and J.W. Koenig, University of Missouri, Rolla, Missouri, p. 403-414.

Alcock, F.J.
1930: Zinc and lead deposits of Canada; Geological Survey of Canada, Economic Geology Series no. 8, 406 p.

Barr, S.M. and Raeside, R.P.
1986: Pre-Carboniferous tectonostratigraphic subdivisions of Cape Breton Island, Nova Scotia; Maritime Sediments and Atlantic Geology, v. 22, p. 252-263.
1989: Tectono-stratigraphic terranes in Cape Breton Island, Nova Scotia: implications for the configuration of the northern Appalachian Orogen; Geology, v. 17, p. 822-825.

Barr, S.M. and Setter, J.R.D.
1984: Petrology of granitoid rocks of the Boisdale Peninsula, central Cape Breton Island, Nova Scotia; Nova Scotia Department of Mines and Energy, Paper 84-1, 75 p.

Barr, S.M., Raeside, R.P., and Jamieson, R.A.
1987a: Geology of the igneous and metamorphic rocks of northern Cape Breton Island, Nova Scotia; Geological Survey of Canada, Open File 1594, 6 maps, scale 1:50 000.

Barr, S.M., Raeside, R.P., and van Breemen, O.
1987b: Grenvillian basement in the northern Cape Breton Highlands; Canadian Journal of Earth Sciences, v. 24, p. 992-997.

Bernier, L., Pouliot, G., and MacLean, W.H.
1987: Geology and metamorphism of the Montauban north gold zone: a metamorphosed polymetallic exhalative deposit, Grenville Province, Quebec; Economic Geology, v. 82, p. 2076-2090.

Binney, W.P., Jenner, K.A., Sangster, A.L., and Zentilli, M.
1986: A stratabound zinc-lead deposit in the Meguma Group metasediments at Eastville, Nova Scotia; Maritime Sediments and Atlantic Geology, v. 22, p. 65-88.

Brockie, D.C., Hare, E.H., and Dingess, P.R.
1968: The geology and ore deposits of the Tri-state district of Missouri, Kansas and Oklahoma; *in* Ore Deposits of the United States, 1933-1937, edited by J.D. Ridge, American Institute of Mining Engineers, p. 401-430.

Burton, J.C., Taylor, L.A., and Chou, I-M.
1982: The fO_2-T and fS_2-T stability relations of hedenbergite and hedenbergite-johannsenite solid solution; Economic Geology, v. 77, p. 764-783.

Carter, T.R.
1984: Metallogeny of the Grenville Province, southeastern Ontario; Ontario Geological Survey, Open File Report 5515, 422 p.

Carter, T.R., Colvine, A.C., and Meyn, H.D.
1979: The geology of base metal, iron and molybdenum deposits in the Pembroke-Renfrew area; Ontario Geological Survey, Open File Report 5275, 349 p.

Chatterjee, A.K.
1977: Tungsten mineralization in the carbonate rocks of the George River Group, Cape Breton Island; Nova Scotia Department of Mines and Energy, Paper 77-7, 26 p.
1979: Geology of the Meat Cove zinc deposit, Cape Breton Island, Nova Scotia; Nova Scotia Department of Mines and Energy, Paper 79-3, 27 p.
1980: Mineralization and associated wallrock alteration in the George River Group, Cape Breton Island, Nova Scotia; Ph.D. thesis, Dalhousie University, Halifax, Nova Scotia, 197 p.

Claypool, G.E., Holser, W.T., Kaplan, I.R., Sakai, H., and Zak, I.
1980: The age curves of sulphur and oxygen isotopes in marine sulphate and their mutual interpretation; Chemical Geology, v. 28, p. 199-260.

Cormier, R.F.
1972: Radiometric ages of granitic rocks, Cape Breton Isand, Nova Scotia; Canadian Journal of Earth Sciences, v. 9, p. 1074-1086.

Crawford, J. and Hoagland, A.D.
1968: The Mascot-Jefferson City zinc district, Tennessee; *in* Ore Deposits of the United States, 1933-1967, edited by J.D. Ridge, American Institute of Mining Engineers, p. 242-256.

Deer, W.A., Howie, R.A., and Zussman, J.
1962: Rock Forming Minerals, Volume 2, Chain Silicates; Longmans, London, 379 p.

deLorraine, W.F. and Dill, D.B.
1982: Structure, stratigraphic controls, and genesis of the Balmat zinc deposits, northwest Adirondacks, New York; *in* Precambrian Sulphide Deposits, edited by R.W. Hutchinson, C.D. Spence, and J.M. Franklin, Geological Association of Canada, Special Paper 25, p. 571-596.

Donohoe, H.V. and Cullen, M.
1983: Deformation, age and regional correlation of the Mount Thom and Bass River complexes, Cobequid Highlands, Nova Scotia; *in* Abstracts with Program, Geological Society of America, Northeastern Section, v. 15, no. 3.

Donohoe, H.V. and Wallace, P.I.
1983: Geological Map of the Cobequid Highlands (4 sheets); Nova Scotia Department of Mines and Energy, Maps 82-06 to -09.

Dunning, G.R. and O'Brien, S.J.
1989: Late Proterozoic-early Paleozoic crust in the Hermitage flexure, Newfoundland Appalachians: U/Pb ages and tectonic significance; Geology, v. 17, p. 548-551.

Dunning, G.R., Barr, S.M., Raeside, R.P., and Jamieson, R.A.
in press: U-Pb zircon, titanite, and monazite ages in the Bras D'Or and Aspy terranes, Cape Breton Island, Nova Scotia: implications for igneous and metamorphic history; Geological Society of America Bulletin.

Easton, R.M. and Bartlett, J.R.
1984: Precambrian geology, Howland area; Ontario Geological Survey, Preliminary Map P-02699.

Einaudi, M.T. and Burt, D.M.
1982: Introduction — Terminology, classification and composition of skarn deposits; Economic Geology, v. 77, p. 745-754.

Einaudi, M.T., Meinert, L.D., and Newberry, R.J.
1981: Skarn deposits; *in* Seventy-Fifth Anniversary Volume, 1905-1980, edited by B.J. Skinner, Society of Economic Geologists, p. 317-391.

Energy, Mines and Resources
1986: Canadian mineral deposits not being mined in 1983; Energy, Mines and Resources Canada, Mineral Bulletin MR 213, 308 p.

Evans, A.M.
1976: Genesis of Irish base-metal deposits; *in* Handbook of Stratabound and Stratiform Sulphide Deposits, v. 5, Regional Studies, edited by K.H. Wolf, Elsevier, Amsterdam, p. 231-256.

Farquhar, R.M. and Haynes, S.J.
1986: Lead isotope data for gold-bearing veins and their host metasedimentary rocks of the Goldenville Formation, eastern Nova Scotia; Maritime Sediments and Atlantic Geology, v. 22, p. 89-100.

Findlay, S., Romer, D.M., and Cazalet, P.C.D.
1984: Lithogeochemical studies around the Navan Zn-Pb orebody, Ireland; *in* Prospecting in Areas of Glaciated Terrain, Institution of Mining and Metallurgy, p. 35-56.

Fletcher, H.
1881: Report on the Richmond, Inverness, Guysborough, and Antigonish counties, Nova Scotia; Geological Survey of Canada, Report of Progress, pt. F, 125 p.

Fletcher, I.R.
1979: A lead isotope study of lead-zinc mineralization associated with the Central Metasedimentary Belt of the Grenville Province; Ph.D. thesis, University of Toronto, Toronto, Ontario, 165 p.

Fletcher, I.R. and Farquhar, R.M.
1982a: Lead isotopic compositions of Balmat ores and their genetic implications; Economic Geology, v. 77, p. 664-673.
1982b: The protocontinental nature and regional variability of the Central Metasedimentary Belt of the Grenville Province: lead isotopic evidence; Canadian Journal of Earth Sciences, v. 19, p. 239-253.

Freeze, A.C.
1966: On the origin of the Sullivan orebody, Kimberly, B.C.; *in* Tectonic History and Mineral Deposits of the Western Cordillera, Canadian Institute of Mining and Metallurgy, Special Volume 8, p. 263-294.

Fritz, P. and Jackson, S.A.
1972: Geochemical and isotopic characteristics of Middle Devonian dolomites from Pine Point, northern Canada; 24th International Geological Congress, 1972, section 6, p. 230-242.

Gauthier, M. and Brown, A.C.
1986: Zinc and iron metallogeny in the Maniwaki-Gracefield district, southwestern Quebec; Economic Geology, v. 81, p. 89-112.

Goodfellow, W.D., Jonasson, I.R., and Morganti, J.M.
1983: Zonation of chalcophile elements about the Howards Pass (XY) Zn-Pb deposit, Selwyn Basin, Yukon; Journal of Geochemical Exploration, v. 19, p. 503-542.

Grogan, R.M. and Bradbury, J.C.
1968: Fluorite-lead-zinc deposits of the Illinois-Kentucky mining district; *in* Ore Deposits of the United States, 1933-1967, edited by J.D. Ridge, American Institute of Mining Engineers, p. 371-400.

Guernsey, T.D.
1928: Geology of the North Mountain, Cape Breton; Geological Survey of Canada, Summary Report 1927, p. 47-82.

Gustafson, L.B. and Williams, N.
1981: Sediment-hosted stratiform deposits of copper, lead and zinc; *in* Seventy-Fifth Anniversary Volume, 1905-1980, edited by B.J. Skinner, Society of Economic Geologists, p. 139-178.

Hagni, R.D.
1976: Tri-state ore deposits: the character of their host rocks and their genesis; *in* Handbook of Stratabound and Stratiform Ore Deposits, v. 6, edited by K.H. Wolf, Elsevier, Amsterdam, p. 462-491.

Hamilton, J.M., Delaney, G.D., Hauser, R.L., and Ransom, P.W.
1983: Geology of the Sulivan deposit, Kimberley, B.C., Canada; *in* Short Course in Sediment-Hosted Stratiform Lead-Zinc Deposits, edited by D.F. Sangster, Mineralogical Association of Canada, p. 31-83.

Hill, J.R.
1987: Geology and geochemistry of Precambrian carbonate rocks, Cape Breton Island, Nova Scotia; Geological Survey of Canada, Open File 1597.
1988: Geochemical differentiation of Precambrian metacarbonate assemblages, Cape Breton Island, Nova Scotia; *in* Current Research, Part B, Geological Survey of Canada, Paper 88-1B, P. 173-185.
1989: Follow-up geology and geochemistry of metacarbonate formations and their contained mineral occurrences, Cape Breton Island, Nova Scotia; Geological Survey of Canada, Open File 2077, 43 p.
1990: A geological and geochemical study of metacarbonate rocks and contained mineral deposits, Cape Breton Island, Nova Scotia; *in* Mineral Deposit Studies in Nova Scotia, Volume 1, edited by A.L. Sangster, Geological Survey of Canada, Paper 90-8, p. 3-29.

Hoagland, A.D.

1976: Appalachian zinc-lead deposits; *in* Handbook of Stratabound and Stratiform Ore Deposits, v. 6, edited by K.H. Wolf, Elsevier, Amsterdam, p. 495-534.

Jamieson, R.A.

1984: Low pressure cordierite-bearing migmatites from Kellys Mountain, Nova Scotia; Contributions to Mineralogy and Petrology, v. 86, p. 309-320.

Jamieson, R.A., Tallman, P.C., Plint, H.E., and Connors, K.A.

1990: Regional geological setting of pre-Carboniferous mineral deposits in the western Cape Breton Highlands, Nova Scotia; *in* Mineral Deposit Studies in Nova Scotia, Volume 1, edited by A.L. Sangster, Geological Survey of Canada, Paper 90-8, p. **-**.

Jolly, J.L. and Heyl, A.V.

1968: Mercury and other trace elements in sphalerite and wallrocks from central Kentucky, Tennessee and Appalachian zinc districts; United States Geological Survey, Bulletin 1252-F, 29 p.

Jonasson, I.R. and Sangster, D.F.

1974: Variations in the mercury content of sphalerite from some Canadian sulphide deposits; *in* Geochemical Exploration '74, Proceedings, 5th International Symposium on Geochemical Exploration, Vancouver, edited by J.L. Elliot, Elsevier, Amsterdam, p. 313-332.

Justino, M.F.

1985: Geology and petrogenesis of the plutonic rocks of North Mountain, Cape Breton Island; Nova Scotia Department of Mines and Energy, Information Series, v. 9, p. 111.

Justino, M.F. and Sangster, A.L.

1987: Geology in the vicinity of the Lime Hill zinc occurrence, southwestern Cape Breton Island, Nova Scotia; *in* Current Research, Part A, Geological Survey of Canada, Paper 87-1A, p. 555-561.

Keating, B.J.

1960: Massive sulphide deposits in Ontario; Canadian Institute of Mining and Metallurgy Bulletin, no. 564, p. 81-87.

Kelly, D.G.

1967: Baddeck and Whycocomagh map areas; Geological Survey of Canada, Memoir 351, 65 p.

Kerr, J.W.

1977: Cornwallis Lead Zinc District; Canadian Journal of Earth Science, v. 14, p. 1402-1426.

Kraume, E., Dahlgrun, F., Ramdohr, P., and Wilke, A.

1955: Die Erzlager des Rammelsberges bei Goslar; Monographien der Deutschen Blei-Zink-Erzlagerstatten, Beihefte zum Geologischen Jahrbuch, v. 18, 394 p.

Kyle, J.R.

1981: Geology of the Pine Point lead-zinc district; *in* Handbook of Stratabound and Stratiform Ore Deposits, v. 9, edited by K.H. Wolf, Elsevier, Amsterdam, p. 709-741.

Large, D.E.

1983: Sediment-hosted massive sulphide lead-zinc deposits: an empirical model; in Short Course in Sediment-Hosted Stratiform Lead-Zinc Deposits, edited by D.F. Sangster, Mineralogical Association of Canada, p. 1-29.

Lea, E.R. and Dill, D.B.

1968: Zinc deposits of the Balmat-Edwards district, New York; *in* Ore Deposits of the United States, 1933-1967, edited by J.D. Ridge, American Institute of Mining Engineers, p. 20-48.

Lydon, J.W.

1983: Chemical parameters controlling the origin and deposition of sediment-hosted stratiform lead-zinc deposits; *in* Short Course in Sediment-Hosted Stratiform Lead-Zinc Deposits, edited by D.F. Sangster, Mineralogical Association of Canada, p. 175-245.

Malcolm, W.

1929: Gold fields of Nova Scotia; Geological Survey of Canada, Memoir 156, 253 p.

Malczak, J., Carter, J.R., and Springer, J.S.

1985: Base metal, molybdenum, and precious metal deposits of the Madoc-Sharbot Lake area, southeastern Ontario; Ontario Geological Survey, Open File Report 5548, 374 p.

Meinert, L.D.

1987: Skarn zonation and fluid evolution in the Groundhog mine, Central Mining District, New Mexico; Economic Geology, v. 82, p. 523-545.

Meyer, W.T. and Evans, D.S.

1973: Dispersion of mercury and associated elements in a glacial drift environment at Keel, Eire; *in* Proceedings Volume, Prospecting in Areas of Glaciated Terrain, Trondheim, Norway, Institution of Mining and Metallurgy, London, p. 127-138.

Miller, C.K.

1979: The geologic setting and environment of ore deposition at the Mindamar mine, Stirling, Richmond County, Nova Scotia; M.Sc. thesis, Dalhousie University, Halifax, Nova Scotia, 223 p.

Milligan, G.C.

1970: Geology of the George River Series, Cape Breton; Nova Scotia Department of Mines and Energy, Memoir 7, 111 p.

Munyanyiwa, H. and Hanson, R.E.

1988: Geochemistry of marbles and calc-silicate rocks in the pan-African Zambesie belt, Zambia; Precambrian Research, v. 38, p. 177-200.

Neale, E.R.W.

1964: Geology, Cape St. Lawrence, Cape Breton Island, Nova Scotia; Geological Survey of Canada, Map 1149A.

O'Brien, S.J., Wardle, R.J., and King, A.F.

1983: The Avalon Zone: a pan-African terrane in the Appalachian orogen of Canada; Geological Journal, v. 18, p. 195-222.

Ohmoto, H., Kaiser, C.J., and Geer, K.A.

in press: Systematics of sulphur isotopes in recent marine sediments and ancient sediment-hosted base metal deposits; *in* International Conference on Stable Isotopes and Fluid Processes in Mineralization, Proceedings, Geological Society of Australia, Special Publication.

Olszewski, W.J., Gaudette, H.E., Keppie, J.D., and Donohoe, H.V.

1981: Rb-Sr whole rock age of the Kellys Mountain basement complex, Cape Breton Island; Geological Society of America, Abstracts with Program, v. 13, p. 169.

Ponsford, M. and Lyttle, N.A.

1984: Metallic mineral occurrences map and data compilation, eastern Nova Scotia - map sheets 11F, 11G, 11J, 11K, 11N; Nova Scotia Department of Mines and Energy, Open File Report 600.

Raeside, R.P.

1989: The Lime Hill gneiss - a basement fragment in the Bras d'Or Zone of Cape Breton Island; Geological Survey of Canada, Open File 1998, 45 p.

1990: Low-pressure metamorphism of the Lime Hill gneissic complex, Bras D'Or Terrane, Cape Breton Island, Nova Scotia; *in* Mineral Deposit Studies in Nova Scotia, Volume 1, edited by A.L. Sangster, Geological Survey of Canada, Paper 90-8, p. 67-76.

Raeside, R.P., Barr, S.M., White, C.E., and Dennis, F.A.R.

1986: Geology of the northernmost Cape Breton Highlands, Nova Scotia; *in* Current Research, Part A, Geological Survey of Canada, Paper 86-1A, p. 291-296.

Sangster, A.L.

1967: Metamorphism of the New Calumet sulphide deposit, Quebec; M.Sc. thesis, Carleton University, Ottawa, Ontario, 142 p.

1970: Metallogeny of base metal, gold and iron deposits of the Grenville Province of southeastern Ontario; Ph.D. thesis, Queen's University, Kingston, Ontario, 356 p.

1990: Metallogeny of the Meguma Terrane; *in* Mineral Deposit Studies in Nova Scotia, Volume 1, edited by A.L. Sangster, Geological Survey of Canada, Paper 90-8, p. 115-162.

Sangster, A.L. and Bourne, J.

1982: Geology of the Grenville Province and regional metallogenesis of the Grenville Supergroup; *in* Precambrian Sulphide Deposits, edited by R.W. Hutchinson, C.D. Spence, and J.M. Franklin, Geological Association of Canada, Special Paper 25, p. 91-126.

Sangster, A.L. and Thorpe, R.I.

1988: Sulphur and lead isotopic studies on two Grenville-type, marble-hosted zinc occurrences, Cape Breton, Nova Scotia; *in* Abstracts with Programs, 1988, Geological Society of America, v. 20, no. 1, p. 67.

Sangster, D.F.
1983: Mississippi Valley-type deposits: a geological melange; *in* International Conference on Mississippi-Valley Type Lead-Zinc Deposits (Proceedings Volume), edited by G. Kisvarsanyi, S.K. Grant, W.P. Pratt, and J.W. Koenig, University of Missouri, Rolla, Missouri, p. 7-19.
in press: MVT and SEDEX lead-zinc deposits: a comparative examination; Institute of Mining and Metallurgy.

Shimizu, M. and Iiyama, J.T.
1982: Zinc-lead skarn deposits of the Nakatatsu mine, central Japan; Economic Geology, v. 77, p. 1000-1012.

Smith, P.K. and Macdonald, A.S.
1981: The Fisset Brook Formation at Lowland Cove, Inverness County, Nova Scotia; Nova Scotia Department of Mines and Energy, Paper 81-1, 18 p.

Snyder, F.G. and Gerdemann, P.E.
1968: Geology of the southeast Missouri lead district; *in* Ore Deposits of the United States, 1933-1967, edited by J.D. Ridge, American Institute of Mining Engineers, p. 327-359.

Soever, A. and Meusy, G.
1986: The Cadieux (Renprior) zinc deposit; *in* Mineral Deposits of the Central Metasedimentary Belt, Grenville Province, Ontario and Quebec, edited by R.M. Easton, T.R. Carter, and J.S. Springer, Geological Association of Canada/Mineralogical Association of Canada, Field Trip 3: Guidebook, p. 43-45.

Sperling, H.
1980: On the metallogenetic setting of the ore deposits in the Hartz; Erzmetall, v. 33, p. 134-136.

Taylor, B.E.
1987: Stable isotope geochemistry of ore-forming fluids; *in* Short Course in Stable Isotope Geochemistry of Low-Temperature Fluids, edited by T.K. Kyser, Mineralogical Association of Canada, v. 13, p. 337-445.

Uglow, W.L.
1916: Ore genesis and contact metamorphism at the Long Lake zinc mine, Ontario; Economic Geology, v. 11, p. 231-245.

Walker, G.D.T.
1988: Mineral chemistry of diopside, garnet and amphiboles from carbonate and calc-silicate rocks, Cape Breton Island, Nova Scotia; B.Sc thesis, Acadia University, Wolfville, Nova Scotia, 137 p.

Weeks, L.J.
1954: Southeast Cape Breton Island, Nova Scotia; Geological Survey of Canada, Memoir 277, 112 p.

Whelan, J.F., Rye, R.O., and deLorraine, W.F.
1984: The Balmat-Edwards zinc-lead deposits - synsedimentary ore from Mississippi Valley-type fluids; Economic Geology, v. 79, p. 239-265.

Winkler, H.G.F.
1979: Petrogenesis of Metamorphic Rocks; Springer-Verlag, New York, 348 p.

Yun, S. and Einaudi, M.T.
1982: Zinc-lead skarns of the Yeonhwa-Ulchin district, South Korea; Economic Geology, v. 77, p. 1013-1032.

Zartman, R.E. and Doe, B.R.
1981: Plumbotectonics - the model; Tectonophysics, v. 75, p. 135-162.

APPENDIX IA

Partial whole rock analyses of unmineralized marble and calc-silicate lithologies Lime Hill and Meat Cove zinc occurrences, Cape Breton Island, Nova Scotia.

SAMPLE#	SiO_2 %	Al_2O_3 %	CaO %	MgO %	Na_2O %	K_2O %	Fe_2O_3 %	MnO %	TiO_2 %	P_2O_5 %
LIME HILL GNEISSIC COMPLEX										
CALC-SILICATE ROCK										
KQS-85-229	17.70	0.66	40.60	9.26	0.13	0.07	0.53	0.06	<0.01	0.07
KQS-85-256C	20.20	1.42	39.40	4.44	0.07	0.02	3.57	0.11	0.03	0.08
KQS-85-271	24.40	1.91	35.70	11.70	0.14	0.79	1.20	0.05	0.06	0.02
KQS-85-251B	31.10	2.26	31.10	16.20	0.16	0.49	1.76	0.04	0.09	0.18
SFB-86-216	34.60	7.42	30.40	5.67	0.73	1.88	3.94	0.07	0.33	0.07
SFB-87-1610	44.50	2.12	39.70	4.27	0.20	1.01	0.52	0.06	0.10	0.03
KQS-85-232	44.90	13.00	23.90	10.10	0.17	0.09	0.93	0.08	0.02	0.06
SFB-86-233	47.30	7.65	36.20	4.26	<0.01	0.19	1.58	0.08	0.18	0.04
KQS-85-262	53.60	3.33	22.40	15.00	0.33	1.74	2.34	0.08	0.13	0.01
CALCITE MARBLE										
SFB-86-217	2.91	0.57	48.20	6.37	<0.01	0.02	0.48	0.02	0.04	0.02
KQS-85-259	4.32	1.63	49.80	4.64	0.07	0.60	1.03	0.03	<0.01	0.13
KQS-85-269	8.10	0.64	47.90	6.30	0.10	0.21	0.24	0.04	<0.01	<0.01
SFB-86-230	10.20	0.37	48.30	4.99	<0.01	0.16	0.45	0.05	0.04	0.20
DOLOMITE MARBLE										
KQS-85-256	0.79	0.25	32.30	20.90	0.07	0.04	0.12	0.02	<0.01	0.07
KQS-85-266	1.51	0.26	33.20	22.00	0.11	0.03	0.19	0.03	0.01	0.04
SFB-86-234	1.53	0.10	31.00	21.10	<0.01	0.01	0.42	0.06	0.02	0.04
KQS-85-218	1.59	0.56	32.00	20.60	0.13	0.06	0.69	0.05	<0.01	0.10
SFB-86-231	1.60	0.11	31.20	21.10	<0.01	0.01	0.57	0.06	0.03	0.01
SFB-86-197	1.61	0.06	31.10	21.20	<0.01	0.01	0.40	0.04	0.02	0.01
SFB-86-199	2.11	0.07	31.50	20.30	<0.01	0.01	0.45	0.06	0.02	0.01
KQS-85-270	2.41	0.46	33.00	20.50	0.11	0.03	0.86	0.07	0.01	0.06
SFB-86-198	2.56	0.18	30.30	21.00	<0.01	0.01	0.93	0.07	0.03	0.01
SFB-86-239	2.82	0.19	31.00	21.00	<0.01	0.01	0.65	0.08	0.03	0.01
KQS-85-258	2.86	0.29	32.30	20.90	0.07	0.02	0.62	0.06	<0.01	0.06
KQS-85-254	2.97	0.71	32.50	19.50	0.09	0.04	2.37	0.11	0.02	0.05
KQS-85-239A	3.05	0.71	32.20	20.40	0.09	0.06	1.62	0.03	<0.01	0.12
KQS-85-267	3.52	0.39	32.50	21.20	0.10	0.04	0.47	0.06	<0.01	0.06
SFB-86-438	3.69	0.05	31.60	21.50	<0.01	0.01	0.15	0.02	0.02	0.01
KQS-85-260	3.75	0.43	34.10	20.40	0.06	0.03	0.49	0.05	0.01	0.12
SERPENTINE-DOLOMITE MARBLE										
KQS-85-264	4.83	3.53	30.00	19.90	0.11	0.08	1.43	0.08	0.06	<0.01
KQS-85-223	5.18	0.36	31.40	20.70	0.10	0.03	0.77	0.06	0.01	0.10
SFB-86-104	6.11	1.51	30.00	21.40	<0.01	0.01	0.44	0.01	0.07	0.02
KQS-85-242	6.59	3.23	32.40	19.40	0.09	0.04	1.93	0.10	0.03	0.12
SFB-87-1604	6.70	0.47	31.20	21.00	<0.01	0.01	1.62	0.08	0.05	0.02
SFB-86-209	7.31	0.06	34.40	16.80	<0.01	0.01	0.48	0.04	0.02	0.01
KQS-85-201A	7.57	0.35	31.20	20.10	0.10	0.07	1.14	0.08	0.02	0.19
KQS-85-204	8.22	1.81	30.00	19.50	0.19	0.32	2.85	0.08	0.04	0.01
KQS-85-220	8.33	0.59	30.00	19.00	0.09	0.07	0.91	0.05	0.03	0.21
KQS-85-255	8.83	0.46	31.40	16.30	0.07	0.04	1.35	0.10	<0.01	0.14
KQS-85-214	12.80	0.64	35.20	16.10	0.08	0.06	0.69	0.05	0.02	0.25
SFB-87-1602	13.20	3.55	27.90	21.90	<0.01	0.02	1.52	0.05	0.17	0.02
KQS-85-252	17.40	3.53	25.20	23.60	0.09	0.04	0.92	0.04	0.04	0.20
KQS-85-265	22.30	1.29	26.40	23.40	0.11	0.09	1.38	0.06	0.05	0.07
WOLLASTONITE MARBLE										
SFB-86-293	16.40	0.60	50.90	0.69	<0.01	0.13	0.09	0.03	0.04	0.02
SFB-87-1605	16.50	1.12	49.60	1.11	<0.01	0.40	0.38	0.01	0.06	0.02
SFB-86-298	21.90	1.57	47.90	0.91	<0.01	1.03	0.32	0.01	0.06	0.03
SFB-87-1614	22.20	0.52	49.10	2.12	<0.01	0.20	0.31	0.03	0.03	0.02
SFB-86-299	24.00	0.31	50.30	0.78	<0.01	0.11	0.09	<0.01	0.02	0.02
SFB-86-294	28.20	2.55	45.50	1.17	<0.01	0.87	0.74	0.02	0.12	0.04
SFB-87-1612	30.50	1.98	45.10	1.39	0.04	1.13	0.51	0.03	0.09	0.03
MEAT COVE ZINC OCCURRENCE										
SERPENTINE-DOLOMITE MARBLE										
SFB-86-583	3.91	0.89	35.90	21.60	<0.01	0.01	1.10	0.08	0.04	0.02
SFB-86-598	6.02	0.54	32.30	22.80	<0.01	0.01	1.36	0.07	0.04	0.01
SFB-86-596	8.54	0.35	31.40	22.00	<0.01	0.04	1.14	0.07	0.03	0.02
SFB-86-582	10.80	1.66	29.50	21.10	0.01	0.01	3.09	0.08	0.07	0.02
SFB-86-579	11.70	0.87	30.00	20.00	<0.01	0.02	3.00	0.07	0.04	0.01
SFB-86-577	11.80	1.30	30.10	17.80	<0.01	0.01	4.46	0.07	0.05	0.02
SFB-86-588	13.40	1.47	31.30	17.40	<0.01	0.02	2.01	0.07	0.04	0.02

APPENDIX IB

Trace element chemical analyses of unmineralized marble and calc-silicate lithologies Lime Hill and Meat Cove zinc occurrences, Cape Breton Island, Nova Scotia.

SAMPLE#	Au PPB	As PPM	Cu PPM	Pb PPM	Zn PPM	Cd PPM	Hg PPB	Ag PPM	Bi PPM	Sb PPM	Sr PPM	Ba PPM	Rb PPM	Ni PPM	Co PPM	Mo PPM	W PPM	Sn PPM	Ga PPM	In PPM	Ge PPM
LIME HILL GNEISSIC COMPLEX																					
CALC-SILICATE ROCK																					
KQS-85-229		3	4	8	463	2		0.3	2.0	3.0		36		6	1	6	5	5			
KQS-85-256C		3	543	13	20	1		0.3	1.0	3.0		7		5	10	5	5	5			
KQS-85-271		3	10	25	73	1		0.3	1.0	3.0		59		7	2	6	5	5	1	<1	<10
KQS-85-251B		3	20	16	89	1		0.7	1.0	3.0		707		11	5	6	5	5			
SFB-86-216	<1	<1	23	2	63	1	5	<0.5	0.1	<0.1	420	160	70	26	14	2	<3	<2	7	1	<10
SFB-87-1610		<1	2	12	14	<1					440	770	20								
KQS-85-232		3	5	44	326	1		0.3	1.0	3.0		40		61	2	7	20	5			
SFB-86-233	<1	2	<1	2	50	<1	15	<0.5	<0.1	<0.1	470	60	20	18	9	3	<3	6	9	1	10
KQS-85-262		3	3	15	213	1		0.3	1.0	3.0		2850		13	6	6	5	5			
CALCITE MARBLE																					
SFB-86-217	<1	<1	2	2	130	<1	8	<0.5	<0.1	<0.1	120	40	10	3	1	<1	<3	<2	<1	2	<10
KQS-85-259		3	7	14	211	1		0.3	1.0	3.0		1540		8	2	7	5	5			
KQS-85-269		3	2	6	7	1		0.3	1.0	3.0		98		4	1	7	5	5			
SFB-86-230	<1	<1	<1	<2	11	<1	<5	<0.5	<0.1	<0.1	590	20	10	4	2	<1	<3	<2	<1	2	<10
DOLOMITE MARBLE																					
KQS-85-256		3	14	5	20	1		0.3	3.0	3.0		68		7	1	4	5	5			
KQS-85-266		3	3	10	22	1		0.3	1.0	3.0		50		3	1	1	5	5			
SFB-86-234	1	<1	<1	<2	6	2	<5	<0.5	<0.1	<0.1	140	<10	<10	3	1	<1	<3	2	<1	2	20
KQS-85-218		3	1	8	11	1		0.3	1.0	3.0		72		6	1	19	5	5	<1	<1	10
SFB-86-231	<1	<1	<1	<2	3	1	<5	<0.5	<0.1	<0.1	50	<10	10	3	2	<1	<3	<2	<1	1	<10
SFB-86-197	<1	<1	<1	<2	29	<1	<5	<0.5	<0.1	<0.1	60	<10	20	<1	<1	<1	3	<2	<1	1	<10
SFB-86-199	<1	<1	<1	<2	360	1	15	<0.5	<0.1	<0.1	60	<10	<10	2	<1	<1	<3	<2	<1	1	<10
KQS-85-270		3	11	16	196	1		0.3	1.0	3.0		25		3	1	2	5	5			
SFB-86-198	<1	<1	<1	<2	2	1	<5	<0.5	<0.1	<0.1	80	<10	20	<1	<1	<1	<3	<2	<1	1	<10
SFB-86-239	<1	<1	<1	<2	3	2	15	<0.5	<0.1	<0.1	190	<10	<10	3	1	<1	3	<2	<1	1	<10
KQS-85-258		3	5	21	571	2		0.3	1.0	3.0		1		5	1	8	5	5	<1	<1	<10
KQS-85-254		3	9	52	331	1		0.3	1.0	3.0		10		8	2	8	5	5			
KQS-85-239A		3	7	15	102	1		0.3	2.0	3.0		7		8	1	11	5	5			
KQS-85-267		3	4	11	53	1		0.3	1.0	3.0		43		8	1	5	5	5			
SFB-86-438	<1	<1	<1	<2	24	4	5	<0.5	<0.1	<0.1	140	<10	<10	13	8	3	<3	<2	<1	2	<10
KQS-85-260		3	7	16	54	1		0.3	1.0	3.0		3		2	1	21	5	5			
SERPENTINE-DOLOMITE MARBLE																					
KQS-85-264		3	3	13	22	1		0.3	1.0	3.0		108		5	1	4	5	5			
KQS-85-223		3	16	18	125	1		0.3	1.0	3.0		14		5	1	6	5	5			
SFB-86-104	<1	<1	<1	<2	8	1	<5	<0.5	<0.1	<0.1	90	<10	20	4	<1	<1	<3	<2	1	2	<10
KQS-85-242		3	8	16	75	1		0.3	1.0	3.0		11		4	1	8	5	5			
SFB-87-1604			9	6	13						70	<10	10								
SFB-86-209	<1		2	<2	140	1	<5	<0.5	<0.1	<0.1	90	130	10	1	<1	<1	<3	<2	<1	2	<10
KQS-85-201A		3	16	11	17	1		0.3	1.0	3.0		17		6	1	1	5	5			
KQS-85-204		3	11	24	71	1		0.3	1.0	3.0		95		7	2	16	5	5			
KQS-85-220		3	11	10	65	1		0.3	1.0	3.0		32		6	1	4	5	5			
KQS-85-255		5	3	5	30	1		0.3	1.0	3.0		3		7	1	6	5	5			
KQS-85-214		3	9	13	31	1		0.3	1.0	3.0		112		5	1	1	5	5			
SFB-87-1602			12	<2	450						90	<10	<10								
KQS-85-252		3	2	12	17	1		0.3	1.0	3.0		36		3	1	6	5	5			
KQS-85-265		6	4	11	84	1		0.3	1.0	3.0		63		8	1	1	5	5			
WOLLASTONITE MARBLE																					
SFB-86-293	<1		<1	6	9	<1	8	<0.5	<0.1	<0.1	1200	20	10	9	5	2	<3	<2	<1	2	<10
SFB-87-1605			2	2	10	<1					1030	80	20								
SFB-86-298	<1		1	16	30	2	5	<0.5	<0.1	<0.1	930	140	30	15	9	3	<3	<2	1	3	<10
SFB-87-1614		<1	2	8	63						440	40	10								
SFB-86-299	<1	<1	<1	24	180	2	19	<0.5	<0.1	<0.1	800	230	<10	16	9	4	<3	<2	<1	2	<10
SFB-86-294	<1	<1	3	16	220	2	8	<0.5	<0.1	<0.1	1190	840	30	19	11	4	<3	<2	3	2	<10
SFB-87-1612		<1	5	8	160						600	70	30								
MEAT COVE ZINC OCCURRENCE																					
SERPENTINE-DOLOMITE MARBLE																					
SFB-86-583	<1	6	<1	<2	260	1	65	<0.5	<0.1	0.1	40	<10	<10	2	3	3	3	<2	<1	2	<10
SFB-86-598	<1	6	<1	24	460	2	31	0.5	<0.1	0.2	60	<10	<10	6	7	7	<3	<2	<1	2	10
SFB-86-596	<1	12	2	28	2400	5	76	<0.5	<0.1	0.3	30	20	20	4	5	7	3	<2	<1	2	<10
SFB-86-582	<1	25	12	4	3400	4	110	0.5	0.1	0.7	30	<10	20	5	13	4	<3	<2	2	1	10
SFB-86-579	<1	20	11	8	2400	3	80	0.5	0.1	0.9	30	<10	10	3	8	5	<3	<2	1	1	<10
SFB-86-577	<1	18	33	8	1000	2	65	<0.5	0.1	0.6	50	<10	10	5	17	5	<3	4	2	1	<10
SFB-86-588	<1	24	8	26	300	3	370	<0.5	<0.1	0.8	70	<10	<10	4	7	6	<3	<2	2	2	<10

APPENDIX IIA

Partial whole rock analyses of sphalerite-bearing marble samples Lime Hill and Meat Cove occurrences, Nova Scotia, and sphalerite-bearing marble samples from Grenville Supergroup occurrences, Ontario and Quebec.

SAMPLE#	SiO_2 %	Al_2O_3 %	CaO %	MgO %	Na_2O %	K_2O %	Fe_2O_3 %	MnO %	TiO_2 %	P_2O_5 %	Zn %
CAPE BRETON ISLAND, NOVA SCOTIA											
LIME HILL ZINC OCCURRENCE											
KQS-85-202	20.00	0.97	8.76	18.10	0.10	0.04	16.80	0.05	0.04	0.07	13.32
KQS-85-203	2.53	0.50	34.00	18.80	0.11	0.04	16.50	0.06	0.02	0.01	5.40
KQS-85-205	16.90	0.86	35.00	17.40	0.11	0.16	3.26	0.02	0.03	0.05	1.00
KQS-85-207	31.00	2.74	6.86	29.60	0.14	0.91	7.04	0.05	0.13	0.09	9.84
KQS-85-212	16.90	4.00	31.00	18.10	0.12	0.82	3.55	0.04	0.17	0.05	0.59
KQS-85-234	3.47	0.25	23.80	18.20	0.09	0.04	3.61	0.08	0.01	0.02	14.96
KQS-85-241	8.37	0.57	4.85	10.30	0.10	0.04	14.90	0.14	0.04	<0.01	27.92
KQS-85-243	19.20	5.51	27.50	15.50	0.17	3.34	4.87	0.04	0.29	0.01	5.24
KQS-85-208	11.90	0.61	17.00	12.50	0.01	0.09	5.02	0.04	0.05	0.02	15.60
SFB-85-223	5.02	0.25	22.20	15.00	0.01	0.02	2.80	0.05	0.03	0.01	12.20
KQS-85-231	3.82	<0.01	16.90	12.70	0.02	0.01	2.68	0.05	0.01	0.01	21.00
KQS-85-236	5.17	0.39	19.00	13.00	0.04	0.01	5.08	0.06	0.05	0.01	14.30
SFB-86-1626	4.87	0.05	19.20	12.60	0.05	0.01	3.79	0.04	0.01	0.01	17.70
SFB-86-1627	2.20	0.14	30.00	19.70	0.01	<0.01	1.32	0.05	0.02	0.01	2.66
SFB-86-1628	2.70	0.15	23.40	15.50	0.01	0.02	2.33	0.10	0.02	0.01	9.32
MEAT COVE ZINC OCCURRENCE											
SFB-86-585	1.49	0.33	30.10	20.40	0.01	0.01	5.71	0.12	0.02	0.01	2.42
SFB-86-569	1.50	0.23	28.60	17.00	0.02	0.01	3.67	0.26	0.02	0.01	6.55
SFB-86-571	1.81	0.24	29.60	13.90	<0.01	0.01	3.49	0.20	0.02	0.01	6.53
SFB-86-590	1.97	0.29	23.40	16.80	<0.01	0.01	3.95	0.32	0.02	0.02	10.90
SFB-86-584	2.22	0.25	30.80	6.15	0.08	0.01	4.23	0.32	0.02	0.01	10.00
SFB-86-603	2.49	0.73	22.80	15.30	0.05	0.01	5.37	0.33	0.04	0.01	10.50
SFB-87-1466	3.22	0.60	31.80	22.90	0.19	<0.01	2.81	0.03	0.02	0.01	0.52
SFB-87-1467	3.82	0.61	32.20	21.70	0.26	<0.01	2.17	0.04	0.01	0.01	1.20
SFB-86-602	3.99	0.64	15.80	9.38	0.01	0.02	6.05	0.40	0.04	0.01	20.80
SFB-86-581	5.54	1.15	32.90	21.70	<0.01	0.01	0.96	0.08	0.04	0.02	1.26
SFB-86-586	5.72	0.74	28.30	20.40	0.01	0.01	2.99	0.12	0.04	0.02	3.14
SFB-86-587	7.70	1.38	23.60	15.20	<0.01	0.01	2.34	0.21	0.04	0.02	9.24
SFB-86-597	8.57	0.47	29.70	19.20	<0.01	0.01	5.24	0.12	0.03	0.02	0.92
SFB-86-570	9.12	1.69	31.70	13.30	<0.01	0.01	1.92	0.15	0.05	0.02	4.18
SFB-87-1462	9.21	0.57	25.10	8.84	2.01	<0.01	4.62	0.13	0.01	0.01	13.00
SFB-86-572	9.74	2.21	25.60	20.10	<0.01	0.01	3.18	0.12	0.07	0.02	3.00
SFB-86-589	11.70	1.63	26.60	19.70	<0.01	0.02	3.33	0.13	0.05	0.02	1.72
SFB-86-591	12.90	1.43	31.50	16.60	<0.01	0.01	2.25	0.08	0.05	0.02	1.39
SFB-86-573	14.20	1.91	23.70	22.00	<0.01	0.02	3.88	0.15	0.06	0.02	1.75
SFB-86-594	21.70	4.29	6.68	11.50	0.01	1.97	13.50	0.26	0.17	0.01	14.90
GRENVILLE SUPERGROUP, QUEBEC											
BOUCHETTE ZINC OCCURRENCE											
SFB-86-1219	23.90	1.21	12.90	11.80	1.90	0.37	39.40	0.69	0.05	0.22	8.68
SFB-86-1220	37.40	2.91	25.00	17.20	0.53	0.38	8.83	0.61	0.21	0.20	0.32
SFB-86-1221	6.74	0.52	31.20	20.70	1.09	0.14	1.08	0.29	0.02	0.13	0.95
LAFONTAINE ZINC OCCURRENCE											
SFB-86-1200	9.24	1.00	2.89	2.12	0.50	0.25	39.00	0.28	0.03	0.29	33.02
SFB-86-1202*	55.40	8.19	5.81	4.07	2.96	4.31	9.27	0.06	0.08	0.76	7.08
SFB-86-1204	15.90	0.98	13.60	8.09	0.19	0.31	42.50	0.13	0.03	0.63	1.02
SFB-86-1206	18.40	0.67	17.60	7.93	0.42	0.07	36.20	0.17	0.03	1.10	13.00
SFB-86-1208	32.70	0.93	31.60	19.70	0.24	0.35	9.67	0.13	0.02	0.40	2.04
SFB-86-1210A	16.60	0.91	29.50	16.20	0.47	0.47	5.33	0.23	0.03	0.39	4.24
SFB-86-1210B	8.20	0.72	40.60	15.90	0.26	0.35	2.72	0.21	0.03	0.40	12.80
SFB-86-1211	8.90	1.07	32.80	17.80	0.85	0.53	3.56	0.16	0.02	0.18	0.34
SFB-86-1214	23.20	0.50	33.90	19.90	0.25	0.04	2.03	0.18	0.02	0.13	1.12

APPENDIX IIA

(continued)

SAMPLE#	SiO_2 %	Al_2O_3 %	CaO %	MgO %	Na_2O %	K_2O %	Fe_2O_3 %	MnO %	TiO_2 %	P_2O_5 %	Zn %
GRENVILLE SUPERGROUP, ONTARIO											
CADIEUX ZINC OCCURRENCE											
SFB-85-239	9.29	0.44	28.30	18.10	0.16	0.12	2.94	0.07	0.02	0.23	16.04
SFB-85-241	29.20	0.42	17.40	12.80	0.19	0.05	3.46	0.06	0.01	0.19	16.16
SFB-86-0001	20.40	1.34	21.50	13.90	0.67	0.27	6.53	0.06	0.06	0.01	4.72
SFB-86-0003	5.50	0.65	20.60	13.60	0.14	0.24	1.64	0.09	0.01	0.01	9.64
SFB-86-0004	5.58	0.81	25.10	13.00	0.23	0.18	1.77	0.09	0.03	0.01	14.36
SFB-86-0006	38.40	0.74	19.70	16.60	0.36	0.11	1.14	0.07	0.01	0.01	7.72
SFB-86-0007	34.20	0.79	13.30	14.10	0.38	0.10	1.87	0.06	0.02	0.06	15.00
SFB-86-0008	35.20	0.89	17.30	12.90	0.37	0.11	2.16	0.06	0.03	0.12	13.48
SFB-86-0010	26.80	0.49	19.80	13.10	0.43	0.14	7.36	0.06	0.01	0.04	7.72
SFB-86-0014	13.20	1.27	20.10	14.00	0.56	0.19	1.05	0.06	0.02	0.05	8.24
SFB-86-0015	24.80	0.61	20.60	12.70	0.84	0.28	1.03	0.06	0.02	0.09	10.64
SFB-86-0016	25.10	0.45	21.90	13.70	0.23	0.09	1.62	0.05	0.01	0.07	12.12
SFB-86-0017	24.20	0.48	27.40	15.70	0.24	0.11	1.40	0.06	0.01	0.07	5.48
SFB-86-0018	9.25	0.76	13.50	8.63	0.23	0.06	6.68	0.06	0.02	0.04	29.25
SFB-86-0025C	12.90	1.44	24.90	16.30	0.21	0.61	4.04	0.09	0.06	0.04	4.96
SFB-86-0240	28.20	0.68	31.60	17.70	0.21	0.13	1.94	0.11	0.02	0.14	15.08
SFB-86-0241	31.40	0.70	22.20	17.50	0.33	0.14	4.13	0.12	0.02	0.21	17.16
SALERNO LAKE ZINC OCCURRENCE											
SFB-86-0034	10.20	1.50	22.50	6.60	0.31	0.42	10.50	0.19	0.03	2.57	20.68
SFB-86-0038	9.10	2.55	27.60	8.96	0.42	1.31	6.22	0.08	0.10	1.30	9.04
SFB-86-0040	14.30	2.91	19.40	6.87	0.38	1.57	5.95	0.12	0.15	3.68	16.84
SFB-86-0042*	52.60	3.53	1.56	4.02	4.34	0.87	5.68	0.07	0.05	1.47	11.88
SFB-86-0043*	56.10	5.30	2.99	4.05	5.62	1.85	8.11	0.09	0.25	3.77	12.92
SFB-86-0049	6.62	1.47	18.80	6.07	0.20	0.57	15.30	0.14	0.06	3.47	16.32
SFB-86-0050	6.61	1.13	23.20	13.20	0.25	0.18	9.50	0.13	0.04	0.45	4.92
SFB-86-0051	5.38	0.86	23.80	12.60	0.19	0.18	6.95	0.35	0.04	0.16	8.20
SPRY ZINC OCCURRENCE, ONTARIO											
SFB-87-1835	35.70	0.14	25.20	18.60	0.34	0.04	0.62	0.09	0.01	0.02	1.90
SFB-87-1836	6.62	0.09	22.40	14.50	1.57	0.04	0.54	0.07	<0.01	0.02	11.00
SFB-87-1837	7.42	0.12	18.30	11.00	2.36	0.02	0.97	0.06	0.02	0.02	18.00
SFB-87-1844	10.10	0.22	20.50	15.10	1.67	0.02	0.79	0.07	0.01	0.03	12.00

* These analyses are for hybrid silicate rocks and are not included in averages cited in text.

APPENDIX IIB

Analyses of selected trace elements in sphalerite-bearing marble samples,
Lime Hill and Meat Cove occurrences, Nova Scotia, and sphalerite-bearing marble samples,
Grenville Supergroup occurrences, Ontario and Quebec.

SAMPLE#	Au PPB	As PPM	Cu PPM	Pb PPM	Cd PPM	Hg PPB	Ag PPM	Bi PPM	Sb PPM	Sr PPM	Ba PPM	Rb PPM	Ni PPM	Co PPM	Mo PPM	W PPM	Sn PPM	Ga PPM	In PPM	Ge PPM
CAPE BRETON ISLAND, NOVA SCOTIA																				
LIME HILL ZINC OCCURRENCE																				
KQS-85-202	19	11	121	53	370	4660	3.7	3.0	3.0		9		27	2	2	5	5	<1	<1	<10
KQS-85-203	5	8	28	24	153	760	1.0	1.0	3.0		18		5	1	1	5	5	<1	<1	<10
KQS-85-205	42	3	29	42	30	70	0.3	1.0	3.0		63		7	1	2	5	5	<1	<1	<10
KQS-85-207	8	3	14	46	246	1885	1.5	1.0	3.0		144		11	1	6	5	5	2	<1	10
KQS-85-212	<1	3	11	22	15	30	0.3	1.0	3.0		147		16	3	4	5	5	2	<1	10
KQS-85-234	4	3	80	1566	403	>5000	3.1	3.0	6.0		18		14	1	1	5	5	2	<1	<10
KQS-85-241	13	6	47	61	1003	>5000	4.5	1.0	3.0		9		16	4	1	5	5	1	1	30
KQS-85-243	1	7	78	72	30	1330	0.3	1.0	3.0		1090		18	4	3	5	5	3	<1	<10
MEAT COVE ZINC OCCURRENCE																				
SFB-86-585	<1	5	27	4	23	270	1.5	<0.1	0.1	20	<10	<10	8	23	8	<3	<2	1	2	10
SFB-86-569	<1	3	8	<2	110	970	<0.5	<0.1	0.1	10	<10	10	8	21	2	<3	<2	1	2	10
SFB-86-571	<1	4	6	<2	71	1410	1.0	<0.1	0.2	50	<10	20	11	18	3	<3	<2	1	1	10
SFB-86-590	<1	6	12	20	110	1410	0.5	<0.1	0.1	10	30	10	2	23	7	<3	<2	3	2	20
SFB-86-584	<1	4	20	20	170	1420	0.5	<0.1	0.3	40	10	<10	8	30	8	<3	<2	1	2	10
SFB-86-603	<1	5	69	34	170	1810	2.5	<0.1	0.2	10	50	<10	2	88	8	<3	<2	4	2	20
SFB-87-1466	2	8	22	4	4	20	<0.5	0.3	0.3	26	<10	11	2	16	1	6	<2	3	<1	10
SFB-87-1467	4	8	11	4	10	220	<0.5	0.3	0.4	38	<10	15	3	19	2	<3	<2	6	<1	20
SFB-86-602	<1	7	12	44	390	2440	3.0	<0.1	0.4	20	130	<10	8	120	13	<3	<2	6	3	60
SFB-86-581	<1	18	1	6	15	140	<0.5	<0.1	0.5	40	<10	<10	4	5	3	<3	<2	2	2	10
SFB-86-586	<1	13	44	6	48	500	0.5	<0.1	0.3	20	<10	20	6	17	6	<3	<2	2	2	10
SFB-86-587	<1	22	4	28	130	960	1.5	<0.1	0.5	20	10	<10	4	29	6	<3	<2	6	2	30
SFB-86-597	2	11	10	22	10	120	<0.5	<0.1	0.2	50	<10	10	6	17	8	<3	<2	<1	2	20
SFB-86-570	<1	26	2	<2	51	410	1.5	<0.1	0.9	40	<10	<10	10	18	3	<3	<2	5	1	20
SFB-87-1462	<1	25	46	210	120	180	1.0	0.4	0.8	86	68	13	3	66	2	81	<2	3	1	30
SFB-86-572	<1	19	9	<2	35	270	1.0	<0.1	0.9	40	<10	20	2	28	2	<3	<2	4	1	20
SFB-86-589	<1	18	10	48	20	220	<0.5	<0.1	0.8	40	<10	20	5	15	7	<3	<2	3	1	<10
SFB-86-591	16	25	13	26	21	370	0.5	<0.1	0.4	20	<10	20	5	15	7	<3	4	3	2	10
SFB-86-573	<1	26	8	<2	25	180	0.5	<0.1	0.8	20	<10	10	3	14	2	<3	<2	3	1	10
SFB-86-594	4	13	42	40	320	400	4.0	0.1	0.8	<10	6130	20	13	100	16	<3	<2	4	2	10
GRENVILLE SUPERGROUP, QUEBEC																				
BOUCHETTE ZINC OCCURRENCE																				
SFB-86-1219	3	19	868	193	54	24000	1.2		1.4	37	130	13	40	3	2	<4	<100			
SFB-86-1220	4	35	460	416	4	7000	1.0		2.4	52	100	10	15	16	4	<1	<100			
SFB-86-1221	7	47	84	8660	10	4000	2.5		7.2	163	25	3	1	<1	2	<1	<100			
LAFONTAINE ZINC OCCURRENCE																				
SFB-86-1200	22	47	210	147	656	57000	1.9		5.4	<1	160	16	25	4	8	<6	180			
SFB-86-1202	2	18	183	121	159	20000	1.8		4.3	143	1600	34	8	2	4	<3	<100			
SFB-86-1204	9	15	257	1334	184	44000	3.1		3.2	53	290	12	35	6	4	<4	<100			
SFB-86-1206	329	12	179	314	313	42000	3.0		2.2	82	25	3	221		2	<4	<100			
SFB-86-1208	9	25	111	152	56	10000	0.5		2.2	148	260	7	11	5	<1	<1	<100			
SFB-86-1210A	56	9	59	7550	326	26000	26.8		4.5	200	420	3	2	4	2	<4	<100			
SFB-86-1210C	8	10	18	2210	90	14000	4.0		2.3	370	350	3	4	2	4	<2	<100			
SFB-86-1211	4	9	22	387	8	9000	0.6		1.1	349	850	9	4	1	3	1	<100			
SFB-86-1214	7	24	24	95	41	9000	0.3		0.7	326	180	3	3	<1	2	<1	<100			

APPENDIX IIB

(continued)

SAMPLE#	Au PPB	As PPM	Cu PPM	Pb PPM	Cd PPM	Hg PPB	Ag PPM	Bi PPM	Sb PPM	Sr PPM	Ba PPM	Rb PPM	Ni PPM	Co PPM	Mo PPM	W PPM	Sn PPM	Ga PPM	In PPM	Ge PPM
GRENVILLE SUPERGROUP, ONTARIO																				
CADIEUX ZINC OCCURRENCE																				
SFB-85-239	<1	7	64	21	66	570	<0.5	<2.0	<5.0		15550		12	5	1	<10	<10			
SFB-85-241	1	15	16	15	236	585	<0.5	<2.0	<5.0		20000		6	<1	1	<10	<10			
SFB-86-0001	10	83	37	1112	103	10000	1.5		5.7	86	56	3	15	5	1	<2	<100			
SFB-86-0003	14	98	62	32	169	9000	0.3		0.8	681	53800	3	7	2	3	4	<100			
SFB-86-0004	3	43	50	36	215	6000	0.3		0.4	218	23100	18	5	<1	3	<3	<100			
SFB-86-0006	4	49	39	14	143	4000	0.3		0.8	172	4300	3	3	<1	<1	<2	<100			
SFB-86-0007	5	30	16	22	229	6000	0.5		0.8	216	18900	3	4	<1	2	5	<100			
SFB-86-0008	3	32	10	10	175	3000	0.3		0.8	207	15700	3	5	<1	<1	<3	<100			
SFB-86-0010	3	33	36	17	102	320	0.3		0.3	266	25300	3	9	1	3	<3	<100			
SFB-86-0014	46	28	31	17290	135	5000	8.5		149.0	645	30900	18	3	<1	1	6	<200			
SFB-86-0015	3	22	60	773	176	6000	0.3		1.8	631	34200	3	4	<1	1	4	<100			
SFB-86-0016	3	25	22	288	176	4000	0.3		0.9	364	23300	7	2	<1	1	3	<100			
SFB-86-0017	3	25	63	104	64	6000	0.3		0.6	305	2000	3	3	<1	3	<1	<100			
SFB-86-0018	4	70	89	7920	929	10000	4.3		24.7	39	710	3	10	2	1	<5	<100			
SFB-86-0025C	35	30	127	6030	116	7000	2.6		37.1	241	280	44	21	6	5	<1	<100			
SFB-86-0240	3	70	15	217	211	9000	0.3		37.1	257	740	3	4	1	1	<4	<100			
SFB-86-0241	3	65	22	337	244	10000	0.3		26.2	181	9720	3	4	1	6	<4	<100			
SALERNO LAKE ZINC OCCURRENCE																				
SFB-86-0034	12	56	139	1283	249	16000	1.2		6.0	466	450	10	15	15	3	<4	<100			
SFB-86-0038	15	61	77	461	226	15000	0.8		3.6	1130	1600	22	9	11	4	4	<100			
SFB-86-0040	20	90	26	181	800	19000	1.0		1.6	1020	2000	38	6	12	3	<4	<100			
SFB-86-0042	16	66	73	311	245	8000	0.5		2.6	601	260	9	11	13	4	<3	<100			
SFB-86-0043	64	205	42	93	364	22000	0.3		2.5	843	510	21	14	15	3	<3	<100			
SFB-86-0049	24	91	37	170	598	20000	1.9		6.1	686	430	26	13	19	3	<4	<100			
SFB-86-0050	12	103	30	143	113	22000	0.3		3.5	517	220	3	7	10	2	<2	<100			
SFB-86-0051	10	53	19	85	176	35000	0.3		0.9	3490	190	7	5	5	2	<3	<100			
SPRY ZINC OCCURRENCE																				
SFB-87-1835	3	5.8	33	4	54	800	<0.5	0.1	7.0	22	29	<10	<1	<1	<1	6	<2			
SFB-87-1836	<1	1	70	6	340	3000	<0.5	<0.1	16.0	22	93	<10	4	2	<1	67	<2			
SFB-87-1837	3	5	150	<2	700	1000	6	<0.1	77.0	16	84	<10	2	2	<1	112	<2			
SFB-87-1844	5	3	58	4	360	1820	4	<0.1	7.0	19	83	<10	2	<1	<1	87	<2			

APPENDIX III

Description of sphalerite-bearing marble samples used in sulphur isotope analyses, Lime Hill and Meat Cove zinc occurrences.

Sample Number	Description	$\delta^{34}S$ ‰ Sphalerite
Lime Hill Samples		
KQS-85-203	East zone, #9 trench: serpentine dolomite with sphalerite	9.5
KQS-85-206	East zone, #9 trench: submassive sphalerite with calcite and serpentine	10.7
KQS-85-231	West zone, #39 trench: interbanded submassive sphalerite in serpentine dolomite	10.8
KQS-85-234	West zone, #39 trench: disseminated sphalerite in white dolomite marble	10.5
KQS-85-241	West zone, #39 trench: submassive sphalerite in serpentine dolomite	10.6
SFB-85-205	East zone, DDH-S9 @ 43 m: disseminated sphalerite in 1 cm band in grey dolomite marble	10.6
SFB-85-209	East zone, DDH-S28 @ 8 m: white dolomite marble with minor disseminated sphalerite and trace pyrite	10.9
SFB-85-220	East zone, DDH-S16 @ 24 m: disseminated sphalerite in grey dolomite marble	12.6
SFB-85-223	East zone, DDH-S18 @ +/− 24 m: massive and disseminated sphalerite in serpentine-dolomite marble	10.6
SFB-85-224	East zone, DDH-S18 @ +/− 40 m: massive sphalerite	12.2
SFB-85-226	West zone, DDH-B11 @ 14 m: disseminated sphalerite in grey dolomite marble	10.5
SFB-85-237	West zone, DDH-B20 @ 28 m: 1 cm band of submassive sphalerite in serpentine-dolomite marble	10.4
Meat Cove Samples		
SFB-86-568	Adit zone dump: brucite-dolomite with minor serpentine and sphalerite	13.1
SFB-86-569	Adit zone dump: brucite-dolomite with sphalerite disseminated in 1 cm bands	12.4
SFB-86-571	Adit zone dump: brucite-dolomite-marble with minor sphalerite	16.7
SFB-86-572	Adit zone dump: serpentine-brucite-dolomite marble with minor sphalerite	16.6
SFB-86-579	Adit zone dump: serpentine-brucite-dolomite-marble with traces of sphalerite	14.8
SFB-86-583	Adit zone dump: serpentine-brucite-dolomite marble with minor disseminated sphalerite	16.4
SFB-86-586	Adit zone dump: serpentine-brucite-dolomite marble with bands of disseminated sphalerite	17.5
SFB-86-590	Adit zone dump: serpentine-brucite-marble with streaks of disseminated sphalerite	16.4
SFB-86-602	Northeast zone: submassive sphalerite with serpentine-brucite-dolomite bands	15.5
SFB-86-603	Northeast zone: brucite marble with 1 cm band of disseminated sphalerite.	16.6

APPENDIX IV

Sulphur isotopic composition ($\delta^{34}S$ ‰) of sphalerite from marble-hosted zinc occurences Cape Breton Island, Nova Scotia and Grenville Supergroup, Ontario, Quebec, and New York

	n	Max.	Min.	Avg.	Source
Nova Scotia Occurrences					
Lime Hill, N.S.	12	12.2	9.5	10.8	1
Meat Cove, N.S.	10	17.5	12.4	15.6	1
Grenville Type IV Occurrences					
Balmat, N.Y.	76	16.6	12.5	14.7	2
Pierrepont, N.Y.	2	14.1	14.2	14.2	3
Salerno Lake, Ontario	16	12.6	4.4	10.9	3
Grenville Type III Occurrences					
Bouchette, Quebec	5	14.7	7.4	11.7	3
Lafontaine, Quebec	13	8.8	6.1	7.5	3
Leitch, Quebec	11	8.1	7.2	7.9	3
Slave Lake, Ontario	11	11.9	8.0	9.8	3
Long Lake, Ontario	8	7.3	5.5	6.5	3

Source of data: 1) this study; 2) Whelan et al., 1984; 3) unpublished data, A.L. Sangster.

APPENDIX V

Galena lead isotopic analyses, Lime Hill and Meat Cove, Nova Scotia.

PB ISOTOPIC RATIOS

	206/204	207/204	208/204
Lime Hill			
KQS-85-234 Dissem. PbS (1566 ppm Pb) in ZnS-bearing marble	17.085	15.567	36.748
SFB-86-206 Dissem. PbS on joint in ZnS-bearing marble	17.000	15.562	36.718
Meat Cove			
SFB-86-595 Dissem. PbS in calc-silicate marble	17.209	15.513	36.376
SFB-86-595R Dissem. PbS in calc-silicate marble	17.166	15.512	36.620
SFB-86-595R Dissem. PbS in calc-silicate marble	17.026	15.480	36.438
TQ-87-54: Dissem. PbS in calc-silicate marble	17.061	15.489	36.477
TQ-87-54R: Dissem. PbS in calc-silicate marble	17.059	15.487	36.499
Boisdale Hills			
SFB-86-1013 Dissem. PbS, ZnS, FeS_2 in quartz-carbonate veins in calcite and dolomite marble	18.501	15.665	38.232
SFB-86-1014 Dissem. PbS, ZnS, FeS_2 in quartz-carbonate veins in calcite and dolomite marble	18.515	15.677	38.269
SFB-86-1016 Dissem. PbS, ZnS, FeS_2 in quartz-carbonate veins in calcite and dolomite marble	18.517	15.675	38.251
SFB-86-1020 Dissem. PbS, ZnS, FeS_2 in quartz-carbonate veins in calcite and dolomite marble	18.530	15.678	38.263
Mill Brook			
SFB-86-564 Dissem. PbS from small quartz stockwork in calcite marble near granite contact	18.428	15.675	38.246
West Bay Road			
SFB-86-560 Galena from quartz vein cutting granite	18.532	15.708	38.500

R = repeat analysis
Analyses by Geospec Consultants Limited, Edmonton, Canada.

Low-pressure metamorphism of the Lime Hill gneissic complex, Bras d'Or Terrane, Cape Breton Island, Nova Scotia[1]

R.P. Raeside[2]

Raeside, R.P., Low-pressure metamorphism of the Lime Hill gneissic complex, Bras d'Or Terrane, Cape Breton Island, Nova Scotia; in Mineral Deposit Studies in Nova Scotia, Volume 1, edited by A.L. Sangster, Geological Survey of Canada, Paper 90-8, p. 67-76, 1990.

Abstract

The Lime Hill gneissic complex of the Bras d'Or Terrane in Cape Breton Island contains migmatitic paragneiss, orthogneiss, amphibolite, and calc-silicate rocks. The dominant lithologies, of upper amphibolite facies, are biotite gneiss and cordierite-biotite gneiss. Based on the analysis of phase relationships, cordierite-K-feldspar-sillimanite anatectic migmatite formed at temperatures above 650°C and pressures below 400 MPa. Geothermobarometry yields conditions of about 750°C and 350 MPa. Minor spinel- and corundum-bearing neosomes in the migmatite indicate similar temperature and pressure conditions. This first metamorphic event may be related to that recorded by the Kellys Mountain Gneiss, and is distinctive of several other areas of gneiss throughout the Bras d'Or Terrane. Extensive retrograde metamorphism, which was probably related to younger intrusive events, occurred at lower amphibolite facies conditions, in the andalusite stability field, and may be associated with the mineralization at the Lime Hill zinc showing. The low-pressure metamorphism and regional extent of gneiss in the Bras d'Or Terrane distinguishes it from other high-grade metamorphic rocks of the Aspy Terrane and from the retrograded granulite facies gneiss of the Grenvillian Blair River Complex.

Résumé

Le complexe gneissique de Lime Hill, au sein du terrane de Bras d'Or, dans l'île du Cap-Breton, renferme du paragneiss migmatitique, de l'orthogneiss, de l'amphibolite et des roches calco-silicatées. Les lithologies prédominantes appartenant au sous-faciès supérieur des amphibolites sont le gneiss à biotite et le gneiss à cordiérite et à biotite. D'après une analyse des rapports de phase, la migmatite anatectique à cordiérite, feldspath potassique et sillimanite s'est formée à des températures dépassant 650°C et à des pressions inférieures à 400 MPa. Des méthodes géothermobarométriques indiquent une température de 750°C et une pression de 350 MPa environ. La présence, dans la migmatite, d'une petite quantité de néosomes contenant du spinelle et du corindon témoigne de l'existence de conditions semblables de température et de pression. Ce premier épisode de métamorphisme pourrait être relié à celui représenté par le gneiss de Kellys Mountain et caractérise plusieurs autres régions de gneiss dans le terrane de Bras d'Or. On note également beaucoup de rétrométamorphisme qui s'est produit aux conditions de température et de pression plus basses du faciès des amphibolites, c'est-à-dire dans le champ de stabilité de l'andalousite; ce métamorphisme est probablement lié à des épisodes subséquents d'intrusion et pourrait être associé à la minéralisation des venues de zinc de Lime Hill. En raison de son étendue et du métamorphisme à faible pression qu'il a subi, le gneiss du terrane de Bras d'Or se distingue des autres roches du terrane d'Aspy soumises à un métamorphisme intense ainsi que du gneiss rétromorphosé du faciès des granulites que l'on retrouve dans le complexe grenvillien de Blair River.

---

[1] Contribution to the Canada – Nova Scotia Mineral Development Agreement, 1984-1989. Project carried by the Mineral Resources Division, Geological Survey of Canada, Project 860008.

[2] Department of Geology, Acadia University, Wolfville, Nova Scotia, B0P 1X0.

INTRODUCTION

The Bras d'Or Terrane of central Cape Breton Island (Fig. 1) is characterized by basement blocks that contain Precambrian stratified rocks, including quartzite, greywacke, slate, marble, and minor mafic metavolcanic rocks, gneiss, and high-grade marble. Previously, all of these lithologies have been assigned to the George River Group. Other significant units include Hadrynian to Cambrian I-type granitoid suites which were generated in a subduction zone environment. Middle Cambrian to Ordovician sedimentary units (e.g. Bourinot Group), which locally overlie the granitoid and gneissic units of the Bras d'Or Terrane, may have been tectonically emplaced, and derived from the Avalon Terrane to the east. Overlying the Precambrian and early Paleozoic rocks are Late Devonian and Carboniferous volcanic and sedimentary rocks (Fisset Brook Formation, Horton and Windsor groups), some of which also occur in the adjacent terranes.

Barr and Raeside (1986) considered the George River Group to be the diagnostic unit of the Bras d'Or Terrane. Although rocks assigned to the George River Group have in the past been described from large areas of northern and central Cape Breton Island (e.g. Milligan, 1970; Wiebe, 1972; Keppie, 1979), detailed mapping has limited the known extent of the unit to the Bras d'Or Terrane (Raeside and Barr, 1987).

The most extensive sections of the George River Group occur in the Creignish Hills and at North Mountain (Fig. 1). In both of these areas metamorphic grade is low, except near postmetamorphic plutons. Relationships in the Georges River area (Boisdale Hills) are less clearly understood because of the limited areal extent of the George River Group, the abundance of severely deformed marble in the George River Group in this area, and the extensive volume of granitoid rocks which have disrupted the stratigraphic continuity. In the North Mountain and Creignish Hills areas, however, gneiss of higher metamorphic grade than that of the George River Group has also been found (Justino and Sangster, 1987; J.E. Campbell, pers. comm., 1989). Similar gneiss has been reported by Armitage (1989) at Whycocomagh Mountain, and by Barr et al. (1982) at Kellys Mountain. Jamieson (1984) described the occurrence at Kellys Mountain of low-pressure cordierite-bearing migmatite which equilibrated under peak metamorphic conditions of 100 to 350 MPa and 580 to 700°C. She interpreted that they formed under conditions of an abnormally high geothermal gradient associated with the intrusion of diorite. The gneiss in the vicinity of the Lime Hill zinc showing at North Mountain bears many petrological and compositional similarities to that at Kellys Mountain and indicates that the conditions suitable for its formation were more widespread than previously thought.

GEOLOGICAL SETTING AND FIELD RELATIONSHIPS, NORTH MOUNTAIN

The area of the North Mountain has been mapped by Kelley (1967), who in common with many earlier workers in central Cape Breton Island (e.g. Guernsey, 1928; Bell and Goranson, 1938) assigned all of the metasedimentary and gneissic rock types in the block to the George River Group (sensu lato). These include low-grade phyllite, greenschist, and crystalline limestone of the George River Group (sensu stricto) as well as the higher grade gneiss and marble. Milligan (1970) mapped much of the area now recognized as the Lime Hill gneissic complex as Paleozoic granite. He interpreted the carbonate and calc-silicate rocks as isolated blocks of marble and calcareous gneiss, respectively. Chatterjee (1977, 1980a, 1980b) described the mineralization at the Lime Hill zinc showing (see Fig. 2) and, based on the known distribution of calc-silicate and carbonate rocks, interpreted these rocks to be roof pendants in felsic intrusive rocks. He analyzed the phase relationships of the calc-silicate minerals and proposed a contact metamorphic origin for both the mineralization and the peak metamorphism of the metasedimentary rocks.

Most recently, the North Mountain has been mapped in detail by Justino (1985) and the Lime Hill zinc showing has been described by Justino and Sangster (1987). These authors recognized that low-grade George River Group rocks (sensu stricto) exist north of a fault extending across the North Mountain, and that higher grade gneiss, amphibolite, and carbonate-bearing rocks constituting the Lime Hill gneissic complex exist south of the fault (Fig. 2). Intruded into the Lime Hill gneissic complex are granodiorite (526 ± 21 Ma, K-Ar, hornblende; M.F. Justino, pers. comm., 1987), alkali-feldspar granite of presumed Cambrian to Devonian age, a wide variety of granitic to quartz dioritic and syenitic sheets, and mafic dykes. Justino and Sangster (1987) postulated that the gneissic complex may represent either a deeper level, more highly metamorphosed, less carbonate-rich sequence of the George River Group or uplifted fault-bounded basement to the George River Group.

Following the detailed mapping and descriptions of M.F. Justino (pers. comm., 1985) and Justino and Sangster (1987), it can no longer be assumed that the agent of metamorphism in the Lime Hill gneissic complex was the heat evolved during the intrusion and crystallization of the associated plutonic rocks. In particular, the extent of gneiss and the wider distribution of high-grade rock types, preclude the assignment of the metamorphism as directly contact related. In this study, the petrology of the metamorphic rocks has been investigated with a view to determining their extent and variability, and the agent of the metamorphism.

THE LIME HILL GNEISSIC COMPLEX

The Lime Hill gneissic complex shows uniformly high metamorphic grade, complex structures, and in some areas, evidence for anatectic migmatization. Four main lithologies can be distinguished by hand specimen and petrographic criteria: biotite gneiss, cordierite-biotite gneiss, amphibolite, and a variety of carbonate-bearing lithologies ranging from calcite marble to multiphase assemblages including combinations of forsterite, diopside, tremolite, talc, brucite, periclase, wollastonite, calcite,

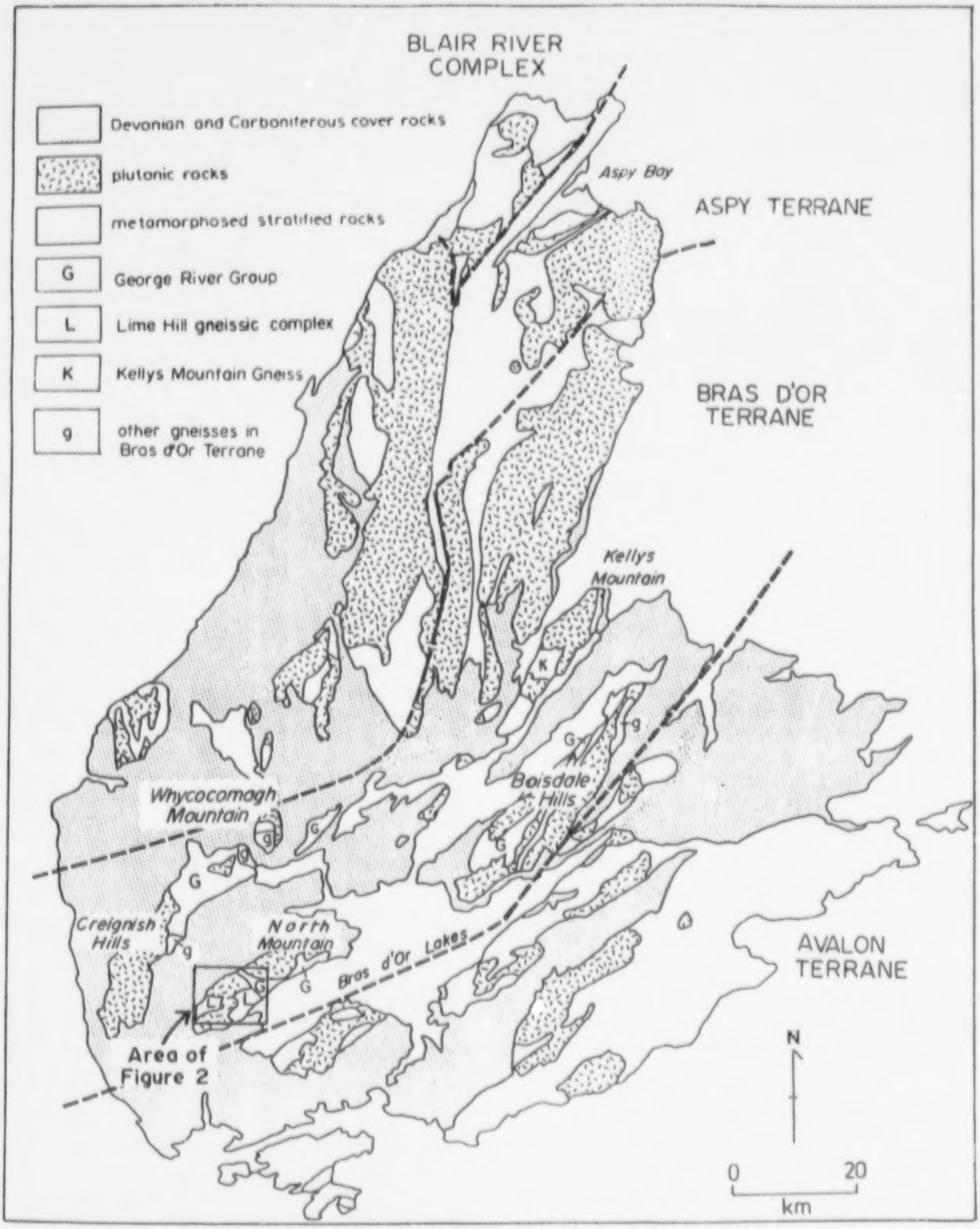
BLAIR RIVER COMPLEX
Devonian and Carboniferous cover rocks
plutonic rocks
metamorphosed stratified rocks
G George River Group
L Lime Hill gneissic complex
K Kellys Mountain Gneiss
g other gneisses in Bras d'Or Terrane
Aspy Bay
ASPY TERRANE
BRAS D'OR TERRANE
Kellys Mountain
K
G
g
Boisdale Hills
Whycocomagh Mountain
Creignish Hills
North Mountain
Bras d'Or Lakes
L
Area of Figure 2
AVALON TERRANE
N
0
20
km

Figure 1. Location of the Lime Hill gneissic complex, other gneissic units, and the George River Group (sensu stricto) in the Bras d'Or Terrane, Cape Breton Island.

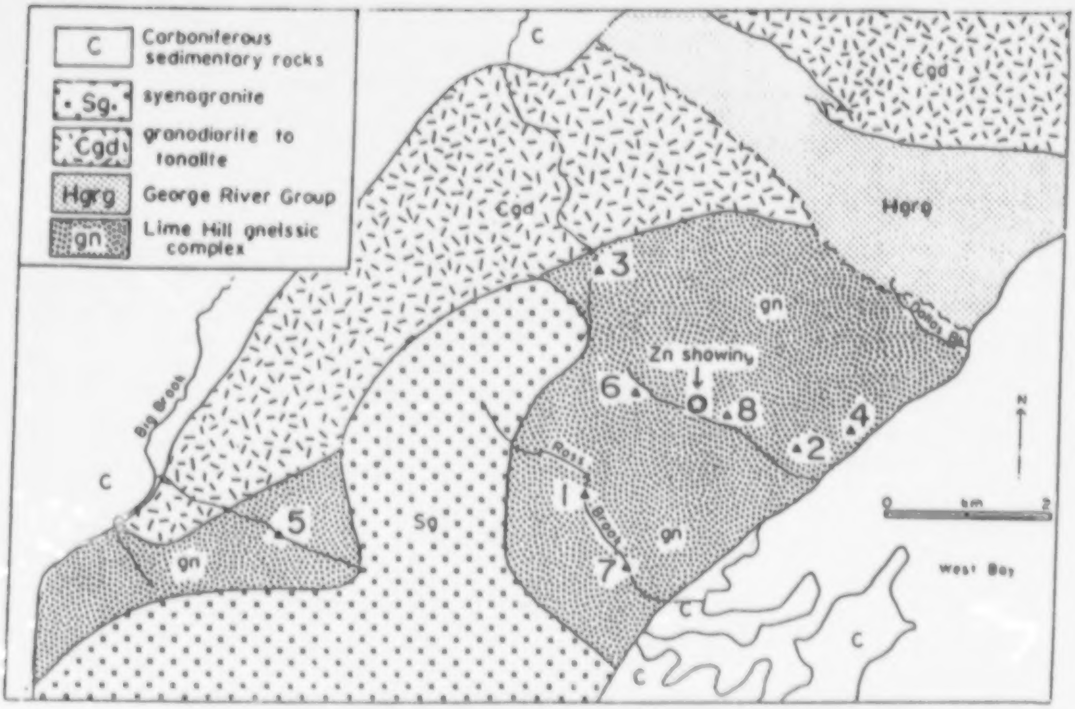

Figure 2. Geology of the Lime Hill gneissic complex (after Justino and Sangster, 1987; M.F. Justino, pers. comm., 1989) and sample locations of analyzed rocks (see Tables 1 and 2).

and dolomite. Amphibolite and carbonate-bearing lithologies are minor constituents, and the complex structure and limited outcrop have prohibited correlation of these rock types across the gneissic complex.

Biotite gneiss typically is a dark, fine to medium grained, well foliated rock with weakly to moderately developed gneissic layering (Justino and Sangster, 1987). Pelitic and quartzofeldspathic varieties appear to represent different protolith compositions. Much of the biotite gneiss contains significant quantities of K-feldspar, commonly microcline perthite, and some also contains small quantities of garnet or pyroxene. K-feldspar-bearing biotite gneiss probably represents metamorphosed plutonic rocks, as K-feldspar is only rarely associated with sillimanite, and most of the K-feldspar-bearing rocks contain lower proportions of mafic minerals than K-feldspar-free biotite gneiss.

Cordierite-biotite gneiss typically is similar in hand specimen appearance to the more pelitic biotite gneiss. Biotite is enriched in the mafic layers and cordierite in the quartzofeldspathic layers, which appear to represent neosomes in a migmatite.

Abundant mafic boudins have been reported from the biotite gneiss (Justino and Sangster, 1987). These are highly variable in their mafic content, but invariably contain hornblende, plagioclase, quartz, and opaque minerals. Justino and Sangster (1987) suggested that the amphibolite represents metamorphosed mafic calc-silicate layers and/or mafic dykes.

Carbonate-bearing lithologies occur in the central part of the Lime Hill gneissic complex, in the area of the Lime Hill zinc showing. These range from dolomite or calcite marble to siliceous marble and carbonate-bearing calc-silicate rocks. They occur as finely layered rocks intercalated with the biotite and cordierite-biotite gneisses. Calc-silicate lithologies occur closely associated with the carbonate-rich lithologies, and are also distributed across the gneissic complex, remote from the areas of known carbonate-rich rock types. The calc-silicate rocks grade into amphibolite and biotite gneiss, and probably represent minor carbonate sedimentation in mafic, pelitic, and semipelitic sequences.

MINERAL ASSEMBLAGES OF THE LIME HILL GNEISSIC COMPLEX

Biotite gneiss

Biotite gneiss is the most abundant unit in the Lime Hill complex. It is typically composed of biotite, K-feldspar, plagioclase, and quartz, with minor amounts of Fe-Ti oxides and zircon. Accessory tourmaline and apatite are present in many specimens, pyroxenes and sillimanite are present in some samples, and garnet is rare. Many samples are moderately to severely retrograded to sericite-chlorite-quartz assemblages, but in unaltered rocks a well developed granoblastic texture has been preserved.

The gneissic fabric is formed by alternating layers of different biotite contents, but in individual layers biotite is randomly oriented. Biotite-rich layers also contain higher concentrations of opaque minerals and quartz. K-feldspar is typically medium to coarse grained and is restricted to the more leucocratic layers. In most samples, it is orthoclase with a poorly developed perthitic structure. In contrast, the dyke phases in the gneissic complex contain nonperthitic microcline. Plagioclase is uniformly distributed throughout the rocks, and occurs as poorly twinned, unzoned xenoblastic crystals. Quartz typically occurs as rounded inclusions or irregular patches in both the leucocratic and biotite-rich layers. Pyroxene forms irregular patches in several samples, and is commonly concentrated in biotite-rich layers. Hypersthene and augite appear to be equally abundant, although only one specimen was found with both pyroxenes in a calc-silicate-free portion of the rock. Diopside is present in calcium-rich layers in some samples. Garnet has been recorded in a few specimens, but constitutes less than 2 percent of any sample.

Cordierite-biotite gneiss

Cordierite-biotite gneiss makes up approximately one third of the quartzofeldspathic rocks examined. It appears to be more abundant in some areas, but it is not possible to delineate zones in which all biotite gneiss contains cordierite, or in which cordierite-biotite gneiss is absent. A wide variety of textures is displayed by the cordierite-biotite gneiss, including disrupted, well layered, and migmatitic varieties, some showing phlebitic, stromatic, schlieren, or ophthalmitic structures (see Mehnert, 1968).

Cordierite occurs in the quartzofeldspathic layers of the gneiss. In some cases these appear to be leucosomes of migmatite, but in many samples cordierite occurs in the leucocratic layers of banded rocks which do not preserve clear evidence of anatectic migmatization. The cordierite occurs as irregular to tabular, coarse grained patches of xenoblastic grains, and as isolated, medium grained, ovoid crystals. Alteration has variably affected cordierite — in some rocks it has been replaced by fine grained aggregates of muscovite and green biotite, in others it is preserved with minor pinitization on the margins. Sillimanite is commonly associated with the cordierite as masses of fibrolite, with increased quantities of Fe-Ti oxides and biotite. Andalusite, spinel, and corundum, all mantled by cordierite, are present in some samples. Other phases in the cordierite-biotite gneiss are texturally similar to those in the biotite gneiss, although in the former the layering is generally more prominent and more clearly defined, and garnet and sillimanite are more abundant in the groundmass.

Amphibolite

Amphibolite, occurring as boudins in biotite gneiss, contains the assemblage hornblende-plagioclase-quartz-opaque minerals. Biotite is common, and K-feldspar is rarely found. Many samples display well preserved relict igneous textures, particularly zoned plagioclase (some with oscillatory zoning) and diabasic or gabbroic textures. A variety of amphibolite shows gneissic layering and contains substantial quantities of biotite. This hornblende-biotite gneiss is typically interlayered with biotite gneiss, and occurs throughout the Lime Hill gneissic complex. It also rarely contains clinopyroxene or K-feldspar and is depleted in mafic minerals compared to amphibolite from boudins. It probably represents a concordant sedimentary unit in the gneiss, which contains a significant mafic component. It does not appear to be metasomatic in origin as it is rarely associated with calc-silicate lithologies.

Retrograde metamorphism has affected most of the samples of amphibolite. In some rocks hornblende has been retrograded to actinolite-chlorite aggregates, and the plagioclase has been extensively sericitized.

Calcareous and calc-silicate lithologies

Carbonate-bearing and calc-silicate rocks are extremely varied in mineralogy and appearance. Pure calcite marble is rare — most of the samples examined contain forsterite (up to 20 percent), commonly partially or completely retrograded to serpentine. Dolomite was encountered in two samples of forsterite-calcite marble. In siliceous marble, and carbonate-bearing and carbonate-free calc-silicate rocks, diopside is almost invariably present, and forsterite (with retrograde serpentine) and talc are common. Various combinations of spinel, periclase, brucite, wollastonite, clinozoisite, scapolite, and sphalerite also occur. Opaque phases include graphite, pyrite, pyrrhotite, and chalcopyrite.

METAMORPHIC PETROLOGY

Retrograde metamorphism

All lithologies of the Lime Hill gneissic complex display the effects of retrograde metamorphism, particularly in the area of the Lime Hill zinc showing. The most obvious effects are extensive sericitization of feldspars and alteration of cordierite to fine grained, nearly-isotropic mats of mica(?). Extensive alteration to chlorite and epidote is restricted to the mafic lithologies, where hornblende and biotite may be completely replaced, although chloritized biotite is common in all lithologies in the area of the zinc showing. Mafic lithologies also display replacement of hornblende by actinolite.

Muscovite is present in some samples of biotite and cordierite-biotite gneiss. In almost all cases, this muscovite occurs as large irregular plates associated with feldspar, aluminosilicate minerals, or cordierite, or as finely intergrown aggregates of biotite and muscovite. It has commonly grown across the boundaries of these minerals and appears to have replaced them. These textural observations indicate that the muscovite is entirely retrograde in the Lime Hill gneiss. As muscovite is a typical phase of lower grade pelitic and semipelitic rocks, its absence as a prograde phase implies that metamorphic conditions exceeded those for its decomposition in the presence of quartz and feldspar, which is in the range of 600 to 700°C, at $P_{H_2O} = P_{total}$, and a pressure of 300 to 500 MPa (Thompson and Algor, 1977).

Andalusite was detected in three samples. In two samples it contains inclusions of magnetite, spinel, or corundum and is closely associated with cordierite. It appears to have formed in these rocks by the breakdown of corundum or spinel, possibly in reaction with cordierite. This reaction appears to have proceeded under retrograde conditions, resulting in overall diminution of grain size, and the mantling of corundum and spinel grains by andalusite. In the third sample, andalusite is a minor phase associated with biotite, plagioclase, garnet, sillimanite, and quartz. In this situation, the andalusite appears to have been formed by the breakdown of sillimanite. It appears to have nucleated preferentially in biotite-rich layers in the gneiss. All three occurrences of andalusite indicate a phase of retrograde metamorphism, sufficiently intense to nucleate and crystallize medium grained andalusite, as well as coarse grained muscovite and chlorite. Maximum pressure-temperature conditions for such an event appear to have been in the amphibolite facies, at pressures less than 400 MPa (the upper stability of andalusite — Holdaway, 1971), and temperatures less than 600 to 700°C (the upper stability of the assemblage muscovite + plagioclase + quartz — Thompson and Algor, 1977). If chlorite was formed simultaneously, the maximum temperature would have been considerably less.

Prograde metamorphism

The largest number of prograde phases that appear to be in textural equilibrium in cordierite-biotite gneiss is biotite, cordierite, plagioclase, K-feldspar, quartz, garnet, ilmenite, magnetite, and melt. Sillimanite is also present in such rocks, although in every case it is isolated from cordierite, and is commonly enclosed by biotite, plagioclase, garnet, and quartz. Using this assemblage it is possible to limit the minimum conditions of peak metamorphism (Fig. 3), based on the reactions:

andalusite or kyanite = sillimanite (Holdaway, 1971)

Al_2SiO_5 + Na-plagioclase + K-feldspar + quartz + H_2O = melt (Thompson and Tracy, 1979)

biotite + K-feldspar + quartz + sillimanite + H_2O = melt (Seifert, 1976)

biotite + sillimanite + quartz = cordierite + K-feldspar + H_2O (Holdaway and Lee, 1977).

Except for the aluminosilicate polymorphic transformation reaction, these reactions are strongly dependent on the water content of the fluid phase and the assumption that $P_{fluid} = P_{total}$. In the Lime Hill area, carbonate rocks are abundant only in a relatively small area near the Lime Hill zinc showing, and dehydration reactions are prevalent. Carbonate minerals are absent from all analyzed samples. Accordingly, XH_2O is assumed to be 1.0 in the derivation of the P-T diagram (Fig. 3). No significant variation in metamorphic grade can be detected across the gneissic complex, based on the examination of mineral assemblages.

The assemblages sillimanite-garnet-corundum-cordierite and sillimanite-garnet-hercynite-cordierite are also useful in limiting the conditions of the prograde metamorphism. Harris (1981) reported the formation of hercynite spinel and corundum by local desilication during anatexis in biotite-sillimanite-quartz-plagioclase-bearing rocks at temperatures below 720°C. Five samples from the Lime Hill gneissic complex appear to have undergone variable amounts of desilication in the neosomes of the migmatite, and have preserved univariant and divariant assemblages around an invariant point involving garnet, Fe-cordierite, hercynite, sillimanite, corundum, and quartz in the Al_2O_3-SiO_2-FeO system (Fig. 3). The position of this invariant point has been calculated at about 650°C, 250 MPa (Harris, 1981).

Physical conditions of metamorphism

Eight samples of biotite and cordierite-biotite gneiss were selected for chemical analysis. Seven of these samples contain the assemblage garnet-biotite-sillimanite (+andalusite)-plagioclase-quartz necessary for the simultaneous determination of metamorphic pressure and temperature conditions based on the garnet-biotite Fe-Mg exchange reaction and the garnet-Al_2SiO_5-plagioclase-quartz solid exchange reaction. Samples were selected from across the outcrop area of the Lime Hill gneissic complex, including the vicinity of the Lime Hill zinc showing.

Mineral analyses were made at the Dalhousie Regional Electron Microprobe Laboratory, Halifax, Nova Scotia, using a JEOL 733 Superprobe. A combined wavelength and energy dispersive analytical technique was used for the analysis of ten major elements. An accelerating voltage of 15 kV, a probe current of about 5×10^{-9} amp, and a beam diameter of about 1×10^{-6} m were used. At least three analyses were made on each grain or portion of a grain. Zoned minerals (garnets) were traversed with successive analyses about 0.01 mm apart, across the largest grains in each polished thin section. Data reduction of raw counts to corrected weight percent of oxides was done using Tracor Northern ZAF software.

Mineral chemistry

Garnet is highly variable in appearance in the eight analyzed samples. Compositional zoning is pronounced in three samples, with the rims being notably richer in the spessartine component, the Mg/(Mg+Fe) ratio being higher in the cores, and pyrope content displaying an antithetic relationship to almandine and spessartine content. In two samples, steep compositional gradients are coincident with textural discontinuities, particularly the density and grain size of inclusions, and the cores were probably not in equilibrium with biotite, plagioclase, sillimanite, and quartz of the matrix. Five samples show minimal or no zoning, except for minor spessartine enrichment in the rims. Grossular (Ca) and spessartine (Mn) contents are low in all samples, generally less than 5 and 10 mol percent, respectively (Table 1).

Biotite occurs as 1 to 4 mm laths in the groundmass of all samples. In each sample, biotite compositions are uniform, and no compositional gradients were detected

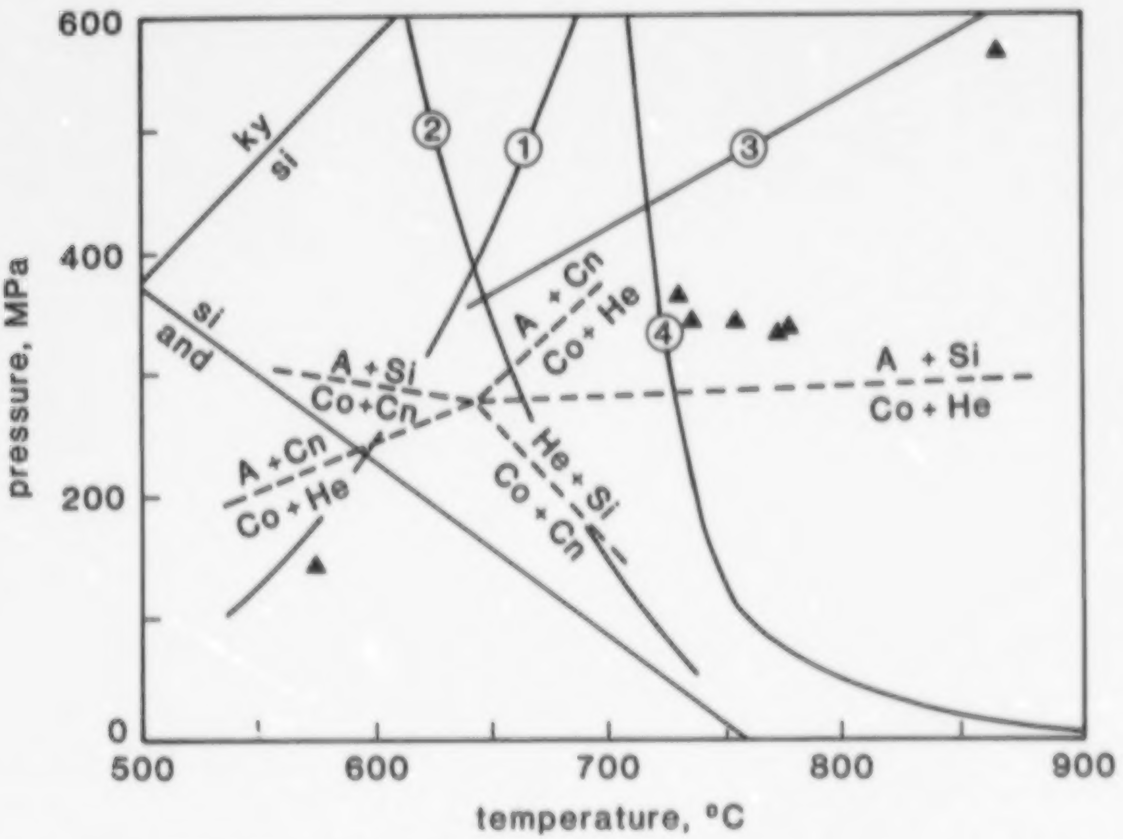

Figure 3. Pressure-temperature diagram with results for analyzed gneiss (filled triangles), using the garnet-biotite calibration of Hodges and Spear (1982) and the anorthite-grossular calibration of Newton and Haselton (1981). Labelled reactions: 1, muscovite + Na-plagioclase + quartz = K-feldspar + Al_2SiO_5 + H_2O (Thompson and Tracy, 1979); 2, Al_2SiO_5 + Na-plagioclase + K-feldspar + quartz + H_2O = melt (Thompson and Tracy, 1979); 3, biotite + Al_2SiO_5 + quartz = cordierite (30 mol % Fe) + K-feldspar + H_2O (Holdaway and Lee, 1977); 4, biotite + K-feldspar + quartz + sillimanite + H_2O = melt (Seifert, 1976). Dashed lines are univariant reactions in the Al_2O_3-SiO_2-FeO system (Harris, 1981): A = almandine, Cn = corundum, Co = Fe-cordierite, He = hercynite spinel, Si = sillimanite, Ky = kyanite. For all water-bearing reactions, P_{H2O} is assumed to equal P_{total}.

Table 1. Garnet-biotite geothermometry, based on the distribution of Mg and Fe between garnet and biotite. Calibrations used: T1, Ferry and Spear (1978); T2, Thompson (1976); T3, Pigage and Greenwood (1982); T4, Indares and Martignole (1985); T5, Hodges and Spear (1982). Abbreviations: ga, garnet; bi, biotite.

Analyzed Sample Site	X^{ga}_{Mg}	X^{ga}_{Fe}	X^{bi}_{Mg}	X^{bi}_{Fe}	X^{ga}_{Ca}	X^{ga}_{Ca}	X^{bi}_{Ti}	$X^{bi}_{Al^{vi}}$	T1, °C	T2, °C	T3, °C	T4, °C	T5, °C
1	0.193	0.700	0.404	0.407	0.025	0.081	0.0567	0.1226	764	734	835	691	776
2 core	0.239	0.652	0.387	0.510	0.041	0.068	0.0365	0.0540	1143	976	1244	1132	1178
2 rim	0.129	0.675			0.041	0.154			715	698	838	768	732
3 core	0.235	0.656	0.361	0.475	0.041	0.068	0.0658	0.0815	1120	962	1220	1023	1154
3 rim	0.138	0.703			0.016	0.143			730	709	829	696	736
4	0.212	0.747	0.369	0.426	0.027	0.013	0.0451	0.1542	853	795	884	731	868
5	0.148	0.762	0.328	0.469	0.032	0.058	0.0722	0.1210	763	732	824	650	777
6	0.096	0.834	0.337	0.462	0.031	0.040	0.0572	0.1388	540	565	578	456	548
7	0.158	0.742	0.353	0.447	0.023	0.076	0.0583	0.1354	746	720	810	661	756
8 core	0.144	0.801	0.334	0.464	0.039	0.016	0.0423	0.1513	703	697	751	622	730
8 rim	0.102	0.834			0.037	0.027			563	584	600	491	574

either within individual biotite grains or with distance from garnet grains.

Plagioclase occurs as an anhedral 1 to 6 mm diameter groundmass phase. Many plagioclase grains show zoning optically, but microprobe analysis of cores and rims commonly reveals differences of less than 5 An percent.

Geothermometry

Temperature determinations based on five calibrations of the garnet-biotite Fe-Mg exchange reaction are listed in Table 1. The patterns displayed by the eight samples appear to be independent of the calibration used, although the absolute temperatures determined from a single sample vary by up to 174°C. Temperatures have been determined using compositional data from both the rims and cores of zoned garnets in three samples. In two of these (samples 2 and 3), the cores yield unrealistically high temperatures, supporting the conclusion reached above that the garnet cores were not in equilibrium with the present composition of biotite. In sample 8, the almandine-rich rim yields a significantly lower temperature than the core, indicating that this feature may be a retrograde effect.

In sample 6, the temperatures calculated by all five calibrations are abnormally low, and are interpreted to represent retrograde re-equilibration. Discounting the nonequilibrium and retrograde temperature determinations, six of the remaining seven samples yielded temperatures ranging from 730 to 777°C (Hodges and Spear, 1982 calibration).

Geobarometry

Pressure was determined from the anorthite-grossular exchange reaction in the assemblage garnet-plagioclase-sillimanite-quartz. Of the eight samples used for geobarometry, seven contain sillimanite, and aluminum saturation has been assumed for these. Pressures determined using the calibration of Newton and Haselton (1981) range from 335 to 363 MPa for five of the samples (Table 2). This is a narrow range, given the uncertainties in the geobarometer, the propagation of analytical uncertainties in the calculation, and the presence of andalusite in some of the samples.

Three pressures were determined that are outside the range of the main cluster. In two cases, these pressures are strongly dependent on the input temperatures and may be spurious, but in the third (sample 6), the distribution coefficient, log Ks (Table 2), is markedly less negative, and may indicate a real variation in the pressure of equilibration.

DISCUSSION

The Lime Hill gneissic complex has reached metamorphic conditions characteristic of the middle to upper amphibolite facies. The inferred temperature-pressure conditions of about 750°C and 350 MPa require a geothermal gradient in the order of 80 to 100°C/km. Such conditions may be attributed to contact metamorphism (as proposed for the Lime Hill area by Chatterjee, 1980a) or to regional perturbations, possibly caused by mafic intrusions at shallow depths or abnormally high heat flow above zones of rifting or continental collision. The uniformity of prograde temperatures across the gneissic complex precludes a direct contact metamorphic origin for the gneiss. All temperatures appear to be within the error limits of the calibration, except the anomalously high temperature for the sample that is farthest from any igneous body. The lowest temperatures, including those interpreted to be due to retrograde re-equilibration, are from samples adjacent to the Lime Hill zinc showing, and the most severely retrograded rocks are also from this area.

It is likely that the agent of metamorphism was of a more regional extent. If the metamorphism involved the intrusion of a large mafic mass, this may be related to the Big Brook granodiorite to tonalite which has been identified west of the Lime Hill gneissic complex (Justino and Sangster, 1987).

The migmatitic nature of the gneiss is particularly significant as it limits the metamorphic conditions to pressures lower than 400 MPa and temperatures above 650°C, the most probable reaction for the development of migmatite being the biotite-breakdown reaction (equation 3,

Table 2. Garnet-plagioclase-Al_2SiO_5-quartz geobarometry, after Ghent (1976). Abbreviations: ga, garnet; pl, plagioclase; gr, grossular; an, anorthite; N & H, Newton and Haselton (1981) calibration.

Analyzed Sample Site	X_{gr}^{ga}	X_{an}^{pl}	a_{gr}^{ga}	a_{an}^{pl}	log Ks Ghent	log Ks N & H	T, K	P, bars Ghent	P, bars N & H
1	0.025	0.348	0.029	0.468	−3.431	−3.624	1049	517	335
2	0.041	0.480	0.046	0.639	−3.205	−3.428	1005	536	363
4	0.027	0.295	0.031	0.355	−3.115	−3.177	1141	790	570
5	0.032	0.445	0.036	0.583	−3.430	−3.628	1050	519	337
6	0.031	0.295	0.035	0.537	−2.935	−3.558	821	328	210
7	0.023	0.298	0.026	0.404	−3.337	−3.574	1029	523	346
8 core	0.039	0.473	0.044	0.634	−3.251	−3.476	1003	516	345
8 rim	0.037	0.473	0.042	0.749	−3.320	−3.754	847	250	131

Fig. 3), which is also responsible for the production of cordierite. The migmatitic leucosomes, therefore, represent anatectic peraluminous granitic melts, some of which may have been extruded from the gneiss and accumulated as granitic magma. The extensive suite of granitic dykes that have intruded the Lime Hill gneissic complex may have been derived from this magma. The dykes may have been responsible for local metamorphism and metasomatism at their contacts with calc-silicate lithologies in the vicinity of the Lime Hill zinc showing. Such local effects may be termed contact metamorphism, and could be responsible for the wide mineralogical variety documented by Chatterjee (1980a).

A phase of dyke intrusion may have been responsible for the extensive retrograde metamorphism observed in many samples from the gneiss, although the significantly lower pressures and temperatures required to stabilize andalusite require a period of uplift prior to the main phase of the retrograde metamorphism. Alternatively, the intrusion of the West Bay alkali-feldspar granite may be responsible for this event.

REGIONAL CORRELATION

The uniformly high metamorphic grade and the distinctive low-pressure style of metamorphism distinguish the Lime Hill gneissic complex from other stratified units in the North Mountain area of Cape Breton Island (i.e. the George River Group, sensu stricto). The contact between the gneiss and the low-grade units is faulted, and it is not possible to correlate one with the other on the basis of this study. The lithological types found in the Lime Hill gneissic complex can be matched to rocks of similar composition in the George River Group, although it appears that the relative abundances are different (Justino and Sangster, 1987). Correlation can be better made between the Lime Hill gneissic complex and the Kellys Mountain Gneiss — both of these units are characterized by low-pressure upper amphibolite facies metamorphism, with abundant development of aluminosilicate-bearing cordierite gneiss (andalusite + sillimanite at Kellys Mountain), and cordierite migmatite (Jamieson, 1984). Other reports of gneiss in the Bras d'Or Terrane of Cape Breton Island include the Boisdale Hills (Barr and Setter, 1984), Whycocomagh Mountain (Armitage, 1989), and the Creignish Hills (J.E. Campbell, pers. comm., 1989). Such blocks of gneiss may be correlative, although it is premature to compare them without a detailed investigation of the metamorphic development and the chemistry of each.

Jamieson (1984) invoked heat evolved from the intrusion of the dioritic bodies as the agent of metamorphism of the Kellys Mountain Gneiss, and the same may be the case for the Lime Hill gneissic complex. However, the recognition of a number of high-grade, low-pressure gneisses in the Bras d'Or Terrane may indicate that a more regional high heat flow was likely for the metamorphism, and that the association with dioritic and granodioritic to tonalitic plutons may be secondary to the original source of the heat.

The distinctive metamorphic style and wide range of lithologies displayed by the Lime Hill gneissic complex and other areas of gneiss in the Bras d'Or Terrane clearly distinguish this gneiss from the retrograded granulite facies Grenvillian rocks of the Blair River Complex in northern Cape Breton Island (Barr et al., 1987), from the high-pressure kyanite-bearing gneiss of the Aspy Terrane (Raeside and Barr, in press), and from the relatively low-grade, predominantly volcanic rocks of the Avalon Terrane in southeastern Cape Breton Island. Instead, the gneisses of the Bras d'Or Terrane may represent the high-temperature, low-pressure metamorphism characteristic of the root zone of an oceanic-oceanic or continental-oceanic collisional zone. Further dating of the metamorphism of the gneiss is required to determine if it represents sedimentary rocks caught up in the subduction zone or if it is the basement lithology of the Bras d'Or Terrane which pre-existed the 555 Ma subduction event (Barr et al., 1988; Raeside and Barr, 1988).

ACKNOWLEDGMENTS

Many of the samples and detailed maps used in this study were made available by M. Justino. Technical assistance was provided by R. MacKay of the Dalhousie Regional Electron Microprobe laboratory and by J. Colwell. Financial support was provided by the Geological Survey of Canada and the Natural Sciences and Engineering Research Council of Canada. The manuscript benefitted from reviews by J. Bourne and an anonymous reviewer.

REFERENCES

Armitage, A.E.
1989: Geology and petrology of the crystalline rocks of the Whycocomagh area, Cape Breton Island, Nova Scotia; B.Sc. thesis, Acadia University, Wolfville, Nova Scotia, 120 p.

Barr, S.M. and Raeside, R.P.
1986: Pre-Carboniferous tectonostratigraphic subdivisions of Cape Breton Island; Maritime Sediments and Atlantic Geology, v. 22, p. 252-263.

Barr, S.M. and Setter, J.R.D.
1984: Petrology of granitoid rocks of the Boisdale Peninsula, central Cape Breton Island, Nova Scotia; Nova Scotia Department of Mines and Energy, Paper 84-1, 75 p.

Barr, S.M., O'Reilly, G.A., and O'Beirne, A.M.
1982: Geology and geochemistry of selected granitoid plutons of Cape Breton Island; Nova Scotia Department of Mines and Energy, Paper 82-1, 176 p.

Barr, S.M., Raeside, R.P., Dunning, G.R., and Jamieson, R.A.
1988: New U-Pb ages from the Cape Breton Highlands and correlations with southern Newfoundland: a Lithoprobe East contribution; Geological and Mineralogical Associations of Canada, Joint Annual Meeting, Program with Abstracts, v. 13, p. A5.

Barr, S.M., Raeside, R.P., and van Breemen, O.
1987: Grenvillian basement in the northern Cape Breton Highlands, Nova Scotia; Canadian Journal of Earth Sciences, v. 24, p. 992-997.

Bell, W.A. and Goranson, E.A.
1938: Bras d'Or map area, Nova Scotia; Geological Survey of Canada, Map 356A, scale 1:63 360.

Chatterjee, A.K.
1977: Tungsten mineralization in the carbonate rocks of the George River Group, Cape Breton Island, Nova Scotia; Nova Scotia Department of Mines, Paper 77-7.

1980a: Mineralization and associated wall rock alteration in the George River Group, Cape Breton Island, Nova Scotia; Ph.D. thesis, Dalhousie University, Halifax, Nova Scotia, 197 p.

1980b: Lime Hill zinc-tungsten mineralization; *in* Mineral Deposits and Mineralogenic Provinces of Nova Scotia, Geological and Mineralogical Associations of Canada, Joint Annual Meeting, Halifax, Nova Scotia, Field Trip Guidebook, p. 45-51.

Ferry, J.M. and Spear, F.S.

1978: Experimental calibration of the partitioning of Fe and Mg between biotite and garnet; Contributions to Mineralogy and Petrology, v. 66, p. 113-117.

Ghent, E.D.

1976: Plagioclase-garnet-Al_2SiO_5-quartz — a potential geobarometer-geothermometer; American Mineralogist, v. 64, p. 874-885.

Guernsey, T.D.

1928: Geology of the North Mountain, Cape Breton; Geological Survey of Canada, Summary Report 1927, Part C, p. 47-82.

Harris, N.

1981: The application of spinel-bearing metapelites to P/T determinations: an example from south India; Contributions to Mineralogy and Petrology, v. 76, p. 229-233.

Hodges, K.V. and Spear, F.S.

1982: Geothermometry, geobarometry and the Al_2SiO_5 triple point at Mt. Moosilauke, New Hampshire; American Mineralogist, v. 67, p. 1118-1134.

Holdaway, M.J.

1971: Stability of andalusite and the aluminum silicate phase diagram; American Journal of Science, v. 271, p. 97-131.

Holdaway, M.J. and Lee, S.M.

1977: Fe-Mg cordierite stability in high-grade pelitic rocks based on experimental, theoretical, and natural observations; Contributions to Mineralogy and Petrology, v. 63, p. 175-198.

Indares, A. and Martignole, J.

1985: Biotite-garnet geothermometry in the granulite facies: the influence of Ti and Al in biotite; American Mineralogist, v. 70, p. 272-278.

Jamieson, R.A.

1984: Low pressure cordierite-bearing migmatites from Kellys Mountain, Nova Scotia; Contributions to Mineralogy and Petrology, v. 86, p. 309-320.

Justino, M.F.

1985: Geology and petrogenesis of the plutonic rocks of North Mountain, Cape Breton Island; Nova Scotia Department of Mines and Energy, Information Series, v. 9, p. 111.

Justino, M.F. and Sangster, A.L.

1987: Geology in the vicinity of the Lime Hill zinc occurrence, southwestern Cape Breton Island, Nova Scotia; Current Research, Part A, Geological Survey of Canada, Paper 87-1A, p. 555-561.

Kelley, D.G.

1967: Baddeck and Whycocomagh map-areas; Geological Survey of Canada, Memoir 351, 65 p.

Keppie, J.D.

1979: Geological map of the Province of Nova Scotia, 1:500 000 scale; Nova Scotia Department of Mines and Energy.

Mehnert, K.R.

1968: Migmatites and the Origin of Granitic Rocks; Elsevier, Amsterdam, 405 p.

Milligan, G.C.

1970: Geology of the George River Series, Cape Breton; Nova Scotia Department of Mines, Memoir 7, 111 p.

Newton, R.C. and Haselton, H.T.

1981: Thermodynamics of the garnet-plagioclase-Al_2SiO_5-quartz geobarometer; *in* Thermodynamics of Minerals and Melts, edited by R.C. Newton, A. Navrotsky, and B.J. Wood, Springer-Verlag, New York, p. 131-147.

Pigage, L.C. and Greenwood, H.J.

1982: Internally consistent estimates of temperature and pressure: the staurolite problem; American Journal of Science, v. 282, p. 943-969.

Raeside, R.P. and Barr, S.M.

1987: Geological map of the igneous and metamorphic rocks of northern Cape Breton Island, Nova Scotia; Geological Survey of Canada, Open File 1594, 6 sheets, scale 1:50 000.

1988: The Bras d'Or Zone: a suspect terrane in Cape Breton Island, Nova Scotia; Geological and Mineralogical Associations of Canada, Joint Annual Meeting, Program with Abstracts, v. 13, p. A102.

in press: Preliminary report on the geology of the northern and eastern Cape Breton Highlands, Nova Scotia; Geological Survey of Canada, Paper 89-14.

Seifert, F.

1976: Stability of the assemblage cordierite + K-feldspar + quartz; Contributions to Mineralogy and Petrology, v. 57, p. 179-185.

Thompson, A.B.

1976: Mineral reactions in pelitic rocks: II. Calculation of some P-T-X(Fe-Mg) phase relations; American Journal of Science, v. 276, p. 425-454.

Thompson, A.B. and Algor, J.R.

1977: Model system for the anatexis of pelitic rocks: I. Theory of melting reactions in the system $KAlO_2$-$NaAlO_2$-Al_2O_3-SiO_2-H_2O; Contributions to Mineralogy and Petrology, v. 63, p. 247-269.

Thompson, A.B. and Tracy, R.J.

1979: Model systems for anatexis of pelitic rocks: II. Facies series melting and reactions in the system CaO-$KAlO_2$-$NaAlO_2$-Al_2O_3-SiO_2-H_2O; Contributions to Mineralogy and Petrology, v. 70, p. 429-438.

Wiebe, R.A.

1972: Igneous and tectonic events in northeastern Cape Breton Island, Nova Scotia; Canadian Journal of Earth Sciences, v. 9, p. 1262-1277.

Regional geological setting of pre-Carboniferous mineral deposits in the western Cape Breton Highlands, Nova Scotia[1]

R.A. Jamieson[2], P.C. Tallman[3], H.E. Plint[4], and K.A. Connors[5]

Jamieson, R.A., Tallman, P.C., Plint, H.E., and Connors, K.A., Regional geological setting of pre-Carboniferous mineral deposits in the western Cape Breton Highlands, Nova Scotia; in Mineral Deposit Studies in Nova Scotia, Volume 1, edited by A.L. Sangster, Geological Survey of Canada, Paper 90-8, p. 77-99, 1990.

Abstract

Silurian to Ordovician phyllites and schists of the Jumping Brook metamorphic suite, western Cape Breton Highlands, host small polymetallic sulphide deposits. The metamorphic rocks include a lower tholeiitic metabasite suite (Faribault Brook metavolcanic rocks), overlain by silicic metasedimentary rocks and felsic tuffs (Barren Brook schist), turbiditic metasedimentary rocks (Dauphinee Brook schist), and the higher grade equivalents of these rocks (Corney Brook schist and Fishing Cove River schist). Regional mapping in the Cape Breton Highlands suggests that equivalent rocks can be found in the Sarach Brook-Middle River area, in the Money Point-Cape North area, and in the Mabou Highlands. Together, these volcanic and sedimentary complexes are characteristic of the Aspy Terrane. Dating of the volcanic and plutonic rocks suggests that Early Silurian silicic volcanism was followed by Early Devonian high-grade metamorphism associated with syntectonic tonalitic to granodioritic intrusions. The metamorphic rocks cooled rapidly and were intruded by posttectonic Devonian granites. The regional geology is consistent with a recently proposed tectonic model involving Silurian subduction south of Newfoundland followed by closure during the Acadian Orogeny.

The sulphide occurrences near Cheticamp are localized near the lithologically and structurally complex transition from mafic volcanic rocks to sedimentary rocks. This transition zone is marked by a thin, complexly deformed felsic tuff-silicic metasedimentary rock horizon which hosts some deposits, and is the locus of late metamorphic and synmetamorphic shearing. Some sulphides were deposited prior to metamorphism and deformation, whereas others appear to have been introduced later; all have undergone complex deformation and remobilization. Retrogression to chlorite-muscovite assemblages is common in, but not restricted to, the vicinity of the sulphide deposits.

Résumé

Les phyllites et les schistes siluriens à ordoviciens de la séquence métamorphique de Jumping Brook, dans l'ouest des hautes-terres du Cap-Breton, logent des gisements de sulfures polymétalliques. Les roches métamorphiques comprennent une séquence inférieure de métabasite tholéiitique (roches volcaniques métamorphisées de Faribault Brook), recouverte par des roches métasédimentaires siliceuses et des tufs felsiques (schiste de Barren Brook), des roches métasédimentaires turbiditiques (schiste du Dauphinée Brook) et les équivalents plus fortement métamorphisés de ces roches (schiste de Corney Brook et schiste de Fishing Cove River). Les travaux de cartographie régionale dans les hautes terres du Cap-Breton permettent de croire à l'existence de roches

---

[1] Contribution to the Canada - Nova Scotia Mineral Development Agreement, 1984-1989. Project carried by the Mineral Resources Division, Geological Survey of Canada, Project 860008.

[2] Department of Geology, Dalhousie University, Halifax, Nova Scotia, B3H 3J5.

[3] Present Address: Noranda Mines, 3 Earl St., Windsor, Newfoundland, A0H 1H0.

[4] Present Address: Department of Geology, University of Alberta, Edmonton, Alberta, T6G 2G6.

[5] Present Address: Department of Geology, Monash University, Melbourne, Australia.

équivalentes dans la zone de Sarach Brook et Middle River, dans la zone de Money Point et Cape North et dans celle des Mabou Highlands. Ensemble, ces complexes de nature volcanique et sédimentaire sont caractéristiques du terrane d'Aspy. La datation des roches volcaniques et plutoniques semble établir qu'un volcanisme silicieux du Silurien inférieur a été suivi au Dévonien inférieur par un métamorphisme très intense associé à des intrusions syntectoniques de nature tonalitique à granodioritique. Les roches métamorphiques se sont refroidies rapidement et ont été pénétrées par des granites post-tectoniques du Dévonien. La géologie régionale s'accorde avec un modèle tectonique récemment avancé qui suppose une subduction silurienne au sud de Terre-Neuve, laquelle aurait été suivie par une fermeture pendant l'orogenèse acadienne.

Les venues de sulfure près de Chéticamp sont situées près de la transition lithologiquement et structuralement complexe qui s'opère des roches mafo-volcaniques aux roches sédimentaires. Cette zone de transition est marquée par un horizon de roches métasédimentaires minces, inextricablement déformées, à caractère felsique et tufo-silicieuse, qui renferme certains gisements et qui est le lieu d'un cisaillement tardimétamorphique et synmétamorphique. Certains sulfures se sont déposés avant les épisodes de métamorphisme et de déformation, tandis que d'autres semblent remonter à une période plus récente: tous ont cependant subi une déformation complexe et une remobilisation. La rétrogression à des assemblages de chloritomuscovite est fréquente au voisinage des gisements de sulfure, sans toutefois leur être exclusive.

INTRODUCTION

The western Cape Breton Highlands, Cape Breton Island, Nova Scotia, are underlain by metamorphic and plutonic rocks, with minor sedimentary and volcanic rocks (Fig. 1). In the vicinity of Cheticamp, numerous polymetallic sulphide occurrences have been documented (e.g. Ponsford and Lyttle, 1984). However, the age, geological setting, and origin of the sulphide deposits is not clear, and their metallogenic affinities and the possible occurrence of similar mineralization elsewhere in the Cape Breton Highlands are not known. The Jumping Brook metamorphic suite in the vicinity of Faribault Brook, west of Cheticamp (Fig. 2 and 3), hosts many of these deposits. This paper discusses the lithology, stratigraphy, structure, metamorphism, age, and regional correlation of this unit, emphasizing factors bearing on the origin and distribution of the mineral occurrences. Other units mapped in the course of this study have been described elsewhere (Plint et al., 1986; Barr et al., 1987a; Jamieson et al., 1987; Plint and Jamieson, 1989) and are discussed here mainly in terms of their relationship to the Jumping Brook metamorphic suite and its mineral deposits.

Previous work

Although early maps of Nova Scotia showed the Cape Breton Highlands to be underlain by metamorphic and plutonic rocks (e.g. Fletcher, 1885), the first systematic reconnaissance work was not done until the 1950s and early 1960s (MacLaren, 1955; Neale, 1963). At this time, the metamorphic rocks of the region were regarded as Precambrian, and correlations with southwestern Newfoundland were suggested (e.g. Neale and Kennedy, 1975). Milligan (1970) and Chatterjee (1980) regarded the rocks of the Cheticamp area as part of the Precambrian "George River Series" recognized in central Cape Breton Island.

Currie (1975, 1982, 1987b), in a study of the igneous and metamorphic rocks of the Cheticamp area, divided the metamorphic rocks into two main units, the high-grade Pleasant Bay complex, which he regarded as late Precambrian, and the lower grade Jumping Brook complex, which he regarded as Ordovician-Silurian. He concluded that there were two important episodes of regional metamorphism separated by emplacement of the Cambrian Cheticamp Pluton, and that both Grenvillian and Avalonian tectonic elements were present in the older rocks (Currie, 1982, 1987a,b).

Jamieson and Craw (1983), Conrod (1984), and Craw (1984) conducted both reconnaissance and detailed mapping in the Cheticamp-Pleasant Bay region. Using structural and metamorphic criteria, they suggested that supracrustal members of the Pleasant Bay gneisses were the high-grade equivalents of the lower grade Jumping Brook rocks. The whole sequence was interpreted as Precambrian based on a presumed intrusive contact between the relatively undeformed Cambrian Cheticamp Pluton and the metamorphic rocks.

The mineral deposits of the Faribault Brook region have been known since the 1890s, and investigated intermittently until the present time (e.g. Ponsford and Lyttle, 1984). Locally significant but highly variable Zn-Pb-Cu-Ag-Au-As-Bi values have been documented in metasedimentary and metavolcanic host rocks. In a detailed study of several showings, Chatterjee (1980) documented paragenetic relationships and alteration, and concluded that they represented polycyclic hydrothermal deposits that postdated the metamorphic host rocks. In the most recent phase of exploration, G. Woods (pers. comm., 1986) emphasized the proximity of the deposits to the Cheticamp Pluton, and concluded that the introduction of the mineralization probably occurred during the early stages of deformation. He interpreted felsic schist near the metabasite-metasedimentary rock transition, recognized by previous workers as being associated with the deposits (e.g. Covey, 1979; Chatterjee, 1980), as mylonite derived in part from granitic rocks, possibly including offshoots from the Cheticamp Pluton.

Thus, by the early 1980s, there were two different interpretations of the regional geology of the western Cape Breton Highlands, and a number of models for the mineral deposits, of which the hydrothermal origin was the most popular. The regional studies had not systematically investigated the mineral deposits, and the mineral deposit studies lacked a regional structural and metamorphic context. Existing radiometric dates had not resolved the problem of the age of the metamorphic rocks or of the deposits (see Jamieson et al., 1986, for review). Both the regional controversy and the most recent mineral deposit models focused on the relationship of the Cheticamp Pluton to the metamorphic rocks of the region. This paper attempts to put the mineral deposits of the Faribault Brook area into their regional context, by documenting the stratigraphy, structure, metamorphism, and age of the rocks in the Cheticamp area, with particular emphasis on the role of the Cheticamp Pluton.

GEOLOGY OF THE JUMPING BROOK METAMORPHIC SUITE

Nomenclature

Jamieson et al. (1987) proposed the name "Jumping Brook metamorphic suite" for the metavolcanic and metasedimentary rocks of the western Cape Breton Highlands, including within the suite the Jumping Brook complex of Currie (1982, 1987b) and correlative rocks to the south and east. The Jumping Brook metamorphic suite was divided into five subunits (Table 1), which are well exposed on the Cheticamp River and its tributaries to the south. Jamieson et al. (1987) retained the term Pleasant Bay complex (Currie, 1982, 1987b) for the gneissic rocks of the region, although the boundaries between the Jumping Brook metamorphic suite and the Pleasant Bay complex are poorly defined in many areas (Plint, 1987). Two subunits within the Pleasant Bay complex, the Belle Cote Road orthogneiss and the McKenzie Mountain megacrystic orthogneiss, have been recognized (Jamieson et al., 1987; Marcotte, 1987; Plint, 1987), but most of the Pleasant Bay complex has not been mapped in detail.

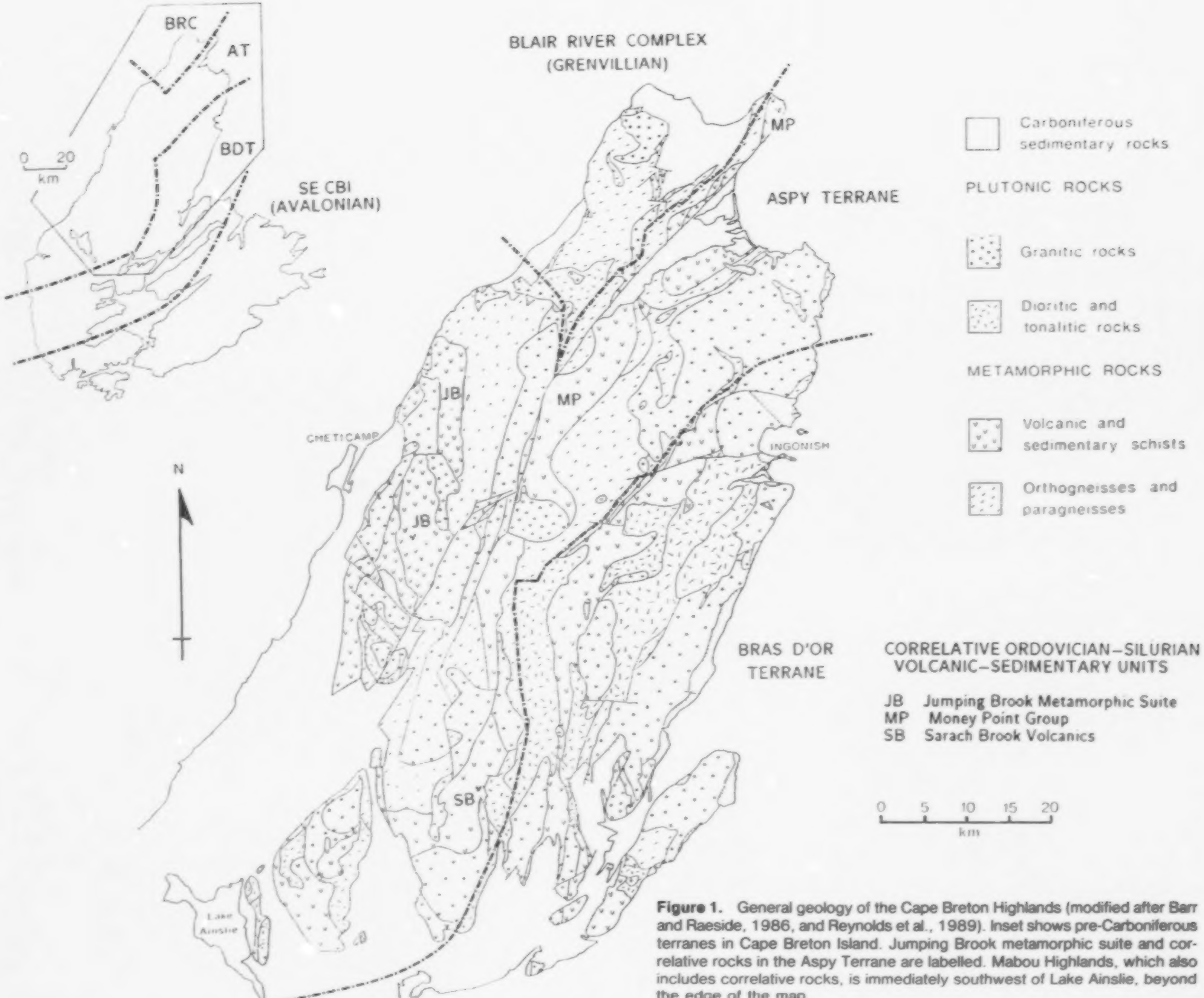
BRC
AT
BDT
0 20
km
SE CBI
(AVALONIAN)
BLAIR RIVER COMPLEX
(GRENVILLIAN)
ASPY TERRANE
BRAS D'OR
TERRANE
MP
MP
JB
JB
SB
CHETICAMP
INGONISH
Lake Ainslie
N
Carboniferous sedimentary rocks
PLUTONIC ROCKS
Granitic rocks
Dioritic and tonalitic rocks
METAMORPHIC ROCKS
Volcanic and sedimentary schists
Orthogneisses and paragneisses
CORRELATIVE ORDOVICIAN–SILURIAN VOLCANIC–SEDIMENTARY UNITS
JB Jumping Brook Metamorphic Suite
MP Money Point Group
SB Sarach Brook Volcanics
0 5 10 15 20
km

Figure 1. General geology of the Cape Breton Highlands (modified after Barr and Raeside, 1986, and Reynolds et al., 1989). Inset shows pre-Carboniferous terranes in Cape Breton Island. Jumping Brook metamorphic suite and correlative rocks in the Aspy Terrane are labelled. Mabou Highlands, which also includes correlative rocks, is immediately southwest of Lake Ainslie, beyond the edge of the map.

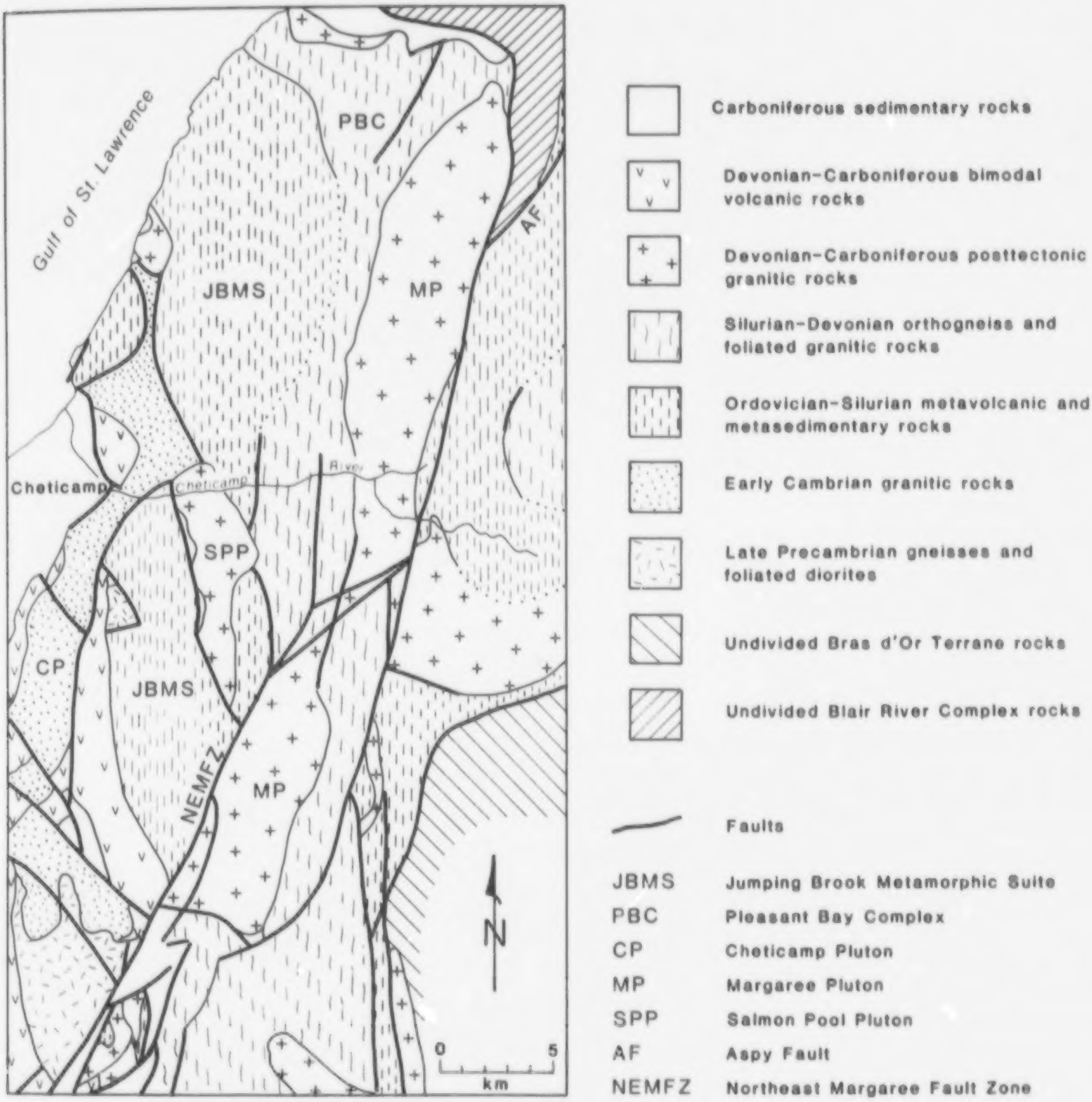
Gulf of St. Lawrence
PBC
JBMS
MP
AF
Cheticamp
Cheticamp River
SPP
CP
JBMS
NEMFZ
MP
N
0
5
km
Carboniferous sedimentary rocks
Devonian-Carboniferous bimodal volcanic rocks
Devonian-Carboniferous posttectonic granitic rocks
Silurian-Devonian orthogneiss and foliated granitic rocks
Ordovician-Silurian metavolcanic and metasedimentary rocks
Early Cambrian granitic rocks
Late Precambrian gneisses and foliated diorites
Undivided Bras d'Or Terrane rocks
Undivided Blair River Complex rocks
Faults
JBMS Jumping Brook Metamorphic Suite
PBC Pleasant Bay Complex
CP Cheticamp Pluton
MP Margaree Pluton
SPP Salmon Pool Pluton
AF Aspy Fault
NEMFZ Northeast Margaree Fault Zone

Figure 2. General geology of the Jumping Brook metamorphic suite and associated rocks (simplified from Plint et al., 1986; Jamieson et al., 1987; Plint, 1987).

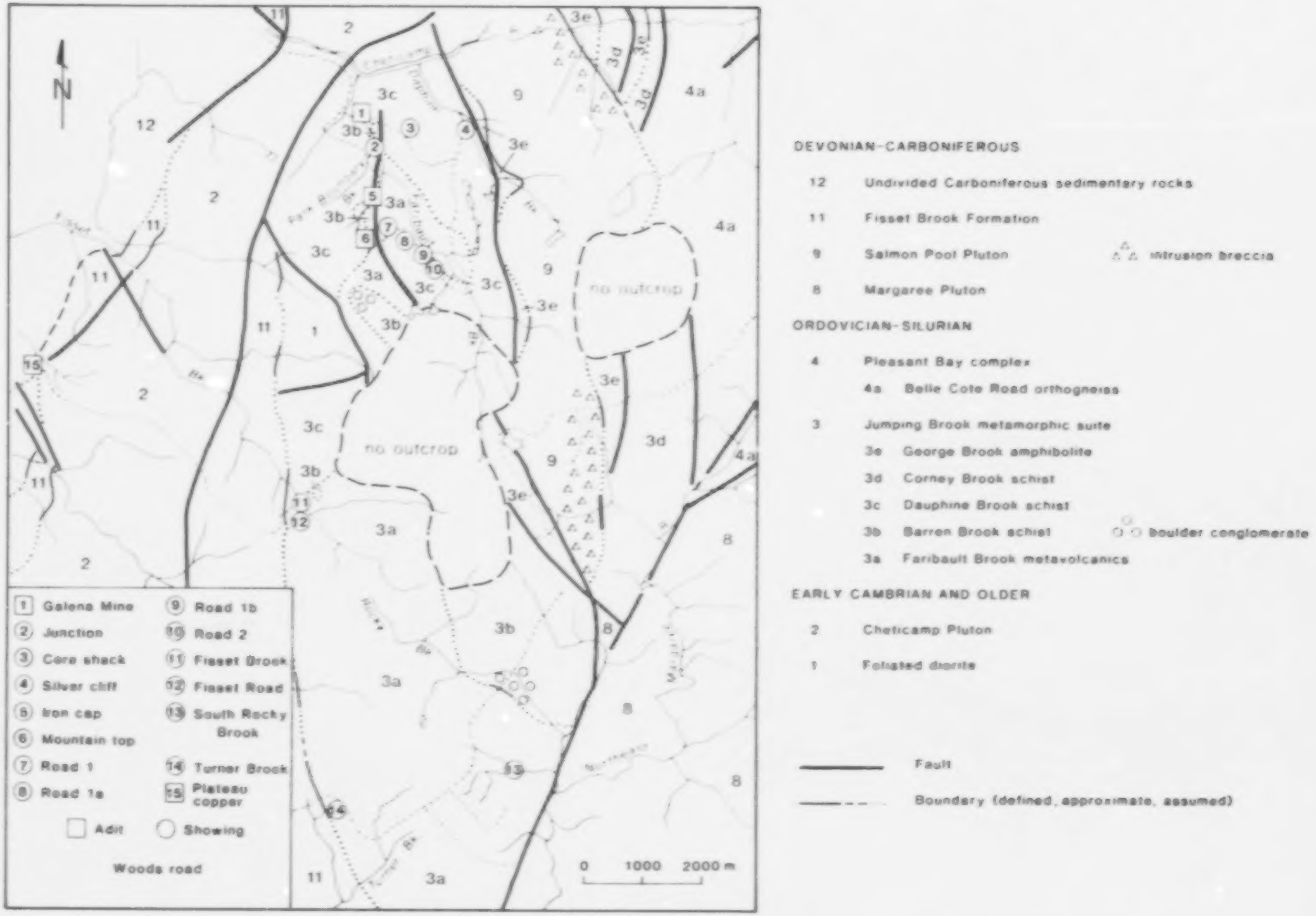
N
DEVONIAN-CARBONIFEROUS
12 Undivided Carboniferous sedimentary rocks
11 Fisset Brook Formation
9 Salmon Pool Pluton
intrusion breccia
8 Margaree Pluton
ORDOVICIAN-SILURIAN
4 Pleasant Bay complex
4a Belle Cote Road orthogneiss
3 Jumping Brook metamorphic suite
3e George Brook amphibolite
3d Corney Brook schist
3c Dauphine Brook schist
3b Barren Brook schist
boulder conglomerate
3a Faribault Brook metavolcanics
EARLY CAMBRIAN AND OLDER
2 Cheticamp Pluton
1 Foliated diorite
Fault
Boundary (defined, approximate, assumed)
1 Galena Mine
2 Junction
3 Core shack
4 Silver cliff
5 Iron cap
6 Mountain top
7 Road 1
8 Road 1a
9 Road 1b
10 Road 2
11 Fisset Brook
12 Fisset Road
13 South Rocky Brook
14 Turner Brook
15 Plateau copper
Adit
Showing
Woods road
no outcrop
no outcrop
0 1000 2000 m

Figure 3. Geology of the southern part of the Jumping Brook metamorphic suite, showing locations of main mineral occurrences. Units numbered according to maps published by Jamieson et al. (1987) and Tallman et al. (1988).

Table 1. Summary of important units in the Cheticamp area (see also Fig. 3).

LATE DEVONIAN-EARLY CARBONIFEROUS

Fisset Brook Formation (Upper Devonian-Tournaisian plant and fish fossils; e.g. Blanchard et al., 1984)
Salmon Pool Pluton (365 +10/-5 Ma, U-Pb zircon, Jamieson et al., 1986)

DEVONIAN

Margaree Pluton (380 Ma, $^{40}Ar/^{39}Ar$ biotite cooling age, Reynolds et al., 1989; 343 + 17 Ma, Rb-Sr isochron probably reflecting alteration, O'Beirne-Ryan et al., 1986)

DEVONIAN-SILURIAN

Pleasant Bay complex: includes
Belle Cote Road orthogneiss (433 ± 20 Ma, U-Pb zircon, Jamieson et al., 1986); approx. 386 Ma, U-Pb titanite, G.R. Dunning, pers. comm., 1989); syntectonic tonalitic intrusion coeval with metamorphism of Jumping Brook metamorphic suite) Undivided gneissic rocks including orthogneiss and minor enclaves of amphibolite and schist that may in part predate the Jumping Brook metamorphic suite

SILURIAN-ORDOVICIAN

George Brook amphibolite (mafic intrusions possibly cogenetic with Jumping Brook metamorphic suite)

Jumping Brook metamorphic suite: includes
  Fishing Cove River schist*
  Corney Brook schist
  Dauphinee Brook schist
  Barren Brook schist
  Faribault Brook metavolcanic rocks
Correlative units in the Cape Breton Highlands include the Money Point Group (Macdonald and Smith, 1980); Sarach Brook-Middle River metamorphic suite (Jamieson and Doucet, 1983) which includes rhyolite dated at 434 Ma (U-Pb zircon, Dunning et al., in press); and Mabou Highlands complex (Barr and Macdonald, 1989).
*The Fishing Cove River schist occurs north of Figure 3. Details of its occurrence are in Jamieson et al., 1987.

CAMBRIAN

Cheticamp Pluton (550 + 8 Ma, U-Pb zircon, Jamieson et al., 1986; 545 Ma, $^{40}Ar/^{39}Ar$ muscovite cooling age, Reynolds et al., 1989)

Lithology and stratigraphy

The Jumping Brook metamorphic suite comprises a belt of low-, medium-, and high-grade metasedimentary, metavolcanic, and metaplutonic rocks extending through the western highlands (Fig. 2) from Pleasant Bay to the Northeast Margaree River. It is bounded on the west by faults against the Cheticamp Pluton and Late Devonian to Carboniferous volcanic and sedimentary rocks, on the east by complex tectonic and locally gradational contacts with gneissic and plutonic rocks of the Pleasant Bay complex (Currie, 1975, 1987a; Craw, 1984; Plint et al., 1986; Marcotte, 1987), and separated from probably equivalent rocks of the Sarach Brook-Middle River area by shear zones and younger intrusions (Jamieson and Doucet, 1983; Jamieson et al., 1987.)

Fine grained, massive to well foliated, mafic to intermediate metavolcanic rocks constitute the Faribault Brook metavolcanic rocks, the structurally lowest unit of the Jumping Brook metamorphic suite. In the middle reaches of Faribault Brook, metabasalts with possible relict pillow structures predominate (Connors, 1986; Plint et al., 1986), although in drill core, interlayering of metasedimentary rocks with metabasite is evident (Tallman et al., 1988). Farther south, massive mafic rocks pass upward into mafic to intermediate metavolcanic rocks with associated fine grained sedimentary rocks and minor lapilli-tuff. Connors (1986) concluded that the metabasites were originally tholeiites formed in an island arc setting. Although there is some compositional variation on a regional scale, the compositions of mafic rocks from the southern part of the study area are also consistent with this interpretation (Fig. 4a).

The Barren Brook schist, which structurally overlies the metabasites, comprises a heterogeneous assemblage of relatively coarse grained, generally silicic metasedimentary rocks, including boulder conglomerate, quartzite, quartz-pebble conglomerate, and quartz-sericite schist (Jamieson et al., 1987). The coarse conglomerate at the base of this unit may mark an unconformity, although it is not regionally extensive, and the rocks on either side have identical structural and metamorphic histories; in any case it marks a significant change in the character of the rocks being deposited. Granite boulders in this conglomerate typically contain large quartz phenocrysts that may be the source of the quartz "eyes" common in the associated, fine grained, silicic metasedimentary rocks; some boulders resemble the nearby Cheticamp Pluton. The Barren Brook schist pinches out northward; in the

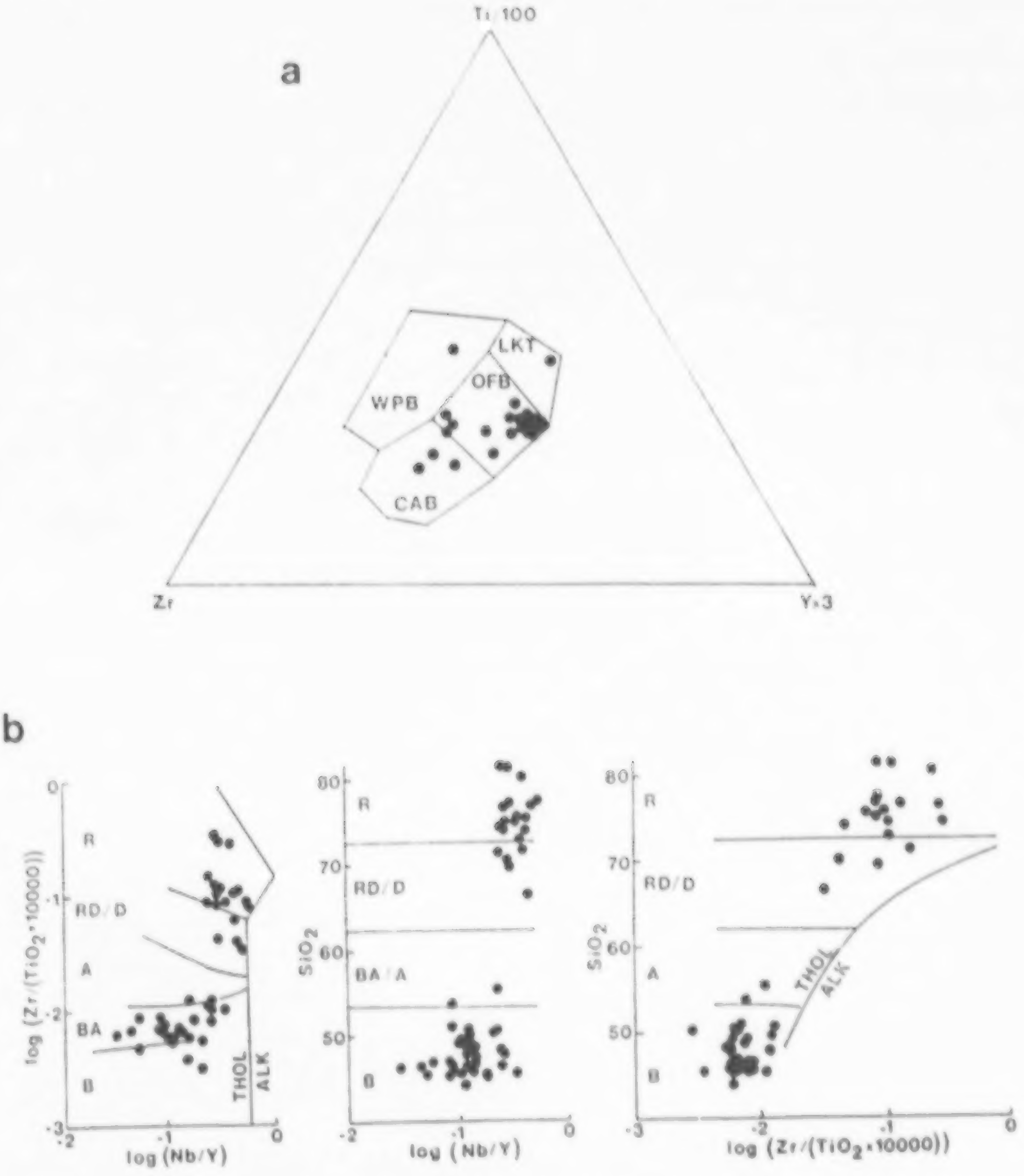

Figure 4. Geochemistry of metavolcanic rocks in the Jumping Brook metamorphic suite and correlative rocks in the southern Cape Breton Highlands. a. Pearce and Cann (1973) diagram showing that metabasites fall mainly in the ocean floor basalt field (after Connors, 1986). WPB = within plate basalt; LKT = low potassium tholeiite; OFB = ocean floor basalt; CAB = calc-alkaline basalt. b. Winchester and Floyd (1977) diagrams showing tholeiitic affinities and range of SiO_2 concentrations of both mafic and felsic rocks. Lack of intermediate compositions may reflect relatively few analyses of pyroclastic rocks. B = basalt; BA = basaltic andesite; A = andesite; D = dacite; RD = rhyodacite; R = rhyolite; THOL = tholeiitic; ALK = alkalic.

Faribault Brook area it forms a thin quartz-sericite schist horizon that is interlayered with other lithologies (Fig. 3; Tallman et al., 1988). These felsic schists are closely associated with the sulphides in many locations (Covey, 1979; Chatterjee, 1980). Although they have been interpreted as mylonitic granitoid rocks (G. Woods, pers. comm., 1986), thin section observations suggest that most of these horizons, including the one that hosts the Galena Mine showing, are foliated silicic pyroclastic rocks and volcanogenic sedimentary rocks (Fig. 5; Connors, 1986). In some localities (e.g. Marleau showing), foliated felsic dykes cut metabasite (e.g. G. Woods, pers. comm., 1986; Tallman et al., 1988). The volcanic members of this unit are high silica rhyolites (Fig. 4b), with highly variable alkali contents that may reflect element mobility before or during metamorphism, or in the case of silicic tuffs, the effects of dilution by other material.

Well foliated, grey, fine to medium grained pelitic, semipelitic, and psammitic phyllites and schists, referred to as the Dauphinee Brook schist, form the upper part of the Jumping Brook metamorphic suite in the Faribault Brook area (Fig. 3), and dominate the lower grade sequence to the north (Currie, 1982, 1987a,b; Conrod, 1984; Plint et al., 1986; Plint, 1987; Plint and Jamieson, 1989). On Faribault Brook, these metasedimentary rocks structurally overlie metabasalts and quartz-sericite schists. The original sedimentary layering in these schists has been strongly modified by tight to isoclinal folds (Fig. 6; Connors, 1986; Jamieson et al., 1987; Plint, 1987), and the interlayering with metavolcanic rocks observed in drill core (Tallman et al., 1988) is at least partly attributable to folding. North of the Cheticamp River, these schists pass into higher grade rocks on the east, but in the Faribault Brook region this transition is obscured by the younger Salmon Pool Pluton (Craw, 1984; Currie, 1987b). Small fault-bounded slivers of similar metasedimentary rocks are common in the central highlands (Jamieson et al., 1987).

Higher grade members of the Jumping Brook metamorphic suite, including the Corney Brook schist and the Fishing Cove River schist, occur north and east of the Faribault Brook area (Plint, 1987). These staurolite- and kyanite-bearing rocks, interpreted by Craw (1984), Jamieson et al. (1987), Plint (1987), and Plint and Jamieson (1989) as the high-grade equivalents of the rocks in the Faribault Brook area, do not contain significant sulphide mineral occurrences and are not discussed further here. For lithological and petrological descriptions of these rocks, as well as discussions of the controversy surrounding their age, the reader is referred to Currie (1982, 1987a,b), Jamieson et al. (1986, 1987), and Plint and Jamieson (1989).

Medium to coarse grained, foliated metabasite, referred to as the George Brook amphibolite, forms large, locally discordant bodies throughout the Jumping Brook metamorphic suite. It typically contains coarse hornblende porphyroblasts in a finer grained plagioclase-biotite-quartz matrix, and commonly has a relict dioritic texture (Plint, 1987). The distribution and texture of these amphibolites suggest that they intruded the Jumping Brook metamorphic suite prior to metamorphism, probably as subvolcanic sills. These rocks locally contain sulphide minerals although no significant concentrations have been documented (Connors, 1986).

Relationship to the Pleasant Bay complex

The relative ages and contact relationships of the Jumping Brook metamorphic suite and the gneisses of the Pleasant Bay complex have been the subject of considerable debate (e.g. Currie, 1982; Jamieson and Craw, 1983; Conrod, 1984; Craw, 1984; Currie, 1987a,b; Plint, 1987; Plint and Jamieson, 1989). Where clearly exposed, most contacts between the two units are synmetamorphic ductile shear zones. However, Craw (1984) and Plint (1987) documented gradational relationships between Jumping Brook metamorphic suite schists and gneisses mapped by Currie (1975, 1982, 1987b) as part of the Pleasant Bay complex. Much of the Pleasant Bay complex consists of tonalitic to granodioritic orthogneiss, interpreted by Jamieson et al. (1986, 1987) and Marcotte (1987) to represent syntectonic intrusions into the Jumping Brook metamorphic suite. This interpretation is supported by the increase in metamorphic grade toward the Pleasant Bay complex from the west, east, and south, and by regionally crosscutting contacts. Although the presence of older enclaves within the Pleasant Bay complex cannot be ruled out, there is currently no unambiguous geological or isotopic evidence that the Pleasant Bay complex represents older basement upon which the Jumping Brook metamorphic suite was deposited.

STRUCTURE AND METAMORPHISM

General aspects

Many of the conflicting hypotheses proposed for the origin and geological setting of the Faribault Brook deposits centre on different interpretations of the structural and metamorphic history of the region. There is general agreement that the deposits have been variably deformed and that sulphides have been remobilized at various stages, but little agreement as to the timing of sulphide deposition with respect to metamorphism, although the role of "alteration" has been emphasized in some studies (e.g. Chatterjee, 1980; G. Woods, pers. comm., 1986). This section summarizes the structural and metamorphic history of the Jumping Brook metamorphic suite.

Deformation

Up to three generations of penetrative structures involving tight to isoclinal folding can be recognized in metasedimentary rocks of the Faribault Brook region (Plint, 1987). Prograde metamorphism to lower amphibolite facies accompanied the first two of these (Plint and Jamieson, 1989); later structures are associated with retrogression of earlier mineral assemblages. Owing to this complex deformation, primary structures preserved in the Jumping Brook metamorphic suite are useful more as a clue to the origin of the rocks than as indicators of stratigraphic younging directions.

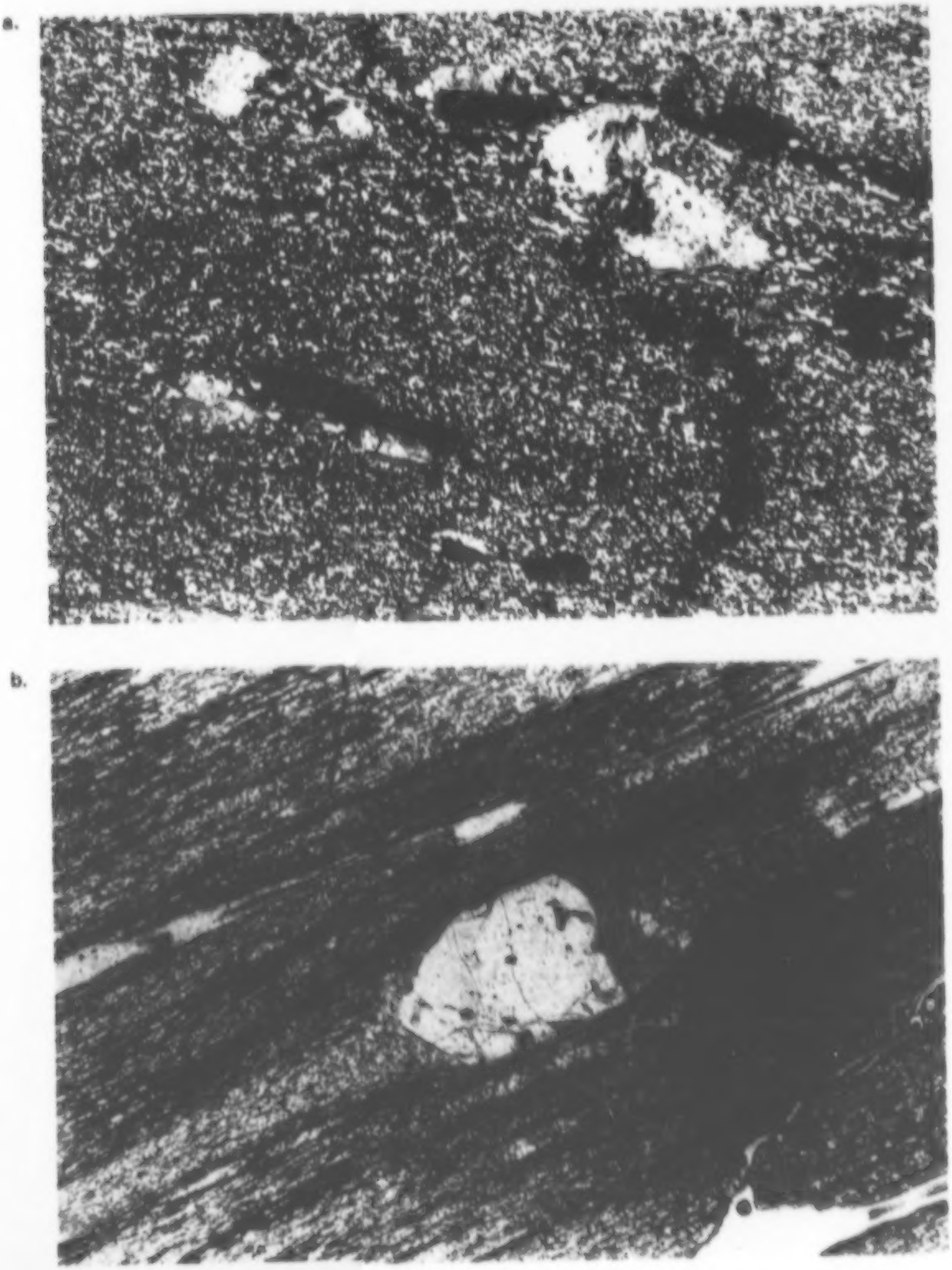

Figure 5. Photomicrographs of Barren Brook schist, showing relict volcanic textures. a) Relict euhedral plagioclase phenocrysts of probable volcanic origin in fine grained felsic horizon interlayered with Dauphinee Brook schist in lower reaches of Faribault Brook. This rock had been interpreted as mylonitized granite, but petrographic observations strongly suggest that it is a deformed felsic tuff. Compare with Sarach Brook and Money Point tuffs, Figure 8b,c (crossed nicols, field of view 10 mm). b) Relict volcanic quartz phenocrysts in a foliated matrix. Despite the strong foliation, the widespread preservation of similar primary features argues against these rocks being mylonitized granites (plane polarized light, field of view 10 mm).

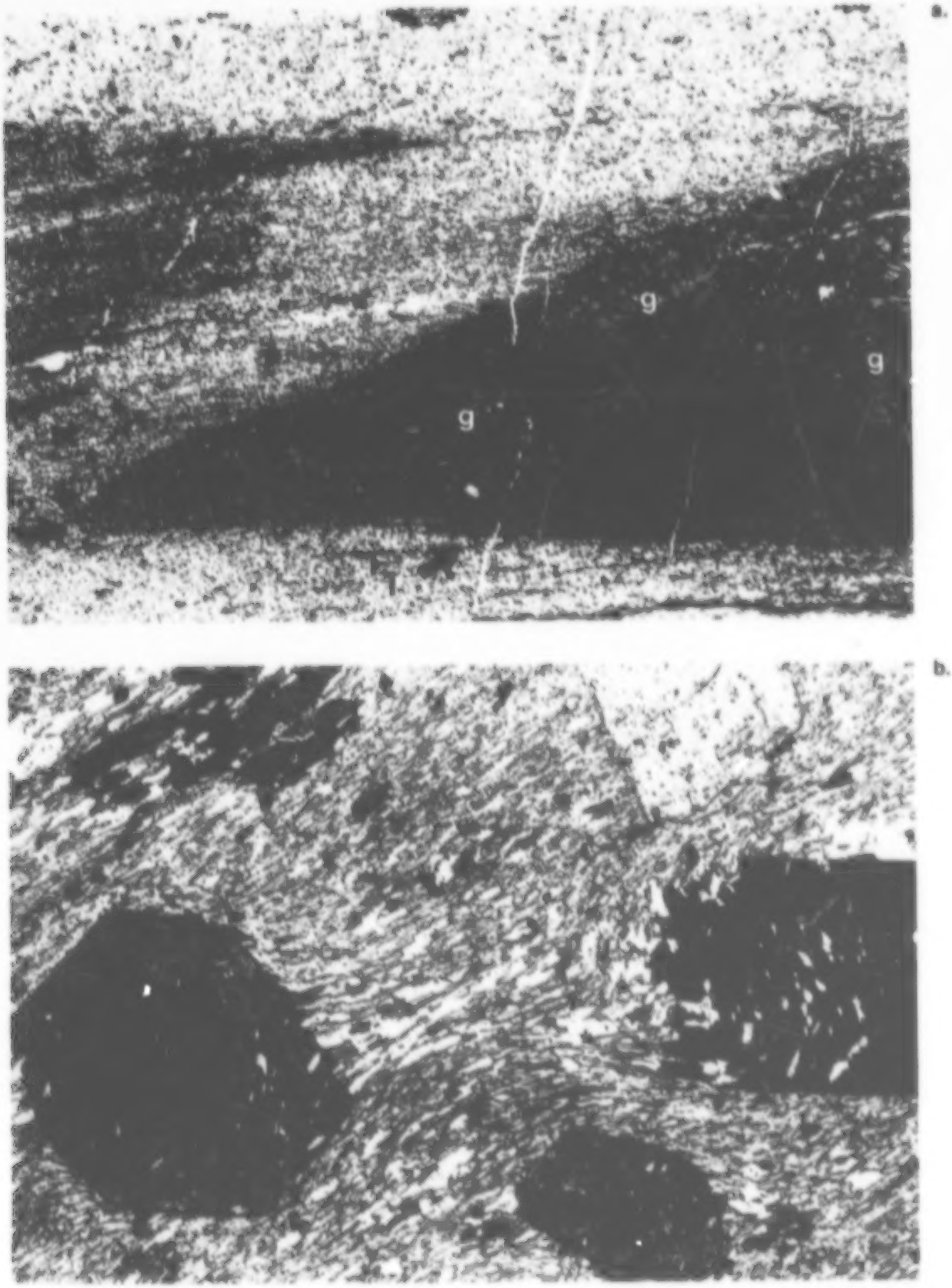

Figure 6. Metamorphic textures in metasedimentary rocks of the Faribault Brook area. Similar relationships are observed throughout the Jumping Brook metamorphic suite (Plint and Jamieson, 1989). a) Complex textures in Dauphinee Brook pelite. The arrow labelled F_1 points to early fold hinge; the main foliation here is S_2, axial planar to the prominent F_2 fold. Garnet porphyroblasts (g) overgrow S_2 (plane polarized light, field of view 10 mm). b) Garnet and biotite porphyroblasts with sigmoidal inclusion trails indicating syntectonic growth. Included fabric is S_1, which is crenulated to form the main matrix fabric, S_2 (plane polarized light, field of view 2.5 mm).

A strong foliation affecting all lithologies is the most prominent fabric in the Faribault Brook area. Field and petrographic observations suggest that in the metasedimentary rocks this is S_2, related to tight to isoclinal folds of a previously folded compositional layering (Fig. 6a). Prograde metamorphic mineral growth occurred during and after the formation of the S_2 foliation (Fig. 6; Plint and Jamieson, 1989).

D_3 deformation produced local tight folds of S_2 and the prominent north-south-trending crenulation lineation characteristic of the Cheticamp River area (Connors, 1986; G. Woods, pers. comm., 1986). This postdated porphyroblast growth (Fig. 7d; Plint and Jamieson, 1989) and was accompanied by retrogression of prograde metamorphic assemblages. It is coaxial with regional-scale north-south-trending antiforms (Conrod, 1984; Craw, 1984; Connors, 1986; Plint, 1987).

Kink bands in the vicinity of Faribault Brook postdate the D_3 crenulation lineation and shear zones, but predate many of the faults in the region. Some retrograde ductile shear zones, quartz veins, and tension gashes with minor sulphides may have formed at about this time. A prominent northeast-southwest-trending fault system is developed, of which the Northeast Margaree Fault Zone is the most important (Fig. 2; Jamieson et al., 1987). The sense of displacement on these faults is not always obvious and may have changed through time, although dextral displacements on the order of several kilometres can be inferred in some places (Jamieson et al., 1987). The age and significance of the numerous small faults within the study area with respect to the Northeast Margaree Fault Zone are not known.

Intense post-Mississippian folding and faulting affected all the rocks along the Gulf of St. Lawrence coast west of the Faribault Brook area. Thrust faults of two different orientations have been documented, as well as normal and strike-slip faults which cut the sequence into slivers in places only a few metres thick (Currie, 1977, 1987b; Barr et al., 1985). This faulting was undoubtedly initiated during the Carboniferous extension that formed the Magdalen Basin (e.g. Bradley, 1982), but the age, geometry, and kinematic history of this complex area have not been investigated in detail.

Metamorphism

A single phase of prograde metamorphic mineral growth produced garnet, chloritoid, biotite, and hornblende porphyroblasts in the Faribault Brook area, with staurolite- and kyanite-bearing assemblages to the north and east (Craw, 1984; Connors, 1986; Currie, 1987a; Plint, 1987; Plint and Jamieson, 1989). Peak metamorphic conditions in the Faribault Brook area probably did not exceed 500°C and 5 kb, whereas near the Jumping Brook metamorphic suite-Pleasant Bay complex transition conditions of 650 to 700°C and 8 to 9 kb have been inferred (Currie, 1987a; Plint and Jamieson, 1989). Porphyroblast growth occurred during the development of S_2 from S_1, and although the porphyroblasts overgrow an early fabric, they are not related to contact metamorphism (Plint, 1987; Plint and Jamieson, 1989). Contact metamorphic effects are restricted to the vicinity of the posttectonic Salmon Pool Pluton, where andalusite, cordierite, and biotite replace porphyroblasts developed during regional metamorphism (Plint and Jamieson, 1989). Regionally developed andalusite, cordierite, and sillimanite were not observed in this study (cf. Chatterjee, 1980; Currie, 1987a,b).

Deformation and metamorphism of sulphides

Several stages of sulphide deposition, involving all the major phases, can be documented through comparison of sulphide textures with the sequence of events established for the regional metamorphism (Fig. 7). These are summarized below.

There is unambiguous evidence of premetamorphic sulphide deposition, in the form of inclusions of sphalerite, arsenopyrite, galena, and chalcopyrite in garnet porphyroblasts that formed during the regional metamorphism (Fig. 7a,b; Connors, 1986). At Galena Mine, sulphide-rich bands are involved in all stages of folding and thus probably formed very early, perhaps during or shortly after deposition of the Barren Brook schist host rocks. Veins that cut compositional layering but are folded by preporphyroblast folds (Fig. 7c) provide additional evidence for sulphide deposition soon after the host rocks were formed.

In metabasites, shear zones commonly host an arsenopyrite-dominated sulphide association. The host rocks have an unusual mineral assemblage including chlorite, biotite, and epidote, with hornblende porphyroblasts that overprint the foliation. The mineral assemblages and textures suggest chemical modification of these rocks prior to the metamorphic peak, with shearing initiated during prograde metamorphism. The arsenopyrite in these rocks forms prominent porphyroblasts, as well as smaller inclusions within garnet (Fig. 7b). Where shearing postdates metamorphism, the arsenopyrite forms porphyroclasts.

Numerous sulphide veins cut both the foliation and porphyroblasts (Fig. 7e). The majority of these are folded by D_3 structures, suggesting that they formed in the waning stages of metamorphism while the rocks were still undergoing ductile deformation. A few undeformed veins, commonly dominated by a very pale honey-brown sphalerite, appear to have formed during the final stages of sulphide deposition.

Extensive retrogression is common in, but not restricted to, the vicinity of the mineral deposits in the Faribault Brook area. This mainly takes the form of chlorite replacing biotite, garnet, hornblende, and chloritoid, and sericite replacing feldspar. Late tourmaline is locally associated with posttectonic sulphide veins, locally resulting in complete replacement of garnet by sulphides (Fig. 7f). These observations suggest that many veins were emplaced under lower greenschist facies conditions, but it is not clear whether this "alteration" is a consequence of regional cooling, or part of a later, unrelated hydrothermal event.

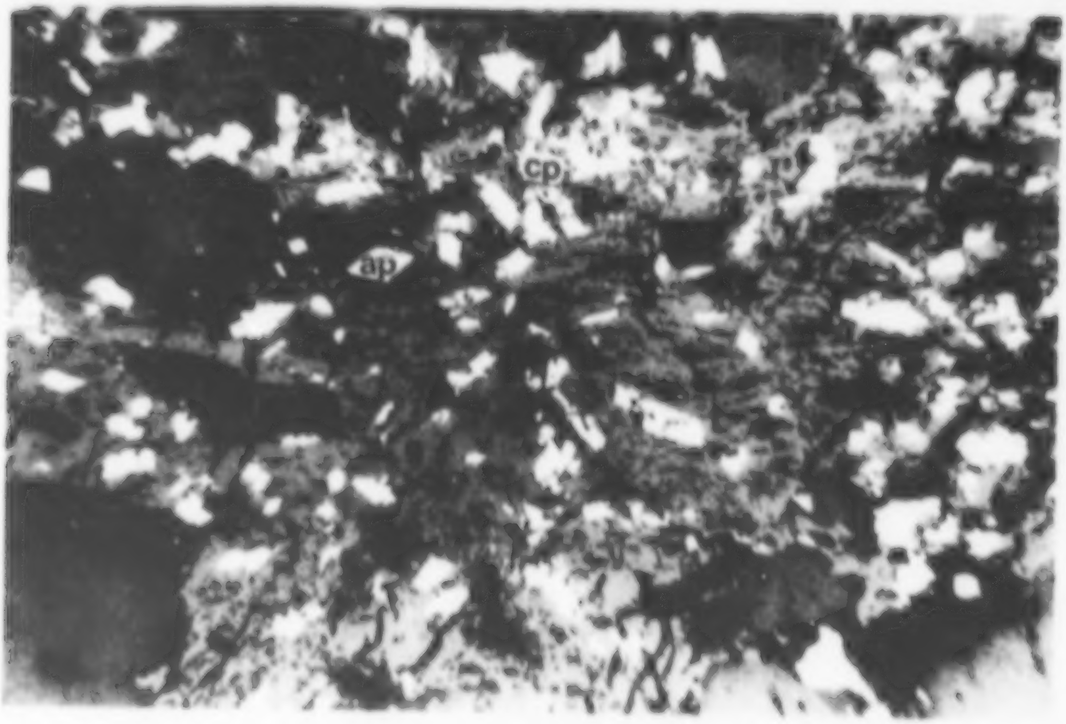

Figure 7. Relationship of sulphides to deformation and metamorphism in the Faribault Brook area. a) Garnet porphyroblast (g) from Galena Mine containing numerous inclusions of arsenopyrite (ap) and chalcopyrite (cp); garnet elsewhere in the same sample also overgrows sphalerite. The garnet is of the same generation as that shown in Fig. 6; the sulphides thus predate the prograde regional metamorphism (reflected light, field of view 2 mm). b) Garnet porphyroblast in metabasite, Highland Mercury drill core, contains inclusions of arsenopyrite, pyrite, and chalcopyrite. Coarse arsenopyrite crystals in the matrix are porphyroblasts that appear to have formed at the same time as the garnet (plane polarized light, field of view 2.5 mm). c) Deformed sulphide band is oblique to bedding (centre left to lower right) but is folded by F_2 (horizontal axial surface); it thus represents a postdeposition, premetamorphic vein (plane polarized light, field of view 15 mm). d) F_3 crenulations (upper left to centre) affecting F_2 fold and S_2 foliation, Dauphinee Brook schist. Sulphide vein cuts F_2 but is folded by F_3 (centre right). Sulphides in folded layer in lower left are associated with a pre-F_2 quartz vein (plane polarized light, field of view 10 mm). e) Late folding (F_3) of sulphide vein, Dauphinee Brook schist. Vein cuts garnet porphyroblast, and is thus post-S_2, and has been affected by post-F_2 flattening that has tightened up the S_2 foliation (plane polarized light, field of view 10 mm). f) Posttectonic sulphides replacing garnet porphyroblasts (lower half of photo); relict garnet (g) largely replaced by chlorite. Tourmaline sprays (for example, at "t") replace plagioclase and overgrow matrix chlorite (plane polarized light, field of view 10 mm).

Figure 7. continued

b.

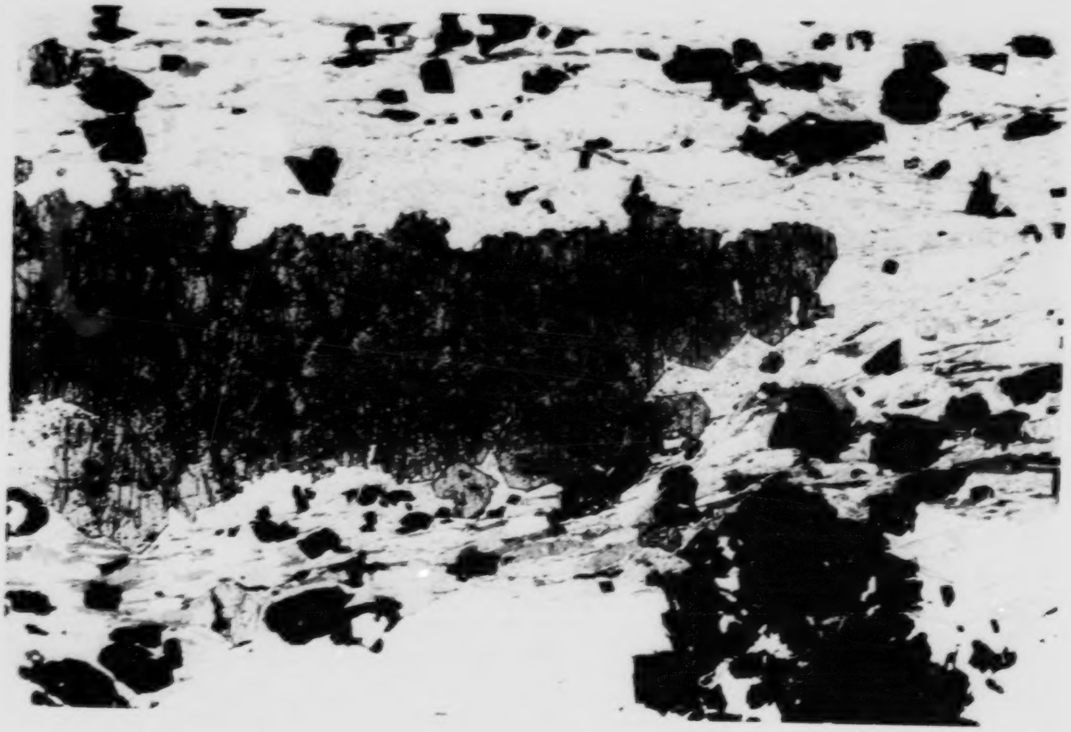

c.

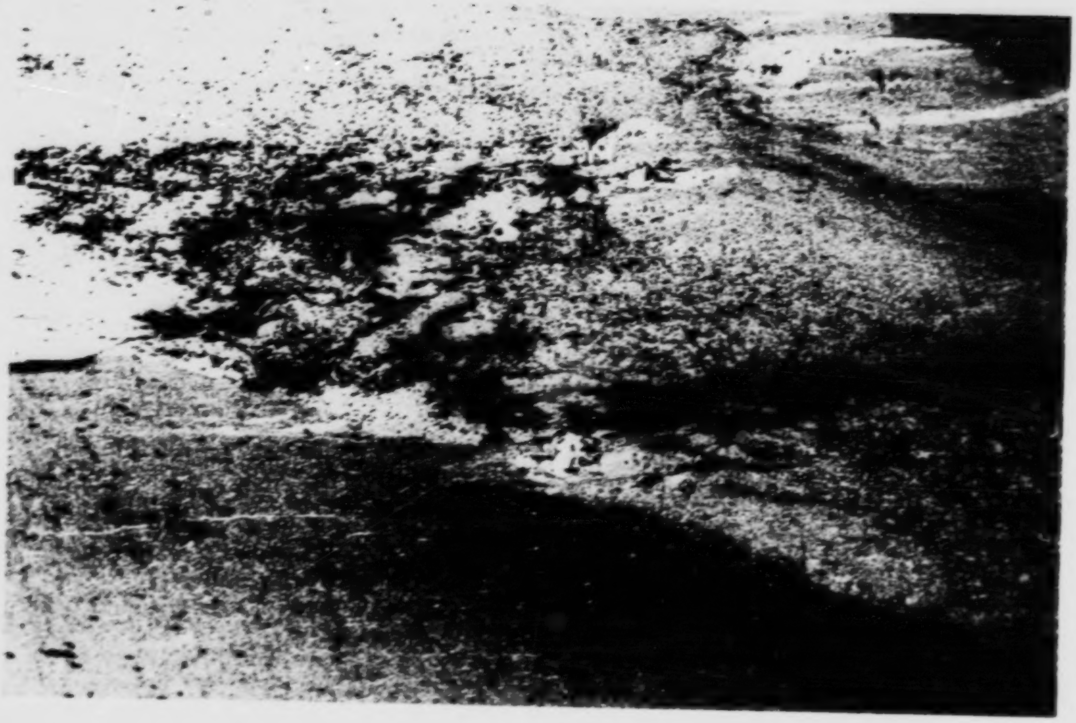

Figure 7. continued

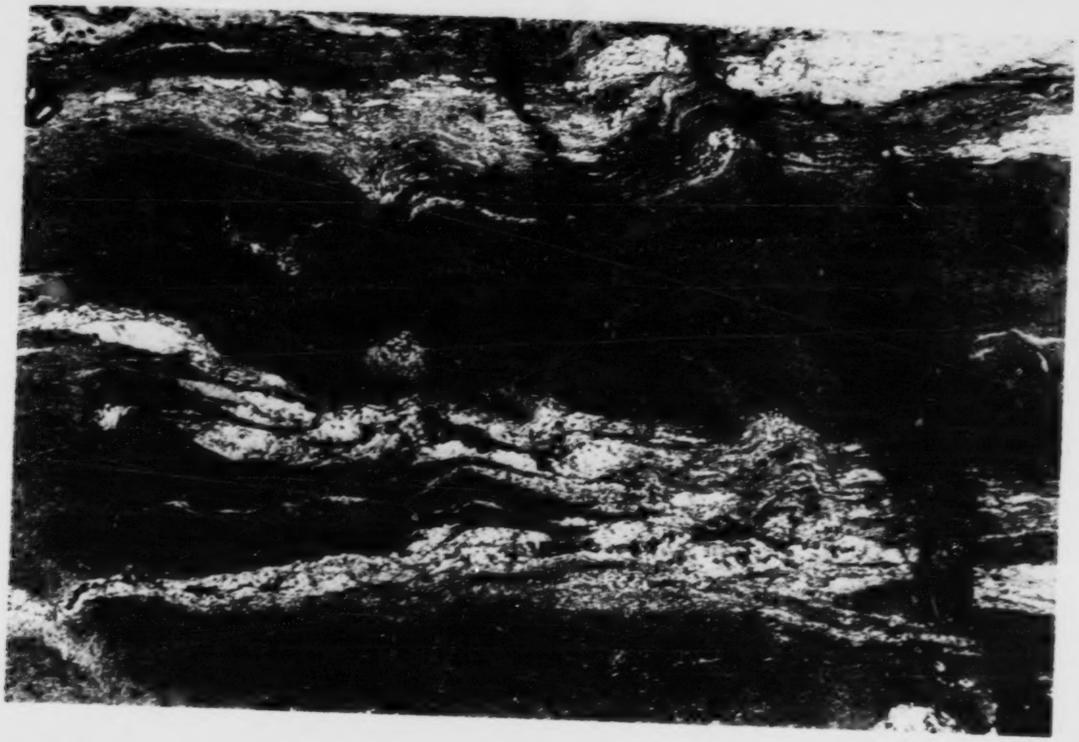

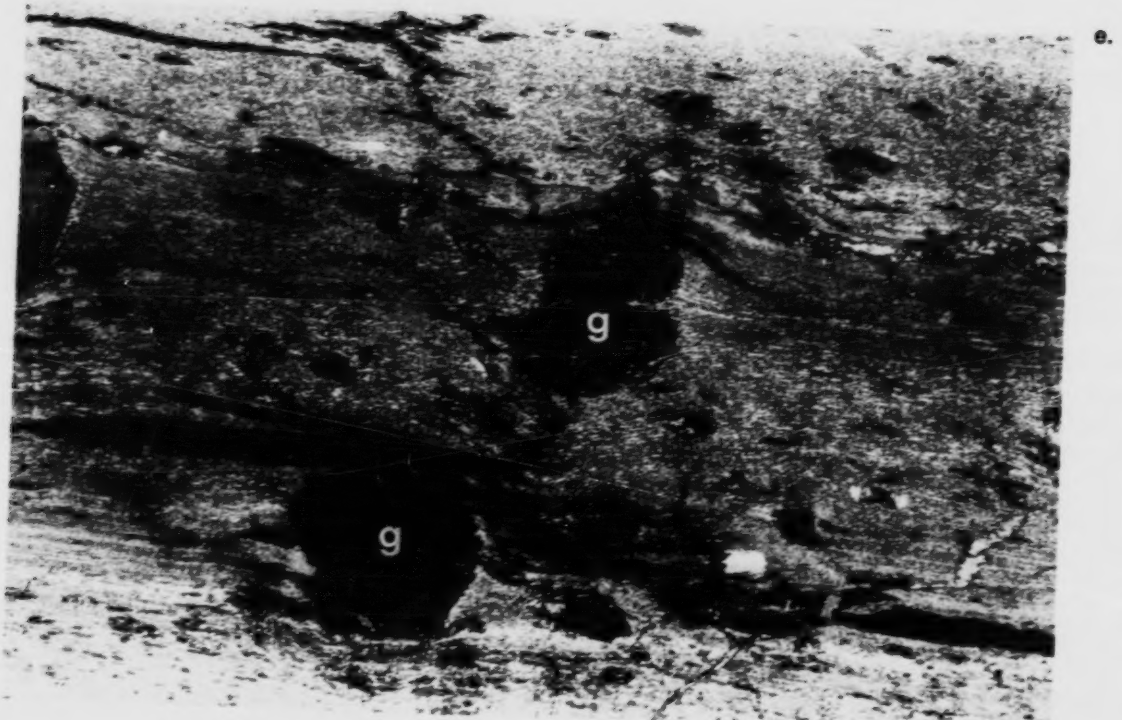

Figure 7. continued

f.

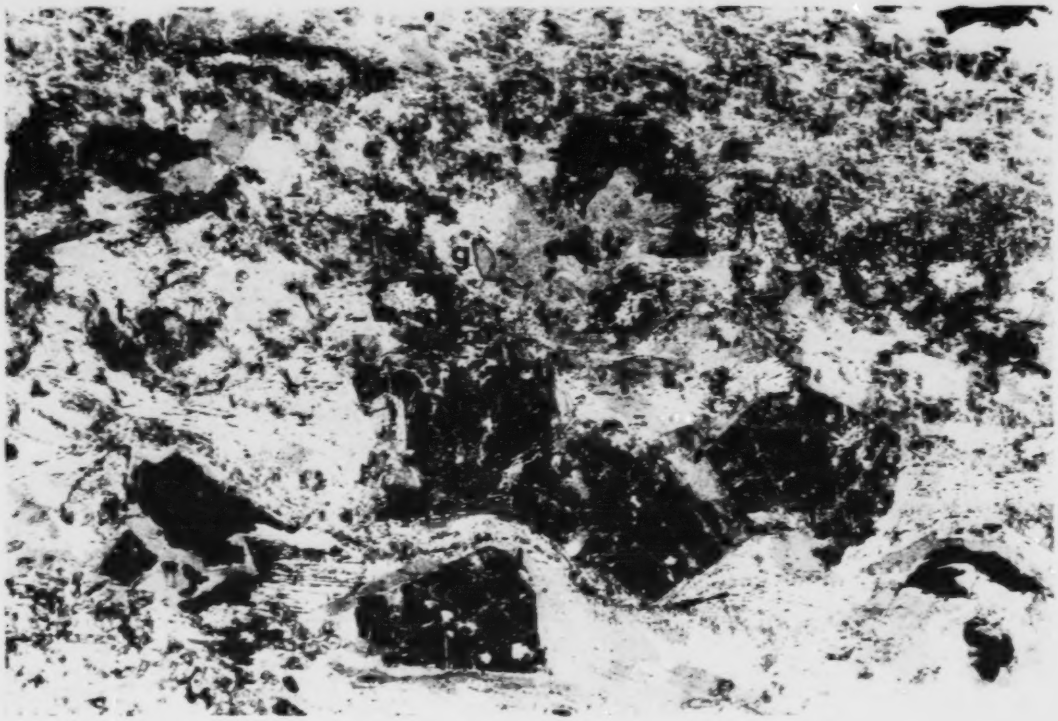

AGE

Age of the Cheticamp Pluton

The Cambrian age of this granodiorite to monzogranite pluton has been established by a U-Pb (zircon) date of 550 ± 8 Ma (Jamieson et al., 1986), two Rb-Sr isochrons (Cormier, 1972; Barr et al., 1986), and a ^{40}Ar/^{39}Ar muscovite cooling age of 545 Ma (Reynolds et al., 1989). It is not penetratively deformed where best studied south of the Cheticamp River (Barr et al., 1986), although its extension north of the Cheticamp River is strongly sheared and locally mylonitized (Currie, 1987b; Plint, 1987). Currie (1982, 1987b) suggested that the pluton intruded the Pleasant Bay complex but is overlain by the Jumping Brook rocks. Although Jamieson et al. (1987) could not confirm an intrusive relationship between the Cheticamp Pluton and the Pleasant Bay complex, they also concluded that it is older than the metamorphic rocks of the Faribault Brook area. Both interpretations are incompatible with the models proposing a genetic relationship between pluton emplacement and mineralization in the Faribault Brook area (cf. G. Woods, pers. comm., 1986).

Age of the Jumping Brook metamorphic suite

Currie (1982, 1987b) suggested an Ordovician-Silurian age for the Jumping Brook metamorphic suite, based on a presumed unconformity between these rocks and the Pleasant Bay complex and a date on a rhyolite dyke inferred to feed the felsic volcanic rocks (Currie et al., 1982). Although the presence of an unconformity has been disputed (e.g. Conrod, 1984; Craw, 1984; Plint et al., 1986; Plint, 1987), Jamieson et al. (1987) agreed with this age, because granite boulders resembling the Cheticamp Pluton occur in metaconglomerate near the base of the Barren Brook schist. Although the rocks in the Faribault Brook area have yet to yield a stratigraphic age, a U-Pb (zircon) date on rhyolitic tuff from the correlative Sarach Brook volcanic rocks in the southern Cape Breton Highlands (Fig. 1 and 8b; Jamieson and Craw, 1983; Jamieson and Doucet, 1983) indicates a primary age of 434 +7/-4 Ma (Dunning et al., in press).

Age of deformation and metamorphism

A number of lines of evidence suggest Acadian (Late Silurian-Early Devonian) deformation and metamorphism of the Jumping Brook metamorphic suite (Plint and Jamieson, 1989). Clearly, deformation and metamorphism can be no older than the age of the rocks, about 434 Ma. A further constraint on the timing of tectonism is provided by the zircon date of 433 ± 20 Ma on the syntectonic Belle Cote Road orthogneiss (Jamieson et al., 1986); concordant titanite from the same outcrop has yielded a U-Pb age of about 386 Ma (G. Dunning, pers. comm., 1989) which probably corresponds to the age of amphibolite facies metamorphism. Hornblende and biotite from the area between the Cheticamp River and Pleasant Bay have yielded Early Devonian ^{40}Ar/^{39}Ar cooling ages between 387 and 379 Ma, indicating very rapid postmetamorphic cooling, probably related to tectonic exhumation (Plint, 1987; Plint and Jamieson, 1989; Reynolds et al., in press). By the time of intrusion of the subvolcanic Salmon Pool Pluton at 365 Ma (Jamieson et al., 1986), the Jumping Brook metamorphic suite was within 10 km of the surface (Plint and Jamieson, 1989).

Age of mineral deposits

The pretectonic Cu-Pb-Zn sulphide deposits associated with the Barren Brook schist presumably formed during or soon after deposition of their Silurian host rocks at about 434 Ma, and before the metamorphic peak at about 400 Ma (Plint and Jamieson, 1989). The time of formation of postmetamorphic sulphide veins and minor replacement deposits associated with tourmaline is not well constrained; these could have formed during mid-Devonian regional cooling and uplift or be related to the younger Salmon Pool Pluton.

REGIONAL CORRELATIONS

Cape Breton

The Jumping Brook metamorphic suite is part of a belt of metavolcanic and metasedimentary rocks that extends through the west-central Cape Breton Highlands from Cape North to Middle River and southwest into the Mabou Highlands (Fig. 1; Barr et al., 1985). These rocks and associated plutons and gneisses are characteristic of the Aspy Terrane, one of four pre-Carboniferous tectonostratigraphic zones recognized in Cape Breton Island (Fig. 1; Barr and Raeside, 1986, 1989; Dunning et al., in press; Reynolds et al., in press). The Aspy Terrane is bounded on the east by late Precambrian to Cambrian dioritic and granitic rocks of the Bras d'Or Terrane (Fig. 1; Barr et al., 1988; Barr and Raeside, 1989; Dunning et al., in press; Raeside and Barr, in press), on the northwest by Grenvillian metaplutonic rocks and gneisses of the Blair River Complex (Barr et al., 1987b), and on the southwest by Cambrian and older granite, diorite, and gneiss which may be related to the Bras d'Or Terrane (Dunning et al., in press; Reynolds et al., 1989).

Similar suites of volcanic and metamorphic rocks occur in the Aspy Terrane of the northern and southern Cape Breton Highlands (Money Point Group, Macdonald and Smith, 1980; Sarach Brook-Middle River metamorphic suite, Jamieson and Doucet, 1983) and the Mabou Highlands (Mabou Highlands complex, Barr and Macdonald, 1989). These rocks are characterized by a similar lithological sequence — lower metabasites, overlain by silicic schists derived from pyroclastic and rhyolitic rocks, followed by metasedimentary rocks. Felsic volcanic rocks, including ash flow and crystal-lithic tuffs and minor flow-banded rhyolite (Fig. 8), dominate the upper part of the sequence in the Sarach Brook region; the relative proportion of silicic volcanic rocks dies out northward, with metatuffs, volcanogenic metasedimentary rocks, and clastic metasedimentary rocks dominant elsewhere. Despite the intense deformation, the overall character of the rocks suggests that they originally represented a felsic volcanic pile constructed on a mafic volcanic base, centred on the Sarach Brook region, and interfingering with sedimentary rocks on its margins. The volcanism appears to have been mainly submarine, judging by the character of the associated sedimentary rocks throughout the belt, and the presence of possible relict pillow structures in the Faribault Brook area (Connors, 1986). However, the volcanic centre in the Sarach Brook region may have been subaerial. Crystal tuffs from the upper part of the Sarach Brook volcanic rocks (Fig. 8b) have yielded a U-Pb (zircon) date of 434 +7/-4 Ma (Dunning et al., in press). The volcanic-sedimentary sequence is thus Early Silurian, as suggested by Currie (1982), although the lower parts probably extend into the Ordovician.

The metasedimentary and metavolcanic rocks are associated with high-grade metamorphic rocks (Cape North Group, Pleasant Bay complex, Middle River metamorphic suite, Mabou Highlands complex); metamorphic grade increases toward the core of the highlands in each region. The relationships between the lower and higher grade rocks are complex, owing to tectonized transition zones (Craw, 1984; Marcotte, 1987) and to a significant orthogneissic component in the high-grade rocks which results in locally crosscutting contacts (Jamieson et al., 1987). However, Plint (1987) demonstrated a continuous progression from low- to high-grade rocks in the area between the Cheticamp River and Pleasant Bay; a similar conclusion was reached by Doucet (1983) for the Middle River area. Plint (1987) compared the metamorphic histories of the Sarach Brook-Middle River and Money Point-Cape North areas with the Jumping Brook-Pleasant Bay region, and found very similar metamorphic and structural patterns, although different mineral assemblages occur locally.

Northern Nova Scotia

In northern mainland Nova Scotia, Silurian bimodal volcanic rocks at Arisaig (Keppie et al., 1978) are approximately the same age as the Aspy Terrane volcanic rocks. The Dunn Point volcanic rocks, which have an alkaline to transitional geochemical character and occur with shallow water sedimentary rocks, have been interpreted as a "within plate" volcanic complex, probably deposited in an extensional environment (Keppie et al., 1978). These rocks and possible equivalents in the Cobequid Highlands (Murphy et al., 1988) escaped the complex Silurian to Devonian deformation and metamorphism that affected the western Cape Breton Highlands. Their original tectonic setting and position relative to the Aspy Terrane volcanic belt is not clear at present.

Newfoundland

Geological, geochronological, and geophysical data strongly suggest that the tectonostratigraphic terranes recognized in Cape Breton can be traced into southwestern Newfoundland (Raeside and Barr, 1988; Dunning et al., in press; Loncarevic et al., in press; Reynolds

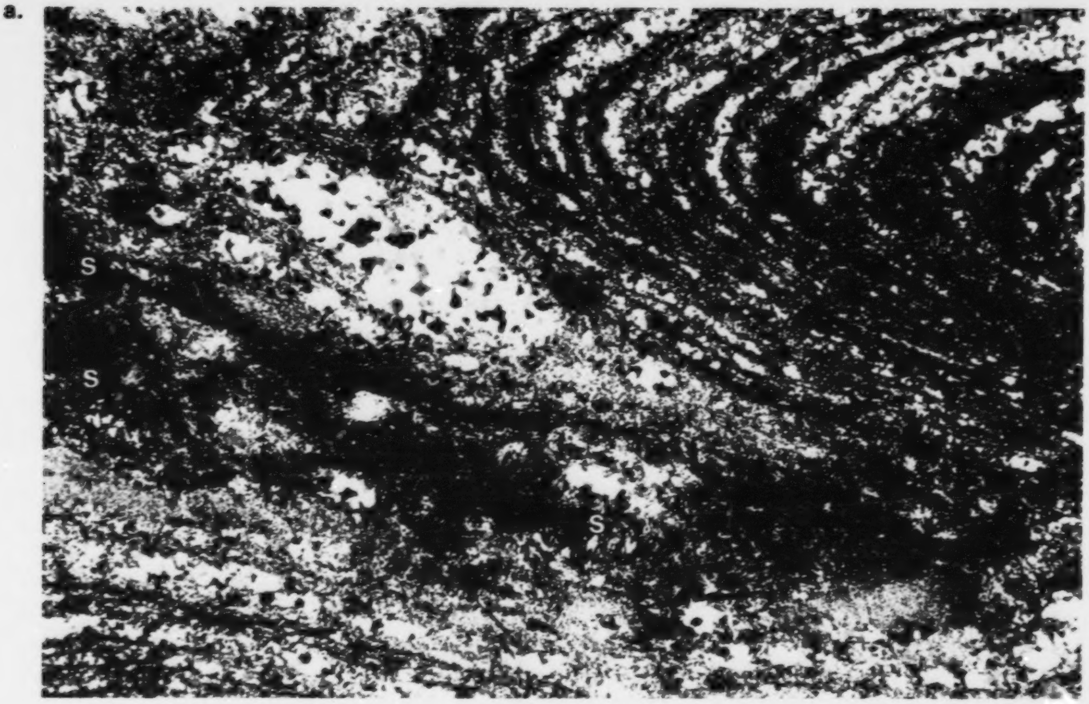

Figure 8. Aspy Terrane volcanic rocks correlative with the felsic members of the Jumping Brook metamorphic suite. a. Deformed flow-banded rhyolite, Sarach Brook volcanic rocks, south-central Cape Breton Highlands (Jamieson and Doucet, 1983). Banding in upper right is deformed flow banding; spherulites (s) are preserved in band running through centre of photo (crossed nicols, field of view 14 mm). b. Foliated crystal tuff, Sarach Brook volcanic rocks, south-central highlands (Jamieson and Doucet, 1983). Note similarity of texture to Barren Brook schist (Fig. 5) and to Money Point tuff (Fig. 8c). Metamorphic garnet (g) overgrows the foliation; identical textures have been observed from felsic horizons in the Faribault Brook area. This sample is from the outcrop that yielded a U-Pb (zircon) date of 434 +7/-4 Ma (Dunning et al., in press) (plane polarized light, field of view 8 mm). c. Foliated crystal tuff, Money Point Group, northern highlands (Macdonald and Smith, 1980). Note textural similarity to Barren Brook schist (Fig. 5) and Sarach Brook tuff (Fig. 8b). A sample from this unit has yielded an Early Silurian U-Pb (zircon) date (T. Krogh, pers. comm., 1986) (crossed nicols, field of view 8 mm).

et al., 1989). Silurian volcanic rocks are common in central Newfoundland, notably in the Springdale and LaPoile regions (e.g. Chandler and Dunning, 1983; Dunning et al., 1986; Chandler et al., 1987; Coyle and Strong, 1987; Dunning et al., 1988). Subaerial Silurian rhyolites and related rocks in the LaPoile area are possibly correlative with the volcanic rocks of the Aspy Terrane (Chorlton, 1983; Dunning et al., in press), and both regions underwent high-grade metamorphism in Late Silurian to Early Devonian times. Raeside and Barr (1988) and Barr and Raeside (1989) documented other similarities between the LaPoile area and the Aspy and Bras d'Or terranes, including the presence of late Precambrian rocks to the southeast (e.g. Dunning and O'Brien, 1989), separated from the Silurian rocks by a major shear zone.

The Springdale Group and its equivalents comprise a calc-alkaline suite ranging from basalts to high silica rhyolites (Coyle and Strong, 1987); it is almost exactly the same age as the Aspy Terrane volcanic rocks (Coyle and Strong, 1988). The geochemistry is also broadly similar, although intermediate volcanic rocks are poorly represented in the Aspy Terrane. In Newfoundland, the Springdale Group and its equivalents have been regarded as postorogenic overlap assemblages (Chandler et al., 1987; Coyle and Strong, 1987), although Silurian metamorphism and deformation were widespread in southern and central Newfoundland (Dunning et al., 1988).

Regional tectonic models

Stockmal et al. (1987) proposed a tectonic model for the Ordovician to Devonian development of the Canadian Appalachians in which collision of an island arc with the

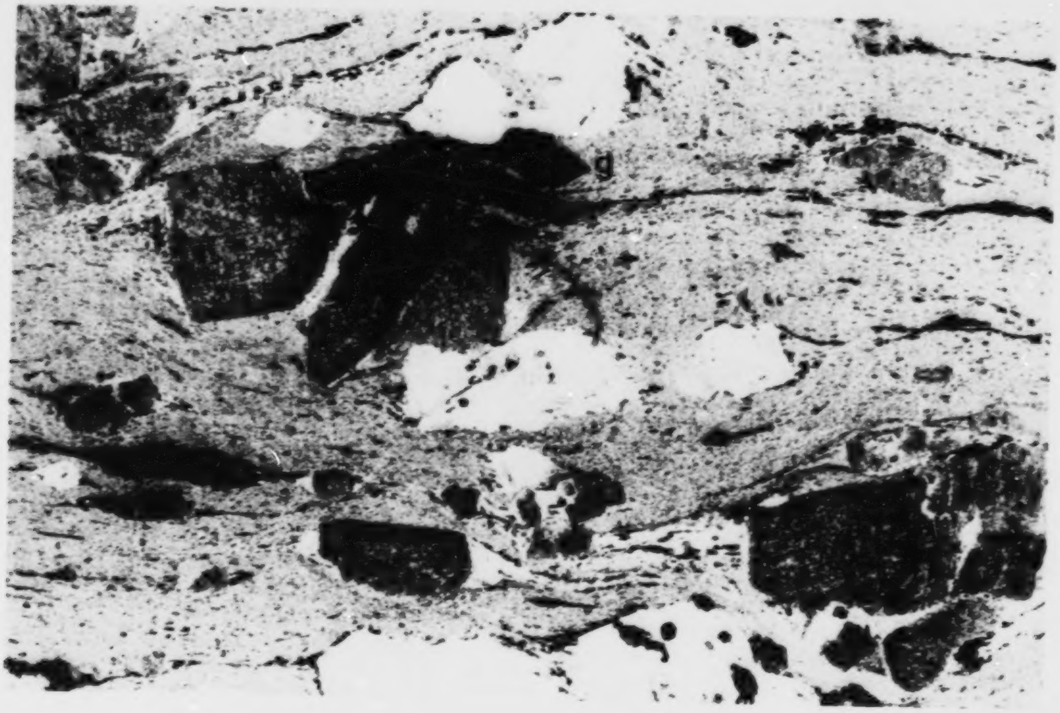

b.

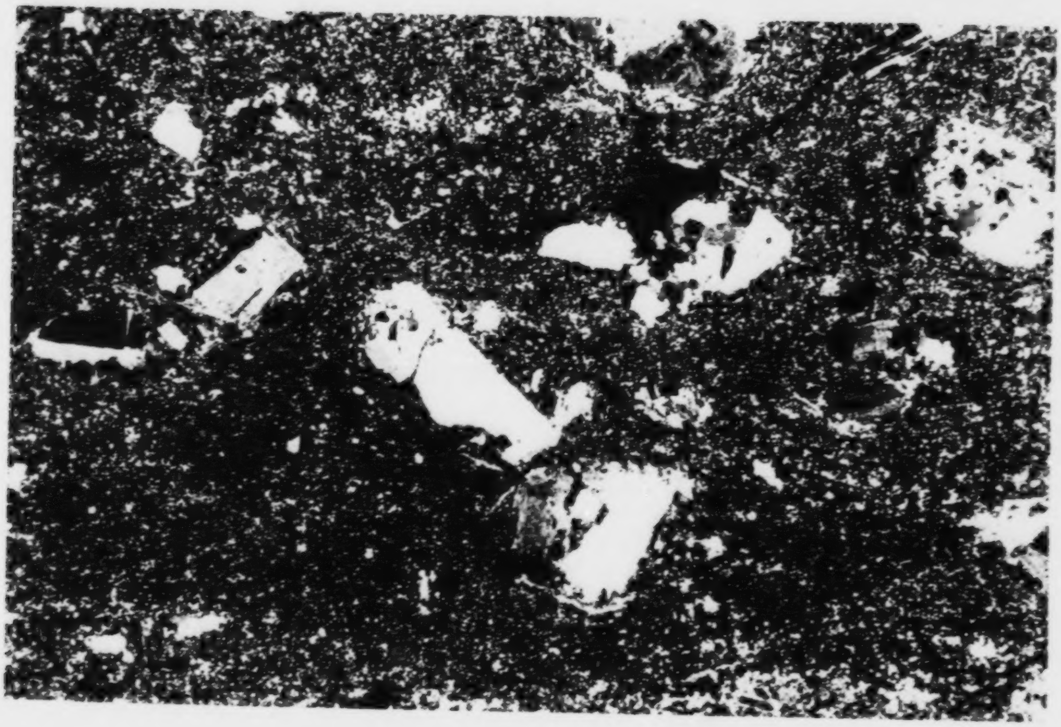

c.

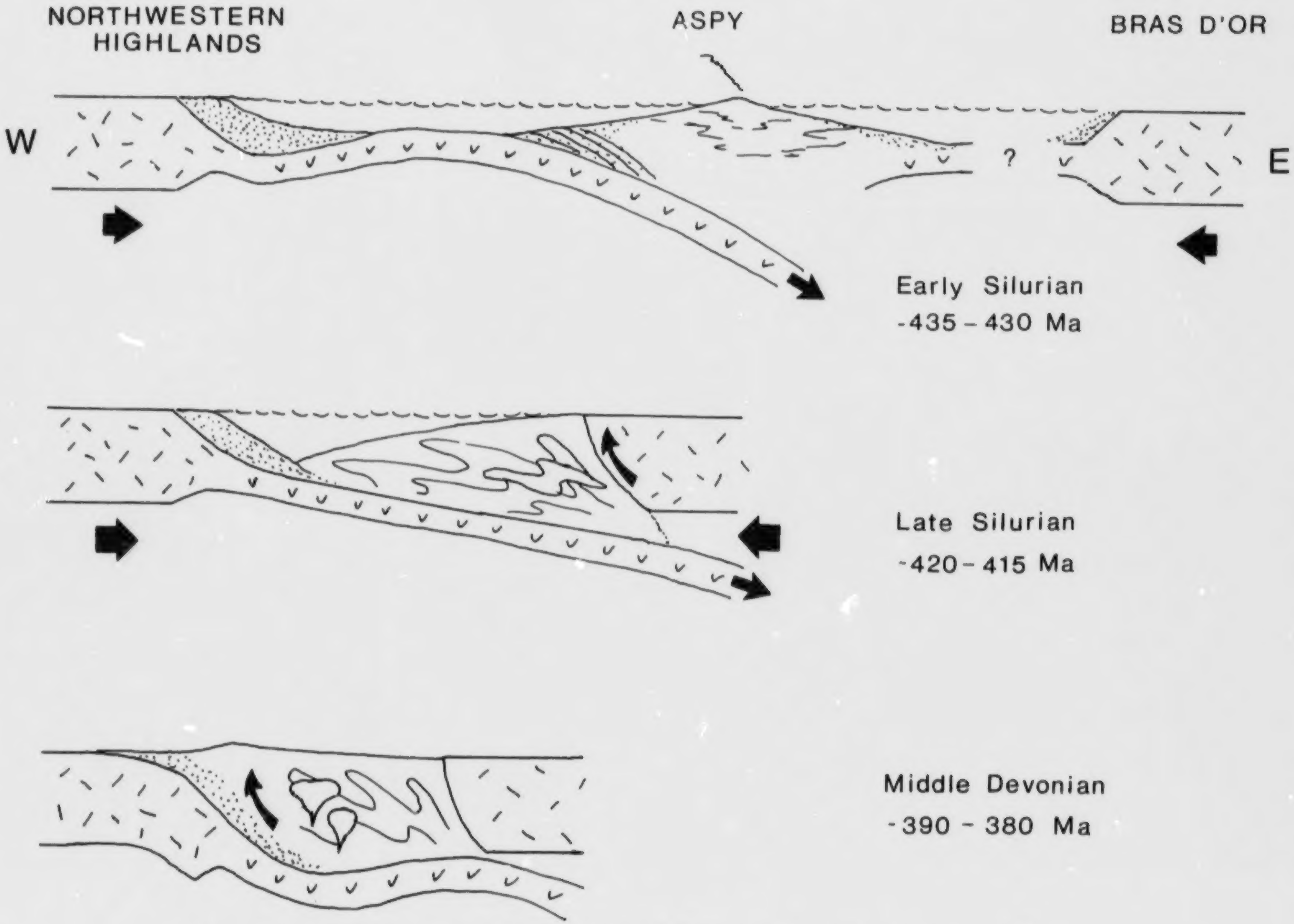
NORTHWESTERN HIGHLANDS
ASPY
BRAS D'OR
W
E
?
Early Silurian
-435 - 430 Ma
Late Silurian
-420 - 415 Ma
Middle Devonian
-390 - 380 Ma

Figure 9. Cartoon illustrating possible tectonic setting for deposition of Jumping Brook metamorphic suite protoliths. For further information, see Stockmal et al. (1987) and Loncarevic et al. (in press).

irregular continental margin of North America during the Taconian Orogeny resulted in incomplete closure of the Iapetus Ocean. In Newfoundland, lithospheric delamination after oceanic closure resulted in Silurian postorogenic volcanism and plutonism, although significant metamorphism and deformation continued in much of the area (Dunning et al., 1988). South of Newfoundland, subduction of oceanic crust continued through the Silurian until collision was completed during the Acadian Orogeny. This model is consistent with the available data from the Jumping Brook metamorphic suite and adjacent rocks, and explains contrasts between the Silurian geology of north-central Newfoundland and Cape Breton.

In this tectonic context, the Jumping Brook metamorphic suite represents a volcanic-sedimentary pile formed close to a Late Ordovician to Silurian subduction zone, which underwent Devonian deformation and high-grade metamorphism in response to Late Silurian to Devonian collision with North America (Fig. 9). Rapid exhumation (Plint and Jamieson, 1989) resulted from thrusting of the Jumping Brook metamorphic suite over the North American margin. The convergent orogenic setting explains the relatively short time span between deposition, metamorphism, and uplift of these rocks, which occurred within about 50 million years.

The tectonic contacts and contrasting age and tectonothermal histories (Reynolds et al., in press) of the Cheticamp Pluton and the Jumping Brook metamorphic suite strongly suggest that they were juxtaposed at a late stage in the accretion of the Jumping Brook metamorphic suite to the eastern Appalachians. However, the Cheticamp Pluton or similar granite was shedding detritus into the Barren Brook schist during the Silurian. The change to felsic volcanism may have coincided with the approach of the Jumping Brook protoliths to a continental margin. The very complex structural relationships between the Cheticamp Pluton and the Jumping Brook metamorphic suite between Pleasant Bay and Cheticamp suggest that the present disposition of these rocks is related to Carboniferous faulting.

IMPLICATIONS FOR MINERAL DEPOSITS

Faribault Brook

This regional study has shown that premetamorphic As-Zn-Pb-Cu deposits are present in the area, particularly associated with felsic tuffs and silicic metasedimentary rocks directly overlying the Faribault Brook metavolcanic rocks. The concentration of deposits in the Faribault Brook area appears to be related to two factors — a regional stratigraphic control related to the interfingering of mafic metavolcanic rocks and metasedimentary rocks with the distal part of a felsic volcanic pile, and the structural and hydrothermal reworking of these deposits in a short-lived but intense metamorphic episode. The stratigraphic situation is unique in the Aspy Terrane; other areas have either higher proportions of felsic volcanic rocks, which in general have very low metal concentrations, or lack significant thicknesses of turbiditic metasedimentary rocks.

Despite the occurrence of correlative units elsewhere in the Aspy Terrane, the Faribault Brook area contains the majority of documented mineral occurrences. However, significant Au and W occurrences have been described from the Sarach Brook region, where they are particularly associated with shear zones. The Eastern Highlands shear zone, which forms the boundary between the Aspy and Bras d'Or terranes, is currently the site of a major exploration effort. This shear zone occupies the same tectonic position as the Cinq Cerf fault zone associated with the Hope Brook gold deposit in Newfoundland (Raeside and Barr, 1988).

CONCLUSIONS

The most important conclusions arising from the regional geological study include the following:

1) The Jumping Brook metamorphic suite is a Silurian volcanic complex, as originally suggested by Currie (1982, 1987b). It is faulted against the Cambrian Cheticamp Pluton on the west, and grades into gneisses of the Pleasant Bay complex on the east. Six mappable units have been identified on a regional scale, of which the most important in the study area are the Faribault Brook metavolcanic rocks, the Barren Brook schist, and the Dauphinee Brook schist.

2) The volcanic rocks probably originated in an oceanic island arc setting, and underwent Devonian deformation, amphibolite facies metamorphism, and rapid cooling as a result of collision with North America.

3) The mineral deposits of the Faribault Brook area include some premetamorphic Cu-Pb-Zn sulphide occurrences associated with the distal part of a felsic volcanic pile where it interfingers with mafic metabasalts and turbiditic metasedimentary rocks. Syntectonic and posttectonic sulphide associations are also present. The geometry and the distribution of the sulphide bodies have been extensively modified by polyphase deformation.

ACKNOWLEDGMENTS

This project has been done under the auspices of the Canada-Nova Scotia Mineral Development Agreement through a contract from the Department of Energy, Mines and Resources to R.A. Jamieson and M. Zentilli. Further financial support has been provided by the Natural Sciences and Engineering Research Council and Dalhousie University. The work has benefitted greatly from discussions in the field with G. Woods (Selco-BP) and A. Sangster (GSC). Numerous discussions over many years with S. Barr, R. Raeside, A. Macdonald, D. Craw, K. Currie, B. Poole, and others, and the work of students at Dalhousie University including J. Marcotte, D. Conrod, S. Dudka, and P. Doucet, have contributed to the regional interpretations presented here.

REFERENCES

Barr, S.M. and Macdonald, A.S.

1989: Geology of the Mabou Highlands; Nova Scotia Department of Mines and Energy, Paper 89-2, 65 p.

Barr, S.M. and Raeside, R.P.

1986: Pre-Carboniferous tectonostratigraphic subdivisions of Cape Breton Island, Nova Scotia; Maritime Sediments and Atlantic Geology, v. 22, p. 252-263.

1989: Tectono-stratigraphic terranes in Cape Breton Island, Nova Scotia: implications for the configuration of the Northern Appalachian orogen; Geology, v. 17, p. 822-825.

Barr, S.M., Jamieson, R.A., and Raeside, R.P.

1985: Igneous and metamorphic geology of the Cape Breton Highlands; Geological Association of Canada-Mineralogical Association of Canada, 1985 Field Guide, Excursion 10, 48 p.

Barr, S.M., Macdonald, A.S., and Blenkinsop, J.

1986: The Cheticamp Pluton: a Cambrian granodioritic intrusion in the western Cape Breton Highlands, Nova Scotia; Canadian Journal of Earth Sciences, v. 23, p. 1686-1699.

Barr, S.M., Raeside, R.P., Dunning, G.R., and Jamieson, R.A.

1988: New U-Pb ages from the Cape Breton Highlands and correlations with southern Newfoundland; Geological Association of Canada-Mineralogical Association of Canada, Program with Abstracts, v. 13, p. A5.

Barr, S.M., Raeside, R.P., and Jamieson, R.A.

1987a: Geological map of the igneous and metamorphic rocks of northern Cape Breton Island, Nova Scotia; Geological Survey of Canada, Open File 1594, 1:50 000 Maps.

Barr, S.M., Raeside, R.P., and van Breemen, O.

1987b: Grenvillian basement in the northern Cape Breton Highlands, Nova Scotia; Canadian Journal of Earth Sciences, v. 24, p. 992-997.

Blanchard, M.C., Jamieson, R.A., and More, E.B.

1984: Late Devonian-Early Carboniferous volcanism in western Cape Breton Island, Nova Scotia; Canadian Journal of Earth Sciences, v. 21, p. 762-774.

Bradley, D.C.

1982: Subsidence in late Paleozoic basins in the northern Appalachians; Tectonics, v. 1, p. 107-123.

Chandler, F.W. and Dunning, G.R.

1983: Fourfold significance of an Early Silurian U-Pb zircon age from rhyolite in redbeds, southwest Newfoundland, NTS 12 A/4; *in* Current Research, Part B, Geological Survey of Canada, Paper 83-1B, p. 419-421.

Chandler, F.W., Sullivan, R.W., and Currie, K.L.

1987: The age of the Springdale Group, western Newfoundland, and correlative rocks — evidence for a Llandovery overlap assemblage in the Canadian Appalachians; Transactions of the Royal Society of Edinburgh: Earth Sciences, v. 78, p. 41-49.

Chatterjee, A.K.

1980: Mineralization and associated wall rock alteration in the George River Group, Cape Breton Island, Nova Scotia; Ph.D. thesis, Dalhousie University, Halifax, Nova Scotia, 197 p.

Chorlton, L.B.

1983: Geological development of the southern Long Range mountains, southwest Newfoundland: a regional synthesis; Ph.D. thesis, Memorial University of Newfoundland, St. John's, 581 p.

Connors, K.A.

1986: Relationships between the sulphide minerals, metamorphism, and deformation in the Faribault Brook area of the Cape Breton Highlands, Nova Scotia; B.Sc. thesis, Dalhousie University, Halifax, Nova Scotia, 105 p.

Conrod, D.M.

1984: The relationship between low and high grade metamorphic rocks in the French Mountain area, Cape Breton Highlands, Nova Scotia; B.Sc. thesis, Dalhousie University, Halifax, Nova Scotia, 214 p.

Cormier, R.F.

1972: Radiometric ages of granitic rocks, Cape Breton Island, Nova Scotia; Canadian Journal of Earth Sciences, v. 9, p. 1074-1085.

Covey, G.

1979: Report on the Cheticamp Project, Amax Minerals Exploration Limited; Nova Scotia Department of Mines and Energy Assessment File 11K/10B, 7-J-09 (48).

Coyle, M.L. and Strong, D.F.

1987: Geology of the Springdale Group: a newly recognized Silurian epicontinental-type caldera in Newfoundland; Canadian Journal of Earth Sciences, v. 24, p. 1135-1148.

1988: Tectonic setting and control of Silurian calderas and associated plutons in western Newfoundland and Scotland; Geological Association of Canada-Mineralogical Association of Canada, Program with Abstracts, v. 13, p. A27.

Craw, D.

1984: Tectonic stacking of metamorphic zones in the Cheticamp River area, Cape Breton Highlands, Nova Scotia; Canadian Journal of Earth Sciences, v. 21, p. 1229-1244.

Currie, K.L.

1975: Studies of granitoid rocks in the Canadian Appalachians; *in* Report of Activities, Part A, Geological Survey of Canada Paper 75-1A, p. 265-270.

1977: A note on post-Mississippian faulting in northwestern Cape Breton Island; Canadian Journal of Earth Sciences, v. 14, p. 2937-2941.

1982: Paleozoic supracrustal rocks near Cheticamp, Nova Scotia; Maritime Sediments and Atlantic Geology, v. 18, p. 94-103.

1987a: Contrasting metamorphic terranes near Cheticamp, Cape Breton Highlands, Nova Scotia; Canadian Journal of Earth Sciences, v. 24, p. 2422-2435.

1987b: Relations between metamorphism and magmatism near Cheticamp, Cape Breton Island, Nova Scotia; Geological Survey of Canada, Paper 85-23, 66 p.

Currie, K.L., Loveridge, W.D., and Sullivan, R.W.

1982: A U-Pb age on zircon from dykes feeding the Jumping Brook complex, northwestern Cape Breton Island, Nova Scotia; *in* Current Research, Part C, Geological Survey of Canada, Paper 82-1C, p. 125-128.

Doucet, P.

1983: The petrology and geochemistry of the Middle River area, Cape Breton Island, Nova Scotia; M.Sc. thesis, Dalhousie University, Halifax, Nova Scotia, 339 p.

Dunning, G.R. and O'Brien, S.J.

1989: Late Proterozoic-early Paleozoic crust in the Hermitage flexure, Newfoundland Appalachians: U/Pb ages and tectonic significance; Geology, v. 17, p. 548-551.

Dunning, G.G., Krogh, T.E., Kean, B.F., O'Brien, S., and Swinden, H.S.

1986: U/Pb zircon ages of volanic groups from the central mobile belt, Newfoundland; *in* Program with Abstracts, Geological Association of Canada-Mineralogical Association of Canada, v. 11, p. 66.

Dunning, G.R., Barr, S.M., Raeside, R.P., and Jamieson, R.A.

in press: U-Pb zircon, titanite, and monazite ages in the Bras d'Or and Aspy terranes of Cape Breton Island, Nova Scotia: implications for magmatic and metamorphic history; Geological Society of America Bulletin.

Dunning, G.R., Krogh, T.E., O'Brien, S.J., and O'Neill, P.

1988: Geochronologic framework for the Central Mobile Belt in southern Newfoundland and the importance of Silurian orogeny; *in* Program with Abstracts, Geological Association of Canada-Mineralogical Association of Canada, v. 13, p. A34.

Fletcher, H.

1885: Report on the geology of northern Cape Breton; Geological Survey of Canada, Report of Progress for 1882-84, part H.

Jamieson, R.A. and Craw, D.

1983: Reconnaissance mapping of the southern Cape Breton Highlands — a preliminary report; *in* Current Research, Part A, Geological Survey of Canada, Paper 83-1A, p. 263-268.

Jamieson, R.A. and Doucet, P.

1983: The Middle River-Crowdis Mountain area, southern Cape Breton Highlands; *in* Current Research, Part A, Geological Survey of Canada, Paper 83-1A, p. 269-275.

Jamieson, R.A., Tallman, P., Marcotte, J.A., Plint, H.E., and Connors, K.A.

1987: Geology of the west-central Cape Breton Highlands; Geological Survey of Canada, Paper 87-13, 11 p.

Jamieson, R.A., van Breemen, O., Sullivan, R.W., and Currie, K.L.

1986: The age of igneous and metamorphic events in the western Cape Breton Highlands, Nova Scotia; Canadian Journal of Earth Sciences, v. 23, p. 1891-1901.

Keppie, J.D., Dostal, J., and Zentilli, M.
1978: Petrology of the Early Silurian Dunn Point and MacGillivray Brook formations, Arisaig, Nova Scotia; Nova Scotia Department of Mines and Energy, Paper 78-5.

Loncarevic, B., Barr, S.M., Raeside, R.P., Keen, C.E., and Marillier, F.
in press: Crustal expression and northeast extension of terranes from Cape Breton Island, Nova Scotia, using geophysical data; Canadian Journal of Earth Sciences.

Macdonald, A.S. and Smith, P.K.
1980: Geology of the Cape North area, northern Cape Breton Island, Nova Scotia; Nova Scotia Department of Mines and Energy, Paper 80-1, 60 p.

MacLaren, A.S.
1955: Cheticamp River, Inverness and Victoria Counties, Cape Breton Island, Nova Scotia; Geological Survey of Canada, Preliminary Map 55-36.

Marcotte, J.A.
1987: Regional mapping and petrographic study of a Silurian gneissic complex, Belle Cote Road, Cape Breton, Nova Scotia; B.Sc. thesis, Dalhousie University, Halifax, Nova Scotia, 93 p.

Milligan, G.C.
1970: Geology of the George River Series, Cape Breton; Nova Scotia Department of Mines, Memoir 7, 111 p.

Murphy, J.B., Pe-Piper, G., Nance, R.D., and Turner, D.
1988: A preliminary report on the geology of the eastern Cobequid Highlands, Nova Scotia; *in* Current Research, Part B, Geological Survey of Canada, Paper 88-1B, p. 99-107.

Neale, E.R.W.
1963: Pleasant Bay map area, Nova Scotia; Geological Survey of Canada, Map 1119A.

Neale, E.R.W. and Kennedy, M.J.
1975: Basement and cover rocks at Cape North, Cape Breton Island, Nova Scotia; Maritime Sediments, v. 11, p. 1-4.

O'Beirne-Ryan, A.M., Barr, S.M., and Jamieson, R.A.
1986: Contrasting petrology and age of two megacrystic granitoid plutons, Cape Breton Island, Nova Scotia; *in* Current Research, Part B, Geological Survey of Canada, Paper 86-1B, p. 179-190.

Pearce, J.A. and Cann, J.R.
1973: Tectonic setting of basic volcanic rocks determined using trace element analysis; Earth and Planetary Science Letters, v. 19, p. 290-300.

Plint, H.E.
1987: Metamorphism of the Jumping Brook metamorphic suite, western Cape Breton Highlands, Nova Scotia: microstructure, P-T-t paths, and tectonic implications; M.Sc. thesis, Dalhousie University, Halifax, Nova Scotia, 368 p.

Plint, H.E. and Jamieson, R.A.
1989: Microstructure, metamorphism, and tectonics of the western Cape Breton Highlands, Nova Scotia; Journal of Metamorphic Geology, v. 7, p. 407-424.

Plint, H.E., Connors, K.A., and Jamieson, R.A.
1986: Geology and mineral occurrences of the Jumping Brook Complex, Cheticamp-Pleasant Bay area, Cape Breton Island, Nova Scotia; *in* Current Research, Part B, Geological Survey of Canada, Paper 86-1B, p. 557-566.

Ponsford, M. and Lyttle, N.A.
1984: Metallic mineral occurrences map and data compilation, eastern Nova Scotia; Nova Scotia Department of Mines and Energy, Open File Report 600.

Raeside, R.P. and Barr, S.M.
1988: The Bras d'Or Zone: a suspect terrane in Cape Breton Island, N.S.; *in* Program with Abstracts, Geological Association of Canada-Mineralogical Association of Canada, v. 13, p. A102.
in press: Preliminary report on the geology of the northern and eastern Cape Breton Highlands; Geological Survey of Canada, Paper 89-14.

Reynolds, P.H., Jamieson, R.A., Barr, S.M., and Raeside, R.P.
1989: A ^{40}Ar/^{39}Ar dating study in the Cape Breton Highlands, Nova Scotia: thermal histories and tectonic implications; Canadian Journal of Earth Sciences, v. 26, p. 2081-2091.

Stockmal, G.S., Colman-Sadd, S.P., Keen, C.E., O'Brien, S.J., and Quinlan, G.
1987: Collision along an irregular margin: a regional plate tectonic interpretation of the Canadian Appalachians; Canadian Journal of Earth Sciences, v. 24, p. 1098-1107.

Tallman, P., Sangster, A.L., and Jamieson, R.A.
1988: Geology and mineralization of the Jumping Brook metamorphic suite, Faribault Brook area, western Cape Breton Island, Nova Scotia; *in* Current Research, Part B, Geological Survey of Canada, Paper 88-1B, p. 109-117.

Winchester, J.A. and Floyd, P.A.
1977: Geochemical discrimination of different magma series and their differentiation products using immobile elements; Chemical Geology, v. 20, p. 325-343.

A reconnaissance lead isotopic study of mineral occurrences in pre-Carboniferous basement rocks of northern and central Cape Breton Island, Nova Scotia[1]

A.L. Sangster[2], R.I. Thorpe[2], and A.K. Chatterjee[3]

Sangster, A.L., Thorpe, R.I., and Chatterjee, A.K., A reconnaissance lead isotopic study of mineral occurrences in pre-Carboniferous basement rocks of northern and central Cape Breton Island, Nova Scotia; in Mineral Deposit Studies in Nova Scotia, Volume 1, edited by A.L. Sangster, Geological Survey of Canada, Paper 90-8, p. 101-114, 1990.

Abstract

Reconnaissance level lead isotopic investigations of galenas from mineral occurrences in central and northern Cape Breton Island provide new data on mineral occurrences and their relationships to specific geological terranes and mineralizing events.

Galenas from mineral occurrences in the Aspy Terrane cluster in two populations, one for sericite schist hosted As-Zn-Pb occurrences with $^{206}\mathrm{Pb}/^{204}\mathrm{Pb}$ *and* $^{207}\mathrm{Pb}/^{204}\mathrm{Pb}$ *compositions in the ranges 18.310 to 18.340 and 15.621 to 15.649, respectively, and a second for trace galenas associated with low-grade stratabound and vein mineralization with* $^{206}\mathrm{Pb}/^{204}\mathrm{Pb}$ *and* $^{207}\mathrm{Pb}/^{204}\mathrm{Pb}$ *compositions in the range 18.307 to 18.362 and 15.587 to 15.626, respectively. The two populations reflect an age difference of about 30 Ma, compatible with an Ordovician-Silurian volcanogenic origin for the more primitive population and metamorphogenic formation of galena 30 Ma later.*

Galenas from the Bras d'Or Terrane form two groups of strikingly different isotopic character. Compositions for galenas from veins in the southeastern Cape Breton Highlands lie on an evolutionary trend between $^{206}\mathrm{Pb}/^{204}\mathrm{Pb} = 18.274$ *and* $^{207}\mathrm{Pb}/^{204}\mathrm{Pb} = 15.634$*, and* $^{206}\mathrm{Pb}/^{204}\mathrm{Pb} = 18.493$ *and* $^{207}\mathrm{Pb}/^{204}\mathrm{Pb} = 15.639$*, compatible with vein formation over a protracted period of time in association with: 1) emplacement of a Cambrian granitoid intrusion (515 Ma); 2) movement on the Eastern Highlands Shear Zone (possibly 425 to 435 Ma); and 3) later events, possibly at 360 to 380 Ma. Vein galenas from granite-related occurrences in the southern Bras d'Or Terrane, on North Mountain, and in the Boisdale Hills, are much more radiogenic, ranging between* $^{206}\mathrm{Pb}/^{204}\mathrm{Pb} = 18.428$ *to 18.532 and* $^{207}\mathrm{Pb}/^{204}\mathrm{Pb} = 15.663$ *to 15.708, and may reflect a different basement source than those in the northern Bras d'Or Terrane.*

Résumé

L'étude, au niveau de reconnaissance, des rapports isotopiques du plomb dans des galènes provenant de manifestations minérales du centre et du nord de l'île du Cap-Breton renseigne sur les manifestations minérales et leurs relations avec des terranes géologiques et des phénomènes de minéralisation particuliers.

Les galènes des manifestations minérales du terrane d'Aspy se répartissent en deux populations : manifestations d'As-Zn-Pb contenues dans des schistes à séricite avec des rapports $^{206}\mathrm{Pb}/^{204}\mathrm{Pb}$ *et* $^{207}\mathrm{Pb}/^{204}\mathrm{Pb}$ *de l'ordre de 18,310 à 18,340 et de 15,621 à 15,649 respectivement, et galènes à l'état de traces associées avec une minéralisation de faible teneur confinées à des strates ou en veines et avec des rapports* $^{206}\mathrm{Pb}/^{204}\mathrm{Pb}$ *et* $^{207}\mathrm{Pb}/^{204}\mathrm{Pb}$ *de l'ordre de 18,307 à 18,362 et de 15,587 à 15,626 respectivement. Les deux populations reflètent une différence d'âge de 30 Ma environ, indiquant que la population la plus ancienne serait d'origine volcanique ordovicienne-silurienne, et l'autre, une formation métamorphique de galène plus jeune de 30 Ma.*

Les galènes du terrane de Bras d'Or forment deux groupes à caractères isotopiques très contrastants. Les compositions des galènes des filons du sud-est des hautes terres du Cap-Breton suivent une tendance comprise entre $^{206}\mathrm{Pb}/^{204}\mathrm{Pb} = 18,274$ *et* $^{207}\mathrm{Pb}/^{204}\mathrm{Pb} = 15,634$*, et* $^{206}\mathrm{Pb}/^{204}\mathrm{Pb} = 18,493$ *et* $^{207}\mathrm{Pb}/^{204}\mathrm{Pb} = 15,639$*, signe qu'une formation filonienne s'est produite pendant une période prolongée en association avec : 1) la mise en place d'une intrusion granitoïde cambrienne (515 Ma); 2) le mouvement dans la zone de cisaillement des hautes terres (peut-être 425 à 435 Ma); et 3) des événements ultérieurs (peut-être 360 à 380 Ma). Les galènes filoniennes des manifestations associées au granite dans le sud du terrane de Bras d'Or, dans la montagne North et dans les collines Boisdale, sont beaucoup plus radiogéniques, allant de* $^{206}\mathrm{Pb}/^{204}\mathrm{Pb} = 18,428$ *à 18,532 et de* $^{207}\mathrm{Pb}/^{204}\mathrm{Pb} = 15,663$ *à 15,708, et pourraient dénoter une source dans le socle différente de celles relevées dans le nord du terrane de Bras d'Or.*

---

[1] Contribution to the Canada - Nova Scotia Mineral Development Agreement, 1984-1989. Project carried by the Mineral Resources Division, Geological Survey of Canada, Project 860008.

[2] Geological Survey of Canada, 601 Booth St., Ottawa, Ontario, K1A 0E8

[3] Nova Scotia Department of Mines and Energy, P.O. Box 1087, Halifax, Nova Scotia, B3J 2X1

INTRODUCTION

The pre-Middle Devonian rocks of the Cape Breton Highlands and adjoining Bras d'Or Lake area have been assigned to three tectono-stratigraphic terranes (Fig. 1) characterized by distinct geological relationships (Barr and Raeside, 1989) and a variety of stratiform and vein base metal and gold occurrences (Ponsford and Lyttle, 1984). The Blair River Complex is characterized by retrograded amphibolite/borderline granulite facies gneisses that have been intruded by a large syenite intrusion with a Grenvillian metamorphic age of 1040 +10/−30 Ma. The Aspy Terrane, in structural contact with the Blair River Complex to the east and south of the complex, is characterized by Ordovician/Silurian metavolcanic and metasedimentary rocks of variable metamorphic grade. The Ordovician/Silurian metamorphic units are in structural juxtaposition with the Cambrian Cheticamp Pluton and have been intruded by a suite of Silurian to Devonian granitoid bodies. The Bras d'Or Terrane lies south of the Aspy Terrane and is composed of late Precambrian metasedimentary rocks and dioritic to granitic intrusions that are dominantly latest Precambrian to Cambrian in age.

This new subdivision of Cape Breton Island basement geology provides a rational basis on which to achieve a regional understanding of the relationships between mineral occurrences. This is, in turn, necessary for creating genetic models and devising mineral exploration programs. The Aspy Terrane contains a variety of mineral occurrences hosted by rocks of different metamorphic grades, including both stratiform sulphide disseminations associated with metavolcanic and metasedimentary rocks, and auriferous sulphide veins. Mineralization in the Bras d'Or Terrane consists of a few, commonly auriferous, base metal-quartz veins. None of these occurrences has a demonstrated economic potential but the area continues to receive substantial mineral exploration effort.

This paper presents an interpretation of new lead isotopic analyses of galenas from mineral occurrences in the Aspy and Bras d'Or terranes of central and northern Cape Breton Island. Lead isotopic compositions for the Meat Cove zinc occurrence, in the Blair River Complex, and the Lime Hill zinc occurrence, in the Lime Hill gneiss, Bras d'Or Terrane, are distinct from those presented here (Sangster et al., 1990) and are reviewed for completeness.

MINERAL OCCURRENCES IN THE ASPY TERRANE

Cheticamp area

The Jumping Brook metamorphic suite in the western Cape Breton Highlands (Fig. 2) consists of a basal assemblage of mafic metavolcanic rocks (Faribault Brook unit), overlain, in turn, by discontinuous felsic metavolcanic rocks and associated metasedimentary rocks (Barren Brook schist), and clastic metasedimentary rocks (Dauphinee Brook schist, Corney Brook schist, Fishing Cove River schist, and George Brook amphibolite) (Jamieson et al., 1989). The Jumping Brook metamorphic suite has been correlated with the Ordovician-Silurian Sarach Brook metavolcanic rocks which have a U-Pb (zircon) age of 433 +7/−4 Ma (Dunning et al., 1990). The proposed correlation is supported by an age of 439 +/−7 Ma (U-Pb zircon; Currie et al., 1982) for a felsic dyke that is interpreted to be a feeder to the Jumping Brook felsic metavolcanic rocks, and by a comparable age of 433 +/−20 Ma for the Belle Cote Road orthogneiss (U-Pb zircon; Jamieson et al., 1986) which has intruded the Jumping Brook rocks.

A.L. Sangster et al. (paper in preparation) have defined five types of mineral occurrences in the Jumping Brook metamorphic suite near Cheticamp. These include (Fig. 2) :

1) Heavily disseminated and banded As-Fe-Zn-Pb +/−Cu sulphides with minor associated vein-quartz-hosted mineralization in or stratigraphically near quartz-sericite schist of the Barren Brook unit. Occurrences are the Core Shack (5)[1], Silver Cliff (6), Galena/Highland Mercury (3), Mountain Top (8), Fisset Brook (7), and Road 2 (10). Another occurrence on Rocky Brook (12) is included in this group because it is hosted by felsic metavolcanic rocks at the top of the Faribault Brook metavolcanic unit which may constitute the unsheared precursor of the Barren Brook sericite schists. However, the mineralization at Rocky Brook is not typical of the occurrences mentioned above in that it is copper-rich and the foliation in the host rocks is much less well developed than in the occurrences near Faribault Brook (Nova Scotia Department of Mines and Energy, Mineral Assessment File 11K/10, 13-J-55).

2) Disseminated pyrite with traces of Zn-Pb-Cu sulphides in sericite schist in metasedimentary rocks not associated with metavolcanic rocks. This type is represented by the Fishing Cove River (14) and Boarsback (15) occurrences.

3) Disseminated pyrrhotite/pyrite with trace amounts of chalcopyrite and rare sphalerite and galena in chlorite and chlorite-biotite schist at and near the top of the Faribault Brook metavolcanic sequence. These include widespread stratabound sulphide zones such as those at the Falls (4), at Pillar Rock (17), and in numerous drillholes in the Faribault Brook area.

4) Massive arsenopyrite veins concordant with the foliation in chlorite and biotite-chlorite schist. Occurrences include Road 1-1 (9) and 90 East Trench (18).

5) Galena and sphalerite in joints and fractures in the Dauphinee Brook schist overlying the Faribault Brook metavolcanic unit. This type of mineralization is widespread near the contact of the Cheticamp Pluton, and occurrences are best exposed in the lower part of Faribault Brook (1), in the Noranda (11) and Amax (2) trenches, and at a few places in the valley of Corney Brook (16).

The age of mineralization in the Cheticamp area has not been directly determined. This mineralization cannot be older than its host rocks (~430 Ma), and is therefore not related to the Cheticamp Pluton, which is of

---

[1] Numbers in parentheses are the identifiers for mineral occurrence locations on Figure 1 (19 to 34) and Figure 2 (1 to 18).

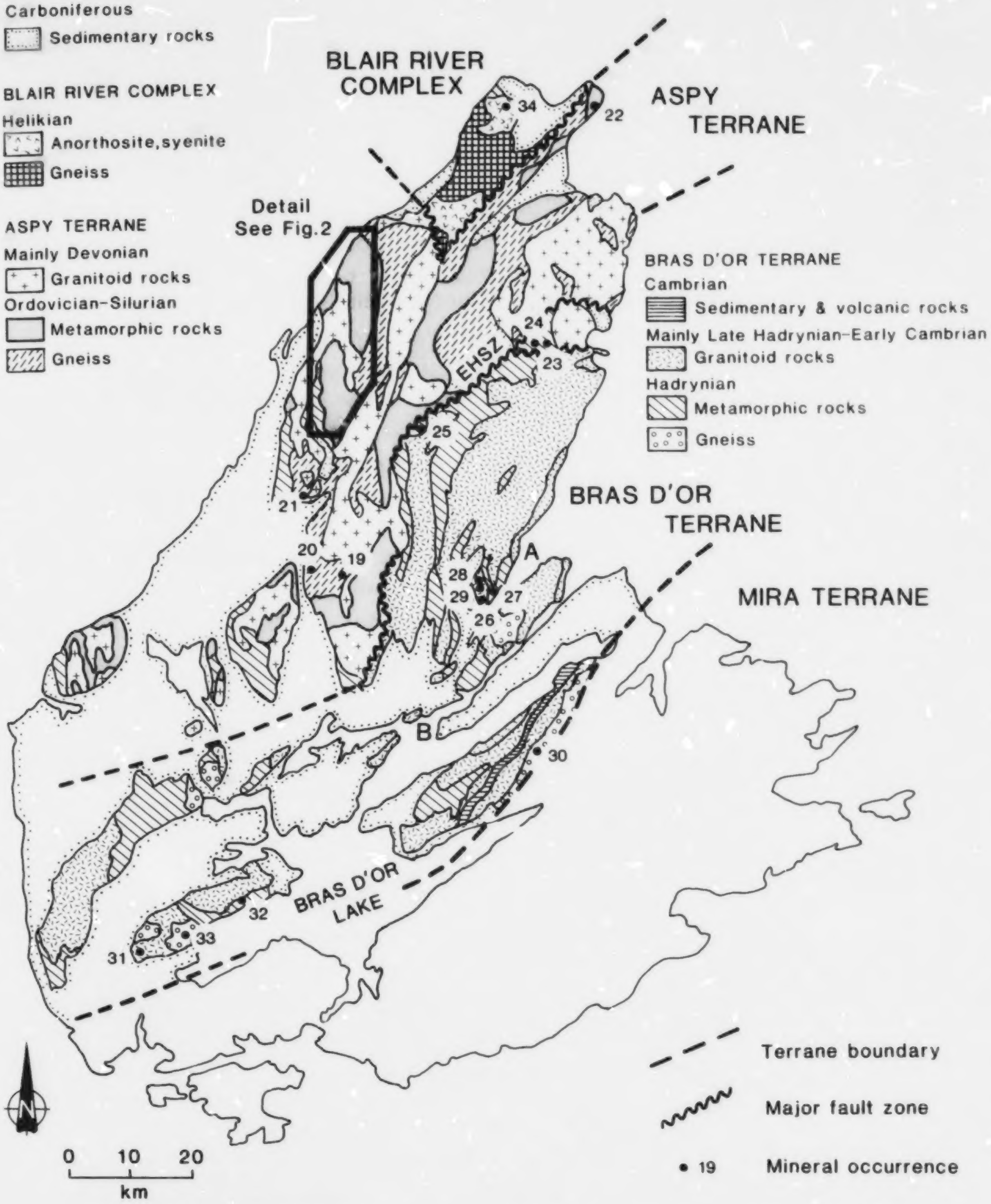
Carboniferous
Sedimentary rocks
BLAIR RIVER COMPLEX
Helikian
Anorthosite,syenite
Gneiss
ASPY TERRANE
Mainly Devonian
Granitoid rocks
Ordovician-Silurian
Metamorphic rocks
Gneiss
BLAIR RIVER COMPLEX
Detail See Fig.2
ASPY TERRANE
BRAS D'OR TERRANE
Cambrian
Sedimentary & volcanic rocks
Mainly Late Hadrynian-Early Cambrian
Granitoid rocks
Hadrynian
Metamorphic rocks
Gneiss
34
22
24
23
EHSZ
25
21
20
19
BRAS D'OR TERRANE
A
28
29
27
26
MIRA TERRANE
B
30
BRAS D'OR LAKE
32
33
31
N
0 10 20
km
Terrane boundary
Major fault zone
• 19 Mineral occurrence

Figure 1. Location of selected mineral occurrences, Aspy and Bras d'Or terranes, Cape Breton Island. Geological base after Barr and Raeside (1989). Mineral occurrence identification: 1-18. Cheticamp area, Figure 2; 19. Sarach Brook; 20. Middle Sister; 21. Sugarloaf Mountain; 22. Money Point; 23. Franey Au; 24. Clyburn Brook; 25. Inco galena; 26. Murray Brook; 27. Prices Point; 28. Elders Brook; 29. Tarbotvale; 30. Rear Boisdale; 31. West Bay Road; 32. Mill Brook; 33. Lime Hill; 34. Meat Cove. EHSZ = Eastern Highlands Shear Zone; A = St. Anns Bay; B = Baddeck Bay.

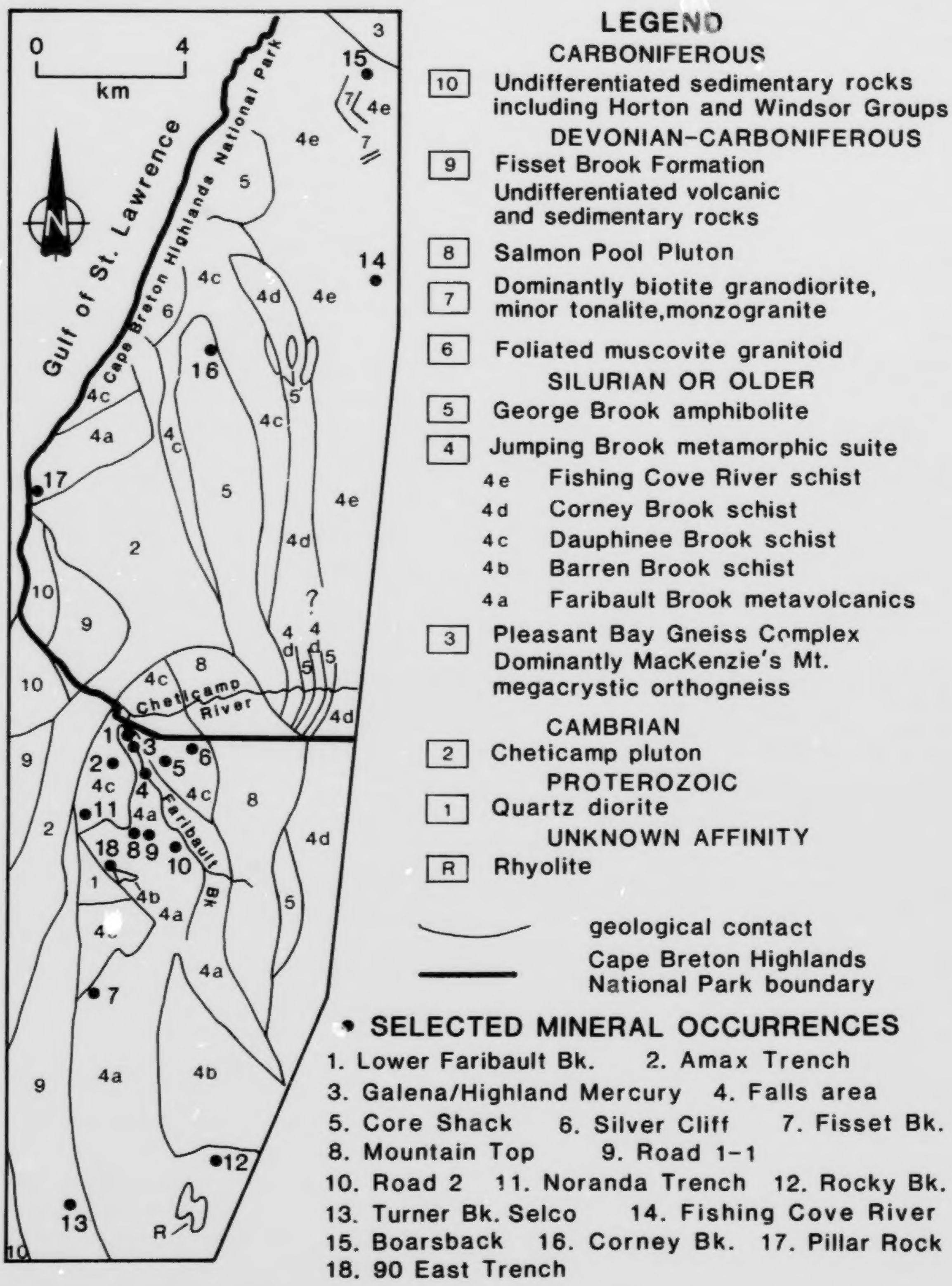
0 4
km
N
Gulf of St. Lawrence
Cape Breton Highlands National Park
Cheticamp River
Faribault Bk
LEGEND
CARBONIFEROUS
10 Undifferentiated sedimentary rocks including Horton and Windsor Groups
DEVONIAN-CARBONIFEROUS
9 Fisset Brook Formation Undifferentiated volcanic and sedimentary rocks
8 Salmon Pool Pluton
7 Dominantly biotite granodiorite, minor tonalite,monzogranite
6 Foliated muscovite granitoid
SILURIAN OR OLDER
5 George Brook amphibolite
4 Jumping Brook metamorphic suite
4e Fishing Cove River schist
4d Corney Brook schist
4c Dauphinee Brook schist
4b Barren Brook schist
4a Faribault Brook metavolcanics
3 Pleasant Bay Gneiss Complex Dominantly MacKenzie's Mt. megacrystic orthogneiss
CAMBRIAN
2 Cheticamp pluton
PROTEROZOIC
1 Quartz diorite
UNKNOWN AFFINITY
R Rhyolite
geological contact
Cape Breton Highlands National Park boundary
• SELECTED MINERAL OCCURRENCES
1. Lower Faribault Bk.
2. Amax Trench
3. Galena/Highland Mercury
4. Falls area
5. Core Shack
6. Silver Cliff
7. Fisset Bk.
8. Mountain Top
9. Road 1-1
10. Road 2
11. Noranda Trench
12. Rocky Bk.
13. Turner Bk. Selco
14. Fishing Cove River
15. Boarsback
16. Corney Bk.
17. Pillar Rock
18. 90 East Trench

Figure 2. Locations of selected mineral occurrences within the Jumping Brook metamorphic suite, Cheticamp area, Cape Breton Highlands. Geological base after Jamieson et al. (1989).

Cambrian age (550 +/−8 Ma; Jamieson et al., 1986). Also, mineralized rock and veins at Cheticamp were highly deformed ~400 Ma ago (Reynolds et al., 1989) and are consequently not related to the Devonian Salmon Pool Pluton (365 +10/−5 Ma, U-Pb zircon; Jamieson et al., 1986), which is posttectonic. They are interpreted to have a genetic relationship to their volcanic host rocks (A.L. Sangster et al., paper in preparation).

Galenas from all mineralization types, except the massive arsenopyrite veins, have been analyzed for their isotopic compositions (Appendix I).

Money Point zinc-lead occurrence (22)

Black argillite within the bimodal Money Point volcanic sequence contains erratically disseminated pyrite with traces of chalcopyrite, galena, and sphalerite, both as disseminations and on joint and fracture surfaces. The argillite contains approximately 20 percent bedding-parallel, barren quartz veins.

An Rb-Sr age of 395 Ma for rhyolite from the Money Point Group (Gaudette et al., 1985) has been interpreted as a metamorphic age. Barr et al. (in press) correlate the Money Point Group with the Ordovician-Silurian Jumping Brook and Sarach Brook (discussed below) metamorphic suites.

Sarach Brook occurrence (19)

The Sarach Brook occurrence consists of erratically disseminated sphalerite and rare galena in a pyritic horizon within porphyroblastic garnet-kyanite-biotite-quartz-feldspar-muscovite schist of the Middle River metamorphic suite. The mineralization was intersected by two drillholes that are represented by core stored in the Drill Core Library of the Nova Scotia Department of Mines and Energy in Stellarton, Nova Scotia. The holes penetrated the central part of a soil geochemical anomaly which is at least 3 km in length and is restricted to a zone 100 m wide which lies 100 to 200 m west of, and parallel to, the faulted contact between the Middle River metamorphic suite and the West Branch North River granite (Sangster and Wowkodaw, 1979; Sangster, 1980). Sphalerite is present in amounts ranging from 0.1 to 1 percent (unpublished data, A.L. Sangster). Trace amounts of galena, chalcopyrite, and arsenopyrite are present locally in the core. The rocks that host the Sarach Brook occurrence are mineralogically similar to the biotite schists/gneisses that host the Boarsback and Fishing Cove occurrences north of Cheticamp, except for the lack of sericite schist associated with pyrite-bearing rock.

Barr et al., (in press) assign an Ordovician-Silurian age to the Middle River metamorphic suite and correlate it with the Sarach Brook metavolanic rocks which are in faulted contact about 6 km to the south. Rhyolites from the Sarach Brook unit have been dated at 433 +7/−4 (U-Pb zircon; Dunning et al., 1990).

Middle Sister occurrence (20)

The Middle Sister occurrence is exposed in a trench on the brow of the middle of three mountains overlooking the Lakes O'Law. The occurrence is poorly exposed, but appears to be in rocks mapped as Middle River gneiss (Barr et al., in press) and consists of very highly deformed sericite schist containing a few percent arsenopyrite and traces of galena. The trenching was carried out during exploration of tungsten anomalies detected in concentrates of detrital heavy minerals and may be associated with small scheelite-bearing vein systems.

Sugarloaf occurrence (21)

The Sugarloaf lead occurrence is located on the southwestern side of the Sugarloaf outlier, which forms a prominent topographic feature protruding through Carboniferous sedimentary rocks in the Margaree Valley. It consists of traces of galena in the sheared contact zone between mafic schist and an unfoliated granite of presumed Devonian age. The mafic schists may be correlatives of the Jumping Brook metamorphic suite.

MINERAL OCCURRENCES IN THE BRAS D'OR TERRANE

St. Anns area (26, 27, 28, 29)

Macdonald and Barr (1985) have documented a large number of base/precious metal occurrences and altered zones in rocks in an area 14 km long by 6 km wide near St. Anns in the southeastern part of the Cape Breton Highlands. Cu-Mo-Au-bearing veins are preferentially hosted by granitoid rocks, whereas Zn-Pb-Cu-Ag-bearing veins are preferentially hosted by a rock sequence containing crystal and lithic-crystal dacitic tuffs and andesitic-dacitic volcanic rocks. Local areas with sericite alteration along joint/fracture surfaces or more pervasively distributed in the rock are common with and without associated pyrite. The principal vein orientation is from north to north-northwest. The veins trending north-northwest have a similar orientation to those, discussed below, hosted by the Kathy Road diorite. The genetic significance of the similar orientation is not known.

The St. Anns leucomonzogranite and Indian Brook granodiorite, which host some mineralized veins, have been dated at 515 +/−17 Ma (Rb-Sr whole rock; Cormier, 1980) and ~570 Ma maximum (U-Pb zircon; Dunning et al., 1990), respectively. Muscovite alteration associated with veins at the Murray Brook Cu-Mo occurrence (26), within the St. Anns leucomonzogranite, has been dated at 517 +/−18 Ma (K-Ar muscovite; Macdonald and Barr, 1985). In the absence of evidence for multiple vein generations, all veins in the St. Anns area have previously been considered to be genetically related to the Cambrian intrusions.

Galena samples for isotopic analyses were obtained from base metal vein occurrences in Tarbotvale (29) (Schoolhouse Brook), at Elders Brook (28 — two occurrences), and at Prices Point (27).

Inco galena vein (25)

Isotopic compositions of galena were obtained for a quartz-galena-altaite-gold-bearing vein which cuts highly deformed Kathy Road diorite. The vein appears to be part of a swarm of similar nongalena-bearing auriferous veins which extend along strike to the southeast at about 150° azimuth. The veins cut the metamorphic foliation of the diorite host, and alteration consisting of hydrothermal white mica and chlorite has been superimposed upon the metamorphic mineralogy of this host. The vein quartz is also highly strained, with subgrain development and zones of extreme cataclasis. The orientation of the vein system suggests that it may be a subsidiary structure to the Eastern Highlands Shear Zone which separates the Aspy and Bras d'Or terranes as defined by Barr and Raeside (1989).

These relationships indicate that the veins are younger than both the Kathy Road diorite (560 +/−2 Ma, U-Pb zircon) and the age of its metamorphism (521 +/−2 Ma, U-Pb titanite) as determined by Dunning et al. (1990). The Eastern Highlands Shear Zone was active both before and after intrusion of the Black Brook granite (S.M. Barr, pers. comm., 1990), which has been dated at 375 +5/−4 Ma (U-Pb zircon; Dunning et al., 1990). Ar-Ar cooling ages (Reynolds et al., 1989) are interpreted to indicate that docking of the Bras d'Or Terrane occurred during the Silurian and Early Devonian. If the gold veins within the Kathy Road diorite are related to the Eastern Highlands Shear Zone, then they are probably of Silurian age and might therefore be slightly younger than the mineralization hosted by the Jumping Brook metamorphic suite near Cheticamp in the Aspy Terrane.

Clyburn Brook veins (23, 24)

Mineralization in the Clyburn Brook area is poorly exposed and its relationships are not understood. Veins are hosted by metamorphic rocks of the MacMillan Flowage Formation (Barr et al., in press), believed to be late Proterozoic to Cambrian in age (Barr and Raeside, 1989). A stream cut at the Franey Au occurrence (23) exposes an east-west-striking, auriferous vein. The vein is highly deformed, suggesting that it is premetamorphic and older than the adjacent Cameron Brook granodiorite (402 +/−3 Ma, U-Pb zircon; Dunning et al., 1990). Galena was not, however, obtained from this vein.

Galena was obtained from a north-south vein exposed in Slate Brook on the northern slope of Clyburn Brook (24) about 2.5 km west of the Franey occurrence and near the contact of the Black Brook granite (375 +5/−4 Ma, U-Pb zircon; Dunning et al., 1990). This vein is concordant with foliation in the host slate and contains a small pocket of heavily disseminated galena in largely barren quartz. A second isotopic composition was obtained from trace quantities of galena from gash veins in rhyolite exposed in Clyburn Brook (200 m south of occurrence 24, Fig. 1) at the mouth of Slate Brook. This rhyolite has been dated at ~412 Ma (Rb-Sr; Keppie and Halliday, 1986). There is no geological evidence for a genetic association between these two galena-bearing units.

North Mountain veins (31,32)

The West Bay Road (31) and Mill Brook (32) veins are spatially related to Cambrian granitoid rocks on North Mountain at the southern end of Bras d'Or Lake. The West Bay Road occurrence consists of minor galena in a small quartz vein cutting West Bay monzogranite within the Lime Hill gneiss complex (Raeside, 1990; Sangster et al., 1990). Small intrusions near the Lime Hill zinc occurrence (33) have yielded Cambrian ages (foliated tonalite, 539 +/−1 Ma; massive granite dyke, 541 +14.5/−23.5 Ma; A.L. Sangster and P.A. Hunt, unpublished data, 1988). The Mill Brook galena was obtained from quartz-carbonate stockwork veins cutting late Proterozoic limestone/marble adjacent to the Marble Mountain granodiorite, presumed to be of Cambrian age.

Boisdale Hills occurrence (30)

The Rear Boisdale occurrence consists of argentiferous galena and sphalerite associated with zones of silicification in late Proterozoic calcite and dolomite marble near the contact with granodiorite of the Boisdale Hills Pluton. The occurrence is not exposed at surface and the geometry of the zones is not known. The age of the occurrence is considered to be about 574 +/−11 Ma by extrapolating the age for the Shunacadie Pluton (Rb-Sr; Poole, 1980) to the similar Boisdale Hills Pluton.

RESULTS OF LEAD ISOTOPIC ANALYSES

All galenas from the Cheticamp area plot within a limited compositional range between $^{206}Pb/^{204}Pb$ = 18.307 to 18.362 and $^{207}Pb/^{204}Pb$ = 15.587 to 15.649 (Appendix I). In detail, however, the lead compositions define two populations (Fig. 3 and 4). A more primitive population includes all occurrences hosted by sericite schist near the top of the Faribault Brook metavolcanic unit, as well as the Boarsback occurrence. The very slightly more radiogenic population includes galena hosted by pyrrhotitic/pyritic chlorite schist, from joints and fractures in the Dauphinee Brook schist, and from the Fishing Cove River occurrence. The occurrences with the more primitive lead compositions are commonly As-Zn-Pb-bearing and contain significant contents of galena associated with sphalerite. The slightly more radiogenic compositions are for trace galenas from pyrrhotitic, and commonly biotitic, chlorite schist, for joint- and fracture-controlled galenas which are clearly later than the primary deposition of their host rocks, and for galenas from the Rocky Brook occurrence.

The compositions of most other galena specimens from occurrences within the Aspy Terrane (Fig. 5) are similar to those from the Cheticamp area described above. Three samples from the Sarach Brook zinc occurrence and four from weakly mineralized black argillite at Money Point all have compositions similar to those of the more radiogenic galenas from Cheticamp occurrences. The isotopic compositions for the small Sugarloaf occurrence are similar to those described above, whereas the isotopic composition of a single galena from the Middle Sister occurrence is much more radiogenic than those from the other occurrences.

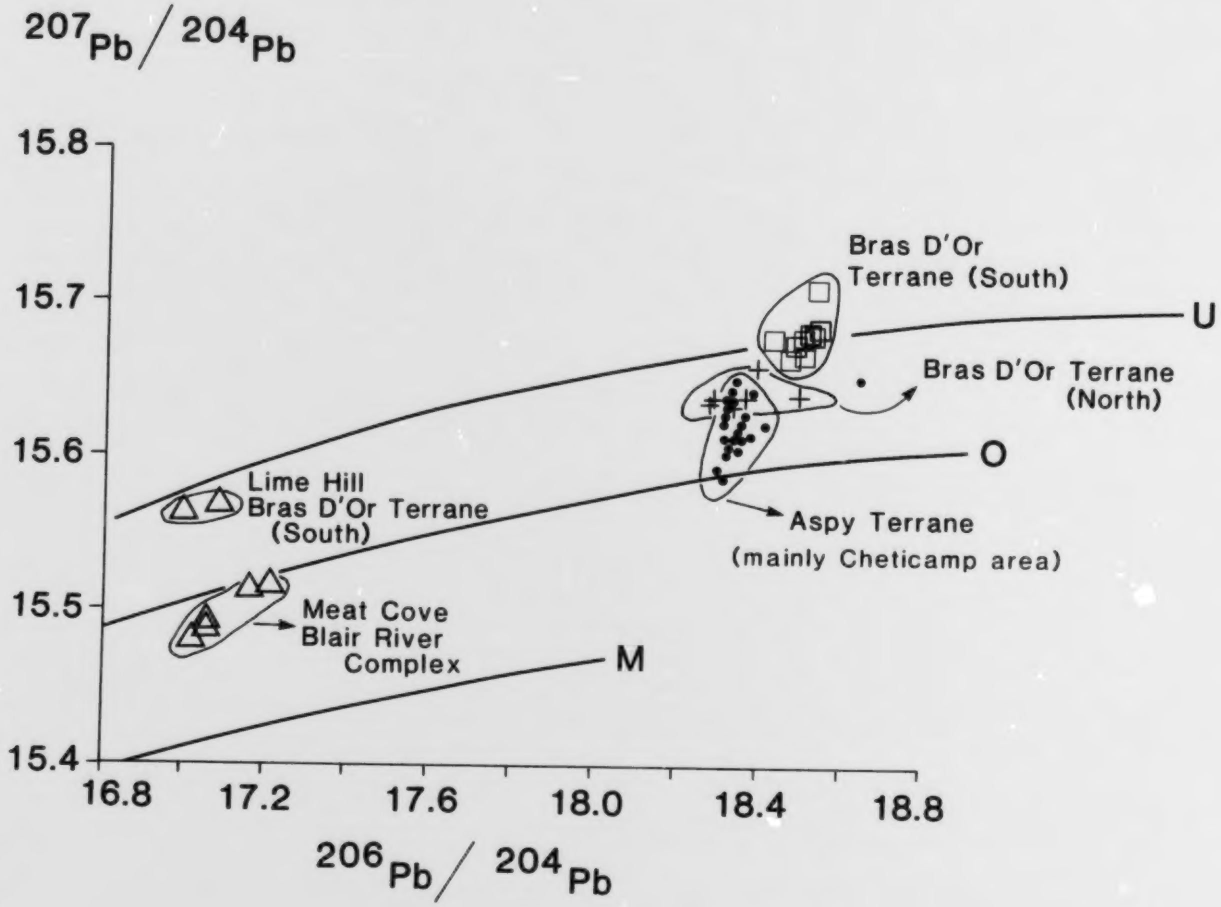

Figure 3. Summary diagram of lead isotopic compositions of galenas from mineral occurrences in pre-Middle Devonian basement rocks from central and northern Cape Breton Island. Evolution curves (mantle = M, orogene = O, upper crust = U) from Zartman and Doe (1981). Lime Hill/Meat Cove data from Sangster et al., 1990.

The isotopic compositions of galena specimens from occurrences in the Bras d'Or Terrane form two distinct groups which are both also distinct from those of the Aspy Terrane (Fig. 6). Those compositions for galenas from vein occurrences in the northern Bras d'Or Terrane form a group with a limited spread in ^{207}Pb/^{204}Pb values, and a relatively larger range in ^{206}Pb/^{204}Pb values from 18.274, lower than compositions for Aspy Terrane galenas, to 18.493. Compositions of galenas from the West Bay Road and Mill Brook occurrences on North Mountain and occurrences in the Boisdale Hills area form a separate population containing much higher levels of radiogenic lead.

DISCUSSION

The lead isotopic composition of galena can provide substantial information on the source and relative age of mineral occurrences. The source of sulphide mineralization can be defined where a relatively uncontaminated mantle source can be postulated or where there is a substantial database of relevant rock-lead isotopic analyses to permit back calculation of present-day compositions of possible source lithologies for comparison with analyses for galenas from mineral occurrences. Such a rock-lead database is not yet available for the Cape Breton intrusions. Model ages are often calculated for galena lead isotopic compositions (e.g. Zartman and Doe, 1981; Fletcher, 1979 for Grenville deposits) but these may be of doubtful value for post-Precambrian deposits when lead contributions to galena may have come from a variety of crustal and mantle sources with different compositions and different lead evolution histories. U-Pb ages, where available, provide a better basis for relating lead isotope systematics to geological events. However, where a single homogeneous source can be assumed, the difference in age between distinct populations of galenas can be calculated with some certainty.

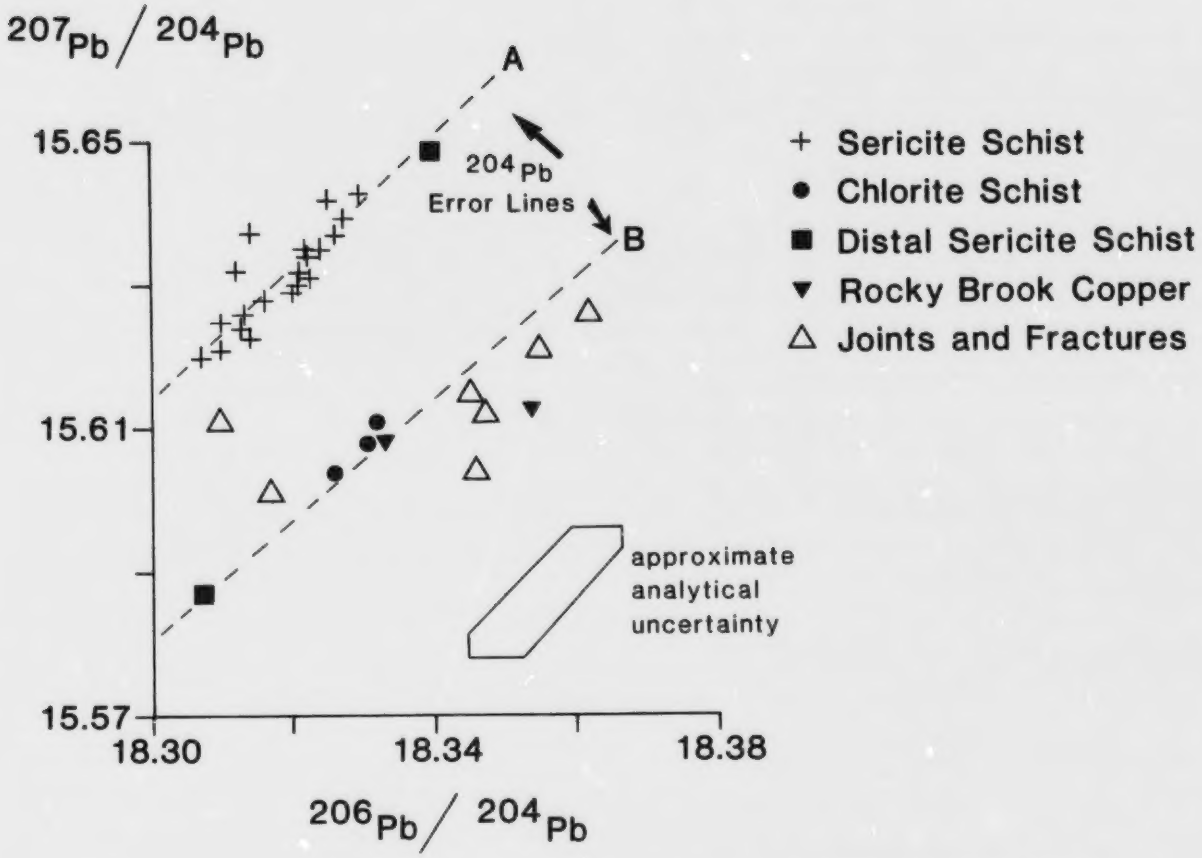

Figure 4. Lead isotopic compositions of galenas from mineral occurrences of various types hosted by the Jumping Brook metamorphic suite. The more primitive compositions (line A) include only sericite schist hosted occurrences. The more evolved population (line B) contains a mixture of joint controlled and trace galenas from mineral occurrences of various types.

Aspy Terrane

The narrow range of lead isotopic compositions exhibited by Cheticamp area galenas (Fig. 3) suggests that all of the galenas from the various types of mineral occurrences were formed from lead derived from a single homogeneous source. Assuming a single source of lead and reasonable $^{238}U/^{204}Pb$ (μ) values for the source in the range of 9 to 10, the calculated difference in age between the two galena populations from the Cheticamp occurrences is about 20 to 40 Ma. This difference in age is in good agreement with the elapsed time between the postulated 430 Ma age of extrusion of the Jumping Brook volcanic rocks (Currie et at., 1982; Jamieson et al., 1990) and their metamorphism at about 400 Ma ago (Reynolds et al., 1989). The coincidence in age thus inferred between the second galena generation and metamorphism means that this galena may have formed from lead liberated from feldspathic minerals during dynamothermal regional metamorphic processes. The presence of abundant biotite in layers within the chlorite schist (A.L. Sangster et al., paper in preparation) probably reflects the presence of a felsic ash component in the mafic volcano-sedimentary rocks from which lead was liberated during metamorphism.

The Rocky Brook galenas are isotopically distinct from those from other occurrences hosted by felsic volcanic rocks and lie within the field for the population interpreted as having a metamorphogenic origin (Fig. 4). Galena is a very minor component of the Rocky Brook occurrence, a characteristic shared by those occurrences from which the galenas have been interpreted above to be metamorphogenic. However, the association with chalcopyrite-pyrrhotite mineralization that is substantially joint/fracture controlled (D. Pollock, pers. comm., 1989) suggests that the mineralization may have been mobilized during metamorphism from a nearby source in mafic metavolcanic or metasedimentary rocks.

Also, the fact that compositions of galena specimens from Money Point argillite, the Sarach Brook zinc occurrence, and the small occurrence on Sugarloaf

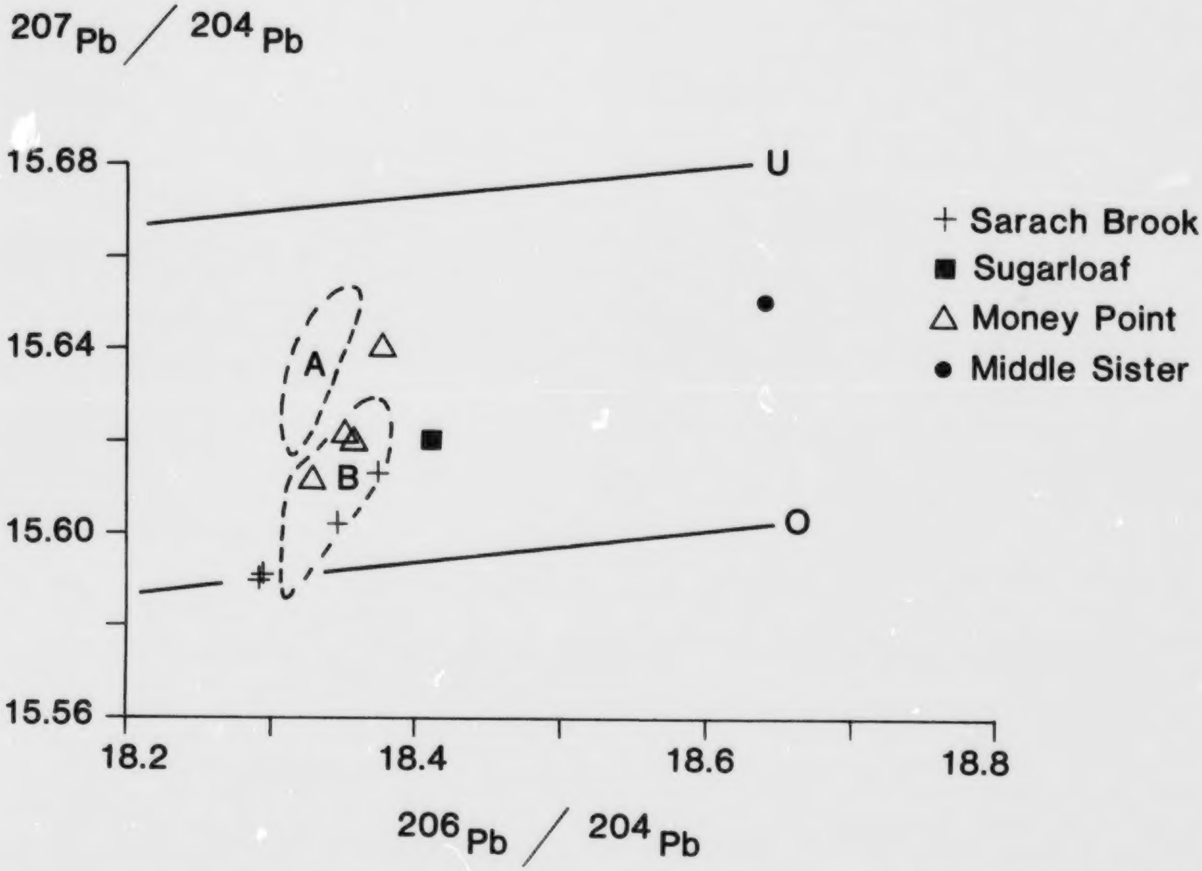

Figure 5. Lead isotopic compositions of galenas from mineral occurrences hosted by the Middle River gneiss and Money Point Group, illustrating the similarity in composition between trace galenas from the widespread occurrences sampled, and the galenas from the Cheticamp area interpreted to be of metamorphogenic origin. Dashed lines outline compositional fields of exhalative galenas "A" and metamorphogenic galenas "B" from Figure 3. Evolution curves (orogene = O, upper crust = U) from Zartman and Doe (1981).

Mountain are similar to those for the second "metamorphogenic" Cheticamp population (Fig. 5) is interpreted as sufficient evidence that these occurrences are genetically comparable. This argument supports the contention of Barr et al. (in press) that all the layered rocks, at different metamorphic grades, in the Aspy zone represent products of Ordovician-Silurian volcanism that were metamorphosed about 400 Ma ago.

The poorly exposed arsenical mineralization at the Middle Sister occurrence resembles some Cheticamp occurrences. The lead, however, is more radiogenic than that of Cheticamp galenas, suggesting that it may have formed during a subsequent event. However, calculations using a Money Point composition (18.378/15.640) suggest that if the source is similar to that for other Aspy Terrane galenas, the Middle Sister galena may have formed as late as 280 to 300 Ma and would represent the youngest known mineralizing event in the Cape Breton Highlands. Otherwise, the Middle Sister galena composition could represent a distinct and more radiogenic source than that for the other galenas.

Bras d'Or Terrane

The two galena populations for mineral occurrences in the Bras d'Or Terrane appear unrelated and are attributed to two distinct sources. The isotopic compositions of vein galenas from the southeastern Cape Breton Highlands (western Bras d'Or Terrane) (Fig. 6) form a group that appears to have evolved over time from a homogeneous source, reflecting the sequential formation of galena in veins over a considerable period of geological time. Assuming isotopically comparable sources, the time represented by the difference in compositions between the Elders Brook and Prices Point galenas is about 130 to 145 Ma (μ = 9 to 10). If it is considered that the Elders Brook veins formed at about 517 Ma (Macdonald and Barr, 1985), the age obtained for alteration associated with the Murray Brook veins, this would imply that formation of the Prices Point vein galena was at about 387 to 372 Ma (Late Devonian), synchronous with some plutonism in the adjacent Aspy and Mira terranes (Dunning et al., 1990). This would seem to be a reasonable possibility. It should also be noted that the Prices Point

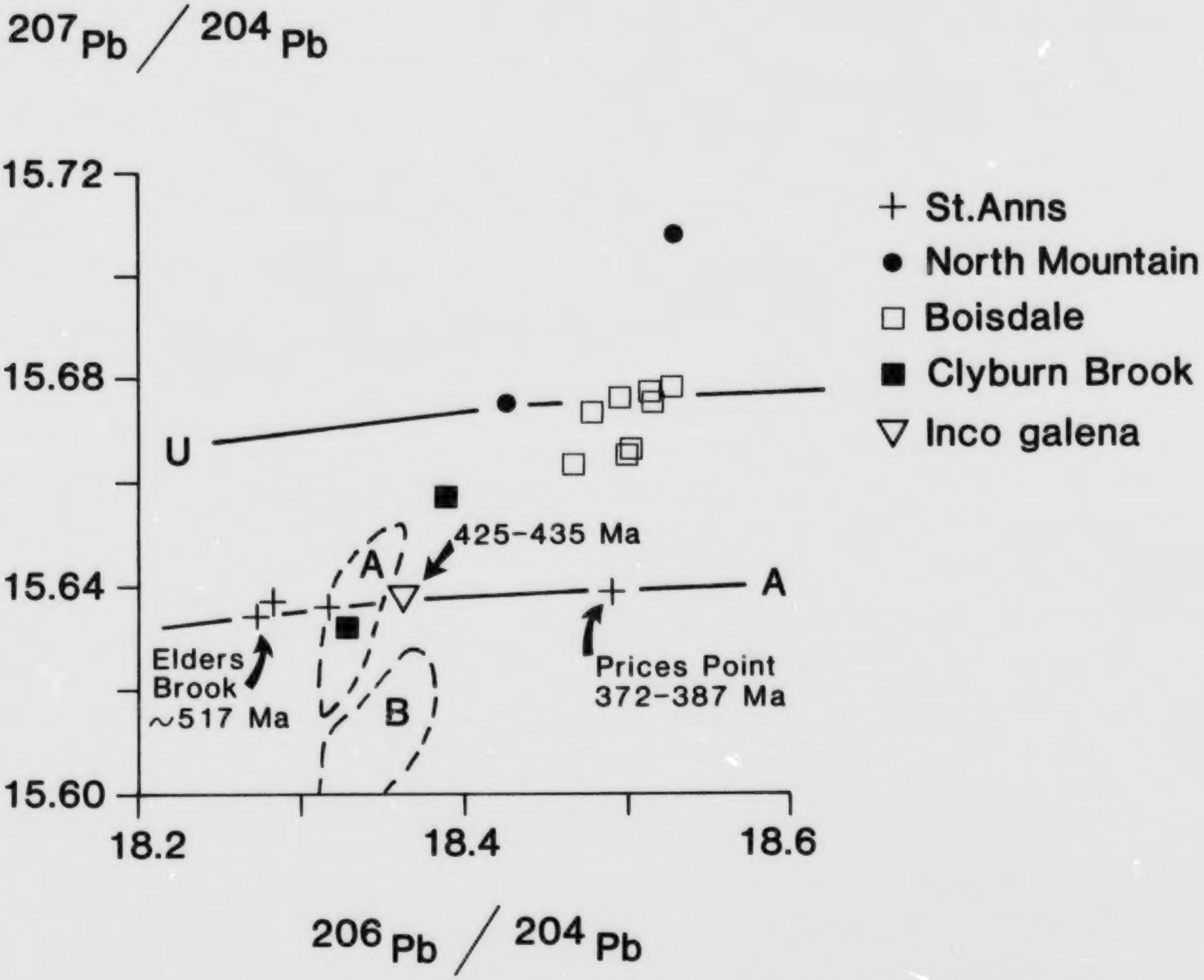

Figure 6. Lead isotopic compositions for galenas from mineral occurrences hosted by rocks of the Bras d'Or Terrane, Cape Breton Highlands/North Mountain/Boisdale Hills areas. Dashed lines outline compositional fields of exhalative galenas "A" and metamorphogenic galenas "B" from Figure 3. Evolution curves for upper crust =U from Zartman and Doe, 1981. Evolution curve (A) has been calculated to fit The Elders Brook and Prices Point isotopic compositions.

occurrence lies on the sea-coast on the western side of a major photo-linear which traverses St. Anns Bay-Baddeck Bay and which may represent a younger structure to which the occurrence may be related. The intermediate compositions cluster within the lower half of the total range of values (Fig. 6), with that for the Inco galena being the most evolved. The Inco vein galena, according to the above interpreted ages, and again assuming an isotopically comparable source, gives an age at about 425 to 435 Ma, which is synchronous with postulated early movement on the Eastern Highlands Shear Zone and corresponds to the age of volcanic rocks in the Jumping Brook metamorphic suite in the Aspy zone. These results permit speculation on an integrated model for mineralization in the Aspy and northwestern Bras d'Or terranes involving: 1) contemporaneous volcanism and formation of stratiform exhalative sulphide zones in the Aspy Terrane (~430 Ma); and 2) formation of gold-base metal veins in the western Bras d'Or Terrane during emplacement of this terrane along fault systems which also served as sites for the veins. This thesis may warrant further study with regard to the importance of models for the regional genetic controls of veins in the design of prospecting programs.

The more radiogenic of the two galena specimens from the Clyburn Brook area is from gash veins in rhyolite, and its composition is not similar to those for other vein occurrences. Its radiogenic character may reflect derivation of its lead from the rhyolitic host.

The galenas from the southern Bras d'Or Terrane are distinctly more radiogenic than those discussed above.

In spite of the fact that some samples from the northwestern Bras d'Or Terrane and all samples from the southern Bras d'Or Terrane appear to be related to Cambrian granitoid plutons, the compositional difference would seem to indicate a distinctly different and more radiogenic source for the southern Bras d'Or galenas, possibly reflecting derivation of lead and associated plutons from isotopically distinct basement.

Lime Hill (33) and Meat Cove (34) occurrences

Sangster et al. (1990) have investigated the compositions of galenas from the Meat Cove occurrence in the Blair River Complex and the Lime Hill occurrence on North Mountain, Bras d'Or Terrane (Fig. 1). Their data are briefly reviewed here to provide a complete overview of the available galena lead isotopic data for pre-Devonian rocks of central and northeastern Cape Breton Island.

The Meat Cove and Lime Hill occurrences consist of both disseminated and massive sphalerite in concordant bands and zones within forsterite marble. They have been interpreted as sedimentary exhalative deposits that formed from Mississippi Valley-type brines (Sangster et al., 1990). The host rocks at Meat Cove are Grenvillian on the basis of a 1040 +30/−40 Ma U-Pb (zircon) metamorphic age and an interpreted 1100 to 1500 Ma intrusive age on associated syenite (Barr et al., 1987), whereas the Lime Hill gneiss is of uncertain Precambrian age, but was intruded and metamorphosed at about 540 Ma (A.L. Sangster, P.A. Hunt, J.K. Mortensen, unpublished data).

Lead from the Meat Cove zinc occurrence is much more primitive in composition (Fig. 3) than that from the occurrences described above. This is compatible with its association with Grenvillian rocks (Barr et al., 1987) and a proposed origin from Mississippi Valley-type brines (Sangster et al., 1990). The isotopic compositions of galenas from Lime Hill are similar to those from Meat Cove (Fig.3) and suggest a similar time of formation from a similar source. The isotopic compositions of both the Lime Hill and Meat Cove galenas are similar to those for leads from similar deposits hosted by Grenville Supergroup marble in Ontario, Quebec, and New York State (see Fig. 13, Sangster et al., 1990). The interpreted origin for the latter Grenvillian deposits (Sangster and Bourne, 1982; Whelan et al., 1984; Gauthier and Brown, 1986) has, in fact, been the one adopted in all essential elements for the Cape Breton deposits. These data suggest that the Meat Cove and Lime Hill deposits are of similar middle Proterozoic age, but, as yet, no independent corroborative evidence has been found. The Lime Hill and Meat Cove galenas are sufficiently distinct isotopically from other Bras d'Or Terrane galenas to exclude Cambrian granite as a source for their mineralizing fluids.

CONCLUSIONS

This review of the isotopic compositions of galenas from mineral occurrences in central and northern Cape Breton Island supports the following conclusions relevant to both mineral deposit and regional geology:

1) The trace amounts of galena found in mineral occurrences at Sarach Brook, and in chlorite schist and in joints and fractures in country rock at Cheticamp and Money Point may very well have formed from lead liberated from felsic volcanic materials during metamorphism about 400 Ma ago. Stratiform mineralization in these areas is likely of exhalative origin and related to volcanism about 430 Ma ago. The conclusions reached here are considered to help substantiate interpretations that all layered rocks in the Aspy Terrane are related to Ordovician-Silurian volcanism and sedimentation.

2) North- to northwest-striking base metal-gold veins in the eastern Bras d'Or Terrane may have formed episodically between Late Cambrian time (~517 Ma) and the time represented by the earliest Silurian (~430 Ma), with the Prices Point vein being possibly as young as Late Devonian. The veins are probably associated with fissures developed during the history of initial breakup (Cambrian?) of a late Precambrian platformal terrane, and emplacement of a piece of it (the Bras d'Or Terrane) in its current structural position at some time during the Silurian/Devonian. This would support a contention that structures associated with the suture, represented by the Eastern Highlands Shear Zone between the Aspy and Bras d'Or terranes, might be preferred sites for gold vein mineralization.

3) The different compositions of galenas associated with Cambrian granitoid intrusions in the eastern and western parts of the Bras d'Or Terrane, in conjunction with very different values obtained from the Lime Hill zinc occurrence, suggest that these occurrences may reflect a basement configuration in the Bras d'Or Terrane of Barr and Raeside (1989) that is more complex than is currently believed.

ACKNOWLEDGMENTS

The authors wish to thank the individuals and companies who have permitted access to their mineral exploration properties and sampling of the mineral occurrences being investigated and for discussions of the geology of those occurrences. In particular gratitude is expressed to Colin MacKenzie and Gary Woods of BP Resources Canada Limited, Bert MacNabb and Mark Slauenwhite of Inco Gold Management Limited, and Gordon Cranton of Gold Brook Developments Limited. We would also like to acknowledge Al Gibb of Parks Canada for permission to visit and sample occurrences in Cape Breton Highlands National Park. The manuscript benefitted from a review by Sandra Barr.

REFERENCES

Barr, S.M. and Raeside, R.P.
1989: Tectono-stratigraphic terranes in Cape Breton Island, Nova Scotia: implications for the configuration of the northern Appalachian orogen; Geology, v. 17, p. 822-825.

Barr, S.M., Raeside, R.P., and Jamieson, R.A.
in press: Geology of northern Cape Breton Island, Nova Scotia; Geological Survey of Canada, Map 1752A. Accompanies Raeside, R.P. and Barr, S.M., in press: Preliminary report on the geology of the Cape Breton Highlands, Nova Scotia; Geological Survey of Canada, Paper 89-14.

Barr, S.M., Raeside, R.P., and van Breemen, O.
1987: Grenvillian basement in the northern Cape Breton Highlands, Nova Scotia; Canadian Journal of Earth Sciences, v. 24, p. 992-997.

Cormier, R.F.
1980: New rubidium/strontium ages in Nova Scotia; *in* Report of Activities, 1979, Nova Scotia Department of Mines and Energy, Report 80-1, p. 223-233.

Currie, K.L., Loveridge, W.D., and Sullivan, R.W.
1982: A U-Pb age on zircon from dikes feeding basal rhyolitic flows of the Jumping Brook complex, northwestern Cape Breton Island, Nova Scotia; *in* Current Research, Part C, Geological Survey of Canada, Paper 82-1C, p. 125-128.

Dunning, G.R., Barr, S.M., Raeside, R.P., and Jamieson, R.A.
1990: U-Pb zircon, titanite, and monazite ages in the Bras d'Or and Aspy terranes of Cape Breton Island, Nova Scotia: Implications for igneous and metamorphic history; Geological Society of America Bulletin, v. 102, p. 322-330.

Fletcher, I.R.
1979: A lead isotopic study of lead-zinc mineralization associated with the central metasedimentary belt of the Grenville Province; Ph.D. thesis, University of Toronto, Toronto, Ontario, 147 p.

Gaudette, H.E., Olszewski, W.J., and Jamieson, R.A.
1985: Rb-Sr ages of some basement rocks, Cape Breton Highlands, Nova Scotia; *in* Program with Abstracts, Geological Association of Canada/Mineralogical Association of Canada, v. 10, p. A20.

Gauthier, M. and Brown, A.C.
1986: Zinc and iron metallogeny in the Maniwaki-Gracefield district, southwestern Quebec; Economic Geology, v. 81, p. 89-112.

Jamieson, R.A., Tallman, P.C., Plint, H.E., and Connors, K.A.
1989: Geological setting of pre-Carboniferous mineral deposits in the western Cape Breton Highlands, Nova Scotia; Geological Survey of Canada, Open File 2008, 72 p.
1990: Regional geological setting of pre-Carboniferous mineral deposits in the western Cape Breton Highlands, Nova Scotia; *in* Mineral Deposit Studies in Nova Scotia, Volume 1, edited by A.L. Sangster, Geological Survey of Canada, Paper 90-8, p. **-**.

Jamieson, R.A., van Breemen, O., Sullivan, R.W., and Currie, K.L.
1986: The age of igneous and metamorphic events in the western Cape Breton Highlands, Nova Scotia; Canadian Journal of Earth Sciences, v. 23, p. 1891-1901.

Keppie, J.D. and Halliday, A.N.
1986: Rb-Sr isotopic data from three suites of igneous rocks, Cape Breton Island, Nova Scotia; Maritime Sediments and Atlantic Geology, v. 22, p. 162-171.

Macdonald, A.S. and Barr, S.M.
1985: Geology and age of polymetallic mineral occurrences in volcanic and granitoid rocks, St. Ann's area, Cape Breton Island, Nova Scotia; *in* Current Research, Part B, Geological Survey of Canada, Paper 85-1B, p. 117-124.

Ponsford, M. and Lyttle, N.A.
1984: Metallic mineral occurrences map and data compilation, eastern Nova Scotia — Map sheets 11F, 11G, 11J, 11K, 11N; Nova Scotia Department of Mines and Energy, Open File Report 600.

Poole, W.H.
1980: Rb-Sr age of the Shunacadie Pluton, central Cape Breton Island, Nova Scotia; *in* Current Research, Part C, Geological Survey of Canada, Paper 80-1C, p. 165-169.

Raeside, R.P.
1990: Low-pressure metamorphism of the Lime Hill gneiss complex, Bras d'Or Terrane, Cape Breton Island, Nova Scotia; *in* Mineral Deposit Studies in Nova Scotia, Volume 1, edited by A.L. Sangster, Geological Survey of Canada, Paper 90-8, p. **-**.

Reynolds, P.H., Jamieson, R.A., Barr, S.M., and Raeside, R.P.
1989: An ^{40}Ar/^{39}Ar study of the Cape Breton Highlands, Nova Scotia: thermal histories and tectonic implications; Canadian Journal of Earch Sciences, v. 26, p. 2081-2091.

Sangster, A.L.
1980: Report on geological, soil and rock geochemical surveys and ground VLF survey, Sarach Brook, Cape Breton Island, St. Joseph Explorations Limited; Nova Scotia Department of Mines and Energy, Assessment File 11K/07B — 07-Q-24(03), 8 p., 12 maps.

Sangster, A.L. and Bourne, J.
1982: Geology of the Grenville Province and regional metallogenesis of the Grenville Supergroup; *in* Precambrian Sulphide Deposits, edited by R.W. Hutchinson, C.D. Spence, and J.M. Franklin, Geological Association of Canada, Special Paper 25, p. 91-126.

Sangster, A.L. and Wowkodaw, O.
1979: Report on geological, soil, rock, stream sediment and heavy mineral geochemical surveys, Sarach Brook, Cape Breton Island, St. Joseph Explorations Limited; Nova Scotia Department of Mines and Energy, Assessment File 11K/07B — 07-Q-24(02), 7 p., 25 maps.

Sangster, A.L., Justino, M.F., and Thorpe, R.I.
1990: Metallogeny of the Proterozoic marble-hosted zinc occurrences at Lime Hill and Meat Cove, Cape Breton Island, Nova Scotia; *in* Mineral Deposit Studies in Nova Scotia, Volume 1, edited by A.L. Sangster, Geological Survey of Canada, Paper 90-8, p. **-**.

Whelan, J.F., Rye, R.O., and deLorraine, W.
1984: The Balmat-Edwards zinc-lead deposits — Synsedimentary ore from Mississippi Valley-type fluids; Economic Geology, v. 79, p. 239-265.

Zartman, R.E. and Doe, B.R.
1981: Plumbotectonics — the model; Tectonophysics, v. 75, p. 135-162.

APPENDIX I. Lead isotopic analyses of galenas from mineral occurrences in the Aspy and Bras d'Or terranes and Blair River Complex, Cape Breton Island. Lead isotopic analyses were carried out at Geospec Consultants Ltd., Edmonton, Alberta.

		Pb Isotopic Ratios		
SAMPLE	**LOCATION**	**206/204**	**207/204**	**208/204**

Aspy Terrane

a) Trace galenas from disseminated pyrrhotite-chalcopyrite occurrences in chlorite schist.

SAMPLE	LOCATION	206/204	207/204	208/204
SFB-86-508	THE FALLS	18.236	15.604	38.175
SFB-86-509	THE FALLS	18.331	15.608	38.187
SFB-86-508A	THE FALLS	18.332	15.611	38.198

b) Galenas from sericite schist hosted arsenopyrite-pyrite-sphalerite-galena mineralization associated with mafic metavolcanic rocks.

SAMPLE	LOCATION	206/204	207/204	208/204
KQS-85-300	ROAD 2	18.310	15.625	38.147
TQ85-70	SILVER CLIFF	18.307	15.620	38.136
TQ85-53	SILVER CLIFF	18.313	15.626	38.153
TQ85-56	SILVER CLIFF	18.323	15.631	38.161
TQ85-65	SILVER CLIFF	18.322	15.635	38.181
TQ85.78	SILVER CLIFF	18.313	15.626	38.153
TQ85-83	SILVER CLIFF	18.321	15.630	38.165
TQ85-88	SILVER CLIFF	18.330	15.643	38.191
TQ85-77	CORE SHACK	18.313	15.624	38.142
TQ85-76	MOUNTAIN TOP	18.314	15.637	38.158
TQ85-86	MOUNTAIN TOP	18.314	15.623	38.151
TQ85-54	FISSET BROOK	18.312	15.632	38.145
TQ85-87	FISSET BROOK	18.325	15.642	38.188
TQ83-134	FISSET BROOK	18.321	15.632	38.169
TQ85-66	GALENA MINE	18.310	15.621	38.134
TQ85-84	GALENA MINE	18.326	15.637	38.180
TQ85-85	GALENA MINE	18.322	15.634	38.169
TQ83-132	GALENA MINE	18.324	15.635	38.174
TQ83-133	HIGHLAND MERCURY	18.327	15.639	38.192
TQ85-60	HIGHLAND MERCURY	18.320	15.629	38.154
TQ85-73	HIGHLAND MERCURY	18.316	15.628	38.153
SFB-86-692*	ROCKY BROOK	18.333	15.608	38.193
SFB-88-581*	ROCKY BROOK	18.354	15.613	38.217

*the Rocky Brook occurrence is hosted by rhyolite at the same stratigraphic position as the sericite-schist-hosted occurrences and could represent their precursor mineralization.

c) Galenas from disseminated pyrite occurrences hosted by sericite schist.

SAMPLE	LOCATION	206/204	207/204	208/204
SFB-87-1356	FISHING COVE BROOK	18.307	15.587	38.150
SFB-87-1351	BOARSBACK	18.340	15.649	38.329

d) Galenas from sphalerite-galena joint coatings in metasedimentary rocks.

SAMPLE	LOCATION	206/204	207/204	208/204
SFB-86-559	CORNEY BROOK	18.317	15.601	38.161
SFB-86-507	L. FARIBAULT BROOK	18.345	15.615	38.218
SFB-86-506	L. FARIBAULT BROOK	18.310	15.611	38.186
SFB-86-503	NORANDA TRENCH	18.346	15.604	38.185
SFB-86-504	NORANDA TRENCH	18.347	15.612	38.230
SFB-86-504R	NORANDA TRENCH	18.355	15.621	38.250
KQS-85-298	AMAX TRENCH	18.362	15.626	38.236

e) Other Aspy Terrane galenas from occurrences described individually in text.

SFB-88-566	MIDDLE SISTER	18.640	15.650	38.434
KQS-85-193	SARACH BROOK	18.346	15.602	38.213
KQS-85-133	SARACH BROOK	18.292	15.590	38.090
KQS-85-189	SURACH BROOK	18.374	15.613	38.245
SFB-85-286	SUGARLOAF	18.411	15.620	38.303
SFB-87-1610	MONEY POINT	18.352	15.621	38.277
SFB-87-1605	MONEY POINT	18.378	15.640	38.335
SFB-87-1606	MONEY POINT	18.330	15.611	38.230
SFB-87-1608	MONEY POINT	18.358	15.619	38.264
SFB-87-1303	*TURNER BROOK (SELCO)	18.434	15.632	38.285
SFB-87-1305	*TURNER BROOK (SELCO)	18.415	15.629	38.291

*These galenas are from a unique occurrence consisting of minor galena disseminations in interflow volcaniclastic sedimentary rocks in vesicular basalt of the Fisset Brook Formation of Middle Devonian age. The isotopic analyses are reported here but not interpreted.

Bras d'Or Terrane

a) Galenas from polymetallic veins in the southeastern Cape Breton Highlands.

SFB-86-893	CLYBURN BROOK	18.391	15.657	38.297
SFB-86-894	SLATE BROOK	18.330	15.632	38.212
SFB-86-927	TARBOTVALE	18.317	15.636	38.113
SFB-86-938	ELDERS BROOK	18.274	15.634	38.045
SFB-86-939	ELDERS BROOK	18.285	15.637	38.047
SFB-87-1009	PRICES POINT	18.493	15.639	38.486
TQ88-25	INCO GALENA	18.364	15.638	38.302

b) Galenas from veins in the Boisdale Hills.

SFB-86-1020	REAR BOISDALE	18.530	15.678	38.263
SFB-86-1016	REAR BOISDALE	18.517	15.675	38.251
SFB-86-1013	REAR BOISDALE	18.501	15.665	38.232
SFB-86-1014	REAR BOISDALE	18.515	15.677	38.269
TQ85-59	REAR BOISDALE	18.504	15.666	38.255
TQ85-61	REAR BOISDALE	18.497	15.676	38.254
TQ85-71	REAR BOISDALE	18.469	15.663	38.205
TQ85-75	REAR BOISDALE	18.480	15.673	38.285

c) Galenas from veins on North Mountain.

SFB-86-564	MILL BROOK	18.428	15.675	38.246
SFB-86-560	WEST BAY ROAD	18.532	15.708	38.500
KQS-85-234	LIME HILL	17.085	15.567	36.748
SFB-86-206	LIME HILL	17.000	15.562	36.718

d) Galenas from stratiform marble-hosted zinc occurrences, Blair River Complex and Lime Hill (from Sangster et al., 1990).

SFB-86-595	MEAT COVE	17.209	15.513	36.376
SFB-86-595R	MEAT COVE	17.166	15.512	36.620
SFB-86-595R	MEAT COVE	17.026	15.480	36.438
TQ-87-54	MEAT COVE	17.061	15.489	36.477
TQ-87-54R	MEAT COVE	17.059	15.487	36.499

Metallogeny of the Meguma Terrane, Nova Scotia[1]

A.L. Sangster[2]

Sangster, A.L., Metallogeny of the Meguma Terrane, Nova Scotia; in Mineral Deposit Studies in Nova Scotia, Volume 1, edited by A.L. Sangster, Geological Survey of Canada, Paper 90-8, p. 115-162, 1990.

116 Abstract/Résumé

119 Geological overview
119 Pre-Middle Devonian
119 Post-Middle Devonian
120 Mineral occurrence overview

Part I: Stratabound mineral occurrences

120 Goldenville-Halifax Formation Transition Zone
120 Introduction
120 Geology of the GHT
120 Geology of the Eastville occurrence
122 Regional mineral occurrences
122 Origin of the coticule
123 Geology of the Torbrook iron formation

Part II: Meguma group gold veins

123 Introduction
124 General geology of the gold districts
127 Structural geology
127 Stratiform veins
129 En echelon veins
130 Angular veins
130 Pegmatitic veins
130 ac veins
130 Northwest faults and veins
130 Miscellaneous structures
130 Mineralogy of the veins
130 Quartz
131 Arsenopyrite
131 Carbonate
131 Gold
132 Accessory minerals
135 Wall-rock alteration
136 Origin of the veins
137 Source of vein materials
139 Timing of vein formation

Part III: Granite-related Sn-W-base metal-U mineralization

140 Introduction
142 Wedgeport-East Kemptville Domain
142 Introduction
142 East Kemptville tin deposit
147 Sediment-hosted tin occurrences
147 Brazil Lake lithium pegmatite
147 New Ross-Vaughan Domain
147 Introduction
147 Greisen
148 Pegmatite
148 Vein and shear zone mineralization
148 Millet Brook uranium deposits
150 Westfield-Caledonia Domain
150 Digby-Gaspereau Domain
150 Shelburne Domain
151 Miscellaneous occurrences
151 West Gore antimony-gold occurrence
152 Liscomb area
152 Eastern Meguma Terrane
152 Musquodoboit pluton
152 Origin of granite-related mineralization
152 Lithophile element deposits
153 Relationship of mineralization to intrusions younger than the SMB
153 Relationship to the Tobeatic Fault Zone
154 Spatial association of mineralization with the Goldenville-Halifax Formation Transition Zone
154 Uranium deposits

Part IV: Regional metallogenic correlation

156 Acknowledgments

156 References

---

[1] Contribution to the Canada – Nova Scotia Mineral Development Agreement, 1984-1989. Project carried by the Mineral Resources Division, Geological Survey of Canada, Project 860008. This review will also be a contribution to the "Geology of the Appalachian Orogen in Canada and Greenland" volume of the Geology of Canada (Decade of North American Geology) series.

[2] Geological Survey of Canada, 601 Booth St., Ottawa, Ontario, K1A 0E8

Abstract

The allochthonous Meguma Terrane consists of major sequences of sandy flysch and shaly flysch of Cambro-Ordovician age overlain locally by Siluro-Devonian clastic metasedimentary and metavolcanic rocks. These rocks are intruded by a batholithic suite of peraluminous granitic rocks with the major event roughly synchronous with the Hercynian intrusive event in Europe. The main batholithic bodies cluster in age about 370 Ma with a younger intrusive suite at 320 to 300 Ma.

Abundant mineral occurrences are associated with both the clastic and intrusive rocks. Metal concentrations that are interpreted to have formed during sedimentation and diagenesis include laterally extensive manganese-bearing strata (in large part coticule) at the transition from the lower Goldenville Formation sandy flysch to the overlying Halifax Formation carbonaceous, sulphidic, shaly flysch. These sediments are variably enriched in a suite of elements including Mn, Total C, Pb, Ba, Au, Zn, Cu, Mo, and W. At Eastville, the basal Halifax Formation immediately overlying the coticule contains subeconomic stratabound concentrations of base metals, which have been interpreted to have a sedimentary exhalative origin.

In the Goldenville Formation, large concordant, arsenical, gold-bearing vein swarms occur in portions of the stratigraphy that contain increased thicknesses of interstratified black argillite. The veins are spatially associated with the crests and flanks of anticlinal domes but most veins are not true saddle reefs in that the veins are not commonly thickened over the crests of anticlines and extend significant distances down fold limbs away from fold hinges. The veins have formed from metamorphically derived fluids. There is considerable current debate whether those fluids were derived from the Meguma Group during the initial stages of metamorphism or later from deep crustal sources at the time of granite emplacement.

Metasedimentary rocks of the Devonian Torbrook Formation contain thin beds of classical oolitic iron formation which has been contact metamorphosed in the thermal aureole of the South Mountain Batholith.

Granite-related mineral occurrences are genetically associated with both the main phase of batholith intrusion and the suite of younger granitoids intruding its contact zones and adjacent Meguma country rock. Occurrences that are probably associated with the main period of batholith intrusion include the major uranium vein occurrences at Millet Brook and a variety of vein and pegmatite occurrences related to the younger leucomonzogranite phase of the main batholithic suite (361 Ma). These occur in the New Ross-Vaughan area and are associated with smaller intrusions of similar character (~370 Ma) in the eastern Meguma Terrane. The larger deposits, particularly of tin and tungsten greisen and vein mineralization, hosted by both granite and Meguma sedimentary rocks, are related to the younger suite of intrusions. The major East Kemptville greisen-tin deposit occurs within the Davis Lake pluton (337 Ma; greisen muscovite 295 Ma) whereas a major occurrence at Plymouth occurs near the contact with the Wedgeport pluton (316 Ma) southwest of the main batholith exposure.

Mineral occurrences in the Meguma Terrane are part of a regional environment reflecting processes extant in a much wider region than the Meguma Terrane. Manganese-rich lithologies are common in Middle Cambrian to Caradocian rocks throughout eastern North America and northwestern Europe, and gold deposits with affinities to those located in the Meguma Group occur within the Appalachian-Caledonian orogen in rocks of similar lithology and age in Ireland and Scottish Uplands as well as farther afield in the Spanish Pyrenees and Victoria mining district of Australia. The major Aguilar Pb-Zn-Ag deposit, Argentina occurs in manganese-rich strata in a quartzite-slate transition of Cambro-Ordovician age. Tin, tungsten, and uranium deposits of the Meguma Terrane are similar in age and general geology to the tin-tungsten and uranium deposits that are related to Hercynian plutonism in western and central Europe.

Résumé

Le terrane allochtone de Meguma se compose de grandes séquences de flysch sableux et de flysch schisteux d'âge cambrien-ordovicien, recouvert par endroits par des roches clastiques siluriennes-dévoniennes, de type métasédimentaire et métavolcanique. Ces roches sont traversées par une série batholitique de roches granitiques hyperalumineuses, et le principal épisode d'intrusions est approximativement contemporain de l'épisode des intrusions hercyniennes en Europe. Les principaux corps batholitiques ont des âges se groupant autour de 370 Ma, et sont accompagnés d'une série intrusive plus jeune datée de 320 à 300 Ma.

D'abondantes minéralisations sont associées à la fois aux roches clastiques et aux roches intrusives. Les concentrations métalliques qui selon les interprétations se seraient formées pendant la sédimentation et la diagénèse, ont en particulier eu lieu dans des strates de grande extension latérale (en grande partie des coticules) riches en Mn, au niveau de la transition entre le flysch sableux du niveau inférieur de la formation de Goldenville et le flysch carboné, sulfuré, schisteux, de la formation sus-jacente de Halifax. Ces sédiments sont diversement enrichis en une série d'éléments, notamment Mn, C total, Pb, Ba, Au, Zn, Cu, Mo et W. À Eastville, la formation basale de Halifax située immédiatement au-dessus de la coticule contient des concentrations de métaux communs se manifestant à l'intérieur d'une seule strate et se situant à un niveau inférieur au seuil de la rentabilité qui, selon les interprétations, seraient d'origine exhalative sédimentaire.

Dans la formation de Goldenville, de grands essaims de filons aurifères concordants, arséniés se manifestent dans des parties de la colonne stratigraphique se caractérisant par des augmentations d'épaisseur de l'argilite noire interstratifiée. Les filons sont spatialement associés avec les crêtes et flancs des dômes anticlinaux, mais la plupart des filons ne sont pas de vrais gîtes de charnière anticlinale, du fait que ces filons ne sont pas généralement épaissis au-dessus des crêtes des anticlinaux et se prolongent à des distances assez importantes le long des flancs des plis, à partir des charnières des plis. Les filons se sont formés à partir de fluides de provenance métamorphique. Actuellement, les chercheurs sont engagés dans un très vif débat visant à établir si ces fluides sont provenus du groupe de Meguma durant les stades initiaux de métamorphisme, ou plus tard de sources crustales profondes à l'époque de la mise en place du granite.

Les roches métasédimentaires de la formation dévonienne de Torbrook contiennent de minces couches d'une formation ferrifère oolitique classique, qui a subi un métamorphisme de contact dans l'auréole de contact du batholite de South Mountain.

Les manifestations minérales apparentées au granite sont génétiquement associées à la fois avec la phase principale de l'intrusion batholitique et avec la série de granitoïdes plus jeunes traversant ces zones de contact et la roche encaissante adjacente de Meguma. Les venues qui sont probablement associées avec la période principale d'intrusion batholitique comprennent les filons uranifères de Millet Brook et diverses manifestations filoniennes et pegmatitiques associées à la phase plus récente du leucomonzogranite de la principale série batholitique (361 Ma). Ces venues se trouvent dans la région de New Ross et Vaughan, et sont associées à de plus petites intrusions de caractère semblable (~370 Ma) dans la partie est du terrane de Meguma. Les plus vastes gîtes, en particulier les minéralisations en Sn et W de greisens et filons, logées à la fois dans le granite et dans les roches sédimentaires de Meguma, sont apparentés à la plus récente série d'intrusions. L'important gisement de Sn dans un greisen, à East Kemptville, se trouve à l'intérieur du pluton de Davis Lake (337 Ma; muscovite du greisen datée à 295 Ma), tandis qu'une importante venue située à Plymouth se manifeste près du contact avec le pluton de Wedgeport (316 Ma) au sud-ouest du principal affleurement batholitique.

Dans le terrane de Meguma, les venues minérales font partie d'un environnement régional qui reflète les processus survenus dans une région beaucoup plus vaste que ce terrane de Meguma. Les lithologies manganifères sont fréquentes dans les roches du Cambrien moyen au Caradocien dans l'ensemble de l'est de l'Amérique du Nord, et dans tout le nord-ouest de l'Europe, et des gisements d'or présentant des affinités avec ceux situés dans le groupe de Meguma se manifestent dans l'orogène appalachien-calédonien dans des roches de lithologie et d'âge comparables en Irlande et sur les hautes terres d'Écosse, ainsi que dans des territoires très éloignés, dans les Pyrénées espagnoles et dans le district minier de Victoria en Australie. Le grand gisement de Pb-Zn-Ag d'Aguilar en Argentine est situé dans des strates manganifères dans une zone de transition entre un quartzite et un schiste ardoisier d'âge cambrien-ordovicien. Les gisements de Sn, W et U du terrane de Meguma ont un âge et une géologie générale comparables à ceux des gisements de Sn, W et U qui sont apparentés au plutonisme hercynien de l'ouest et du centre de l'Europe.

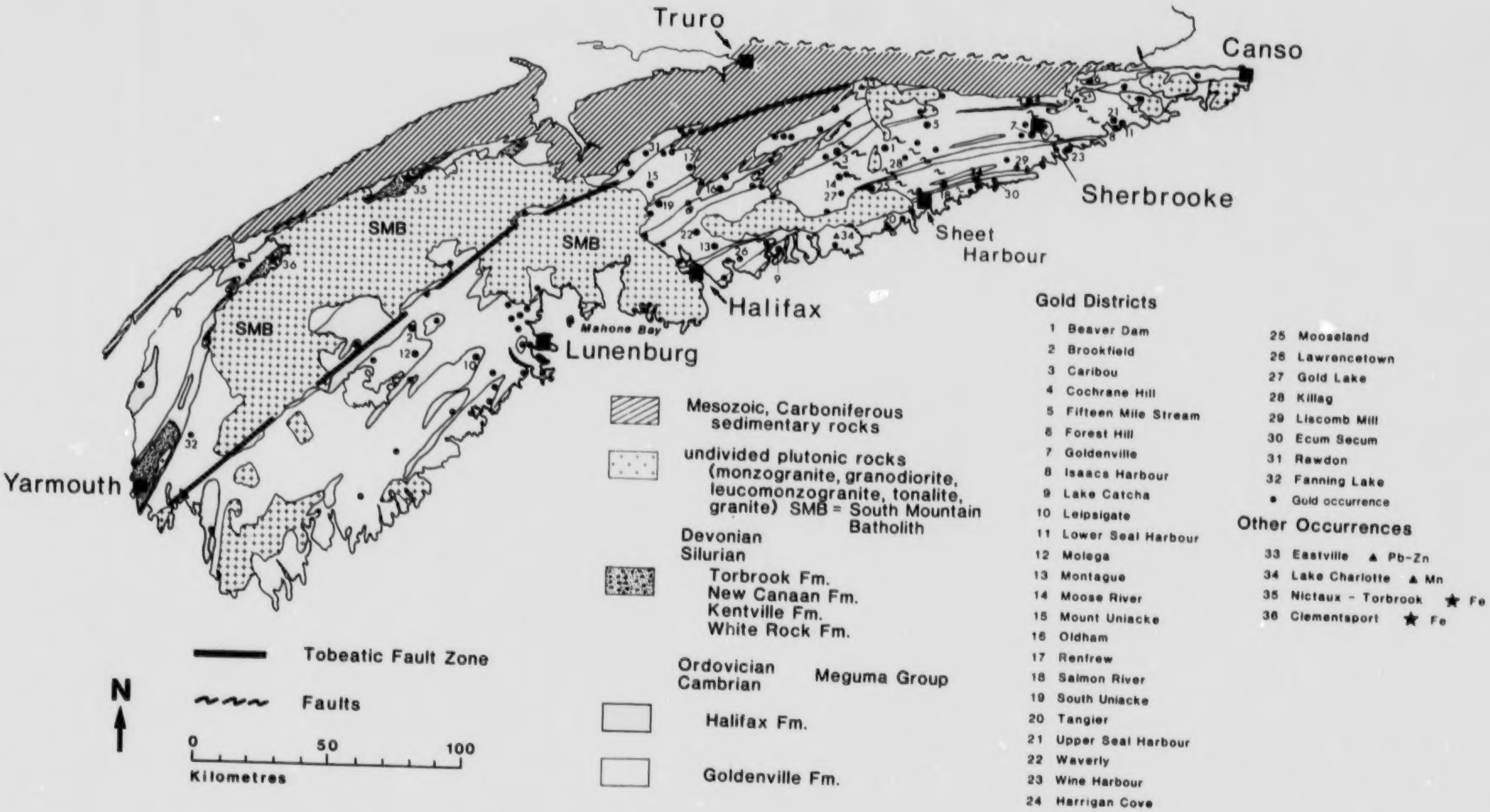
Truro
Canso
Sherbrooke
Sheet Harbour
Halifax
Mahone Bay
Lunenburg
Yarmouth
SMB
SMB
SMB
Mesozoic, Carboniferous sedimentary rocks
undivided plutonic rocks (monzogranite, granodiorite, leucomonzogranite, tonalite, granite) SMB = South Mountain Batholith
Devonian
Silurian
Torbrook Fm.
New Canaan Fm.
Kentville Fm.
White Rock Fm.
Ordovician
Cambrian
Meguma Group
Halifax Fm.
Goldenville Fm.
Tobeatic Fault Zone
Faults
N
0
50
100
Kilometres
Gold Districts
1 Beaver Dam
2 Brookfield
3 Caribou
4 Cochrane Hill
5 Fifteen Mile Stream
6 Forest Hill
7 Goldenville
8 Isaacs Harbour
9 Lake Catcha
10 Leipsigate
11 Lower Seal Harbour
12 Molega
13 Montague
14 Moose River
15 Mount Uniacke
16 Oldham
17 Renfrew
18 Salmon River
19 South Uniacke
20 Tangier
21 Upper Seal Harbour
22 Waverly
23 Wine Harbour
24 Harrigan Cove
25 Mooseland
26 Lawrencetown
27 Gold Lake
28 Killag
29 Liscomb Mill
30 Ecum Secum
31 Rawdon
32 Fanning Lake
● Gold occurrence
Other Occurrences
33 Eastville ▲ Pb-Zn
34 Lake Charlotte ▲ Mn
35 Nictaux - Torbrook ★ Fe
36 Clementsport ★ Fe

Figure 1. Geology and nongranite-related mineral occurrences of the Meguma Terrane.

GEOLOGICAL OVERVIEW

The Meguma Terrane is a slim wedge of allochthonous crust 440 km long and up to 110 km wide that forms the southwestern part of the Province of Nova Scotia (Fig. 1). This "suspect terrane" docked with the eastern side of the Avalon Platform during the Middle Devonian (Keppie, 1985). As a result, the pre-Middle Devonian history of the Meguma Terrane is distinct from the history of adjacent areas whereas its post-Middle Devonian history is shared with the region in which it occurs. Schenk (1971, 1973) proposed a source for the Meguma clastic sediments in proximity to the current position of North Africa.

Pre-Middle Devonian

The Meguma zone was folded about northeasterly trending, subhorizontal axes during the Early Devonian Acadian Orogeny. The folds tend to be broad and open and can normally be traced along strike for 100 km or more. Wavelengths are of the order of 10 km.

The pre-Middle Devonian history of the Meguma Terrane is represented by a sequence of sedimentary rocks giving a more or less complete record of deposition from the Cambrian to Lower Devonian. The Cambro-Ordovician Meguma Group constitutes approximately 90 percent of the exposed sedimentary sequence. The sequence consists of the basal Goldenville Formation quartz wacke and the overlying Halifax Formation slate. The age of Meguma sedimentation is constrained by the presence of 560 to 650 Ma detrital zircons in the Goldenville Formation (Krogh and Keppie, 1988) and by the rare occurrence of Tremadocian graptolites believed to be from a stratum near the top of the Halifax Formation (Cumming, 1985). A second detrital zircon population in the Goldenville Formation, giving ages between 2050 and 2300 Ma (Krogh and Keppie, 1988), is believed to confirm northern Africa as a suitable source for Meguma sediments as proposed by Schenk (1971, 1973). The Halifax Formation is overlain in the west and northeast by infolded keels of Silurian to Lower Devonian clastic sedimentary and volcanic rocks of the White Rock, Kentville, New Canaan, and Torbrook formations.

Although its base is not exposed, the Upper Cambrian (?) Goldenville Formation has a minimum thickness of 5500 m (18 000 feet) and consists of massive, thick bedded, sandy flysch with thin interbeds of chloritic slate and siltstone. Sandstone beds range from a few metres to tens of metres thick whereas the slate beds are 0.1 to 2 m thick. The overlying Ordovician Halifax Formation contains approximately 3700 m (12 000 feet) of grey to black slate with thin interbeds of crosslaminated silty flysch. The slate beds are commonly carbonaceous and contain several percent of pyrrhotite, with minor pyrite in coarser grained, less carbonaceous beds. The transition from the Goldenville to Halifax Formation (GHT) consists of interstratified slate and sandstone and represents a change from noncarbonaceous, sulphide-poor rocks to carbonaceous, sulphide-rich rocks. This transition also contains a calcareous argillite enriched in Mn, coticule in part (i.e. spessartine-rich quartzite), and is locally anomalous in Zn, Pb, Ba, As, and Au (Bishop and Wright, 1974; Binney et al., 1986; Zentilli et al., 1986). Regional work by Schenk (1970) has indicated that the sandy flysch of the Goldenville Formation may represent an abyssal plain deposit and the overlying Halifax Formation shaly flysch may represent the lower part of a continental rise prism. Waldron and Jenson (1985) identified the existence of submarine fan deposits in part of the Goldenville Formation.

Silurian and Lower Devonian rocks are folded into the Halifax Formation in a belt that extends discontinuously along the northwestern flank of the South Mountain Batholith (Fig. 1). The basal White Rock Formation is defined in most areas by the presence of white quartzite (Taylor, 1965). The formation also contains bimodal, rift related, alkalic-tholeiitic volcanic rocks (Keppie and Dostal, 1980). The overlying Kentville, New Canaan, and Torbrook formations represent a concordant Upper Silurian to Lower Devonian sedimentary sequence. The Kentville Formation consists of about 500 to 600 m of siltstone and slate with minor argillaceous quartzite. These rocks grade upward into the New Canaan Formation, consisting of about 300 m of volcanic and siltstone-fragment breccia in a calcareous matrix (Taylor, 1965). The overlying Torbrook Formation consists of slate, siltstone, quartzite (Smitheringale, 1973), and thin beds of Clinton-type iron formation.

Post-Middle Devonian

Post-Middle Devonian rocks overlie both the Meguma zone and the adjacent Avalon Terrane. In the north-central Meguma zone, these include Upper Devonian to Mississippian continental clastic sedimentary rocks of the Horton Group and evaporites (anhydrite, salt) with lesser amounts of limestone and fine grained red clastic sedimentary rocks of the Windsor Group. The northwestern flank of the Meguma zone is overlain by Triassic to Jurassic redbeds and basalts that are related to the development of the Fundy graben.

The pre-Middle Devonian strata in the Meguma zone are intruded by a chemically related suite of posttectonic, peraluminous, S-type, Devono-Carboniferous granitoids (Clarke et al., 1980, 1985). These intrusions consist of granite, granodiorite and granodiorite porphyry, and two-mica monzogranite. Lesser amounts of tonalite and trondhjemite are locally present. The intrusive rocks vary in composition from tonalite to leucomonzogranite with quartz diorite and biotite monzogranite being the most common compositions. Their size varies from bodies of a few square kilometres to composite intrusions of batholithic scale.

Regional metamorphism associated with the earliest phases of Acadian plutonism postdated the development of regional folding (Keppie, 1985). $^{40}Ar/^{39}Ar$ studies (Muecke et al., 1988) suggest that the main Acadian regional metamorphism occurred at 405 to 390 Ma with significant thermal overprinting events associated with plutonism at 385 to 360 Ma and 320 to 300 Ma. Regional metamorphic grade is typically greenschist facies but increases in areas of greater Acadian plutonism. Almandine-amphibolite facies (Taylor, 1967) and cordierite-amphibolite facies (Hill, 1986b) are observed in the extreme southwestern and eastern portions of the Meguma zone.

Brittle and ductile faulting have extensively affected rocks of the Meguma Terrane. Intrusions in the northeastern Meguma zone were foliated during a dynamothermal event related to dextral movement along the southern margin of the Carboniferous St. Marys Graben (Chedabucto Fault Zone; Keppie, 1985). Structural trends of Early Devonian (Acadian) folds are segmented by a prominent northwest-trending sinistral fault system. Giles (1985) has recently proposed a major strike-slip fault (Tobeatic Fault) which divides the Meguma Terrane into northwest and southeast structural zones along a trace subparallel to the long axis of the zone.

Mineral occurrence overview

There are three fundamental classes of mineral occurrences in the Meguma Terrane:

1) Concordant deposits that formed during sedimentation or diagenesis. This includes mineralization related to the Goldenville-Halifax Formation Transition Zone (i.e. subeconomic base metal occurrences in the Eastville area, and regional manganese-rich strata) as well as Clinton-type iron occurrences within the Torbrook Formation.

2) Structurally controlled deposits of hydrothermal origin that show no direct relationship to igneous processes. Deposits of this type include the widely known concordant gold-bearing quartz veins hosted by the Goldenville Formation and other small stratabound and crosscutting veins.

3) Deposits that are spatially and genetically related to Acadian plutons. This class includes several types of endogranitic and exogranitic Sn-W-base metal-U occurrences including the East Kemptville tin deposit and the Millet Brook uranium deposit.

PART I: STRATABOUND MINERAL OCCURRENCES

Goldenville-Halifax Formation Transition Zone

Introduction

The Goldenville-Halifax Formation Transition Zone (GHT) is a package of distinctive lithologies occurring in the uppermost part of the Goldenville Formation at the transition from sandy flysch to shaly flysch of the Halifax Formation. The GHT is of variable thickness and is poorly exposed over a strike extent of 1700 km in the Meguma Terrane (Fig. 1). The upper portion of the transition zone contains a manganese- and carbonate-rich unit that is anomalous in a variety of elements that are commonly related to shale-hosted metal deposits. Extensive, low-grade lead-zinc mineralization, as defined by exploration drilling between 1977 and 1983, occurs along a 10 km strike length of the GHT near Eastville.

Geology of the GHT

The stratigraphy of the transition zone is best examined in the Mahone Bay area (O'Brien, 1985b, 1986; Zentilli et al., 1986) and at Eastville (Binney et al., 1986). At Mahone Bay, the GHT (Green Bay Formation of O'Brien) is up to 2 km thick and consists of variable proportions of interstratified grey to green argillite and grey-green to buff quartz sandstone (Rissers Beach, Tancook, and West Dublin members) overlain by rhythmically laminated (millimetre to centimetre scale) green and grey-green sandstone (Moshers Island Member) containing pink and brown laminae rich in manganese garnets and manganese oxides (O'Brien, 1986). Zentilli et al. (1986) indicated that the Moshers Island Member was enriched in Mn, Ba, Cu, Pb, and Zn compared to other units of the GHT at Mahone Bay.

The GHT at Eastville is 35 to 45 m thick in contrast to the 2 km section at Mahone Bay (Binney et al., 1986). The basal units of the transition zone consist of massive quartz metawacke interstratified with grey to black sulphidic slate, resting sharply on massive, grey to greenish-grey Goldenville Formation quartz metawacke. The slate forms 10 to 50 percent of this unit and displays abrupt facies changes with siltier lithologies (Fig. 2). This is overlain by 7 to 10 m of banded, sulphide-bearing, calcareous spessartine-rich quartzite (i.e. coticule). Individual bands contain up to 14 percent Mn in spessartine garnet. The coticule beds are intensely contorted (Fig. 3) in contrast to the relatively planar stratification present in both the overlying and underlying sedimentary rocks. The coticule is overlain by a 5 to 15 m thick, massive, black, pyrrhotite-rich argillite which is defined as the base of the Halifax Formation (Binney et al., 1986). Elsewhere, in areas of lowest metamorphic grade, manganese-rich carbonate occurs at this horizon.

Geology of the Eastville occurrence

The base metal mineralization at Eastville (Binney et al., 1986; MacInnis, 1986) occurs mainly within the basal beds of the Halifax Formation and to a lesser extent in manganese-rich lithologies along a 10 km strike length of GHT. To the west, the mineralized horizon extends beneath the edge of the Carboniferous Windsor Group rocks; to the east, it is truncated by the Liscomb pluton and/or the St. Marys fault. The stratabound mineralization is confined to the transition zone and the base of the Halifax Formation, dropping sharply in grade at its lower contact with the Goldenville Formation and decreasing from highest grade near the base of the Halifax Formation to 100 to 200 ppm Pb + Zn 10 to 100 m higher in the stratigraphy. Mineralization within the transition zone itself tends to be rather low grade and very erratic. Values in the calcareous quartzite (coticule) are anomalous compared to the regional rocks but are the lowest tenor within the anomalous stratigraphy. Combined Pb-Zn values tend to average 0.5 to 1.5 percent over

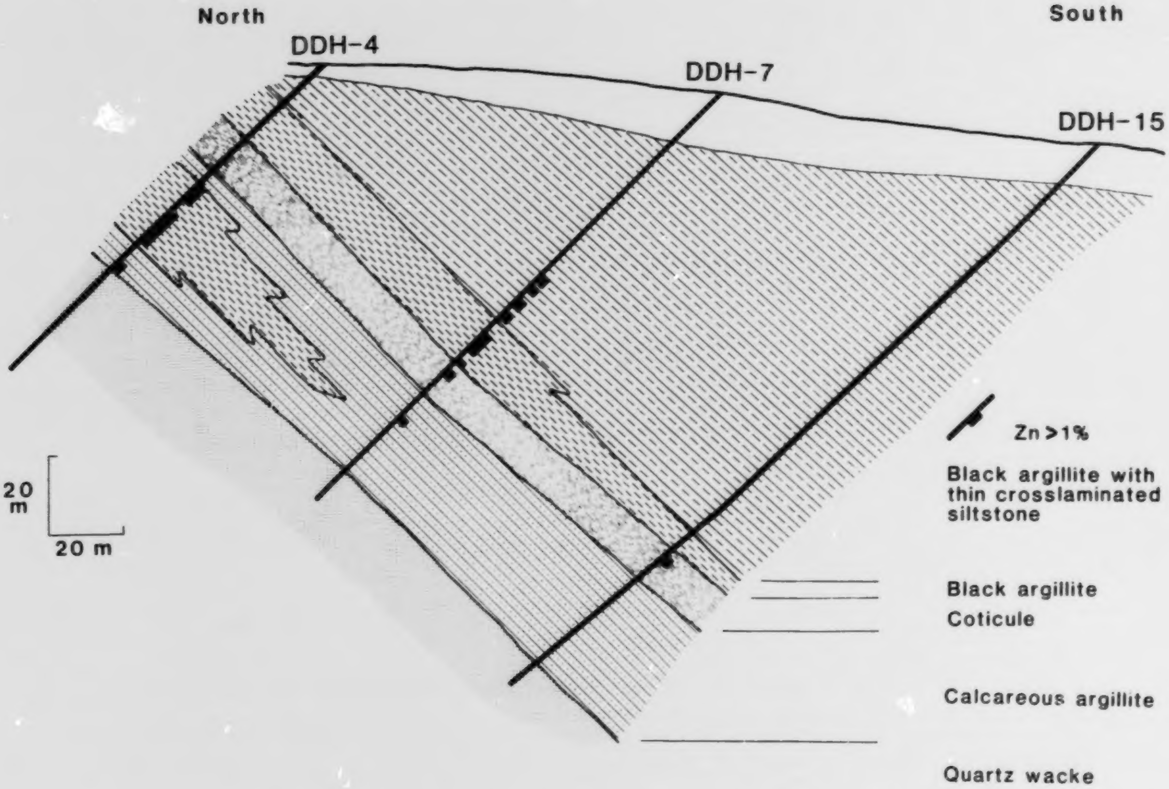
North
South
DDH-4
DDH-7
DDH-15
Zn >1%
Black argillite with thin crosslaminated siltstone
Black argillite
Coticule
Calcareous argillite
Quartz wacke
20 m
20 m

Figure 2. Vertical diamond-drill section through the Goldenville-Halifax Transition Zone, Eastville Zn-Pb-Mn occurrence, Nova Scotia (modified after Binney et al., 1986).

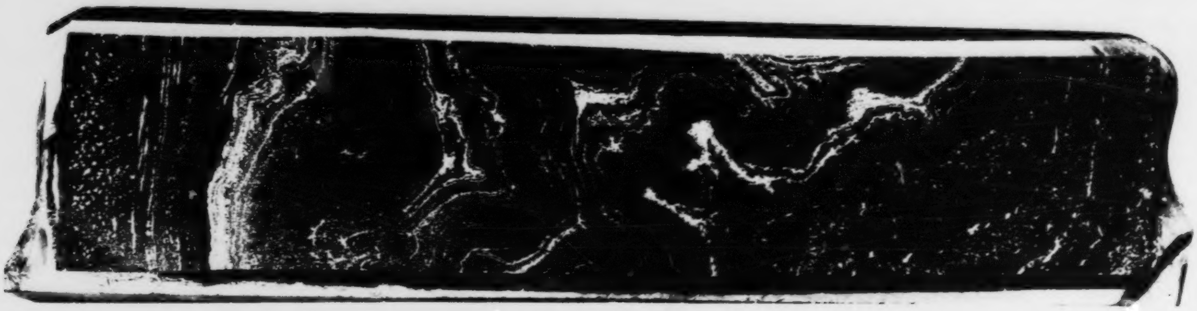

Figure 3. Highly deformed coticule from Eastville, DDH 224-27. Drill core diameter is 3.0 cm (GSC 204943-A).

thicknesses up to 100 m though thicknesses of 2 to 20 m are common. Higher grades of 2 to 4 percent Pb + Zn occur locally where low-grade stratabound mineralization has been remobilized into millimetre-scale fractures and calcite veins. Pyrrhotite, in amounts up to 10 percent, with minor pyrite, are the only sulphides normally visible at combined metal values below 1.5 percent. Higher grade material consists of galena with lesser sphalerite associated with pyrrhotite in small, 1 to 2 mm by 2 to 5 mm ovoid sulphide blebs within the slate. Minor dark sphalerite occurs with pyrite and pyrrhotite in sulphide-rich layers in the carbonaceous argillite and with pyrite as films on cleavage and joint surfaces. The iron sulphides occur either as fine grained, even disseminations or as 1 to 10 mm beds which may be disrupted, with individual sulphide segments forming en echelon lenses parallel to cleavage. Locally, hairline fractures and small breccia zones contain calcite and light coloured sphalerite. Element distributions in the Eastville strata are portrayed in Figure 4.

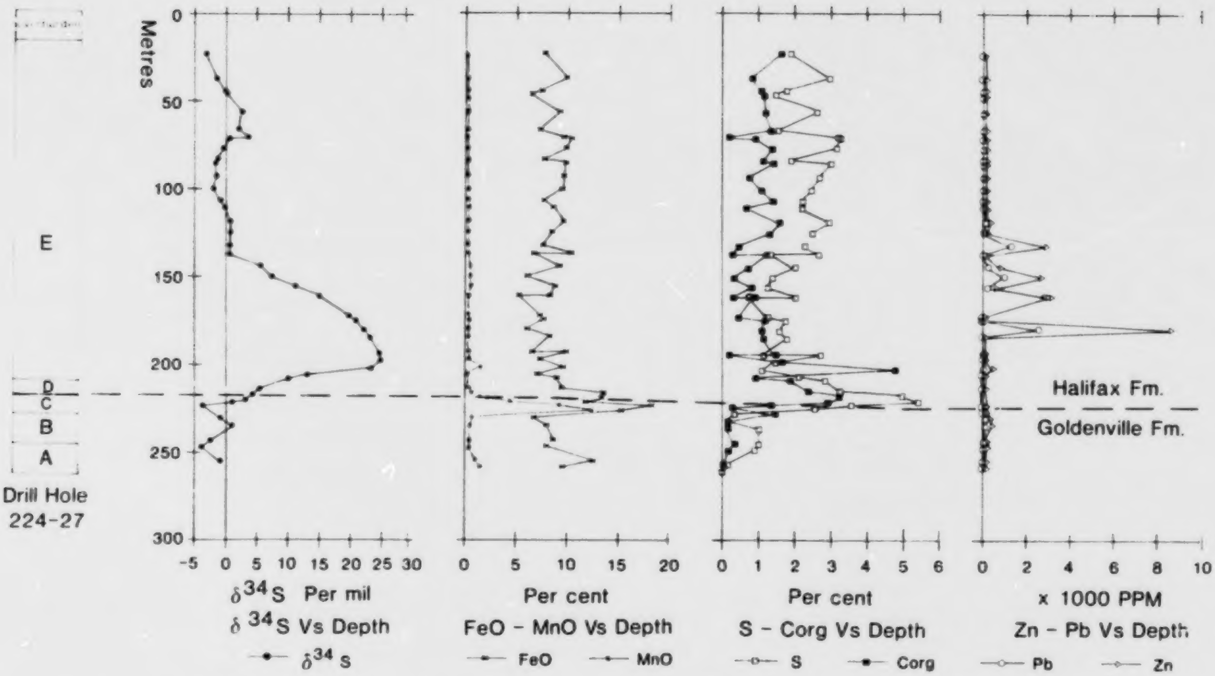

Figure 4. S isotopic and Fe, Mn, S, C_{org}, Pb, and Zn geochemical profiles through the GHT in DDH 224-27, Eastville Zn-Pb-Mn occurrence, Nova Scotia. A=quartz wacke, B=calcareous argillite, C=manganiferous calcareous argillite, D=black sulphidic argillite, E=black sulphidic argillite with interbedded crosslaminated siltstone. $\delta^{34}S$ values elsewhere increase with depth to levels of +10 to +25 per mil which are typial of Goldenville Formation sulphides.

Regional mineral occurrences

Little regional work has been done on the relationship between GHT rocks and spatially associated mineralization. Zentilli et al. (1986) point out that significant occurrences of manganese (Hingston, 1985), tungsten (Shaw, 1983; Fisher, 1984), and tin (Wolfson, 1983) occur within the transition zone rocks which may constitute a stratigraphic control on metallogenesis.

Origin of the coticule

Geochemical data from the GHT established the presence of a regional manganiferous horizon enriched in Mn, Ba, Cu, Pb, and Zn. Zentilli et al. (1986) and Graves and Zentilli (1988a) indicated that the chemical data for the transition zone most closely resembles some Pacific metalliferous sediments; the whole rock compositions of the GHT approach Average Shale and Average Deep Sea Sediment of Lalou (1983), possibly indicating the predominance of a pelagic depositional environment. Zentilli et al. (1986) concluded that the manganiferous sedimentary rocks of the GHT had a sedimentary protolith and are thus not related to volcanic or hydrothermal processes.

Manganese accumulates as chemical sediment in anoxic seawater where the oxic-anoxic interface intersects bottom sediment (Force and Cannon, 1988). The presence of anoxic conditions during Cambro-Ordovician time (Berry and Wilde, 1978) is indicated by a sulphur isotope stratigraphy defined in Meguma Group sedimentary rocks (Sangster, 1987; Sangster et al., 1988, 1989). Sulphur isotopic ratios throughout the Goldenville Formation vary between +8 and +28 per mil. The enrichment in heavy sulphur suggests that the sulphides formed by biogenic fractionation in a closed system stratified ocean basin, where the sulphate source was also enriched in heavy sulphur. These conditions also resulted in the reservoir being enriched in dissolved manganese. A rapid decrease in $\delta^{34}S$ to -5 per mil coincident with deposition of the manganiferous calcareous argillite in the GHT reflects a change in sulphate source to more oxic seawater in a regime open to seawater sulphate during manganese deposition (Sangster et al., 1988, 1989).

The major portion of the base metal mineralization at Eastville is within carbonaceous sulphidic argillite of the basal Halifax Formation immediately overlying the coticule. These beds are characterized by a return to anoxic water conditions and $\delta^{34}S$ ratios greater than +20 per mil. Unlike the manganese anomaly, the zinc-lead anomaly is local and weak or nonexistent in other GHT sections studied at the Caribou gold mine and the Lake Charlotte manganese occurrence (Graves and Zentilli, 1988b). This indicates that the processes relating to the accumulation of the zinc-lead mineralization at Eastville were local, rather than regional, and have been attributed to sedimentary exhalative brines (Binney et al., 1986; Graves and Zentilli, 1988a). The lead isotopic composition of galena from Eastville is similar to some Appalachian volcanogenic massive sulphide deposits formed at about the same time (Bathurst, Stirling) and is compatible with a sedimentary exhalative origin in Cambro-Ordovician sedimentary rocks (R. Thorpe, pers. comm., 1989; Fig. 5).

Geology of the Torbrook iron formation

Sedimentary iron formation occurs within the Lower Devonian Torbrook Formation in the Clementsport and Nictaux-Torbrook basins (Fig. 1; Gross, 1967; Smitheringale, 1973; Wright, 1975). The deposits produced 350 000 tons of iron ore between 1825 and 1913. Grades varied between 35 and 50 percent Fe, 15 to 25 percent Si, 0.5 to 1.5 percent P, and 0.05 to 0.2 percent S. The iron ores consist of stratified hematite and/or magnetite intercalated with quartzite and slate over strike lengths of up to 4 km. Individual units up to 3 m thick occur at several distinct stratigraphic horizons. The hematite is locally oolitic and occurs with iron silicate, detrital quartz, and argillaceous material (Smitheringale, 1973). Gross (1967) classified the deposits as "oolitic-textured hematite-chamosite-siderite iron formation" similar to that mined at Wabana in Newfoundland. The magnetite content has resulted from the thermal metamorphism of the Fe-bearing beds by the South Mountain Batholith.

PART II: MEGUMA GROUP GOLD VEINS

Introduction

The first discovery of nonplacer gold in the Meguma Terrane was by Lieutenant C. L'Estrange at Mooseland in 1858. The discovery of gold at Tangier in 1860 resulted in a rush of people into the Mooseland and Tangier areas.

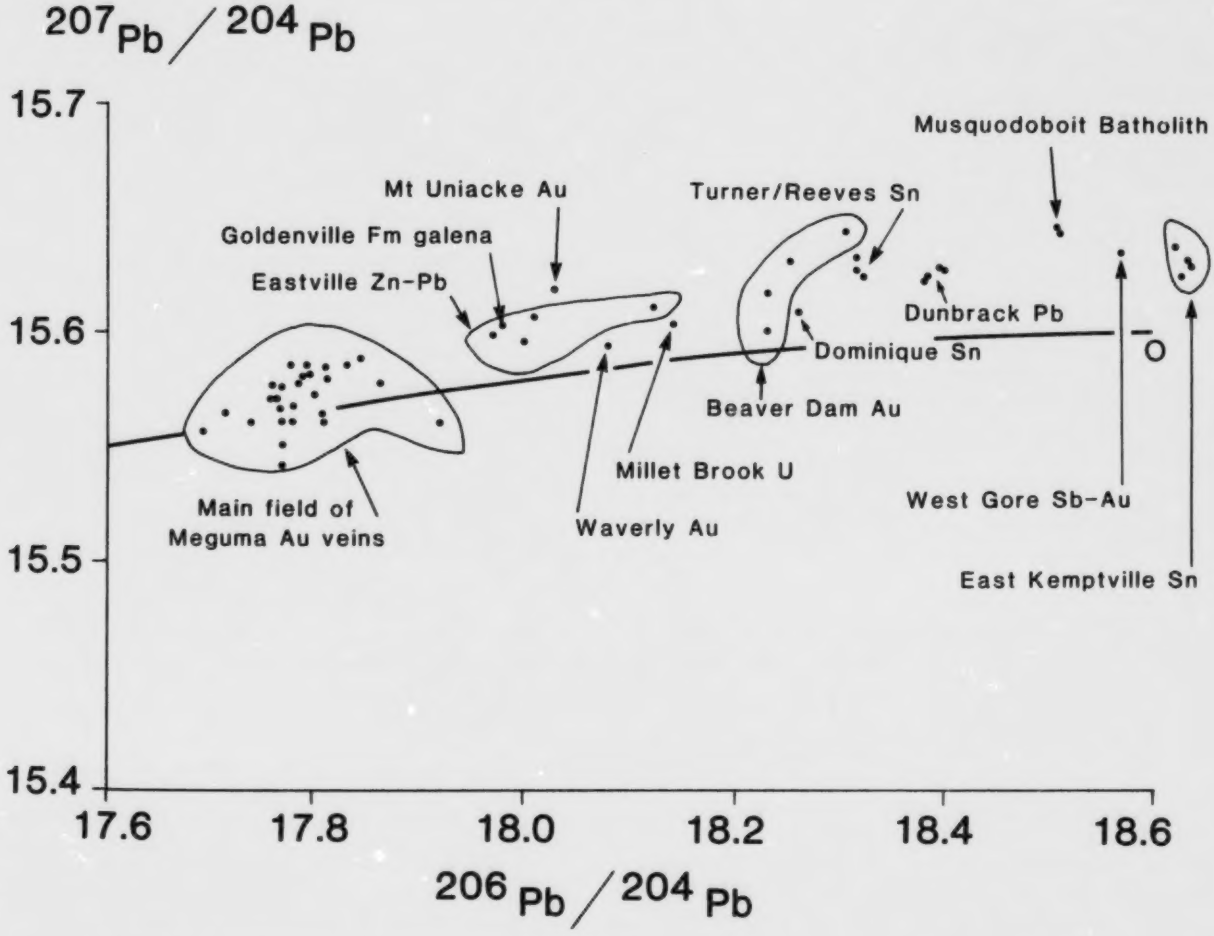

Figure 5. Lead isotope compositions of galenas from Meguma Terrane mineral occurrences (compiled from Farquhar and Haynes, 1986; R. Thorpe, unpublished data on samples collected by A.K. Chatterjee, M. Zentilli, J.M. Richardson, and A.L. Sangster). "Main Field Of Meguma Au Veins" contains Pb ratios determined on galenas from the following districts: Caribou, Oldham, Killag, Montague, Dufferin, Cochrane Hill, Mount Uniacke, Lacy, Gold Lake, Barney Point, Goldenville, Sinclair Lake, Cream Pot, Upper Seal Harbour, Waverly, Wine Harbour, Isaacs Harbour, Forest Hill, Widow Point, and a sample of galena from Goldenville Formation quartz wacke not related to known gold mineralization. Reference curve (O) is the orogene of Zartman and Doe (1981).

By the end of 1861, gold had also been discovered at Goldenville, Wine Harbour, Lawrencetown, Oldham, and Waverly as well as several other localities. By 1900, the Government of Nova Scotia had declared more than 60 formal gold districts. Production began in 1862 (7275 ounces) and continued at a level of 10 000 to 30 000 ounces per year until 1910 (Table 1). With the exception of a minor period of production in the Caribou and Goldenville districts from 1937 to 1942, gold mining in Nova Scotia has seen only limited prospecting and production since 1916 until the late 1970s. Total recorded production to 1985 was 1 400 000 ounces of gold with 15 percent of that coming from the Goldenville district and an additional 56 percent from 17 districts with recorded production in excess of 20 000 ounces each. A resurgence in exploration activity between 1983 and 1987 resulted in the production of 11 859 ounces of gold during 1987 and 1988.

Table 1. Total production from some Nova Scotia gold districts. Production figures courtesy of Nova Scotia Department of Mines and Energy.

District	Past Production	Ounces Gold
1) Beaver Dam	1890-1906	966
2) Brookfield	1887-1938	43 041
3) Caribou	1869-1945	91 381
4) Cochrane Hill	1888-1928	1 192
5) Fifteen Mile Stream	1883-1911	19 740
6) Forest Hill	1895-1935	25 102
7) Goldenville	1862-1942	210 152
8) Isaacs Harbour	1862-1940	39 654
9) Lake Catcha	1887-1942	17 951
10) Leipsigate	1888-1942	12 083
11) Lower Seal Harbour	1894-1942	34 295
12) Molega	1888-1950	34 876
13) Montague	1863-1938	68 139
14) Moose River	1870-1937	25 984
15) Mount Uniacke	1867-1941	27 739
16) Oldham	1862-1938	85 295
17) Renfrew	1862-1939	51 965
18) Salmon River	1881-1942	41 631
19) South Uniacke	1888-1946	20 762
20) Tangier	1862-1919	26 078
21) Upper Seal Harbour	1893-1944	57 027
22) Waverly	1862-1938	73 353
23) Wine Harbour	1862-1939	42 726

The work of E.R. Faribault between 1886 and 1939, compiled and reported by Malcolm and Faribault (1912) and Malcolm (1929, reprinted 1976) is most valuable in any consideration of the geology of the Meguma gold veins. The reader is referred to these publications for unreferenced general historical and descriptive geological details of individual gold veins and districts, many of which are no longer accessible for observation. An abundance of new work on the geology of the gold veins has been initiated within the last few years. Unfortunately, many recent studies have not had access to mine workings and consequently have been limited to sparse outcrop on the fringe of old mining areas, mine dump rock, and a few pits, trenches, and drillholes. Major contributions involving the documentation of gold districts will result from data generated in the current exploration boom and resulting underground developments.

General geology of the gold districts

Stratabound gold-bearing vein arrays occur mainly in the Meguma Terrane northeast of Halifax (Fig. 1), and throughout the total exposed Goldenville stratigraphy (Table 2). The veins occur mostly on the flanks and crests of domes on regional anticlines (Fig. 6 and 7). Vein arrays that form the districts range from 1 to 4 km in length and 0.1 to 0.5 km in width. The Goldenville district was the largest (maximum dimensions indicated above) with 105 veins exposed over a 518 m section across the anticline (Malcolm, 1976).

Table 2. Depth of Meguma gold districts below the Goldenville-Halifax Formation Transition Zone (modified after Malcolm, 1976). There is no stratigraphic correlation implied between gold occurrences at a particular depth below the GHT.

Depth below GHT Kilometres	Gold districts
about 5.6	Moose River
4.4	Tangier
4.0	Fifteen Mile Stream, Beaver Dam
3.2	Lawrencetown
2.4	Goldenville, Harrigan Cove, Gold Lake, Forest Hill
2.0	Waverly, Renfrew
1.6	Mooseland, Killag, Liscomb Mill, Richardson (Seal Harbour), Lower Isaacs Harbour, Wine Harbour, Montague
1.2	Ecum Secum, Middle Isaacs Harbour, Cochrane Hill, Lake Catcha, Oldham
0.8	Salmon River (Dufferin)
0	Caribou

Regional controls on the distribution of gold districts have been discussed extensively. Most of the districts occur within greenschist facies rocks (Taylor and Schiller, 1966) and east of the South Mountain Batholith. However, some major occurrences (e.g. Cochrane Hill, Forest Hill, Mile Lake (in Forest Hill district)) are within amphibolite grade metamorphic rocks that are spatially associated with numerous Devono-Carboniferous granitic intrusions. Fyfe and Henley (1973) and Henley (1973) have suggested that gold may be metamorphically mobilized under amphibolite facies metamorphic conditions. In the Meguma zone, there is some consensus that the chlorite-biotite isograd may be important in the localization of many gold deposits (Graves, 1976; Mawer, 1986) but its location has only been defined locally.

Most gold occurrences are strongly associated with thicker than normal argillite beds interstratified with the Goldenville Formation quartz wacke. Woodman (1904) estimated that the argillaceous component of the Goldenville Formation composed only 3 percent of the total

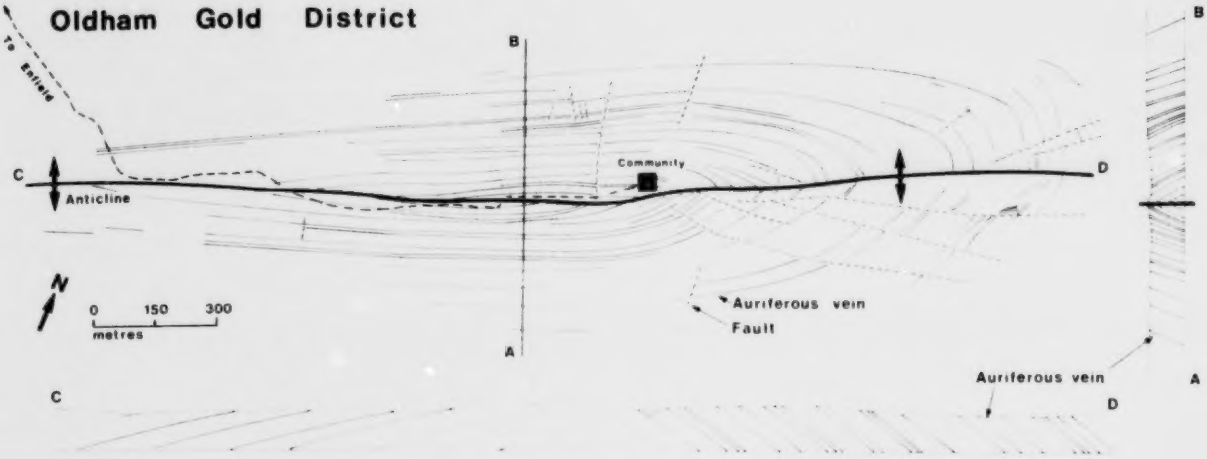
Oldham Gold District
To Enfield
B
C
Anticline
Community
D
N
0 150 300
metres
A
Auriferous vein
Fault
B
A
Auriferous vein
C
D

Figure 6. Generalized geological plan of the Oldham gold district, Nova Scotia (modified from Faribault, 1898). At Oldham, the gold-bearing vein array forms a tight cluster around the dome of the anticline.

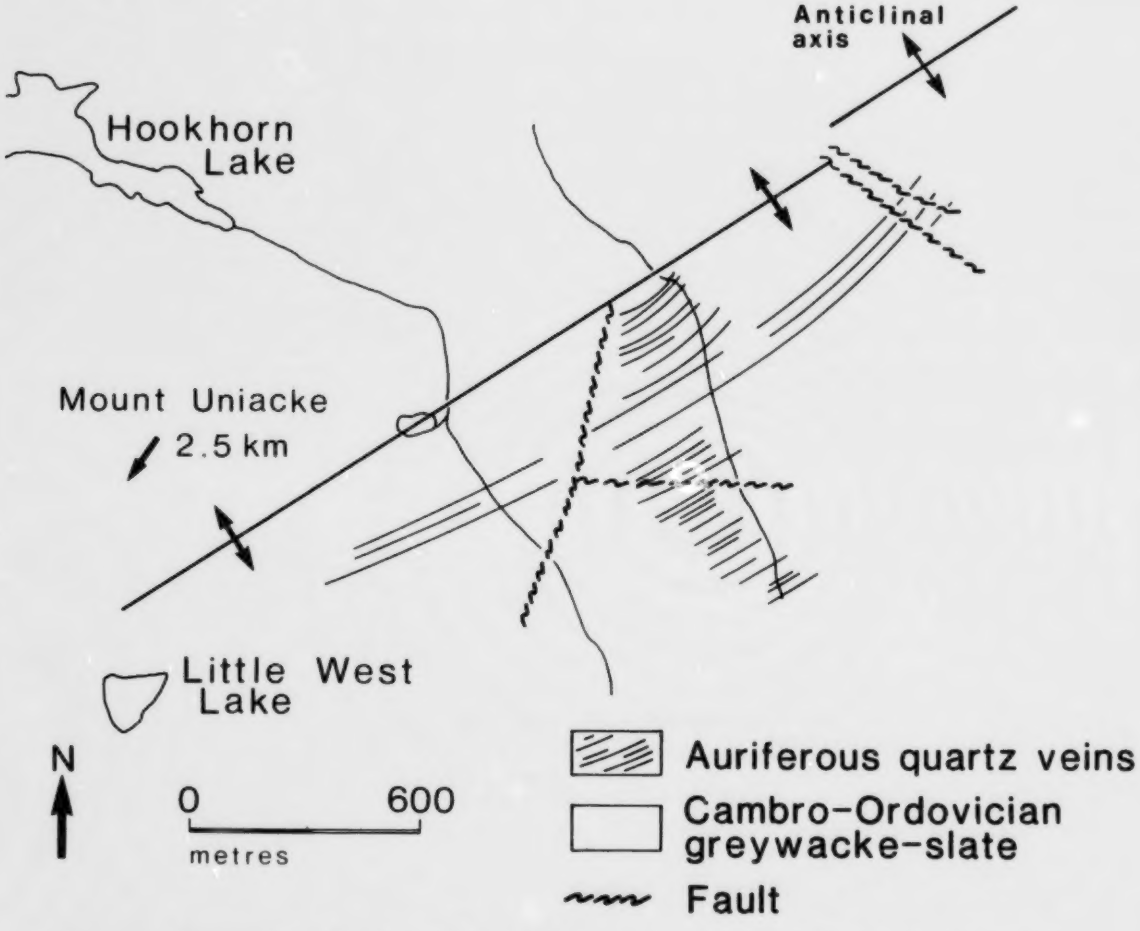
Anticlinal axis
Hookhorn Lake
Mount Uniacke
2.5 km
Little West Lake
N
0 600
metres
Auriferous quartz veins
Cambro-Ordovician greywacke-slate
Fault

Figure 7. Geological plan of the Mount Uniacke gold district, Nova Scotia (modified after Faribault, 1901). At Mount Uniacke, the veins occur only on the southern flank of the anticline and are not known to cross the anticlinal hinge.

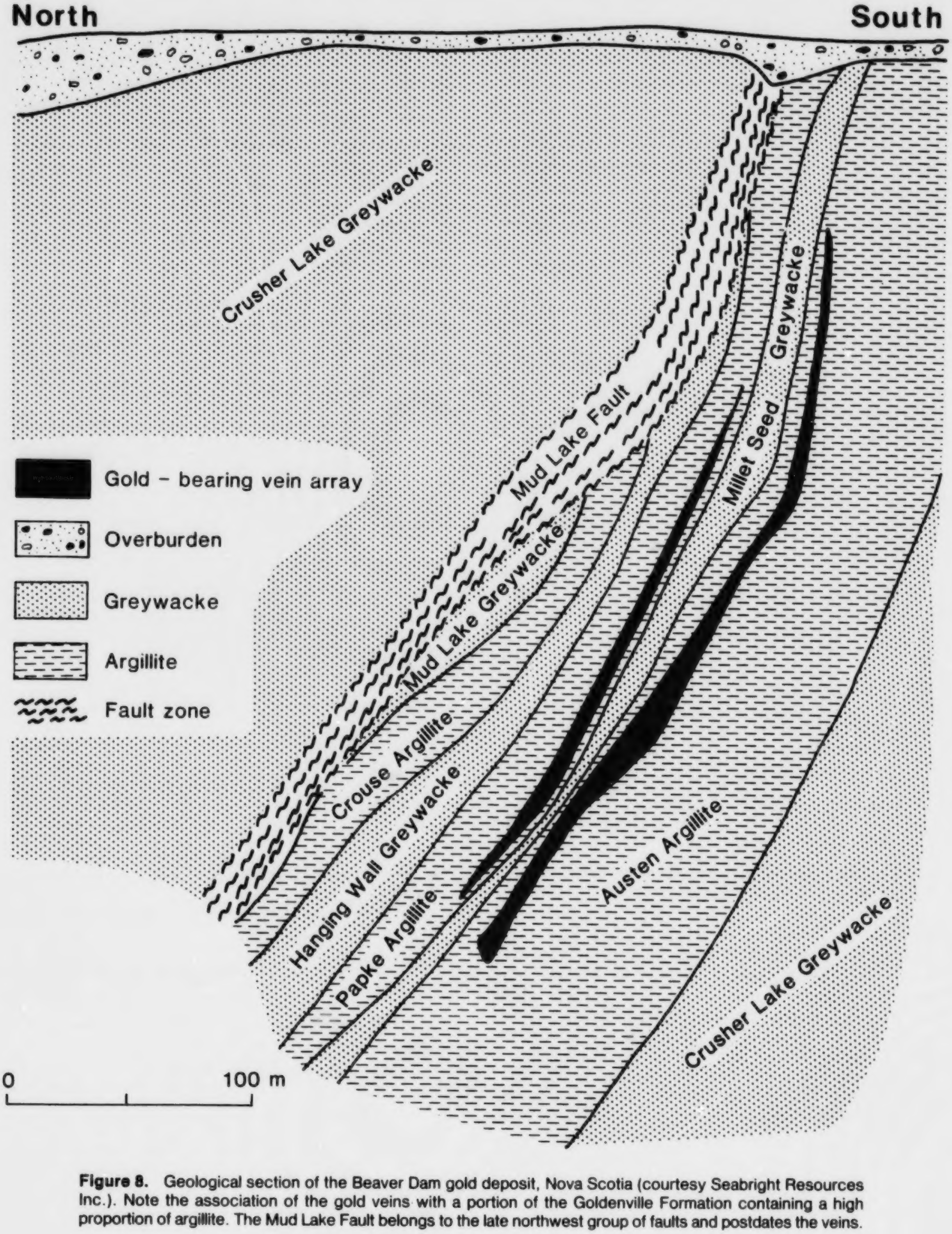
North
South
Crusher Lake Greywacke
Mud Lake Fault
Mud Lake Greywacke
Crouse Argillite
Hanging Wall Greywacke
Papke Argillite
Millet Seed Greywacke
Austen Argillite
Crusher Lake Greywacke
Gold - bearing vein array
Overburden
Greywacke
Argillite
Fault zone
0
100 m

Figure 8. Geological section of the Beaver Dam gold deposit, Nova Scotia (courtesy Seabright Resources Inc.). Note the association of the gold veins with a portion of the Goldenville Formation containing a high proportion of argillite. The Mud Lake Fault belongs to the late northwest group of faults and postdates the veins.

thickness. These are typically thin interbeds, a few centimetres to a few metres thick, of grey-green to grey laminated slate and crosslaminated silty slate (Malcolm, 1929; Waldron and Jenson, 1985). In the gold districts, the slate is commonly argillaceous rather than silty, and is carbon-rich and sulphidic with abundant pyrrhotite and arsenopyrite (Brunton, 1928; Malcolm, 1929; Smith, 1984a,b). At the Beaver Dam deposit, gold-bearing veins occur in strata consisting of about 75 percent argillite over a thickness of 150 m (Fig. 8).

Mawer (1986) described a positive correlation between the location of 120 Meguma gold occurrences and horizontal distance for each from 1) the Goldenville-Halifax Formation Transition Zone, 2) the chlorite-biotite isograd, and 3) Devono-Carboniferous granitic intrusions. He did not differentiate, however, between major and minor occurrences or reduce data with regard to the relative percentages of productive rocks present.

Structural geology

Meguma gold-bearing bedding-parallel veins are located within or immediately below the upper margins of incompetent, impermeable argillite horizons in the Goldenville Formation quartz wacke. Many of the districts are located on the steeper limb of a fold, e.g. Beaver Dam, Goldenville, Tangier (Smith and Kontak, 1986) or in a satellitic structure on the limb of a larger fold (e.g. Dufferin mine; Fig. 9). The Meguma deposits are mistakenly referred to as saddle reefs (Henderson and Henderson, 1986). True saddle reefs (Herman, 1914 in Boyle, 1986, Fig. 2; Ramsay, 1967) are restricted to fold hinges and are considerably thickened in the axial zones with only minor down limb extension. The Meguma veins are normally of constant thickness around the fold hinge and have significant downdip extent beyond the fold hinge (Dufferin mine (Fig. 9) and Richardson vein, Upper Seal Harbour district are exceptions). Most researchers contend that several generations of veins are present (Fyson, 1966; Graves, 1976; Haynes and Smith, 1983; O'Brien, 1985a; Henderson et al., 1986a,b; Mawer, 1986) representing semicontinuous vein development throughout an extended period of time. However, Smith and Kontak (1988a,b) have proposed that all gold-bearing veins formed simultaneously. Although vein types are similar both regionally and in the gold districts, the abundance of veins is considerably greater in the gold districts. The greater vein density is associated with an increase in slate content of the Goldenville Formation wacke and the gold, arsenopyrite, and pyrrhotite contents of both the slates and wackes. Vein system complexity may increase with the metamorphic grade of their host rocks (Smith, 1983b). South of the St. Marys and Cobequid-Chedabucto fault zones, intense dextral shear has significantly modified earlier wall rock and vein geometries (e.g. Cochrane Hill, Smith, 1984a,b).

Several classifications of veins have been proposed within individual districts (Henderson, 1983; Smith, 1983b; Haynes, 1986; Henderson et al., 1986b). The following summary combines elements of these classifications.

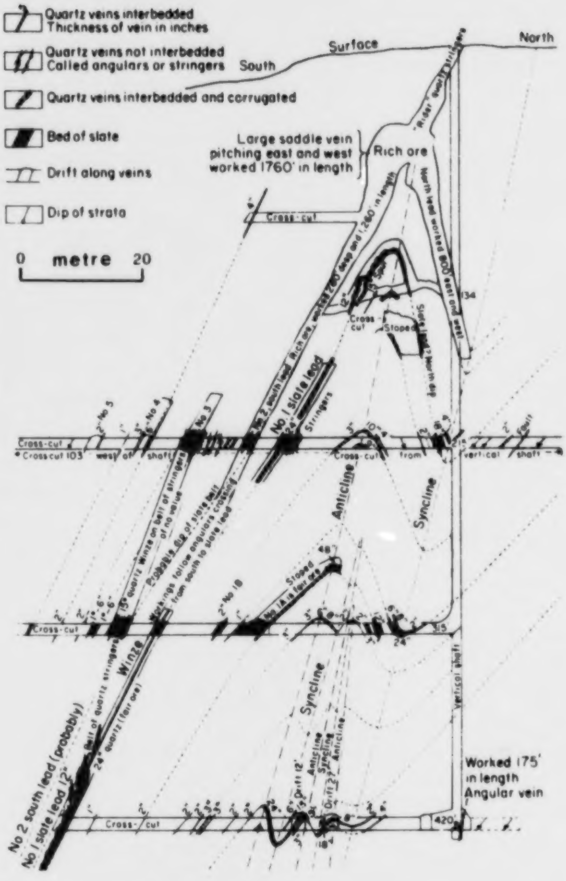
Quartz veins interbedded Thickness of vein in inches
Quartz veins not interbedded Called angulars or stringers
Quartz veins interbedded and corrugated
Bed of slate
Drift along veins
Dip of strata
0 metre 20
Surface
South
North
Large saddle vein pitching east and west worked 1760' in length
Rich ore
"Rider" quartz stringers
North lead worked 800' east and west
Cross-cut
Stoped
134
No 1 slate lead
Stringers
Anticline
Syncline
Winze
Vertical shaft
Worked 175' in length Angular vein
No 2 south lead (probably)
No 1 slate lead 12"
Cross-cut 103' west of shaft
420

Figure 9. Geological section of the Dufferin mine, Nova Scotia. The productive veins were found on the crest of a secondary fold on the southern flank of the main anticline. The vein in the fold crest labelled "Rich ore" was one of the few true "saddle-reefs" recognized in Meguma gold occurrences (modified by Guilbert and Park, 1986; after Malcolm and Faribault, 1912).

Stratiform veins

These are the earliest vein structures and consist of bedding-parallel laminated veins with crack-seal texture (cf. Ramsay, 1980) that formed during a period of episodic hydraulic overpressure (Faribault, 1899; Graves, 1976; Graves and Zentilli, 1982; Henderson, 1983; Mawer, 1985, 1986, 1987; O'Brien, 1985a; Henderson et al., 1986a,b). The veins vary from a centimetre to a few metres in thickness and persist along strike for hundreds to thousands of metres. These veins are regionally concordant and rarely cross from one stratigraphic horizon to another. The internal structure of the laminated veins is complex (Mawer, 1985, 1987). The laminations consist of 20 to 100 um thick layers of quartz alternating with 2 to 20 um thick layers of white mica and/or chlorite. The laminae commonly enclose fragments of wall-rock slate with contact relationships similar to vein-wall rock contacts. The phyllosilicate laminae mimic vein wall topography. Microscopic evidence for deformation of the bedding-parallel veins includes the presence of tectonic stylolites, extensive straining, and recrystallization of quartz.

Some laminated veins display extensive mesoscale deformation and recrystallization. Pinch and swell structure and boudinage, usually of the "chocolate-tablet type", is common with milky "bull" vein quartz in the neck of the pinch (Fig. 10a). Intense buckle folding of laminated veins has produced an apparently anomalous situation where the veins and their immediate host rocks have been intensely folded (Fig. 10b,c) whereas the enclosing beds have retained their planar form. This may have resulted from shortening of the sedimentary rocks under lateral compression with differential solution of

a.

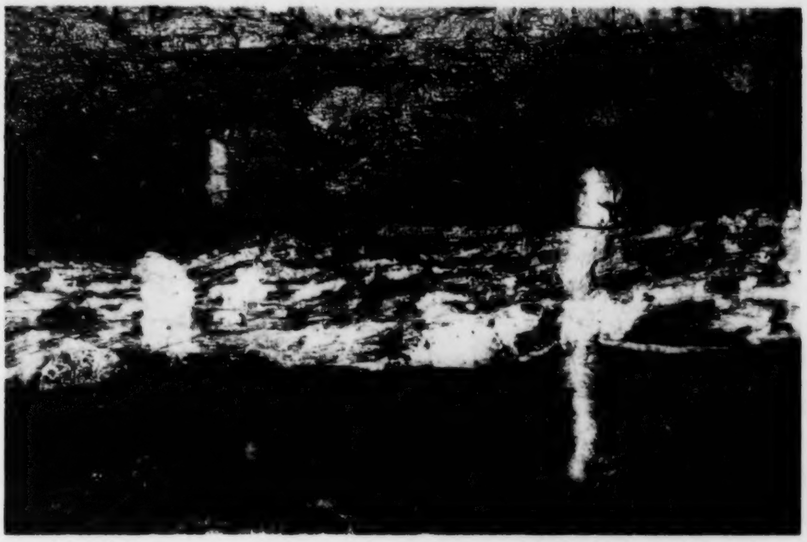

b.

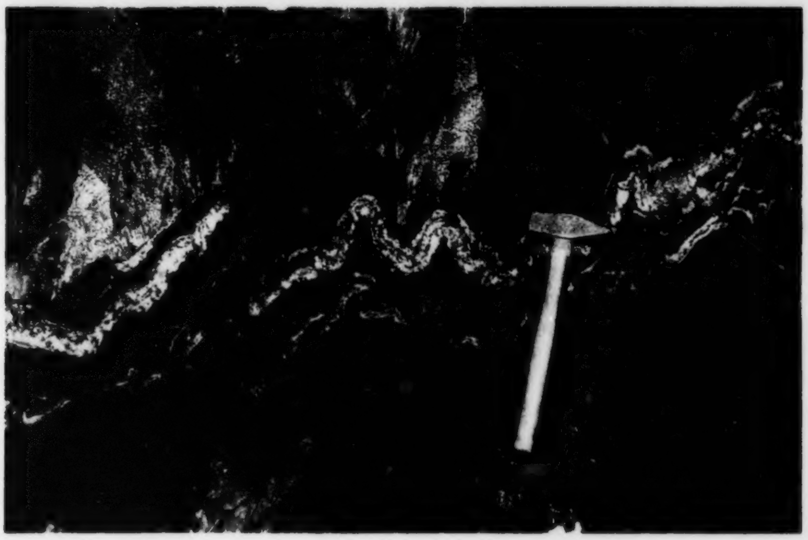

Figure 10. a) Marker vein, Tangier gold district, showing bedding-parallel crack-seal vein. Note the 'pinch and swell' with recrystallized quartz in the pinch. Three-dimensional exposure in the mine indicates this is a section through chocolate-tablet boudinage. Long axis of photo is parallel to the length of the vein dipping 45° south exposed in the back of a raise. Left side of photo is up, looking north. Vein thickness is 25 cm (GSC 204390-R). b) Twin vein, Tangier gold district, showing two thin buckled veins in slate below their contact with the overlying wacke, on the crest of the Tangier anticline. Hammer handle is 30 cm in length (GSC 204390-S). c) Dunbrack vein, Oldham gold district, showing buckle folding of the vein at intersections with pressure solution cleavage evident in the underlying slate. Scale unknown: veins of this type are commonly 5 to 25 cm thick (photograph courtesy of National Archives of Canada, #PA 161565). d) Nugget vein, Tangier gold district, showing apparently chaotic vein textures resulting from the development of superimposed, variably rotated en echelon veins in black, organic-rich, arsenopyrite-rich slate. Painted numbers "65" are 25 cm high (GSC 204390-T).

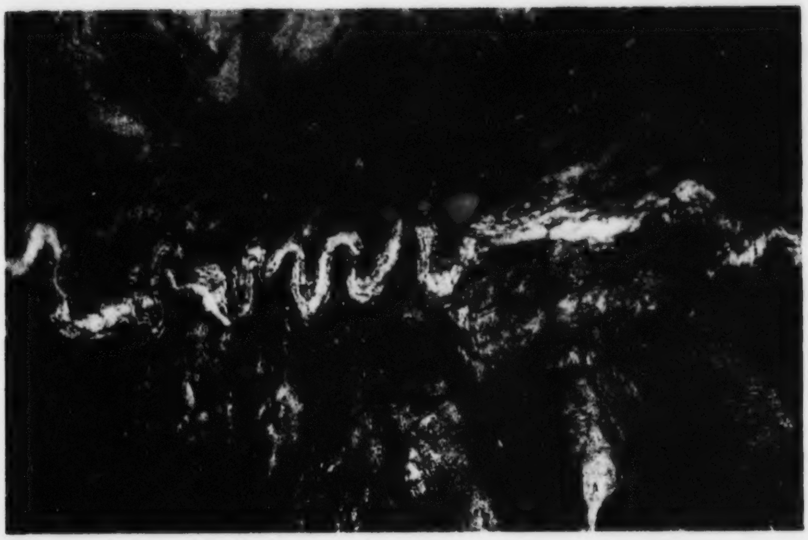

c.

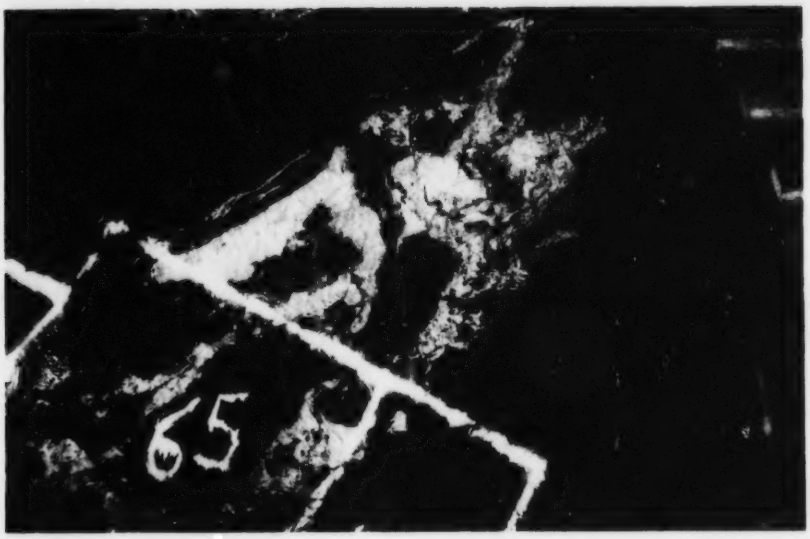

d.

quartz from the phyllosilicate-rich sedimentary rocks along a well developed pressure solution cleavage (Clifford et al., 1983; Henderson et al., 1986a) whereas the quartz veins shortened by buckle folding. In some districts, nonbuckled bedding-parallel crack-seal veins and thin white quartz veins (recrystallized or thicker crack-seal) occur with highly buckled veins suggesting that the process of hydraulic fracturing was protracted over the period of vein formation and that in some districts, nonbuckled stratiform veins may have formed late in the period of bedding-parallel vein formation. Some early veins possibly underwent shortening by pressure solution rather than buckle folding. This may be the case for early veins adjacent to sandstone beds rather than those enclosed in slate.

En echelon veins

En echelon veins formed in slate or siltstone beds between massive wacke on the limbs of major folds. The veins fill extensional fractures which formed as a result of bedding-parallel shear during folding (Henderson et al., 1986b). Many of the locally crosscutting but stratabound white quartz veins in slate horizons are attributed to this process (J.R. Henderson, pers. comm., 1989) including a spectrum of cases from simple en echelon veins to the apparent chaotic development of "bull quartz" within a single stratigraphic horizon (Fig. 10d). The latter represents superimposed en echelon veins in various stages of rotation, compression, and extension.

Angular veins

Some laterally extensive veins, which rarely exceed a few centimetres in thickness, resemble en echelon veins except that they crosscut several stratigraphic horizons and are continuous both above and below bedding-parallel veins. These veins are the "angulars" referred to in the older literature as "feeders" and "robbers", referring to their association with grade changes at their intersection with the auriferous bedding-parallel veins. They crosscut the stratiform and stratabound en echelon veins. At Cochrane Hill, the angular veins have been related to deformation during the late stages of Acadian amphibolite facies metamorphism (Smith, 1983b).

Pegmatitic veins

Pegmatitic veins are restricted to areas around granitic intrusions and areas of higher grade metamorphism. At Cochrane Hill, pegmatite occurs both within and outside the pit area. Mineralogically, the veins contain quartz, orthoclase, plagioclase, muscovite, biotite, andalusite, and traces of gold (Smith, 1983b).

ac veins

Late extension parallel to the regional fold axes has produced quartz-filled ac joints in the metawacke (Henderson, 1983). These are regional features and occur irrespective of the presence of gold-bearing veins but may contain traces of gold where they occur within gold districts.

Northwest faults and veins

Subvertical quartz-calcite veins, vein breccias, and sinistral kink bands are parallel to regional northwest sinistral faults and cut all structures in the Meguma Terrane. They have a significant effect on gold distribution in some districts. Gold grades in some bedding-parallel veins at the Tangier deposit increase near intersections with northwest faults (D. Forgeron, pers. comm., 1986). In the Brookfield, Caribou, and Rawdon districts (among others) the northwest faults host past producing, gold-bearing veins where they cut slate which hosts mineralized bedding-parallel veins (Fig. 11).

Miscellaneous structures

Some important gold mineralization is associated with locally developed structures. At the Mount Uniacke gold district, gold occurs in intersections of bedding-parallel veins and barren veins developed along a normal fault associated with a secondary fold (Fig. 12). At the Caribou mine, significant gold was mined from bedding-parallel veins and vein breccias in a structural discordance on the flank of the major fold (Fig. 13). In both the Leipsigate and Ecum Secum gold districts, gold mineralization was found in faults subparallel to the fold axes. Similar structures are locally common in other gold districts (Malcolm, 1976).

Mineralogy of the veins

Quartz

Quartz, the most abundant vein mineral, occurs in two forms: grey to black, laminated, inclusion-rich and white,

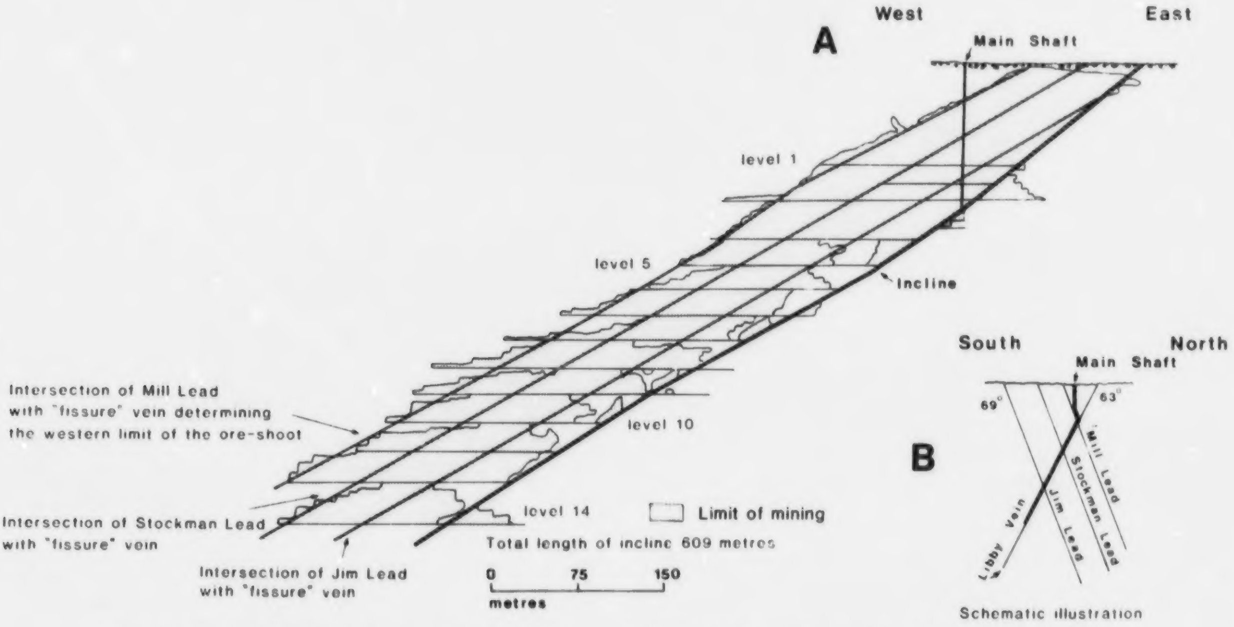
West
East
A
Main Shaft
level 1
level 5
Incline
level 10
level 14
Intersection of Mill Lead with "fissure" vein determining the western limit of the ore-shoot
Intersection of Stockman Lead with "fissure" vein
Intersection of Jim Lead with "fissure" vein
Limit of mining
Total length of incline 609 metres
0
75
150
metres
South
North
Main Shaft
69°
63°
B
Mill Lead
Stockman Lead
Jim Lead
Libby Vein
Schematic illustration

Figure 11. Longitudinal section of the Libby fissure vein, Brookfield gold district, showing the restriction of gold ore to the intersection of the fissure with the Mill, Stockman, and Jim interbedded veins (modified after Malcolm and Faribault, 1912).

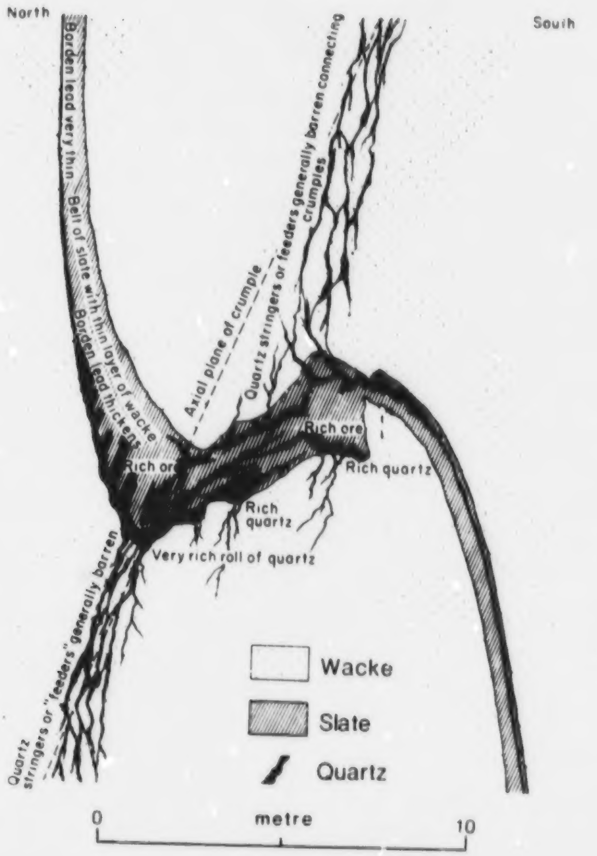

Figure 12. Geological section of a folded auriferous bedding-parallel vein and late barren veining in a normal breccia fault zone, Mount Uniacke gold district, Nova Scotia. Note the gold enrichment in the bedding-parallel vein near the secondary barren quartz. This phenomenon is commonly interpreted as a product of remobilization of gold from the bedding-parallel vein into the area of its intersection with the later crosscutting structure (modified by Guilbert and Park, 1986; after Malcolm and Faribault, 1912).

nonlaminated varieties. The grey quartz, the earliest variety, only occurs in laminated crack-seal veins. It is relatively coarse grained with fibrous crystals perpendicular to vein walls, and exhibits a platy, lamellar, or columnar structure (Fig. 14a,b) in shades of grey and black (O'Brien, 1985a; Mawer, 1986, 1987). The grey quartz is normally mineralized and the colour, in combination with a greasy luster, can be used as a prospecting tool for gold (Malcolm, 1976). White quartz occurs marbled within laminated grey quartz veins, in stratabound nonstratiform veins and vein breccias, and in varieties of crosscutting vein and tension fracture fillings. Some coarse grained white quartz veins are vuggy.

Arsenopyrite

Arsenopyrite is present in all gold districts in variable amounts up to a maximum of about 5 percent. It is most abundant in wall rocks but does occur within the veins. Its habit varies with the host rock composition. Arsenopyrite in quartz wacke is normally coarse grained and evenly disseminated within the rock (Fig. 15a) with well formed, twinned crystals up to 2 cm in diameter. Pronounced, quartz-filled pressure shadows with long axes aligned with cleavage (Fig. 15b), rarely containing gold (C. Miller, pers. comm., 1985), are common around precleavage arsenopyrite. Arsenopyrite in slate is finer grained and commonly occurs as 1 to 5 mm crystals that are disseminated in bands parallel to lithological layering, with the long axis of the crystals oriented in the axial plane cleavage (Fig. 15c). Arsenopyrite also forms large, very coarsely crystalline grain aggregates or individual crystals within the veins or along the vein-wall rock contacts.

Carbonate

Carbonate is fine to coarse grained, distinctively brown weathered, and varies among calcite, ankerite, and ferroan dolomite in composition (Kontak and Smith, 1988a). Its mode of occurrence varies with its host. Carbonate in quartz wacke is fine to medium grained and evenly disseminated throughout the wacke matrix, imparting a subtle light brown colour to the normal light to medium grey rocks. In slate, the carbonate is also fine grained and evenly disseminated where present in minor amounts (Fig. 16a). Where quantities increase, grain size coarsens and the carbonate tends to occur in layer-parallel bands (e.g. Lake Catcha gold district), visually resembling some carbonate facies iron formations. In veins, carbonate has several habits, occurring as fine disseminations to coarse clots interstitial to vein quartz and as layer-parallel bands within laminated quartz veins (Fig. 16b).

Gold

Gold occurs as fine grained films between crack-seal laminae or along vein-wall rock contacts, and as medium to coarse grained aggregates in white quartz. Where gold occurs with arsenopyrite, it is most commonly present as fracture fillings or coatings on arsenopyrite crystals. Coarser grained gold occurs with coarse grained quartz in bedding-parallel veins or at intersections of later structures (e.g. angulars, en echelon veins, northwest veins) and early veins. Gold grades in this structural setting may be spectacularly high, but are typically erratic and difficult to evaluate. More consistent grades occur in areas where buckling of the vein has increased the proportion of vein present per linear metre of mine working. Gold assays approaching ore grades have been reported in arsenopyritic slate or quartzite associated with quartz veins and in the absence of significant veining (e.g. Torquoy zone, Moose River district, G. Isenor, pers. comm., 1989). Meguma gold commonly contains traces to 5 percent Ag but occurrences with as much as 20 percent are known (Malcolm, 1976).

Occurrences of gold and associated minerals are highly variable and many veins have distinctive characteristics which distinguish them from veins only a few metres

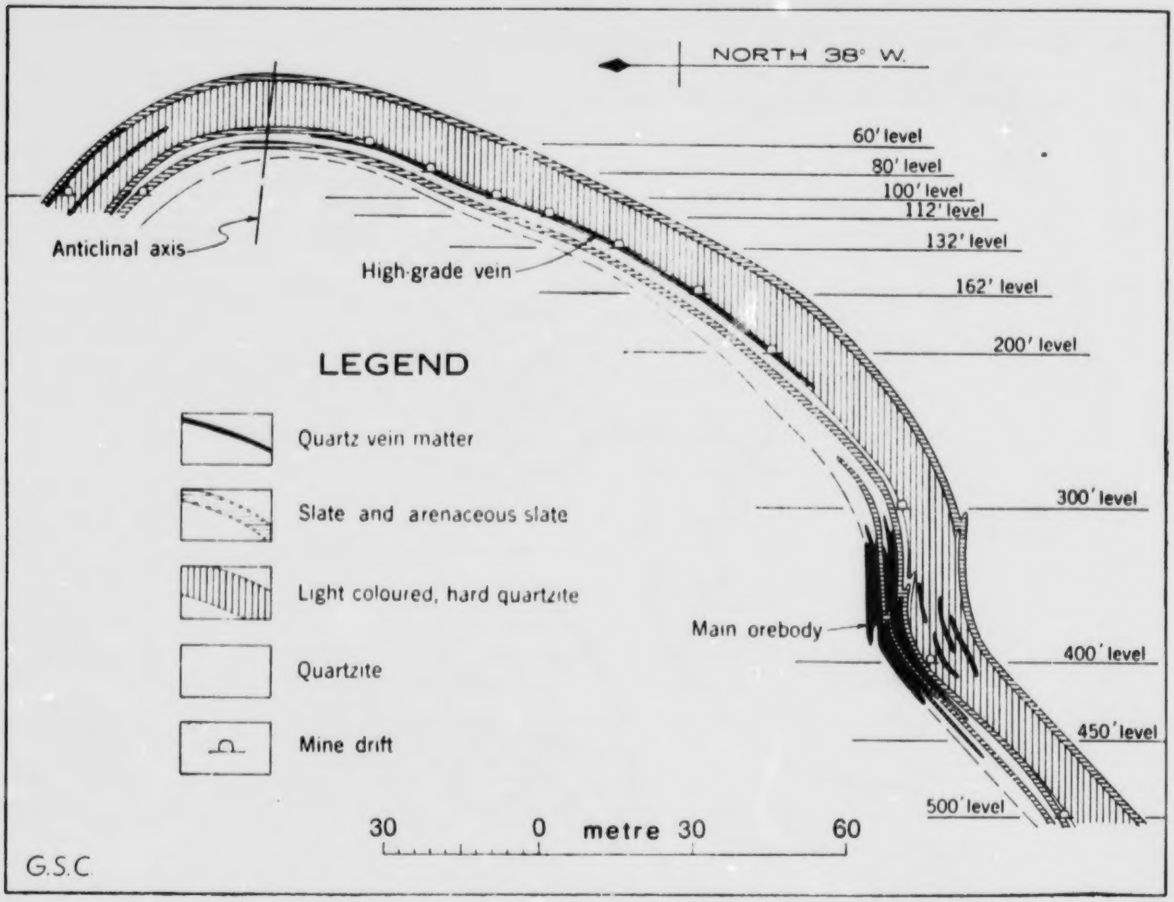
NORTH 38° W.
60' level
80' level
100' level
112' level
132' level
162' level
200' level
300' level
400' level
450' level
500' level
Anticlinal axis
High-grade vein
Main orebody
LEGEND
Quartz vein matter
Slate and arenaceous slate
Light coloured, hard quartzite
Quartzite
Mine drift
30 0 metre 30 60
G.S.C.

Figure 13. Geological section of the Caribou mine, Nova Scotia. Note the main ore zone associated with flexure in anticlinal limb and bedding-parallel veins (from Bell, 1948).

away. Recent underground exploration of the Marker, Twin, and Nugget veins in the Tangier gold district illustrates this point. These auriferous veins occur over a stratigraphic interval of about 25 m near the crest, but on the southern flank of the Tangier anticline. The lower Nugget lead (Fig. 10d) is 0.5 to 1 m thick and consists of a 10 cm basal crack-seal vein and numerous white quartz-filled en echelon veins in the overlying arsenopyritic slate. The Twin lead (Fig. 10b), 10 m stratigraphically higher, consists of two veins, each 1 to 2 cm in thickness, which occur within a 10 cm thick slate bed. The two veins consist predominantly of white quartz with local remnants of crack-seal texture. The lower vein is poorly mineralized whereas the upper vein contains 5 to 10 percent combined pyrrhotite and chalcopyrite as well as abundant visible gold. Both veins are buckle folded. The Marker vein (Fig. 10a), overlying the Twin vein at the top of the section, is about 25 to 30 cm thick and consists of a planar (i.e. not folded) grey-white banded crack-seal vein which displays excellent development of "chocolate-tablet" boudinage. Most of the gold is associated with a few percent pyrrhotite at the upper vein contact. Traces of arsenopyrite are disseminated within the overlying wacke bed. The veins retain their dimensions, physical character, and mineralogy over a strike length of at least 3000 m (D. Forgeron, pers. comm., 1986).

The crack-seal veins have historically been the most productive gold-bearing vein type (Malcolm, 1929).

Accessory minerals

A large number of accessory minerals occur within the veins. The gold distribution within the veins typically varies directly with the occurrence of sulphide minerals. Arsenopyrite is common in gold-bearing areas but is a poor guide to the presence of gold on a local scale (Kerswill, 1988). On the other hand significant quantities of pyrrhotite with traces of galena, sphalerite, and chalcopyrite occur with gold-bearing veins but are absent in barren veins. Pyrite is present in minor amounts and may locally be a major component. Gold has been noted in a pyritic sericite schist in the Salmon River (Dufferin) district (Nova Scotia Department of Mines and Energy, Assessment File 21-H-63) and small-scale mining in the late 1970s at Renfrew was from four thin, heavily pyritic

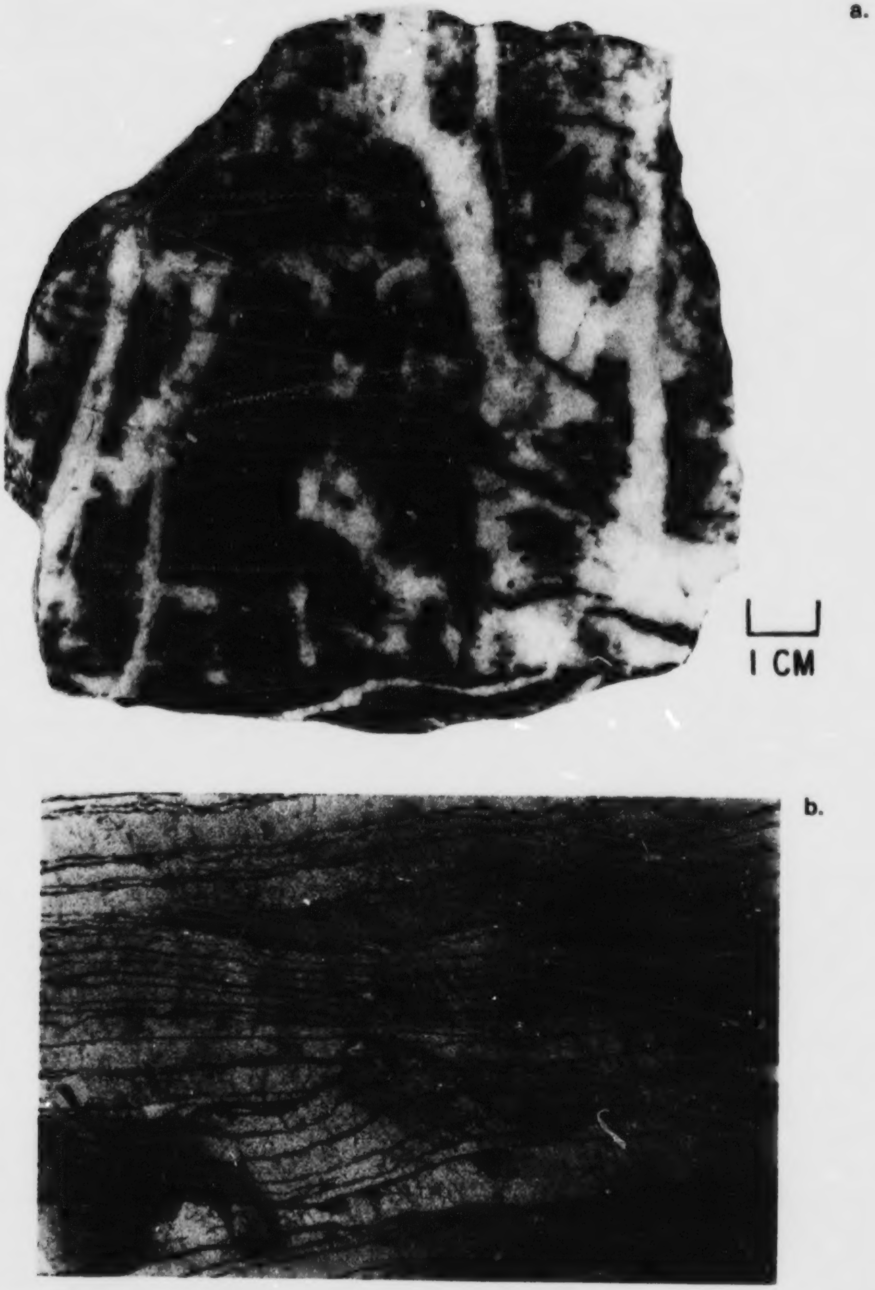

Figure 14. a) Hand specimen from the Gold River gold district showing grey-white mottled "speckled hen" vein typical of crack-seal textures in bedding-parallel veins. Colour variation is due to the relative abundance of solid and fluid inclusions in the vein quartz (GSC 204390-D). b) Photomicrograph of crack-seal textures showing phyllosilicate lamination and tectonic stylolites (arrows). Length of view is 0.45 mm; from Mawer, 1987.

quartz veins in a 1 m thick slate bed which carried up to 1 ounce gold per ton over that width. Pyrrhotite occurs predominantly in the host rocks of many deposits and in the veins of others. Its habit is similar to arsenopyrite, occurring as bedding-parallel disseminated ovoid blebs with the long dimension oriented parallel to cleavage. Scheelite is common in the Moose River veins and is an accessory in a few occurrences, locally with accompanying traces of stibnite (Smith and Kontak, 1986). Argentite, tetrahedrite, loellingite, molybdenite, and tellurides (Kontak and Smith, 1987b; Smith and Kontak, 1988c) have been identified in trace amounts in a few deposits.

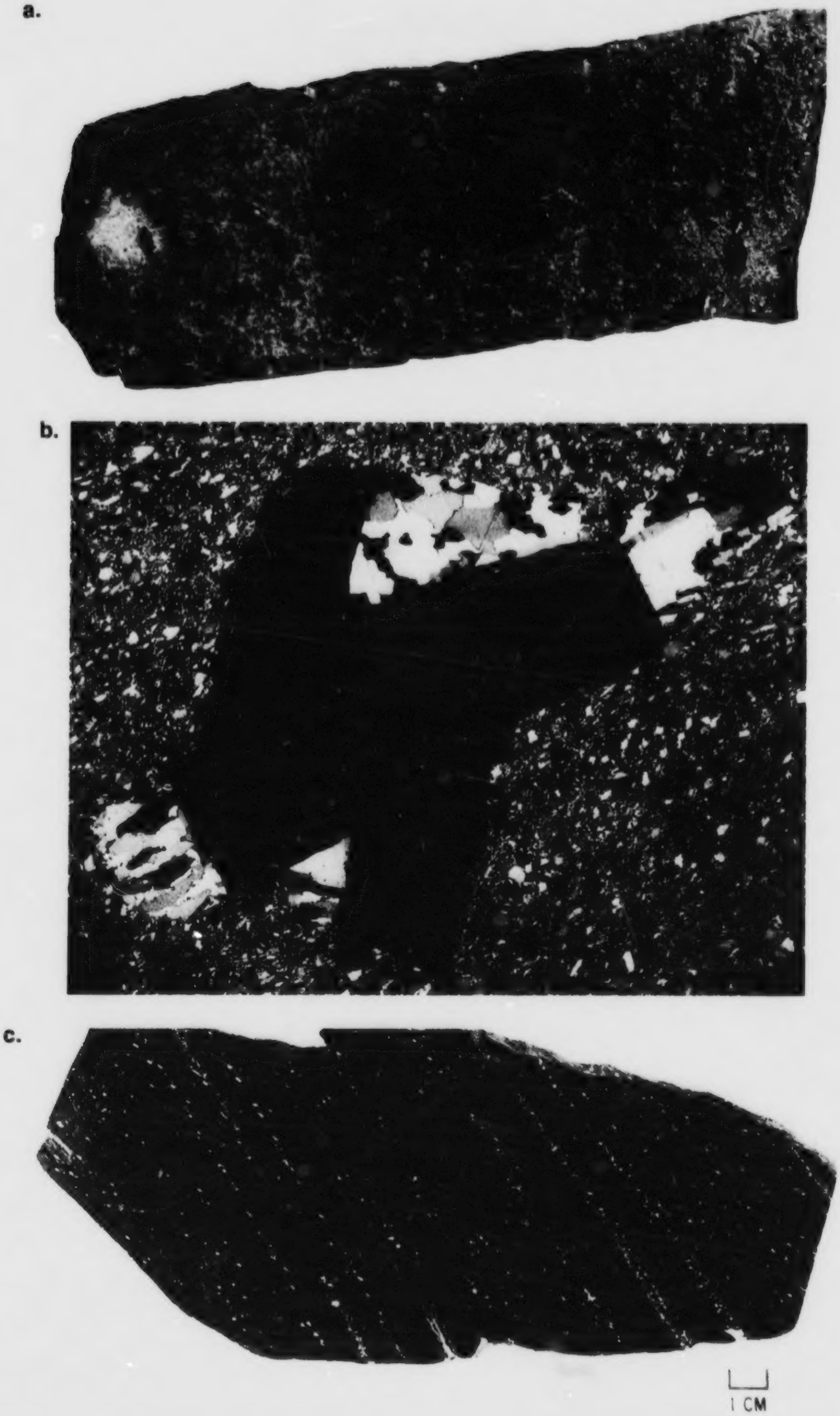

Figure 15. a) Evenly disseminated, coarse grained arsenopyrite (dark grey) in quartz wacke, Caribou gold district. Sample length is 15 cm (GSC 204390-A). b) Photomicrograph of arsenopyrite and associated unstrained quartz pressure shadows in calcareous quartz wacke, Caribou gold district. Arsenopyrite crystal is 7 mm long (GSC 204390-U). c) Arsenopyrite disseminated in bands parallel to lithological layering in argillite, Lawrencetown gold district. Note long axes of arsenopyrite crystals are oriented parallel to cleavage (GSC 204390-E).

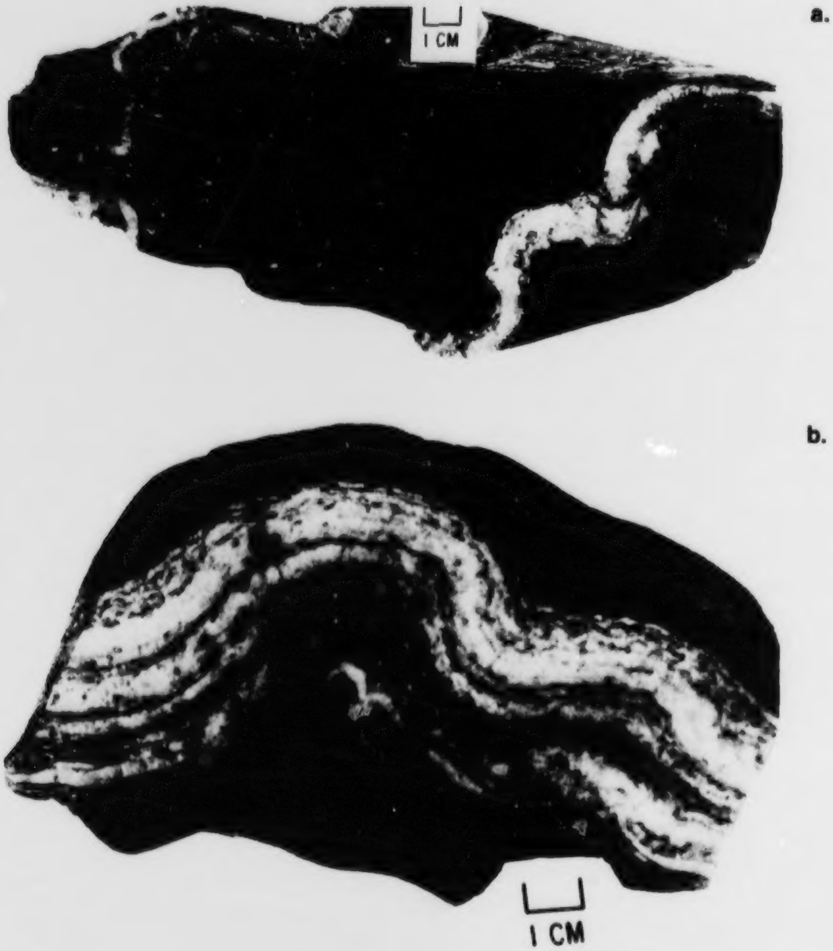

Figure 16. a) Arsenopyrite (white specks) and banded carbonate-bearing and carbonate-free argillite (lighter and darker grey bands respectively) associated with buckled bedding-parallel quartz veins, Lawrencetown gold district (GSC 204390-C). b) Banded bedding-parallel quartz-carbonate-chlorite vein in argillite, Lake Catcha gold district (GSC 204390-B).

In most districts, veins may contain sparse potassium feldspar and sericite. Chlorite occurs as selvages along the margins of all veins in the pelitic rocks. Plagioclase, tremolite/actinolite, biotite, muscovite, garnet, andalusite, rutile, sphene, ilmenite, tourmaline, and epidote occur in veins in host rocks of higher metamorphic grade (Smith, 1983a,b; Haynes et al., 1986). These minerals may be present in accessory amounts in many veins except in late pegmatoid veins where they may be major components.

Little attention has been paid to the presence of carbon in rocks associated with gold-bearing veins. Older literature commonly refers simply to the black slate or argillite host. Malcolm (1976), referring to the host rocks of better grade veins, observed that "These are generally black and are frequently impregnated with arsenopyrite, pyrite, or pyrrhotite, and the interstratified veins that can be worked with profit are usually found in beds of this character. In some cases the cross veins also are found to be enriched where they lie in contact with strata of this class." There are no published analytical data on the carbon content of rocks associated with the gold veins; however, the presence of a high carbon content in argillite interbeds in the Goldenville Formation may be a useful prospecting guide.

Wall-rock alteration

The presence of large volumes of rock containing disseminated, iron-rich carbonate and arsenopyrite adjacent to veins has long been recognized but has always been described without substantial interpretation, leading to the assumption that the carbonate and arsenopyrite are a primary component of the rocks in which they occur. A thorough study of the significance of alteration has yet to be carried out and references to alteration are of limited extent.

Boyle (1979) analyzed greywacke adjacent to a gold vein at the Caribou mine and determined that the adjacent greywacke was depleted in SiO_2, H_2O, and MnO but showed major enrichment of K_2O, CO_2, P_2O_5, and CaO, and lesser enrichment of Al_2O_3, FeO, Fe_2O_3, MgO, TiO_2, and S. Haynes (1983, 1986, 1987) tabulated wall-rock alteration and mineral associations for various vein types. He described thin zones of silicification and sericite-arsenopyrite alteration adjacent to some vein types.

Smith and Kontak (1986) and Kontak and Smith (1987a) report wall-rock alteration associated with gold-quartz vein mineralization in 29 of 30 gold districts studied in the eastern Meguma. They report silicification with accompanying depletion of alumina and alkalies as the dominant alteration type, forming zones measured in millimetres to tens of metres thick near gold-bearing veins. At the Beaver Dam deposit, they report a zone of silica enrichment for the full extent (800 m x 650 m) of the known deposit. However, they also report that the intensity of alteration is highly variable, is not uniquely related to quartz veining, is relatively sulphide-free, and is best characterized visually rather than chemically (Kontak and Smith, 1987a). However, unpublished regional lithogeochemical data (J. Kerswill, pers. comm., 1989) show that the range of compositions of SiO_2 and Al_2O_3 in regional and gold-bearing Goldenville Formation is similar, suggesting that most silica redistribution is due to processes of intergranular pressure solution during diagenesis (Houseknecht and Hathon, 1987; Houseknecht, 1988) and formation of the pervasive pressure solution cleavage (Fueten, 1985; Fueten et al., 1986; Henderson and Henderson, 1986; Henderson et al., 1986a). The principal chemical feature demonstrated to have a chemical relationship to gold distribution is an increase in K_2O/Na_2O in the wall rocks to gold veins (Kerswill, 1988), attributed to depletion in Na_2O rather than enrichment in K_2O.

Origin of the veins

Three general mechanisms have been proposed for the origin of the gold veins: 1) syngenetic hydrothermal deposition on the seafloor; 2) early syntectonic deposition from hydrothermal fluids of diverse origins; and 3) late syntectonic deposition from magmatic or deep crustal hydrothermal fluids.

Hunt (1868) was the first to propose a syngenetic origin for the quartz vein materials within the enclosing sediment. Hind (1869, 1870, 1872) supported Hunt's (1868) proposal for the laminated veins, but attributed other bedding-parallel veins to later processes. McBride (1978) reported a pyrite- and carbonate-rich stratum 1300 m below the GHT that contains several small gold occurrences and proposed a syngenetic origin for the gold. Haynes and Smith (1983) and Haynes (1983, 1986, 1987) proposed a complex, hydrothermal, hot spring model. Haynes (1987) interpreted the laminated, concordant veins as fumarole-related geyserite, and the crosscutting and semiconcordant mineralized veins as subsurface feeders and parasites of the hydrothermal system. Documentation of structural features (Henderson and Henderson, 1986; Henderson et al., 1986b; Mawer, 1986, 1987) does not support a synsedimentary origin for these veins though it has been argued (see below) that synsedimentary components have been mobilized to form the veins.

Theories involving early syntectonic processes have been commonly used to explain the origin of the veins. Early workers, including Campbell and Poole (1862), Campbell (1863), Selwyn (1872), Gilpin (1888), Faribault (1899), Malcolm and Faribault (1912), and Malcolm (1929) stressed the value of structure as a controlling factor and considered derivation of vein materials from enclosing sedimentary rocks, and "ascending" or "descending" hydrothermal fluids as transporting agents. Boyle (1966, 1979) supported a lateral secretion model. Modern variants of these theories support an early syntectonic, pregranite, and prefolding origin for the veins, a source for the vein materials in the enclosing sedimentary rocks, and material movement and deposition from fluids derived during the initial phases of prograde metamorphism (Graves, 1976; Graves and Zentilli, 1982; Henderson, 1983; Henderson and Henderson, 1986; Henderson et al., 1986a; Sangster et al., 1989).

Theories using late syntectonic mechanisms to explain vein genesis include magmatic hydrothermal processes related to Acadian granites and vein formation from deep, crustally derived metamorphic fluids at the time of Acadian plutonism but not directly from a magmatic source. A simple magmatic hydrothermal source for the vein materials and gold was proposed by Rickard (1927), Newhouse (1936), Emmons (1937), Bell (1948), and Douglas (1948). Recent proposals allow for a source of vein materials either directly from a granitic source, from the lower crust or mantle or from the enclosing sedimentary rocks, mobilized by magmatic or deep crustal metamorphic fluids driven by magmatic heat (Mawer, 1985, 1986, 1987; Hy and Williams, 1986; Smith and Kontak, 1986; Kontak and Smith, 1987a,b, 1988b).

The different hypotheses can be discussed by considering the source of vein materials and timing of vein formation.

Source of vein materials

A geological overview of the association between gold districts and Goldenville Formation stratigraphy provides substantial support for a source within the associated sedimentary rocks. The repetitive occurrence of the gold districts, on a regional scale, with the more carbonaceous, sulphidic, and argillaceous portions of the stratigraphic sequence indicates a possible genetic association between the gold districts and the stratigraphy. Pyrrhotite and arsenopyrite textures in wall rocks to the gold-bearing veins are identical to the pyrrhotite-pyrite-slate textures of acknowledged synsedimentary origin in the overlying Halifax Formation (Sangster et al., 1988). The random dissemination of large (1 to 2 cm) twinned arsenopyrite crystals in quartz wacke and quartzite, which retain detrital textures and unaltered feldspars, supports an early diagenetic/metamorphic origin for the arsenopyrite. An origin of these crystals as porphyroblasts formed at low metamorphic grade is supported by the very regular, widely spaced (5 to +/− 50 cm centres) dissemination of the arsenopyrite, the absence of controlling structure, and the presence of strained quartz pressure shadows.

Interpretations of extensive structural and geochemical studies of the regional and vein host lithologies support a source of all vein materials from the Goldenville Formation. There is substantial evidence that silica, the major vein component, was mobile during late diagenesis and prograde metamorphism (Fueten, 1985; Henderson et al., 1986a,b); silica derived by pressure solution from the quartz wacke may represent the largest portion of vein quartz (Clifford et al., 1983; Crocket et al., 1983).

Crocket et al. (1983, 1986a,b) determined that gold and arsenic contents in slate and wacke in some gold districts were increased by about 0.5 and 2.5 orders of magnitude over regional background levels for similar rocks (Table 3). Smith (1983a) noted strongly anomalous Au (10 ppb to 100 ppm) and As (100 to 50 000 ppm) contents in both meta-argillite and metawacke associated with gold-bearing veins at Cochrane Hill. Boyle (1966) reported values up to 0.5 ppm and 2.0 ppm Au and 0.5 and 1.2 ppm Ag in sedimentary pyrite and arsenopyrite, respectively, from Goldenville Formation slate and greywacke.

Two possible mechanisms are available for derivation of As from the Goldenville Formation. Kubilius and Perry (1989) have demonstrated that the greenschist facies rocks average 8 ppm As, whereas similar rocks at amphibolite facies metamorphic grades average 0.2 ppm As. This suggests that Goldenville Formation rocks undergoing the transition to amphibolite facies metamorphic grade could have been a source for As mobilized by metamorphically derived fluids. A second potential As source is within the carbonaceous sedimentary rocks that host the gold deposits. The ability of marine organic material to complex available As is well documented (Leventhal, 1983). Oxidation of these organic complexes during regional metamorphism, to produce C or CO_2, would release the complexed As, permitting reaction with biogenic pyrrhotite to produce arsenopyrite. This scenario indicates that the source of the As could have been within the carbonaceous host rocks to the veins, rather than a more regional source as proposed by Kubilius and Perry (1989).

Perhaps the best evidence supporting the Goldenville Formation as a source for the vein materials has been provided by recent sulphur, carbon, and oxygen stable isotope studies on vein and wall rock sulphides, vein carbonates, and by lead isotopic studies of vein galenas.

$\delta^{34}S$ values for sulphides from Meguma gold deposits are heavy, with district averages ranging from +9 to +20 per mil (Sangster, 1987, and unpublished data). Variations in sulphur isotopic compositions within individual districts are small, normally +/− 1 to 3 per mil, and pyrrhotite and arsenopyrite from veins, slates and wackes within individual gold districts are isotopically similar. The ranges of $\delta^{34}S$ values for gold-vein-related rocks and for regional Goldenville Formation rocks (Kubilius, 1983) are similar (Sangster et al., 1988, 1989). These data support the derivation of sulphur in sulphides associated with gold deposits from the host sedimentary rocks (Sangster, 1987; Kontak and Smith, in press). Sangster et al. (1988, 1989) have interpreted the heavy isotopic signature to reflect the diagenetic formation of the primary sulphide from isotopically heavy sulphate derived from oxygen deficient water in a stratified Iapetus ocean.

The carbon and oxygen isotopic ratios for carbonates from Meguma gold veins (Kontak et al., 1988b,c) show a compositional provinciality for each deposit averaging

Table 3. Comparison of average gold and arsenic contents of slates and greywackes from Harrigan Cove and Goldenville with unmineralized Meguma Group rocks and literature averages (from Crocket et al., 1986a).

Area or Sample	Lithology	Au ppb	As ppm	Reference
Harrigan Cove	greywacke	8.7	972	Crocket et al., 1986a
	slate	8.0	549	"
Goldenville	slate	10.5	523	"
Unmineralized Meguma Group rocks				
Ruth Falls Syncline Ecum Secum area	greywacke	1.2	2.3	Crocket et al., 1983
	slate	1.7	2.5	"
Oldham area (core several hundred metres from nearest mineralization)	greywacke	0.62	—	Thorpe and Thomas, 1976
	slate	2.0	—	"
Sherbrooke area	whole rocks (slate, greywacke, granite)	1.0	—	Brooks et al., 1982
Literature survey	sandstone	3.0	1	Crocket, 1974
	shale	2.5	13	Onishi, 1969

-20 to -24 per mil and +12 to +18 per mil respectively, for all Meguma deposits analyzed. These $\delta^{13}C$ values are lighter than those for carbonates from Precambrian gold deposit carbonates (-8 to -2 per mil) (Kontak et al., 1988c), a fact that they explained through a complex interaction of deep, exotic fluids with Meguma Group rocks. However, the carbon and oxygen isotopic ratios are similar to those for carbonates, interpreted to contain carbon from an oxidized organic carbon source, that occur in the GHT and Halifax Formation at Eastville (MacInnis, 1986). Also, the compositions of carbonates from Meguma gold veins (Fig. 17) lie on the extrapolation of the thermally dependant C/O isotopic equilibrium curve of Franks and Forester (1988), at a position that could represent temperatures of vein filling, possibly in the range between 300 and 400°C (Graves, 1976; Kontak et al., 1988a; Kontak and Smith, 1989). This relationship strongly suggests that the vein carbonate was derived by oxidation of organic carbon during diagenesis and prograde regional metamorphism. Since the presence of organic carbon is essential to the process of bacterial reduction of sulphate, the oxidation of organic carbon to produce CO_2 and CO_3^{2-} species probably occurred in combination with the diagenetic reduction of sulphate to sulphide (Holser et al., 1988) and supplied the CO_2 found in fluid inclusions in the gold-bearing veins. Regional vein quartz, hosted by noncarbonaceous quartz wacke and argillite away from gold districts, does not contain CO_2-rich fluid inclusions (Sheets, 1987).

Farquhar and Haynes (1986) and R. Thorpe (pers. comm., 1988) have obtained ore lead isotope determinations from numerous Meguma Group-hosted gold veins. Their data (Fig. 5) show that the isotopic ratios for most of the districts containing stratabound gold veins cluster about $^{207}Pb/^{204}Pb = 15.57$ and $^{206}Pb/^{204}Pb = 17.80$.

Chatterjee and Strong (1985) point out the more radiogenic character of the majority of the galenas from granite-related deposits (East Kemptville tin greisen, Dunbrack lead-quartz vein; Fig. 5) in relation to those from Meguma gold vein deposits. This is interpreted to be compatible with derivation of the vein materials by leaching from the host Goldenville Formation sedimentary rocks.

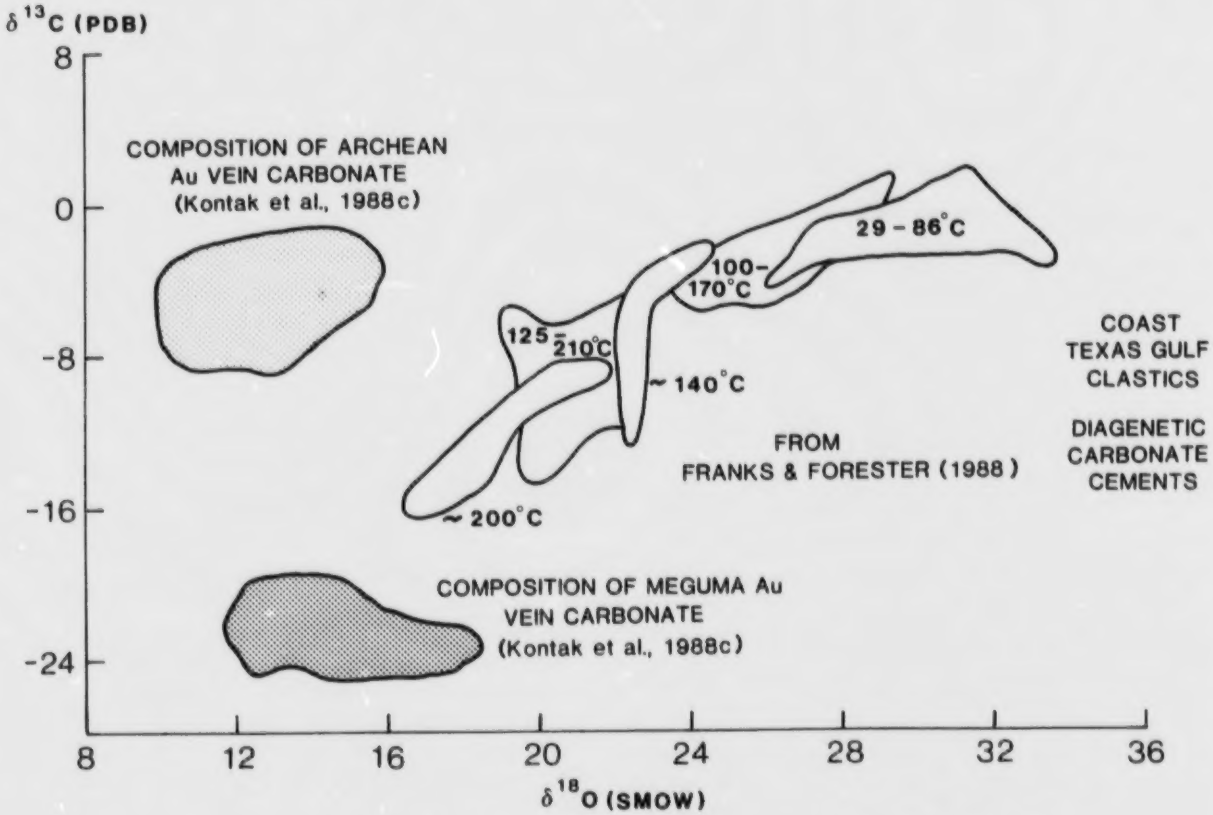

Figure 17. C-O isotopic composition of diagenetic carbonate cements (after Franks and Forester, 1988) with composition of Meguma gold vein carbonate and Precambrian gold vein carbonate (data from Kontak et al., 1988c). Meguma gold vein carbonate C-O isotopic compositions (data from Kontak and Smith, 1988c) lie on the extrapolation of the thermal evolution curve for diagenetic carbonate cements indicated by data from Gulf Coast clastics (Franks and Forester, 1988). This suggests that the Meguma gold vein carbonate is a product of late diagenetic/early metamorphic oxidation of organic carbon. The Meguma vein carbonate compositions are distinctly different from Archean gold vein carbonates.

Furthermore, the data lie close to the orogene growth curve of Doe and Zartman (1979) and Zartman and Doe (1981); the least radiogenic leads give model ages that approximate the period of Goldenville sedimentation (Farquhar and Haynes, 1986), though the data cannot be used for precise age calculations.

Lead isotope analyses for single samples from each of the Isaacs Harbour, Mount Uniacke, and Waverly districts, and four from the Beaver Dam occurrence, are more radiogenic than most of the leads analyzed from the gold veins, but are still less radiogenic than the least radiogenic granite-hosted base metal vein (Dunbrack). The first three occurrences also have other lead analyses lying within the main data cluster, suggesting that higher ratios represent galenas formed during a period of vein formation that is younger than that represented by the less radiogenic galenas. All of the more radiogenic occurrences are in or near biotite or staurolite-andalusite metamorphic zones associated with Devonian plutons and it is probable in these cases that a second generation of galena has been formed during the intrusive/metamorphic event. At the Beaver Dam site, the recently defined large gold-bearing vein system lies partially within the aureole of the River Lake pluton. Crack-seal veins, interpreted as indicative of an early metamorphic origin (Henderson and Henderson, 1986; Henderson et al., 1986b), are present. However, vein-related postgranite hydrothermal alteration has affected the minerals within the contact aureole (D. Duncan, Seabright Resources Inc., pers. comm., 1987). This supports the interpretation of a complex history for the more radiogenic galenas from the gold veins.

The direct generation of the veins from a magmatically derived fluid has been proposed by Douglas (1948) and Mawer (1986) but is considered unlikely by Kontak et al. (1988b). Lithophile element deposits related to Acadian plutonism are widespread within both the Meguma Terrane (O'Reilly et al., 1982; Logothetis, 1985; Richardson, 1988a,b) and adjacent areas of the Avalon, Gander, and/or Dunnage terranes in New Brunswick and Newfoundland. The Acadian granite-related deposits are characterized by widely varied mineral assemblages including Sn, W, Sb, F, Cu, Zn, Li, Be, etc. Arsenic is of major importance only in the case of the Mount Pleasant deposit in New Brunswick and Au occurs at elevated background levels in only a few areas (O'Reilly et al., 1982; Charest et al., 1985; Logothetis, 1985; Rogers et al., 1985). In contrast, the Meguma gold-quartz-carbonate veins have a comparatively simple ore mineralogy with arsenopyrite, pyrrhotite, native gold, pyrite, and traces of galena, chalcopyrite, and scheelite. The assemblage is constant, with only minor variations throughout some 70 districts. Also, known granite-related deposits occur in a variety of different forms, including greisens, veins, pegmatites, breccia zones, and subvolcanic breccia pipes. They are highly variable from area to area and even within an area (Logothetis, 1985). In contrast, Meguma gold veins demonstrate similar structures from district to district, as described above. The consistency of both mineralogy and structural development within the group of Meguma gold deposits in contrast to the wide mineralogical and structural variability of the confirmed granite-related deposits, is the strongest argument for genetically disassociating the gold veins from magmatic-hydrothermal processes. The broad scatter of lead isotopic data does not suggest derivation of the lead by magmatic processes, which tend to homogenize lead compositions, but rather support metamorphic derivation either from an inhomogeneous source or over a prolonged geological time span.

Timing of vein formation

Two metamorphogenic regimes for genesis of Meguma gold-bearing veins are currently the subject of considerable discussion. These include:
1) formation of the early bedding-parallel veins during the initial phase of metamorphism, and with continued episodic formation of bedding-parallel, en echelon, and other vein types throughout the period of Acadian metamorphism and plutonism, which culminated 400 and 370 Ma ago respectively (Muecke et al., 1988);
2) formation of all major veins at 370 Ma, subsequent to metamorphism and simultaneous with Acadian plutonism, from lower crustal fluids focused along major ductile shear zones.

Proponents of early-syntectonic models (Graves, 1976; Graves and Zentilli, 1982; Crocket et al., 1986a,b; Henderson and Henderson, 1986; Henderson et al., 1986a,b) have advocated the emplacement of the bedding-parallel gold-bearing veins into a horizontal stratigraphic sequence prior to folding, cleavage formation, and intrusion. This model relies on fluids mobilized by initial horizontal tectonic compression and greenschist facies metamorphism to provide the episodic hydraulic overpressures which resulted in regional crack-seal vein formation and pressure solution cleavage. Such a model satisfactorily explains the observed buckle folding in bedding-parallel veins by at least 50 percent volume loss (Fueten, 1985; Henderson et al., 1986b) during pressure solution cleavage formation (Fig. 18). Subsequent formation of pinch and swell and boudinage structures in the early veins, and the sequential formation of the later en echelon veins, are believed to be related to processes of bedding-parallel shear during fold amplification. The ac veins are related to extension parallel to fold axes.

Others have provided less convincing evidence for the emplacement of the initial vein systems and gold into folded beds during the intrusion of the Acadian granites. Mawer (1986, 1987) documented extensive microscale deformation textures in bedding-parallel veins including: pervasive undulose extinction, deformation bands, subgrains, and deformation lamellae in quartz; dynamically recrystallized quartz; and several generations of tectonic stylolites. These features overprint well preserved primary textures in the veins, and seem also to provide evidence for an early rather than late vein origin.

Hy and Williams (1986), Smith and Kontak (1986, 1988a,b), and Kontak and Smith (1987a,b, 1988b) have published preliminary accounts of work that relate gold distribution to syngranite ductile shear zones. The zones

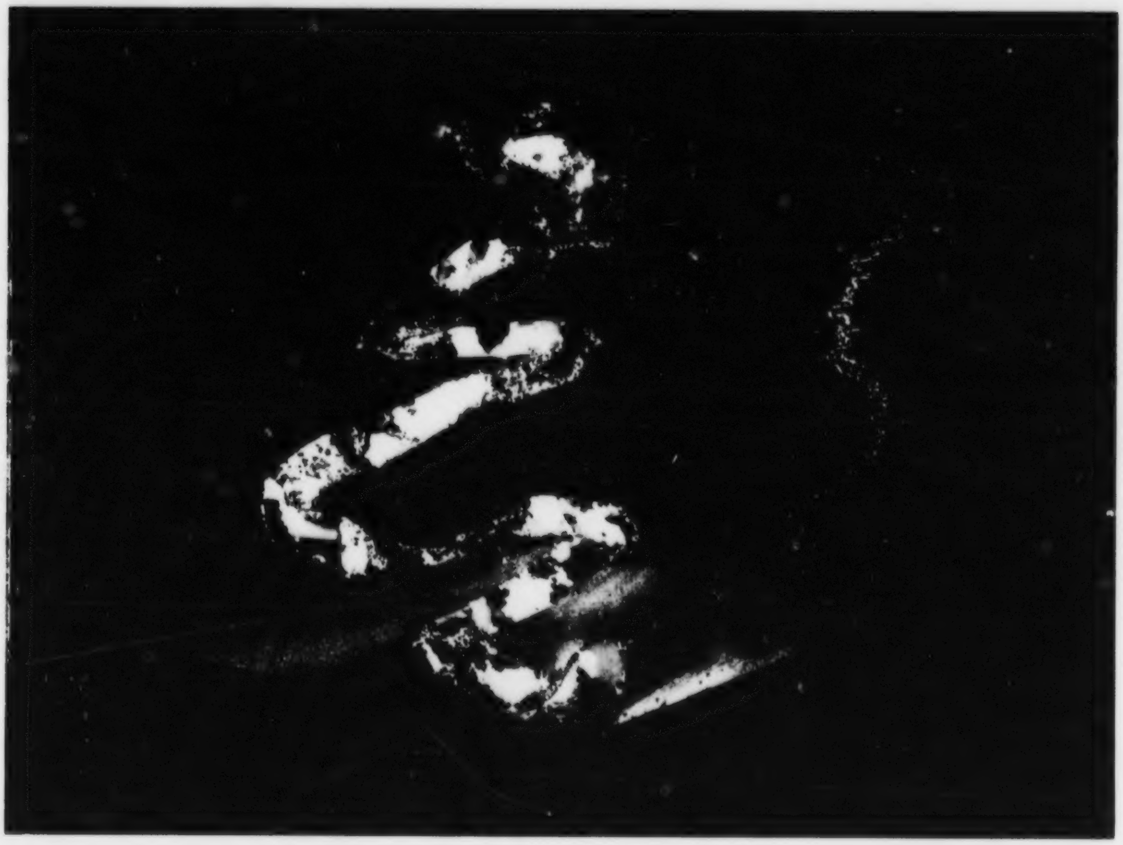

Figure 18. Photomicrograph of oversize thick section of two buckle veins in argillite, Moose River gold district. Note particularly the following features: 1) the occurrence of auriferous pyrrhotite (opaque) in crests of buckles in larger vein; 2) strained coarse grained quartz; 3) fine grained mosaics of unstrained secondary quartz related to margins of pyrrhotite grains and vein walls; 4) the location of the pressure solution cleavage planes adjacent to buckle fold limbs; and 5) the proportional spacing of the pressure solution lamellae with regard to the vein thicknesses (i.e. thicker vein, centre, versus thinner vein at right). Diamond-drill core sample from Moose River gold district. These features indicate that the vein formed prior to cleavage formation and folding. Sample width is 6 cm. Crossed nicols (GSC 204261-G).

are defined by the presence of a steeply dipping mineral lineation, commonly displayed by carbonate, arsenopyrite, or quartz-orthoclase (C. Hy, pers. comm., 1987) that occurs in highly carbonaceous argillite in many gold districts. These authors interpret the lineation to indicate a large component of downdip ductile shearing at elevated temperatures, indicating thermal doming and vertical tectonic processes associated with granite intrusion and thus compatible with the interpretation that gold was introduced by fluids from the deep crust or mantle. Kontak et al. (1988d, 1989) reported $^{40}Ar/^{39}Ar$ plateau ages of 370 Ma on muscovite from quartz veins from the Beaver Dam and Fifteen Mile Stream gold districts in support of the syngranite emplacement interpretation. However, these ages could be related to extensive regional thermal overprinting of Meguma rocks during Acadian plutonism (385 to 360 Ma) as documented by Muecke et al. (1988). Thermal resetting must be considered a possible alternative interpretation for these data since the Beaver Dam and Fifteen Mile Stream occurrences are close to thermal centres represented by the River Lake and Sloanes Lake plutons, respectively.

PART III: GRANITE-RELATED SN-W-BASE METAL-U MINERALIZATION

Introduction

Most of the principal granite-related mineral occurrences are spatially associated with the South Mountain Batholith (SMB) which is the major plutonic feature of southern Nova Scotia (Fig. 19). The batholith is a composite intrusion containing older biotite granodiorite and granodiorite porphyry phases (age = 372 ± 2 Ma) that are cut by younger and smaller bodies of two-mica monzogranite and leucomonzogranite which have been dated at 364 ± 1 Ma and 361 ± 1 Ma respectively (Tables 4 and 5; Clarke and Halliday, 1980; Clarke et al., 1985).

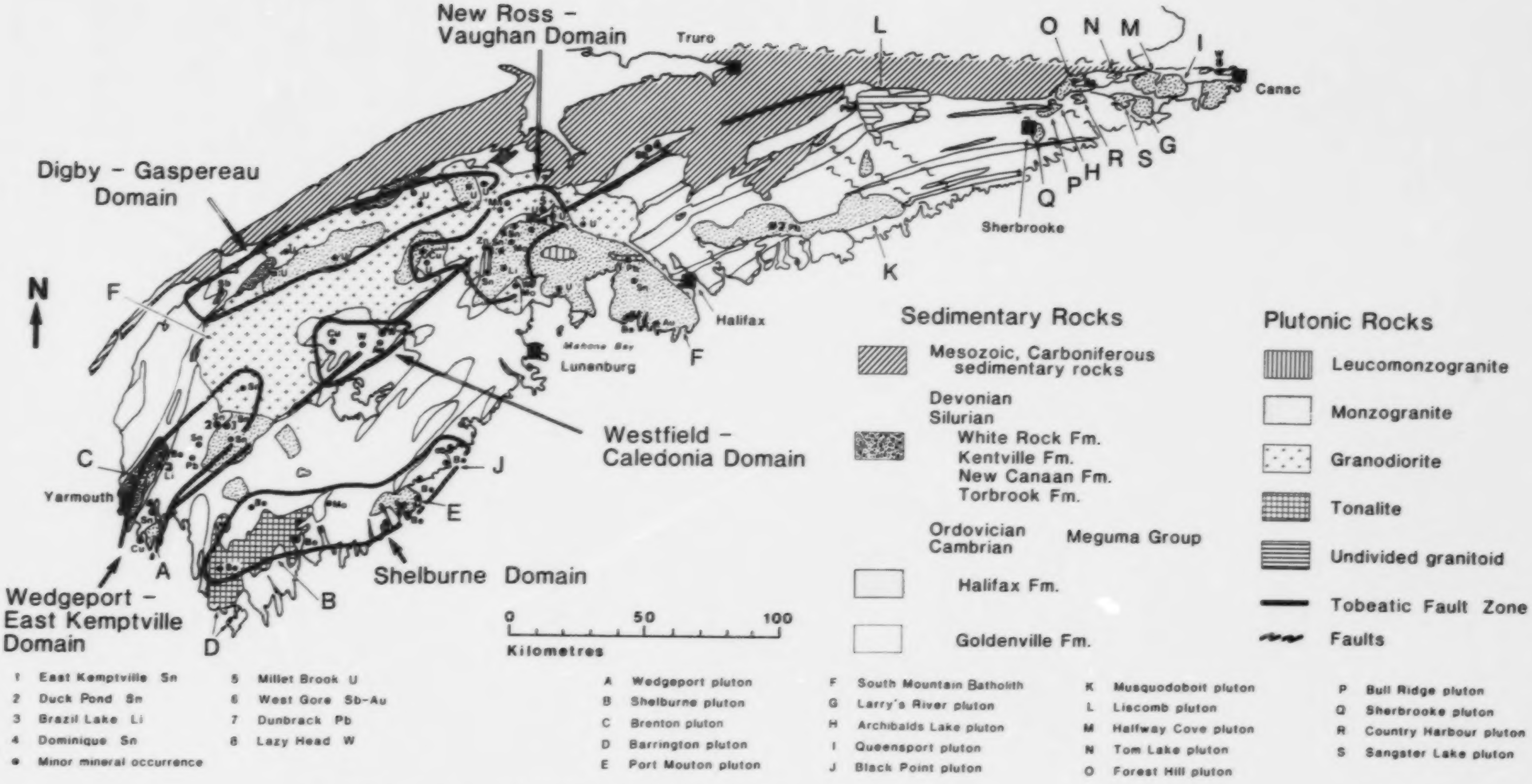
New Ross - Vaughan Domain
Truro
L
O N M
I
Canso
Digby - Gaspereau Domain
R S G
P H
Q
Sherbrooke
K
N
F
Halifax
Mahone Bay
Lunenburg
F
Westfield - Caledonia Domain
C
J
Yarmouth
E
A
Shelburne Domain
Wedgeport - East Kemptville Domain
B
D
0 50 100
Kilometres
Sedimentary Rocks
Mesozoic, Carboniferous sedimentary rocks
Devonian
Silurian
White Rock Fm.
Kentville Fm.
New Canaan Fm.
Torbrook Fm.
Ordovician
Cambrian
Meguma Group
Halifax Fm.
Goldenville Fm.
Plutonic Rocks
Leucomonzogranite
Monzogranite
Granodiorite
Tonalite
Undivided granitoid
Tobeatic Fault Zone
Faults
1 East Kemptville Sn
2 Duck Pond Sn
3 Brazil Lake Li
4 Dominique Sn
● Minor mineral occurrence
5 Millet Brook U
6 West Gore Sb-Au
7 Dunbrack Pb
8 Lazy Head W
A Wedgeport pluton
B Shelburne pluton
C Brenton pluton
D Barrington pluton
E Port Mouton pluton
F South Mountain Batholith
G Larry's River pluton
H Archibalds Lake pluton
I Queensport pluton
J Black Point pluton
K Musquodoboit pluton
L Liscomb pluton
M Halfway Cove pluton
N Tom Lake pluton
O Forest Hill pluton
P Bull Ridge pluton
Q Sherbrooke pluton
R Country Harbour pluton
S Sangster Lake pluton

Figure 19. Geology and granite-related mineral deposits of the Meguma Terrane. Geology modified after O'Reilly et al. (1982), Chatterjee (1983a), and Richardson (1988a,b).

Smaller plutons of similar composition and age occur east of the SMB (Clarke et al., 1980; Rogers, 1985; Hill, 1986a,b). These include the Musquodoboit Batholith (MacDonald and Clarke, 1985), the composite mafic/felsic Liscomb Complex (Giles and Chatterjee, 1987), and a number of smaller intrusions scattered throughout the eastern Meguma Terrane, particularly in the Canso area. A second group of smaller intrusions of broadly similar composition and with ages ranging between 330 and 300 Ma locally intrude the contact zone of the SMB and the Meguma rocks south and west of the batholith. Examples of this period of plutonic activity include the Davis Lake, Wedgeport, and Port Mouton plutons. Alteration products in granitic rocks related to granite-hosted mineral occurrences relate to this later period of activity (Table 4).

The source of the magma that formed the SMB has been the subject of a number of studies (summarized in Clarke et al., 1988). The peraluminous nature of the SMB, the abundance of magmatic and xenocrystic garnet and cordierite (Allan and Clarke, 1981; Maillet and Clarke, 1985), the presence of abundant reacted Meguma xenoliths in the intrusion (Jamieson, 1974; Allan and Clarke, 1981; Woodend, 1985), and the generally high $\delta^{18}O$ values found in the intrusion (Longstaffe et al., 1980) suggest that a major portion of the granodiorite magma may have resulted from partial melting of Meguma-like sedimentary rocks. However, initial Sr ratio data (Clarke and Halliday, 1980), refined and interpreted with Nd isotopic data (Clarke et al., 1988), suggest that the SMB magma might either be a hybrid with a large portion of both crustal- and mantle-derived material including a large portion of mantle-derived Nd and Sr, or was derived from crustal sedimentary rocks with more evolved $^{87}Sr/^{86}Sr$ and higher Sm/Nd than the observed Meguma sedimentary rocks.

Granite-related mineral deposits and occurrences are located in and peripheral to younger two-mica monzogranite intrusions which intrude the margins of the SMB or adjacent Meguma Group metasedimentary rocks. These are highly evolved or "specialized" intrusions (Tischendorf, 1977) and contain distinctive trace element values that are diagnostic of potentially metalliferous granites. Chatterjee et al. (1983) used statistical discriminant analysis to further subdivide these specialized granites into stanniferous and uraniferous types. The classification of tin or uranium specialization is based on relative enrichment in Rb, K_2O, F, Li, W, P_2O_5, and Be, and Cu, Sn, Mn, and Zn, respectively. These two types of enrichment are attributed to late stage magmatic processes including albitization and greisenization in the case of tin, and late stage hydrothermal processes leading to the concentration of uranium.

Chatterjee (1983a) proposed several metallogenic domains for the SMB which are the basis of this outline. Geographic names have, where possible, been used for the domains in accord with previous informal usage. Major groups of deposits are discussed within the context of the geographic domains in which they occur.

Wedgeport-East Kemptville Domain

Introduction

The Wedgeport-East Kemptville Domain extends 80 km east-northeast of Yarmouth, Nova Scotia. It includes the Wedgeport pluton, Davis Lake pluton, and Meguma Group metasedimentary rocks. The domain is characterized by polymetallic tin-base metal occurrences in the granitic and associated metasedimentary rocks (Wolfson, 1983; Chatterjee et al., 1985a; Richardson, 1985a,b, 1988a,b; Fig. 19). The East Kemptville tin deposit is the largest granophile element mineral deposit in the domain. Large, but currently noncommercial, sediment-hosted tin-base metal occurrences are present in the associated metasedimentary rocks.

East Kemptville tin deposit

The East Kemptville tin deposit is located 54 km northeast of Yarmouth, Nova Scotia. It lies within the Davis Lake pluton, a younger biotite monzogranite/leucomonzogranite which has intruded the southwestern apex of the SMB (Fig. 20). The tin deposit was discovered by heavy mineral surveys and follow-up boulder prospecting carried out by Shell Canada Resources Limited in 1978. After completion of a feasibility study, the deposit was sold to Rio Algom Ltd., who defined a reserve of 56 million tonnes of ore grading 0.165 percent Sn at a cutoff grade of 0.08 percent Sn. Production from the deposit began in October 1985. Since its discovery, the East Kemptville deposit has been studied extensively. The description presented here is primarily from Richardson et al. (1982), Chatterjee et al. (1985a), and Richardson (1985a,b, 1988a,b).

The greisen mineralization at East Kemptville is similar in some respects to that of other large tonnage tin deposits, particularly those in the Krusne hory Mountains, Erzgebirge district of Czechoslovakia (Richardson et al., 1982). These deposits, however, are commonly cupola-related; the East Kemptville deposit is different in that it occurs below a horizontal inflection on the steeply dipping contact of the Davis Lake pluton.

At East Kemptville, meta-argillite and metawacke of the Cambro-Ordovician Meguma Group were folded about northeast-southwest fold axes during the Acadian Orogeny and subsequently intruded by the SMB and younger granitic intrusions. At the northwestern contact of the Davis Lake pluton, steeply dipping, north-facing Goldenville Formation metawacke is overlain by calcareous meta-argillite of the transition zone between the Goldenville and Halifax formations and this is in turn overlain by Halifax Formation meta-argillite. The transition zone (GHT) is characterized by a distinctive manganese-rich (coticule-bearing) stratum which is regionally anomalous in Au, Pb, Zn, Ba, and As (Binney et al., 1986; Zentilli et al., 1986).

Various studies suggest that the Davis Lake pluton (Fig. 20) is a single, highly differentiated intrusion that

Table 4. Selected ages for granitoid rocks of the Meguma Terrane. In part extracted from summary by Clarke et al. (1980). The reader should exercise caution in interpreting the analyses: old, and possibly imprecise, data are presented with recent age determinations. Age determinations by several methods, each with its own limitations, are included. Abbreviations - wr=whole rock, bi=biotite, zr=zircon, qpl=quartz plagioclase, ms=muscovite, kf=K-feldspar, phl=phlogopite, pl=plagioclase.

Intrusion	Age(Ma)	Method	Initial Sr	Reference
SOUTH MOUNTAIN BATHOLITH				
Regional				
Leucomonzogranite	361±1	Rb-Sr wr	0.7102	Clarke and Halliday (1980)
Two-mica monzogranite	364±1	bi ms kf	0.7094	"
Biotite granodiorite	372±2	pl	0.7081	"
Mineral occurrences				
-Long Lake W-Mo-Cu-Ag Two-mica granite	332±10	Rb-Sr wr	0.70837	O'Reilly et al. (1985)
-Westfield W-Mo-Sn-Ag-Au K-feldspathized granite porphyry	270±14	Rb-Sr wr	0.71672	O'Reilly et al. (1985)
-Lake Darling Cu Greisen	281±5	Rb-Sr ms		O'Reilly et al. (1985)
-East Kemptville Sn Davis Lake Complex				
Biotite monzogranite	330±7	Rb-Sr-wr	0.727	Richardson (1988b)
Quartz-topaz greisen	337±5	Rb-Sr wr	0.729	Richardson (1988b)
Quartz-topaz greisen	295±5	Ar-Ar ms		Zentilli and Reynolds (1985)
PLUTONS EAST OF THE SMB				
Larrys River				
Two-mica monzogranite	333	Rb-Sr		Fairbairn et al. (1960)
	328-369	K-Ar bi ms		"
	372	U-Pb zr		Krogh and Keppie (1988)
Halfway Cove				
Two-mica monzogranite	372	U-Pb zr		"
Archibalds Lake				
Granite	298±10	Rb-Sr wr		Fairbairn et al. (1960)
	347	K-Ar ms		"
Queensport				
Two-mica monzogranite	367-391	K-Ar bi ms		Wanless et al. (1968)
	362-386	Rb-Sr wr		Fairbairn et al. (1964)
Musquodoboit				
Two-mica monzogranite	368-391	Rb-Sr ms bi		Wanless et al. (1968)
	377	K-Ar bi		"
Adamellite	362	Ar-Ar bi		Reynolds et al. (1981)
Sericite-Dunbrack vein	304	Ar-Ar		Reynolds et al. (1981)
Liscomb				
Biotite granodiorite	389	K-Ar bi		Fairbairn et al. (1960)
PLUTONS SOUTHWEST OF THE SMB				
Wedgeport				
Biotite monzogranite	316±5	U-Pb zr		Cormier et al. (1988)
	323±12	Rb-Sr wr	0.7137	"
internal isochron	257±8	Rb-Sr bi kf wr qpl	0.716 to 0.759	"
Shelburne				
Trondhjemite	306	K-Ar bi		Fairbairn et al. (1960)
Two-mica granite	323	Rb-Sr bi		"
Granite	302	Ar-Ar bi		Reynolds et al. (1981)
Meladiorite	353	K-Ar bi		Reynolds et al. (1981)
Brenton				
Monzogranite	325±9	Ar-Ar bi ms		O'Reilly (1976)
Foliated granite	314-328	Ar-Ar bi ms		Reynolds et al. (1981)
Barrington				
Biotite tonalite	318	Rb-Sr bi		Fairbairn et al. (1960)
	348	K-Ar bi		"
Quartz diorite	306-308	Ar-Ar bi		Reynolds et al. (1981)
Port Mouton				
Two-mica granodiorite and two-mica granite	340±23	Rb-Sr wr		Cormier and Smith (1973)
Monzonite	297-300	Ar-Ar bi		Reynolds et al. (1981)
Black Point				
Norite	366±16	K-Ar phl		Wanless et al. (1968)

Table 5. Summary chemical analyses of granitic rock types associated with granite-hosted mineral occurrences.

	South Mountain Batholith*				Davis Lake pluton**								Misc. Greisen*		Westfield Caledonia****			
	Gd n=4-11	MG n=5-30	LMG n=3-25	A/P n=4-12	MGSN n=2	QTGSN n=12	BMG n=8	ABMG n=4	BMCMG n=4	MAG n=1	BLM n=5	LM n=6	Turner Tin n=2-10	U Mineralized Granite*** n=4	PG n=3	AG n=5	K-feld n=9	QACP n=5
SiO_2	69.38	74.06	74.45	73.78	40.00	71.63	75.87	75.57	75.41	71.90	75.90	74.15	72.95	68.92	71.68	70.98	70.93	72.93
TiO_2	0.61	0.20	0.07	0.07	0.07	0.04	0.18	0.20	0.11	0.21	0.08	0.06	0.06	0.61	0.38	0.58	0.42	0.23
Al_2O_3	14.36	13.62	14.06	14.73	25.02	14.28	12.58	13.10	12.94	14.80	13.50	14.85	15.43	13.69	14.31	14.42	14.57	14.45
Fe_2O_3	0.44	0.16	0.21	0.24	3.14	2.05	0.66	0.67	1.15	1.07	0.32	0.29	0.56	6.06	0.27	0.77	0.51	2.11
FeO	3.53	1.51	0.81	0.72	3.00	1.80	1.20	1.07	1.10	0.90	1.04	1.03	1.75	2.77	2.55	2.65	2.21	1.85
MnO	0.10	0.04	0.03	0.03	0.44	0.06	0.04	0.02	0.03	0.02	0.05	0.07	0.93	0.06	0.07	0.37	0.06	0.05
MgO	1.02	0.28	0.10	0.10	0.23	0.06	0.30	0.42	0.22	0.37	0.12	0.08	0.14	1.14	0.67	0.82	0.76	0.57
CaO	1.93	0.59	0.51	0.46	5.16	0.05	0.56	0.37	0.41	0.57	0.33	0.61	0.46	1.24	1.30	1.06	1.13	1.33
Na_2O	3.29	3.45	4.11	3.98	0.21	0.43	3.33	3.29	3.12	8.42	3.61	3.93	0.89	3.04	3.10	2.86	3.38	1.69
K_2O	3.86	4.72	4.32	4.95	9.26	1.39	4.60	4.05	4.59	0.60	4.24	3.87	5.26	3.45	4.26	4.08	4.66	3.65
P_2O_5	0.10	0.14	0.26	0.24	3.21	.033	0.10	0.11	0.22	0.17	0.23	0.41	0.22	0.22	0.19	0.21	0.16	0.31
H_2O	0.88	0.80	0.84	0.81									--	--	1.00	1.42	1.07	1.33
F	0.07	0.15	0.40	0.27	2.10	3.00	1.76	1.68	1.90	0.05	0.43	1.03	--	0.04	0.04	0.11	0.07	0.05
Ba	689	181	57	57	60	115	189	212	146	120	91	24	44	505	520	604	420	538
Sr	140	25	15	14	278	28	42	37	28	62	18	44	18	106	111	134	102	98
Rb	142	388	760	653	2412	507	435	479	427	84	768	963	879	136	181	180	186	169
Li	124	277	628	559	1215	366	111	166	103	32	379	589	--	97	82	93	85	65
Sn	12	22	44	40	26850	4823	15	33	20	22	35	196	--	4	5	10	10	22
W	2	1	2	--	56	8	8	8	0	<10	22	33	--	2	<4	<4	17	5
Mo	3	2	2	2	3	2	2	1	1	<1	2	4	--	4	4	5	3	2
Cu	11	8	13	5	26	2975	7	7	8	3	14	151	--	264	4	20	37	199
Pb	--	--	--	--	134	17	17	32	17	34	9	12	--	44	21	23	20	15
Zn	68	60	55	39	176	5228	69	63	39	23	73	266	--	417	57	58	90	25
U	--	--	--	--	45	22	15	10	21	<10	24	24	--	668	7	7	4	14
Th	11	11	4	3	43	15	20	15	22	25	16	4	4	8	10	10	15	5
Cs	11	24	34	24	47	14	12	11	12	6	25	23	62	--	--	--	--	--
Sc	11	4	2	2	0	1	4	4	--	--	3	2	3	--	--	--	--	--
Ta	2	4	7	7	14	2	1	1	--	--	2	4	5	--	--	--	--	--
Hf	6	3	2	2	4	2	3	3	--	--	2	2	2	--	--	--	--	--
Zr					58	7	101	108	62	100	42	21		--	250	141	78	119
Y					22	1	37	35	13	20	13	10		--	--	--	--	--
Nb					20	26	15	17	17	30	19	38		--	--	--	--	--
As					26	7	5	169	0	<5	8	7		--	9	26	--	10
Bi					12	34	1	4	8	36	10	4		<1	<1	3	1	6
Be					11	<2	15	10	--	--	9	7		2	5	5	3	6
B					50	1	23	38	--	--	20	38		50	13	30	12	60
Au					--	1ppb	9ppb	1ppb	--	--	1ppb	1ppb			10ppb	6ppb	1218ppb	42ppb
Ag					1	6	<1	<1	<1	<1	<1	--			<1	<1	7	<1
Sb					<2	2	7	6	<5	<5	3	--						

Gd=granodiorite; MG=monzogranite; LMG=leucomonzogranite; A/P=applite/pegmatite; MGSN=muscovite greisen; GTGSN=quartz-topaz greisen; BMG=biotite monzogranite; ABMG=altered biotite monzogranite; BMCMG=biotite-chlorite-muscovite monzogranite; MAG=magnetic monzogranite; BLM=blue leucomonzogranite; LM=leucomonzogranite; PG=porphyritic granodiorite; AG=altered granodiorite; K-feld=K-feldspathized porphyry; QACP=quartz-albite-chlorite-pyrite porphyry.

*from compilation by Clarke et al., 1985; **from Richardson, 1988b; ***from Chatterjee et al., 1985c; ****from O'Reilly, 1985.

Major element oxides and F reported as percent; trace elements reported as ppm except Au as ppb.

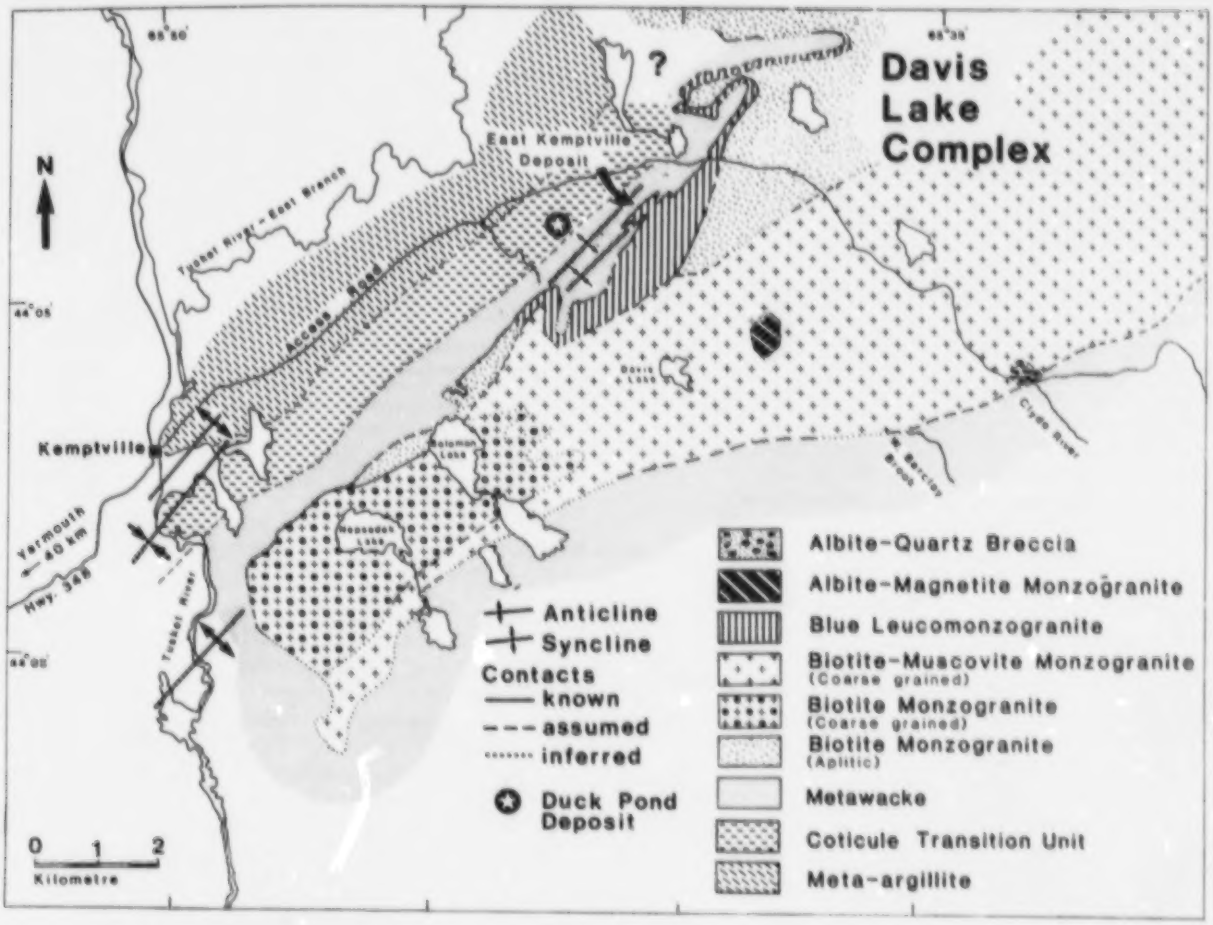
65°50'
65°35'
44°05'
44°00'
?
Davis Lake Complex
N
East Kemptville Deposit
Tusket River – East Branch
Access Road
Kemptville
Yarmouth 40 km
Hwy. 340
Tusket River
Davis Lake
Solomon Lake
Clyde River
Barclay Brook
Anticline
Syncline
Contacts
known
assumed
inferred
Duck Pond Deposit
0 1 2
Kilometre
Albite-Quartz Breccia
Albite-Magnetite Monzogranite
Blue Leucomonzogranite
Biotite-Muscovite Monzogranite (Coarse grained)
Biotite Monzogranite (Coarse grained)
Biotite Monzogranite (Aplitic)
Metawacke
Coticule Transition Unit
Meta-argillite

Figure 20. Geology of the Davis Lake complex and location of the East Kemptville tin deposit (modified after Richardson, 1988b).

has been modified by late magmatic processes (Chatterjee and Strong, 1985; Chatterjee et al., 1985a; Richardson, 1985a,b, 1988a,b; Kontak, 1987). The least altered rock consists of coarse grained biotite monzogranite. Weak sericitic alteration of microcline perthite and plagioclase, and chloritic alteration of biotite pervades even the freshest rocks. Near the deposit, pervasive sericite alteration has been overprinted by late magmatic albite and white mica (blue leucomonzogranite). This alteration is most intense within and beneath the deposit. The tin greisens at East Kemptville crosscut the albite-white mica alteration (Richardson, 1988a).

The East Kemptville deposit is a horizontal tabular zone 1500 m by 500 m by 100 m thick consisting of massive greisen and greisen-bordered veins and stockworks within blue leucomonzogranite of the Davis Lake pluton. The deposit formed immediately below a horizontal roll in the steeply dipping contact between the intrusive rocks and enclosing Meguma Group metawacke (Fig. 21). Ore grade tin mineralization is restricted to the granite. The greisen-bordered vein and microfracture system is steeply dipping and is oriented subparallel and perpendicular to the main contact (Richardson et al., 1982; Richardson, 1985a). Greisen-bordered veins occur over an area of 15 km^2, but only at the East Kemptville site do they occur in sufficient density to constitute a commercial deposit (Chatterjee et al., 1985a).

The greisens that host the tin ores are the end product of hydrothermal alteration that has affected much of the Davis Lake pluton. Essential minerals of the greisens are fine to very fine grained bluish quartz, topaz, and greenish to silver mica (muscovite and zinnwaldite). Other minerals include cassiterite, pyrite, sphalerite, chalcopyrite, pyrrhotite, arsenopyrite, molybdenite, galena, wolframite, and fluorite.

Individual greisen zones bordering veins and fractures are 0.5 to 40 cm wide, but may be in excess of 20 m long. Their mineralogical composition changes gradationally along strike. The essential minerals occur as a series of mineralogically and chemically zoned envelopes about a central quartz-topaz vein or fracture (Richardson et al.,

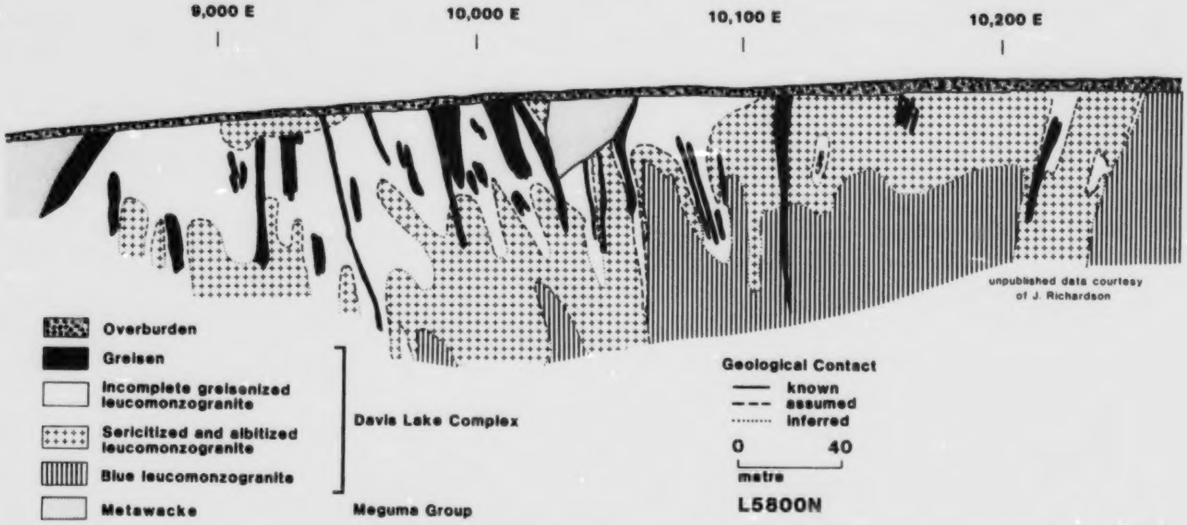
9,000 E
10,000 E
10,100 E
10,200 E
unpublished data courtesy of J. Richardson
Overburden
Greisen
Incomplete greisenized leucomonzogranite
Sericitized and albitized leucomonzogranite
Blue leucomonzogranite
Metawacke
Davis Lake Complex
Megume Group
Geological Contact
known
assumed
inferred
0
40
metre
L5800N

Figure 21. Vertical section 5800N, East Kemptville tin deposit (modified after Richardson, 1988b).

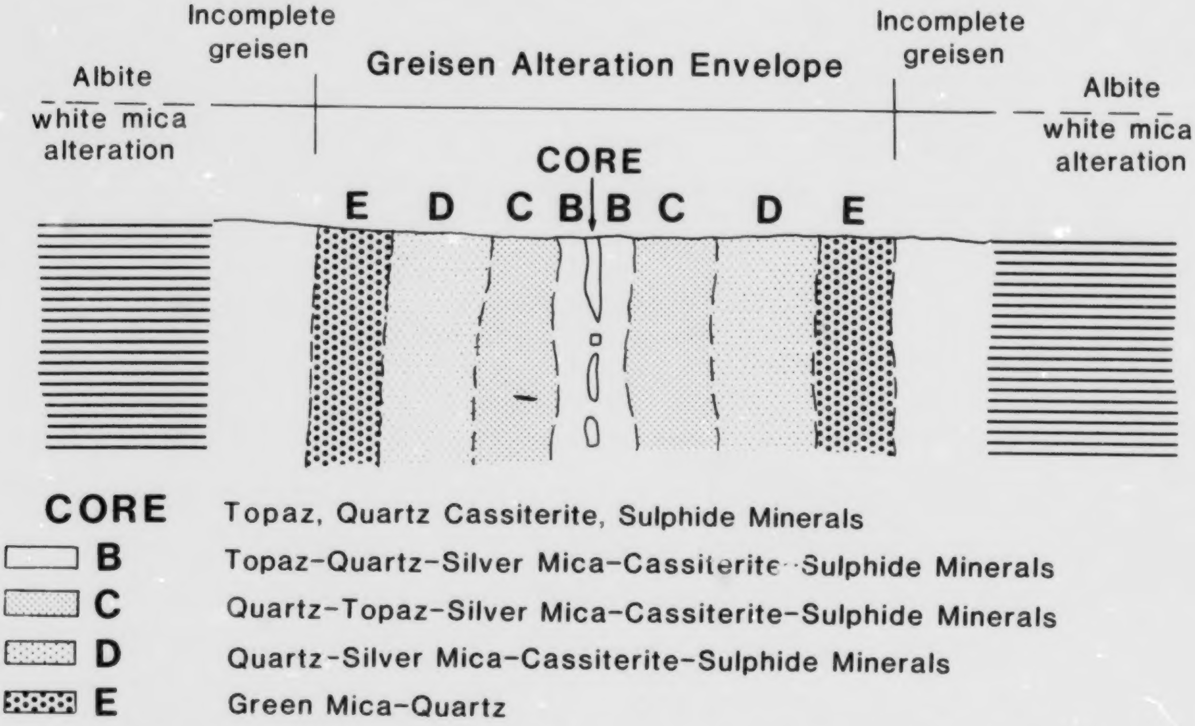
Incomplete greisen
Greisen Alteration Envelope
Incomplete greisen
Albite
white mica alteration
Albite
white mica alteration
CORE
E D C B B C D E
CORE Topaz, Quartz Cassiterite, Sulphide Minerals
B Topaz-Quartz-Silver Mica-Cassiterite-Sulphide Minerals
C Quartz-Topaz-Silver Mica-Cassiterite-Sulphide Minerals
D Quartz-Silver Mica-Cassiterite-Sulphide Minerals
E Green Mica-Quartz

Figure 22. Schematic illustration of greisen alteration envelopes, East Kemptville tin deposit (modified after Richardson, 1985a). Minerals in each zone listed in decreasing order of abundance.

1982, Richardson, 1985a; Fig. 22). The core quartz-topaz veins are highly varied in composition and in some cases grade through several related mineral assemblages over short distances (Table 6). Massive greisen zones are as much as 4 to 6 m wide and 40 m long in local areas of high vein density.

The core veins are succeeded outward by mineralogical zones characterized by decreasing topaz and increasing quartz and mica contents. Sulphides and oxides are disseminated throughout the envelope but cassiterite content decreases toward the margins (Table 7). Pyrite, chalcopyrite, and pyrrhotite are in most cases preferentially

Table 6. Mineral assemblages in greisen-bordered quartz veins.

a) quartz — cassiterite
b) sphalerite — pyrite — cassiterite
c) arsenopyrite ± wolframite ± cassiterite
d) topaz — cassiterite — chalcopyrite — sphalerite
e) crystals of cassiterite and/or pyrite along a central microfracture

Table 7. Sn distribution in greisen-bordered vein phases (after Richardson et al., 1982).

Core	2.5 Sn
Quartz-topaz-mica-sulphide envelope	0.1 to 0.5 Sn
Altered granite	0.05 Sn

concentrated outside the core. Richardson (1988a) described two types of alteration outside the greisen envelopes. Incompletely greisenized leucomonzogranite in which approximately 75 percent of all feldspars have been replaced, borders the greisen. Peripheral to this is white or blue leucomonzogranite that shows pervasive albite-white mica alteration. Tin grades are high in the core veins and decrease with decreasing intensity of alteration away from the core veins (Table 7).

Richardson (1985a) subdivided areas of massive greisen by colour. Dark grey greisen contains topaz, cassiterite, chalcopyrite, sphalerite, and pyrite. Light grey greisen contains quartz, mica, and only minor topaz, cassiterite, chalcopyrite, and pyrite. Rare green greisen contains predominant green mica and quartz with cassiterite, sphalerite, and fluorite. Contacts between the various types of massive greisen and greisen-bordered vein zones are gradational.

Sediment-hosted tin occurrences

Polymetallic tin-base metal occurrences are present in sedimentary rocks of the Goldenville-Halifax Formation Transition Zone near Duck Pond Brook, 1 km west of the East Kemptville deposit (Pitre, 1987) and in the Dominique-Plymouth area near the northern end of the Wedgeport pluton (Wolfson, 1983). In both areas, the main type of tin mineralization consists of sulphide-cassiterite veinlets, crosscutting foliation, with associated chloritic and/or biotitic alteration. Wolfson (1983) also described stratiform sulphide-cassiterite mineralization in silicified and calcareous layers within the sedimentary rocks. The transition zone and associated carbonaceous meta-argillite is commonly pyrrhotite-rich and in the Plymouth area contains associated arsenopyrite and traces of chalcopyrite. The concordant tin-bearing zones occur over a thick stratigraphic interval but individual veinlets are commonly only about 1 cm thick. Cassiterite in some cases forms as much as 30 percent of these thin units. Pyrite, rather than the regionally present pyrrhotite, is dominant in the cassiterite bands. Other sulphide minerals present include sphalerite, pyrrhotite, arsenopyrite, and chalcopyrite. Alteration associated with the stratabound cassiterite bodies is restricted to some silicification and development of chlorite (Wolfson, 1983; Pitre, 1987). In a few rare instances, cassiterite grains in these bodies have a clastic detrital appearance (Wolfson, 1983; p. 183).

The southeastern part of the Wedgeport pluton contains greisen-bordered sulphide-cassiterite veinlets and small zones of massive greisen with very different compositions. Chatterjee et al. (1985b) listed the major gangue minerals as quartz, muscovite, topaz, fluorite, beryl, tourmaline, and carbonates with minor metallic phases, including sphalerite, chalcopyrite, arsenopyrite, cassiterite, wolframite, scheelite, native bismuth, argentite, pyrite, and pyrrhotite.

Brazil Lake lithium pegmatite

The Wedgeport-East Kemptville domain hosts a distinctive lithium-bearing pegmatite which cuts Silurian White Rock Formation quartzite 15 km northeast of Yarmouth (Taylor, 1967). The pegmatite consists of quartz, feldspar (cleavelandite), and spodumene, with accessory hornblende, apatite, beryl, columbite-tantalite, cassiterite, and holmquistite (Hutchinson, 1982). The pegmatite is poorly exposed and is not known to contain commercial quantities of lithium.

New Ross-Vaughan Domain

Introduction

The New Ross-Vaughan complex, located approximately 75 km west of Halifax (Fig. 23) is a composite phase of the SMB containing a petrologically and chemically diverse suite of monzogranite intrusions which cut SMB granodiorite. The younger intrusive phases include monzogranite, monzogranite porphyry, leucomonzogranite, aplitic monzogranite, and pegmatite (Charest et al., 1985). Three main types of metallic mineralization are known: greisen, pegmatite, and fissure veins and shear zones (O'Reilly et al., 1982; Logothetis, 1985; Table 8). The Millet Brook uranium deposit is the largest of these occurrences.

Greisen

The polymetallic quartz-sericite and quartz-sericite-pyrite-fluorite greisens form selvages bordering quartz-sulphide veins or irregular zones of pervasive alteration (O'Reilly et al., 1982; Logothetis, 1985). The occurrences contain varied amounts of Sn, W, Mo, Cu, and Zn and, to a lesser extent, U, Be, As, Nb, and Ta. Two larger greisen occurrences (Long Lake and Turner Tin; Fig. 23, Table 8) are associated with apogranites (O'Reilly et al., 1982; p. 84) and are the result of mineralization processes similar to but much less intense than those that occurred at the East Kemptville deposit.

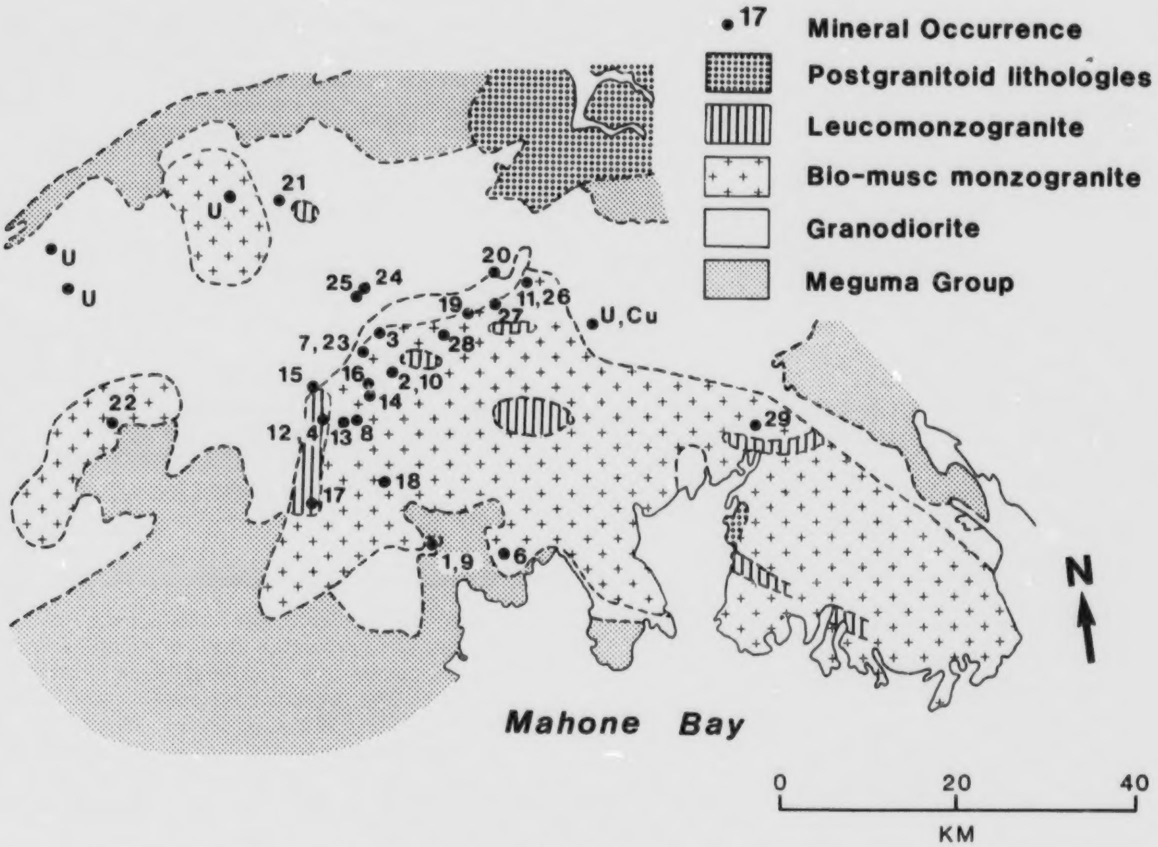

Figure 23. Geology and mineral occurrences of the New Ross-Vaughan complex (modified after Logothetis, 1985; mineral occurrence numbers are keyed to Table 8).

Pegmatite

The pegmatites of the New Ross-Vaughan complex are small lensoid bodies with maximum dimensions in the tens of metres. They are spatially associated with the later, more evolved phases of the SMB, commonly the leucomonzonite (Charest, 1976). Where a spatial association with leucomonzonite is less obvious, the pegmatites contain leucogranitic or aplitic phases, which are probably related to the same period of intrusive activity. The pegmatites probably formed during a single period from late, residual leucomonzonite-derived volatiles.

Metallic and associated mineralization in the pegmatites is similar to that found in greisen deposits. Two types of pegmatites are present: 1) Mo-bearing pegmatites; and 2) Sn-W-F-bearing pegmatites with accessory Li, U, Ta, Nb, and Cu.

Vein and shear zone mineralization

Late, hydrothermally derived mineralization occurs in veins, shears, joints, and fractures within intrusive and, less commonly, Meguma metasedimentary rocks. Several mineral assemblages are common. Quartz-fluorite and quartz-calcite-molybdenite veins likely formed from late magmatic fluids and are probably related to the period of pegmatite intrusion (Logothetis, 1985). Uranium-phosphate-bearing shear zones cut granodiorite at the Millet Brook occurrence (described below). Manganese veins also cut sheared, hematite-stained, and argillically altered granodiorite. These contain pods and veinlets of massive pyrolusite, manganite, and psilomelane which are attributed to either meteoric or hypogene hydrothermal origin by various authors (O'Reilly et al., 1982; Logothetis, 1985).

Millet Brook uranium deposits

The Millet Brook uranium deposits (Fig. 24) occur within the biotite granodiorite phase of the SMB. They were discovered in the late 1970s following airborne radiometric surveys and ground scintillometer prospecting follow-up. The deposits are about 3 km north of the two-mica monzogranites of the New Ross-Vaughan complex (Charest et al., 1985) and are separated from the complex by a large roof pendant of Meguma metasedimentary rocks. The deposits consist of a number of small individual fracture zones. Three main zones of steeply dipping, pitchblende-bearing fractures were identified within an area 8 by 12 km² (Robertson and Duncan, 1982).

Table 8. Metallic mineral occurrences and prospects of the New Ross-Vaughan complex and from elsewhere in the SMB. The occurrences are listed under the headings of the principal types of mineralization discussed in the text. The number associated with each occurrence may be used to locate its position on Figure 23. Table modified after Logothetis, 1985).

Polymetallic tin mineralization:		
1. Long Lake	W,Sn,Zn,Cu,Mo, Ag,(Rb,Cs,Li,REE)	greisens (irregular pods and veins), greisenized leucomonzogranite, and Mo-bearing pegmatite
2. Walker Moly	Mo,W,Sn,Cu,Bi,Sb, Zn,U	massive greisens, greisenized leucomonzogranite host, and Mo-bearing pegmatite
3. Wallaback Lake	Sn,Zn,Li	irregular greisen patches, greisenized leucomonzogranite, and pegmatite
4. Keddy	Ta,Nb,Mo	pervasively greisenized leucomonzogranite, and Mobearing pegmatite.
5. East Kemptville*	Sn,Cu,Zn	greisenized leucomonzogranite and greisen-bordered quartz veins
6. QSPF	Fe,Cu,fluorite	greisen-bordered quartz veins in biotite-muscovite monzogranite
7. Turner Tin	Sn,Zn,Cu,Fe,Bi	greisen-bordered quartz veins in biotite-muscovite monzogranite, and associated elvan veins with greisenized borders
8. Lake Darling	Cu,(Mo)	Mo-bearing quartz-feldspar vein with greisen selvages in biotite-muscovite monzogranite
Molybdenum:		
9. Long Lake	Mo	molybdenite-rich metasomatic "pegmatite"
10. Walker Moly	Mo	molybdenite-rich pegmatite
11. Swinimer occurrence	Mo	quartz veins in Meguma Group
12. Keddy	Mo	molybdenite-bearing pegmatite and leucomonzogranite
13. Lake Darling	Mo	molybdenite-bearing quartz vein
Pegmatite-hosted occurrences:		
14. Morley's Pegmatite	Sn,W,Li,F	pegmatite dykes and associated breccia (jasper breccia) in leucomonzogranite and monzogranite
15. Reeves Pegmatite	Sn,Li,F	pegmatite in leucomonzogranite
16. Mill Brook	F,Li	pegmatite dyke in biotite-muscovite monzogranite
17. Nevertell Lake	Sn,W	pegmatite dyke in leucomonzogranite
18. Seffernville pegmatite	Li	quartz and pegmatite dykes in monzogranite
Uranium:		
19. Vaughan Episyenites	U,Zn,(P)	mineralized episyenite pods or lenses in biotite-muscovite monzogranite developed next to fine grained (porphyritic) monzogranite dykes
20. Millet Brook	U	uraniferous shear/fracture zones in granodiorite
21. Gaspereau Lake	U	uraniferous shear/fracture zones in leucomonzogranite
22. East Dalhousie	U	autunite-bearing fractures and/or shear zones in altered biotite-muscovite monzogranite
23. Many occurrences (e.g. Turner Tin)	U	associated with greisen-hosted polymetallic tin mineralization
Manganese:		
24. Cain-Riddle Mine	Mn	manganiferous shear/fracture zones in granodiorite
25. Dean and Chapter Mine	Mn	manganiferous shear zone
Fluorite ± sulphide veins:		
26. Leminster	F	fluorite veins
27. Canoe Lake	F	fluorite veins
28. Lake Lewis	F	fluorite veins
29. Upper Tantallon	Zn,F	fluorite ± sphalerite veins

*The East Kemptville tin mine is located 70 km east southeast of the western margin of Figure 23.

Reserves are reported at 1.0 million pounds of contained U_3O_8 (Chatterjee et al., 1985c).

At Millet Brook the host rock is a massive to faintly foliated, medium to coarse grained, porphyritic biotite granodiorite that is typical of much of the SMB (Chatterjee et al., 1985c). Biotite occurs as aggregates that form a network texture around the lighter coloured silicate minerals. Phenocrysts of plagioclase and potassium feldspar as much as 4 cm across are common.

The Upper Salter Lake zone (Fig. 24a,b) is the largest of the mineralized zones discovered to date. Drilling has defined three parallel veins over a width of 90 m, for a combined strike length of 210 m and to a depth of 150 m. The deposit is open in all directions. Two additional zones, the C1 and C2, occur about 1.5 km east of the Upper Salter Lake deposit. These zones have strike lengths of 90 and 300 m, respectively, with uranium mineralization over widths as great as 8 m. All veins strike northeast and have subvertical dips.

Sooty pitchblende is the most important uranium mineral in the veins. Accessory coffinite, carnotite, and Pb-autunite are common. Within 50 m of the surface, the uranium is present as supergene metatorbernite and autunite. Gangue minerals include vein carbonate and minor pyrite and chalcopyrite (Robertson and Duncan, 1982), as well as sphalerite, proustite, quartz, phyllosilicates, and tourmaline (Chatterjee et al., 1985c). Hydrothermal alteration minerals in the host rocks adjacent to the veins include hematite, albite, and kaolin, and minor muscovite, chlorite, and quartz. Cataclastic textures are present in the host rocks immediately adjacent to the veins.

Westfield-Caledonia Domain

In the Westfield-Caledonia area (Fig. 25), K-feldspathized albite-bearing porphyry, albitized porphyry, and greisenized granitoids are associated with a granodiorite-monzogranite prominence of the SMB that intruded slate and greywacke of the Meguma Group (O'Reilly, 1985). The altered rocks locally host greisen zones, quartz veins, and quartz vein stockworks containing scheelite, cassiterite, molybdenite, arsenopyrite, and pyrite. The altered rocks also contain as much as 50 ppb Au, compared to a maximum of 15 ppb in unaltered granitoid rocks (O'Reilly, 1985). The Meguma Group slates south of the prominence contain several quartz veins with associated greisen envelopes and quartz vein stockworks. These veins contain scheelite-cassiterite mineralization with associated base metal sulphides, arsenopyrite, pyrite, marcasite, gold, and silver.

This occurrence is unique because of the presence of anomalous Au with Sn and a lack of Rb-U specialization of the host granitic rocks. O'Reilly (1985) attributed this to the early loss of a fluid phase from the granodioritic magma and subsequent metasomatism of crystallized granodiorite by the Rb-U-poor residual volatiles.

Digby-Gaspereau Domain

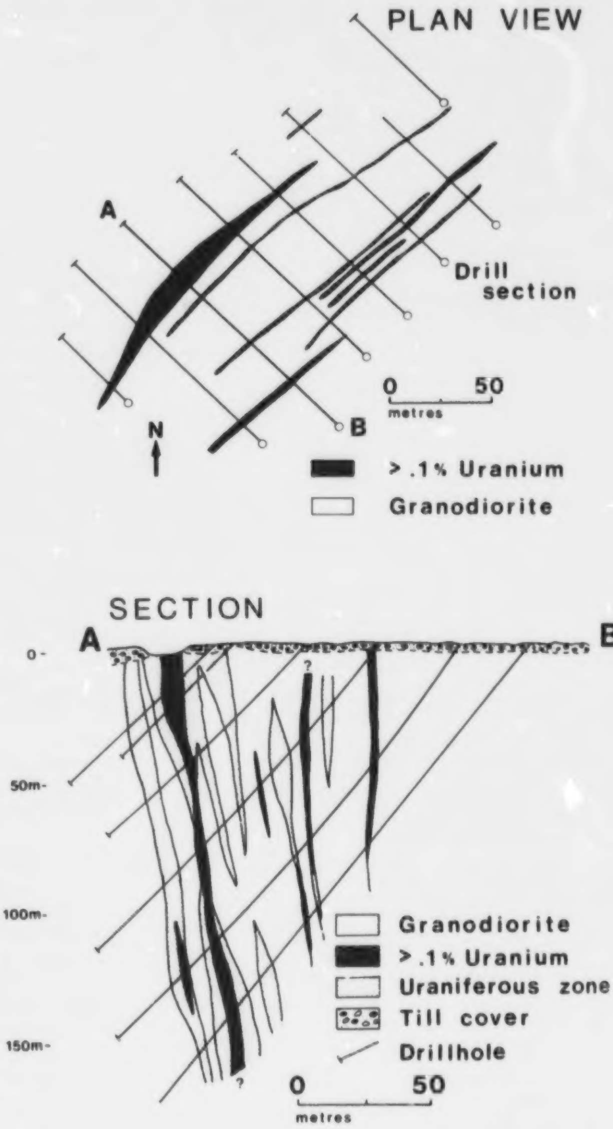

Figure 24. Geological plan and section of the Upper Salter Lake deposit, Millet Brook (modified after Robertson and Duncan, 1982).

The Digby-Gaspereau Domain contains a number of small uranium prospects characterized by a U-Cu (± Ag ± P) elemental association. These occurrences are similar to the Millet Brook deposits having formed as en echelon pods within shear and fracture zones in the SMB. The uranium mineralization is dominated by pitchblende and accessory amounts of torbernite and autunite. Associated sulphides include pyrite, chalcopyrite, bornite, covellite, galena, chalcocite, sphalerite, and wolframite. Alteration minerals include albite, muscovite, biotite, chlorite, orthoclase, carbonates, and tourmaline (Chatterjee, 1983b).

Shelburne Domain

Minor occurrences of beryl are associated with pegmatites and quartz veins in spatial association with the Port Mouton and Shelburne plutons (Taylor, 1967). Chatterjee (1983a) defined a mineralized domain based on these occurrences which is here referred to as the Shelburne Domain (Fig. 19).

Miscellaneous occurrences

Numerous small occurrences and geochemically anomalous areas are associated with granites other than the SMB (Fig. 19). Most have not been investigated in detail but are described in unpublished mineral exploration assessment file reports.

West Gore antimony-gold occurrence

Auriferous stibnite-quartz veins fill fissures and constitute the matrix of slate breccia within northwest-striking fracture zones that cut Halifax Formation slate (Fig. 26). The veins dip steeply and average 30 cm or less in thickness. However, one shoot with a maximum thickness of

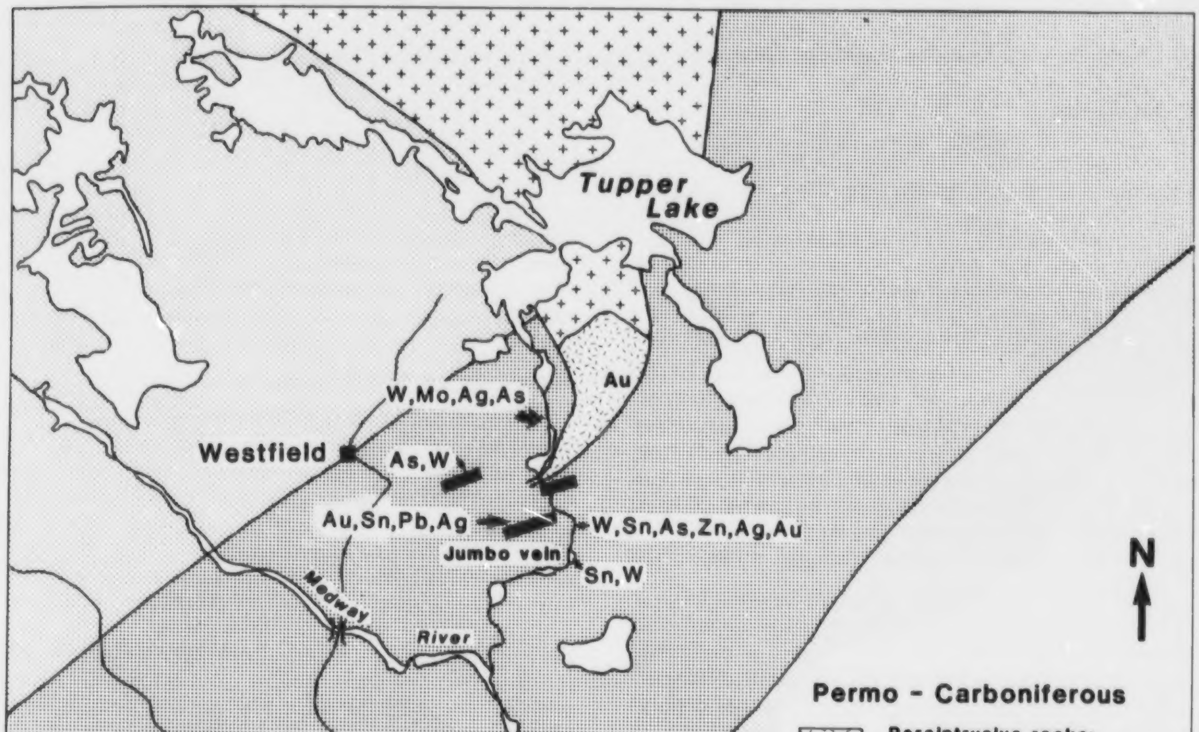
Tupper Lake
Au
W,Mo,Ag,As
Westfield
As,W
Au,Sn,Pb,Ag
Jumbo vein
W,Sn,As,Zn,Ag,Au
Sn,W
Medway
River
N
Caledonia
North Brookfield
composite albite-bearing granitoid dyke
Sn,W
quartz-albite-chlorite - pyrite porphyry
Area of gravity low and contact metamorphism
0 1 2 3
Kilometre
Permo - Carboniferous
Paraintrusive rocks: K - feldspathized, albitized and greisenized granite
Devonian
Biotite granodiorite - monzogranite
Cambro - Ordovician
Meguma Group
Halifax Formation: slate, minor quartzite and metawacke
Goldenville Formation: metawacke, quartzite and minor slate
Quartz vein and/or granitoid dyke

Figure 25. Geology of the Westfield-Caledonia area (modified after O'Reilly, 1985).

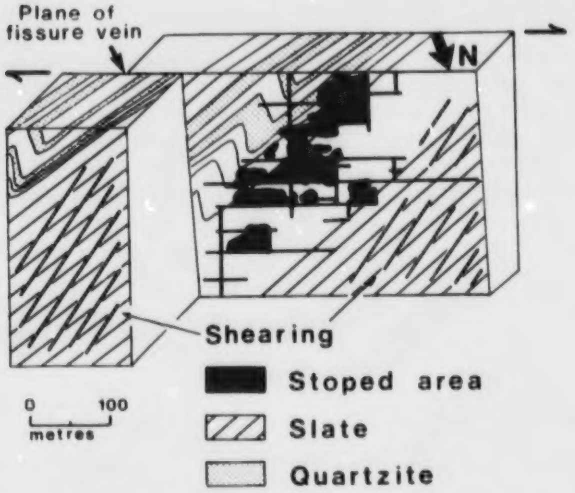

Figure 26. Longitudinal section of fissure vein at West Gore. Note the control of the mineralized ore shoot exerted by the fault plane intersection with a secondary anticline (modified after Douglas, 1940).

2 m has been recorded (Askwith, 1901). Antimony and gold grades are variable, but are generally high within the veins. Askwith (1901) reported values to 40 percent Sb and 10 oz/t Au from high-grade mining in the late 1800s. Sb concentrates shipped to England between 1914 and 1917 averaged 1.4 oz/t Au (Douglas, 1940).

These veins are similar in style and mineralogy to a larger antimony deposit at Lake George, New Brunswick (Morrissey and Ruitenberg, 1980; Scratch et al., 1984; Seal et al., 1988). Scratch et al. (1984) attributed the genesis of the New Brunswick deposit to either: 1) deposition from a late stage magmatic fluid originating in a satellitic intrusion to the Devonian Pokiok batholith; or 2) deposition from convectively driven meteoric fluids. Lead isotope analyses (R. Thorpe, pers. comm., 1988) show a strong similarity between West Gore galena and galena from the East Kemptville tin deposit, indicating a probable late magmatic source for the West Gore mineralization.

Liscomb area

The Liscomb complex (Fig. 19) consists of a suite of Devono-Carboniferous granitoid rocks which have intruded Meguma Group metasedimentary rocks and gabbroic and gneissic rocks of uncertain origin (Giles and Chatterjee, 1986). Two Pb-Zn-Ag +/− Sb occurrences are present near the western margin of the complex. Mineral exploration assessment files contain records of anomalous U, W, and Sn analyses associated with unclassified phases of the intrusion.

Eastern Meguma Terrane

Several mineral occurrences of possible igneous metasomatic origin are associated with small monzogranite plutons between Sherbrooke and Canso. At Lazy Head, disseminated scheelite is associated with pyrite, pyrrhotite, and chalcopyrite within spessartine-rich rocks of the GHT. The coticule-hosted mineralization is cut by quartz-microcline veinlets containing erratically disseminated scheelite, sphalerite, and pyrite (Shaw, 1983). The occurrence is close to the contact of a two-mica monzogranite, but Shaw (1983) concluded that the tungsten predates the granitic rocks and was redistributed by them.

Anomalous uranium has been recorded from lake sediments over or adjacent to some of the plutons in the eastern Meguma Terrane (Garrett and Keppie, 1982); however, no occurrences of uranium minerals have been located. Ford and Ballantyne (1983) measured high eU/eTh ratios over the Sangster Lake granite but were unable to confirm the presence of uranium in a limited surficial geochemical survey. Lithogeochemical analyses of eastern Meguma granites indicate that some phases of several intrusions have element distributions characteristic of increased differentiation with high background contents of elements such as Sn and Be (Ford and Ballantyne, 1983).

Musquodoboit pluton

MacDonald and Clarke (1985) attributed a moderate economic potential to the Musquodoboit monzogranite. The intrusion lacks late stage differentiates but is hydrothermally altered (greisenized and albitized), and the Ba/Rb, Li/K, and Li/Zn geochemical indicators are higher than average (MacDonald and Clarke, 1985). Lake sediment geochemical samples over parts of the Musquodoboit pluton are anomalous in uranium (Garrett and Keppie, 1982), tungsten, and gold (Rogers et al., 1985). High background uranium is common in lake sediments over the monzogranite and probably reflects the more highly evolved nature of the intrusion. Several small quartz-scheelite showings have been reported in the west-central part of the intrusion. A small hydrothermal Pb-Zn-Ag-Cu-bearing quartz vein, the Dunbrack occurrence, cuts cordierite-bearing monzogranite within the intrusion (MacMichail, 1975; Dickie, 1978).

Origin of granite-related mineralization

The widespread occurrence of concentrations of lithophile elements within or near the SMB and the presence of uranium-bearing veins within the older granodiorite phase of the batholith has logically lead to the assumption that the deposits are genetically related to late-magmatic volatiles that evolved during crystallization of the SMB. The detailed studies carried out within the last five years have, however, indicated that this model is oversimplified.

Lithophile element deposits

Extensive chemical work by Chatterjee et al. (1985a) and Richardson (1985a, 1988b) has indicated that hydrothermal alteration and mineralization in the Davis Lake pluton resulted from an apparently continuous process of chemical evolution beginning with magmatic differentiation and ending with evolution of a fluorine-rich volatile phase. Richardson (1985a) concluded that "In the

Davis Lake complex, the excellent correlation among the spatial location, degree of fractionation, intensity of albite-white mica alteration and greisen, and degree of mineralization suggests that a progressive process of interaction between ongoing fractionation, crystallization, fluid phase separation, collection and subsequent alteration played an important role in the genesis of the East Kemptville deposit". The recent documentation that most ages for mineralization and the associated intrusions are substantially younger than the SMB, the documentation of ages of alteration products synchronous with postulated movement on the Tobeatic Fault Zone (Richardson, 1988b), and the observation that much lithophile element mineralization is spatially associated with the transition zone between the Goldenville and Halifax formations all suggest a significantly greater element of complexity to the mineralizing system than is evident from a simple magmatic differentiation model involving a single SMB magma protolith.

Relationship of mineralization to intrusions younger than the SMB

Geochronological studies (Table 4) are beginning to unravel complex age relationships among various intrusive and alteration events in the Meguma Terrane. Ages on the intrusions associated with mineralization (Davis Lake, Wedgeport, etc.) indicate that the mineralizing plutons are as much as 40 to 50 Ma younger than rocks of the SMB and must therefore have evolved independently. The chemical character of the Davis Lake pluton is considered to be a function of primary magmatic composition and not due to evolution of the SMB magma. The distinctive siliceous fluorine- and metal-rich nature of the Davis Lake magma is considered to be similar to A-type granite magmas and to have formed by a second partial melting of the same parent material from which the SMB magma was derived (Richardson, 1988b).

Various types of isotopic studies provide information on the provenance of the SMB and Davis Lake magmas and contained metals and provide conflicting evidence on the possible contribution of Meguma rocks. Initial $^{87}Sr/^{86}Sr$ of 0.727 ± 0.004 for the Davis Lake pluton is the highest reported for an Appalachian granite (Richardson, 1988b). Such a high value precludes formation of the Davis Lake pluton entirely from Meguma Group rocks with Sr isotopic ratios similar to those found in rocks at surface (metawacke = 0.071282, meta-argillite = 0.71733; data of Clarke and Halliday, 1980 from Richardson, 1988b). However, anomalously high ϵ'_{Nd} (-5.2 to -1.4) compared to measured Meguma rocks (-11.2 to -8.7) was interpreted by Clarke et al. (1988) to indicate that the SMB magma is either a hybrid with both crustal and mantle components or was derived from deeper metasedimentary crust with younger model ages or higher Nd/Sm ratios than the upper crust. The maximum involvement of Meguma rocks satisfying Nd and Sr isotopic data for the SMB would occur if the "metasedimentary rocks of the Meguma Zone represent an inverted time sequence where the younger rocks of a former crustal segment were eroded first and buried beneath older materials eroded later from the same, or another, source..." (Clarke et al., 1988). This would permit an origin of the Davis Lake pluton, and other younger magmas, by a second remelting event (Richardson, 1988b) possibly involving a significant component of Meguma rocks as suggested by Wolfson (1983) in southwestern Nova Scotia.

Evidence from lead isotopic studies provides additional evidence for the origin of granite-hosted mineralization in a lower crust below the Meguma Group. The isotopic compositions of galena lead from granite-related deposits (Millet Brook, Dunbrack, East Kemptville, West Gore) compare favourably with published lead isotopic compositions of feldspars from late orogenic granites (325 to 400 Ma) in the U.S. Appalachians (Michard-Vitrac et al., 1981; Kish and Feiss, 1982; LeHuray, 1982) and are significantly more highly evolved than Meguma leads. The significance of this is twofold. First, it indicates that the Meguma rocks in general and the GHT (see GHT discussion below) are an unlikely source for the lead contained within the granite-related mineral deposits. Secondly, it indicates that the main granitic source was within a basement to the Meguma Group which is common to larger areas of the Appalachians, and that the Meguma allochthon therefore must either have been emplaced together with a basement isotopically similar to that elsewhere along the Appalachians or was emplaced over existing, in situ, Appalachian basement.

Elsewhere in the Meguma, Clarke and Chatterjee (1988) have shown that the Nd isotopic composition of intrusions in the Liscomb complex are intermediate between the mafic/felsic "basement" gneisses and Meguma rocks and concluded that the magma may have been derived from the gneisses and reflect substantial contamination by Meguma Group rocks. In the Canso area, the Larrys River and Halfway Cove plutons contain zircon populations that appear to have been inherited only from the Goldenville Formation suggesting magma derivation from it (Krogh and Keppie, 1988).

These data indicate that individual Meguma granite magmas may have been derived from either Meguma rocks, a lower crust, or combinations of the two. Mineralized plutons such as the Davis Lake may have contained larger volumes of magma derived from lower crustal materials than elsewhere.

Relationship to the Tobeatic Fault Zone

Giles (1985) proposed the existence of the Tobeatic Fault Zone traversing the length of southern Nova Scotia (Fig. 19). Post-Visean sinistral movement on the fault, during the period after 330 Ma ago, is estimated at 110 km and has displaced portions of the SMB and younger Carboniferous sedimentary sequences. Latest movement on the fault may have been pre-Triassic based on concordance of paleomagnetic declinations determined on Triassic rocks north and south of the fault. The proposed fault provides a significant new aspect to geological reconstructions in southern Nova Scotia for two reasons. First, the proposed age of major movement on the fault (post-Visean) coincides with the spectrum of ages on the younger plutons which are spatially associated with mineralization, and in some cases with the age of sericite alteration associated with mineralization (Reynolds et al., 1981; Zentilli and Reynolds, 1985; Reynolds et al., 1987). Secondly, the Wedgeport-East Kemptville, Westfield-Caledonia, and New Ross-Vaughan metallogenic domains lie on or near the trace of the proposed fault and parallel to it, implying a genetic relationship to processes associated with the faulting. Giles (1985) suggested that frictional heating along the fault may have been responsible for magma generation and mineralization as proposed by Strong and Hanmer (1981) for granites in Brittany. Sibson (1979) has shown that frictional heating along faults is generally insufficient to generate large volumes of magma.

These data do, nevertheless, indicate an interdependence of intrusion, faulting, and mineralization which Richardson (1988b) attributed to the creation of pull-apart crustal structures by regional dextral shear during the Maritime Disturbance (320 to 300 Ma). The origin of the Davis Lake and other late granites by a second partial melting event is compatible with this model.

Spatial association of mineralization with the Goldenville-Halifax Formation Transition Zone

A commonly overlooked feature of the granite-related mineralization in the Meguma Terrane is its persistent location in or adjacent to the Goldenville-Halifax Transition Zone. The GHT contains a Mn-rich calcareous argillite horizon that is enriched in a variety of metals throughout much of the Meguma Terrane (Binney et al., 1983; Zentilli et al., 1985, 1986; Binney et al., 1986). The Wedgeport-East Kemptville domain parallels and includes the GHT. The East Kemptville deposit lies only 900 m southeast of the GHT and several smaller showings, including the Dominique occurrence near Yarmouth (Wolfson, 1983), and the Pearl Lake, Gardiners Meadow, Duck Pond, and East Branch occurrences near East Kemptville (Richardson, 1988b; Fig. 1-1) are within rocks of the GHT. The altered intrusive rocks and their associated mineralization in the Westfield-Caledonia domain cut the GHT (O'Reilly, 1985; Fig. 12.1 and 12.2) and a large number of occurrences in the New Ross-Vaughan domain and the Long Lake greisen occur on the projections of the GHT through the SMB. In the eastern Meguma Terrane the coincidence is less evident, but a base metal occurrence on the western side of the Liscomb complex and a tungsten occurrence at Canso occur in the GHT near granite. This repetitive geological association may indicate at least a partial metal source for some of the granite-related mineral deposits within the GHT that would either require a significant component of Meguma involvement in magma generation, as discussed above, or extensive volatile transfer between the late granitic magmas and the GHT.

Uranium deposits

The Millet Brook uranium deposit is similar in character and probable origin to known granite-hosted intrabatholithic and peribatholithic uranium veins of the Bohemian, Central, Amorician, and Iberian massifs of Europe (Robertson and Duncan, 1982). These deposits are thought to be products of late stage magmatic processes. At Millet Brook, the host granodiorite is an unlikely source of uranium because the uranium content resides in early refractory minerals. Chatterjee et al. (1982, 1985c) related the origin of the veins to late stage magmatic fluids derived from a concealed two-mica leucomonzogranite beneath the deposit but similar in character to the Lewis Lake pluton, which is 10 km southeast of the Millet Brook deposit. Unaltered phases of the Lewis Lake pluton average about 10 ppm U and about 25 percent of that is present in nonrefractory minerals (such as biotite). In portions of the intrusion that have been affected by late, hydrothermal autometasomatism by carbonate-rich fluids, the uranium content averages approximately 70 percent of that in unaltered leucomonzogranite. Chatterjee et al. (1985c) proposed that the uranium was mobilized from a uraniferous leucomonzogranite as carbonate complexes and transported along sheared zones in the enclosing granodiorite. They attributed deposition to conditions favorable for exsolution of CO_2 from the fluid and for wall-rock reaction, in accord with mechanisms proposed by Cuney (1978) and Leroy (1978). If formation of the Millet Brook deposit is related to late deuteric phases of the leucomonzogranite intrusions which are recognized as the latest phases of the SMB and were emplaced at about 361 ± 1 Ma, then uranium occurrences may represent the only mineralization related to the main intrusive phases of the SMB.

PART IV: REGIONAL METALLOGENIC CORRELATION

The data and interpretations presented here document a specialized sedimentary regime during the Cambro-Ordovician Period which resulted in the local deposition of metal-rich, carbonaceous shale of the Goldenville Formation in basins and laterally extensive sedimentary rocks, rich in manganese and locally base metals, at the transition to the overlying Halifax Formation. Vein gold-arsenopyrite concentrations in the Goldenville Formation are the result of fluid flow induced by compaction and regional stress, probably associated with the transport and docking of the Meguma Terrane on the outboard side of the Avalon platform rocks along the Cobequid-Chedabucto Fault (Keppie, 1985). The time span involved may have extended from the onset of metamorphism circa 400 Ma ago to the Hercynian Orogeny circa 300 Ma ago. Granophile element deposits were formed in association with hydrothermal processes following the intrusion of the SMB and during emplacement of younger satellitic intrusions.

A brief summary of the regional occurrence of related deposits is presented here in order to provide the reader with a wider context for understanding the Meguma Group deposits and occurrences.

During Meguma sedimentation, geological processes were active within and beyond the Appalachian orogen which resulted in the formation of mineralization similar to that discussed previously in this paper. Manganese coticules and related tourmalinites are widespread throughout the Appalachians of northeastern North America and Caledonides of northwestern Europe, i.e. Cape Cod to Norway (Kennan and Kennedy, 1983). In part, the coticules are associated with belts of volcanic rocks, which are in turn associated with massive sulphides. Examples include the Cambro-Ordovician volcanic rocks and massive sulphides in the Eastern Townships of Quebec, Bathurst district of New Brunswick, and Avoca (Leinster) area, Ireland (Bruck et al., 1974, 1978). The Meguma coticules, however, are in a group that is not associated with a volcanic environment and which includes occurrences in the Gander Group of Newfoundland, in the Harlech Dome in Wales, and in the type locality for coticules in the Ardennes in Belgium (Kennan and Kennedy, 1983). Both groups of manganese-rich rock occur over a narrow stratigraphic range between late Middle Cambrian and Caradocian. The widespread geographic distribution and limited stratigraphic range of manganese-rich strata suggest the presence of specialized chemical conditions during the lowermost Paleozoic, and support the proposals of Berry and Wilde (1978) that anoxic conditions, which resulted in the concentration of manganese, were widespread during the Cambrian and Early Ordovician. As a result, the sulphur isotopic profile which is so distinctive of the GHT in the Meguma Terrane (Sangster et al., 1988, 1989) should be regionally extensive. Recently, Botsford and Sangster (in press) investigated a similar but less well developed sulphur isotope stratigraphy associated with iron and base metal enrichment in the Humber Group of western Newfoundland. The Meguma and Humber Group occurrences may represent geographic locations on opposite sides of Iapetus.

Most Cambro-Ordovician base/precious metal mineralization related to the regional coticules is associated with volcanic rocks and is absent in the Meguma Terrane. Rocks that are lithologically similar to Meguma Group rocks and that are of Cambro-Ordovician age host gold mineralization within and outside the Appalachian-Caledonian orogen. Flysch-hosted gold occurrences are known at Clontibret, Ireland and throughout the Ordovician of the Southern Uplands zone of Scotland (Steed and Morris, 1986) though the deposits are considered to be Devonian in age. Lower Paleozoic flysch-hosted gold occurrences are known in slate near McAdam in southwestern New Brunswick (Fyffe, 1988) and in the Davisville Group rocks in the Gander area of Newfoundland.

Beyond the Appalachian-Caledonian orogen, important deposits occur in rocks of similar age. A major sedimentary exhalative Zn-Pb-Ag deposit occurs at El Aguilar in the northwestern Argentine Andes. The stratigraphic setting of the deposit is comparable to the Eastville occurrence with the manganese-rich (bustamite, rhodochrosite) ore zones (A.L. Sangster, unpublished data) occurring in the transition between the lower Aguilar quartzite and upper Acoite slate of Cambro-Ordovician age (Gemmell and Zantrop, 1987). Sulphur (+10.8 to +26.5 per mil) and lead isotopes ($Pb^{206}/Pb^{204} = 18.04$; $Pb^{207}/Pb^{204} = 15.64$) (Gemmell et al., 1988) are similar to those for the Eastville occurrence reported above. Arsenical gold mineralization occurs in pre-Caradocian flysch in the Spanish Pyrenees (Ayora and Casas, 1986) and in Cambro-Ordovician flysch in the Victoria goldfields, Australia (McAndrew, 1965; Singleton, 1965; Sandiford and Keays, 1986) where sedimentary pyrite in the host rocks to the gold mineralization contains anomalously heavy $\delta^{34}S$ as observed in the Goldenville Formation (R.R. Keays, pers. comm., 1989). Both groups of occurrences bear substantial similarity to Meguma vein gold deposits though different genetic systematics may apply in each case.

Granophile element deposits are widespread within the Canadian Appalachians, associated with the extensive Devono-Carboniferous plutonism. Detailed information on many smaller occurrences can be obtained in the assessment files of the Provincial Departments of Mines.

The Mount Pleasant deposit in New Brunswick, located on the northeastern margin of the St. George Batholith, is the largest known deposit other than East Kemptville. It contains complex W-Bi-Mo-As-F and Sn-Zn-Pb-Cu porphyry, breccia, replacement, and vein-hosted mineralization related to various granitoid phases of a subvolcanic (caldera) complex (Kooiman et al., 1986; Sinclair et al., 1988) which has been dated at about 336 Ma (Kooiman et al., 1986). Other eastern Canadian deposits of lithophile elements related to similar, but possibly deeper level intrusions include:
1) Lake George, New Brunswick where Sb-quartz veins and associated high level W-Au-Mo breccias and skarns (Seal et al., 1988) adjacent to the southern margin of the Pokiok batholith cut both Silurian metasedimentary rocks and rocks of a genetically related granite cupola. Age data suggest the cupola granitoid rocks are Silurian and thus conflict with an apparent Early Devonian age for the adjacent Pokiok batholith with which the cupola is considered to be associated (McCutcheon et al., 1981; Procyshyn and Morrissy, 1989);
2) deposits at Sisson Brook and Burnt Hill, New Brunswick, which consist of a variety of W-Mo-, W-Cu-, W-Zn-, and Mo-W-bearing veins and vein breccias related to Late Silurian to Middle Devonian granitoid intrusions into a Cambro-Ordovician volcano-sedimentary sequence (Ruitenberg and McCutcheon, 1985; Gardiner, 1989);
3) deposits at Grey River, Newfoundland which consist of multiply injected quartz lodes and greisens containing a variety of mineral suites containing Mo-W-Ag-Pb-Zn-F-Ba (Higgins, 1985). The deposits are associated with a Devonian megacrystic granite which intrudes gneissic metasedimentary rocks of probable Early Ordovician age.

Northeastern North America is part of a larger geological region that encompasses western Europe and includes major deposits that add to the variety of granophile element deposits that are of similar age and geology to those in the Meguma. Significant uranium occurrences of the type described at Millet Brook, Nova Scotia are unknown elsewhere in eastern Canada but are common in parts of Europe. Best known of these are the uranium vein deposits of the Massif Central, France where large numbers of uranium-bearing veins are associated with Hercynian (~350 Ma) peraluminous granitic intrusions (Nash et al., 1981).

Tin and tungsten mineralization is widespread in western and central Europe with major concentrations associated with Hercynian granites at Cornwall in southwestern England (Dines, 1956), the Erzgebirge in Czechoslovakia and East Germany (Taylor, 1979), and at Panasqueira in Portugal (Kelly and Rye, 1979). Both the Erzgebirge and Portugese deposits are associated with intrusions that cut latest Precambrian to Cambrian metasedimentary rocks. Ages for mineralizing events in the European deposits are generally in the range measured for deposits in the Meguma Terrane described above, i.e. Cornwall — 282 Ma; Erzgebirge — 360 to 310 Ma (quoted in Taylor, 1979); and Panasqueira — 290 to 296 Ma (Ar-Ar)(Snee et al., 1988).

ACKNOWLEDGMENTS

The author is indebted to his colleagues at the Geological Survey of Canada and Nova Scotia Department of Mines for their interest and constructive comments, during the preparation of this manuscript. In particular, Mariette and Jack Henderson, John Kerswill, Howard Poulsen, Ralph Thorpe, Dave Sinclair, and Jim Franklin of the G.S.C. discussed various aspects of Nova Scotia geology with the author and each reviewed all or part of this manuscript. Discussions with Paul Smith and Dan Kontak of the Nova Scotia Department of Mines and Energy and Paul Williams and Charlotte Hy of the University of New Brunswick served to enhance the author's appreciation of the scope of the problems involved in understanding Meguma vein genesis. The author also wishes to thank representatives of mining and mineral exploration companies in the area for open discussion of the geology of individual properties. In particular the author thanks Dennis Forgeron and Alister MacIntyre of Coxheath Gold Holdings Ltd. and Dave Duncan, Jim Fortin, Ken Adams, and Mike Cullen of Seabright Resources Inc. Others, particularly Milton Graves of Cuesta Research Ltd., Marcos Zentilli of Dalhousie University, and Craig Miller formerly of the Nova Scotia Department of Mines and Energy, freely shared their long experience in the Nova Scotia gold fields. The author is grateful to Jean Richardson of McMaster University for access to much of her unpublished information on the East Kemptville deposit, including illustrations which are reproduced here. An early version of the manuscript benefitted greatly from her knowledge of the East Kemptville deposit and Davis Lake pluton. A.K. Chatterjee of the Nova Scotia Department of Mines and Energy shared his substantial knowledge of the granophile deposits and Don Pollock, Dave Duncan, and Jamie Robertson discussed aspects of the Millet Brook deposits. Various editorial and figure preparation tasks were efficiently executed by Bob Bretzlaff and Ross Knight. The author is solely responsible for the content of this manuscript.

REFERENCES

Allan, B.D. and Clarke, D.B.
1981: Occurrence and origin of garnets in the South Mountain Batholith, Nova Scotia; Canadian Mineralogist, v. 19, p. 19-24.

Askwith, W.R.
1901: The West Gore antimony deposits; Transactions of the Mining Society of Nova Scotia, v. 6, p. 80-86.

Ayora, C. and Casas, J.M.
1986: Strata-bound As-Au mineralization in pre-Caradocian rocks from the Vall de Ribes, eastern Pyrenees, Spain; Mineralium Deposita, v. 21, p. 278-287.

Bell, L.V.
1948: Caribou mine; *in* Structural Geology of Canadian Ore Deposits, Canadian Institute of Mining and Metallurgy, Jubilee Volume, p. 927-936.

Berry, W.B.N. and Wilde, P.
1978: Progressive ventilation of the oceans — an explanation for the distribution of the lower Paleozoic black shales; American Journal of Science, v. 278, p. 257-275.

Binney, P., Sangster, A.L., and Zentilli, M.
1983: A lead-zinc deposit in metasediments of the Meguma group, Eastville, Colchester County, Nova Scotia (abstract); Symposium on Stratabound Sulfides of the Appalachian-Caledonian Orogen, Ottawa, September 16-17, International Geological Correlation Programme, Project No. 60, CCSS, Program and Abstracts, p. 8.

Binney, W.P., Jenner, K.A., Sangster, A.L., and Zentilli, M.
1986: A stratabound lead-zinc deposit in Meguma Group metasediments at Eastville, Nova Scotia; *in* Contributions to the Geology of the Meguma Terrane, Nova Scotia, Maritime Sediments and Atlantic Geology, v. 22, p. 65-88.

Bishop, D.G. and Wright, J.D.
1974: Geology and trace element studies of manganese occurrences in Nova Scotia; Nova Scotia Department of Mines, Economic Geology Series 74-1, 255 p.

Botsford, J.W. and Sangster, D.F.
in press: Metal precipitation related to Lower Ordovician oceanic changes: geochemical evidence from deep-water sedimentary sequences in western Newfoundland; *in* Mechanics of Metal Concentration in Sedimentary Basins, International Association of Sedimentologists, Special Publication.

Boyle, R.W.
1966: Origin of gold and silver deposits of the Meguma Series, Nova Scotia; Geological Association of Canada/Mineralogical Association of Canada, Program, Annual Meeting.
1979: The geochemistry of gold and its deposits; Geological Survey of Canada, Bulletin 280, 584 p.
1986: Gold deposits in turbidite sequences: their geology, geochemistry, and history of the theories of their origin; *in* Turbidite-Hosted Gold Deposits, edited by J.D. Keppie, R.W. Boyle, and S.J. Haynes, Geological Association of Canada, Special Paper 32, p. 1-14.

Brooks, R.R., Chatterjee, A.K., Smith, P.K., Ryan, D.E., and Zhang, H.P.
1982: The distribution of gold in rocks and minerals of the Meguma Group of Nova Scotia, Canada; Chemical Geology, v. 35, p. 87-95.

Bruck, P.M., Gardiner, P.R.R., Max, M.D., and Stillman, C.J.
1978: Field guide to the Caledonian and pre-Caledonian rocks of south-east Ireland; The Geological Survey of Ireland, Guide Series No. 2, 87 p.

Bruck, P.M., Potter, T.L., and Downie, C.
1974: The Lower Paleozoic stratigraphy of the northern part of the Leinster Massif; Proceedings of the Royal Irish Academy, v. 74, sect. B, p. 75-84.

Brunton, S. Sir
1928: Some observations on a so-called interbedded vein at Tangier, N.S.; Mining Society of Nova Scotia-Annual Meeting, p. 784-803.

Campbell, J.S.
1863: Nova Scotia gold fields; a report to the Honourable Joseph Howe, Provincial Secretary, Halifax, 12 p.

Campbell, J.S. and Poole, H.
1862: Report on the goldfields; a report to the Commissioner of the Crown Lands, Halifax, 36 p.

Charest, M.H.

1976: Petrology, geochemistry and mineralization of the New Ross area, Lunenburg County, Nova Scotia; M.Sc. thesis, Dalhousie University, Halifax, Nova Scotia.

Charest, M.H., Farley, E.J., and Clarke, D.B.

1985: The northwestern part of the New Ross-Vaughan complex: petrology, geochemistry and mineral deposits; *in* Guide to the Granites and Mineral Deposits of Southwestern Nova Scotia, edited by A.K. Chatterjee and D.B. Clarke, Nova Scotia Department of Mines and Energy, Paper 85-3, preprint, p. 29-40.

Chatterjee, A.K.

1983a: Metallogenic map of the Province of Nova Scotia; Nova Scotia Department of Mines and Energy, Halifax.

1983b: Mineral deposit studies: contrasting granophile (Sn:W:Mo:Cu:U) deposits of Nova Scotia; *in* Mines and Minerals Branch Report of Activities 1982, Nova Scotia Department of Mines and Energy, Report 83-1, p. 49-51.

Chatterjee, A.K. and Strong, D.F.

1985: Geochemical characteristics of the polymetallic tin domain, southwestern Nova Scotia, Canada; *in* Granite-Related Mineral Deposits, CIM Geology Division, Extended Abstracts Volume, Granite-Related Mineral Deposits Symposium, Halifax, p. 41-52.

Chatterjee, A.K., Robertson, J., and Pollock, D.

1982: A summary of the petrometallogenesis of the uranium mineralization at Millet Brook, South Mountain Batholith, Nova Scotia; *in* Mines and Minerals Branch Report of Activities 1981, Nova Scotia Department of Mines and Energy, Report 82-1, p. 57-66.

Chatterjee, A.K., Strong, D.F., and Muecke, G.K.

1983: A multivariate approach to geochemical distinction between tin-specialized granites of southern Nova Scotia; Canadian Journal of Earth Sciences, v. 20, p. 420-430.

Chatterjee, A.K., Strong, D.F., and Clarke, D.B.

1985a: Petrology of the polymetallic quartz-topaz greisen at East Kemptville; *in* Guide to the Granites and Mineral Deposits of Southwestern Nova Scotia, edited by A.K. Chatterjee and D.B. Clarke, Nova Scotia Department of Mines and Energy, Paper 85-3, preprint, p. 149-196.

Chatterjee, A.K., Strong, D.F., Clarke, D.B., and Keppie, J.D.

1985b: Geology and geochemistry of the Carboniferous Wedgeport pluton hosting Sn-W mineralization; *in* Guide to the Granites and Mineral Deposits of Southwestern Nova Scotia, edited by A.K. Chatterjee and D.B. Clarke, Nova Scotia Department of Mines and Energy, Paper 85-3, preprint, p. 201-216.

Chatterjee, A.K., Strong, D.F., Clarke, D.B., Robertson, J., Pollock, D., and Muecke, G.K.

1985c: Geochemistry of the granodiorite hosting uranium mineralization at Millet Brook; *in* Guide to the Granites and Mineral Deposits of Southwestern Nova Scotia, edited by A.K. Chatterjee and D.B. Clarke, Nova Scotia Department of Mines and Energy, Paper 85-3, preprint, p. 63-114.

Clarke, D.B. and Chatterjee, A.K.

1988: Meguma Zone basement I: Sr-Nd isotopic study of the Liscomb complex and the origin of peraluminous granites of the Meguma Zone; Geological Association of Canada/Mineralogical Association of Canada, Program with Abstracts, v. 13, p. A21.

Clarke, D.B. and Halliday, A.N.

1980: Strontium isotope geology of the South Mountain Batholith; Geochimica et Cosmochimica Acta, v. 44, no. 8, p. 1045-1058.

Clarke, D.B., Barr, S.M., and Donohoe, H.V.

1980: Granitoid and other plutonic rocks of Nova Scotia; *in* Proceedings: The Caledonides in the U.S.A., edited by D.R. Wones, I.G.C.P. Project 27: Caledonide Orogen, Department of Geological Science, Virginia Polytechnic Institute and State University, Memoir no. 2, p. 107-116.

Clarke, D.B., Halliday, A.N., and Hamilton, P.J.

1988: Neodymium and strontium isotopic constraints on the origin of the peraluminous granitoids of the South Mountain Batholith, Nova Scotia, Canada; Chemical Geology (Isotope Geoscience Section), v. 73, p. 15-24.

Clarke, D.B., Muecke, G.K., and Chatterjee, A.K.

1985: The South Mountain Batholith: geology, petrology and geochemistry; *in* Guide to the Granites and Mineral Deposits of Southwestern Nova Scotia, edited by A.K. Chatterjee and D.B. Clarke, Nova Scotia Department of Mines and Energy, Paper 85-3, preprint, p. 1-14.

Clifford, P.M., Crocket, J.H., and Fueten, F.

1983: Distribution and localization of gold in Meguma Group rocks, Nova Scotia. Part 1: Structural effects and pressure solution-preliminary results; *in* Current Research, Part B, Geological Survey of Canada, Paper 83-1B, p. 279-283.

Cormier, R.F. and Smith, T.E.

1973: Radiometric ages of granitic rocks in southwestern Nova Scotia; Canadian Journal of Earth Sciences, v. 10, p. 1201-1210.

Cormier, R.F., Keppie, J.D., and Odom, A.L.

1988: U-Pb and Rb-Sr geochronology of the Wedgeport granitoid pluton, southwestern Nova Scotia; Canadian Journal of Earth Sciences, v. 25, p. 255-261.

Crocket, J.H.

1974: Gold; *in* Handbook of Geochemistry, edited by K.H. Wedepohl, chapter 79, sections B-O, v. 11/5, Springer-Verlag, Berlin.

Crocket, J.H., Clifford, P.M., Fueten, F., and Kabir, A.

1983: Distribution and localization of gold in Meguma Group rocks, Nova Scotia. Part 2: implications of background geochemistry and cleavage development — a preliminary report; *in* Current Research, Part B, Geological Survey of Canada, Paper 83-1B, p. 285-290.

Crocket, J.H., Fueten, F., Clifford, P.M., Kabir, A., and Henderson, J.R.

1986a: Distribution of gold and arsenic in turbidites at Harrigan Cove, Nova Scotia; *in* Turbidite-Hosted Gold Deposits, edited by J.D. Keppie, R.W. Boyle, and S.J. Haynes, Geological Association of Canada, Special Paper 32, p. 149-160.

Crocket, J.H., Fueten, F., Kabir, A., and Clifford, P.M.

1986b: Distribution and localization of gold in Meguma Group rocks, Nova Scotia; *in* Contributions to the Geology of the Meguma Terrane, Nova Scotia, Maritime Sediments and Atlantic Geology, v. 22, p. 15-34.

Cumming, L.M.

1985: A Halifax slate graptolite locality, Nova Scotia; *in* Current Research, Part A, Geological Survey of Canada, Paper 85-1A, p. 215-221.

Cuney, M.

1978: Geologic environment, mineralogy, and fluid inclusions of the Bois Noirs-Limouzat uranium vein, Forez, France; Economic Geology, v. 73, no. 8, p. 1567-1610.

Dickie, J.R.

1978: Geological, mineralogical and fluid inclusion studies at the Dunbrack lead-silver deposit, Musquodoboit Harbour, Halifax County, Nova Scotia; B.Sc. thesis, Dalhousie University, Halifax, Nova Scotia.

Dines, H.G.

1956: The metalliferous mining region of south-west England; Memoirs of the Geological Survey of Great Britain, London, 2 volumes.

Doe, B.R. and Zartman, R.E.

1979: Plumbotectonics, the Phanerozoic; *in* Geochemistry of Hydrothermal Ore Deposits, edited by H.L. Barnes, John Wiley and Sons, New York, p. 22-70.

Douglas, G.V.

1940: Antimony at West Gore; Nova Scotia Department of Mines, Annual Report on Mines, 1939, part 2, p. 37-49.

1948: Structure of the gold veins of Nova Scotia; *in* Structural Geology of Canadian Ore Deposits, Canadian Institute of Mining and Metallurgy, Jubilee Volume, p. 919-926.

Emmons, E.R.

1937: Gold Deposits of the World; McGraw-Hill, New York, 562 p.

Fairbairn, H.W., Hurley, P.M. and Pinson, W.H.

1964: Preliminary age study and initial $^{87}Sr/^{86}Sr$ of Nova Scotia granitic rocks by the Rb-Sr whole rock method; Geological Society of America Bulletin, v. 75, p. 253-258.

Fairbairn, H.W., Hurley, P.M., Pinson, W.H., and Cormier, R.F.

1960: Age of granitic rocks of Nova Scotia; Geological Society of America Bulletin, v. 71, p. 399-419.

Faribault, E.R.

1898: Map of the Oldham gold district; Geological Survey of Canada, Map 642.

1899: The gold measures of Nova Scotia and deep mining; Journal of the Canadian Mining Institute, v. 2, p. 119-129.

1901: Map of the Mount Uniacke gold district; Geological Survey of Canada, Map 709.

Farquhar, R.M. and Haynes, S.J.

1986: Lead isotope data for gold-bearing veins and their host metasedimentary rocks of the Goldenville Formation, eastern Nova Scotia; *in* Contributions to the Geology of the Meguma Terrane, Nova Scotia, Maritime Sediments and Atlantic Geology, v. 22, p. 89-100.

Fisher, B.E.

1984: A regional investigation of scheelite occurrences in the Meguma Group of Nova Scotia; B.Sc. thesis, Dalhousie University, Halifax, Nova Scotia, 210 p.

Force, E.R. and Cannon, W.F.

1988: Depositional model for shallow-marine manganese deposits around black shale basins; Economic Geology, v. 83, p. 99-117.

Ford, K.L. and Ballantyne, S.B.

1983: Uranium and thorium distribution patterns and lithogeochemistry of Devonian granites in the Chedabucto Bay area, Nova Scotia; *in* Current Research, Part A, Geological Survey of Canada, Paper 83-1A, p. 109-119.

Franks, S.G. and Forester, R.W.

1988: Relationships among secondary porosity, pore fluid chemistry, and carbon dioxide, Texas Gulf Coast; *in* Clastic Diagenesis, edited by D.A. McDonald and R.C. Surdham, American Association of Petroleum Geologists, Memoir 37, p. 63-79.

Fueten, F.

1985: Spaced cleavage development in the metagreywackes of the Goldenville Formation, Meguma Group, Nova Scotia; M.Sc. thesis, McMaster University, Hamilton, Ontario.

Fueten, F., Clifford, P.M., Pryer, L.L., Thompson, M.J., and Crocket, J.H.

1986: Formation of spaced cleavage and concurrent mass removal of SiO_2, Meguma Group metawackes, Goldenville, Nova Scotia; Maritime Sediments and Atlantic Geology, v. 22, p. 35-50.

Fyfe, W.S. and Henley, R.W.

1973: Some thoughts on chemical transport processes, with particular reference to gold; Minerals Science and Engineering, v. 5, p. 295-303.

Fyffe, L.R.

1988: Bedrock geology of the McAdam-St. Croix area; New Brunswick Department of Natural Resources and Energy, Thirteenth Annual Review of Activities, p. 70-75.

Fyson, W.K.

1966: Structures in the Lower Paleozoic Meguma Group, Nova Scotia; Geological Society of America Bulletin, v. 77, p. 931-943.

Gardiner, W.W.

1989: The Burnt Hill granites and related tungsten-molybdenum and tin deposits; *in* Mineral Deposits Associated with Siluro-Devonian Plutonism in New Brunswick-Gaspé Sector, Geological Association of Canada/Mineralogical Association of Canada, Field Trip Guidebook B5, p. 51-62.

Garrett, R.G. and Keppie, J.D.

1982: National geochemical reconnaissance, Meguma Terrane, southern mainland, Nova Scotia; Geological Survey of Canada, Open File Report 847, 7 p.

Gemmell, J.B. and Zantrop, H.

1987: Geology and mineral deposits of the Aguilar Mine, Jujuy, Argentina; Geological Society of America, Abstracts with Programs, v. 19, no. 7, p. 674.

Gemmell, J.B., Zantrop, H., Barbero, B.A., and Chamberlain, C.P.

1988: Genesis of the stratabound Aguilar deposits, Argentina: a sulphur, lead, carbon and oxygen isotope investigation; Geological Society of America, Abstracts with Program, v. 20, no. 7, p. A38.

Giles, P.S.

1985: A major post-Visean sinistral shear zone — new perspectives on Devonian and Carboniferous rocks of southern Nova Scotia; *in* Guide to the Granites and Mineral Deposits of Southwestern Nova Scotia, edited by A.K. Chatterjee and D.B. Clarke, Nova Scotia Department of Mines and Energy, Paper 85-3, preprint, p. 233-248.

Giles, P.S. and Chatterjee, A.K.

1986: Peraluminous granites of the Liscomb complex; *in* Tenth Annual Open House and Review of Activities, Program and Summaries, Nova Scotia Department of Mines and Energy, Information Series No. 12, p. 83-90.

1987: Peraluminous granites of the Liscomb complex; *in* Report of Activities 1986, Nova Scotia Department of Mines and Energy, Report 87-1, p. 95-98.

Gilpin, E.

1888: Notes on the Nova Scotia gold veins; Transactions of the Royal Society of Canada, v. 6, sect. 4, p. 63-70.

Graves, M.C.

1976: The formation of gold-bearing quartz veins in Nova Scotia; M.Sc. Thesis, Dalhousie University, Halifax, Nova Scotia, 166 p.

Graves, M.C. and Zentilli, M.

1982: A review of the geology of gold in Nova Scotia; *in* Geology of Canadian Gold Deposits, edited by R.W. Hodder and W. Petruk, Canadian Institute of Mining and Metallurgy, Special Volume 24, p. 233-242.

1988a: The lithochemistry of metal enriched coticules in the Goldenville-Halifax Transition Zone of the Meguma Group, Nova Scotia; *in* Current Research, Part A, Geological Survey of Canada, Paper 88-1A, p. 251-262.

1988b: Geochemical characterization of the Goldenville Formation-Halifax Formation Transition of the Meguma Group, Nova Scotia: data tables and sample location maps; Geological Survey of Canada, Open File Report 1829, 110 p.

Gross, G.A.

1967: Iron deposits in the Appalachian and Grenville regions of Canada; *in* Geology and Iron Deposits of Canada, Volume 2, Geological Survey of Canada, Economic Geology Report 22, 111 p.

Guilbert, J.M. and Park, C.F.

1986: Geology of Ore Deposits; W.H. Freeman, New York, 985 p.

Haynes, S.J.

1983: Typomorphism of turbidite-hosted auriferous quartz veins, southern Guysborough County; *in* Report of Activities 1982, Nova Scotia Department of Mines and Energy, Report 83-1, p. 183-224.

1986: Geology and geochemistry of turbidite-hosted gold deposits, greenschist facies, eastern Nova Scotia; *in* Turbidite-Hosted Gold Deposits, edited by J.D. Keppie, R.W. Boyle, and S.J. Haynes, Geological Association of Canada, Special Paper 32, p. 161-178.

1987: Classification of quartz veins in turbidite-hosted gold deposits, greenschist facies, eastern Nova Scotia; Canadian Institute of Mining and Metallurgy Bulletin, v. 80, no. 898, p. 37-51.

Haynes, S.J. and Smith, P.K.

1983: Gold potential of the Meguma Group: new concepts; Maritime Sediments and Atlantic Geology, v. 19, p. 96.

Haynes, S.J., Reilly, B.A., and Keilly, L.A.

1986: Structural setting of the Mile Lake gold prospect, Guysborough County, Nova Scotia; *in* Current Research, Part A, Geological Survey of Canada, Paper 86-1A, p. 141-150.

Henderson, J.R.

1983: Analysis of structure as a factor controlling gold mineralization in Nova Scotia; *in* Mines and Minerals Branch, Report of Activities 1982, Nova Scotia Department of Mines and Energy, Report 83-1, p. 265-282.

Henderson, J.R., Henderson, M.N., Mawer, C.K., Crocket, J.H., Clifford, P.M., and Fueten, F.

1986a: Timing and origin of auriferous quartz veins, Meguma Terrane, Nova Scotia; *in* Poster Volume, Gold '86; Geological Association of Canada, Mineral Deposits Division, p. 70-71.

Henderson, J.R., Wright, T.O., and Henderson, M.N.

1986b: A history of cleavage and folding: an example from the Goldenville Formation, Nova Scotia; Geological Society of America Bulletin, v. 97, p. 1354-1366.

Henderson, M.N. and Henderson, J.R.

1986: Constraints on the origin of gold in the Meguma zone, Ecum Secum area, Nova Scotia; *in* Contributions to the Geology of the Meguma Terrane, Nova Scotia, Maritime Sediments and Atlantic Geology, v. 22, p. 1-14.

Henley, R.W.

1973: Solubility of gold in hydrothermal chloride solutions; Chemical Geology, v. 11, p. 73-87.

Herman, H.

1914: Economic geology and mineral deposits of Victoria; Victoria (Australia) Geological Survey, Bulletin 34, 36 p.

Higgins, N.C.
1985: Wolframite deposition in a hydrothermal vein system: the Grey River tungsten prospect, Newfoundland, Canada; Economic Geology, v. 80, p. 1297-1327.

Hill, J.D.
1986a: Granitoid plutons of the Canso area, Nova Scotia; *in* Current Research, Part A, Geological Survey of Canada, Paper 86-1A, p. 185-192.
1986b: Geology of the Guysborough-Country Harbour area; *in* Tenth Annual Open House and Review of Activities, Program and Summaries, Nova Scotia Department of Mines and Energy, Information Series No. 12, p. 182-183.

Hind, H.Y.
1869: Notes on the structure of the Nova Scotia gold district; Transactions of the Nova Scotia Institute of National Science, v. 2, part. 3, p. 102-109.
1870: On two gneissoid series in Nova Scotia and New Brunswick, supposed to be the equivalents of the Huronian (Cambrian) and Laurentian; Quarterly Journal, Geological Society of London, v. 26, p. 468-479.
1872: Report on the Mt. Uniacke, Oldham, and Renfrew gold mining districts; Halifax, p. 136.

Hingston, R.W.
1985: The manganiferous slates of the Cambro-Ordovician Meguma Group at Lake Charlotte, Halifax County, Nova Scotia; B.Sc. thesis, Dalhousie University, Halifax, Nova Scotia, 67 p.

Holser, W.T., Schidlow, M., Mackenzie, F.T., and Maynard, J.B.
1988: Biogeochemical cycles of carbon and sulphur; *in* Chemical Cycles in the Evolution of the Earth, edited by C.B. Gregor, R.M. Garrels, F.T. Mackenzie, and J.B. Maynard, John Wylie and Sons, Toronto, p. 105-174.

Houseknecht, D.W.
1988: Intergranular pressure solution in four quartzose sandstones; Journal of Sedimentary Petrology, v. 58, p. 228-246.

Houseknecht, D.W. and Hathon, L.A.
1987: Petrographic constraints on models of intergranular pressure solution in quartzose sandstones; Applied Geochemistry, v. 2, p. 507-524.

Hunt, T.S.
1868: Report on the gold region of Nova Scotia; Geological Survey of Canada, 48 p.

Hutchinson, H.E.
1982: Geology, geochemistry and genesis of the Brazil Lake pegmatites, Yarmouth County, Nova Scotia; B.Sc. thesis, Dalhousie University, Halifax, Nova Scotia, 105 p.

Hy, C. and Williams, P.F.
1986: Meguma quartz veins, Tangier area; *in* Tenth Annual Open House and Review of Activities, Nova Scotia Department of Mines and Energy, Information Series No. 10, p. 202-205.

Jamieson, R.A.
1974: The contact of the South Mountain Batholith near Mount Uniacke, Nova Scotia; B.Sc. thesis, Dalhousie University, Halifax, Nova Scotia, 52 p.

Kelly, W.C. and Rye, R.O.
1979: Geologic, fluid inclusion, and stable isotope studies of the tin-tungsten deposits of Panasquiera, Portugal; Economic Geology, v. 74, p. 1721-1822.

Kennan, P.S. and Kennedy, M.J.
1983: Coticules — a key to correlation along the Appalachian- Caledonian orogen; *in* Regional Trends in the Geology of the Appalachian-Caledonian-Hercynian-Mauritanide Orogen, edited by P.E. Schenk, Nato ASI Series, Series C: Mathematical and Physical Sciences Volume 116, p. 355-361.

Keppie, J.D.
1985: Geology and tectonics of Nova Scotia; *in* Excursion 1 — Appalachian Geotraverse, edited by J.D. Keppie, K.L. Currie, J.B. Murphy, R.K. Pickerell, L.R. Fyffe, and P. St. Julian, Geological Association of Canada/Mineralogical Association of Canada, Fredericton 85, p. 181.

Keppie, J.D. and Dostal, J.
1980: Palaeozoic volcanic rocks of Nova Scotia; *in* International Geological Correlation Project 27, Virginia Polytechnical Institute and State University, Memoir 2, p. 249-256.

Kerswill, J.A.
1988: Lithogeochemical indicators of gold potential in the eastern Meguma Terrane of Nova Scotia; Nova Scotia Department of Mines and Energy, Report 88-3, p. 215-217.

Kish, S.A. and Feiss, P.G.
1982: Application of lead isotopic studies to massive sulphide vein deposits of the Carolina Slate Belt; Economic Geology, v. 77, p. 352-363.

Kontak, D.J.
1987: East Kemptville leucogranite: a possible mid-Carboniferous topaz granite; *in* Report of Activities 1986, Nova Scotia Department of Mines and Energy, Report 87-1, p. 81-94.

Kontak, D.J. and Smith, P.K.
1987a: Alteration haloes and their implications for gold mineralization in the Meguma zone, Nova Scotia; *in* Report of Activities 1987, Nova Scotia Department of Mines and Energy, Report 87-1, p. 65-74.
1987b: Meguma gold: the best kept secret in the Canadian mining industry; Prospectors and Developers Association of Canada, Annual Meeting, March, 1987, 14 p.
1988a: Meguma gold studies IV: chemistry of vein mineralogy; *in* Mines and Minerals Branch, Report of Activities 1987, Part B, Nova Scotia Department of Mines and Energy, Report 88-1, p. 85-101.
1988b: Meguma gold studies VI: integrated model for the genesis of Meguma-hosted lode gold deposits; *in* Mines and Minerals Branch, Report of Activities 1987, Part B, Nova Scotia Department of Mines and Energy, Report 88-1, p. 111-119.
1989: Fluid inclusion study of quartz vein polytypes in the Beaver Dam gold deposit, Meguma Terrane, Nova Scotia, Canada; Pan-American Conference on Research on Fluid Inclusions (Second Biennial; PACROFI 2), v. 2, p. 38.
in press: Sulphur isotopic composition of sulphides from the Beaver Dam and other Meguma Group-hosted gold deposits, Nova Scotia; Canadian Journal of Earth Sciences.

Kontak, D.J., MacDonald, D., and Smith, P.K.
1988a: Fluid inclusion study of the Beaver Dam gold deposit, Meguma Terrane, Nova Scotia; *in* Mines and Minerals Branch Report of Activities 1988, Part A, Nova Scotia Department of Mines and Energy, Report 88-3, p. 63-70.

Kontak, D.J., Smith, P.K., and Kerrich, R.
1988b: Meguma gold studies V: Carbon, strontium, oxygen, and sulphur isotopic compositions of vein materials: implications for source reservoirs and fluid:rock ratios attending vein formation; *in* Mines and Minerals Branch, Report of Activities 1987, Part B, Nova Scotia Department of Mines and Energy, Report 88-1, p. 101-110.

Kontak, D.J., Smith, P.K., Kerrich, R. and King, R.W.
1988c: Distribution of carbonate $\delta^{13}C$ and $^{87}Sr/^{86}Sr$ in gold deposits of the Meguma Terrane, Nova Scotia and Superior Province, Canada: implications for C and Sr source reservoirs; *in* Extended Abstracts Oral Programme, Bicentennial Gold '88, Geological Society of Australia, Abstract no. 22.

Kontak, D.J., Smith, P.K., and Reynolds, P.H.
1988d: Meguma gold studies III: timing of mineralization at the Beaver Dam gold deposit, eastern Meguma Terrane, Nova Scotia: implications for Meguma gold deposits; *in* Mines and Minerals Branch, Report of Activities 1987, Part B, Nova Scotia Department of Mines and Energy, Report 88-1, p. 77-83.

Kontak, D.J., Smith, P.K., Chatterjee, A.K., Giles, P.S., and Reynolds, P.H.
1989: $^{40}Ar/^{39}Ar$ geochemical studies in the Beaver Dam-Liscomb area, southern Nova Scotia: recognition of a major 370 Ma magmatic-metallogenic event; Geological Association of Canada/Mineralogical Association of Canada, Program with Abstracts, v. 14, p. A11.

Kooiman, G.J.A., McLeod, M.J., and Sinclair, W.D.
1986: Porphyry tungsten-molybdenum orebodies, polymetallic veins and replacement bodies, and tin-bearing greisen zones in the Fire Tower zone, Mount Pleasant, New Brunswick; Economic Geology, v. 81, p. 1386-1373.

Krogh, T.E. and Keppie, J.D.
1988: U-Pb ages of single zircon cores imply a pan African source for two Meguma granites; Geological Association of Canada/Mineralogical Association of Canada, Program with Abstracts, v. 13, p. A69.

Kubilius, W.P.

1983: Sulphur isotopic evidence for country rock contamination of granitoids in southwestern Nova Scotia; M.Sc. thesis, Pennsylvania State University, University Park, Pennsylvania, 108 p.

Kubilius, W.P. and Perry, J.M.

1989: Oxidation and arsenic loss during regional metamorphism of the Meguma Group, Nova Scotia; Geological Association of Canada, Program with Abstracts, v. 14, p. A2.

Lalou, C.

1983: Genesis of ferromanganese deposits: hydrothermal origin; *in* Hydrothermal Processes at Seafloor Spreading Centres, edited by P.A. Rona, K. Bostrom, L. Laubier, and K.L. Smith, Jr., NATO Conference Series, Plenum Press, New York, p. 503-534.

LeHuray, A.P.

1982: Lead isotopic patterns of galena in the Piedmont and Blue Ridge ore deposits, southern Appalachians; Economic Geology, v. 77, p. 335-351.

Leroy, J.

1978: The Margnac and Fanay uranium deposits of the La Crouzille District (Western Massif Central, France): geologic and fluid inclusion studies; Economic Geology, v. 73, no. 8, p. 1611-1634.

Leventhal, J.S.

1983: Organic carbon, sulphur, and iron relationships as an aid to understanding depositional environments and syngenetic metals in recent and ancient sediments; *in* Paleoclimate and Mineral Deposits, United States Geological Survey, Circular 822, p. 34-36.

Logothetis, J.

1985: Economic geology of the New Ross-Vaughan complex; *in* Guide to the Granites and Mineral Deposits of Southwestern Nova Scotia, edited by A.K. Chatterjee and D.B. Clarke, Nova Scotia Department of Mines and Energy, Paper 85-3, preprint, p. 41-62.

Longstaffe, F.J., Smith, T.E., and Muehlenbachs, K.

1980: Oxygen isotope evidence for the genesis of Upper Paleozoic granitoids from southwestern Nova Scotia; Canadian Journal of Earth Sciences, v. 17, p. 132-141.

MacDonald, M.A. and Clarke, D.B.

1985: The petrology, geochemistry and economic potential of the Musquodoboit batholith, Nova Scotia; Canadian Journal of Earth Sciences, v. 22, no. 11, p. 1633-1642.

MacInnis, I.N.

1986: Lithogeochemistry of the Goldenville-Halifax Transition (GHT) of the Meguma Group in the manganiferous zinc-lead deposit at Eastville, Nova Scotia; B.Sc. thesis, Dalhousie University, Halifax, Nova Scotia, 138 p.

MacMichail, T.F.

1975: The origin of the lead-zinc-silver ores and alteration of the surrounding granite at the Dunbrack mine, Musquodoboit Harbour, Nova Scotia; B.Sc. thesis, Dalhousie University, Halifax, Nova Scotia.

Maillet, L.A. and Clarke, D.B.

1985: Cordierite in the peraluminous granites of the Meguma Zone, Nova Scotia, Canada; Mineralogical Magazine, v. 49, p. 695-702.

Malcolm, W.

1929: Gold fields of Nova Scotia; Geological Survey of Canada, Memoir 156, 253 p.

1976: Gold fields of Nova Scotia; Geological Survey of Canada, Memoir 385 (reprint of Memoir 156 without plates or maps), 253 p.

Malcolm, W. and Faribault, E.R.

1912: Gold fields of Nova Scotia; Geological Survey of Canada, Memoir 20-E, 331 p.

Mawer, C.K.

1985: Origin of bedding-concordant auriferous quartz veins, Meguma Terrane, Nova Scotia; Geological Survey of Canada, unpublished internal report, 19 p.

1986: The bedding-concordant gold-quartz veins of the Meguma Group, Nova Scotia; *in* Turbidite-Hosted Gold Deposits, edited by J.D. Keppie, R.W. Boyle, and S.J. Haynes, Geological Association of Canada, Special Paper 32, p. 135-148.

1987: Mechanics of formation of gold-bearing quartz veins, Nova Scotia, Canada; Tectonophysics, v. 135, p. 99-119.

McAndrew, J.

1965: Gold deposits of Victoria; *in* Geology of Australian Ore Deposits, edited by J. McAndrew and R.T. Madigan, Eighth Commonwealth Mining and Metallurgical Congress, v. 1, p. 450-457.

McBride, D.E.

1978: Geology of the Ecum Secum area, Halifax and Guysborough counties, Nova Scotia; Nova Scotia Department of Mines and Energy, Report 78-1, 12 p.

McCutcheon, S.R., Lutes, G., Gauthier, G., and Brooks, C.

1981: The Pokiok Batholith: a contaminated Acadian intrusion with an anomalous Rb/Sr age; Canadian Journal of Earth Sciences, v. 18, p. 910-918.

Michard-Vitrac, A., Albarede, F., and Allègre, C.J.

1981: Lead isotopic composition of Hercynian granitic K-feldspars constrains continental genesis; Nature, v. 291, p. 460-464.

Morrissy, C.J. and Ruitenberg, A.A.

1980: Geology of the Lake George antimony deposit, southern New Brunswick; CIM Bulletin, v. 73, no. 822, p. 79-84.

Muecke, G.K., Elias, P., and Reynolds, P.H.

1988: Hercynian/Alleghanian overprinting of an Acadian terrane: ^{40}Ar/^{39}Ar studies in the Meguma Zone, Nova Scotia, Canada; Chemical Geology (Isotope Geoscience Section), v. 73, p. 153-167.

Nash, J.T., Granger, H.C., and Adams, S.S.

1981: Geology and concepts of genesis of important types of uranium deposits; *in* Seventy-Fifth Anniversary Volume, Economic Geology, p. 63-116.

Newhouse, W.H.

1936: A zonal gold distribution in Nova Scotia; Economic Geology, v. 31, p. 805-831.

O'Brien, B.H.

1985a: The formation of veins in greenschist facies rocks and the early deformation of the Meguma Group, eastern Nova Scotia; Nova Scotia Department of Mines and Energy, Paper 85-2, 35 p.

1985b: Preliminary report on the geology of the LaHave River area, Nova Scotia; *in* Current Research, Part A, Geological Survey of Canada, Paper 85-1A, p. 789-794.

1986: Preliminary report on the geology of the Mahone Bay area; *in* Current Research, Part A, Geological Survey of Canada, Paper 86-1A, p. 439-444.

Onishi, H.

1969: Arsenic; *in* Handbook of Geochemistry, edited by K.H. Wedepohl, sections B-M, v. 11/4, Springer-Verlag, Berlin.

O'Reilly, G.A.

1976: The petrology of the Brenton pluton, Yarmouth County, Nova Scotia; B.Sc. thesis, Dalhousie University, Halifax, Nova Scotia.

1985: Alkali metasomatism associated with W-Sn-Ag-Au mineralization in the granitoid rocks of the Westfield-Caledonia area, Queens County, Nova Scotia; *in* Guide to the Granites and Mineral Deposits of Southwestern Nova Scotia, edited by A.K. Chatterjee and D.B. Clarke, Nova Scotia Department of Mines and Energy, Paper 85-3, preprint, p. 217-232.

O'Reilly, G.A., Farley, E.J., and Charest, M.H.

1982: Metasomatic-hydrothermal mineral deposits of the New Ross-Mahone Bay area, Nova Scotia; Nova Scotia Department of Mines and Energy, Paper 82-2, 96 p.

O'Reilly, G.A., Gauthier, G., and Brooks, C.

1985: Three Permo-Carboniferous Rb-Sr age determinations from the South Mountain Batholith, southwestern Nova Scotia; *in* Mines and Minerals Branch, Report of Activities 1984, Nova Scotia Department of Mines and Energy, Report 85-1, p. 143-152.

Pitre, C.V.

1987: Paragenesis of sediment-hosted tin mineralization at the Duck Pond prospect, East Kemptville, Yarmouth County, N.S.; B.Sc. thesis, Carleton University, Ottawa, Ontario, 55 p.

Procyshyn, E.L. and Morrissy, C.J.

1989: Geology of the Lake George mine, southern New Brunswick; *in* Mineral Deposits Associated with Siluro-Devonian Plutonism in New Brunswick-Gaspé Sector, Geological Association of Canada/Mineralogical Assoiation of Canada, Field Trip Guidebook B5, p. 40-51.

Ramsay, J.G.

1967: Folding and Fracturing in Rocks; McGraw-Hill, London, 568 p.

1980: The crack-seal mechanism of rock deformation; Nature, v. 284, p. 135-139.

Reynolds, P.H., Elias, P., Muecke, G.K., and Grist, A.M.
1987: Thermal history of the southwest Meguma zone, Nova Scotia, from a ^{40}Ar/^{39}Ar and fission track dating study of intrusive rocks; Canadian Journal of Earth Sciences, v. 24, p. 1952-1965.

Reynolds, P.H., Zentilli, M., and Muecke, G.K.
1981: K-Ar and ^{40}Ar/^{39}Ar geochronology of granitoid rocks from southern Nova Scotia: its bearing on the geological evolution of the Meguma zone of the Appalachians; Canadian Journal of Earth Sciences, v. 18, p. 386-394.

Richardson, J.M.
1985a: Magmatic fractionation and metasomatic alteration of the Davis Lake-East Kemptville complex and its relationship to the rest of the South Mountain Batholith; *in* Guide to the Granites and Mineral Deposits of Southwestern Nova Scotia, edited by A.K. Chatterjee and D.B. Clarke, Nova Scotia Department of Mines and Energy, Paper 85-3, preprint, p. 131-148.
1985b: The East Kemptville greisen-hosted tin deposit, Nova Scotia: overview of the geological relationships and geochemistry; *in* Granite-Related Mineral Deposits: Geology, Petrogenesis and Tectonic Setting, Canadian Institute of Mining and Metallurgy, Geology Division, Extended Abstracts, Conference on Granite-Related Mineral Deposits, September 15-18, Halifax, Canada, p. 203-204.
1988a: Field and textural relationships of alteration and greisen-hosted mineralization at the East Kemptville tin deposit, Davis Lake monzogranite, southwest Nova Scotia; *in* Recent Advances in the Geology of Granite-Related Mineral Deposits, Canadian Institute of Mining and Metallurgy, Special Volume 39, p. 265-279.
1988b: Genesis of the East Kemptville greisen-hosted tin deposit, Davis Lake Complex, southwestern Nova Scotia, Canada; Ph.D. thesis, Carleton University, Ottawa, Ontario, 293 p.

Richardson, J.M., Spooner, E.T.C., and McAuslin, D.A.
1982: The East Kemptville tin deposit, Nova Scotia: an example of a large tonnage, low grade, greisen-hosted tin deposit in the endocontact zone of a granite batholith; *in* Current Research, Part B, Geological Survey of Canada, Paper 82-1B, p. 27-32.

Rickard, T.A.
1927: Gold mining in Nova Scotia; Nova Scotia Department of Public Works and Mines, Report on the Mines, 1926, p. 163-177.

Robertson, D.J. and Duncan, D.R.
1982: Geology and exploration history of the Millet Brook uranium deposit (abstract and reprint of presentation); CIM Bulletin, v. 75, no. 839, p. 130.

Rogers, H.D.
1985: Geology of the igneous-metamorphic complex of Shelburne and eastern Yarmouth counties, Nova Scotia; *in* Current Research, Part A, Geological Survey of Canada, Paper 85-1A, p. 773-777.

Rogers, P.J., MacDonald, M.A., and Rigby, D.W.
1985: Regional lake sediment survey of the Meguma zone, southern Nova Scotia: new analytical data; Nova Scotia Department of Mines and Energy, Open File Report 605, 65 p.

Ruitenberg, A.A. and McCutcheon, S.R.
1985: Tungsten, molybdenum and tin deposits in New Brunswick; Geological Association of Canada/Mineralogial Association of Canada, Field Trip Guidebook 13, Fredericton, New Brunswick, 36 p.

Sandiford, M. and Keays, R.R.
1986: Structural and tectonic constraints on the origin of gold deposits in the Ballarat Slate Belt, Victoria; *in* Turbidite-Hosted Gold Deposits, edited by J.D. Keppie, R.W. Boyle, and S.J. Haynes, Geological Association of Canada, Special Paper 32, p. 15-24.

Sangster, A.L.
1987: Sulphur isotope studies, Meguma Terrane, Nova Scotia: a preliminary report; *in* Report of Activities 1987, Part A, Nova Scotia Department of Mines and Energy, Paper 87-5, p. 207-208.

Sangster, A.L., Bretzlaff, R., Graves, M.C., and Zentilli, M.
1989: Stratigraphic variation of δ^{34}S compositions in the Meguma Group: implications for paleoenvironment and mineralization; Atlantic Geoscience Society, Colloquium '89, Program and Abstracts.

Sangster, A.L., Graves, M.C., and Zentilli, M.
1988: Sulphur isotopic variation in Mn-As-Au-Zn-Pb-bearing strata: sedimentation and diagenesis in an anoxic basin in Cambro-Ordovician flysch of the Meguma Group, Nova Scotia, Canada; Geological Society of America, Annual Meeting, Abstracts with Program, v. 20, no. 7, p. A301.

Schenk, P.E.
1970: Regional variation of the flysch-like Meguma Group (Lower Paleozoic) of Nova Scotia compared to recent sedimentation of the Scotia Shelf; Geological Association of Canada, Special Paper 7, p. 127-153.
1971: Southeastern Atlantic Canada, Northwestern Africa, and continental drifts; Canadian Journal of Earth Sciences, v. 8, p. 1218-1251.
1973: Nova Scotia, Morocco, and continental drift; *in* Earth Sciences Symposium on Offshore Eastern Canada; Geological Survey of Canada, Paper 71-23, p. 219-222.

Scratch, R.B., Watson, G.P., Kerrich, R., and Hutchinson, R.W.
1984: Fracture-controlled antimony-quartz mineralization, Lake George deposit, New Brunswick; Economic Geology, v. 79, no. 5, p. 1159-1186.

Seal, R.R., Clark, A.H., and Morrissy, C.J.
1988: Lake George, southwestern New Brunswick: a Silurian, multistage, polymetallic (Sb-W-Mo-Au-base metal) hydrothermal centre; *in* Recent Advances in the Geology of Granite-Related Mineral Deposits, Canadian Institute of Mining and Metallurgy, Special Volume 39, p. 252-264.

Selwyn, A.R.C.
1872: Notes and observations on the goldfields of Quebec and Nova Scotia; Geological Survey of Canada, Report of Progress, 1870-71, p. 252-282.

Shaw, W.G.
1983: A geological investigation of the Lazy Head tungsten deposit, Guysborough County, and a comparison with the Moose River deposit, Halifax County, Nova Scotia; M.Sc. thesis, Dalhousie University, Halifax, Nova Scotia, 229 p.

Sheets, R.W.
1987: Fluid inclusion study of quartz veins in the Ecum Secum area, Nova Scotia, Canada; M.Sc. thesis, Ohio State University, Columbus, Ohio, 166 p.

Sibson, R.H.
1979: Fault rocks and fault mechanisms; Journal of the Geological Society of London, v. 133, p. 191-213.

Sinclair, W.D., Kooiman, G.J.A., and Martin, D.A.
1988: Geological setting of granites and related tin deposits in the North Zone, Mount Pleasant, New Brunswick; *in* Current Research, Part B, Geological Survey of Canada, Paper 88-1B, p. 201-208.

Singleton, O.P.
1965: Geology and mineralization of Victoria; *in* Geology of Australian Ore Deposits, edited by J. McAndrew and R.T. Madigan, Eighth Commonwealth Mining and Metallurgical Congress, v. 1, p. 440-449.

Smith, P.K.
1983a: Stop 3-5: Cochrane Hill gold mine; *in* Gold Deposits of the Meguma Terrane of Nova Scotia, Canadian Institute of Mining and Metallurgy, CIM Geology Division, Excursion Guidebook, p. 72-104.
1983b: Geology of the Cochrane Hill gold deposit, Guysborough County, Nova Scotia; *in* Mines and Minerals Branch, Report of Activities 1982, Nova Scotia Department of Mines and Energy, Report 83-1, p. 225-256.
1984a: Geology and lithogeochemistry of the Cochrane Hill gold deposit — an indication of metalliferous source beds; Nova Scotia Department of Mines and Energy, Report 84-1, p. 203-214.
1984b: Geological map of the Cochrane Hill open-pit gold deposit; Nova Scotia Department of Mines and Energy, Map 84-1.

Smith, P.K. and Kontak, D.J.
1986: Meguma gold studies: advances in geological insight as an aid to gold exploration; *in* Tenth Annual Open House and Review of Activities, Program and Summaries, Nova Scotia Department of Mines and Energy, Information Series No. 12, p. 105-114.
1988a: Meguma gold studies I: generalized geological aspects of the Beaver Dam gold deposit, eastern Meguma zone, Nova Scotia; *in* Mines and Minerals Branch, Report of Activities 1987, Part B, Nova Scotia Department of Mines And Energy, Report 88-1, p. 45-60.
1988b: Meguma gold studies II: vein morphology, classification and information, a new interpretation of "crack seal" quartz veins; *in* Mines and Minerals Branch, Report of Activities 1987, Part B, Nova Scotia Department of Mines And Energy, Report 88-1, p. 61-76.

1988c: Bismuth-tellurium-silver-tungsten association at the Beaver Dam gold deposit, eastern Nova Scotia; *in* Mines and Minerals Branch, Report of Activities 1988, Part A, Nova Scotia Department of Mines and Energy, Report 88-3, p. 71-81.

Smitheringale, W.G.

1973: Geology of parts of Digby, Bridgetown, and Gaspereau Lake map areas, Nova Scotia; Geological Survey of Canada, Memoir 375, 78 p.

Snee, L.W., Sutter, J.F., and Kelly, W.C.

1988: Thermochronology of economic mineral deposits: dating the stages of mineralization at Panasquiera, Portugal, by high-precision ^{40}Ar/^{39}Ar age spectrum techniques on muscovite; Economic Geology, v. 83, p. 335-354.

Steed, G.M. and Morris, J.H.

1986: Gold mineralization in Ordovician greywackes, Clontibret, Ireland; *in* Turbidite-Hosted Gold Deposits, edited by J.D. Keppie, R.W. Boyle, and S.J. Haynes, Geological Association of Canada, Special Paper 32, p. 67-86.

Strong, D.F. and Hanmer, S.K.

1981: The leucogranites of southern Brittany: origin by faulting, frictional heating, fluid flux and fractional melting; Canadian Mineralogist, v. 19, p. 163-176.

Taylor, F.C.

1965: Silurian-Ordovician relationships and Silurian stratigraphy in southwestern Nova Scotia; Geological Survey of Canada, Paper 64-13, 24 p.

1967: Reconnaissance geology of Shelburne map area, Queens, Shelburne, and Yarmouth counties, Nova Scotia; Geological Survey of Canada, Memoir 349, 83 p.

Taylor, F.C. and Schiller, E.A.

1966: Metamorphism of the Meguma Group of Nova Scotia; Canadian Journal of Earth Sciences, v. 3, p. 959-974.

Taylor, R.G.

1979: Geology of tin deposits; Developments in Economic Geology 11, Elsevier Scientific Publishing Company, New York, 543 p.

Thorpe, R.I. and Thomas, G.M.

1976: Gold content of greywacke and slate of the Goldenville Formation, Nova Scotia, as determined by neutron activation analysis; *in* Report of Activities, Part A, Geological Survey of Canada, Paper 76-1A, p. 314-328.

Tischendorf, G.

1977: Geochemical and petrographic characters of silicic magmatic rocks associated with rare-element mineralization; *in* Metallization Associated with Acid Magmatism, edited by M. Stemprok et al., Czechoslovakia Geological Survey, Prague, v. 2, p. 41-96.

Waldron, J.W.F. and Jenson, L.R.

1985: Sedimentology of the Goldenville Formation, Eastern Shore, Nova Scotia; Geological Survey of Canada, Paper 85-15, 31 p.

Wanless, R.K., Stevens, R.D., Lachance, G.R., and Edmonds, C.M.

1968: Age determinations and geological studies, K-Ar isotopic ages; Geological Survey of Canada, Paper 67-2A, p. 141.

Wolfson, I.

1983: Geology, mineralogy and geochemistry of tin mineralization in the Dominique-Plymouth area, Yarmouth County, Nova Scotia; M.Sc. thesis, Dalhousie University, Halifax, Nova Scotia, 411 p.

Woodend, S.L.

1985: Port Mouton pluton; *in* Guide to the Granites and Mineral Deposits of Southwestern Nova Scotia, edited by A.K. Chatterjee and D.B. Clarke, Nova Scotia Department of Mines and Energy, Paper 85-3, preprint, p. 115-120.

Woodman, J.E.

1904: The sediments of the Meguma Series of Nova Scotia; American Geologist, v. 34, July.

Wright, J.D.

1975: Iron deposits of Nova Scotia; Nova Scotia Department of Mines, Economic Geology Series 75-1, 154 p.

Zartman, R.E. and Doe, B.R.

1981: Plumbotectonics — the model; Tectonophysics, v. 75, p. 135-162.

Zentilli, M. and Reynolds, P.H.

1985: ^{40}Ar/^{39}Ar dating of micas from the East Kemptville tin deposit, Yarmouth County, Nova Scotia; Canadian Journal of Earth Sciences, v. 22, p. 1546-1548.

Zentilli, M., Graves, M.C., Mulja, T., and MacInnes, I.

1986: Geochemical characterization of the Halifax-Goldenville Transition of the Meguma Group of Nova Scotia: preliminary report; *in* Current Research, Part A, Geological Survey of Canada, Paper 86-1A, p. 423-428.

Zentilli, M., MacInnis, I.N., and Reynolds, P.H.

1985: Geochemistry of lead-zinc-manganese mineralization associated with the Goldenville-Halifax Transition of the Cambro-Ordovician Meguma Group at Eastville, Nova Scotia (abstract); Geological Association of Canada/Mineralogical Association of Canada, Annual Meeting, Fredericton, Program with Abstracts, p. A71.

Crack-seal texture in bedding-parallel, gold-bearing, columnar-quartz veins: evidence of fossil water sills[1]

J.R. Henderson[2] and M.N. Henderson[3]

Henderson, J.R. and Henderson, M.N., Crack-seal texture in bedding-parallel, gold-bearing, columnar-quartz veins: evidence of fossil water sills; in Mineral Deposit Studies in Nova Scotia, Volume 1, edited by A.L. Sangster, Geological Survey of Canada, Paper 90-8, p. 163-168, 1990.

Abstract

Numerous examples of fibrous-mineral veins showing inclusion-band fabric have been attributed to episodic hydraulic fracturing and sealing. Here we describe an unusual solid-inclusion band fabric exhibited by 1 to 2 cm diameter, subhedral columnar quartz crystals composing 10 to 20 cm wide, bedding-parallel, barren and auriferous veins in the Cambro-Ordovician Meguma Group, Nova Scotia. The columnar crystals tend to be oriented normal to the vein walls, and display Brazil twins which we regard as evidence of primary fabric. Twinned crystals commonly show hexagonal sections with dark grey, mica-rich centres and milky-white, fluid inclusion-rich rims. Viewed in a plane perpendicular to bedding, the dark centres of crystals exhibit 0.05 to 0.1 mm thick quartz plates bounded by micrometre-thick bands of white micas. The inclusion bands are aligned parallel to the vein walls and terminate within single crystals which have an outer zone of milky quartz. Deformed quartz veins occur on limbs and hinges of folds, particularly anticlines.

These observations lead us to conclude that: (1) the solid-inclusion banded quartz resulted from episodic hydraulic fracturing and incremental growth of columnar crystals dispersed in a water sill; (2) the crystals formed bridges across the largely fluid-filled fracture; (3) between pulses of hydraulic fracturing, fluid pressure equalled lithostatic pressure; (4) the milky quartz displaced the fluid by growing in optical continuity with the solid-inclusion banded quartz; and (5) localization of bedding-parallel quartz veins in the region of anticlines may be due to ponding of water beneath very broad, open domes formed by differential compaction beneath impermeable layers in the Goldenville Formation, and during tectonic shortening these intensely veined rocks became the loci of some of the major anticlines.

Résumé

De nombreux exemples de veines contenant des minéraux fibreux, et présentant une fabrique à bandes d'inclusions ont été attribués à la fracturation hydraulique et au scellement épisodiques de la roche. Nous décrivons ici une fabrique inhabituelle à bandes d'inclusions solides présentée par des cristaux de quartz hypidiomorphes, prismatiques, qui constituent des veines stériles et des veines aurifères de 10 à 20 cm de large, parallèles au litage, dans le Groupe cambrien-ordovicien de Meguma en Nouvelle-Écosse. Les cristaux prismatiques sont généralement orientés perpendiculairement aux parois des veines, et présentent des macles du Brésil, que nous considérons comme un indice d'une fabrique primaire. Les cristaux maclés ont souvent une section hexagonale à centres gris sombre riches en mica, et des bordures blanc laiteux, riches en inclusion fluides. Observés dans un plan perpendiculaire au litage, les centres sombres des monocristaux sont caractérisés par des lamelles de quartz de 0,05 à 0,1 mm d'épaisseur, limitées par des bandes de mica blanc de l'ordre du millimètre. Les bandes d'inclusions sont alignées parallèlement aux parois des veines et se terminent dans la périphérie laiteuse de ces monocristaux. Les veines de quartz déformées sont situées sur les flancs et charnières des plis, en particulier des anticlinaux.

Ces observations nous mènent à la conclusion suivante : 1) le quartz à bandes d'inclusions solides est le résultat de la fracturation hydraulique épisodique et de la croissance incrémentale des cristaux prismatiques dispersés dans un filon-couche aqueux; 2) les cristaux ont constitué des ponts traversant la fracture largement remplie de fluides; 3) entre les épisodes de fracturation hydraulique, la pression exercée par les fluides a été égale à la pression lithostatique; 4) le quartz laiteux a déplacé le fluide en se développant en continuité optique avec le quartz à bandes d'inclusions solides; et 5) la localisation des veines de quartz parallèles au litage dans la région des anticlinaux est peut-être due à la retenue de l'eau au-dessous de dômes ouverts, très vastes, formés par compaction différentielle au-dessous de couches imperméables de la Formation de Goldenville; pendant le raccourcissement tectonique, plusieurs des grands anticlinaux ont été localisés sur ces roches intensément veinées.

---

[1] Contribution to the Canada - Nova Scotia Mineral Development Agreement, 1984-1989. Project carried by the Lithosphere and Canadian Shield Division, Geological Survey of Canada, Project 760027.

[2] Geological Survey of Canada, 580 Booth Street, Ottawa, Ontario, K1A 0E4.

[3] Geological Survey of Canada, 601 Booth Street, Ottawa, Ontario, K1A 0E8.

INTRODUCTION

Hydraulic fractures form when the fluid pressure within the rock pore space exceeds the least principal stress (σ_3) (Hubbert and Willis, 1957; Hubbert and Rubey, 1959; Gretener, 1969). In natural fractures connected to the surface water table, hydrostatic pressure is about 40 percent lithostatic pressure ($P_{fluid}/P_{lithostatic} = \lambda = 0.4$). Below several kilometres depth in the presence of an overlying aquaclude, pore-space reduction due to cementation, in conjunction with thermal expansion of water, may cause abnormally-high fluid pressure (Bradley, 1975). Fluid pressures in excess of 0.9 lithostatic pressure ($\lambda > 0.9$) have been measured in deep wells sealed by impermeable layers (Hubbert and Rubey, 1959), and it is generally assumed (Fyfe et al., 1978) that in the realm of regional metamorphism, $\lambda = 1$.

Recognition of hydraulic-fracture induced veining is based on geometry and fabric. Hydraulic fractures should form approximately perpendicular to σ_3. In areas of active tectonic compression σ_3 should be vertical, and horizontal hydraulic fractures should form when $\lambda > 1$ (Hubbert and Willis, 1957). Price (1975) suggested that in a series of horizontal sediments with the lowest tensile strength coincident with bedding surfaces, water sills may develop by dewatering beneath a slightly flexed impermeable layer. Should water sills drain before mineralization, their existence would be unrecorded.

Bedding-parallel, fibrous-mineral veins in flat-lying rocks have been attributed to hydraulic fracturing (Shearman et al., 1972; Stoneley, 1983) and in deformed rocks, bedding-parallel veins oriented perpendicular to the deduced σ_3 direction have been attributed to hydraulic fracturing by Phillips (1972), Nelson (1981), and Fitches et al. (1986).

Certain vein textures have been interpreted to be indicative of the hydraulic fracturing mechanism. Commonly these are "dirty" veins, such as wall rock-breccia veins (Phillips, 1972; Fyfe et al., 1978; Swager, 1985). However, the most commonly cited evidence in support of hydraulic fracturing as a deformation mechanism is the presence of oriented inclusions of fluid or solid phases within fibrous-mineral filled veins ("crack-seal" veins; Ramsay, 1980; Cox and Etheridge, 1983). Fibrous crack-seal veins are never more than hairline fractures, and the period during which the fracture is held open by fluid pressure is (geologically) very short. Vein thickness is related to the number of episodes of microcracking and sealing. If each crack is formed between the vein and the wall rock, metamorphic minerals may be detached from the wall rock in planar arrays (inclusion bands) and incorporated into the incrementally widening vein.

In drill core from horizontal East Texas Basin sandstone, Laubach (1988) described vertical fractures with discontinuous quartz pillars showing crack-seal fluid-inclusion bands which he attributed to intermittent hydraulic fracturing and sealing. Laubach (1988) recognized the inclusion-banded quartz as having formed bridges between the incrementally widening water-filled dykes which subsequently were partly filled with post-kinematic ankerite and clay.

We have seen hundreds of bedding-parallel quartz veins in the Goldenville Formation with fabrics seemingly identical to the vertical veins described by Laubach (1988). They range in thickness from less than a millimetre to more than a metre. Some of the bedding-parallel veins are partly filled by columnar quartz crystals with solid-inclusion bands parallel to bedding (Fig. 1). We consider the inclusion-banded columnar quartz as evidence of the crack-seal mechanism of deformation. A later infilling of milky quartz (see below) is believed to be proof of the existence of water sills during vein formation.

Most of mainland Nova Scotia is underlain by the Meguma Group, comprising the Goldenville Formation sandy flysch and the overlying Halifax Formation silty flysch. The Meguma zone was initially shortened by cleavage and folding during the Early Devonian Acadian Orogeny, and subsequently underwent granitic intrusion and several dextral-shear related deformations (Henderson, 1986; Henderson et al., 1986). Historically, bedding-parallel veins in the Goldenville Formation were the most significant gold producers (Graves and Zentilli, 1982), and although other vein geometries occur (e.g. en échelon, saddle-reef, and ac veins), in this paper we are concerned only with the origin of certain bedding-parallel veins.

BEDDING-PARALLEL VEIN DISTRIBUTION AND GEOMETRY

Bedding-parallel quartz (+/- carbonate, sulphide, and gold) veins occur throughout the Meguma zone within the Goldenville Formation, most commonly near the top of shale (slate) beds in the sandstone-siltstone-shale flysch. Bedding-parallel veins are rare in the overlying black and grey siltstone-shale flysch of the Halifax Formation. The veins are very extensive parallel to the bedding surface. Rarely, the veins truncate bedding, such as where a bedding-parallel vein in a slate bed intersects a scour filled by sand of an overlying bed. Some millimetre-thick veins conform perfectly to the cross laminated tops of Bouma C divisions in turbidite beds. Bedding-parallel

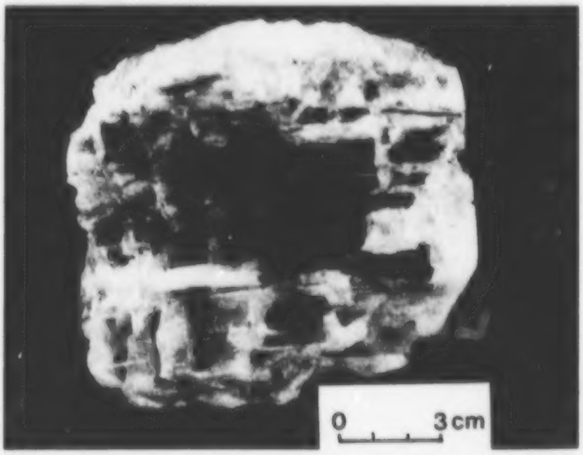

veins in slate beds occurring on major fold hinges exhibit intrafolial folds indicating 50 to 60 percent layer-parallel shortening (Fig. 2). Where bedding-parallel veins occur between thick metasandstone beds they are not folded intrafolially (Fig. 3). Although bedding-parallel veins appear to be ubiquitous, their density seems greatest in shale-rich facies located on hinges and limbs of major anticlines in the Goldenville Formation.

FABRIC OF BEDDING-PARALLEL VEINS

Most bedding-parallel veins are composed of both milky-white and oily-grey quartz, although many of the relatively thick veins occurring between metasandstone beds are entirely milky-white quartz (Fig. 3). The veins composed of both varieties of quartz have a striking mottled black-and-white appearance in the plane of the vein (Fig. 4), and are called ''speckled-hen'' or ''turtle-shell'' veins in the Caribou Mine where they are auriferous (M. Cullen, pers. comm., 1988). The dark ''specks'' compose about 30 percent of the veins, and commonly show hexagonal outlines.

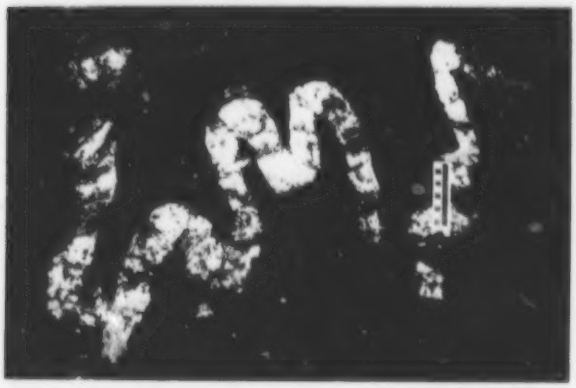

Figure 2. Folded bedding-parallel, auriferous crack-seal quartz vein contained within slate exposed in the Dr. Sutherland Mine on the crest of the Moose River anticline (GSC 204867-L).

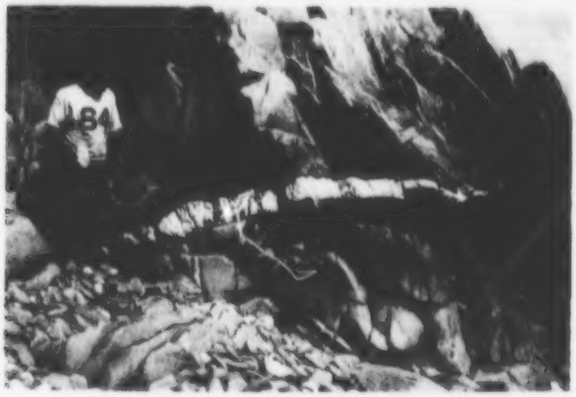

Figure 3. Barren milky-quartz vein contained between metasandstone beds, Tuffin Island, near the crest of the Southern anticline (GSC 204124-Z).

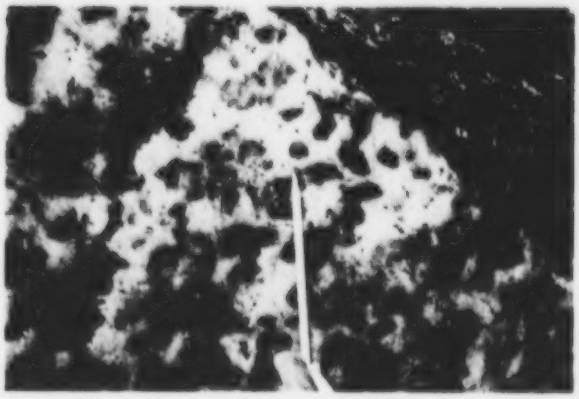

Figure 4. Base of a bedding-parallel, auriferous ''speckled-hen'' quartz vein exposed on the back of a drift in the Caribou Mine on the southeastern limb of the Caribou anticline. ''Speckled-hen'' is a term applied locally by miners in reference to the distinctive surface appearance of these veins (GSC 204867-P).

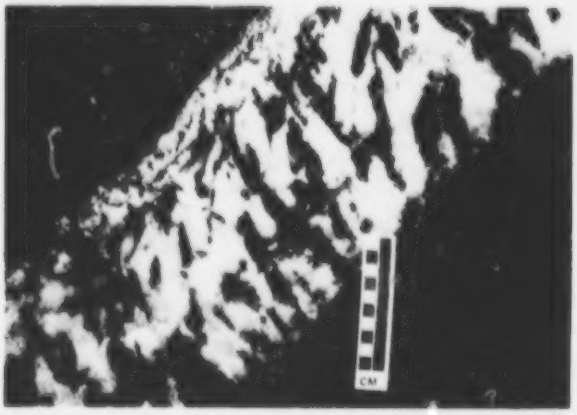

Figure 5. Profile of an auriferous, bedding-parallel, ''speckled-hen'' quartz vein exposed in a crosscut in the Caribou Mine on the northwestern limb of the Caribou anticline. Note that the dark, solid-inclusion filled crystals are oriented at a large angle to the vein walls, and tend to taper toward the hanging wall of the vein. See text for discussion (GSC 204867-M).

In Figure 5, a ''speckled-hen'' vein is exposed in profile in a crosscut in the Caribou Mine. The specks can be seen to compose columns oriented at a large angle to the bedding. Some of the columns appear to taper upward in the vein shown, but this may be due to ''cut effects''. However, based on observations of many veins we believe there is a real tendency for the columns to taper preferentially both upward and downward in different veins, and this may indicate that the vein opened preferentially on the side with the larger crystals. The vein in Figure 5 is more deformed near the top, where the crystals are more narrow, than near the bottom, and the columns bend progressively updip in the upper 5 cm of the vein.

Veins similar in appearance to the "speckled-hen" variety at Caribou Mine are exposed in trenches at the Harrigan Cove Mine. One of these veins is shown in outcrop in Figure 6, and in hand specimen in Figure 1. Vugs occur within a thick "pillow" in a vertical vein showing "chocolate-tablet" pinch-and-swell. Within the vugs, subhedral quartz columns composed of hundreds of millimetre-thick quartz plates oriented parallel to the vein walls and nearly perpendicular to the columns can be seen. Figure 7, a photomicrograph of a thin section from the vein in Figure 6, shows that the quartz columns form single crystals exhibiting undulose extinction in polarized light, and showing slight offsets parallel to some of the plates (cf. also Fig. 6 and 9 in Henderson and Henderson, 1986, and Fig. 6 and 9 in Mawer, 1986).

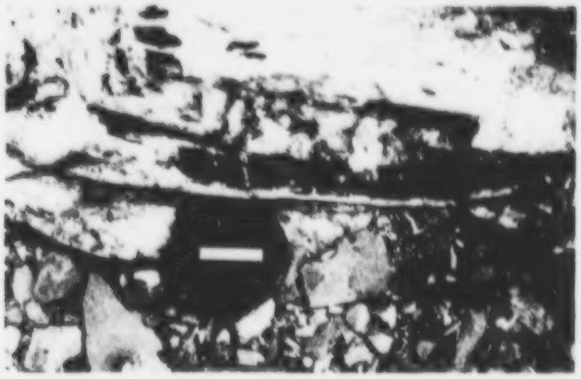

Figure 6. Vuggy, bedding-parallel, auriferous crack-seal vein exposed in a trench at the Harrigan Cove Mine, on the vertical southern limb of the Tangier anticline. Figure 1 shows a hand specimen of this vein (GSC 203683-Z).

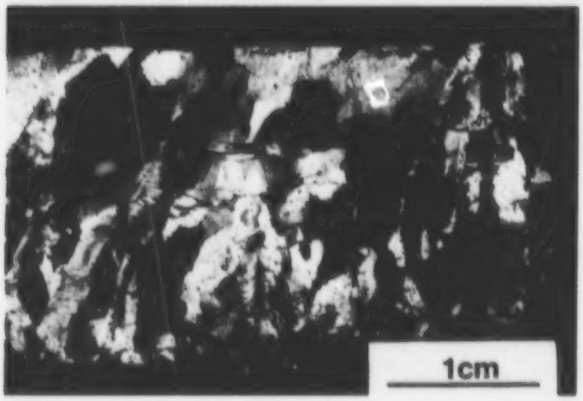

Figure 7. Photomicrograph of a thin section (crossed nicols) of the vein shown in Figures 1 and 6. The section is cut in the plane perpendicular to the fold axis. Columnar quartz crystals are divided by numerous bedding-parallel mica inclusion bands. Note that the inclusion bands are weakly folded, and the columnar crystals display undulatory extinction and are slightly offset across some inclusion bands (GSC 202510-P).

A photomicrograph of a thin section of the "speckled-hen" vein in Figure 4 is shown in Figure 8. The picture, taken in partly polarized light, shows basal sections of quartz crystals (almost in extinction) that are twinned according to the Brazil law. The crystal in the centre of the photo has a core containing inclusion bands of white micas, and an outer zone of milky quartz. Mawer (1986, 1988) considered Brazil-twinned quartz crystals from bedding-parallel veins in the Goldenville Formation to indicate primary crystal fabric. We concur, and further consider that the primary twinned crystals show a two-stage growth history: initially the crystals increased in length by the mechanism of incremental hydraulic fracturing and sealing as the fracture widened, and later overgrowths of milky quartz increased their width until the fracture was filled.

The postulated two-stage growth history of primary crystals in the "speckled-hen" veins means that the hydraulic fractures not only widened incrementally, but also fluid pressure maintained open fractures (water sills) until the milky quartz filled in the cavities or vugs. Note that the vugs in the vein shown in Figures 1 and 6 may have remained fluid-filled cavities or were filled originally by soluble carbonate minerals. Critical evidence in support of the water sill hypothesis is exhibited by a vein

Figure 8. Photomicrograph of a thin section (partly crossed nicols) of the "speckled-hen" vein shown in Figure 4. The section is cut parallel to bedding and shows basal sections of several Brazil-twinned quartz crystals. The large central crystal has a triangular central area displaying mica inclusion-bands suggesting a two-stage growth history. See text for discussion (GSC 204869).

shown in Figure 9. The vein is the "speckled-hen" variety made up of both milky and inclusion-banded quartz, and the latter form subhedral crystals that commonly extend beyond the top and bottom of the vein. This is displayed in a close view of the vein (Fig. 10) which reveals numerous quartz-crystal "pegs" embedded in the underlying siltstone where the vein has been detached.

Figure 11 summarizes our conception of "speckled-hen" vein development by incremental widening of a water sill with dispersed columnar quartz bridges. Slight reduction in fluid pressure (Fig. 11D) allowed the relatively ductile wall rock to intrude the fracture until $P_f = P_l$ was restored.

Figure 9. Photograph taken perpendicular to bedding showing noncylindrical folds in a barren bedding-parallel quartz vein exposed on a horizontal enveloping surface. Basins in the folded vein preserve vertically cleaved slate of the overlying bed. The outcrop is located on the crest of the Southern anticline on the southern shore of Sober Island (GSC 204867-H).

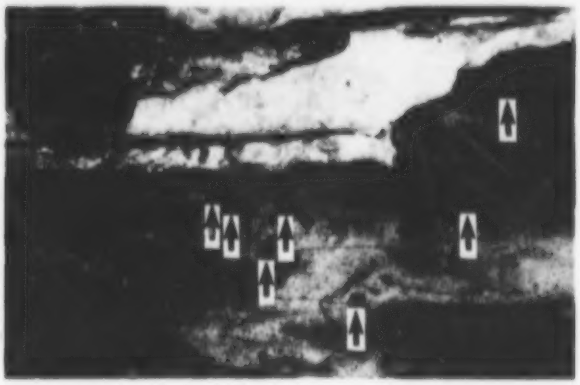

Figure 10. Photograph taken perpendicular to bedding showing a close-view of the metasiltstone bed underlying the vein pictured in Figure 9. The vein has been detached from the bedding surface shown in the lower half of the photograph, and columnar-quartz crystals dispersed within the vein penetrate the underlying bed (arrowed) (GSC 204867-S).

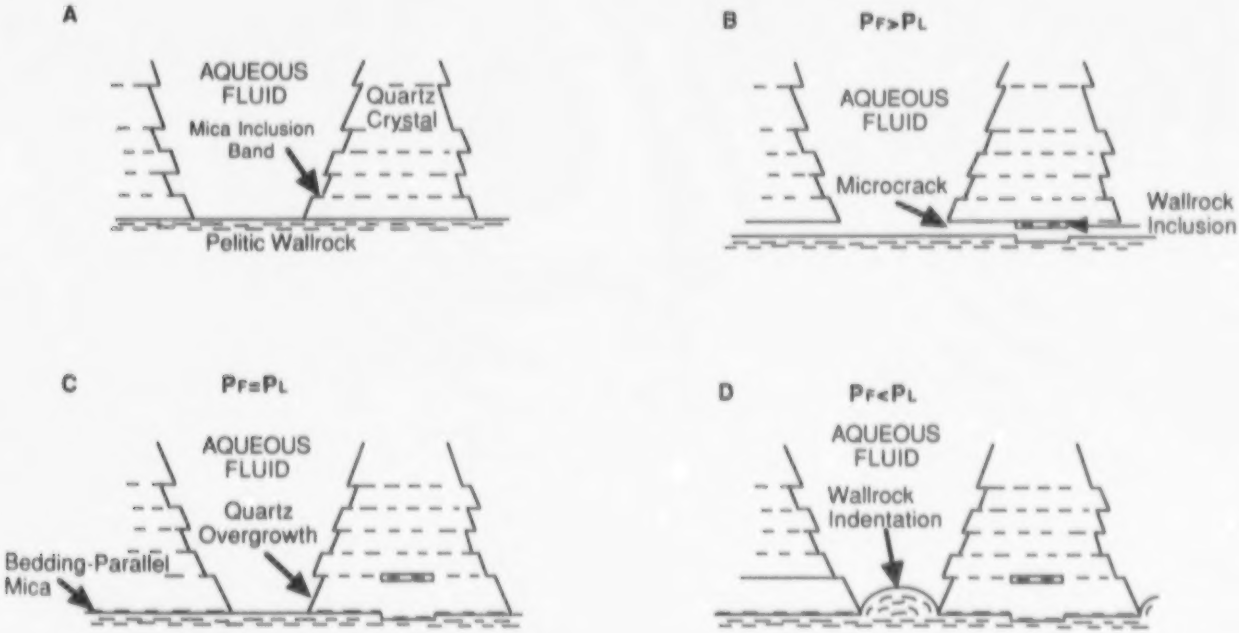
A
AQUEOUS FLUID
Quartz Crystal
Mica Inclusion Band
Pelitic Wallrock
B
$P_F > P_L$
AQUEOUS FLUID
Microcrack
Wallrock Inclusion
C
$P_F = P_L$
AQUEOUS FLUID
Quartz Overgrowth
Bedding-Parallel Mica
D
$P_F < P_L$
AQUEOUS FLUID
Wallrock Indentation

Figure 11. Conceptual model of the progressive widening of a water sill. (A) Lower half of a water sill with dispersed columnar-quartz bridges. (B) Transient microcracking event ($P_{fluid} > P_{lithostatic}$) causing an incremental widening of the water sill, and inclusion of a wall-rock chip into the cavity. (C) Resealing of the quartz bridge, with inclusion of the wall-rock chip and formation of a bedding-parallel metamorphic mica inclusion-band. (D) Transient decrease in fluid pressure permitting intrusion of ductile wall rock into the fluid-filled part of the cavity.

CONCLUSIONS

The water sill hypothesis of bedding-parallel vein formation implies that there was no bedding-parallel shear until the water sill was sufficiently mineralized to act competently or the fragile quartz bridges would have been broken. That the veins were competent during folding is shown by the preservation of their primary fabric (e.g. Fig. 1, 7, and 8).

All bedding-parallel veins that we have examined, however, show some evidence of deformation. Microscopic-scale deformation is revealed by undulose extinction of primary quartz columns, folding of inclusion-bands, and subgrain formation along borders of primary crystals. On the hinges of major folds, bedding-parallel veins in slate beds show 50 to 60 percent shortening by folding, whereas the enclosing slates shortened by pressure-solution cleavage formation (Fig. 2; see also Henderson et al., 1986). On limbs of major folds, bedding-parallel veins show evidence of heterogeneous strain; they are more recrystallized along their margins than in their centres (Fig. 5), and tectonic stylolites, common in most veins, indicate pressure solution.

Gold occurs in bedding-parallel columnar crack-seal veins at Caribou, Moose River, and Harrigan Cove; gold probably is associated with this type of bedding-parallel vein at other localities, and as development of gold prospects continues in the Meguma zone this is a viable target. If the water sill hypothesis is true, gold must have been introduced along with the primary mineralizing waters after compaction, and before the regional folding. The crack-seal veins described here definitely predate fold amplification, granite intrusion, and dextral shearing.

Localization of bedding-parallel quartz veins in the region of anticlines may be due to ponding of water beneath broad open domes formed by differential compaction beneath impermeable layers (cf. Price, 1975) in the Goldenville Formation. Subsequently, during tectonic shortening, these intensely veined rocks became the loci of some of the major anticlines.

ACKNOWLEDGMENTS

Tom Wright shares credit for many of the ideas expressed in this paper. We thank Seabright Explorations, Inc. for permission to visit its properties at Caribou and Moose River. Mike Cullen is thanked specifically for providing us with the plans of the Holman Mine, and generally for the fine hospitality during our stay at Caribou. We are grateful to Al Sangster and John Kerswill for encouraging us to write up our ideas on the origin of the "speckled-hen" veins. Bill Fyson and Howard Poulsen are thanked for helpful reviews of the paper.

REFERENCES

Bradley, J.S.
1975: Abnormal formation pressure; American Association of Petroleum Geologists Bulletin, v. 59, p. 957-973.
Cox, S.F. and Etheridge, M.A.
1983: Crack-seal fibre growth mechanisms and their significance in the development of oriented layer silicate microstructures; Tectonophysics, v. 92, p. 147-170.
Fitches, W.R., Cave, R., Craig, J., and Maltman, A.J.
1986: Early veins as evidence of detachment in the Lower Paleozoic rocks of the Welsh Basin; Journal of Structural Geology, v. 8, p. 607-620.
Fyfe, W.S., Price, N.J., and Thompson, A.B.
1978: Fluids in the Earth's Crust; Elsevier, Amsterdam.
Graves, M.C. and Zentilli, M.
1982: A review of the geology of gold in Nova Scotia; *in* Geology of Canadian Gold Deposits, edited by R.W. Hodder and W. Petruk, Canadian Institute of Mining and Metallurgy, Special Paper 24, p. 233-244.
Gretener, P.E.
1969: Fluid pressure in porous media — its importance in geology: a review; Bulletin of Canadian Petroleum Geology, v. 17, p. 255-295.
Henderson, J.R.
1986: Geology, Ecum Secum area, Nova Scotia; Geological Survey of Canada, Map 1648A, scale 1:50 000.
Henderson, J.R., Wright, T.O., and Henderson, M.N.
1986: A history of cleavage and folding: an example from the Goldenville Formation, Nova Scotia; Geological Society of America Bulletin, v. 97, p. 1354-1366.
Henderson, M.N. and Henderson, J.R.
1986: Constraints on the origin of gold in the Meguma zone, Ecum Secum area, Nova Scotia; Maritime Sediments and Atlantic Geology, v. 22, p. 1-13.
Hubbert, M.K. and Rubey, W.W.
1959: Role of fluid pressure in mechanics of overthrust faulting, Part I, Mechanics of fluid-filled porous solids and its application to overthrust faulting; Geological Society of America Bulletin, v. 70, p. 115-166.
Hubbert, M.K. and Willis, D.G.
1957: Mechanics of hydraulic fracturing; Petroleum Transactions of the American Institute of Mechanical Engineers, v. 210, p. 153-163.
Laubach, S.E.
1988: Subsurface fractures and their relationship to stress history in East Texas Basin sandstone; Tectonophysics, v. 156, p. 37-49.
Mawer, C.K.
1986: The bedding-concordant gold-quartz veins of the Meguma Group, Nova Scotia; *in* Turbidite-Hosted Gold Deposits, edited by J.D. Keppie, R.W. Boyle, and S.J. Haynes, Geological Association of Canada, Special Paper 32, p. 135-148.
1988: Mechanics of formation of gold-bearing quartz veins, Nova Scotia, Canada; Tectonophysics, v. 135, p. 99-119.
Nelson, R.A.
1981: Significance of fracture sets associated with stylolite zones; American Association of Petroleum Geologists Bulletin, v. 65, p. 2417-2425.
Phillips, W.J.
1972: Hydraulic fracturing and mineralization; Journal of the Geological Society of London, v. 128, p. 337-359.
Price, N.J.
1975: Fluids in the crust; Science Progress, v. 62, p. 59-87.
Ramsay, J.G.
1980: The crack-seal mechanism of rock deformation; Nature, v. 284, p. 135-139.
Shearman, D.J., Mossop, G., Dunsmore, H., and Martin, M.
1972: Origin of gypsum veins by hydraulic fracture; Institute of Mining and Metallurgy Transactions, v. 81, p. B149-155.
Stoneley, R.
1983: Fibrous calcite veins, overpressures, and primary oil migration; American Association of Petroleum Geologists Bulletin, v. 67, p. 1427-1428.
Swager, C.P.
1985: Syndeformational carbonate-replacement model for the copper mineralization at Mount Isa, Northwest Queensland: a microstructural study; Economic Geology, v. 80, p. 107-125.

Origin and deformational and metamorphic history of gold-bearing quartz veins on the Eastern Shore of Nova Scotia[1]

P.F. Williams[2] **and C. Hy**[3]

Williams, P.F. and Hy, C., Origin and deformational and metamorphic history of gold-bearing quartz veins on the Eastern Shore of Nova Scotia; in Mineral Deposit Studies in Nova Scotia, Volume 1, edited by A.L. Sangster, Geological Survey of Canada, Paper 90-8, p. 169-194, 1990.

Abstract

The metamorphic and deformational history of an area between Sheet Harbour and Lake Charlotte on the Eastern Shore of Nova Scotia has been studied, paying special attention to the quartz veins.

Regional folds (F_1) and their axial plane cleavage are developed in Meguma turbidites and shales. The folds are intruded by Devonian granitoids and overprinted by dip-slip, ductile shear zones. Many of the shear zones are found in the contact aureoles of the granitoids and may have formed during contact metamorphism. Irrespective of the time of formation, they were certainly active during contact metamorphism. The remainder of the shear zones are interpreted as being the same age and are associated with concentrations of carbonate that are believed to be a product of metasomatism. A group of predominantly brittle faults overprint all older structures and are interpreted as Triassic, or younger, transfer faults associated with the opening of the Atlantic Ocean. These faults exploit older (Devonian) ac joints.

All of the gold occurrences that we have visited are associated with ductile shear zones despite the fact that such shear zones are not common elsewhere in the study area.

It has long been recognized that the best occurrences of gold are in bedding-parallel veins and we find that these veins are generally composite where they are gold-bearing. The late bedding-parallel vein influxes are believed to be approximately the same age as late- to postfolding saddle reefs and ac veins, both of which are mineralized locally. Earlier en échelon veins, which are approximately coeval with the early influxes of the bedding-parallel veins, are also locally mineralized. We conclude that the gold was a late addition to the bedding-parallel and en échelon veins introduced at about the same time as emplacement of the saddle reef and ac veins and that the gold-bearing veins and granitoids were different products of a thermal dome that developed in the Meguma Terrane in Devonian times. The older veins were probably not gold-bearing but they acted as competent bodies during the late faulting and therefore tended to become the locus of brittle fractures and thus also the locus of gold-bearing quartz veins.

Résumé

Le métamorphisme et la déformation d'une zone située entre Sheet Harbour et Lake Charlotte sur la côte est de la Nouvelle-Écosse ont été analysés en portant une attention spéciale aux filons de quartz.

Les plis régionaux (F_1) et leur clivage ardoisier axial se sont formés dans des turbidites et schistes argileux de Meguma. Les plis sont recoupés par des intrusions de granitoïdes dévoniens

---

[1] Contribution to the Canada - Nova Scotia Mineral Development Agreement, 1984-1989. Project carried by the Mineral Resources Division, Geological Survey of Canada, Project 860008.

[2] Department of Geology, University of New Brunswick, P.O. Box 4400, Fredericton, New Brunswick, E3B 5A3

[3] Gold Quest NL, P.O. Box #1, Inglewood, Victoria 3517, Australia

sur lesquels se superposent des zones de cisaillement ductile à rejet incliné. Les zones de cisaillement se retrouvent pour la plupart dans les auréoles de contact des granitoïdes et ont pu se former durant le métamorphisme de contact. Peu importe à quand remonte leur formation, elles ont sûrement été actives durant le métamorphisme de contact. Les autres zones de cisaillement seraient, selon les interprétations, du même âge que les concentrations de carbonate que l'on croyait être le produit du métasomatisme, concentrations auxquelles elles seraient associées. Un groupe de failles en grande partie cassantes se superposent à toutes les autres structures plus anciennes; il s'agirait de failles de transfert triasique ou plus récentes associées à l'ouverture de l'océan Atlantique. Ces failles exploitent des diaclases croisées plus anciennes (Dévonien).

Tous les gîtes d'or observés sont associés à des zones de cisaillement ductiles en dépit du fait que ces dernières soient peu nombreuses ailleurs.

Les meilleurs gîtes d'or se retrouvent, on le sait depuis longtemps, dans des filons parallèles à la stratification qui sont, selon les auteurs, généralement composites. Les plus récents filons parallèles à la stratification seraient chronologiquement équivalents aux gîtes de charnière anticlinale et aux filons croisés datant de la fin du plissement et postérieurement, tous deux minéralisés localement. Des filons en échelon plus anciens, à peu près contemporains à la formation initiale des filons parallèles à la stratification, sont également minéralisés localement. En conclusion, l'or n'est apparu dans les filons parallèles à la stratification et en échelon qu'en dernier lieu, vers la même époque environ que la mise en place des gîtes de charnière anticlinale et des filons croisés; de plus, les filons et granitoïdes aurifères sont des produits différents d'un dôme thermique formé dans le terrane de Meguma durant le Dévonien. Les filons plus anciens n'étaient probablement pas aurifères mais ils ont joué le rôle de massifs compétents durant la dernière période de formation de failles et, par conséquent, ont eu tendance à devenir le siège de fractures cassantes et, de ce fait, un lien propice à la formation de filons de quartz aurifères.

INTRODUCTION

The project reported on here was primarily aimed at understanding the history and origin of the gold-bearing quartz veins on the Eastern Shore of Nova Scotia (Fig. 1). However, it was felt that the veins needed to be studied in the context of the general geological history of the area and more particularly in terms of the metamorphic and structural history. We therefore have remapped a portion of the area (Fig. 2) emphasizing the collection of metamorphic and structural data as well as any data at all pertaining to the veins. We have subdivided the veins into groups and have mapped the distribution of each group.

The area is one of Cambro-Ordovician metasedimentary rocks comprising the lower Goldenville Formation, a turbidite sequence with thick sandstones and thin slates, and the upper Halifax Formation, a predominantly slate sequence (Schenk, 1971, 1975). These metasedimentary rocks were folded (F_1) during Acadian times (Keppie, 1976, 1979, 1982a; Clarke and Halliday, 1980) into large folds with wavelengths of several kilometres. Mesoscopic F_1 folds in bedding are rare. There is a regional axial plane cleavage (S_1), which we believe began to form prior to the development of the folds (see also Henderson, 1983; Henderson et al., 1986). It is characterized by greenschist facies mineralogy. This deformed metamorphic sequence was intruded by posttectonic Devonian plutons (Clarke and Halliday, 1980; Reynolds et al., 1981; MacDonald and Clarke, 1985) which truncate the regional folds (Fig. 2). Contact metamorphic minerals overgrew the regional foliation and in a few places where there is outcrop within the aureole, close to the contact, a syncontact metamorphic shear zone is developed. It is parallel to the contact and kinematic indicators consistently indicate that the granitoid has moved up relative to the country rock. These shear zones persist away from the granitoid and are characterized by a new foliation (S_2) and a steeply plunging stretching lineation.

Outcrop in the area mapped is excellent along the coast and locally very good along the lake shores. Manmade outcrop in road cuttings and old mine sites is also good but very localized. Elsewhere the outcrop is generally poor and from the point of view of structural observations practically nonexistent. Our interpretation therefore is partly dependant on the use of the total field and vertical gradient magnetic maps (Geological Survey of Canada, 1986a) and, for the Ship Harbour area, on the gamma ray spectrometric map (Geological Survey of Canada, 1986b). In general, areas of Goldenville Formation are characterized by total magnetic fields less than 54700nT whereas areas of Halifax Formation are characterized by fields in excess of 54700nT. On the vertical gradient maps the strike of bedding is very well marked by continuous linear anomalies. Quite large positive and negative anomalies occur within the Goldenville Formation but the largest positive anomalies are associated with the Halifax Formation, and mapping shows that the transition from Goldenville to Halifax coincides with the vertical gradient 0nT/m contour. The granitoid is marked by a very high total field magnetic anomaly (>54800nT) and a low vertical gradient (between −0.05 and +0.05nT/m). These general relationships were checked wherever outcrop allowed.

The resolution of the spectrometric data is lower than that of the magnetic data and the spectrometric maps cannot be used to accurately position geological contacts. The data were used, however, to check interpretations based on the magnetic data.

In the following paragraphs we describe the veins in the context of the deformational and metamorphic history of the area. We show that the occurrence of gold is related not only to periclinal anticlines as previously recognized (Malcolm, 1929), but also to the S_2 shear zones, and suggest that the gold was transported along the shear zones during S_2 deformation and approximately coeval emplacement of the granitoids by fluids moving ahead of the granitoids.

METAMORPHISM

Earlier workers (e.g. Newhouse, 1936; Mawer, 1985) have pointed to the proximity of the known gold occurrences, on the Eastern Shore, to the granitoids and more specifically to biotite of suspected contact metamorphic origin. The granitoids are not metamorphosed in the area that we have mapped (Fig. 2), so that any metamorphism recognizable in the sedimentary rocks has to be of pregranitoid regional origin or contact origin and the only known source of possible contact metamorphism is the granitoids. Our study of metamorphism is concentrated in the area around the eastern end of the Musquodoboit pluton (Fig. 2).

In the lowest grade areas the sedimentary rocks are composed essentially of quartz, chlorite, muscovite, and inherited plagioclase. Such areas are well away from the granitoids and in approaching the Musquodoboit pluton, for example, biotite makes an appearance. Keppie and Muecke (1979) considered the biotite to be a product of regional metamorphism, but our petrological and microstructural work indicates that it is post-F_1 deformation and is of the same origin as cordierite and andalusite. The latter minerals, particularly the cordierite, are quite clearly limited to a narrow aureole around the batholith. Biotite, however, is less clearly related to the batholith because it defines a much wider zone, but wherever we have observed it, it is younger than the regional axial plane cleavage. For example, at Mooseland, on the northern side of the pluton, biotite overprints the axial plane cleavage of the Mooseland-Gegogan anticline. At Beaver Dam (Fig. 1), on the eastern side of the River Lake Pluton, several generations of biotite, probably all related to the same metamorphism, overprint the regional foliation.

In the Ship Harbour area, biotite occurs in a zone parallel to the contact of the granitoid and is found up to 1.5 km, measured horizontally, from the pluton. It has a preferred orientation but nevertheless overprints the low greenschist facies regional cleavage (Fig. 3). In a ductile

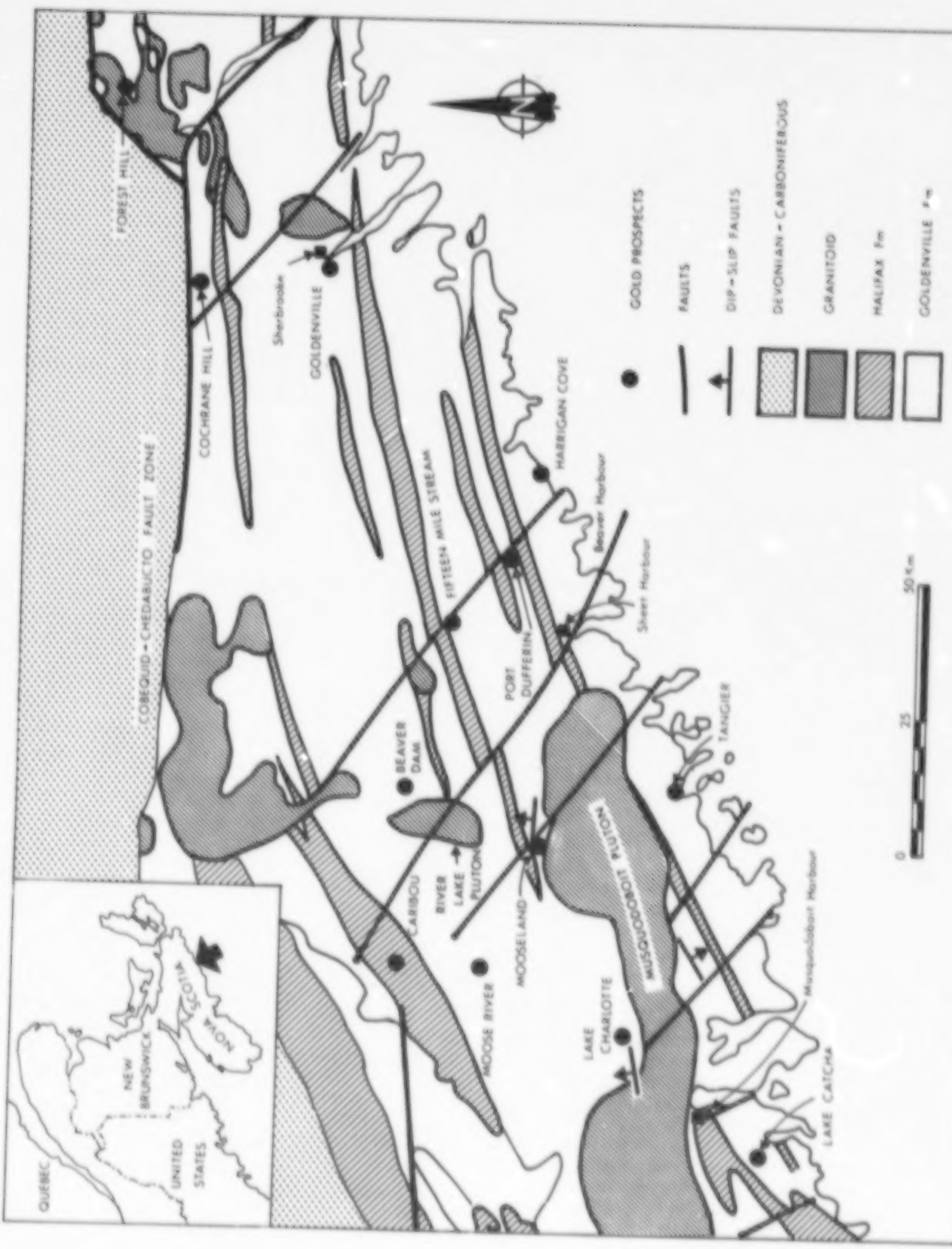
QUEBEC
NEW BRUNSWICK
UNITED STATES
NOVA SCOTIA
FOREST HILL
COBEQUID - CHEDABUCTO FAULT ZONE
COCHRANE HILL
Sherbrooke
GOLDENVILLE
FIFTEEN MILE STREAM
HARRIGAN COVE
Beaver Harbour
Sheet Harbour
PORT DUFFERIN
BEAVER DAM
TANGIER
CARIBOU
RIVER LAKE PLUTON
MOOSELAND
MUSQUODOBOIT PLUTON
MOOSE RIVER
LAKE CHARLOTTE
Musquodoboit Harbour
LAKE CATCHA
0
25
50 Km
N
GOLD PROSPECTS
FAULTS
DIP-SLIP FAULTS
DEVONIAN - CARBONIFEROUS
GRANITOID
HALIFAX Fm
GOLDENVILLE Fm

Figure 1. Eastern Shore of

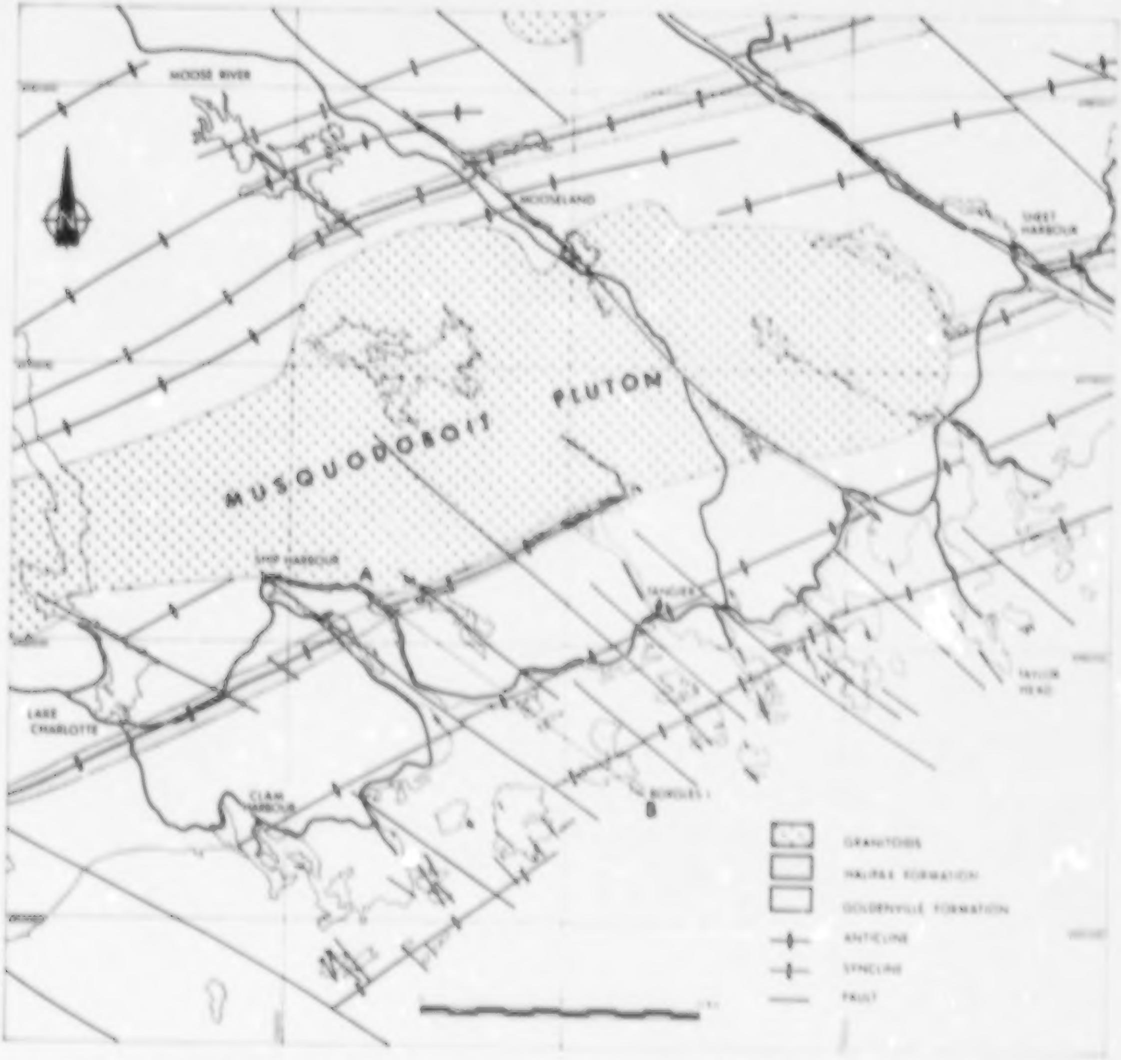

Figure 2. Geological map of the area examined in detail. The significance of section A-B is discussed in the text.

shear zone associated with the contact (see below), within the biotite zone, as many as three generations of biotite can be recognized in a single outcrop (Fig. 4). The first generation is aligned parallel to a foliation and is overgrown by late cordierite porphyroblasts which are also aligned parallel to the foliation and are deformed. The second generation of biotite has a preferred orientation of (001) perpendicular to the foliation and together with the first generation is overgrown by andalusite with which a third generation of biotite is associated (Fig. 4). We interpret these relationships as indicating continued growth of biotite during contact metamorphism and progressive shear. This conclusion is supported by the fact that probe analyses of the three generations of biotite, including grains from both types of porphyroblast as well as from the matrix, show the same composition without any zoning despite their association with cordierite and andalusite (see Thompson, 1976).

FAULTS

Two groups of faults are common in the Meguma Terrane of the Eastern Shore. The most apparent and most common are northwest trending and they greatly influence the topography of the area. Many rivers follow these faults and the numerous bays and strings of coastal islands are aligned parallel to them (Fig. 2). They come in all lengths from a few decimetres to tens of kilometres and, where a movement direction can be demonstrated, they are generally transcurrent and commonly sinistral. They formed under brittle to brittle-ductile transition conditions and are the youngest regionally important structures known in the area.

The second group comprises less obvious brittle-ductile faults or shear zones. In the area of interest the zones are mostly northeasterly trending, but the largest example, the Cobequid-Chedabucto Fault just to the

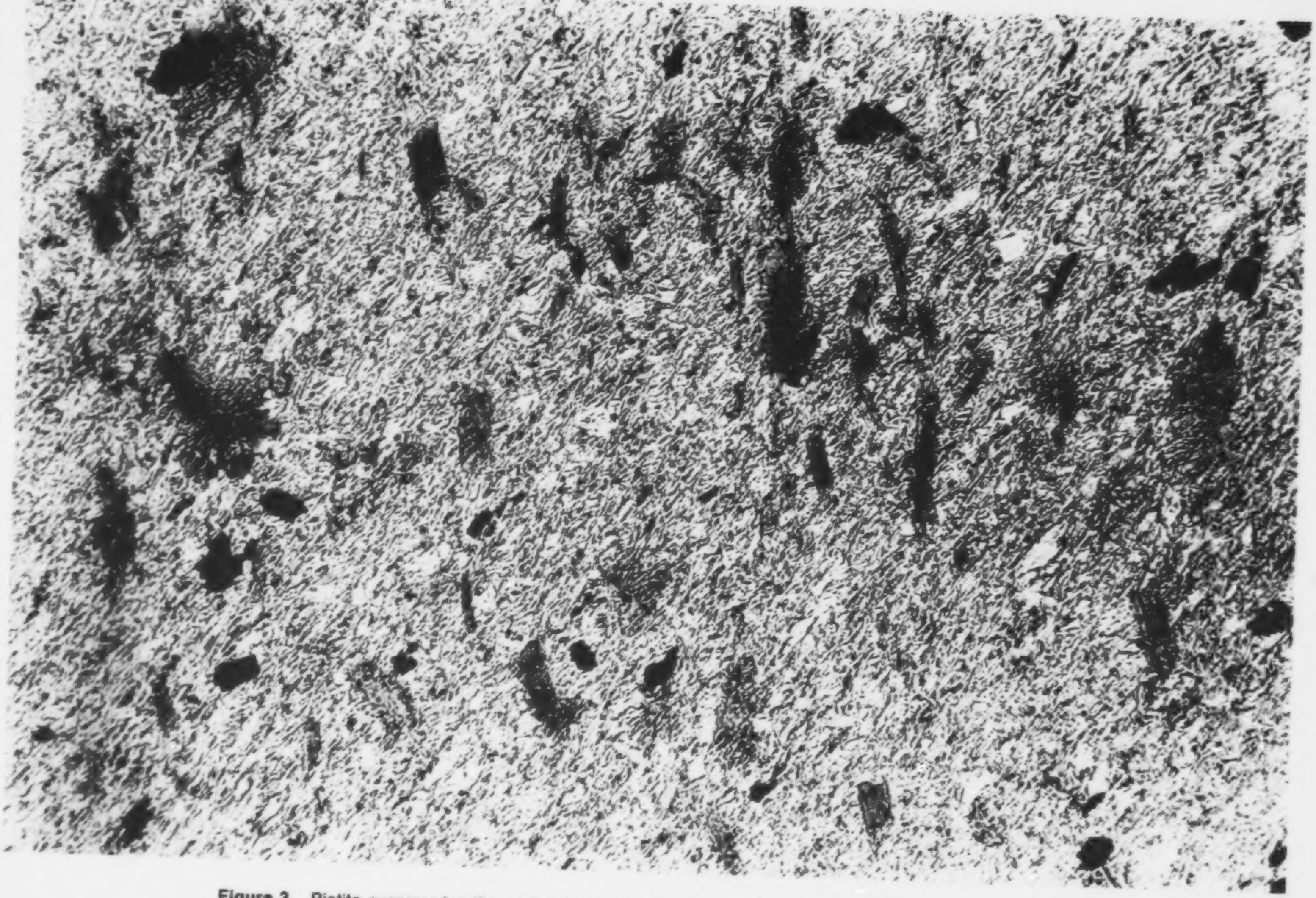

Figure 3. Biotite overgrowing the regional foliation (S_1) in the Goldenville Formation close to the contact with the southern side of the Halifax Formation at Ship Harbour. The biotite shows a preferred orientation about a line trending slightly west of north and S_1 trends approximately northeast. The horizontal edge of the photograph represents a length of 3 mm. Crossed nicols (GSC 205075).

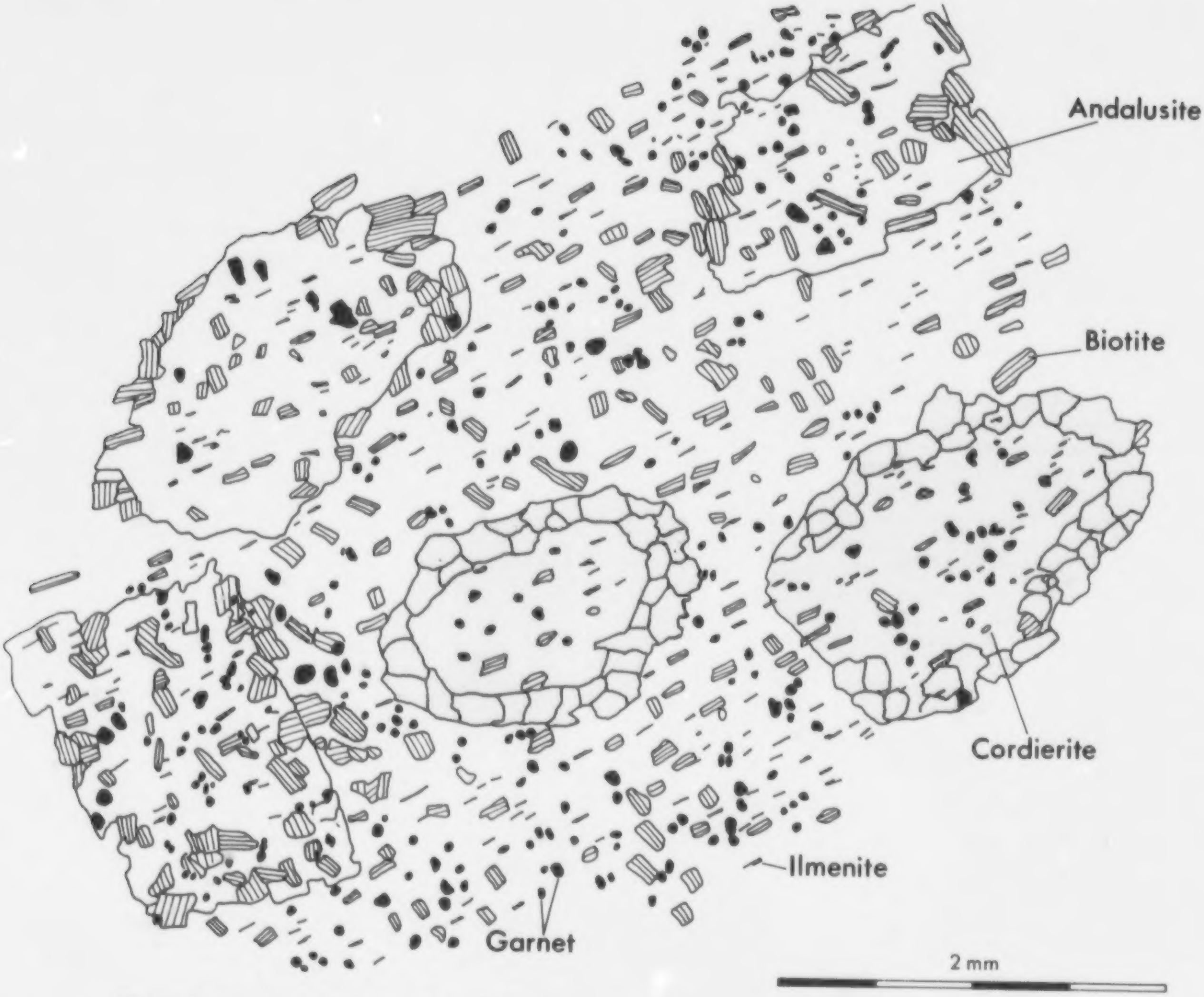

Figure 4. Specimen from the Goldenville Formation, close to the contact with the Musquodoboit pluton in Ship Harbour, showing three generations of biotite: (1) The oldest is preserved in the cordierite porphyroblasts as well as in the matrix and defines a foliation trending approximately northeast; (2) The next generation has a preferred orientation approximately perpendicular to the early foliation; (3) The youngest is less well oriented, is coarser on average, and is associated with the andalusite.

north of the area, is east-west striking. These faults are generally described as transcurrent and it is certainly true that the Cobequid-Chedabucto Fault is primarily a transcurrent ductile fault (Eisbacher, 1970; Keppie, 1982b; Mawer and Williams, 1986; Mawer and White, 1987). The northeasterly striking shear zones in the area of interest, however, are primarily dip-slip features though some also show transcurrent components of movement. There is a definite correlation between these structures and gold occurrence.

We describe the two groups of faults in more detail below under separate headings.

Northwest-trending faults

In outcrop these faults occur as single vertical to steeply dipping fractures, as zones of tension gashes, which may be discrete (Fig. 5a,b) or linked by a through-going fracture (Fig. 5d), and as zones of kinks and kinkbands (Fig. 5i). Where some of the long faults cut the coast there are zones of kinking that are several metres wide. For example, a minor fault marked by a 4 km long aerial photograph lineament outcrops approximately 1 km east of the eastern head of Ship Harbour (Black Point) and comprises a 10 to 20 m wide zone of kinks, kinkbands, and minor faults.

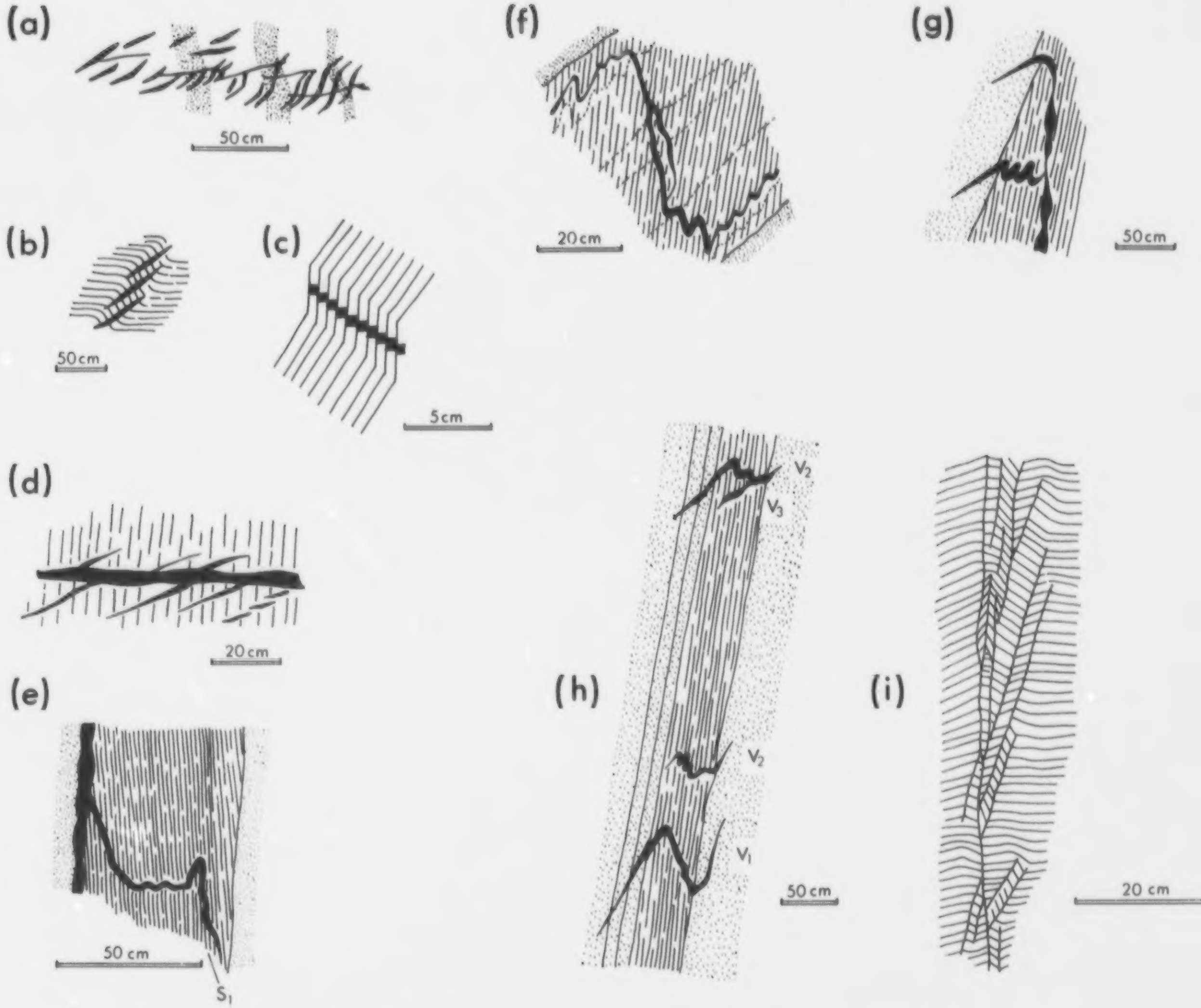

Figure 5. Various quartz veins all shown in solid black. Sandstones are represented by stippling and S_1 is represented by closely spaced parallel lines. (a to d) Veins related to northwest-trending brittle faults. (a, b) Tension gashes. (c) A vein in a fault-related kinkband. The vein has been segmented by slip on the kinked foliation (S_1). (d) Thick vein infill in a sinistral fault. The fault displaces S_1 and older tension gashes. (e) Bedding-parallel vein, at the contact between two Bouma graded beds, with a deformed "feeder" vein. (f) Discordant segment of a bedding-parallel vein. The vein persists, parallel to bedding, for several metres on either side of the sketch. (g, h) En échelon veins in pelitic beds. The veins show various amounts of shear reflecting differences of age. The relative ages for a given bed are indicated by V1 to V3. (i) Kinkbands associated with a minor northwest-trending fault. The fault is strike-slip and the sense of movement probably sinistral.

The tension gashes are generally vertical to steeply dipping indicating that the movement vector was generally horizontal, but locally there is evidence of minor dip-slip movement also. The fractures are mostly quartz-filled and some of the faults are marked by quartz-matrix breccia zones that can be a few decimetres thick.

Sinistral movements predominate, but, as was already evident in 1896 from maps of Tangier Mine (Faribault, 1896, 1927, 1928), both sinistral and dextral movements occur. In mesoscopic outcrop the faults tend to occur in dextral or sinistral spatial groupings.

At the regional scale the faults are very clear on the vertical gradient maps (Geological Survey of Canada, 1985, 1986a), locally appearing, on the map, as sharp features suggesting a single fracture, whereas elsewhere they are seen to be broad regional kinkband structures; both variants can be found along the trace of a single fault. It is possible to recognize a similar variation in their sharpness on a much smaller scale, in outcrop.

These faults are common in the granitoids, where they occur only as brittle features. They are therefore relatively young structures and in fact are known to displace Triassic or Jurassic dykes elsewhere in the region (Keppie, 1979). We interpret them as transfer faults (Gibbs, 1984) associated with the opening of the Atlantic Ocean. It has been suggested that one of these faults, the Canso Fault, was active in Devonian times (McCutcheon and Robinson, 1987). However, this interpretation is based on the assumption that it is the same age as the Oak Bay Fault in New Brunswick, which has been interpreted by Stringer and Burke (1985) as having first been active in Middle Devonian times. Interpreting the two faults as coeval is reasonable, but Stringer and Burke's (1985) interpretation relies on the assumption that the Oak Bay Fault is purely transcurrent. However, a slight dip-slip component, such as we observe locally in minor faults of this group, makes it possible to interpret the Oak Bay Fault as post-Devonian. A younger limit is placed on the fault by the fact that it does not appear to displace a Late Triassic-Early Jurassic dyke of the suite generally cut by the northwest-striking faults (Stringer and Burke, 1985). This would be consistent with the faults and dykes being approximately coeval and is therefore consistent with our interpretation of the faults as Atlantic Ocean-opening transfer faults.

Within the area considered, the northwest-striking faults are abundant. Small examples are commonly only a few metres apart and locally even closer together. Where there are no markers to demonstrate displacement the faults have the appearance and frequency of ac joints and in fact it is quite probable that they initially developed as such. However, where there are suitable markers practically all of the "joints" appear to have been activated as faults. Displacement on the small faults is commonly only a few millimetres or centimetres. Faults of the same orientation with horizontal separations of hundreds of metres occur on an average spacing of less than 10 km (Fig. 2).

The large fault passing through Taylor Head and Mooseland shows a change in horizontal separation from sinistral to dextral back to sinistral along its length; this can be explained by adding a dip-slip component to the fault and assuming that the direction of dip of the markers varies along the length of the fault (Fig. 6a). It can also be explained, however, by invoking the presence of listric normal faults (Fig. 6b). Such faults do occur in the region (Hutchinson et al., 1988) and are generally (e.g. Lister et al., 1986) associated with transfer faults. We have no direct evidence of their existence in the area that we have mapped, but have observed horizontal faults in Beaver Harbour, farther to the east, where the hanging wall has moved to the east.

The only deformed grains of gold of which we are aware come from one of the northwest-trending faults at Tangier (A. McIntyre, pers. comm., 1987), indicating that the fault was active after gold emplacement. This could be interpreted as an indication that the ac veins were responsible for the introduction of gold and that younger faulting along the veins deformed the gold. Alternatively it might be argued that the faults were responsible for introduction of the gold (i.e. gold introduction was syntectonic).

Shear zones

Both Forest Hill and Cochrane Hill (Fig. 1) are situated within the zone of transposition associated with the Cobequid-Chedabucto Fault and have the structure of dextral transcurrent shear zones (Smith, 1983, 1984). Although the main movement in both cases is strike-slip there is evidence of local dip-slip components. In both mines the mineralization is concentrated in bedding-parallel leads which are transposed along with all other markers. The relationship between mineralization and shearing in these two areas is not clear. They could be coeval or the mineralization could be older and simply incorporated in the shear zone when the latter developed. At Forest Hill the leads have undergone a long history of stretching and folding so that if they were coeval with the shear zone they developed early enough in its history to have been affected by much of the progressive deformation. Despite the obvious differences in these possible interpretations, the geology of these two mines is not inconsistent with our interpretation of the origin of the mineralization. However, because we have done no detailed work in either mine, we will not comment further.

In the area that we have mapped, away from the direct influence of the Cobequid-Chedabucto Fault, the ductile faults are northeasterly trending. They are not ubiquitous like the northwest-trending faults and in fact are rare in much of the area. For example in an almost continuously exposed section from the Musquodoboit pluton in Ship Harbour to Borgles Island (Fig. 2, A-B), a distance of 12 km, we have recorded only one broad (ca. 0.5 km) shear zone adjacent to the granitoid and a second zone, just a few metres wide, on the coast. Both zones are near vertical and have a large dip-slip component of movement with the northwest side up.

Despite the paucity of shear zones along the well exposed coastline we find evidence of dip-slip shear zones at all of the mineralized mines and prospects that we have visited including Beaver Dam, Caribou, Fifteen Mile Stream, Goldenville, Harrigan Cove, Lake Catcha, Lake Charlotte, Mooseland, Moose River, Port Dufferin, and Tangier (Fig. 1). We do not see shear zones outcropping in all of these areas, but although there is no outcrop there are rocks on the mine dumps that have a microstructure characteristic of outcrops found only within shear zones. We interpret this as an indication that shear zones were intersected by the mines.

The shear zone rocks are typically and consistently well foliated and have a strong mineral lineation (seen nowhere else) defined by elongate porphyroblasts and locally by porphyroblasts and related pressure shadows. Wherever the shear zones outcrop, their foliation (S_2) is steeply dipping and generally parallel to bedding, and their lineation is steeply plunging. Where shear zone rocks are found on the mine dumps, we are able to infer that

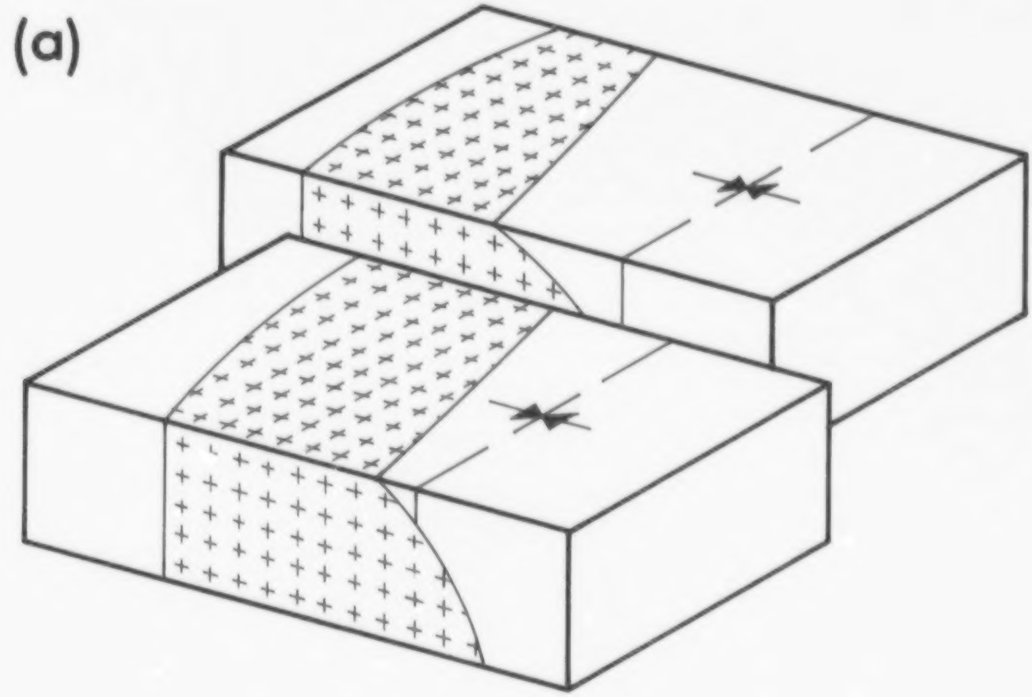

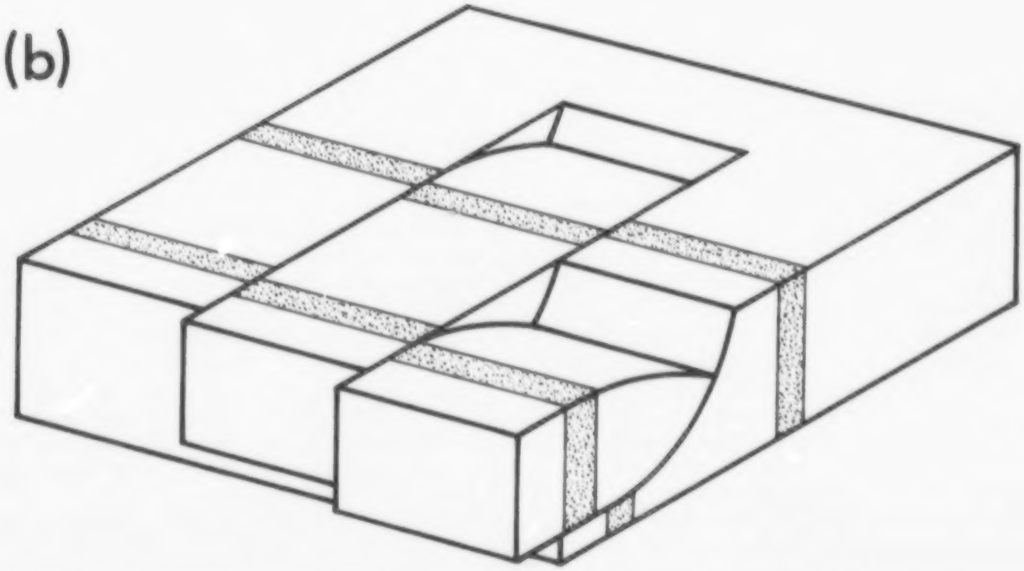

Figure 6. Variation in the apparent sense of movement on strike-slip faults due to: (a) the effect of a vertical component of movement on variously dipping markers; (b) the presence of detachment faults that terminate at the strike-slip (transfer) fault.

the lineation was steeply plunging, because it is approximately perpendicular to the bedding/cleavage intersection lineation which in outcrop, consistently has a shallow plunge. Where outcrop is good, as in Ship Harbour, it can be seen that the shear zone foliation is a new surface that overprints the regional foliation. It is very well developed in the more pelitic beds and, at best, only weakly developed in the psammites. In Ship Harbour, for example, bedding dips steeply, and cleavage in the pelites (S_2) dips one way whereas cleavage in the psammites (S_1) dips the other, producing a herringbone pattern with bedding parallel to the "backbone". Rotated porphyroblasts associated with the new foliation indicate northwest-side-up movement at this particular locality, with the granitoid on the upthrown side.

The porphyroblasts that define the lineation have been shown to be synkinematic with the development of the shear zone foliation (Hy and Williams, 1986). At Beaver Dam the porphyroblasts are mainly biotite and andalusite, at Lake Charlotte they are mainly cordierite, and at Mooseland they are mainly biotite, plus a little cordierite away from the anticline. All are a product of contact metamorphism related to the granitoids. Figure 7 shows an example of synkinematically rotated cordierite in a shear zone north of the Musquodoboit pluton at Lake Charlotte. The specimen is viewed looking easterly so that the pluton is on the upthrown side of the shear zone, as it is at Mooseland, which is similarly located (Fig. 2). At Beaver Dam, less than 750 m east of the River Lake Pluton, there is also a shear zone, and the pluton is again on the upthrown side.

Thus the sense of movement on the shear zones varies, depending on whether the shear zones lie north or south of the plutons, and the plutons are consistently exposed on the upthrown side.

At Caribou, Lake Catcha, and Tangier the downdip lineation is defined by carbonate porphyroblasts and aggregates of chlorite. From their localized distribution we surmise that the carbonates are a product of metasomatism along the faults (paper in preparation by authors). Figure 8 shows an example of a rotated ankerite porphyroblast in a specimen collected from the dump at Caribou Mine.

We have not looked at samples from the other mines in the same detail that we have examined samples from the six mine sites referred to in the previous three paragraphs. However, our preliminary examination indicates that the shear zone fabric, on all of the sites that we have visited, is the same as the contact or carbonate porphyroblast fabrics described above. The only difference between the two types is in mineralogy; we detect no differences in the structure or microstructure. Thus we suggest that all of the shear zones are of common origin and that the mineralogical differences simply reflect differences in contact metamorphic grade (paper in preparation by authors). This implies that all of the shear zones are coeval with the granitoids and suggests that the carbonate metasomatism may also be coeval and indirectly related to the granitoids.

The area mapped seems unusual in that the shear zones are predominantly dip-slip rather than transcurrent zones; the latter are common throughout the northern Appalachians (Webb, 1969; Anderson, 1972; Bradley, 1982; Johnson and Wones, 1984; Leger and Williams, 1986, 1988; Ludman, 1986; Mawer and White, 1987) and are also reported from the Meguma (Eisbacher, 1970; Benson, 1974; Keppie, 1982b; Mawer and Williams, 1986; Hwang and Williams, 1988). There are, to our knowledge, no major strike-slip shear zones in the area that we have mapped. However, we do find evidence of minor strike-slip movement and it is commonly, but not always, sinistral.

For example, within the Ship Harbour shear zone there are ductile and brittle faults, concentrated in the pelites, that displace vertical ac veins horizontally in a sinistral sense. In one outcrop, slickenside striae indicate that the movement was truly transcurrent and not just oblique. The faults and shear zones are steeply dipping and parallel to bedding as far as they can be followed. Displacement on the faults cannot be determined, due to the narrowness of the roadcut, but one shear zone, less than 10 cm wide, has a displacement in excess of 40 cm.

Similarly, in outcrops at Mooseland, vertical veins with an approximate north strike are displaced horizontally. In steeply dipping psammitic beds the veins are at a high angle to bedding, and are folded. In the intercalated pelitic beds they are rotated anticlockwise, are acutely inclined to bedding, and are boudinaged indicating that there has been sinistral shear parallel to bedding.

Not all of the strike-slip movements are sinistral. Some bedding-parallel veins are boudinaged with a steeply plunging boudin axis indicating horizontal extension. Such extension is compatible with transcurrent shear, and on Taylor Head boudinaged veins are anticlockwise of bedding indicating dextral movement. Mawer (1987) has also reported evidence of dextral offset in bedding-parallel veins and according to his interpretation offset developed during emplacement of the veins, during the late stages of folding.

VEINS

Various types of veins have been recognized and different mechanisms have been suggested for their emplacement. There are the "bedding-parallel" veins which have previously been interpreted as syngenetic geyserite deposits that were subsequently modified by metamorphism (Haynes, 1983, 1987). We agree with Henderson (1983) and Mawer (1985) and find this an untenable interpretation for several reasons, not least of which is the fact that the bedding-parallel veins quite commonly bifurcate or "jump", by means of a short discordant segment, from one bed to another (Fig. 5f). We therefore do not consider the hypothesis of a syngenetic origin further. There are two types of bedding-parallel veins with one type interpreted as crack-seal veins emplaced prior to, or during, folding and regional metamorphism (Malcolm, 1929; Graves and Zentilli, 1982; Henderson, 1983;

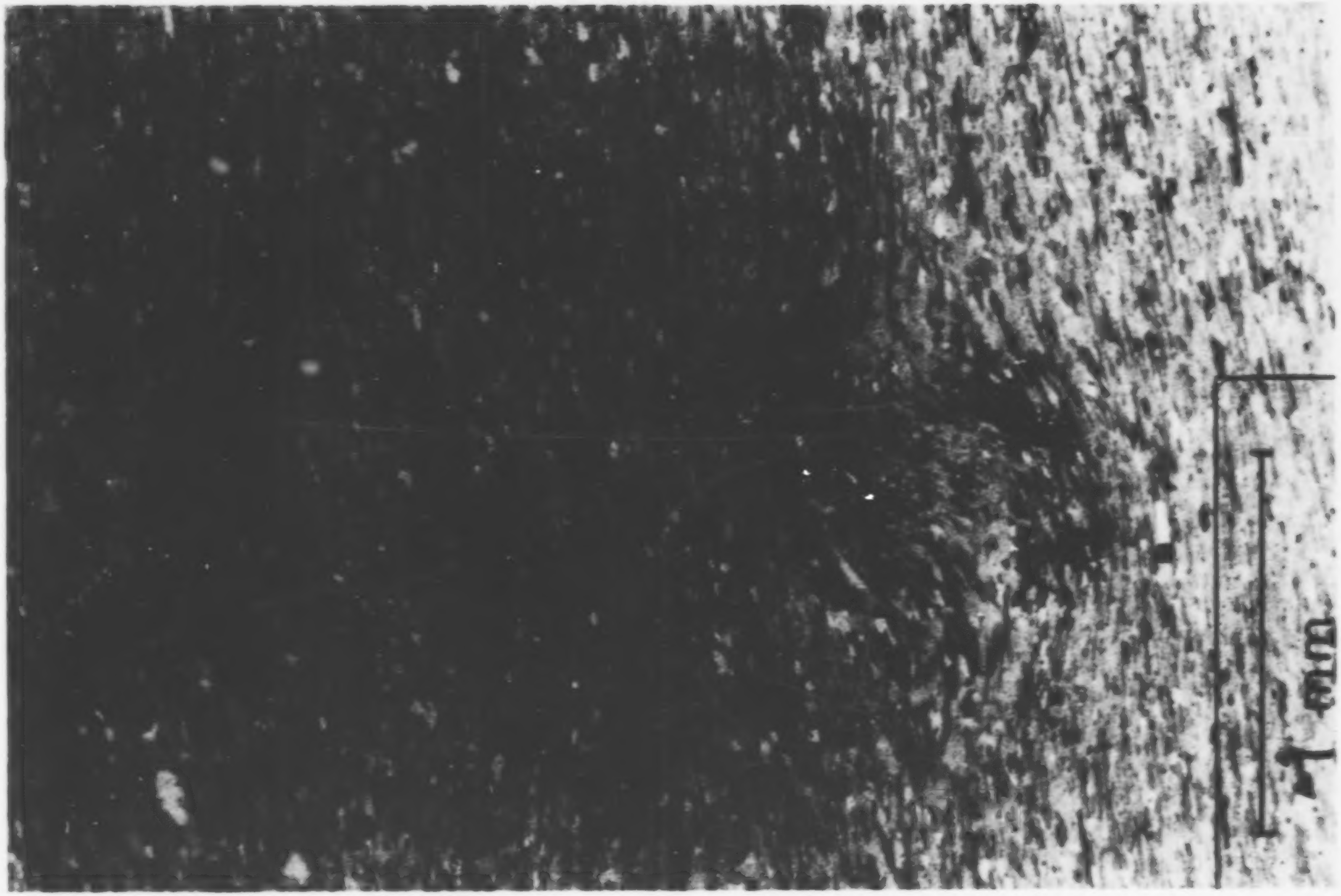

Figure 7. Rotated cordierite porphyroblasts. Foliation is steeply dipping and is defined by biotite and muscovite. The photograph is viewed looking east and rotation is anticlockwise indicating south side up. See text for discussion. Plane polarized light (GSC 205075-E).

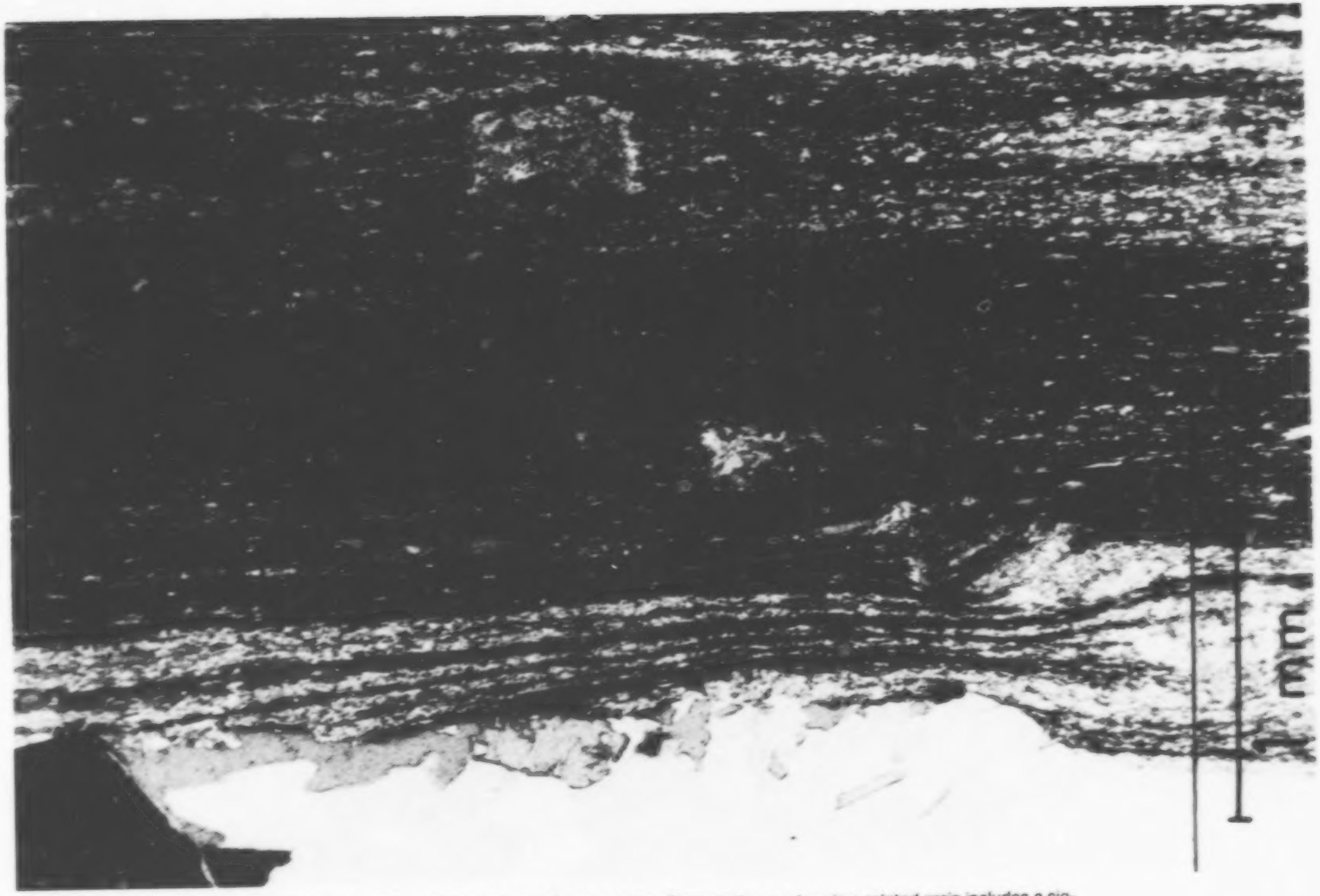

Figure 8. Synkinematic ankerite from Caribou Mine. Close to the quartz vein a rotated grain includes a sigmoidal foliation. Plane polarized light (GSC 205075-D).

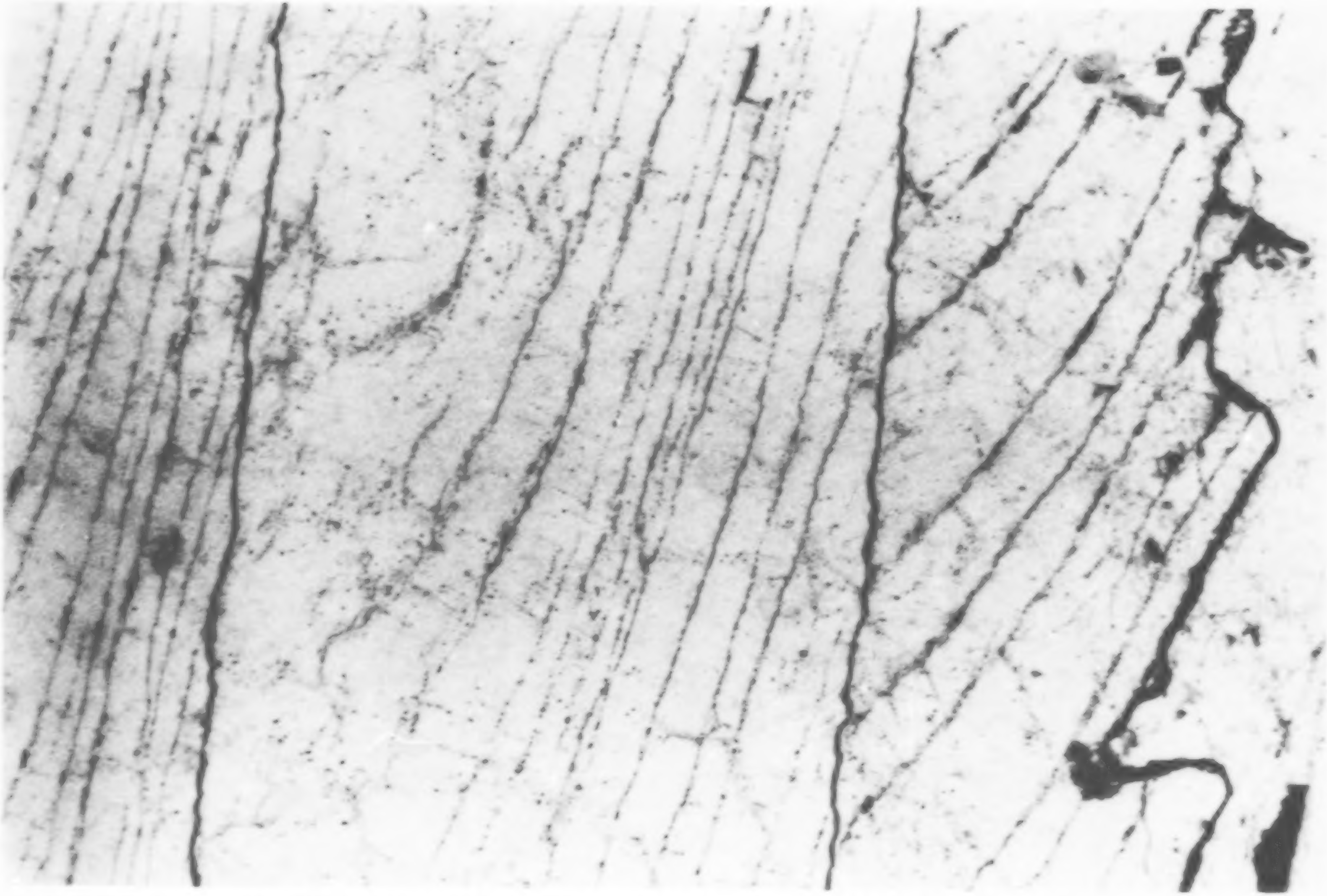

Figure 9. Quartz vein showing curved inclusion bands (numerous faint lines) and stylolites (three dark lines trending north/south). Horizontal edge of photograph represents 1 mm. Plane polarized light (GSC 205075-C).

Mawer, 1985, 1987; O'Brien, 1985; Henderson and Henderson, 1986; Henderson et al., 1986). The other, referred to as the saddle reef type, is different in appearance to typical bedding-parallel veins. Members of this group are interpreted to have been emplaced in a single pulse into the fold hinges late during or after folding (Faribault, 1896, 1897, 1903; Keppie, 1976).

Henderson (1983), Henderson and Henderson (1986), and Henderson et al. (1986) have described two types of discordant veins. One, referred to as en échelon veins, occurs mainly in pelitic layers and shows a variety of morphologies consistent with formation during folding. The folds are assumed to be flexural slip structures and the veins are interpreted to be tension gashes, related to the flexure-induced shear in the incompetent layers (Henderson, 1983; Henderson and Henderson, 1986; Henderson et al., 1986). The second type comprises ac veins related to the regional folding.

Largely following earlier workers, we recognize the following seven types of veins, distinguishing them on the basis of their morphology, relationship to bedding, and overprinting relationships. We indicate whether or not they are gold-bearing:

1) Early discordant veins. Not generally gold-bearing but gold has shown up in an assay of rock containing such a vein at Beaver Dam (Mine geological staff, pers. comm., 1986). However, how and exactly where the gold occurred is not known.
2) Bedding-parallel folded veins. The main gold leads.
3) En échelon veins. Gold is reported by Hedley (1941) in what Henderson and Henderson (1986) interpret as en échelon veins.
4) Saddle reef veins. Generally barren, but locally gold-bearing (e.g. Dufferin Mine, Malcolm, 1929).
5) ac veins. Generally poor in gold.
6) Late discordant veins. No gold.
7) Breccia veins. No gold.

Along the coast we found large areas where veins are very rare and generally thin. In such areas the abundant ac joints, for example, are open and commonly have displacement on them, but generally lack vein filling or are only partially filled with well terminated crystals projecting into an open vein. There are even larger areas where the only veins observed are very thin ac veins. In areas where veins are developed, however, it is remarkable that a variety of types commonly occur together. This suggests that all of the veins were intruded together or that the same channelways have been used repeatedly for emplacement of vein material.

The following paragraphs give a brief description of the general characteristics and overprinting relationships of each group.

1) Early discordant veins are generally < 1 cm thick, and can occur anywhere in the folded sequence; they show no preference for regional fold hinges. They are commonly tight to isoclinally folded with the regional S_1 cleavage parallel to their axial plane, and wavelengths and amplitudes are generally less than 1 cm and 0.5 cm respectively. They are cut by bedding-parallel, en échelon, and ac veins. No overprinting relationships have been recorded between them and the remaining veins, but because the latter can all be shown to overprint the bedding-parallel veins, the early discordant veins are the oldest group that we recognize. Microscopically they are strongly deformed and recrystallized to a foam texture. In rare instances there is a suggestion of the inclusion bands typical of crack-seal veins (Ramsay and Huber, 1983) but recrystallization is too pervasive to be sure of this microstructure.

2) Bedding-parallel veins, in general, are spatially related to anticlines and therefore occur in association with the saddle reef veins. The two, however, are generally easy to distinguish in that the bedding-parallel veins are rich in inclusions, dark in colour, and long and narrow, whereas the saddle reef veins are very white, and tend to be thick and locally crescent-shaped. The bedding-parallel veins are locally deformed, being folded, particularly in regional fold hinges, and boudinaged. The boudins commonly indicate horizontal extension which may or may not be combined with vertical extension. Locally they have spurs or "feeder" veins that are strongly discordant and, on regional fold limbs, these segments of the veins are generally folded (Fig. 5e).

These veins have a complex microstructure indicating that they developed as composite veins filled by many pulses of quartz. They are overprinted by the breccia, ac, and saddle reef veins. At Mooseland, for example, a bedding-parallel vein is partially (on one limb of the fold but not the other) contained within a saddle reef type vein. The latter encloses the bedding-parallel vein and also cuts through it so that the bedding-parallel vein has a boudinaged appearance. An anomalous observation was made at Mooseland where a composite bedding-parallel vein cuts through an ac vein.

As indicated above, these are the veins in which most of the gold occurs. They have recently been described in detail by Mawer (1985, 1987) and Henderson and Henderson (1986), and our observations are generally in agreement with theirs. Bedding-parallel veins are locally rich in inclusion bands of very fine grained mica, opaque phases, and locally chlorite. The bands are commonly parallel to the vein walls, but locally are clearly discordant and in such veins are generally curved (Fig. 9). The bands are commonly truncated by several generations of vein-parallel stylolites suggesting compression perpendicular to the vein walls (Mawer, 1987 and Fig. 9). This interpretation is strengthened by the presence of healed extension fractures, marked by fluid inclusion trails, approximately perpendicular to the stylolites (Mawer, 1987) and by larger fractures now occupied by clear white quartz. Such areas of clear quartz have the appearance of a small vein perpendicular to the host vein and completely contained within the latter. There are also less regular areas of clear quartz that surround single crystals of quartz that are rich in inclusion bands (Fig. 10). These clear quartz grains are not a product of recrystallization but are due to emplacement of new quartz, as can be shown, where locally, the fluid inclusions in adjacent examples of the two types of quartz have different compositions (paper in preparation by C. Hy). Large

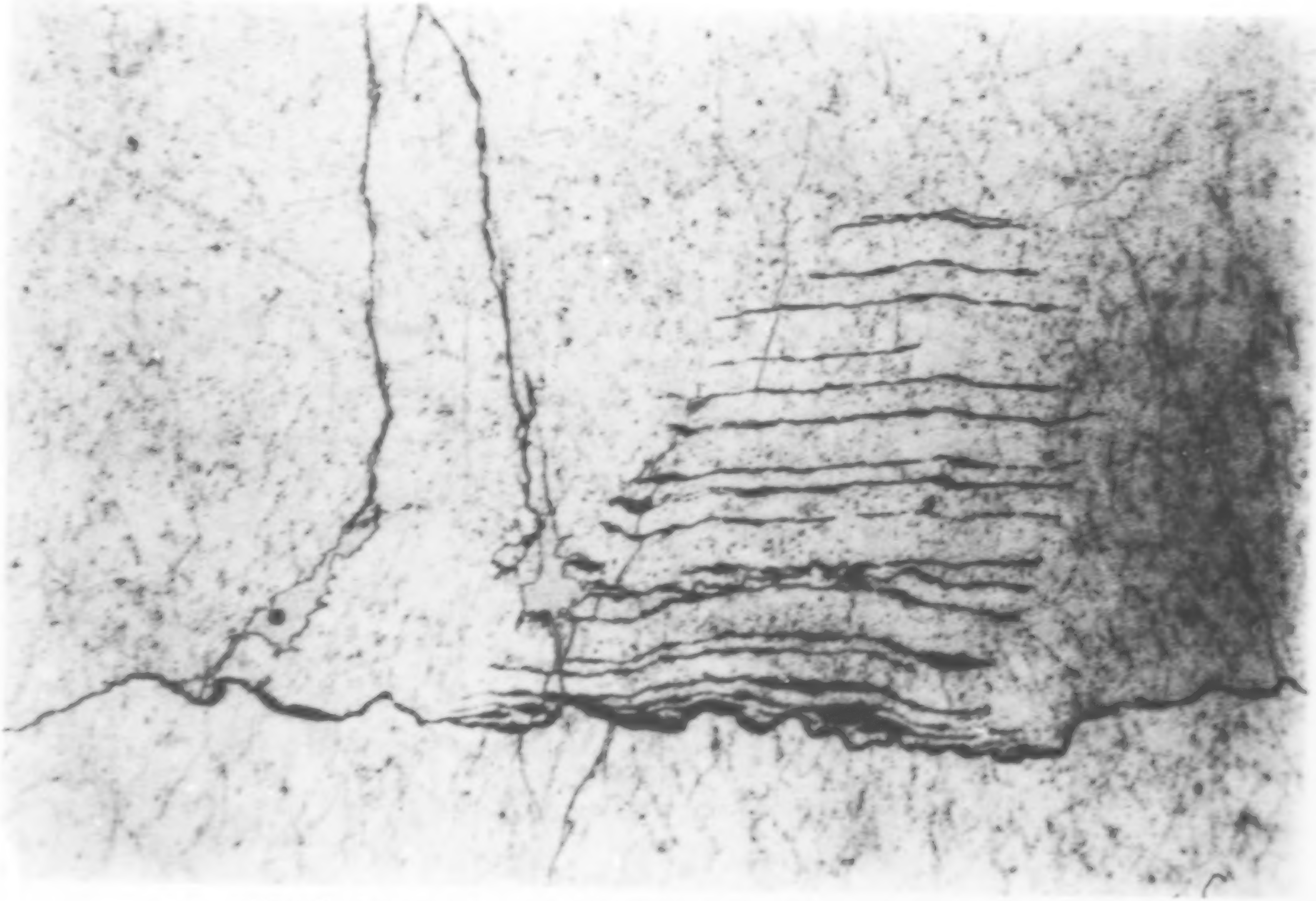

Figure 10. Crack-seal vein segment with inclusion bands surrounded by massive quartz free of inclusion bands. Note that the inclusion bands are locally stylolitized. Horizontal edge of photograph represents 1.2 mm. Plane polarized light (GSC 205075-B).

cavities (up to ca. 4 cm) can also be found in these composite veins, and in hand specimen the veins typically have a mottled appearance due to alternation of the dark inclusion-rich quartz and white inclusion-free quartz. The white quartz shows no evidence of having been deformed. The late white quartz cannot be distinguished from the saddle reef quartz and in fact could be from the same source. Locally this can be demonstrated where the late quartz in a composite bedding-parallel vein is continuous with a saddle reef vein. Carbonate is a major constituent of some veins and is consistently a late fracture filling in the older quartz (Fig. 11) and locally in arsenopyrite. This is consistent with our suggestion that the carbonate is introduced late, along the shear zones.

Not all bedding-parallel veins are composite, with stylolites, fractures, and alternating patches of white and dark quartz. In our experience such composite veins are common where gold has been found and occur nowhere else. Away from the gold, the bedding-parallel veins may be crack-seal types or may be composed of recrystallized polygonal grains with locally preserved crack-seal or palisade microstructure.

As noted by Mawer (1987), the bedding-parallel veins display two types of microstructure: microstructures resulting from vein growth, and microstructures resulting from subsequent deformation. The secondary deformational structures, including recrystallized polygonal aggregates, are developed wherever the veins are tightly folded or boudinaged. In the planar limbs of regional folds, the primary structures are best developed and weak undulose extinction may be the only evidence of post-vein deformation on the scale of individual grains. It is significant that these veins are not everywhere deformed because it indicates that at least some of these veins formed late in the folding history. It also indicates that the lack of small parasitic folds in the veins on the limbs of larger folds, is a primary feature and not due to late unfolding of early-formed folds.

3) En échelon veins as stated above, occur mainly in pelitic beds and are found only on fold limbs, being related to the bedding-parallel shear resulting from flexural slip folding. They are emplaced as tension gashes at about 45° to bedding, and, as they rotate progressively in response to shearing, they fold and then unfold and/or boudinage (Henderson, 1983; Henderson and Henderson, 1986; Henderson et al., 1986). All stages of this deformational history can be found in one planar segment of a pelitic bed, indicating that the veins were emplaced at different times during the folding, probably throughout the folding history (Fig. 5g,h). They are overprinted by ac, late discordant, and brecciated veins. Their relationship to bedding-parallel veins is unclear; we have not seen any overprinting relationships but the "feeder" spurs of the bedding-parallel veins, described above, have the same distribution and same morphology as the variously deformed en échelon veins. This suggests that the two may be contemporary or overlapping at least. We have not observed undeformed spurs whereas undeformed en échelon veins do occur. The spurs are rare so that our sample may not be fully representative. If it is, however, it indicates that emplacement of the en échelon veins continued later than emplacement of bedding-parallel veins.

Microstructurally, these veins are mostly composed of clear quartz that lacks solid inclusions. The quartz grains are generally elongate and define a shape fabric parallel to S_1. Various intensities of deformation are recorded in microstructures that vary from undulose extinction, through core and mantle structure, to completely recrystallized polygonal aggregates. There is a rough positive correlation between the intensity of deformation indicated by the microstructure and the intensity of deformation indicated by mesoscopic folds and boudinage. In some veins, sparse quartz grains that appear green in hand specimen contain inclusion lamellae parallel to the vein wall. In one vein there is a single grain thick, discontinuous selvedge of such crack-seal grains on either side of a vein composed otherwise of clear quartz.

4) Saddle reefs occur only in anticlinal hinges and were observed at Dufferin Mine (Malcolm, 1929), Harrigan Cove, Mooseland, and at the tip of Taylor Head. They are composed of coarse grained white quartz which is free of solid inclusions but contains large fluid inclusions. Extinction is usually only very weakly undulose and grain boundaries are straight.

In very localized areas these veins do show optical evidence of deformation which varies in intensity. At the low end of the spectrum it is marked by strong undulose extinction, greater intensity is marked by serrated boundaries with nucleating new grains in the bulges, and finally the most intensely deformed grains have a core and mantle texture. Despite the local recrystallization, the intensity of deformation observed in these veins is, in general, significantly less than that observed in the three types of veins described above with the exception of some composite veins.

The saddle reef veins are cut by ac and brecciated veins. No relationship with the late discordant veins was observed.

5) ac veins are widespread and fairly common. They show no preference for position in the regional structure and cut through pelites and psammites alike (cf. Henderson and Henderson, 1986). They are commonly only a few millimetres thick, but scattered throughout the area are decimetre-thick ac veins that persist across strike for tens of metres.

It is not clear whether the veins are related to ac joints (sensu stricto) or to the northwest-striking faults which probably originated as joints and were later activated as faults. However, we draw attention to the following observations: (i) some of the veins occupy what are still joints (sensu stricto); (ii) where there is clear displacement involved the veins commonly occur as tension gash arrays, with individual veins approximately vertical, rather than as a single fault-parallel vein (Fig. 5a); (iii) some ac veins are brecciated, suggesting postvein faulting; and (iv) a northwest-striking fault just north of Ship Harbour outcrops on the coast as a zone of asymmetrical kinkbands

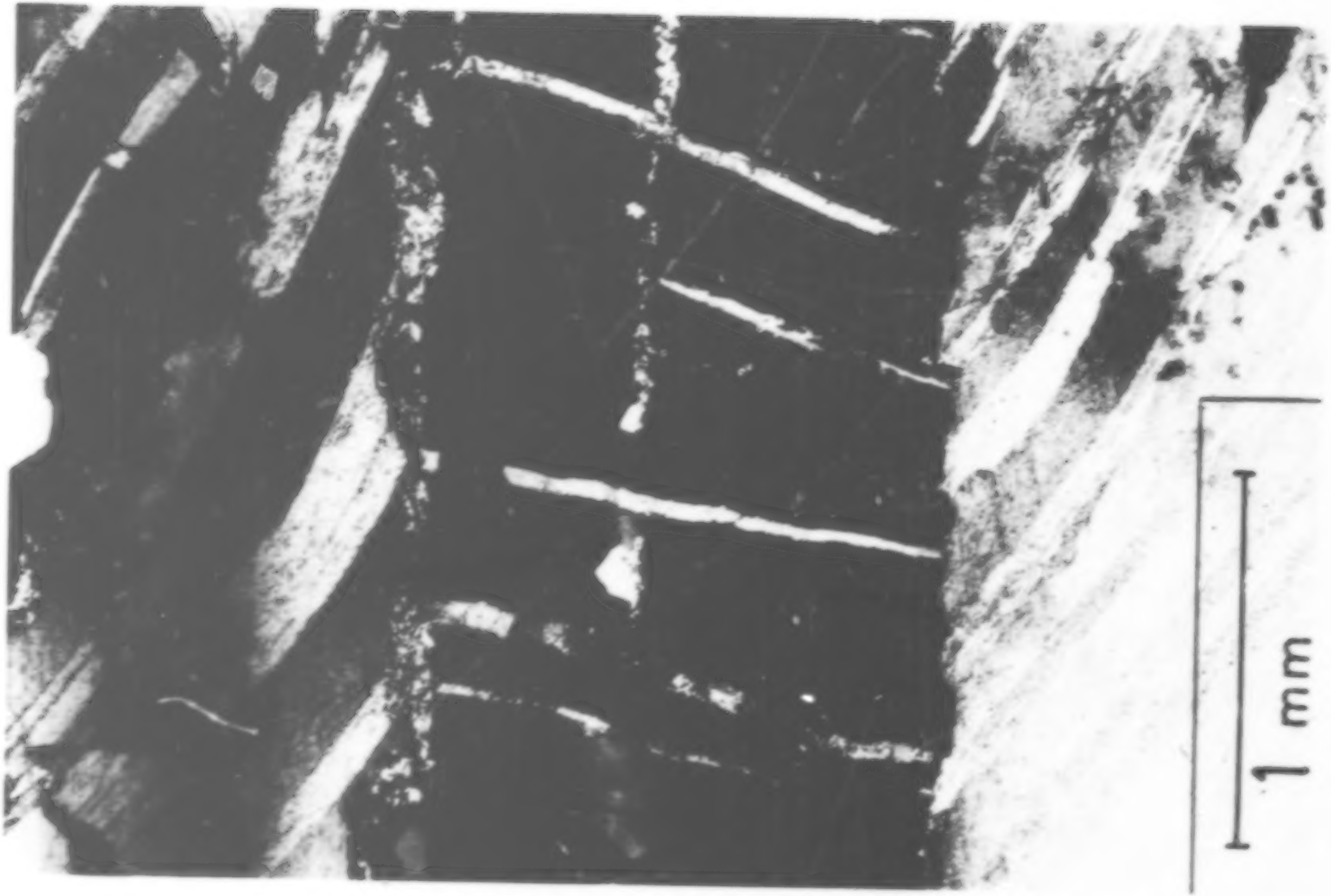

Figure 11. Mixed calcite and quartz vein with calcite filling cracks in the central quartz portion. Crossed nicols (GSC 205075-A).

and minor faults. S_1-parallel slip associated with development of the kinkbands is seen to deform ac veins which are parallel or approximately parallel to the kinkbands (Fig. 5c). We thus consider it probable that there are two generations of veins associated with the ac structures: an early one that invaded the ac joints, and a younger generation that is not strictly an ac vein set but a set of tension gash arrays associated with transcurrent faulting parallel to the joints. Further work is required to clarify this point.

The quartz in the veins is commonly deformed, and undulose extinction, serrated boundaries, and incipient recrystallization are widespread. Less common are core and mantle structure and complete recrystallization to equant grains. The quartz grains are commonly elongate and define a steeply plunging lineation.

6) Late discordant veins are approximately horizontal and show no preference for position with respect to the regional structure. They cut through pelites and psammites alike and show no signs of mesoscopic scale deformation. In thin section, the quartz grains are prismatic and elongate in the plane of the vein such that they define a weak east-northeast-trending lineation. The grains have straight boundaries that are perpendicular to the vein wall and show no evidence of significant deformation.

7) Breccia veins strike approximately 160 to 170° and show no relationship to the regional structure. They comprise angular fragments of the wall rock in a matrix of quartz and commonly have a stockwork appearance between fairly planar outer boundaries. They are consistently oriented clockwise of the northwest-striking faults and appear to be spatially related to the more strongly developed faults. On Borgles Island, for example, one such vein strikes 017° and converges on a vertical fault zone striking 147°; however, the outcrop ends before they actually intersect. Offsets on minor splays and a general bending of S_1 into the fault both indicate that the fault movement vector has a horizontal dextral component; the vein in this example could therefore be interpreted as a tension gash-type splay related to dextral faulting.

In thin section these veins are composed of large prismatic crystals which have euhedral terminations, locally in vugs. There are many inpurities along the grain boundaries and many of the veins are pink. They have a different mineralogy than any of the other veins, as can be seen from Table 1. We have seen no evidence of plastic deformation of the breccia veins, but there is some younger, very localized, brittle deformation.

MINERALOGY AND FLUID INCLUSION CHEMISTRY OF THE VEINS

The mineralogy of the veins is simple and, with the exception of the breccia veins, shows little variation (Table 1). The main minerals present are quartz, albite-andesine, chlorite, biotite, arsenopyrite, apatite, and zircon. The latter are rounded and presumably derived from the country rock. Some variations in mineralogy are related to proximity to the granitoids and are reflected in the country rocks. For example, in bedding-parallel veins from Mooseland, arsenopyrite and biotite are common both in the veins and in the country rock, because Mooseland lies within the biotite isograd. In bedding-parallel veins at Tangier, on the other hand, chlorite and carbonates are common in both the veins and the country rock and the carbonate is believed to have been introduced with fluids along the shear zone. There is no biotite, however, in either the veins or the country rock. These observations indicate that the veins must be pre- or syn-contact metamorphism.

Table 1. Mineralogy of the veins. Vein types: (1) early discordant; (2) bedding-parallel; (3) en échelon; (4) saddle reef; (5) ac; (6) late discordant; (7) breccia.

VEIN TYPES	1	2	3	4	5	6
MINERALOGY						
QUARTZ	x	x	x	x	x	x
CHLORITE	x	x	x	x	x	
BIOTITE	x	x	x		x	
WHITE MICA	x	x	x		x	
PLAGIOCLASE		x	x		x	
APATITE	x	x	x			
CARBONATE		x	x		x	
DIOPSIDE		x				
EPIDOTE			x			
GARNET		x				
GEDRITE		x				
SPHENE	x	x	x		x	x
TOURMALINE		x	x		x	
ZIRCON	x	x	x			
ZOISITE		x				
ARSENOPYRITE	x	x			x	
CHALCOPYRITE		o				
GALENA		o				
GOETHITE		x				
GRAPHITE	x					
HEMATITE	x	x			x	
ILMENITE	x					
MAGNETITE		x			x	
PYRITE	x	o			x	
PYRRHOTITE	x	x	o			
SPHALERITE		o				

x - observed.

o - reported in unpublished reports by P.K. Smith and D. Kontak, Nova Scotia Department of Mines and Energy, or reported by mine geologists.

We have made a study of fluid inclusions, but our data set is incomplete. For example, we have data for the bedding-parallel and en échelon veins, but not for the bedding-parallel vein spurs or "feeder" veins (which have very similar geometry to the en échelon veins). We also lack data for the breccia veins. Work to date indicates that a more detailed study is worthwhile and in this article we simply summarize our present results.

Two types of fluid inclusions have been recognized in most veins. There are inclusions that occur singly in undeformed vein quartz and there are others that occur in linear arrays which commonly cut across grain boundaries. We refer to these as primary (sensu Roedder, 1984) and secondary inclusions respectively. The secondary inclusions are interpreted to lie along the traces of healed cracks.

The composition of the primary fluid inclusions varies systematically, allowing us to combine the vein types into three groups: (1) The early discordant and crack-seal bedding-parallel veins have two types of two-phase (liquid plus gas at room temperature) inclusions. One comprises CO_2-filled inclusions and the other comprises saline H_2O-filled inclusions; (2) The inclusions in saddle reef veins and in clear quartz of bedding-parallel veins are three-phase (two liquids plus a gas) at room temperature and contain moderately saline mixtures of H_2O and CO_2; (3) En échelon, ac, and late discordant veins all have inclusions composed of saline H_2O and contain no CO_2.

Homogenization temperatures of primary inclusions indicate that all of the vein material was deposited from fluids at temperatures in excess of 300°C. These saline fluids were therefore all capable of transporting gold and thus capable of introducing the gold or of remobilizing it.

Secondary inclusions from all but the breccia veins were analyzed and found to be saline H_2O solutions that vary only slightly in composition. Their homogenization temperatures indicate generally lower temperatures of entrapment, but they are still in excess of 300°C, indicating the presence of fluids capable of transporting gold at the time that they formed. Thus, at least throughout the pre-breccia vein history of fluid inclusion development, the fluids were capable of depositing or remobilizing gold.

DISCUSSION

Timing of vein emplacement

The evidence presented above makes it possible to order the veins in terms of their relative ages. On the basis of overprinting alone, the oldest are the early discordant veins, followed by the bedding-parallel veins. Saddle reefs and en échelon veins are younger, but they cannot be dated relative to one another. Similarly, the ac, breccia, and late discordant veins are youngest, but cannot be dated relative to one another. The fact that en échelon veins are generally deformed whereas the saddle reefs are only very locally deformed strongly suggests that the en échelon veins are older than the saddle reefs. Similarly the ac veins are deformed whereas the late discordant and breccia veins are not, suggesting that the ac veins are the older of the three. However, this argument is equivocal because the ac veins are probably deformed by late transfer fault movement parallel to the veins and such deformation would not generally have affected the rock body between the veins. The deformation could therefore have occurred after emplacement of the late discordant and breccia veins. However, as a working hypothesis we assume that these two deformation arguments are correct and that the ac veins are older than the other two.

The fact that the saddle reefs are essentially undeformed suggests that they were emplaced after, or very late during the development of the folds. Folding of the early discordant veins and folding and boudinage of the bedding-parallel veins on the other hand indicates that they developed before or during the folding history. The variety of structures seen in the en échelon veins, even within a single pelite bed, indicates that the en échelon veins developed at various times during the regional folding history (Henderson and Henderson, 1986). The bedding-parallel vein spurs suggest a common origin for the bedding-parallel veins and the en échelon veins, but the fluid inclusion work indicates that the two constitute distinct groups. It may be that the spurs and en échelon veins represent veins forming coevally, in response to the same stress, from fluids of different origin. Alternatively both sets of veins may have formed during folding but at slightly different times, the spurs (and the bedding-parallel veins therefore) forming earlier and the en échelon veins forming later.

Henderson (1983), Henderson and Henderson (1986), and Henderson et al. (1986) have suggested that development of the bedding-parallel veins started before the development of the S_1 cleavage which they believe was pre-regional folding and involved at least 50 percent shortening (ibid). We agree that domainal slaty cleavages like S_1 are initiated before large-scale folding, but believe that, like crenulation cleavages, they continue to evolve throughout folding (Hobbs et al., 1976, p. 242; Williams and Schoneveld, 1981). Henderson et al. (1986) themselves refer to stretching parallel to the S_1 cleavage, during flexural flow associated with the development of the folds. Their evidence (ibid) for early development of S_1 is that "micas" in the inclusion bands are commonly aligned parallel to the length of the band and to the vein wall (cf. Mawer, 1987). They argue that the new grains are epitaxial on country rock grains and that their observation therefore indicates that the country rock foliation was parallel to bedding at the time of formation of the inclusions. This is a very reasonable argument if the micas are strictly parallel, but there are other possible explanations. First, even in the present slaty cleavage, except in areas of very large strain, the layer silicates in the quartz-rich domains (sensu Hobbs et al., 1976, p. 242) are parallel to bedding. Because of the orientation of the weak (001) plane these grains are the ones most likely to split away from the wall as each new crack-seal increment forms. The less mature the cleavage, the greater the percentage of layer silicate grains that would tend to be parallel to the vein wall. Thus it is conceivable that the inclusion bands could be mimicking a domainal slaty cleavage at some stage, including a late stage, in its development. Second, it is possible that the orientation of the layer silicates was modified by shear at the time of their growth in the veins. In the inclusion bands that we have seen, in which the layer silicates are oriented preferentially parallel to the vein wall, the preferred orientation varies from one band to another in a nonsystematic way. If the Henderson (1983) and Henderson and Henderson (1986) interpretation is correct we would expect, in a situation where the degree of preferred orientation varies, the preferred orientation to vary from bedding-parallel in the centre of the vein to cleavage-parallel at the margin of the vein. In fact some of the best cleavage-parallel orientations are observed in bands near the centre of the veins that are flanked on both sides by bands in which the preferred orientation is parallel to the vein walls.

Orientation also could be modified by the development of stylolitic seams along individual inclusion bands (Mawer, 1987). We observe many inclusion bands that have been modified in this manner. Where the seams are castellated they are obviously stylolitized, but such seams grade into almost planar ones that are not obviously stylolitic and these in turn grade into normal inclusion bands. Wherever stylolitization can be demonstrated the layer silicate grains are preferentially oriented parallel to the length of the seam and we interpret this as indicating rotation of the grains during stylolite formation. Where they grade into inclusion bands the layer silicates become progressively more inclined to the band.

Yet another possibility is inherent in recent descriptions by Cox (1987) of some interesting veins in which inclusion bands have developed during vein-parallel shear. He has shown that inclusion bands can grow lengthwise from steps in the vein wall such that the age of the inclusion band varies progressively along its length. In this situation the orientation of the layer silicates in the inclusion band depends essentially on whether the step is within a microlithon or a septum. Thus different steps can produce inclusion bands of different orientations and each band represents one parent grain rather than many grains of the same orientation.

Finally, secondary surfaces of deformational origin, in which the layer silicate grains are oriented parallel to bedding, are known to form during folding in layered rocks (Williams, 1972) and such surfaces would be natural places for veins to develop. We thus do not consider parallelism of layer silicate grains, inclusion bands, and vein walls to be compelling evidence for the age of the veins.

Mawer (1987) suggests that the bedding-parallel veins are late syntectonic, i.e. they developed after initiation of the regional folds. As evidence he cites the following facts: (1) They are generally associated with domal anticlines and not with synclines (Malcolm, 1929 cited in Mawer, 1987), suggesting a physical trap; (2) The veins are equally undeformed in the regional fold hinges as in the limbs and there is much undeformed vein material; and (3) Isolated, included fragments of country rock have the same cleavage and the same cleavage orientation as the adjacent country rock.

We agree with Mawer's (1987) interpretation and as further evidence add the following points: (1) We agree that the veins are commonly insufficiently deformed but in contrast to his observation we point out that, whereas bedding-parallel veins are locally undeformed in regional fold hinges, they are generally much more strongly and more periodically folded in regional fold hinges than in regional fold limbs. If the veins were present before cleavage development they should have undergone considerable shortening before the onset of regional folding (Hobbs et al., 1976, p.242; Henderson et al., 1986) and should therefore be much more uniformly folded on a small scale than they are (see Ramberg, 1964). On the other hand if they were emplaced after the initiation of the regional folds we would expect the observed distribution of small-scale folds. Our reasoning is that the veins would be in a vein-parallel shortening orientation in the regional fold hinges, throughout the history of folding, but in the limbs they would start in a less advantageous orientation for folding and would progressively rotate into a vein-parallel extensional orientation; and (2) The spurs or "feeder" veins associated with the bedding-parallel veins show similar variation in geometry to that observed in the en échelon veins. This indicates that, like the en échelon veins, they formed during much of the folding history.

The ac veins sensu stricto must postdate the folding because they are unaffected by that deformation and they predate the northwest-striking faults as discussed above. They are essentially planar in the Ship Harbour shear zone, where most of the movement is related to granitoid emplacement, but are deformed by the younger transcurrent movement. They could thus be late syngranitoid or postgranitoid. The fact that an ac vein at Mooseland is cut by a composite bedding-parallel vein, indicates that they can be older than the youngest addition to the bedding-parallel veins. In view of arguments presented below this would make them syngranitoid to late syngranitoid.

If the breccia veins are related to the northwest-striking faults, and if the faults are transfer faults as suggested above, then both are probably of Triassic age or younger (cf. Tankard and Welsink, 1987) and formed during opening of the Atlantic Ocean. We have no evidence for the absolute age of the late discordant veins.

In summary, we suggest that early discordant veins were emplaced before the onset of regional folding. Early in the folding history, when bedding dips may have been as low as 10 to 15°, fluids migrating through the sequence became trapped in hydraulic fractures concentrated in the incipient domes below relatively impermeable sandstones (Mawer, 1987). These fractures were mostly bedding-parallel but locally cut across the bedding, parallel to the tension gash orientation associated with bedding-parallel shear (Fig. 5e,f). The en échelon veins also formed during folding. The two groups of veins may have been forming at the same time from different fluid sources (the bedding-parallel veins from an exotic source and the en échelon veins from solutions derived locally within the host pelites), or the crack-seal portion of the bedding-parallel veins may have been emplaced earlier during folding than the en échelon veins. After folding, or very late in the folding history, the saddle reefs were emplaced, accompanied, or followed closely by ac veins and the undeformed clear quartz portions of the bedding-parallel veins. The northwest-striking faults and, subsequently, the late discordant and breccia veins came last. We do not know when the northeast-striking shear zones were initiated, but they were active as dip-slip structures during emplacement of the granitoids in the Devonian and continued to be active, at least as transcurrent faults, until after emplacement of the ac veins.

The observed differences in the morphology of the bedding-parallel veins and the saddle reefs fits very well with the suggested history of emplacement. If veins are intruded during folding it is to be expected that they will be preferentially located in antiforms and further that they will become progressively more localized in the fold hinge. While bedding dips are shallow there is not such a volume problem in the hinge as at later stages of folding, and the bedding-normal stresses on the limbs are not so high as when bedding dips are steep. Thus it makes good sense for the early veins to extend well down the limbs (bedding-parallel veins) and for the late veins to be more localized in the fold hinge (saddle reefs) and in such extensional sites as boudin necks in older veins (bedding-parallel composite veins). Further, heterogeneity of movement on any late bedding-parallel movement zones could cause opening of voids in adjacent pre-existing fold closures, thus giving rise to postfold saddle reefs.

Timing of gold emplacement

One of the big problems in a study of this type is a lack of detailed knowledge of the exact relationship between the gold, the veins, and the country rock in which the gold is found (this situation is aggravated by the sampling problem that is always associated with gold). We know for example that gold is most common in the bedding-parallel veins, but they are composite structures and we do not know which influx of vein material brought the gold with it. Gold occurs in the wall rock of the auriferous veins indicating that the gold was able, by one means or another, to permeate the rock surrounding the main fracture along which it was introduced. The occurrence of gold in the crack-seal portion of a vein, therefore, cannot be considered evidence that that particular gold came in with one of the crack-seal increments, any more than the presence of gold in the wall rock can be interpreted as indicating a syngenetic origin.

In looking for the origin of the gold there are a number of associations that must be considered: (1) The gold occurs typically within the biotite isograd (i.e. in biotite or higher grade rocks, cf. Mawer, 1985), or is associated with carbonate metasomatism; (2) All significant mineralization, that we are aware of, is spatially associated with shear zones that have a vertical stretching lineation (paper in preparation by authors). These shear zones are not so common in the Meguma that the relationship can be explained as coincidental. Their vertical displacement is a result of granitoid emplacement which implies that they root in the granitoids; and (3) The gold is most commonly found in economic concentrations in bedding-parallel veins that contain late, generally undeformed, coarse grained quartz (i.e. in the composite veins). We are not aware of any significant mineralization in simple crack-seal bedding-parallel veins.

Associations (1) and (2) strongly suggest a causal relationship between the granitoids and the gold mineralization. We have no direct evidence that the gold was added during emplacement of the granitoids, just evidence that the fluid migration and the deformation were related to the same shear zones that enabled emplacement of the granitoids and the assumption that migration occurred while the zones were active. We interpret this as an indication that gold and granitoid emplacement were essentially contemporaneous, and recent dating of vein minerals supports this conclusion (Kontak et al., 1988b). This might suggest that the gold, and the fluids carrying it, were derived from the granitoids. However, stable isotope work (Kontak and Smith, in press) has shown that this is not likely to be so, but rather, that the fluids are derived from metamorphic dehydration reactions in rocks underlying the Meguma Terrane (see also Kontak et al., 1988a). The same metamorphism was responsible for melting deep-seated rocks to produce the granitoid magma (Kontak et al., 1988b).

Association (3) suggests that the late addition to the bedding-parallel veins carried the gold. We therefore suggest that bedding-parallel veins comprised areally extensive layers of competent material which fractured during fault-related deformation, providing a sink for the gold-bearing fluids. Basic dykes played a similar role in the formation of "ladder veins" in the Woods Point deposits in Australia (Edwards, 1953).

Gold has been reported from all of the early veins (all but the late discordant and breccia veins) and it has been pointed out above that all of these veins were precipitated from fluids capable of transporting gold. A possible explanation for the gold distribution is that all of the early veins have acted locally as brittle hosts for the late mineralizing fluids which may have been contemporary or overlapping in time with the ac veins. In addition, any of the veins could have been deposited from fluids that remobilized gold from older deposits. It might be asked why the bedding-parallel veins are particularly rich in gold if the gold-carrying fluids were added so late in the history. A possible explanation is that they were a preferred host because of a pre-existing concentration of sulphides not found in the other veins. It has been suggested that the gold could have been concentrated by earlier deposited arsenopyrite (Crocket et al., 1986). A second possibility is considered below.

Our interpretation is consistent with the conclusions of Bonham-Carter et al. (1985). They analyzed the statistical relationship between known gold occurrences and two types of linear structure. The latter included lineaments derived from satellite image analysis, and major fold axes based on geological mapping, as derived from Keppie (1982a). Bonham-Carter et al. (1985) claim that their work indicates a significant correlation between mineralization and anticlines and mineralization and east-northeast- to northeast-, and north-northwest- to northwest-striking lineaments. They interpret the second of the two lineaments as a series of faults and the first as the trace of bedding. We agree that the second may be due to faulting but it may also be due to ac master joints. Either way we suggest that the significance of the correlation is that it indicates a relationship between mineralization and ac veins. We suggest that the first lineament represents the trace of the northeast-trending shear zones and faults, rather than bedding, and that the correlation therefore indicates a relationship between mineralization, shear zones, and faults.

Model for the emplacement of the mineralized veins

The scenario that we envisage is one of a thermal dome developing below an area of F_1-folded, steeply dipping Meguma strata that, like rocks throughout the region, were probably already cut by transcurrent shear zones. These rocks already contained barren early discordant, bedding-parallel, and en échelon veins that developed prior to, or during, folding as a product of low-grade regional metamorphism. Fluids, derived from younger metamorphic reactions associated with the thermal dome and containing gold, migrated along the existing shear zones which were reactivated, in response to the thermal dome activity, as dip-slip faults. These solutions heated the Meguma strata giving rise to metasomatic and thermal metamorphic effects and locally deposited gold in new fractures in various types of pre-existing veins.

The fractures developed in and around the shear zones in response to the renewed deformation. Bedding-parallel shear zones developed in the limbs of folds must sooner or later intersect an antiformal fold hinge. A synthetic movement (i.e. for an antiform, a left-side-down movement on the left-hand limb or a right-side-down movement on the right-hand limb) on such a ductile fault would impose a stretch parallel to the limb, and competent layers would therefore tend to boudinage, forming sinks for migrating fluids. Pre-existing bedding-parallel veins, concentrated around such antiformal hinges, would be a perfect medium to concentrate brittle extensional fractures in the areas of stretching and therefore might be expected to be the most common sink for the incoming fluids. Other pre-existing veins such as the en échelon and early discordant veins were probably less favourably oriented for extension and therefore less likely to fracture and become auriferous. The walking-stick form of many of the bedding-parallel veins (i.e. elongate on one limb and short on the other) might be explained by the vein being stretched on one limb and not on the other or by hinge migration associated with the younger deformation.

An antithetic movement might also give rise to mineralized veins because such a movement would tend to separate the beds of the anticlinal hinge and might produce minor buckles as observed in some of the gold-producing areas. Either way, solutions would tend to migrate away from the fault up into the anticline or minor buckle and become trapped there (Fig. 12a). This also

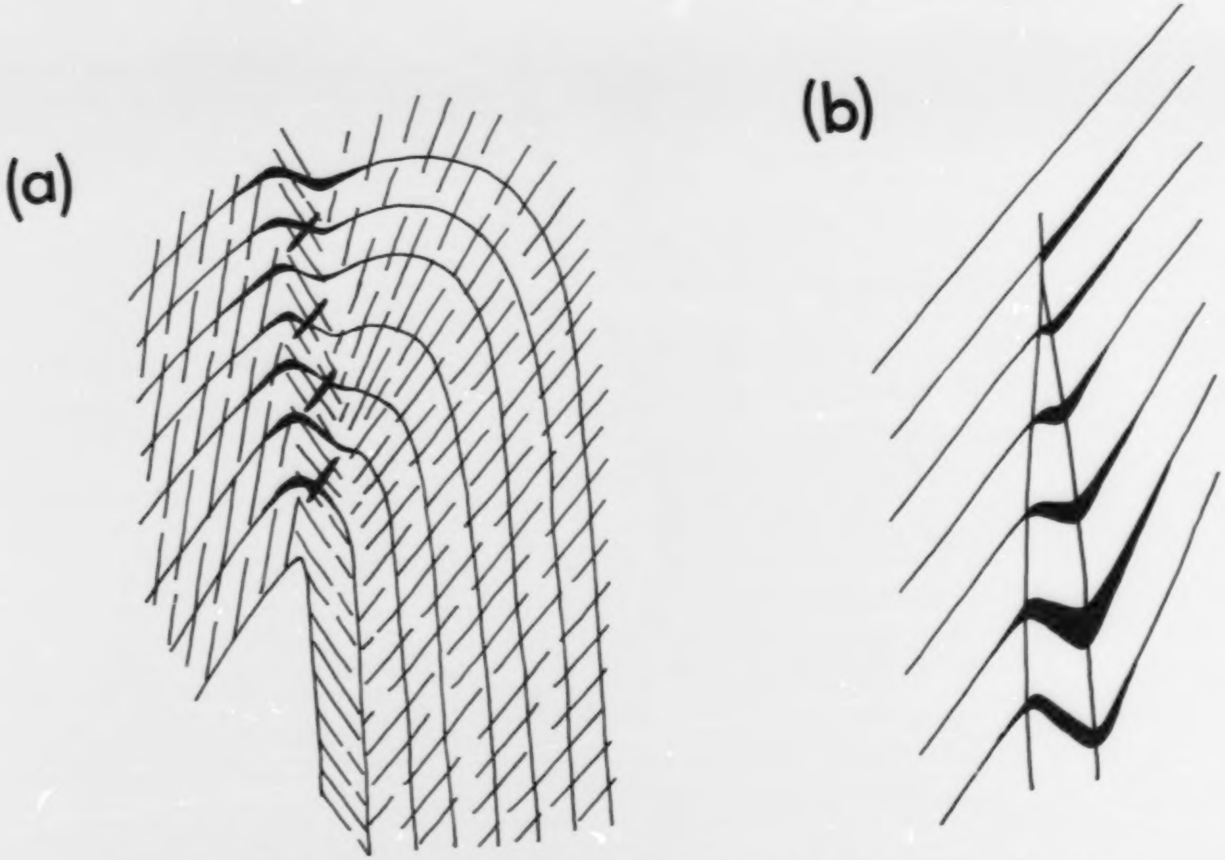

Figure 12. Diagrams representing possible models for the development of vein concentrations in the vicinity of shear zones. See text for discussion.

would tend to produce veins on one side of the folds rather than symmetrical saddle reefs, unless large quantities of fluid were introduced at one time.

Other possible traps can be envisaged; for example, some of the ductile shear zones may not have reached the surface but may have died out within the rock body. In such a situation, fluids rising along the shear zone may have caused high fluid pressures, and therefore brittle behaviour and vein development, at or near their terminations (Fig. 12b). Such a deposit might appear as a stockwork of veins associated with minor faults and the shear zone might not be visible. We would expect such stockworks to be preferentially developed parallel to bedding, but because shear zones are probably not everywhere parallel to bedding the stockworks could conceivably cut across the general trend.

We have emphasized the role of shear zones in the above discussion, but with reasonable fluid pressure we would expect such zones to have developed close to the brittle-ductile transition so that we would expect brittle faulting to overlap in time and space with the ductile shearing. Evidence for early-formed brittle faults will be obscured by younger ductile movement. The few brittle faults that we see everywhere overprint the ductile fabrics, giving the impression that brittle faulting followed ductile shear and was of minor significance. However, it is conceivable that brittle faults, coeval with ductile shear, have played a greater role in transporting the mineralizing fluids than the ductile shear zones themselves.

Late in the history of emplacement of the veins the granitoid magma migrated upward tracking the fluids by invading the warmer parts of the crust. Intrusion probably involved some stoping but the main emplacement mechanism involved lifting the roof of a developing magma chamber, by movement of the roof block on the existing shear zones. Thus the granitoids were constrained to be elongate parallel to the general strike of the Meguma Terrane strata and the continuing deformation further established the plumbing. We have no information on the cross-strike terminations of the plutons and it is possible that they simply taper, in the vertical plane, in that direction.

During emplacement, the granitoids intruded the metamorphic zones of the thermal dome and continued the metamorphic process, producing aureoles continuous with the earlier thermal dome effects. Thus what we have called contact metamorphism is in part due to the thermal dome and as such not strictly contact metamorphism. However, because the two are continuous we do not believe that they are regionally separable but point out that this interpretation is compatible with local overprinting relationships.

The thermal dome gave rise to a topographic high and as the high was reduced by erosion, stress release lead to opening of the ac joints and their partial infilling by residual fluids and exploitation by mafic dykes (Owen et al., 1988).

The model proposed here can be tested and we suggest that there is the need to look at individual mines in detail and to integrate geochemical and structural work.

ACKNOWLEDGMENTS

This work was carried out under GSC contract OST85-00061. We have benefitted greatly from discussions with many government and company geologists working in the area and would particularly like to thank Jack and Marriette Henderson, Howard Poulsen, Duncan Keppie, John Kerswill, Al Sangster, and Paul Smith. We also wish to thank Laurel Goodwin, Jack Henderson, Dan Kontak, and Chris Mawer for critical reviews of this manuscript. Word processing was done by Sherri Townsend and drafting by Angel Gomez.

REFERENCES

Anderson, F.D.
1972: The Catamaran fault, north-central New Brunswick; Canadian Journal of Earth Sciences, v. 9, p. 1278-1286.

Bonham-Carter, G.F., Rencz, A.N., Harris, J.R., and Bercha, F.G.
1985: Spatial relationship of gold occurrences with lineaments derived from LANDSAT and SEASAT imagery, Meguma Group, Nova Scotia; *in* Proceedings, Fourth Thematic Conference, Remote Sensing for Exploration Geology, San Francisco, California, p. 755-768.

Benson, D.G.
1974: Geology of the Antigonish Highlands, Nova Scotia; Geological Survey of Canada, Memoir 376, 92 p.

Bradley, D.C.
1982: Subsidence in late Paleozoic basins in the northern Appalachians; Tectonics, v. 1, p. 107-123.

Clarke, D.B. and Halliday, A.N.
1980: Strontium isotope geology of the South Mountain Batholith, Nova Scotia; Geochimica et Cosmochimica Acta, v. 44, p. 1045-1058.

Cox, S.F.
1987: Anitaxial crack-seal vein microstructures and their relationship to displacement paths; Journal of Structural Geology, v. 9, p. 779-787.

Crocket, J.H., Fueten, F., Kabir, A., and Clifford, P.M.
1986: Distribution and localization of gold in Meguma Group rocks, Nova Scotia: implications of metal distribution patterns in quartz veins and host rocks on mineralization processes of Harrigan Cove, Halifax County; Maritime Sediments and Atlantic Geology, v. 22, p. 15-33.

Edwards, A.B.
1953: Mines of the Walhalla-Woods Point auriferous belt; *in* Geology of Australian Ore Deposits, edited by A.B. Edwards, Australian Institute for Mining and Metallurgy, Melbourne, p. 1061-1076.

Eisbacher, G.H.
1970: Deformation mechanics of mylonitic rocks and fractured granites in the Cobequid Mountains, Nova Scotia, Canada; Geological Society of America Bulletin, v. 81, p. 2009-2020.

Faribault, E.R.
1896: Tangier sheet; Geological Survey of Canada, Map 565.
1897: Sheet Harbour sheet; Geological Survey of Canada, Map 592.
1903: Deep Gold Mining in Nova Scotia; Government of Nova Scotia, The Commissioner of Public Works and Mines, Kings Printer, 16 p.
1927: Hand drawn map held by Geological Survey of Canada, Ottawa.
1928: Hand drawn map held by Geological Survey of Canada, Ottawa.

Geological Survey of Canada
1985: Geophysical Series, Aeromagnetic vertical gradient maps, Nova Scotia sheets 11D/16; 11E/1,8; 11F/4; 11C/13; and 11F/5.
1986a: Geophysical Series, Aeromagnetic vertical gradient map, Nova Scotia sheets 11E/2,3,7; and 11D/10,11,14,15.
1986b: Airborne Geophysical Survey, Ship Harbour area, gamma ray spectrometric map, Nova Scotia NTS 11D/15 (part of).

Gibbs, A.D.
1984: Structural evolution of extensional basin margins; Journal of the Geological Society of London, v. 141, p. 609-620.

Graves, M.C. and Zentilli, M.

1982: A review of the geology of gold in Nova Scotia; *in* Geology of Canadian Gold Deposits, edited by R.W. Hodder and W. Petruk, Canadian Institute of Mining and Metallurgy, Special Paper 24, p. 233-242.

Haynes, S.J.

1983: Typomorphism of turbidite-hosted auriferous quartz veins, southern Guysborough County; *in* Report of Activities, 1982, Nova Scotia Department of Mines and Energy, Report 83-1, p. 183-224.

1987: Classification of quartz veins in turbidite-hosted gold deposits, greenschist facies, eastern Nova Scotia; Canadian Institute of Mining and Metallurgy Bulletin, v. 22, no. 898, p. 37-51.

Hedley, P.M.

1941: Geology and structure as related to mining, Guysborough Mines Limited, Goldenville, Nova Scotia; Transactions, Canadian Institute of Mining and Metallurgy, v. 44, p. 251-258.

Henderson, J.R.

1983: Analyses of structure as a factor controlling gold mineralization in Nova Scotia; *in* Current Research, Part B, Geological Survey of Canada, Paper 83-1B, p. 13-21.

Henderson, J.R., Wright, T.O., and Henderson, M.N.

1986: A history of cleavage and folding: an example from the Goldenville Formation, Nova Scotia; Geological Society of America Bulletin, v. 97, p. 1354-1366.

Henderson, M.N. and Henderson, J.R.

1986: Constraints on the origin of gold in the Meguma zone, Ecum Secum area, Nova Scotia; Maritime Sediments and Atlantic Geology, v. 22, p. 1-13.

Hobbs, B.E., Means, W.D., and Williams, P.F.

1976: An Outline of Structural Geology; John Wiley and Sons, New York, 571 p.

Hutchinson, D.R., Klitgord, K.D., Lee, M.W., and Trehu, A.M.

1988: U.S. Geological Survey deep seismic reflection profile across the Gulf of Maine; Geological Society of America Bulletin, v. 100, p. 172-184.

Hwang, S.G. and Williams, P.F.

1988: Overprinted shear zones in southern Nova Scotia, Shelburne-Barrington area; *in* Program with Abstracts, Geological Association of Canada/Mineralogical Association of Canada, Annual Meeting, v. 13, p. A59.

Hy, C. and Williams, P.F.

1986: Timing of quartz emplacement in the Meguma Terrane, Nova Scotia; *in* Abstracts with Program, Toronto International Conference Gold '86, p. 75-76.

Johnson, T.D. and Wones, D.R.

1984: Sense and mode of shearing along the Norumbega fault zone, Eastern Maine; *in* Abstracts with Program, 19th Annual Meeting, Northeastern Section, Geological Society of America, v. 16, p. 27.

Keppie, J.D.

1976: Structural model for saddle reef and associated gold veins in the Meguma Group, Nova Scotia; Nova Scotia Department of Mines, Paper 76-1, 34 p.

1979: Geological map of Nova Scotia, 1:500 000 scale; Nova Scotia Department of Mines and Energy.

1982a: Tectonic map of the province of Nova Scotia (1:500 000); Nova Scotia Department of Mines and Energy.

1982b: The Minas Geofracture; *in* Major Structural Zones and Faults of the Northern Appalachians, edited by P. St. Julien and J. Beland, Geological Association of Canada, Special Paper 24, p. 263-280.

Keppie, J.D. and Muecke, G.K.

1979: Metamorphic map of Nova Scotia; Nova Scotia Department of Mines and Energy, scale 1:1 000 000.

Kontak, D.J. and Smith, P.K.

in press: Sulphur isotopic composition of sulphides from the Beaver Dam and other Meguma-hosted gold deposits, Nova Scotia: implications for genetic models; Canadian Journal of Earth Sciences.

Kontak, D.J., Smith, P.K., and Kerrich, R.

1988a: Meguma gold studies V: carbon, strontium, oxygen and sulphur isotopic compositions of vein minerals: implications for source reservoirs and fluid:rock ratios attending vein formation; *in* Report of Activities, 1987, Part B, Nova Scotia Department of Mines and Energy, Report 88-1, p. 101-110.

Kontak, D.J., Smith, P.K., and Reynolds, P.H.

1988b: Meguma gold studies III: timing of mineralization at the Beaver Dam gold deposit, eastern Meguma Terrane, Nova Scotia: implications for Meguma gold deposits, Nova Scotia; *in* Report of Activities, 1987, Part B, Nova Scotia Department of Mines and Energy, Report 88-1, p. 77-84.

Leger, A. and Williams, P.F.

1986: Transcurrent faulting history of southern New Brunswick, *in* Current Research, Part B, Geological Survey of Canada, Paper 86-1B, p. 111-120.

1988: Comment on "Model for the Precambrian evolution of the Avalon terrane, southern New Brunswick, Canada"; Geology, v. 16, p. 475.

Lister, G.S., Etheridge, M.A., and Symonds, P.A.

1986: Detachment faulting and the evolution of passive continental margins; Geology, v. 14, p. 246-250.

Ludman, A.

1986: Timing of terrane accretion in eastern and east-central Maine; Geology, v. 14, p. 411-414.

MacDonald, M.A. and Clarke, D.B.

1985: The petrology, geochemistry, and economical potential of the Musquodoboit batholith, Nova Scotia; Canadian Journal of Earth Sciences, v. 22, p. 1633-1642.

Malcolm, W.

1929: Gold fields of Nova Scotia; Geological Survey of Canada, Memoir 156, 253 p. (reprinted in 1976 as Memoir 385).

Mawer, C.K.

1985: Origin of bedding-concordant auriferous quartz veins, Meguma Terrane, Nova Scotia; Maritime Sediments and Atlantic Geology, v. 21, p. 1-9.

1987: Mechanics of formation of gold-bearing quartz veins, Nova Scotia, Canada; Tectonophysics, v. 135, p. 99-119.

Mawer, C.K. and White, J.C.

1987: Sense of displacement on the Cobequid-Chedabucto fault system, Nova Scotia, Canada; Canadian Journal of Earth Sciences, v. 24, p. 217-223.

Mawer, C.K. and Williams, P.F.

1986: Structural study of highly deformed Meguma phyllite and granite, vicinity of White Head Village, S.E. Nova Scotia; Maritime Sediments and Atlantic Geology, v. 22, p. 51-64.

McCutcheon, S.R. and Robinson, P.T.

1987: Geological constraints on the genesis of the Maritimes Basin, Atlantic Canada; *in* Sedimentary Basins and Basin-Forming Mechanisms, edited by C. Beaumont and A.J. Tankard, Canadian Society of Petroleum Geologists, Memoir 12, p. 287-297.

Newhouse, W.H.

1936: A zonal gold mineralization in Nova Scotia; Economic Geology, v. 31, p. 805-831.

O'Brien, B.H.

1985: The formation of veins in greenschist facies rocks and the early deformation of the Meguma Group, Eastern Nova Scotia; Nova Scotia Department of Mines and Energy, Paper 85-2, p. 75-77.

Owen, J.V., Greenough, J.D., Hy, C., and Ruffman, A.

1988: Xenoliths in a mafic dyke at Popes Harbour, Nova Scotia: implications for the basement to the Meguma Group; Canadian Journal of Earth Sciences, v. 25, p. 1464-1471.

Ramberg, H.

1964: Selective buckling of composite layers with contrasted rheological properties. A theory for simultaneous formation of several orders of folds; Tectonophysics, v. 1, p. 307-341.

Ramsay, J.G. and Huber, M.I.

1983: Strain analysis; *in* The Techniques of Modern Structural Geology, v. 1, Academic Press, London, 307 p.

Reynolds, P.H., Zentilli, M., and Muecke, G.K.

1981: K-Ar and ^{40}Ar-^{39}Ar geochronology of granitoid rocks from southern Nova Scotia: its bearing on the geological evolution of the Meguma zone of the Appalachians; Canadian Journal of Earth Sciences, v. 18, p. 386-394.

Roedder, E.

1984: Fluid inclusions; Reviews in Mineralogy, v. 12, Mineralogical Society of America, Washington, 644 p.

Schenk, P.E.
1971: Southeastern Atlantic Canada, northwestern Africa, and continental drift; Canadian Journal of Earth Sciences, v. 8, p. 1218-1251.
1975: A regional synthesis; Maritime Sediments and Atlantic Geology, v. 11, p. 17-24.

Smith, P.K.
1983: Geology of Cochrane Hill gold deposit; *in* Report of Activities, 1982, Nova Scotia Department of Mines and Energy, Report 83-1, p. 225-256.
1984: Cochrane Hill open-pit gold deposit, Guysborough County, Nova Scotia; Nova Scotia Department of Mines and Energy, Map 84-1.

Stringer, P. and Burke, K.B.S.
1985: Structure in southwest New Brunswick; *in* Excursion 9, Fredericton '85, Geological Association of Canada, University of New Brunswick, 34 p.

Tankard, A.J. and Welsink, H.J.
1987: Extensional tectonics and stratigraphy of Hibernia oil field, Grand Banks, Newfoundland; The American Association of Petroleum Geologists Bulletin, v. 71, p. 1210-1232.

Thompson, A.B.
1976: Mineral reactions in pelitic rocks: I. Prediction of P-T-X(Fe-Mg) phase relations; American Journal of Science, v. 276, p. 401-424.

Webb, G.W.
1969: Paleozoic wrench faults in the Canadian Appalachians; American Association of Petroleum Geologists, Memoir 12, p. 754-786.

Williams, P.F.
1972: Development of metamorphic layering and cleavage in low-grade metamorphic rocks at Bermagui, Australia; American Journal of Science, v. 272, p. 1-47.

Williams, P.F. and Schoneveld, Chr.
1981: Garnet rotation and the development of axial plane crenulation cleavage; Tectonophysics, v. 78, p. 307-334.

Borehole geophysical logging at the Lake Charlotte manganese prospect, Meguma Group, Nova Scotia[1]

C.J. Mwenifumbo[2], P.G. Killeen[2], and M.C. Graves[3]

Mwenifumbo, C.J., Killeen, P.G., and Graves, M.C., Borehole geophysical logging at the Lake Charlotte manganese prospect, Meguma Group, Nova Scotia; in Mineral Deposit Studies in Nova Scotia, Volume 1, edited by A.L. Sangster, Geological Survey of Canada, Paper 90-8, p. 195-202, 1990.

Abstract

Multiparameter borehole geophysical measurements (natural gamma-ray spectrometry, spectral gamma-gamma, induced polarization (IP), resistivity, magnetic susceptibility, temperature, and temperature gradient) were made in hole LC86-1 at the Lake Charlotte manganese prospect. The hole intersects carbonaceous, pyrrhotite- and pyrite-rich black slates of the Halifax Formation and a manganese-rich, calcareous banded argillite. The slates are characterized by a much higher gamma-ray count rate than the argillites. Argillites with manganese mineralization have a higher density and spectral gamma-gamma ratio (SGG), and a lower potassium content than the slates. An apparent correlation between amplitudes in the SGG ratio and concentration of manganese suggests that the SGG ratio could be used for directly detecting manganese mineralization. The pyrrhotite/pyrite-rich slates that overlie the manganiferous argillites have higher magnetic susceptibility, lower resistivity, and have a stronger IP effect and high natural gamma radioactivity. It may be possible to map the black slates and the adjacent manganiferous argillites by using these parameters in surface geophysical surveys.

Résumé

Dans le sondage LC86-1 foré dans la zone d'intérêt manganésifère de Lake Charlotte, on a mesuré plusieurs paramètres géophysiques (spectrométrie des rayons gamma naturels, diagraphie spectrale de rayons gamma-gamma, polarisation provoquée (PP), résistivité, susceptibilité magnétique, température et gradient de température). Le sondage recoupe des schistes ardoisiers noirs, carbonés, riches en pyrrhotite et pyrite de la formation de Halifax et une argilite rubanée calcaire riche en manganèse. Les ardoises sont caractérisées par un taux de comptage des rayons gamma beaucoup plus élevé que celui des argilites. Les argilites avec une minéralisation de manganèse ont une densité et un rapport spectral gamma-gamma (SGG) plus élevés que les ardoises, mais leur teneur en potassium est plus faible. Une corrélation apparente entre les rapports SGG et la concentration en manganèse semble indiquer que le rapport SGG pourrait servir à détecter de façon directe les minéralisations de manganèse. Les ardoises riches en pyrrholite et pyrite qui reposent sur les argilites manganésifères présentent une susceptibilité magnétique plus élevée, une résistivité plus faible, un effet PP plus important et une radioactivité gamma naturelle élevée. La cartographie des ardoises noires et des argilites manganésifères adjacentes pourrait être réalisable en ayant recours à ces paramètres dans les levés géophysiques de surface.

---

[1] Contribution to the Canada – Nova Scotia Mineral Development Agreement, 1984-1989. Project carried by the Mineral Resources Division, Geological Survey of Canada, Projects 860008 and 860062.

[2] Borehole Geophysics Section, Geological Survey of Canada, 601 Booth Street, Ottawa, Ontario, K1A 0E8.

[3] Cuesta Research, 154 Victoria Road, Dartmouth, Nova Scotia, B3A 1V8.

INTRODUCTION

A 275 m deep, NQ size hole (LC86-1) was drilled for scientific purposes at the Lake Charlotte manganese prospect, Meguma Terrane, Nova Scotia. The objective was to obtain a stratigraphic section through the contact between the Goldenville and Halifax formations of the Meguma Group and to assess the stratigraphic significance of the stratabound manganese mineralization along this contact. The hole intersected two major lithologies: 1) a highly carbonaceous, pyrrhotite/pyrite-rich black slate belonging to the Cunard member of the Halifax Formation; and 2) a calcareous banded argillite of the Moshers Island member of the Goldenville-Halifax Formation Transition Zone (Graves and Zentilli, 1988). Manganese mineralization occurs within the calcareous argillites. Base metal sulphides and oxides occur mainly in the carbonaceous slates. The sulphides include disseminated pyrrhotite and pyrite, and the oxides consist of iron-titanium oxides including titanomagnetite, ilmenite, and rutile. Details of the geology and geochemistry of hole LC86-1 is given in Graves and Zentilli (1988).

Multiparameter borehole logging measurements were made to demonstrate their use in interpreting the stratigraphy and lithology intersected by the hole and to delineate mineralized horizons. The borehole geophysical measurements included the following:

1) natural gamma-ray spectrometry (total [illegible]t, K, U, Th);
2) spectral gamma gamma density (density, SGG ratio);
3) resistivity;
4) induced polarization (IP);
5) magnetic susceptibility (MS);
6) temperature and temperature gradient.

These measurements were made using the Geological Survey of Canada research and development borehole logging system.

LOG RESPONSE CHARACTERISTICS

Borehole geophysical measurements record changes in the physical and chemical properties of the formations along the length of the borehole. Detailed descriptions of the physical principles and properties of these parameters are given in a number of publications (e.g. Glenn and Nelson, 1979; Hearst and Nelson, 1985; Killeen and Mwenifumbo, 1987). The following is a summary of the response characteristics of the parameters measured in hole LC86-1.

Natural gamma-ray spectrometry

Gamma-ray measurements detect variations in the natural radioactivity due to changes in concentration of trace elements of uranium (U) and thorium (Th), as well as changes in the concentration of the major element potassium (K). In igneous and metamorphic environments, K, U, and Th may contribute about equally to the total gamma radiation detected by the gamma probe. In some sedimentary rock formations, much of the natural radioactivity emanates from the radioactive isotope, ^{40}K, in clay minerals and potassium feldspars. Changes in the clay mineral content are characteristic of certain rock formation and, therefore, the natural gamma-ray log may be used to identify and distinguish different lithologies. The lithologies intersected in LC86-1 are argillites and slates and the principal source of the natural gamma radiation is most likely due to clay minerals. Spectrometric data from this hole shows quantitatively the K, U, and Th contributions.

Spectral gamma gamma density

The spectral gamma gamma density tool consists of a radioactive source (^{60}Co or ^{137}Cs) and a sodium iodide or cesium iodide scintillation detector. Gamma rays emitted by the source collide with electrons and lose energy by photoelectric absorption and Compton Scattering. The scattered gamma rays are then counted at the detector at a fixed distance from the source. Gamma ray spectra are recorded over the energy range from 0.0 to 1.0 MeV. Density information is determined from the count rate in an energy window between 100 keV and 500 keV. This window relates to Compton Scattering which is a function of electron density in the surrounding material. The electron density is related to the bulk density of the material. Information about the elemental composition of the rock can be obtained from the ratio of the count rates in two energy windows, one at a high energy and one at a low energy. Count rates within the low energy window are mainly influenced by photoelectric absorption which is a function of the atomic number, Z, and by Compton Scattering. The ratio of counts in the high energy window (density window) to counts in the low energy window (density and Z effect window) is called the spectral gamma gamma ratio (SGG ratio) and can be used to obtain information on changes in Z. This ratio increases through zones containing high Z material.

The density log responses are highly variable and not particularly diagnostic of specific lithological changes. In the environment studied, however, the presence of iron sulphides and oxides, and the high percentage of organic carbon within the carbonaceous slate, should significantly alter the density of this rock unit. Manganese and iron sulphide mineralization with atomic numbers 25 and 26 should be reflected in the SGG profile along the borehole.

Resistivity and induced polarization

The electrical resistivity of rocks depends on several factors. Rocks are usually poor conductors, and their resistivities are primarily determined by the porosity, the degree of saturation of the pore spaces, and the salinity of the pore fluid. Conductive minerals such as metallic sulphides and oxides, and graphite in the rock have a strong influence on the resistivity. Decreases in resistivity may, therefore, be a result of either significant concentration of sulphides and oxides or an increase in porosity due to fracturing. The presence of clay minerals also reduces the resistivity of the formation and therefore, alteration processes that result in the formation of clay minerals may be easily detected on a resistivity log. Induced polarization measurements primarily respond to the presence of polarizable and conductive minerals. Polarizable minerals intersected in hole LC86-1 consist of disseminated pyrrhotite/pyrite and iron-titanium oxides (titanomagnetite and ilmenite).

Magnetic susceptibility

The magnetic susceptibility of a volume of rock is a ratio of the intensity of magnetization produced in the rock to the strength of the external magnetic field. It is primarily dependent on the ferromagnetic minerals (magnetite and/or pyrrhotite) present within the rock mass. Magnetic susceptibility measurements can provide a rapid estimate of the amount of magnetic minerals present. The variations in the content of these minerals can be interpreted to reflect lithological changes, degree of homogeneity, and the presence of alteration zones of a rock mass. Pyrrhotite mineralization intersected in LC86-1 is easily detected by downhole magnetic susceptibility measurements. Since these minerals seem to be specific to the carbonaceous slates, the magnetic susceptibility measurements may be used to characterize this rock member.

Temperature logging

The temperature log in a borehole is affected by a number of factors. In mineral exploration these include drilling fluid circulation (if hole is logged immediately after drilling), groundwater flow, and variations in thermal conductivity of the wall rock. The latter may be used to detect changes in lithology where different thermal conductivity exists along the borehole. Fractures or shear zones may provide pathways for groundwater to flow if hydrological gradients exist within the rock mass. Groundwater movements produce some characteristic anomalies that may help locate open fractures.

DISCUSSION OF RESULTS

Figure 1 shows the lithology, total count gamma ray, resistivity, induced polarization, magnetic susceptibility, gamma gamma density, SGG ratio, temperature, and temperature gradient logs for hole LC86-1. The density log is in arbitrary units because the probe was not calibrated to read bulk densities in g/cm^3. The electrical logs (resistivity and IP) were acquired with a 10-cm normal array. The resistivity is presented on two scales: a linear scale and also on a logarithmic scale to emphasize the lower values. Temperature gradient is determined from the temperature data by means of a gradient operator. Temperature logging is always the first one done and is run downhole. Table 1 summarizes the logging parameters for the different logging tools used.

Lithology and mineralization

Both the upper and lower calcareous banded argillites (Moshers Island member) are clearly distinguished from the carbonaceous slates (Cunard member). The argillites are characterized by comparatively lower radioactivity, higher resistivity, lower IP, lower MS, higher density, and higher SGG ratio. Small fluctuations in the resistivity log probably result from thinly bedded carbonaceous materials and/or pyrite which may occur as layers of grains in the bedding planes (see upper argillites, Fig. 1). Most of the manganese mineralization occurs within the argillites in the form of manganese-bearing calcite ($CaMn(CO_3)_2$), manganese oxides consisting mainly of manganese-bearing ilmenite (FeTiMn-oxides), and in the form of silicates such as spessartine garnet. Alteration of these minerals to produce manganese oxide — possibly manganite and pyrolusite — is common. The enrichment in manganese mineralization may explain the higher SGG ratios observed in this lithological unit.

The slates contain disseminated pyrrhotite and pyrite, and thus exhibit lower resistivity, higher induced polarization and higher magnetic susceptibility than the argillites. The lower density and lower SGG ratio within this unit may be attributed to the amount of organic carbon (>5 weight percent C, Graves and Zentilli, 1988), even though the concentration of iron sulphides is high. Normally this would tend to increase the values of these parameters. The overall bulk density and effective atomic number is reduced by the presence of carbon. The slate is divided into two units by a noncarbonaceous unit. This noncarbonaceous slate (between 75.5 and 80.5 m) is more resistive and less radioactive than the carbonaceous slate. The upper section (between 59.0 and 75.5 m) has a slightly lower radioactivity and higher resistivity than the lower section (between 80.5 and 100 m). The higher resistivity may be due to quartz veins and silicification in this section. The natural gamma radioactivity is also higher within the slates, mainly as a result of potassium. Figure 2 shows the spectral gamma-ray logs (K, U, and Th) beside the chemical assay logs of K_2O, U, and Th. The sparse distribution of the chemical assay data makes it difficult to compare the assay to the log data. Differences in sample volume may contribute to discrepancies in the two data sets. The Cunard slate is characterized by fairly uniform, high potassium. The U and Th contents are, however, variable being lower in the upper section and higher in the lower section. This explains the difference in total radioactivity in these two sections. The process of silicification may have leached out uranium from the upper section, assuming that the upper and lower sections belong to the same unit (see discussion on stratigraphy and structure).

The lower Moshers Island argillite may be divided into three subunits. An expanded section of this argillite unit is shown in Figure 3. The upper subunit is characterized by slightly lower gamma radioactivity and by slightly higher magnetic susceptibility, density, and SGG ratio. This subunit is fairly similar to the upper argillites. The resistivity is fairly high except for a wide low resistivity zone between 110 and 120 m which is probably due to a fracture zone. This zone is also mineralized as indicated by an increase in IP effect (see Fig. 1). The middle subunit of the lower argillite exhibits a slightly different signature. The natural gamma radioactivity increases slightly, and the MS, density, and SGG ratio decreases

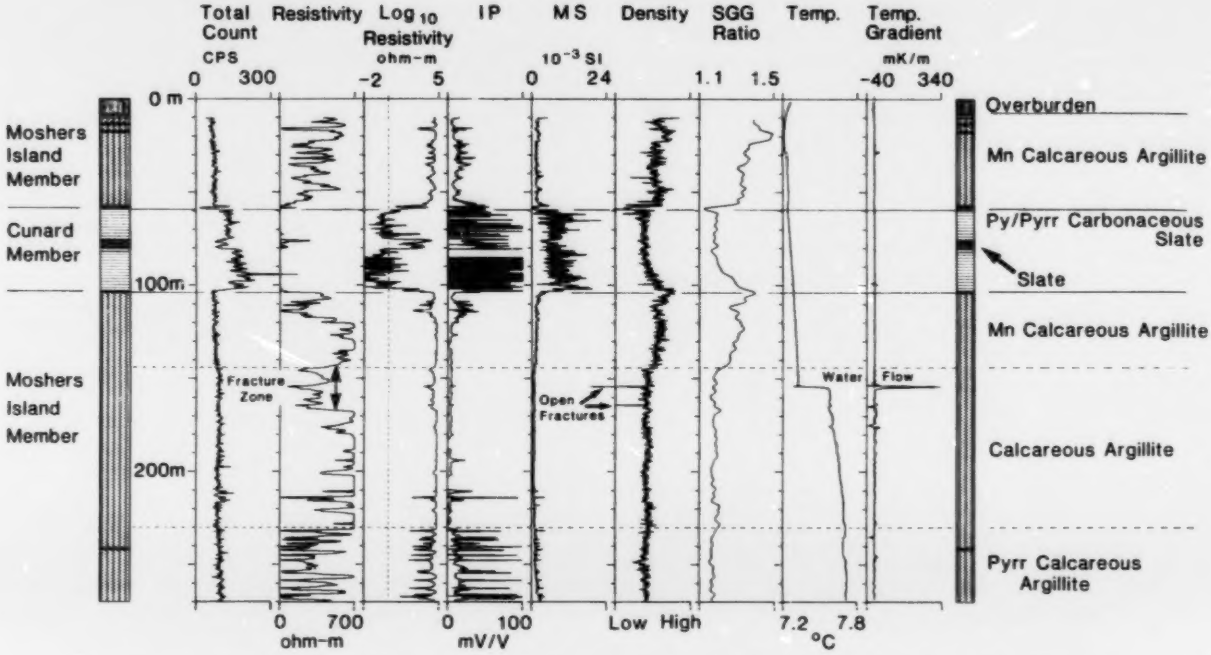

Figure 1. Geological log, total count (TC), 10-cm normal resistivity and induced polarization (IP), magnetic susceptibility (MS), density, SGG ratio, temperature, and temperature gradient logs recorded in hole LC86-1. The density log is in arbitrary units. A linear and logarithmic resistivity log are shown. The logarithmic plot of resistivity is presented in order to emphasize the variations in low resistivity within carbonaceous slate. All the logging parameters clearly define the carbonaceous pyrrhotite/pyrite slates. The prominent change in temperature and temperature gradient at 154 m is caused by water entering the borehole at this point.

Table 1. Logging parameters for the different logging tools used in hole LC86-1.

LOGGING TOOL	PARAMETER MEASURED	LOGGING SPEED	SAMPLE INTERVAL
Spectral gamma-ray	Total count (CPS) K (%) U (ppm) Th (ppm)	3 m/minute	20 cm
Spectral gamma gamma	density SGG ratio	3 m/minute	10 cm
Induced polarization	IP (mV/V) Res (ohm-m)	3 m/minute	5 cm
Magnetic susceptibility	MS (SI)	6 m/minute	2 cm
Temperature	T (°C) TG (mK/m)	6 m/minute 6 m/minute	3 cm 3 cm

SGG – spectral gamma gamma
IP – induced polarization
Res – resistivity
MS – magnetic susceptibility
TG – temperature gradient
CPS – counts per second
mV/V – milliVolt per Volt
mK/m – milliKelvin per metre
SI – SI units

appreciably within this subunit. The decrease in the SGG ratio is probably due to lack of or reduced concentrations of manganese mineralization (see Fig. 4). The resistivities are again very high except for a wide low resistivity zone between 145 and 165 m probably due a fracture zone indicated by the groundwater flow on the temperature log (see section on fracture zones and water flow). The lower subunit, between 230 and 275 m (Fig. 1), is not that much different from the middle subunit, especially in percent K (Fig. 2). The major difference between the upper and lower subunits are in the percent K values and SGG ratio. The lower subunit is a calcareous banded argillite containing disseminated and banded pyrrhotite and pyrite. The iron sulphide bands tend to lower the resistivity and increase the IP effect and magnetic susceptibility. The increase in magnetic susceptibility is due to the presence of pyrrhotite and/or ilmenite.

SGG ratio and manganese mineralization

Figure 4 shows the SGG ratio log with drill core assays of manganese oxide (MnO), arsenic, organic carbon, and sulphur(S). High SGG ratios reflect increases in the effective atomic number, Z, in the lithology. There is a good correlation between the SGG ratio and MnO. High SGG ratios correspond to increases in the concentration of manganese minerals. Even though the slates are enriched in iron sulphides, the SGG ratios within this unit are lower than those observed within the argillites. The

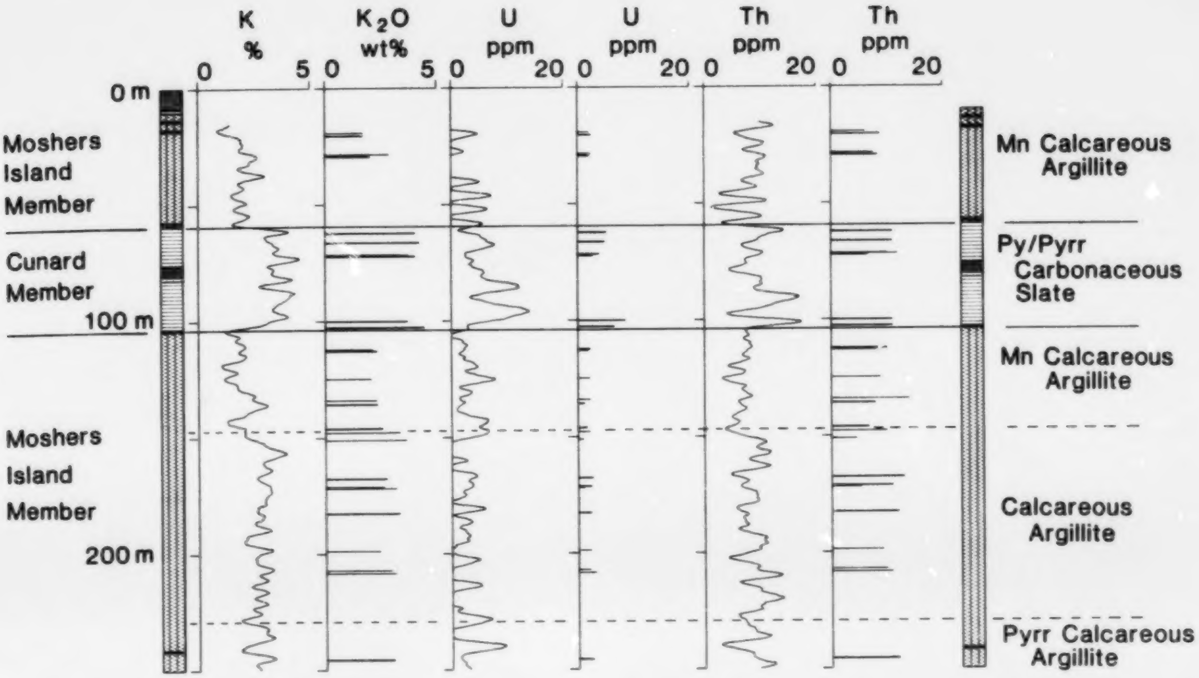

Figure 2. Geological log and spectral gamma-ray logs (percent K, U ppm, and Th ppm) plotted alongside the chemical assays of weight percent K_2O, U ppm, and Th ppm. The two types of logs correlate fairly well despite the sparse distribution of the assay data.

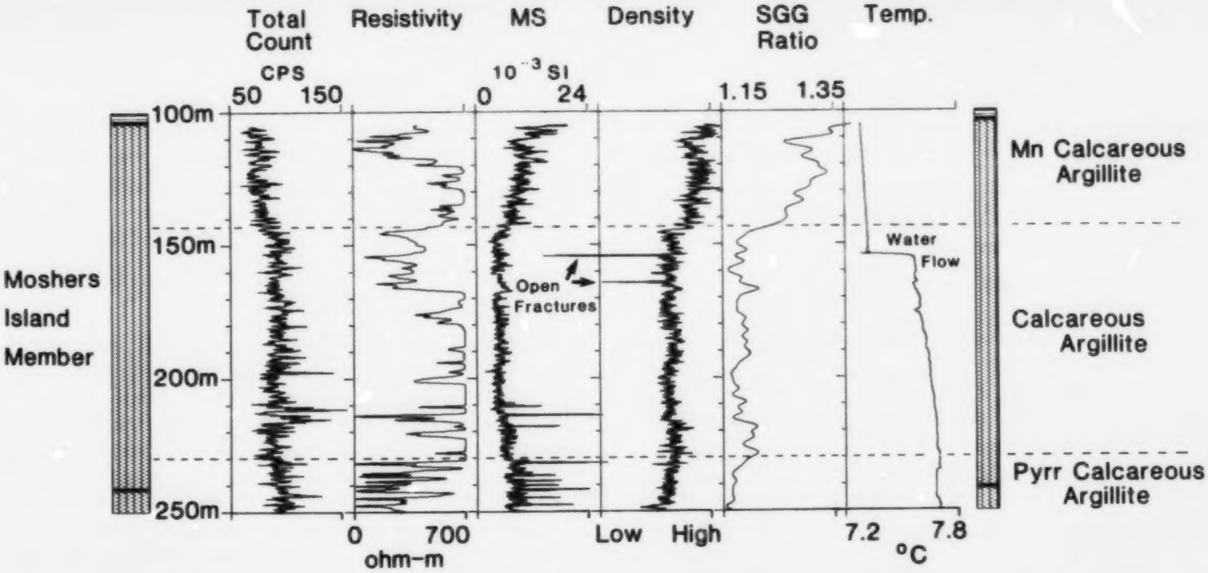

Figure 3. An expanded section of the lower Moshers Island banded calcareous argillites showing the division of this unit into three subunits based on differences in the geophysical logs. The fracture zone with flowing water at 154 m gives a characteristic response shown in the temperature, density, and resistivity logs.

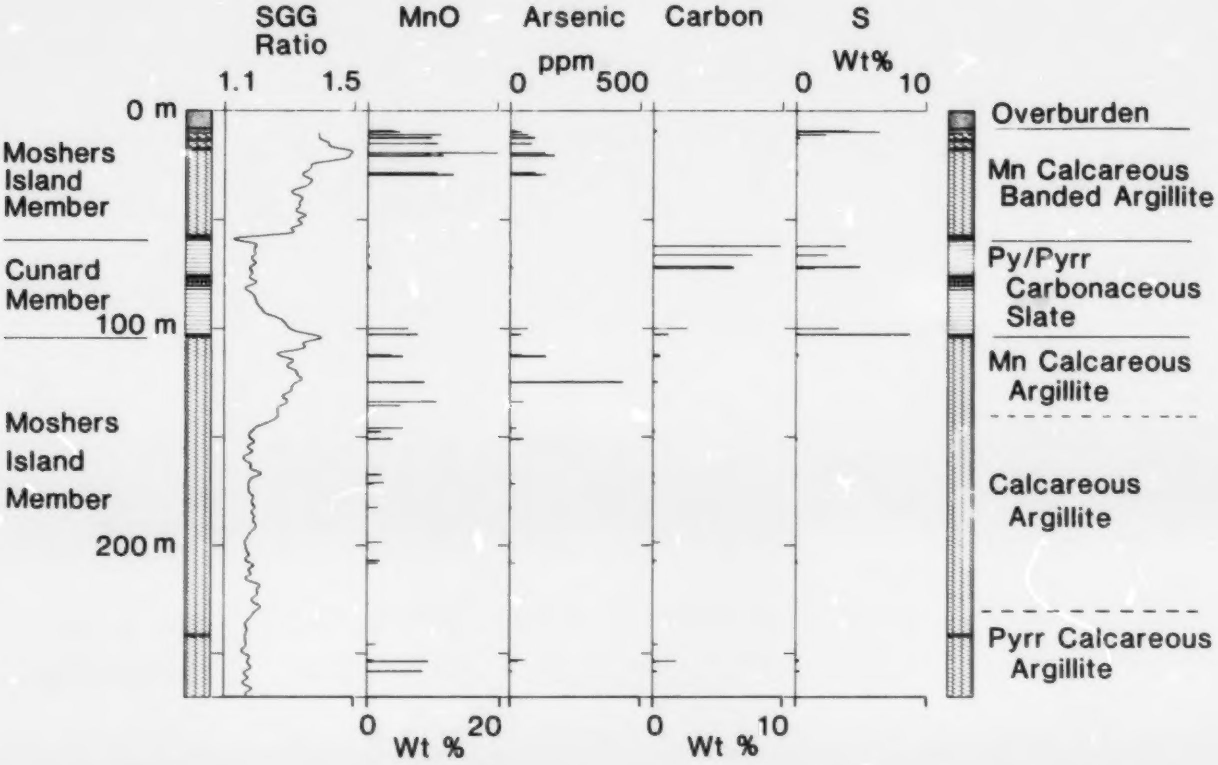

Figure 4. Geological and SGG ratio logs plotted with drill core assays of MnO, As, $C_{organic}$, and S. MnO and As correlate with the high SGG ratios which reflect increases in the effective atomic number, Z, of the calcareous argillites due mainly to manganese mineralization. Despite the high iron sulphide content (high S), the SGG ratio shows a decrease in the slates due to a high organic carbon content.

high percentage of organic carbon in the slates (an average of about 5 weight percent C) with a low Z value of 6, reduces the effective Z value of the lithology and hence the SGG ratio.

Stratigraphy and structure

Hole LC86-1 was drilled on the northern limb of the Lake Charlotte syncline. The Cunard slates of the Halifax Formation are stratigraphically higher than the Moshers Island argillite which occurs within the Goldenville-Halifax Formation Transition Zone (Zentilli et al., 1986). The occurrence of the Moshers Island argillite above and below the Cunard slate presents some difficulties in interpreting the stratigraphy and structure along hole LC86-1. There are several possible explanations for the occurrence of Cunard slate sandwiched between the Moshers Island argillite. The most probable explanation, which is supported by the geophysical measurements, is that the hole may have been drilled through a minor fold within the limb of the syncline. There appears to be some symmetry in the geophysical log responses centred around the noncarbonaceous slate within the Cunard member at about 75 m. High resistivity, density, and SGG ratio, and low radioactivity are characteristic of the lithologies above and below this member. Log symmetry is also observed within the Cunard slate. The slight asymmetry in the geophysical response characteristics between the lower and upper Cunard slate — notably total count gamma ray, resistivity, and SGG ratio — is mainly due to the secondary silicification in the upper slates (see Fig. 1).

Fracture zones and water flow

Although there are no indications of fault or fracture zones in the description of the drill core, the downhole geophysical logs indicate a number of zones where geophysical responses are characteristic of fracture or alteration zones. There may be one such zone near the upper contact between the Moshers Island argillite and the Cunard slate (about 58 m). Figure 5 is an expanded section of some of the geophysical logs showing the upper contact. The natural gamma radioactivity, magnetic susceptibility, density, SGG ratio, and resistivity are anomalously low, coinciding with chloritic argillite. The temperature log also indicates water flow around this zone.

A wide fracture zone between 145 and 165 m is indicated by low resistivity (Fig. 3). The density log does not show a corresponding wide, low density zone. However,

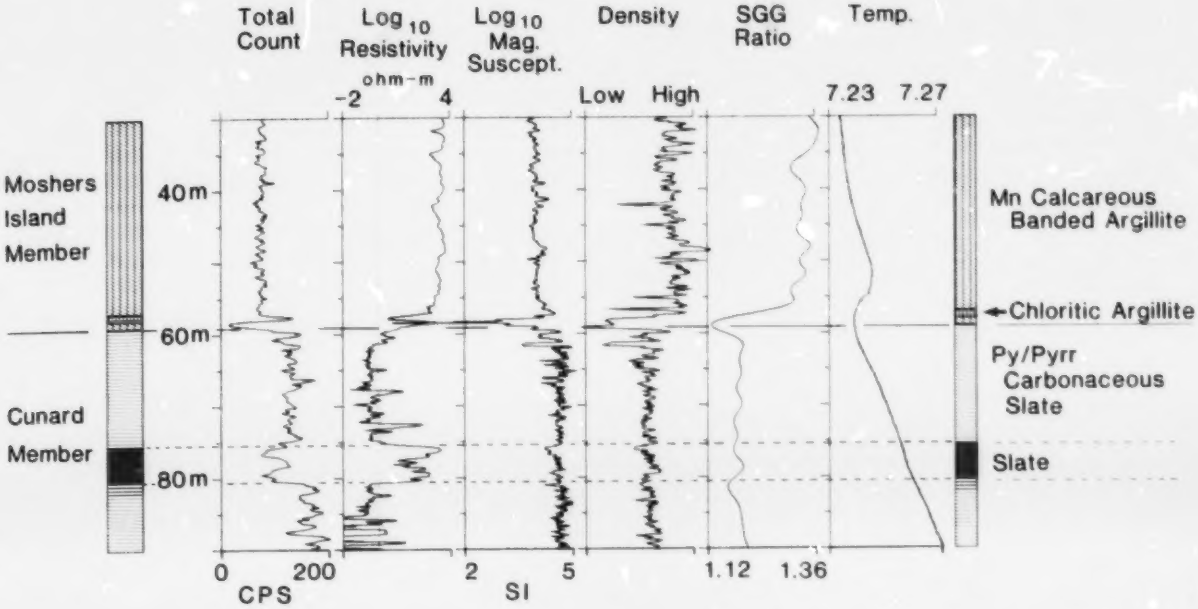

Figure 5. An expanded section with the geophysical logs showing the contact between the upper Moshers Island argillite and Cunard slates with a prominent fracture/alteration zone. The magnetic susceptibility is plotted on a logarithmic scale to emphasize the low susceptibility zone. An anomalously low gamma ray, magnetic susceptibility, density, and SGG ratio zone at approximately 58 m coincides with the chloritic argillite and is probably an alteration zone.

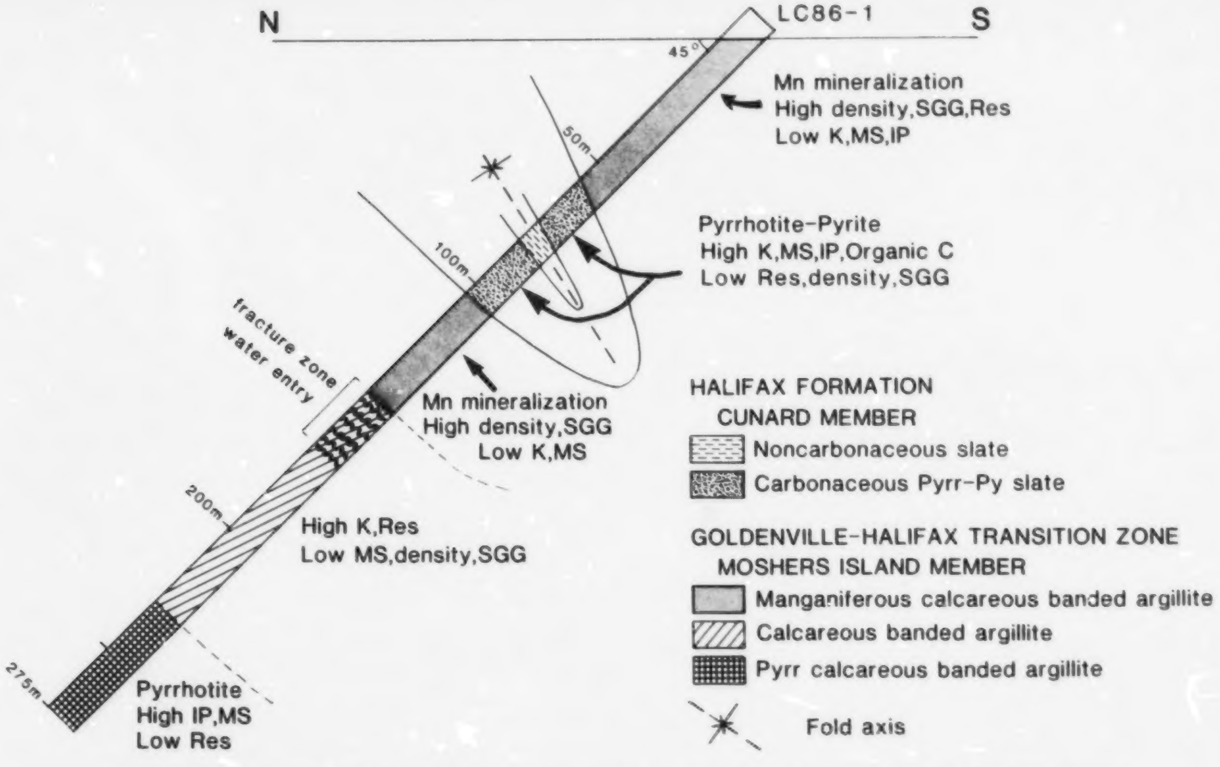
N
LC86-1
S
45°
50m
100m
200m
275m
Mn mineralization
High density,SGG,Res
Low K,MS,IP
Pyrrhotite-Pyrite
High K,MS,IP,Organic C
Low Res,density,SGG
fracture zone
water entry
Mn mineralization
High density,SGG
Low K,MS
High K,Res
Low MS,density,SGG
Pyrrhotite
High IP,MS
Low Res
HALIFAX FORMATION
CUNARD MEMBER
Noncarbonaceous slate
Carbonaceous Pyrr-Py slate
GOLDENVILLE-HALIFAX TRANSITION ZONE
MOSHERS ISLAND MEMBER
Manganiferous calcareous banded argillite
Calcareous banded argillite
Pyrr calcareous banded argillite
Fold axis

Figure 6. Diagrammatic interpretation of the stratigraphy and structure intersected along hole LC86-1 based on drill core geological information, assays, and geophysical measurements.

two narrow, fairly low density zones are indicated at approximately 155 and 164 m within this broader resistivity low. These two zones are probably due to an increase in hole diameter of open fractures. Density logs were repeated in this hole to confirm this pattern. The temperature and temperature gradient logs indicate water production at 155 m and in fact the hole is a flowing artesian.

SUMMARY OF RESULTS

Figure 6 shows a summary of the interpretation of the stratigraphy and structure of the formations intersected along hole LC86-1 based on drill core geological information, chemical assays, and geophysical measurements. The lithologies intersected are easily mapped using geophysical measurements. As well as complimenting the geological and geochemical data, geophysics provides some new information, especially about the lower Moshers Island calcareous banded argillite. The manganiferous argillite has a characteristic geophysical signature of high density, high SGG ratio, and low potassium. An increase in the SGG ratio appears to indicate the presence of manganese mineralization. This assumes the absence of significant concentrations of iron sulphides and other elements with high Z values. Arsenic is well correlated with manganese mineralization which makes it easy to interpret the SGG ratio.

Temperature logs can be used to detect fluid flow in drillholes. The detection of fracture zones with fluid movement is important in the event that the holes need to be cemented to avoid mixing of groundwater between different aquifers.

Surface magnetic surveys (Shea, 1957) indicate a close spatial relationship between the magnetic highs and manganese occurrences. The magnetic highs are probably caused by pyrrhotite mineralization in the carbonaceous Cunard slates. The other geophysical parameters, resistivity, IP, and natural gamma ray, also show distinct signatures within the Cunard slates and may be useful in surface geophysical surveys to map these slates and the underlying manganiferous argillites.

CONCLUSION

Borehole logging measurements at the Lake Charlotte manganese prospect have shown that manganiferous argillites may be detected easily and a better definition of the lithological boundaries may be made. Because the atomic number of manganese is fairly high compared to most of the major elements that constitute the host rock, it may be possible to estimate the manganese content using the SGG ratio, provided that the effective atomic number of the host rock is fairly constant and lower. The presence of iron sulphides may complicate the interpretation. The mineralized and nonmineralized Moshers Island argillites show some distinct differences in geophysical responses that could provide useful information to a geologist collecting samples for assay. Present assay samples from the drill core were randomly distributed along the hole and did not provide a good representation of the variations in mineralization and lithology. It is highly recommended that downhole logging measurements be carried out first before any comprehensive sampling for assaying is done. This will ensure a representative sampling of the major lithological units and mineralized sections.

ACKNOWLEDGMENTS

We wish to thank Bill Hyatt for the field data acquisition, and Barbara Elliott and Angela Tchen for assistance in computer data processing. The work was done under the Canada-Nova Scotia Mineral Development Agreement.

REFERENCES

Glenn, W.E. and Nelson, P.H.
1979: Borehole logging techniques applied to base metal ore deposits; *in* Geophysics and Geochemistry in Search for Metallic Ores, edited by P.J. Hood, Geological Survey of Canada, Economic Geology Report 31, p. 273-294.

Graves, M.C. and Zentilli, M.
1988: Geochemical characterization of the Goldenville-Halifax Formation Transition Zone of the Meguma Group, Nova Scotia: Part 1 - Location maps, sample sections and major elements, Harker variation diagrams; Part 2 - Data tables and sample descriptions; Geological Survey of Canada, Open File 1829, 110 p.

Hearst, J.R. and Nelson, P.H.
1985: Well Logging for Physical Properties; McGraw-Hill Book Company, New York, 571 p.

Killeen, P.G. and Mwenifumbo, C.J.
1987: Interpretation of new generation geophysical logs in Canadian Mineral exploration, *in* Proceedings of the Second International Symposium on Borehole Geophysics for Minerals, Geotechnical, and Groundwater Application, October 6-8, 1987, Golden, Colorado.

Shea, F.S.
1957: Manganese, Lake Charlotte, Halifax County, Nova Scotia: Magnet Cove Barium Corporation Exploration reports; Nova Scotia Department of Mines and Energy, Assessment Report 11D15B 31H29(05).

Zentilli, M., Graves, M.C., Mulja, T., and MacInnis, I.
1986: Geochemical characterization of the Goldenville-Halifax Transition Zone of the Meguma Group of Nova Scotia: preliminary report; *in* Current Research, Part A, Geological Survey of Canada, Paper 86-1A, p. 423-428.

Geology of the Yava sandstone-lead deposit, Cape Breton Island, Nova Scotia, Canada[1]

D.F. Sangster[2] and P.D. Vaillancourt[3]

Sangster, D.F. and Vaillancourt, P.D., Geology of the Yava sandstone-lead deposit, Cape Breton Island, Nova Scotia, Canada; in Mineral Deposit Studies in Nova Scotia, Volume 1, edited by A.L. Sangster, Geological Survey of Canada, Paper 90-8, p. 203-244, 1990.

- 204 Abstract
- 205 Résumé
- 206 Introduction
- 207 Salmon River Basin Geology
  - 207 Intrusive rocks
    - 207 Chisholm Book granodiorite
    - 207 Salmon River porphyry
  - 207 Sedimentary rocks
    - 207 Stratigraphy
    - 209 Windsor and Canso groups
      - 211 MacKeigan Lake Formation
    - 211 Riversdale Group
      - 211 Silver Mine Formation
    - 212 Morien Group
      - 212 Big Barren Formation
      - 212 Glengarry Valley Formation
  - 212 Base metal occurrences
- 213 Yava Mine Geology
  - 213 Local geology
  - 214 Ore zones
    - 215 West Zone
    - 217 Central Zone
    - 217 East Zone
  - 219 Host rock petrography and mineralogy
    - 219 Quartz
    - 219 Feldspar
    - 219 Carbonate
    - 219 Heavy minerals
    - 219 Silica overgrowths
    - 219 Muscovite
    - 219 Clay minerals
      - 219 Clay in sandstone
      - 222 Clay in shale
  - 222 Mineralization
    - 222 Distribution
    - 223 Sulphide petrography in sandstone
    - 224 Sulphide petrography in coaly material
    - 226 Hydrocarbon alteration
    - 226 Paragenesis
  - 226 Lead isotopes
  - 229 Sulphur isotopes
    - 229 Sulphide
      - 229 Yava
      - 231 Other areas
    - 231 Sulphates
      - 231 Barite
      - 231 Gypsum
- 231 Discussion
  - 231 Timing of mineralization
  - 231 Controls
  - 233 Direction of flow of mineralizing fluids
  - 233 Temperature of ore deposition
  - 233 Sources of sulphur and lead
  - 235 Diagenetic processes in Silver Mine sandstone
- 235 Genesis
- 239 Summary and Conclusions
- 239 Acknowledgments
- 240 References
- 241 Appendices
  - 241 Appendix A — Clay mineral determinations
  - 241 Appendix B — Lead isotope determinations
  - 242 Appendix C — Sulphur isotope determinations

---

[1] Contribution to the Canada - Nova Scotia Mineral Development Agreement, 1984-1989. Project carried by the Mineral Resources Division, Geological Survey of Canada, Project 860008.

[2] Geological Survey of Canada, 601 Booth St., Ottawa, Ontario, K1A 0E8; and Derry Laboratory for Sedimentary Geochemistry and Mineral Deposits, Ottawa-Carleton Geoscience Centre, Ottawa, Ontario

[3] Present address: Noranda Exploration, Suite 1300, 4 King St. West, Toronto, Ontario, M5H 1B6

Abstract

The Yava lead deposit is contained in Upper Carboniferous fluviatile sandstones lying disconformably on Lower Carboniferous sedimentary rocks and nonconformably on Cambrian and Upper Devonian sialic intrusions. Mineralization occurs exclusively in a characteristic grey sandstone in the lower sandstone unit of the Silver Mine Formation; an overlying green sandstone in the same unit is virtually devoid of galena. Quartz and clay are the most abundant minerals in the Silver Mine Formation sandstone with kaolinite being the most common clay mineral in the grey sandstone member. Both members contain abundant organic material, much of it as coalified debris of Calamites and Lepidodendron. Relict potassium feldspar grains suggest that the original sediment was likely close to a feldspathic sandstone in composition.

Proven geological reserves (1981) at Yava were 3 500 000 tonnes of 4.12% Pb (3% cutoff) distributed over three zones (West, Central, and East). During a two and one-half year period prior to 1981, 388 000 tonnes of 4.75% Pb were mined from the West Zone.

Galena characteristically occurs as cement between detrital quartz grains, producing a low-grade, disseminated style of mineralization; higher grade material appears to have resulted from replacement of quartz and/or carbonate grains. Much lesser amounts of sphalerite and pyrite are usually associated with the abundant coaly material in the sandstone. Intercalated shale units are seldom mineralized. Sulphide-filled wood cells retain their original shape indicating that mineralization took place during earliest diagenesis and before compaction of this material. Detailed studies of the organic matter revealed an abnormal evolution of reflectance gradients attributable to chemical, rather than thermal, alteration by ore-bearing fluids.

Highest lead grades occur in sandstone overlying channel-shaped depressions in felsic basement rocks. These buried depressions, in turn, correlate in position with modern streams in areas of basement exposure, suggesting that the latter are at least partially controlled by an exhumed Pennsylvanian topography.

Lead isotope ratios in ore-stage galena and basement igneous rocks indicate that lead was derived from both Chisholm Brook granodiorite and Salmon River porphyry. Sulphur isotope data indicate sulphur in the Yava deposit was derived by dissolution of gypsum in underlying MacKeigan Lake Formation shales, followed by bacterial reduction in the coal-bearing grey sandstone host.

Continued passage of meteoric water through the sandstone is suggested as the mechanism by which potash feldspar was altered to kaolinite. This process released lead from the feldspar lattice to combine with reduced sulphur and precipitate galena as cement in the porous sandstone. Silica released by the same breakdown of feldspar was also precipitated, slightly earlier than the galena, as the characteristic secondary overgrowths on detrital quartz grains. Mafic minerals, likely derived from the Chisholm Brook granodiorite, are suggested as the source of the minor zinc and iron in the deposit.

Résumé

Le gisement de plomb Yava se trouve dans les grès fluviatiles du Carbonifère supérieur reposant en discordance sur des roches sédimentaires du Carbonifère inférieur et des intrusions sialiques du Cambrien et du Dévonien supérieur. Il y a minéralisation exclusivement dans un membre caractéristique de grès gris de l'unité grèseuse inférieure; une unité sus-jacente de grès vert ne renferme pratiquement aucune galène. Le quartz et l'argile sont les minéraux les plus abondants dans la formation grèseuse de Silver Mine et la kaolinite est le minéral argileux le plus courant dans le membre de grès gris. Les deux membres renferment une quantité de matière organique en grande partie sous forme de débris houillifiés de Calamites et le Lepidodendrons. La présence de grains résiduels de feldspath potassique semble indiquer que la composition des sédiments originaux était vraisemblablement apparentée à celle du grès feldspathique.

Les réserves géologiques prouvées (1981) au gisement Yava s'établissaient à 3 500 000 tonnes renfermant 4,12% de Pb (teneur de coupure 3%) et se répartissaient en trois zones (de l'Ouest, du Centre et de l'Est). Pendant un intervalle de deux ans et demi avant 1981, on a extrait de la zone de l'Ouest 388 000 tonnes de minerai renfermant 4,75% de Pb.

La galène est de manière caractéristique présente sous forme de ciment entre les grains de quartz détritique et forme ainsi une minéralisation à faible teneur de type disséminée; la formation d'un matériau de plus forte teneur semble avoir résulté du remplacement de grains de quartz ou de carbonate, ou des deux. Des quantités beaucoup moindres de sphalérite et de pyrite sont habituellement associées à l'abondant matériau charbonneux dans le grès. Les unités intercalaires de schiste argileux sont rarement minéralisées. Les cellules ligneuses remplies de sulfures ont conservé leur forme originale, signe que la minéralisation s'est effectuée pendant le tout début de la diagenèse et avant la compaction de ce matériau. Des études détaillées de la matière organique ont révélé une évolution anormale des gradients de réflectance attribuable à une altération chimique, plutôt que thermique, causée par des fluides minéralisés.

Les teneurs en plomb les plus élevées se rencontrent dans le grès recouvrant des dépressions en forme de chevaux dans les roches felsiques du socle. Il existe d'autre part une corrélation entre la position de ces dépressions enfouies et celle des cours d'eau contemporains dans la région, phénomène qui semble indiquer que le cours de ces derniers est, du moins en partie, déterminé par un relief du Pennsylvanien exhumé.

Les rapports entre les isotopes du plomb dans la galène et les roches ignées du socle de l'étage du minerai indiquent que ce plomb provient de la granodiorite de Chisholm Brook et du prophyre de Salmon River. Les données sur les isotopes du soufre indiquent que le soufre du gisement Yava a été formé par une dissolution du gypse des schistes argileux de la formation sous-jacente de MacKeigan Lake suivie d'une réduction bactérienne dans le grès gris carbonifère hôte.

On considère que le passage en continu d'eau atmosphérique dans le grès est le mécanisme par lequel le feldspath potassique a été altéré en kaolinite. Ce processus a libéré le plomb du réseau cristallin du feldspath pour lui permettre de se combiner au soufre réduit et de précipiter la galène sous forme de ciment dans le grès poreux. La silice libérée par la même décomposition du feldspath a également précipité, légèrement plus tôt que la galène, sous forme d'accroissements secondaires caractéristiques sur les grains de quartz détritique. Les auteurs proposent en outre que l'altération de matériaux mafiques, provenant vraisemblablement de la granodiorite de Chisholm Brook, est la source des quantités mineures de zinc et de fer que renferme le gisement.

INTRODUCTION

The Yava deposit, a former lead producer in southeastern Cape Breton Island, Nova Scotia, is hosted in Pennsylvanian fluviatile sandstones. It is one of the few sandstone-lead deposits of continental affiliation; the majority are hosted in marine sandstones (Bjørlkke and Sangster, 1981).

The Yava area lies in the Salmon River Basin (Fig. 1), also referred to as the Glengarry Half-Graben (Prime and Boehner, 1984), situated on the southern margin of the Maritimes Basin of the Avalon zone in the Appalachian Structural Province (Poole, 1967; Williams et al., 1972; Williams, 1979).

The Maritimes Basin extends from the Gulf of Maine northward through Western Newfoundland. The basin contains a complex of rift valleys bounded by high-angle faults or sharp downflexures, surrounded by relatively stable platforms (Belt, 1968). Carboniferous sedimentation was localized mainly in successor basins, developed upon the earlier Taconic and Acadian deformed zones, characterized by the development of synsedimentary horsts and grabens. The horsts, in general, behaved as sporadically active, local positive elements that shed vast amounts of nonmarine detritus into adjacent, interconnected, yoked grabens and half-grabens (McCabe and Schenk, 1982). Thus the sedimentary succession in the Maritimes Basin consists of thick terrestrial clastics, predominantly redbeds with minor marine units, ranging in age from Middle Devonian to Early Permian.

Within the basin, the Lower to Upper Carboniferous Windsor and Canso groups are most relevant to the Yava area. The Visean Windsor Group is a kilometre-thick lithostratigraphic unit distinguished by perhaps a dozen cycles, each usually of marine carbonate overlain by gypsum/anhydrite, and capped by red siliciclastics. The lower part of the Windsor Group is a thin laminated carbonate overlain by 100 to 400 m (maximum) of anhydrite, and 300 m of halite followed by several much thinner cyclic units. The basal portion of the Windsor Group is studded with carbonate mud mounds reaching 100 m in thickness (McCabe and Schenk, 1982).

Strata of the overlying Namurian to lower Westphalian Canso Group suggest re-establishment of similar environmental conditions to those in the Early Carboniferous, with lakes in the low areas and local alluvial fans along basin margins. The climate, which had been predominantly arid during the Visean, shifted toward moderate rainfall during the Namurian to Westphalian resulting in grey, coal-bearing siliciclastics of alluvial affiliation. The wetter climate resulted in derivation of sediment from more distant sources: the coarse fluvial facies of Belt (1965).

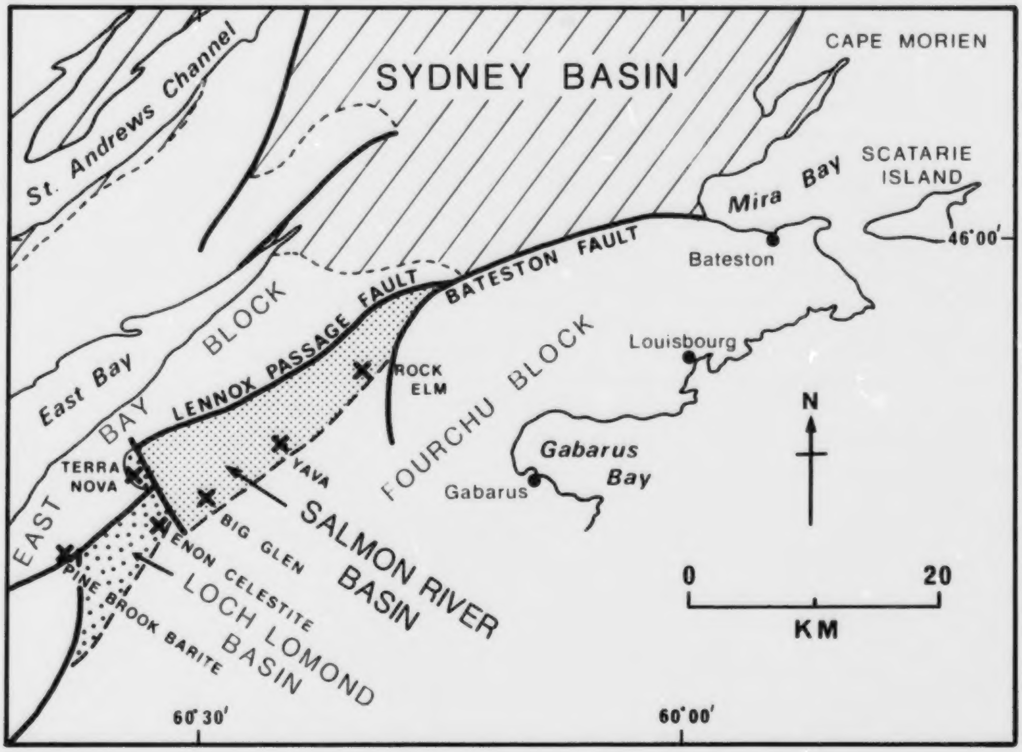
CAPE MORIEN
SYDNEY BASIN
St. Andrews Channel
Mira Bay
SCATARIE ISLAND
46°00'
Bateston
BATESTON FAULT
LENNOX PASSAGE FAULT
East Bay
EAST BAY BLOCK
ROCK ELM
FOURCHU BLOCK
Louisbourg
N
Gabarus Bay
Gabarus
TERRA NOVA
YAVA
BIG GLEN
SALMON RIVER BASIN
ENON CELESTITE
PINE BROOK BARITE
LOCH LOMOND BASIN
0
20
KM
60°30'
60°00'

Figure 1. Location of Salmon River and Loch Lomond basins, southeastern Cape Breton Island, Nova Scotia (modified from Prime and Boehner, 1984).

SALMON RIVER BASIN GEOLOGY

The Yava deposit is located at the southeastern margin of the Salmon River Basin (Keppie, 1982; Prime and Boehner, 1984). This small Carboniferous structural basin in southeastern Cape Breton Island is situated southwest of the Sydney Basin. The wedge-shaped Salmon River Basin trends northeast-southwest, is almost 25 km long and a maximum of 8 km wide, and covers an area of approximately 125 km^2 (Fig. 2). It contains up to 1500 m of Visean to upper Westphalian strata dominantly of nonmarine origin.

The Salmon River Basin is fault bounded on the southwest with marine Visean Windsor Group rocks of the contiguous Loch Lomond Basin. The southeastern border with the Fourchu Block is an onlap unconformity-nonconformity with Cambrian and Devonian rocks of the Loch Lomond plutonic complex and Ordovician clastic metasedimentary rocks of the Kelvin Glen Group. The northwestern border of the basin is in fault contact with Lower Cambrian volcanic rocks of the Fourchu Group and the Devonian Huntington Mountain Pluton of the East Bay Block.

Intrusive rocks

The Loch Lomond plutonic complex is the largest granitoid body in southeastern Cape Breton Island. The main body is approximately 26 km long with a maximum width of 7 km and consists of three suites: 1) the Chisholm Brook granodiorite, originally considered to be of Early Cambrian age (Rb/Sr = 544 +/−21 Ma; Barr et al., 1984) but recently shown to be late Precambrian (U/Pb = 620 Ma; S.M. Barr, pers. comm., 1989; 2) the Salmon River porphyry, Late Devonian (Rb/Sr = 368 +/−30 Ma; Barr et al., 1984); and 3) the Miller's Brook monzodiorite (McMullin, 1984).

Chisholm Brook granodiorite

The granodiorite of the Loch Lomond complex area is medium grained and inequigranular. Subhedral to euhedral plagioclase is set in a finer grained matrix of quartz and potassium feldspar. Although plagioclase is commonly zoned, it is generally of oligioclase composition. In the immediate Terra Nova area, the matrix contains abundant calcite. Most of the mafic material is chloritized biotite and amphibolite.

The granodiorite is commonly transected by highly altered mafic dykes; chloritization of mafic material is the most common type of alteration.

Salmon River porphyry

The Salmon River porphyry, the northern half of the Loch Lomond igneous complex, is a pink to orange-red aphanitic rock with abundant phenocrysts of quartz and feldspar in a fine grained groundmass; the relative proportions of phenocrysts to groundmass range from 50:50 to 25:75 (Barr et al., 1984). The porphyry breaks with a clean subconchoidal fracture and is relatively unweathered. There are also minor occurrences of deep red coarser grained rocks which break with a rougher fracture, referred to by McMullin (1984) as microgranite.

Homogeneous round quartz phenocrysts, from 0.5 to 2 mm in diameter, exhibit partial resorption at their margins, some of which are sericitized. Feldspar occurs as grain clusters or anhedral to euhedral phenocrysts from 0.2 to 0.6 mm in diameter. Although potassium feldspar is abundant in the groundmass, feldspar phenocrysts are generally albitic. Muscovite phenocrysts range from 0.2 to 1 mm in length and occur in tabular or in fan-shape forms with unaltered grains containing small inclusions of heavy minerals, mostly rutile and zircon. The groundmass consists of microcrystalline quartz (0.05 mm) and unidentified clay minerals. The porphyry is generally variably altered; sericitization, pervasive in most samples, is most notable in feldspar phenocrysts, which have a "cloudy" appearance owing to the presence of fine grained sericite. Although some of the albite grains are heavily sericitized and may appear inhomogeneous with clay mineral inclusions, the general outline of the grains is well preserved. The average composition of the porphyry is shown in Table 1.

Sedimentary rocks

Stratigraphy

The strata within the Salmon River Basin form an asymmetrical southwest-plunging syncline. Bedding generally dips 10 to 20 degrees northwest, except along the steep Lennox Passage Fault where sediments dip 75 degrees to the southeast.

In the Yava area, rocks of the Salmon River Basin (Glengarry Half-Graben of Prime and Boehner, 1984) are dominated by Windsor Group marine evaporites, minor carbonate, and shales (possibly of nonmarine origin) and Canso Group/Riversdale Group and Morien Group marginal marine to fluvial sediments (Fig. 3). Near the centre of the basin, these rocks have a maximum projected thickness of more than 1500 m and range in age from Visean to late Westphalian (Prime and Boehner, 1984). Along the unconformity defining the southeastern border of the basin, there is a progressive onlap of basin fill sedimentary rocks against the basement in the area southwest of Yava and stratified basement northeast of Yava, resulting from a Carboniferous onlap along a basal unconformity (Fig. 4).

The major rock units above the Salmon River porphyry in the Yava area are marine carbonates and siliciclastics of the Uist Formation, the shale-dominated transitional assemblage of the MacKeigan Lake Formation, and disconformably overlying continental sandstones of the Silver Mine Formation. Toward the centre of the basin, this sequence is overlain by conglomerate of the Big Barren Formation and by coal-bearing sandstone of the Glengarry Valley Formation (Fig. 2).

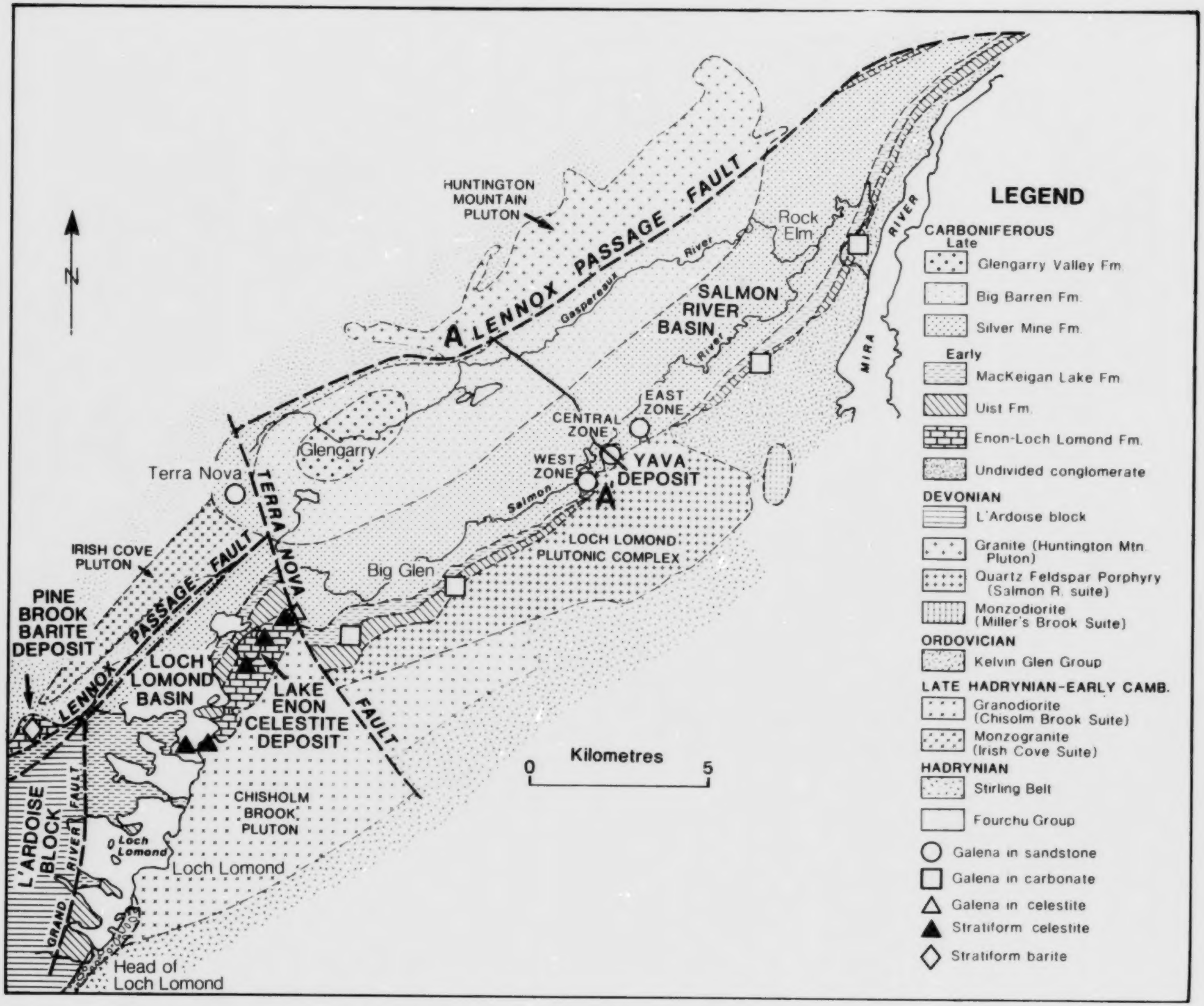
N
HUNTINGTON MOUNTAIN PLUTON
LENNOX PASSAGE FAULT
A
Gaspereaux River
SALMON RIVER BASIN
River
Rock Elm
MIRA RIVER
Glengarry
Terra Nova
TERRA NOVA FAULT
EAST ZONE
CENTRAL ZONE
WEST ZONE
YAVA DEPOSIT
Salmon
LOCH LOMOND PLUTONIC COMPLEX
IRISH COVE PLUTON
Big Glen
PINE BROOK BARITE DEPOSIT
LENNOX PASSAGE FAULT
LOCH LOMOND BASIN
LAKE ENON CELESTITE DEPOSIT
L'ARDOISE BLOCK
GRAND RIVER FAULT
CHISHOLM BROOK PLUTON
Loch Lomond
Loch Lomond
Head of Loch Lomond
Kilometres
0
5
LEGEND
CARBONIFEROUS
Late
Glengarry Valley Fm.
Big Barren Fm.
Silver Mine Fm.
Early
MacKeigan Lake Fm.
Uist Fm.
Enon-Loch Lomond Fm.
Undivided conglomerate
DEVONIAN
L'Ardoise block
Granite (Huntington Mtn. Pluton)
Quartz Feldspar Porphyry (Salmon R. suite)
Monzodiorite (Miller's Brook Suite)
ORDOVICIAN
Kelvin Glen Group
LATE HADRYNIAN-EARLY CAMB.
Granodiorite (Chisolm Brook Suite)
Monzogranite (Irish Cove Suite)
HADRYNIAN
Stirling Belt
Fourchu Group
Galena in sandstone
Galena in carbonate
Galena in celestite
Stratiform celestite
Stratiform barite

Figure 2. Geology of the Salmon River Basin and surrounding area with locations of major sulphide and sulphate deposits (from Vaillancourt and Sangster, 1986).

Table 1. Means and standard deviation of major and trace element analyses, Lock Lomond plutonic complex (Barr et al., 1984).

	CHISHOLM BROOK Granodiorite n = 12			SALMON RIVER Porphyry n = 18		
SiO_2	70.8	±	1.3	74.3	±	0.6
TiO_2	0.41	±	0.06	0.06	±	0.01
Al_2O_3	14.7	±	0.5	14.0	±	0.4
Fe_2O_3	1.4	±	0.4	0.7	±	0.3
FeO	1.4	±	0.1	0.6	±	0.2
MnO	0.12	±	0.04	0.02	±	0.02
MgO	0.86	±	0.15	0.12	±	0.08
CaO	1.87	±	0.12	0.36	±	0.12
Na_2O	3.76	±	0.30	3.49	±	0.39
K_2O	3.11	±	0.34	4.80	±	0.51
P_2O_5	0.12	±	0.03	0.01	±	0.01
B	6	±	2	9	±	3
Ba	770	±	80	176	±	282
Cu	10	±	3	13	±	5
F	390	±	30	300	±	140
Li	9	±	5	15	±	12
Mo	0.9	±	0.2	0.8	±	0.2
Pb	8	±	8	30	±	9
Rb	76	±	21	200	±	42
Sn	1.8	±	0.6	2.3	±	0.9
Sr	241	±	58	53	±	19
Th	12	±	2	25	±	6
U	2.7	±	0.3	4.5	±	2.7
Zn	62	±	9	31	±	10

Windsor and Canso groups

Uist Formation

The Uist Formation is a complex wedge of porphyry breccia (best developed in the Yava mine area), coarse angular to subrounded conglomerate, and minor limestone-dolostone varying in thickness from 92 to 140 m (Prime and Boehner, 1984). The breccia reaches a maximum thickness of 15 m, and is a poorly lithified, inhomogeneous rock composed of angular to subangular fragments of porphyry of mixed cobble to pebble size in a matrix of massive olive-green silty clay transected by minor calcite veins. Feldspar clasts consist of almost equal proportions of albite and microcline. Sericitization of feldspars is the major alteration and ranges from moderate to extreme, with albite being more affected than microcline. In the most heavily altered samples, sericitization occupies cleavage and twinning planes of feldspars but otherwise forms a network around most grains. The matrix of the breccia consists of calcite, microgranular quartz, clay, and sericite. Calcite in places forms up to 75 percent of the matrix, has varying grain sizes but is typically between 0.2 and 0.4 mm. Veins in the breccia are also calcitic and, in places, contain minor amounts of galena.

The porphyry breccia is overlain by a variable thickness (0-18 m) of conglomerate in areas mostly outside of the Yava mine area. The red to brown conglomerate contains pebbles of quartz, limestone, volcanics, and granite, with local thin beds of gritty sandstone and shale. The overlying unit (Big Glen Member; Boehner, 1983), of variable thickness (0-15 m), forms massive resistant outcrops of finely crystalline dolostone with cavities partly lined by coarse grained calcite. It is grey to brown and locally bioclastic containing crinoid and brachiopod debris as well as sparsely disseminated galena. Fossils and organic material are most notable as concentric forms with a diameter of 0.2 to 0.4 mm that are very likely mollusc and ostracod fragments. These concentric forms are lined with sparry calcite and contain sphalerite grains. Botryoidal pyrite also occurs with the organic matter. Coarse grained gypsum aggregates and random veins of celestite transect the matrix.

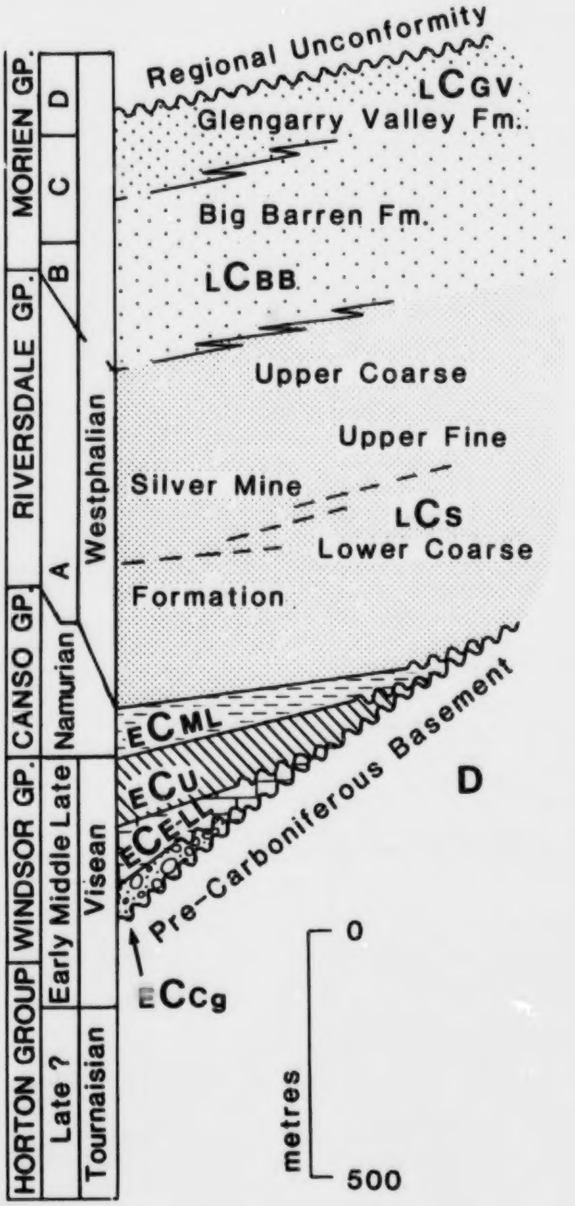
MORIEN GP.
RIVERSDALE GP.
CANSO GP.
WINDSOR GP.
HORTON GROUP
D
C
B
A
Late
Namurian
Early Middle Late
Late ?
Westphalian
Visean
Tournaisian
Regional Unconformity
LCGV
Glengarry Valley Fm.
Big Barren Fm.
LCBB
Upper Coarse
Upper Fine
Silver Mine
LCs
Lower Coarse
Formation
ECML
ECU
ECELL
ECCg
D
Pre-Carboniferous Basement
0
metres
500

Figure 3. Stratigraphic section, Salmon River Basin (modified from Prime and Boehner, 1984). Unit symbols as in Figure 5.

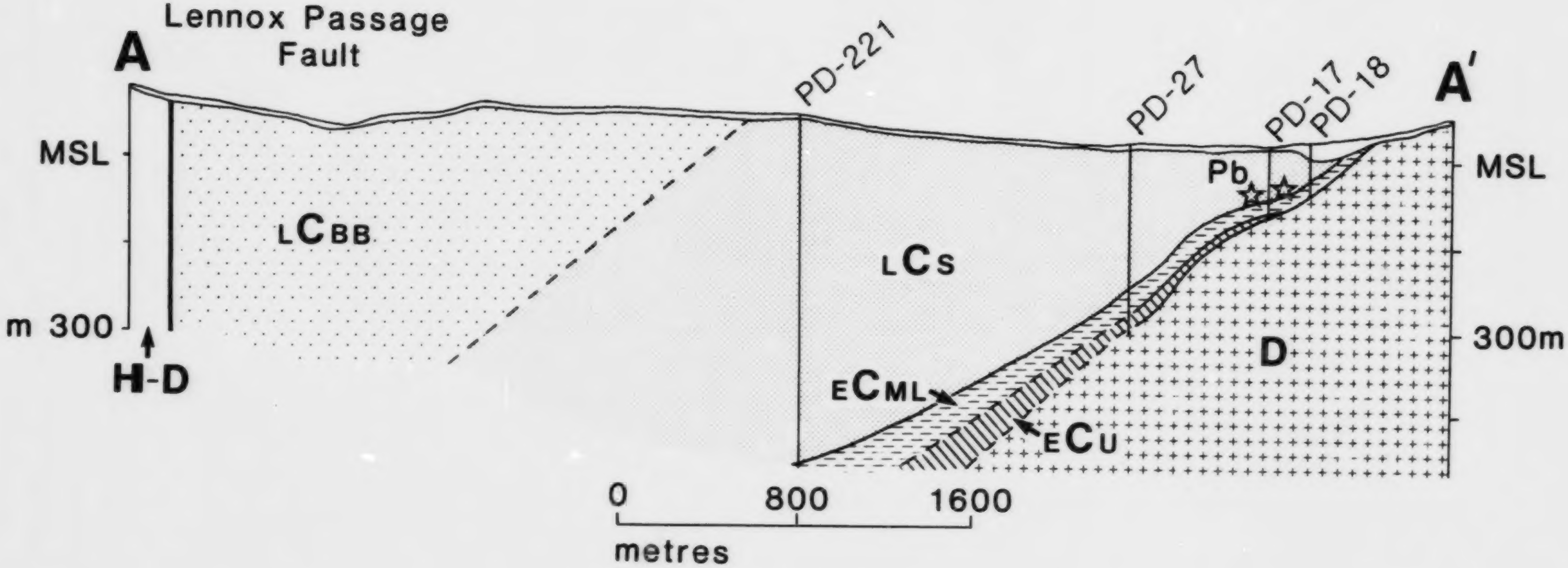
A
Lennox Passage
Fault
MSL
m 300
H-D
$_{L}C_{BB}$
PD-221
$_{L}C_{S}$
$_{E}C_{ML}$
PD-27
PD-17
PD-18
Pb
$_{E}C_{U}$
D
A′
MSL
300m
0
800
1600
metres

Figure 4. Cross-section, Salmon River Basin. Position of section A-A′ shown in Figure 2 (modified from Prime and Boehner, 1984). Unit symbols as in Figure 5.

MacKeigan Lake Formation

The MacKeigan Lake Formation conformably overlies the limestone at the top of the Uist Formation. The formation extends the full length of the basin except locally at the Yava deposit where it is overstepped by the Silver Mine Formation.

The MacKeigan Lake Formation consists of three to four distinct subunits. At the base is red siltstone (<4 m) overlain by interbedded grey shale, limestone, and gypsum (<78 m). The gypsum gradually decreases in abundance upward and the unit is transitional into an upper section of fine grained, green and red sandstone and mudstone (<33 m) (Prime and Boehner, 1984).

The MacKeigan Lake Formation lies between marine carbonates of the Uist Formation and continental sandstone of the Silver Mine Formation. As such, the depositional environment of the formation may have been transitional between marine and continental. Although no marine fossils have yet been identified in the formation, the abundant gypsum, occurring as beds and nodules, attests to at least periodic marine flooding. The simplest interpretation of the MacKeigan Lake lithologies, therefore, is a lagoonal mud flat subjected to occasional inundations by the sea.

In the Yava mine area, a calcareous unit up to 2 m thick overlies the MacKeigan Lake Formation. This unit is a light grey, inhomogeneous, friable rock consisting of interlocking fragments of pink to grey, cryptocrystalline calcite in a clay matrix that Bonham (1982) interpreted as a calcrete. The fragments are of various sizes from several millimetres to 15 cm and are separated by irregular cracks and fractures filled with either soft green to grey clay or white sparry calcite (Bonham, 1982). The unit has a consistent vertical profile, comprising an irregular transitional nodular central part and a cap of locally preserved laminar bedded carbonate up to 10 cm in thickness (Bonham, 1982). Throughout most of the rock, there is in situ replacement of micron-sized grains of calcite and aragonite by sparry calcite with decimicron- to centimicron-sized crystals. Numerous coarser grained calcite veins and vugs occur throughout in addition to abundant fractures and stylolites. The rock also contains a variable amount of mud clasts and aggregates of gypsum and celestite.

Riversdale Group

Silver Mine Formation

The Silver Mine Formation disconformably overlies calcrete of the MacKeigan Lake Formation. A three-part subdivision of the Silver Mine Formation was recognized by Prime and Boehner (1984):

1) a lower unit of medium to coarse grained green-grey sandstone (>225 m) that displays a subtle transition upward into;

2) a middle unit of red to grey-green, fine grained sandstone with mudstone and minor coal (>335 m); and

3) an upper unit of coarse sandstone (>60 m).

In the Yava mine area, the lower sandstone unit is underlain by a limestone pebble conglomerate, shale flake conglomerate, or coal lag. Generally, the conglomerate is characterized by rounded carbonate clasts with a diameter between 2 mm and 3 cm, minor coal particles, and quartz clasts between 0.5 and 2 mm in a sandy matrix of feldspar, carbonate, microcrystalline quartz, chert fragments, and clay. Feldspar is generally altered to calcite. Where the rock is mostly carbonate, quartz grains are engulfed in a matrix of calcite. The 1 to 3 m thick conglomerate grades upward into a medium- to coarse-grained grey sandstone. Typically, the lower sandstone unit grades from grey and galena-bearing at its base to green and nongalena-bearing higher in the sequence (Vaillancourt, 1985). The grey sandstone is characterized by bands of galena and by pyrite-galena-sphalerite-rich woody fragments at its base. The green sandstone, which constitutes the bulk of the Silver Mine Formation, is generally sulphide-poor relative to the grey sandstone, and very homogeneous, with minor coaly fragments that are never or rarely sulphide-bearing. Although both sandstones contain pyrite, the manner in which it occurs in each is different: in the grey sandstone, the pyrite is commonly associated with coal, while in the green sandstone the pyrite occurs as isolated clusters. Minor carbonate, usually as cement, is ubiquitous throughout the section. Randomly distributed feldspar grains occur in both sandstone types.

The distinction between the two sandstone types within the lower unit is important because ore-grade galena is restricted to the grey sandstone; only minor galena occurs in the green sandstone. To better characterize the two sandstone types, porosity and mineral composition of each were determined by image processing on the Jeol Microprobe at the Continental Shelf Institute, Trondheim, Norway. Porosity of the green sandstone ranges from 8 to 10 percent whereas that of grey sandstone is more variable; in strongly mineralized sections it is between 1 and 5 percent, while throughout the rest of the rock, it ranges from 15 to 22 percent. Apart from the galena, the most important compositional difference between the grey and green sandstone is clay content which ranges from 1 to 15 percent in the grey galena-bearing sandstone, but from 15 to 25 percent in the green sandstone. A summary of the petrographic and lithological features of the two sandstone members is presented in Table 2.

The precise stratigraphic relationship between the green and grey sandstones, and its sedimentological and metallogenetic significance, is not known with any certainty. Because the present study was initiated after the Yava mine closed, the green-grey transition could only be examined in drill core. Even if access to the mine were possible, it is doubtful if the mine workings ever exposed the transition because all ore-grade material occurs in the grey sandstone. In his description of the Yava mine, based largely on underground exposures, Bonham (1983) did not mention green sandstone or its relationship with the ore-bearing grey sandstone. Recognition and petrographic descriptions of the two sandstone types were, in fact, not made until two years later (Vaillancourt, 1985).

Table 2. Summary of major petrographic and lithological features characterizing the grey and green sandstone members, Silver Mine Formation (Vaillancourt, 1985).

	Porosity	Quartz grains	Clay content	Clay mineralogy	Sulphide, sulphate mineralogy	Coaly debris	Other minerals
GREY SANDSTONE	1-5% in galena-rich portion 15-22% in galena poor portion	Medium to coarse Mature, well rounded Overgrowths common	1-15%	High kaolinite/ chlorite ratio	galena pyrite sphalerite barite	-Abundant at base of fluvial cycles -abundant pyrite, sphalerite, galena	-heavy minerals -K-Feldspar common -muscovite
GREEN SANDSTONE	8-10%	Medium grained Immature, angular Overgrowths not common	15-25%	Low kaolinite/ chlorite ratio	pyrite	-present in minor amounts -nonsilicified -minor pyrite	-only minor amounts

Although it has been suggested that the grey sandstone may represent a form of diagenetic alteration of the green sandstone (B. Rust, pers. comm., 1988; R.C. Boehner, pers. comm., 1989), the authors prefer to attribute the differences to differing source provenances for the two sandstone types. The chlorite-poor and kaolinite-rich grey sandstone is best developed in the immediate Yava area, close to the mafic-poor, potassium-rich Salmon River porphyry (Fig. 2). In contrast, the more abundant chlorite-bearing Chisholm Brook granodiorite and Irish Cove monzogranite on the southwestern end of the Salmon River Basin are obvious and likely sources for the chloritic green sandstone. Grey sandstone, for example, was not noted in the Terra Nova deposit which occurs in the southwestern extension of the basin where it is underlain by the Irish Cove pluton (Fig. 2).

These preliminary observations suggest that the grey sandstone was derived largely from the porphyry and may, in fact, be distributed only as a local detrital apron or pediment close to the porphyry source. It is obvious that much more study on the nature and distribution of the two sandstone types is required before their relationship, and its significance, is understood.

The middle unit of the Silver Mine Formation, which is devoid of sulphide material and generally absent in the mine area, consists of mudstone, siltstone, and sandstone which may be green, grey-green, or red. The percentage of fines within the middle unit is substantially greater than in the lower unit, with coal seams and carbonaceous shales being prominent, averaging 1 to 2 cm in thickness.

The upper unit of the Silver Mine Formation exhibits a return to a coarse grained grey sandstone similar to the basal unit, although it is not galena-bearing. The unit is 60 m thick, contains coal fragments, and is transitional into the overlying Big Barren Formation.

Morien Group

Big Barren Formation

This formation has a maximum projected thickness of 700 m (Prime and Boehner, 1984) and consists of interbedded red conglomerate, sandstone, and mudstone. The conglomerate clasts are well rounded, clast supported, well sorted, and consist predominantly of quartzite. These features contrast with those of the Uist Formation and other older conglomerates which are typically immature, poorly sorted, subangular, and commonly granitoid-rich.

Glengarry Valley Formation

The Glengarry Valley Formation is conformable, transitional, and interstratified with the underlying Big Barren Formation. It ranges in thickness from 210 to 300 m and consists of fine grained green-grey and red sandstone, with siltstone and shale interbeds and minor coal seams (Prime and Boehner, 1984).

The formation is confined to a relatively small elliptical area in the northwestern portion of Glengarry Valley where Carboniferous sediments of the Salmon River Basin reach their maximum thickness.

Base metal occurrences

Base metal occurrences in the Salmon River Basin occur at or near unconformity pinchouts of several stratigraphic units in contact with basement (Fig. 5). Although the Yava sandstone-lead deposit is the major occurrence in the Salmon River Basin and was examined in greatest detail, drill core from the Big Glen and Rock Elm occurrences were also briefly examined (Fig. 2).

Big Glen and Rock Elm are located southwest and northeast of Yava, respectively. Although galena in sandstone commonly occurs in these occurrences, the Silver

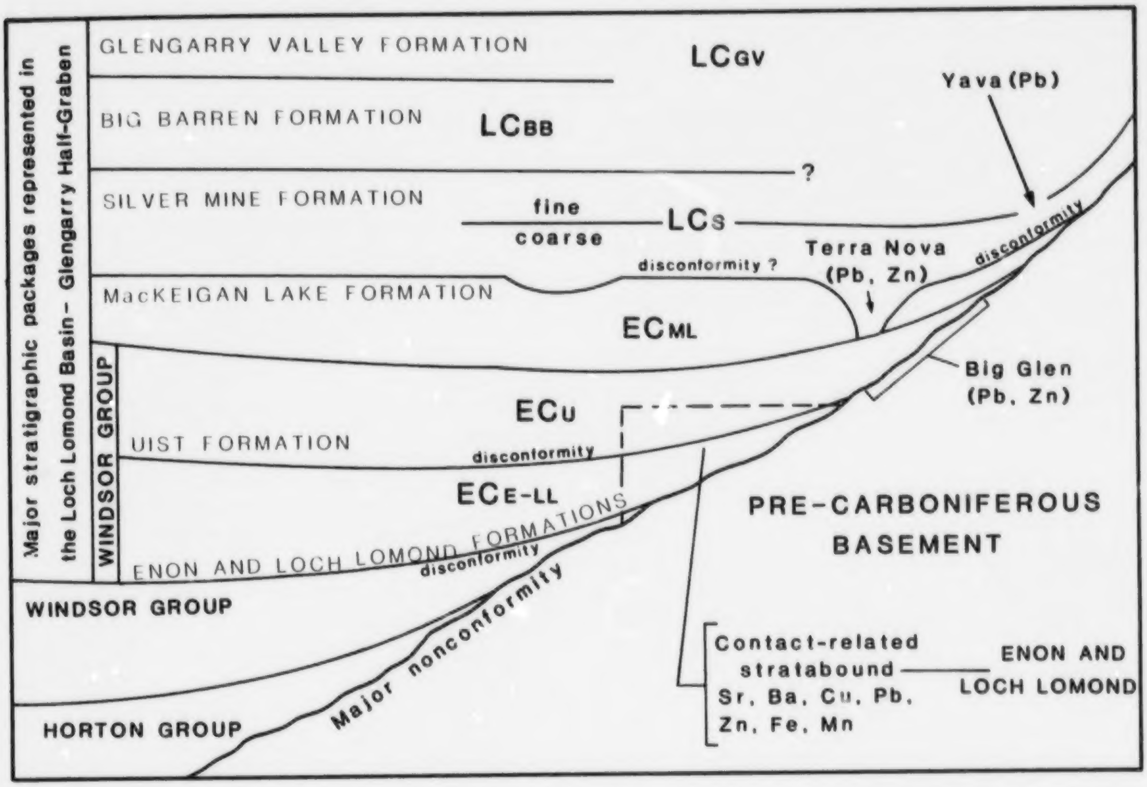
Major stratigraphic packages represented in the Loch Lomond Basin – Glengarry Half-Graben
GLENGARRY VALLEY FORMATION
LCGV
BIG BARREN FORMATION
LCBB
?
SILVER MINE FORMATION
fine
coarse
LCS
Yava (Pb)
disconformity
Terra Nova (Pb, Zn)
disconformity ?
MacKEIGAN LAKE FORMATION
ECML
WINDSOR GROUP
Big Glen (Pb, Zn)
ECU
UIST FORMATION
disconformity
ECE-LL
ENON AND LOCH LOMOND FORMATIONS
disconformity
PRE-CARBONIFEROUS BASEMENT
WINDSOR GROUP
Major nonconformity
Contact-related stratabound Sr, Ba, Cu, Pb, Zn, Fe, Mn
ENON AND LOCH LOMOND
HORTON GROUP

Figure 5. Relationship of mineral occurrences to stratigraphy and basement onlap, Salmon River Basin (modified from Prime and Boehner, 1984).

Mine Formation is not in contact with basement igneous rocks. In fact, galena mineralization in Uist Formation carbonate rocks is more characteristic of these areas. Where galena does occur in sandstone, it is as very minor disseminations in green sandstone devoid of coaly material.

The Terra Nova deposit occurs west of the Terra Nova Fault in an outlier of the Salmon River Basin (Fig. 2). Galena occurs as fine disseminations in green sandstone at the base of the sedimentary sequence. Galena concentrations occur in paleochannels, possibly reflecting ancient stream channels. Terra Nova differs from Yava in several aspects: 1) it has a lower grade of mineralization; 2) the sandstone stratigraphy, specifically coaly or organic material, is rare; and 3) the Zn/Pb ratio is higher, with sphalerite mineralization more pervasive overall.

Within the Loch Lomond Basin (Fig. 2), the Pine Brook barite and Lake Enon (Kaiser) celestite deposits were also examined and sampled, as they contain minor to trace base metal sulphides. Pine Brook is a small stratiform barite deposit within Windsor Group carbonates that was briefly accessible during open-pit mining. The Lake Enon deposits were mined for celestite which occurs as lenses and layers in Windsor Group carbonates and evaporites (Forgeron, 1977).

YAVA MINE GEOLOGY

Local geology

The Salmon River porphyry forms a topographic high, presently up to 50 m above the basin nonconformity, along the southeastern edge of the Salmon River Basin (Fig. 2). Although Yava lies in sandstone of the Silver Mine Formation above depressions in the porphyry, it is separated from the porphyry by shales of the MacKeigan Lake Formation. The sandstones also onlap the porphyry on paleotopographic ridges; in these areas, mineralization is lower grade or absent. Thicker sections of the MacKeigan Lake Formation shales and the Big Glen dolostone of the Uist Formation lie nonconformably on the basement east and west of Yava. The Yava deposit is therefore located at the apex of the onlap sequence in the Salmon River Basin. The thickness of underlying stratigraphic units increases not only to the southwest but also in a northwesterly and northeasterly direction.

Although basement relief is considered to be the primary control on mineral distribution, three other aspects influence grade (Bonham, 1982, p. 15):
1) Lithology — within the interbedded units of conglomerate, sandstone, and shale, mineralization is confined to sandstone and the sandy matrix of the

conglomerates. Mineralization does not occur in shale or as replacement of any of the conglomerate clasts. The galena forms as a cement, filling open pore spaces in the sandstone.

2) Early diagenetic effects — throughout the sandstones, concretions occur where an early diagenetic cement of calcite and siderite has formed. These features cut bedding, but predate mineralization. They effectively seal porosity and apparently prevented deposition of galena.

3) Organic content — coaly lag horizons, which occur as discontinuous interbeds at or near the base of fining upward cycles within the sandstone, generally carry lead grades that are up to twice that of the surrounding host sandstone.

Ore zones

Yava consists of three ore zones (West, Central, and East) which are situated along strike over a distance of 3000 m and extend downdip for 600 m. Ore reserves have been estimated to be 3.5 million tonnes at 4.1% Pb at a 3% Pb cutoff (Table 3).

Table 3. Ore reserves, Yava deposit (Bonham, 1982)

Proven geological reserves as of July 1, 1981

Zone	3.5% cutoff Tonnes	%Pb	3.0% cutoff Tonnes	%Pb
WEST ZONE				
Unmined areas	629 651	4.95	773 600	4.68
Recoverable pillars in first pass areas	97 488	4.87	97 488	4.87
Crown pillars (surface)	97 521	5.69	97 521	5.69
EAST ZONE				
Crown pillar (surface)	331 385	4.34	443 743	4.07
East Zone to 115 m depth excluding crown pilar	804 539	4.14	1 757 619	3.74
Downdip probable in East Zone	383 162	3.96		
CENTRAL ZONE				
Central Zone	217 250	4.38	217 250	4.38
Crown pillar (surface)	127 324	4.29	127 324	4.29
Total Yava	2 688 320	4.44	3 514 625	4.12

Preproduction ore reserves as of June 1979
West Zone proven geological reserves to 4% cutoff at start of mining:

517 000 tonnes at 6.2% Pb
+594 000 tonnes at 5.1% Pb (probable)

Total 1 111 000 tonnes at 5.6% Pb

Total mine production August 1979 - June 1981

344,193 tonnes at 4.68% Pb (mill head grade)

Overall reserves for all three zones (proven, probable, and potential)
Preproduction 1970

Cut-off	Reserves
4% cut-off	3.97 m tonnes at 5.3% Pb 1.63 m tonnes at 4.9% Pb (additional)
3.5% cut-off	6.46 m tonnes at 4.1% Pb 4.44 m tonnes at 3.9% Pb (additional)
2.5% cut-off	11.0 m tonnes at 3.5% Pb 5.9 m tonnes at 3.3% Pb (additional)

Paleotopography of the porphyry basement, reconstructed from drillhole data, shows that these zones of higher grade lead coincide with basement depressions (Bonham, 1983) even though galena-bearing sandstone of the Silver Mine Formation is separated from the basement by the MacKeigan Lake Formation (Fig. 6). Contours of lead grade, averaged over a 3.6 m mining thickness, are, in all three zones, oriented roughly perpendicular to the northeast trend of the sandstone-basement contact (Fig. 6). In common with other sandstone-lead deposits of the world, these linear zones of higher grade lead at Yava have been interpreted as the position of former stream channels in the sandstone (Sangster and Vaillancourt, in press).

In a detailed examination of the relationship between paleotopography and zones of high galena concentration, Sangster and Vaillancourt (1990) showed that the buried depressions at Yava correlate in position with modern streams in areas of basement exposure (Fig. 7). This correspondence led the authors to suggest that the positions of the modern streams are largely controlled by an exhumed Pennsylvanian topography.

All the ore zones occur exclusively in the grey sandstone of the lower unit of the Silver Mine Formation; minor amounts of mineralization also occur in the MacKeigan Lake shales of the stratigraphic footwall. The zones have a high-grade core grading laterally into lower grade margins. Although the style and nature of mineralization is the same in all three zones, the location of the ore zone within the Silver Mine Formation may change slightly from one zone to the next.

A sketch of the wall in No. 2 Decline, West Zone (Fig. 8) illustrates how the ore zone follows the Silver Mine Formation-MacKeigan Lake Formation disconformable contact. Because the sandstone host rock progressively onlaps onto the shales and porphyry, the ore zone is broadly discordant. This is particularly evident in the south-southwestern end of the decline shown in Figure 8. Here, the ore zone, although essentially conformable with the underlying contact with MacKeigan Lake Formation, crosses several beds of the Silver Mine Formation comprising complex fining upward cycles of conglomerate, sandstone, and mudstone (Bonham, 1983).

West Zone

The West Zone is the only one that has been mined, and extends for 360 m along strike and 500 m downdip. The zone consists of two northwest-trending lobes: the portal lobe and the southeastern lobe which merge into a central ore area downdip (Bonham, 1982). The overall ore

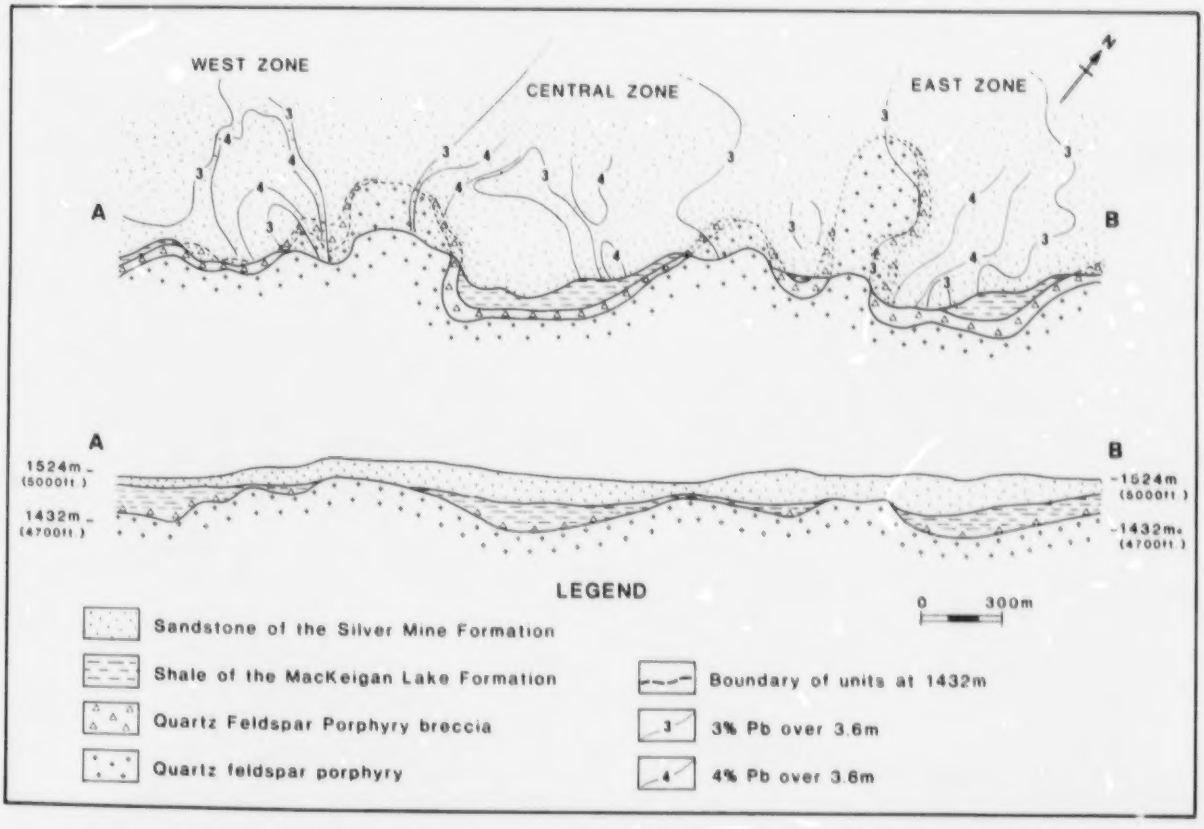
WEST ZONE
CENTRAL ZONE
EAST ZONE
N
A
B
3
4
1524m
(5000ft)
1432m
(4700ft)
LEGEND
Sandstone of the Silver Mine Formation
Shale of the MacKeigan Lake Formation
Quartz Feldspar Porphyry breccia
Quartz feldspar porphyry
Boundary of units at 1432m
3% Pb over 3.6m
4% Pb over 3.6m
0
300m

Figure 6. Generalized map and longitudinal cross-section, Yava deposit (from Vaillancourt, 1985).

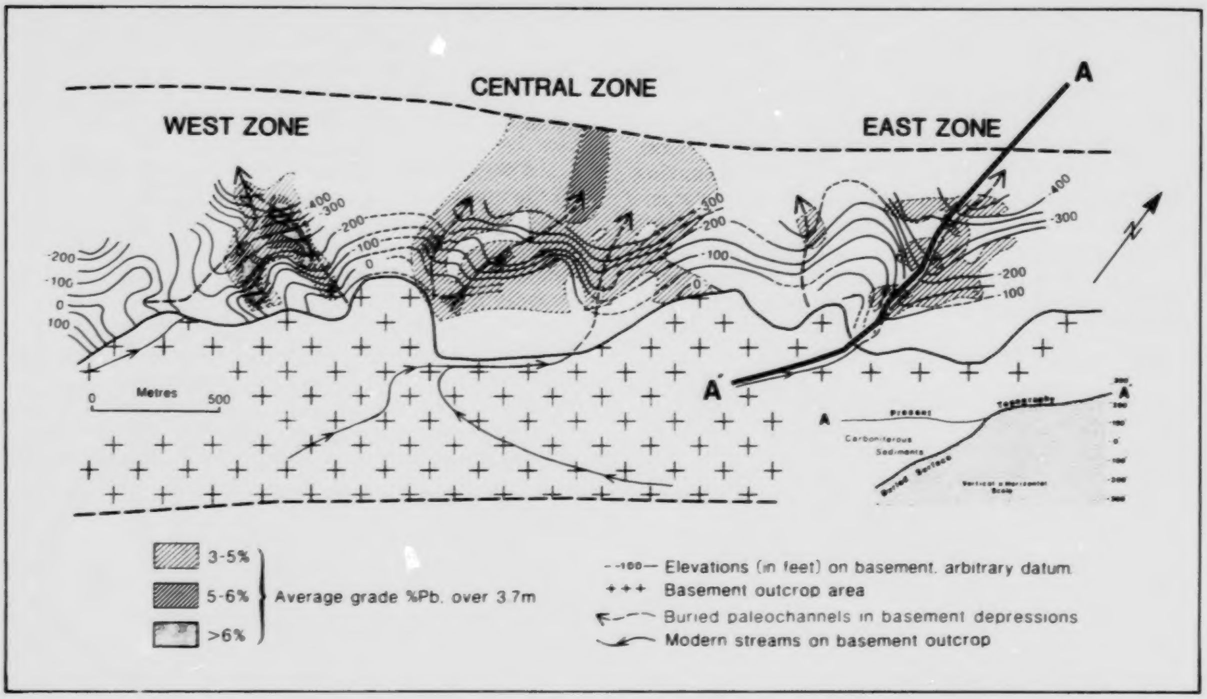
CENTRAL ZONE
WEST ZONE
EAST ZONE
A
A′
N
-400
-300
-200
-100
0
100
0 Metres 500
A
Present Topography
Carboniferous Sediments
Buried Surface
Vertical = Horizontal Scale
3-5%
5-6%
>6%
Average grade %Pb. over 3.7m
--100— Elevations (in feet) on basement. arbitrary datum
+++ Basement outcrop area
Buried paleochannels in basement depressions
Modern streams on basement outcrop

Figure 7. Map of the Yava deposit showing the location of paleochannels and modern streams in relation to mineralization. Inset shows topographic profile along line A-A′ suggesting postexhumation erosion has decreased the gradient in modern streams relative to that in the original paleostream (from Sangster and Vaillancourt, 1990).

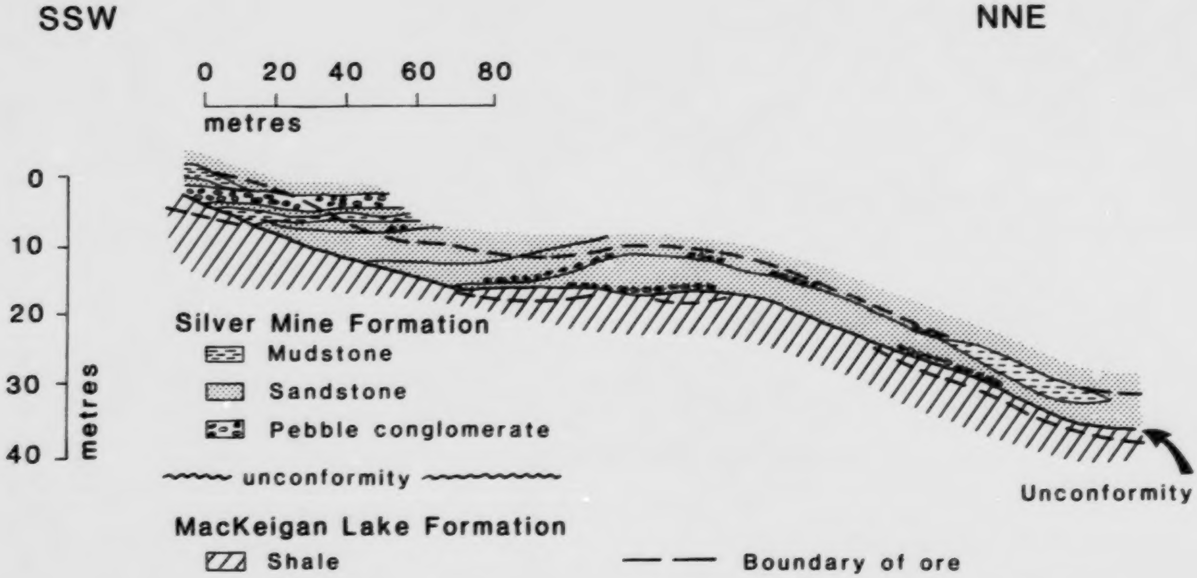
SSW
NNE
0 20 40 60 80
metres
0
10
20
30
40
metres
Silver Mine Formation
Mudstone
Sandstone
Pebble conglomerate
unconformity
MacKeigan Lake Formation
Shale
Boundary of ore
Unconformity

Figure 8. Geology of part of the updip wall, No. 2 Decline, West Zone, Yava. Note that the ore zone follows the MacKeigan Lake-Silver Mine contact and, in doing so, because of the onlapping relationship of the Silver Mine Formation, cuts across several lithological units within it. Position of No. 2 Decline is shown in Figure 9 (from Bonham, 1983).

reserves for this zone were originally calculated by Patterson (1979) to be 1.1 million tonnes at 5.6% Pb (4% cutoff).

As a result of drilling by the Nova Scotia Department of Mines and Energy in 1986 and 1987, Patterson (1987) was able to demonstrate that a low-grade Zn-rich zone extended southwest of the Yava West Zone (Fig. 9). The drilling also showed that: 1) expressed in terms of feet-percent metal, Zn values increase antipathetically with Pb values (Fig. 9); 2) in common with the Pb mineralization, distribution of Zn is controlled by the presence of topographic lows in the basement porphyry; and 3) relative to the Pb-rich West Zone, the Zn-rich extension lies farther out in the Salmon River Basin and at a slightly higher stratigraphic position in the grey sandstone member of the Silver Mine Formation (Fig. 10). Although a Zn-rich upper portion in the outer reaches of the West Zone had been previously reported on the basis of a single drillhole (Bjørlykke and Sangster, 1981, p. 189), the recent drilling at Yava appears to firmly establish a distinct Zn zone adjacent to the Pb-rich West Zone. The position of this Zn zone (i.e. farther into the basin and stratigraphically higher) is a feature also noted at the Mechernich (Germany), Laisvall and Vassbo (Sweden), and Largentiere (France) sandstone-lead deposits (Bjørlykke and Sangster, 1981).

Central Zone

The undeveloped Central Zone is a larger but poorly understood area of apparently diffuse mineralization underlying a surface area of 900 by 600 m^2. Early drilling indicated that mineralization occurs at two different levels. To the west and updip, ore occurs in footwall contact with shale of the MacKeigan Lake Formation. To the east and downdip, the ore is located within the sandstones at a position 5 m above the contact with MacKeigan Lake sediments. The zone was estimated by Metallgesellschaft in 1981 to contain 340 000 tonnes of 4.34% Pb at 3% Pb cutoff (Table 3).

East Zone

Ore grade in the East Zone occurs as a single elongate lobe, 360 m wide, extending downdip for 500 m. The ore has a variable footwall ranging from 1) direct contact with MacKeigan Lake shales to the east, 2) 8.5 m above the contact in the centre, to 3) directly on porphyry basement in the western part. The sandstone host in this area is coarser grained and contains more coaly material and fewer shale interbeds than the West or Central zones (Bonham, 1982). The East Zone crown pillar is estimated to contain approximately 440 000 tonnes of 4.07% Pb at 3% Pb cutoff. It is, however, open downdip and hence has a high potential for containing additional reserves (Table 3).

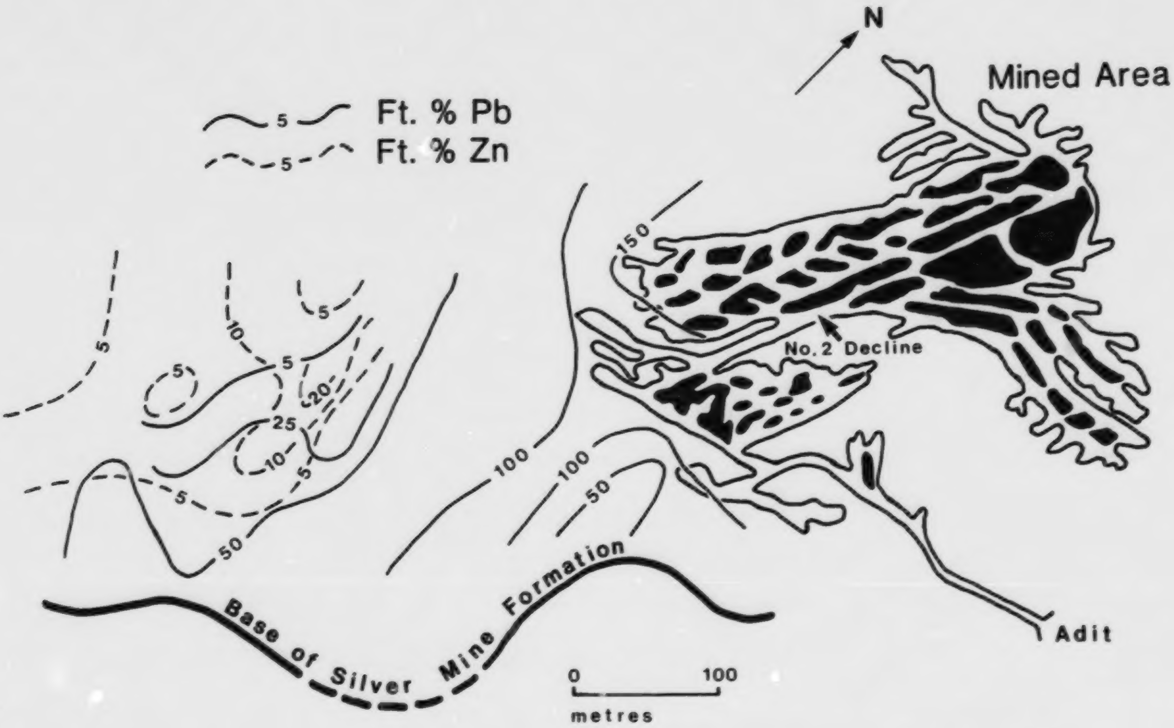

Figure 9. Position of the Zn-rich extension of the West Zone (dashed line contours) relative to the Pb-rich mined area (from Patterson, 1987 and Bonham, 1982).

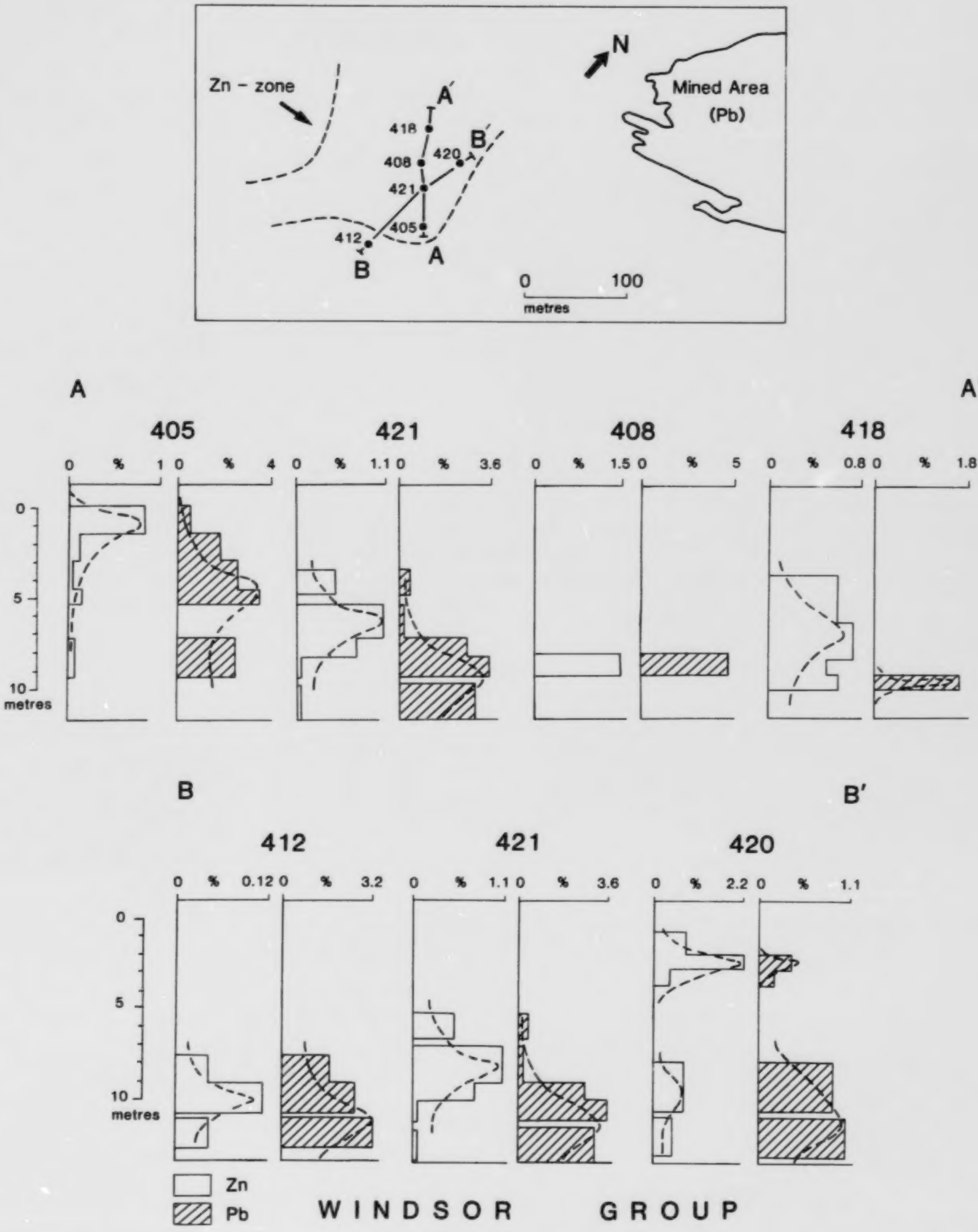

Figure 10. Assay profiles A-A′ and B-B′ through the Zn-rich extension of the West Zone, Yava. Note that zinc, in most cases, is situated slightly stratigraphically higher than the lead. Dashed lines on histograms are for emphasis only; they have no statistical significance.

Host rock petrography and mineralogy

Quartz

The grey sandstone consists of angular to semirounded mineral grains. Quartz composes between 65 and 85 percent of the rock; grain sizes range from 0.1 to 1.5 mm but are most commonly in the 0.25 to 0.5 mm range. Quartz is generally coarser grained where galena is present.

Feldspar

Feldspar is erratically distributed and constitutes probably no more than 1 percent of the sandstone. Although feldspar occurs throughout the stratigraphic succession, it is more common in the grey sandstone. Microcline, the predominant feldspar, is generally altered along cleavage and twinning planes and displays poorly defined grain boundaries corroded by carbonate and clay minerals (Fig. 11). Albite is less common than potassium feldspar. No differences were noted in feldspar composition between mineralized and unmineralized sandstone.

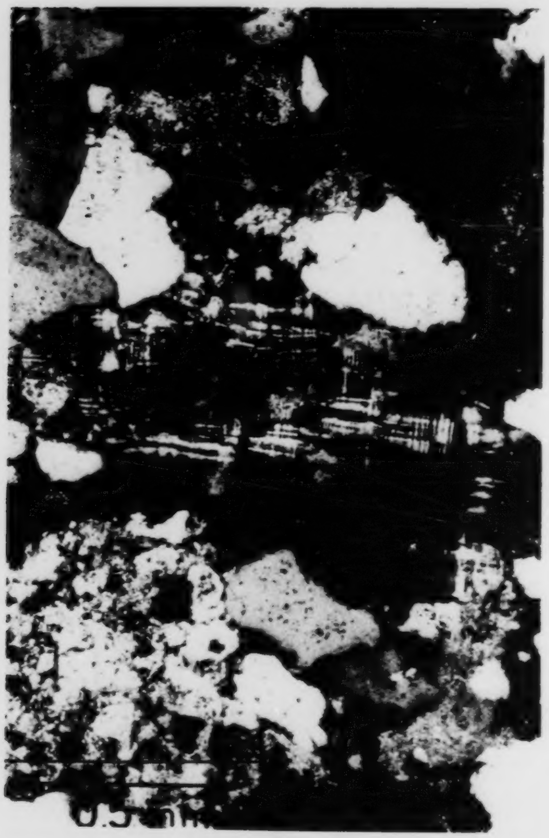

Figure 11. Detrital grid-twinned microcline grain partially altered to carbonate and clay minerals at grain boundaries, grey sandstone member, Yava (GSC 204077-I).

Carbonate

Carbonate, generally calcite, is ubiquitous throughout the stratigraphic section and most commonly occurs as cement. It is especially abundant where coal is present and occurs as both calcite and dolomite. In both the grey and green sandstone, calcite occurs as microsparite. In addition, in the grey sandstone, sparry calcite commonly fills pore spaces, conforming to straight edges of pre-existing silica overgrowths and galena. Calcite also replaces microcline along grain margins. Large calcite concretions up to 0.5 m in diameter were also encountered in the mining operations.

Heavy minerals

Within the galena-rich bands, there are concentrations of up to 25 percent of other heavy minerals; in order of decreasing abundance these are rutile, zircon, ilmenite, magnetite, and chromite. They are distinctive in thin section by their rounded prismatic habits and, in the case of rutile, yellowish to reddish-brown colour. They have very distinct grain boundaries and may be fractured. Beyond the galena-rich bands, heavy minerals are significantly less abundant, constituting no more than 3 percent by volume. Heavy minerals also occur only in trace amounts in the green sandstone.

Silica overgrowths

In addition to the presence of galena, one of the more characteristic aspects of the grey sandstone is the occurrence of silica overgrowths on detrital quartz grains (Fig. 12). Silica overgrowths are not always associated with galena or sulphide minerals nor does galena only occur where there is secondary silica, but the association between galena and secondary silica is common, especially in well mineralized sections (Fig. 13). Overgrowths also occur in the green sandstone where they are associated with pyrite, but do not fill entire pore spaces.

Muscovite

Detrital muscovite grains occur in the sandstone as large flakes along bedding planes. Petrographically the muscovite is characterized by its anomalous size (up to 2.5 mm) and birefringence. Elongate tabular blades, most common in the grey sandstone, splay out at their extremities and are commonly altered to illite.

Clay minerals

Clay in sandstone

As discussed previously, the most characteristic feature of the Silver Mine Formation sandstone at Yava is the transition from the grey sandstone at the base to the green sandstone higher in the sequence. From petrographic observations, it appears the colour change is due to a variation in clay mineral ratios from a kaolinite-enriched grey sandstone to a chlorite-enriched green sandstone. From X-ray diffraction analyses on 66 samples of both grey and

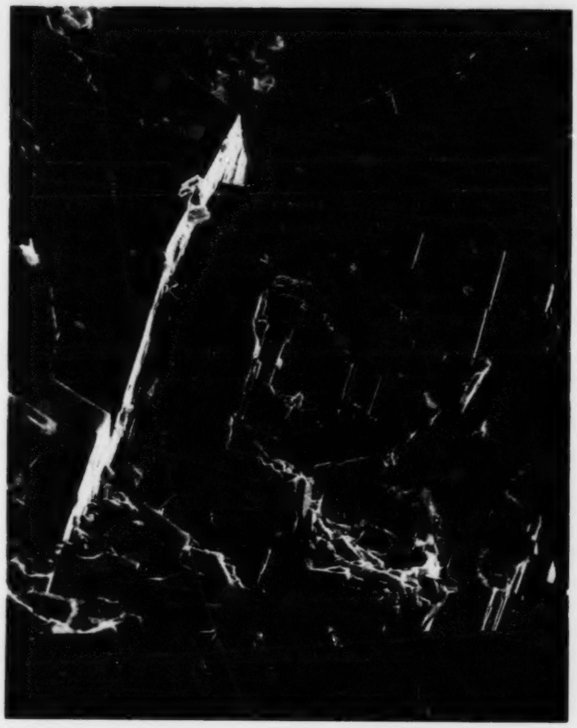

Figure 12. Scanning electron photomicrograph showing detrital quartz grain (centre) with euhedral silica overgrowth (on left) in contact with galena cement (on right). Vermicular-textured mineral at top centre is kaolinite. Bar scale is 10μ.

green sandstone at Yava, the average clay composition of all mineralized and nonmineralized samples is: kaolinite — 50% (ranging from 23 to 75%); illite — 35% (ranging from 15 to 64%) and chlorite — 15% (ranging from 5 to 39%).

Kaolinite is most abundant in pore spaces of the grey sandstone and appears as fine masses of crystals or as individual grains. It is colourless to pale yellow and has a weak birefringence. Scanning electron microscopy observations reveal a vermicular form that is well preserved as individual platelets (Fig. 12).

Illite is also common in the grey sandstone, usually in the form of acicular crystals displaying a bright yellow internal reflectance. The mineral occurs, in association with kaolinite, in pore spaces of the grey sandstone but also as flakes on altered feldspar and muscovite grains. Many of the larger muscovite grains have broken edges which have been replaced by illite; in some instances, entire muscovite flakes have altered to illite.

Chlorite occurs in two forms: detrital and diagenetic. Detrital chlorite is most common in shale and green sandstone. Minute chlorite crystals occur as rounded aggregates which appear to be mudclasts. Diagenetic chlorite occurs throughout the sandstone sequence as well defined flakes or blade-like crystals with a blue internal reflectance. The flakes are common as aggregates in the green and grey sandstones where they occupy pore spaces and occur in contact with detrital grains. Under high magnification, the chlorite flakes appear as rosettes.

Although a relationship between the presence of galena and kaolinite at the Yava sandstone-lead deposit has been proposed previously (Vaillancourt and Sangster, 1984), relatively little detailed clay mineralogy was done at the time. To remedy this, 66 samples were selected from the Yava deposit of which 53 were from the West Zone. To provide regional coverage and contrast Yava with the surrounding areas, further sampling was carried out in Terra Nova (23 samples), Big Glen (14 samples), Rock Elm (6 samples), and the Loch Lomond Basin (4 samples from Lake Enon celestite deposit and 4 samples from Pine Brook barite deposit). Sample preparation and determination methods are described in Appendix A.

Montmorillonite group clays are notably absent. When the Yava samples are divided into galena-rich and galena-poor groups, two distinctive patterns appear. In sandstones that contain 5% Pb or more, the average clay mineral abundances are: 48% kaolinite, 41% illite, and 11% chlorite. In sandstones with less than 2% Pb, the

Figure 13. Photomicrograph illustrating detrital quartz grains (light grey) partially surrounded by silica overgrowths (dark grey) in characteristic straight-edge contact with galena cement (white), Yava (GSC 204077-F).

average kaolinite content drops to 41%, illite to 36%, while chlorite increases to 23%. Thus, progressing from the stratigraphically lower galena-bearing grey sandstone to the stratigraphically higher nongalena-bearing green sandstone, chlorite abundance increases relative to kaolinite and illite (Table 4). Of the minerals illite and kaolinite, kaolinite shows the best correlation with galena and was also noted to be abundant near mineralized wood fragments.

Thus Yava, with the greatest abundance of lead, is characterized by the highest ratio of kaolinite to chlorite. Although kaolinite is present in variable proportions throughout the Yava area, kaolinitization at Yava is most intense within the grey sandstone member. On a triangular plot of kaolinite-illite-chlorite, most Yava samples plot near the kaolinite-illite axis (Fig. 14). In general, the kaolinite/chlorite ratio increases with galena abundance (Fig. 15) although considerable scatter is observed. For example, above 5% Pb, the relationship between kaolinite/chlorite and Pb is much more variable than at lower levels of Pb. At Yava, in sandstone samples with Pb grades from 0 to 0.9%, the kaolinite-to-chlorite ratio is 2.78; for Pb grades from 1 to 2.9%, it is 4.73, and for sandstone samples with a Pb grade greater than 3%, the kaolinite-to-chlorite ratio is 7.97 (Fig. 15). The grey sandstone samples averaged 5.19% Pb with average kaolinite/chlorite ratio of 7.11, while the green sandstone samples averaged 0.35% Pb, and an average kaolinite/chlorite ratio of 3.09 (Table 4). The relationship between kaolinite/chlorite ratios and Pb values at Yava is further demonstrated when the heavily mineralized West Zone is compared with the Central and East zones. For all West Zone samples, kaolinite-to-chlorite ratios average 4.55 whereas in the Central and East zones, the ratios average 3.98.

Compared to Yava, the Terra Nova deposit, hosted in green sandstone, contains much less organic material and both lead grade and kaolinite abundance are lower. Of 23 sandstone samples from eight drillholes at Terra Nova, kaolinite represents an average of only 18% of the clay content, illite 55%, and chlorite 27%. Eight Terra Nova samples have no kaolinite and, as a result, the average kaolinite-to-chlorite ratio at Terra Nova (0.68) is much lower than Yava. In contrast with Yava, Terra Nova has proportionately more samples near the illite end member as well as a number along the illite-chlorite axis, signifying a lack of kaolinite (Fig. 16). Although there

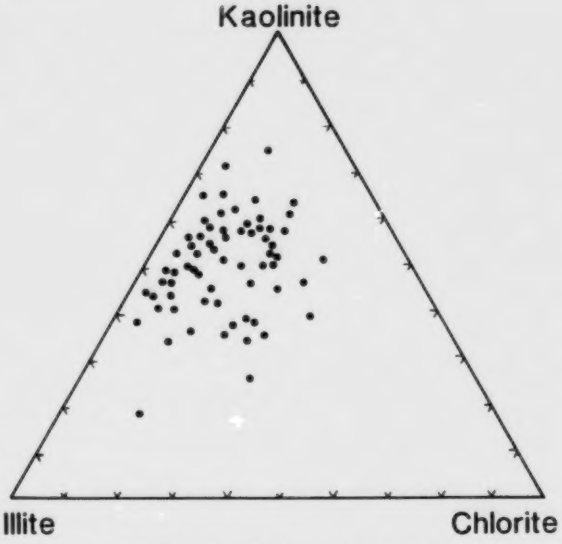

Figure 14. Relative abundances of kaolinite-illite-chlorite in grey sandstone, Yava deposit.

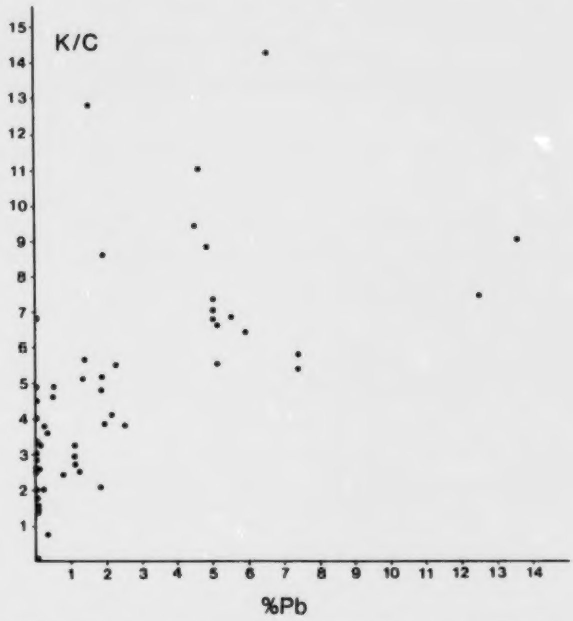

Figure 15. Kaolinite-chlorite ratio (K/C) versus %Pb, Yava deposit.

Table 4. Clay abundances, Yava deposit. Abbreviations as follows: Ill. = illite; Chl. = chlorite; Kaol. = kaolinite; K/C = kaolinite to chlorite ratio.

	n	Avg. Ill.	Avg. Chl.	Avg. Kaol.	Avg. K/C	Pb%
Silver Mine Fm.(avg.)	65	34.69	15.48	49.50	4.51	
Grey Sandstone	23	38.65	8.13	52.65	7.11	5.19
Green Sandstone	42	32.52	19.50	47.90	3.09	0.35

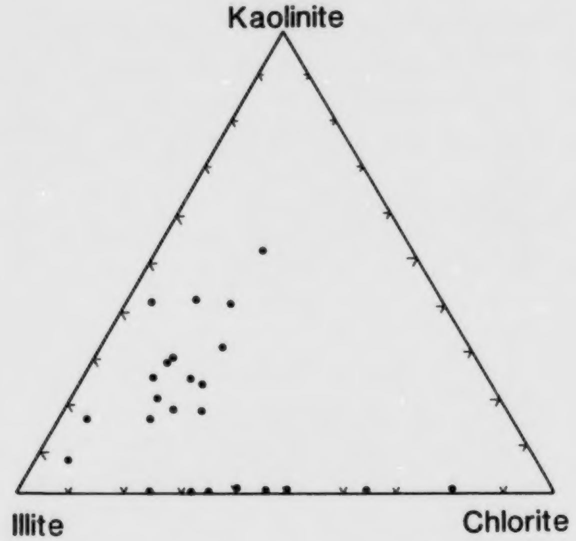

Figure 16. Relative abundances of kaolinite-illite-chlorite (mostly green sandstone), Terra Nova deposit.

are no systematic data available on lead content for the Terra Nova samples, higher illite abundances generally correlate with the presence of visible galena.

The relative clay abundances in Silver Mine Formation sandstones from the remaining areas in the Salmon River and Loch Lomond basins are shown in Figure 17. The points are generally scattered and, in contrast to the Yava and Terra Nova samples, no clear pattern emerges for these other areas. Of 31 sandstone samples from 10 drillholes in the remaining areas of the Salmon River and Loch Lomond basins, kaolinite represents 33% of the clay, illite 40% and chlorite 27%; the kaolinite to chlorite ratio in these areas is 1.22.

From the above observations, three types of clay assemblages occur within mineralized sandstone: 1) kaolinite-dominant with a high illite component (e.g. Yava mine area) and a strong correlation with galena; 2) an illite-dominated composition and a relatively high chlorite content (e.g. Terra Nova). Terra Nova is unlike Yava in that there is no grey sandstone, very little organic material, and lead grades are much lower; and 3) other occurrences in the Salmon River and Loch Lomond basins make up the third type of clay distribution with subequal proportions of kaolinite, illite, and chlorite. In these areas, galena is only weakly disseminated, sandstone is no longer the dominant lithology, and mineralization, where present, occurs in carbonate or sulphate host rocks as well as in sandstone.

Clay in shale

Shale, occurring as thin, sometimes discontinuous, lenses forms roughly 11% of the grey sandstone of the Silver Mine Formation in the Yava area (Bonham, 1983). The shale contains illite and chlorite but not kaolinite.

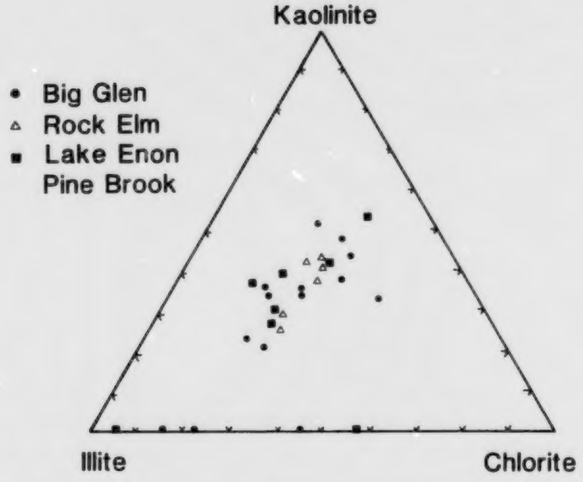

Figure 17. Relative abundances of kaolinite-illite-chlorite (mostly green sandstone) in other base metal occurrences, Salmon River and Loch Lomond basins.

Average composition of the shale is 37% quartz (ranging from 8 to 53%), 34% illite (9 to 52%), 23% chlorite (2 to 33%), 4% plagioclase feldspar (0 to 12%), and 3% potassium feldspar (0 to 11%). Of the clays, illite represents 60% while chlorite represents 40%.

In order to assess the character of clay in these shales relative to clay in sandstone at Yava, 24 shale samples from thin seams and beds within the Silver Mine Formation sandstone as well as from the MacKeigan Lake Formation underlying the three zones at Yava were analyzed for their clay content. The clays from these samples are distinctive in that they do not contain smectite group clays or kaolinite. The average clay composition of the shales is 61% illite and 39% chlorite and is fairly constant throughout the section.

Mineralization

Distribution

Yava is an essentially monomineralic deposit with galena as the major sulphide mineral; pyrite and sphalerite occur in very minor amounts. Metal ratios for typical ore are as follows: Pb:Zn = 19:1, Pb:Ag (%/g/t) = 1:1, Zn:Ag (%/g/t) = 1:20. Ore concentrate averaged 68 g/t Ag (Bonham, 1982).

Galena is present throughout the grey unit as disseminations and bands (Fig. 18). The bands are characterized by increased concentrations of detrital heavy minerals (rutile and zircon) and barite cement. Sphalerite may also occur in association with galena. Pyrite is abundant only in the presence of coaly material.

Disseminated galena occurs in the green sandstone but is much less abundant and never reaches ore grade. Sphalerite is not common. In contrast to that in grey sandstone, coaly material in green sandstone is never

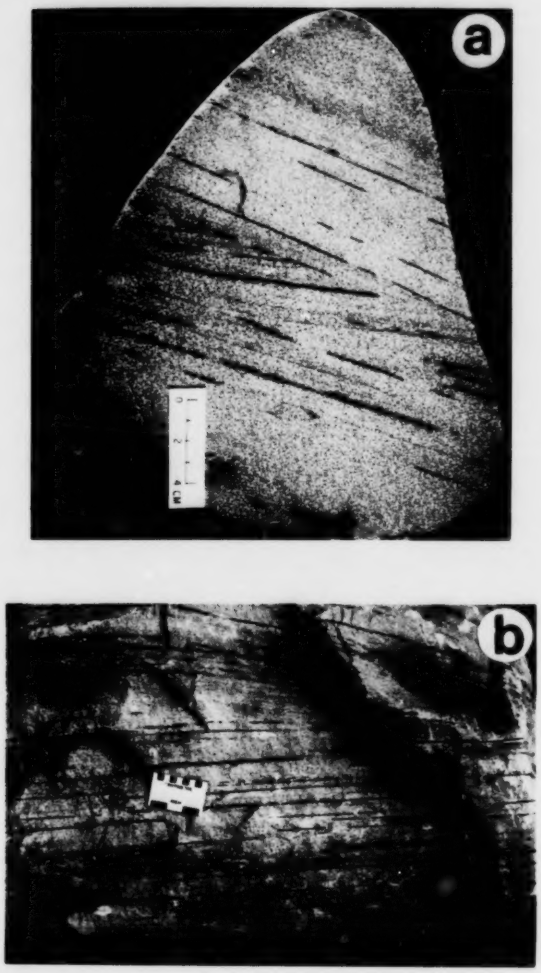

Figure 18. Silver Mine Formation grey sandstone with galena and organic particulate distributed parallel to bedding and crossbedding. a) Hand-sized specimen illustrating both horizontal and crossbedding (GSC 205002-C); b) Boulder in Yava dump illustrating extent of continuity of galena-carbon layers along bedding planes in sandstone (GSC 205002-B).

Sulphide petrography in sandstone

The sulphide mineral assemblage at Yava consists of galena, pyrite, and sphalerite, with rare chalcopyrite. Galena is the dominant sulphide mineral and occurs mostly as anhedral grains up to 0.4 mm but averages 0.2 mm. The grains, which partially to wholly fill pore spaces, are interstitial between clastic quartz grains and clay matrix. Generally, galena appears as isolated grains but these may also coalesce to form interconnected aggregates within the sandstone. In areas of galena mineralization, quartz grains have secondary silica overgrowth features and galena typically forms straight edge boundaries with the overgrowths. This style of mineralization is characterized by re-entrant angles between galena and the overgrowths (Fig. 13). Galena may contain inclusions of pyrite or sphalerite although, more commonly, the inclusions are small concentrations of clay material.

Pyrite is present as isolated patches in the sandstone sequence although it is much less abundant and more localized than the galena. In the unmineralized sandstone above the galena-bearing units, pyrite characteristically appears as clusters up to 2 cm in diameter in an otherwise barren green sandstone.

Locally, pyrite can be much more abundant than galena and may act as a cement supporting individual clastic grains (Fig. 19). The pyrite cement may occur as a galena-bearing although it may contain pyrite. In nongalena-bearing green sandstone, the only visible sulphide mineral is pyrite which occurs as spots and clusters, randomly distributed throughout the rock. This type of pyrite distribution has not been observed in the grey sandstone.

Mineralization in the Yava deposit is characterized by a low-grade or unmineralized footwall, a high-grade basal section, and a rapid transition to a lower grade upper section. Galena most commonly occurs in sandstone as disseminations or bands that are concordant as well as discordant with sedimentary features. It also occurs as discordant spots, cusps, arrowheads, and roll fronts or concordant bands and layers (Bonham, 1982). Whether disseminated or concentrated, the galena occurs as cement, filling open pore spaces in the sandy sediment.

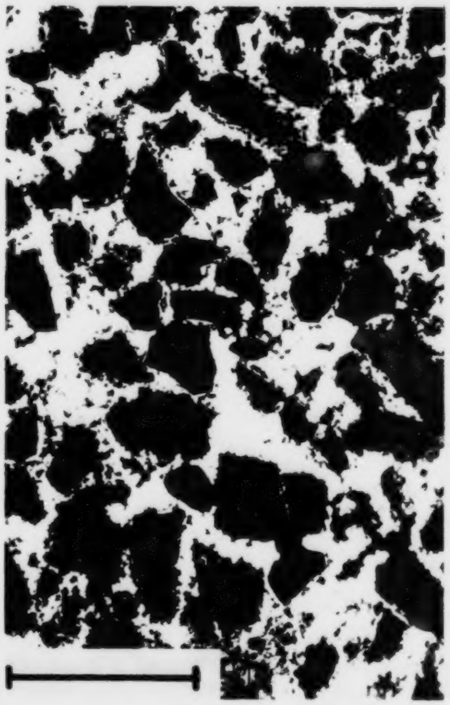

Figure 19. Photomicrograph of detrital quartz grains (light grey and black) cemented and partially replaced by pyrite (white). Note darker grey silica overgrowths partially surrounding quartz grains. Scale bar is 0.5 mm (GSC 204077-E).

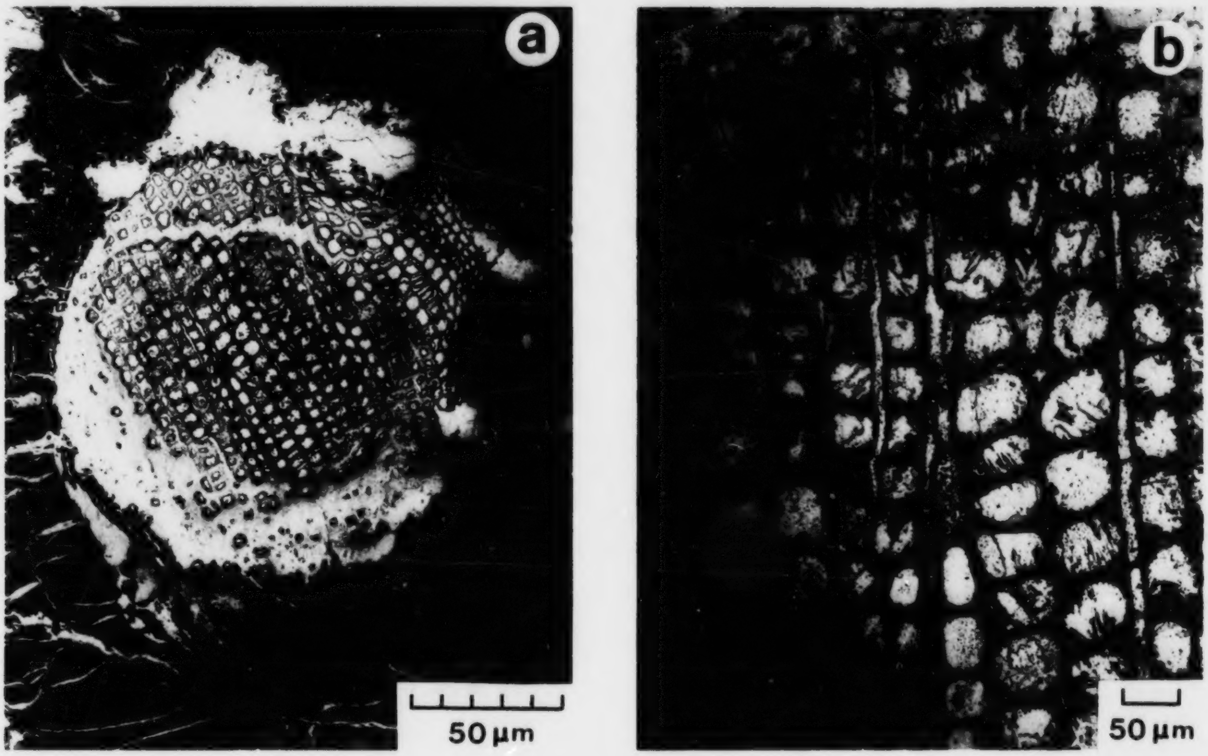

Figure 20. Photomicrographs of sulphide-filled cells in noncompacted woody material, Yava. a) Low-power view showing galena-filled (white) cleats in organic material (black) surrounding central cellular structure. Cells are mainly filled with pyrite; cell walls consist of unreplaced organic matter (black and stippled grey). Large white area between cleat-filled organic material and central cellular structure is largely galena (GSC Photo 205002-F); b) Close-up of portion of above showing unreplaced cell walls (stippled grey and black); cells are filled mainly with pyrite (white) with minor galena (light grey) and sphalerite (dark grey) (GSC 200502-D); c) Detail of sulphide-filled cells showing textural relationships between pyrite (white), galena (light grey), and sphalerite (dark grey). Note that many cells have galena around the inside edge with alternating pyrite-sphalerite in the middle. Cell in lower left quadrant shows alternating pyrite-galena (GSC 205002-E).

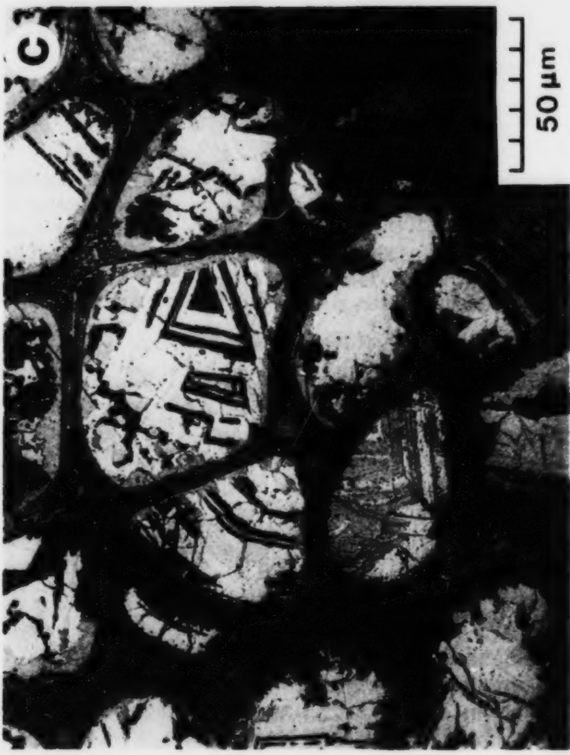

homogeneous mass but usually has a fractured appearance with numerous disaggregated and broken grains, an occurrence most favorable for galena and sphalerite replacement.

Carbonate is also generally more abundant in sandstone near pyrite than galena although this style is not ubiquitous. In general, calcite is more noticeable than pyrite near coal.

Sphalerite is not visible in hand-sized specimen but, when observed microscopically, is usually associated with pyrite or galena and only rarely occurs as individual grains. It is generally not abundant in the sandstone and represents not more than 5 to 10 percent of the total sulphide content. Within masses of galena, sphalerite occurs mostly as well defined anhedral inclusions from 0.05

mm to 0.2 mm. Sphalerite is most abundant with galena where silica overgrowths on quartz grains are relatively insignificant and where galena forms irregular anhedral masses instead of straight edge contacts with quartz. Sphalerite also occurs as inclusions in pyrite but is more typical as a replacement along grain boundaries or margins of fractured pyrite grains.

Sulphide petrography in coaly material

The coaly material at Yava has special significance because it occurs in the form of randomly oriented debris around, and in which, there is abundant galena, pyrite, and sphalerite. Although mineralization in coaly material represents only 15 percent of the total sulphide content at Yava (Bonham, 1983), it is nevertheless important because it contributes to the understanding of paragenesis and shows some important mineral relationships.

Mineralization textures range from open cellular fill to deformed or cataclastic and fractured. In the cellular fill mineralization, a network of near-circular cells, mainly filled with pyrite, are surrounded by galena (Fig. 20a). Galena may occur as thin veins running through the cell structure, as partial cell filling, or as infilling of cleats in coaly material. The pyrite core may be in various stages of replacement; sphalerite occurs as thin bands 0.01 mm thick forming alternating geometric zones with pyrite within each cell (Fig. 20b,c). The sphalerite-pyrite growth bands are oriented independently of the cavity walls and appear to have grown as a separate phase. Rare pyrite-galena geometric zones can also be found as cell filling (Fig. 20c). Sphalerite also serves as a groundmass for isolated pyrite framboids, spherical clusters of pyrite grains from 0.01 to 0.05 mm in diameter. When replacement is in an advanced stage, the entire pyrite core may be replaced by sphalerite. Sulphide-filled undeformed cellular structures such as this are important clues to timing of mineralization. Mineralization thus clearly occurred, at least partly, before compaction of the weak *Calamites* and *Lepidodendron* (Bonham, 1983) cellular structure.

Coaly material displaying a higher degree of deformation has a different mineralization style and a higher degree of pyrite replacment (Fig. 21). Coaly material is crushed and fractured, leaving broken fragments and contorted remnants of coal and coal cells. Galena replacement is more pervasive, forming envelopes around pyrite patches where the original wood cells may only remain as faint outlines or are nonexistent. In the most deformed areas, there are no visible cell cavities. Galena is also widespread filling fractures and cleats in coal (Fig. 20, 21, and 22).

Sphalerite replacement varies greatly but occurs predominantly in the heavily fractured areas along the margins of galena-filled cleats and fractures. Sphalerite also occurs in the outer areas of galena envelopes surrounding pyrite (Fig. 22).

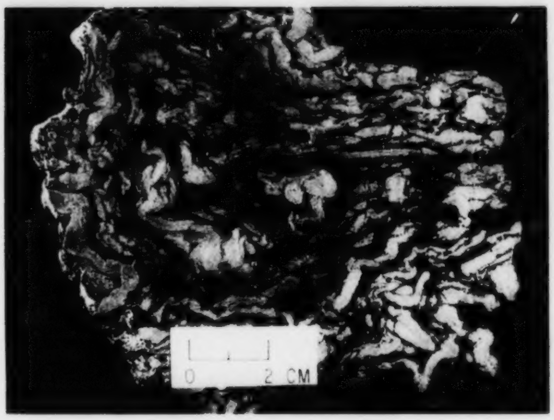

Figure 21. Pyrite-coal aggregate. Light-coloured irregular masses consist of pyrite replacing woody material. Black areas are masses of high-reflectance "coal" containing short, galena-filled cleats (white) (GSC 204007).

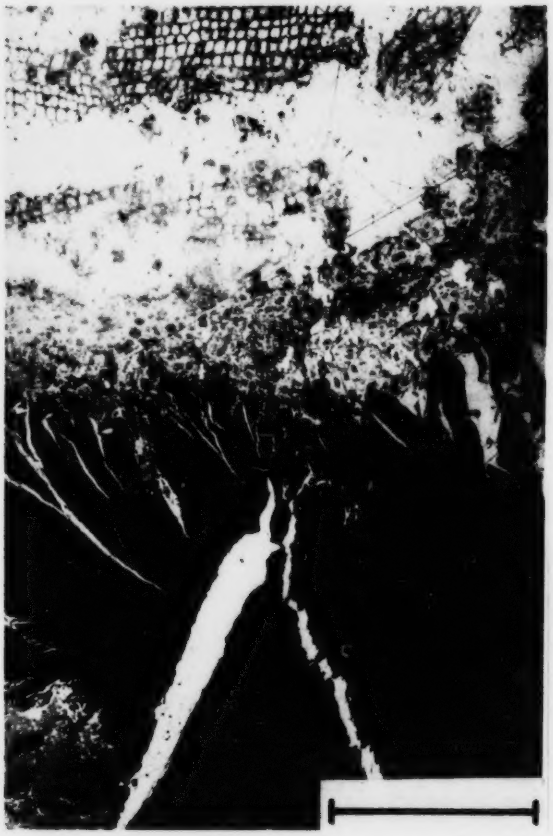

Figure 22. Photomicrograph of galena-filled (white) cleats in organic matter (black). Note main mass of cellular-textured portion is filled with, and replaced by, pyrite (white). Sphalerite (dark grey) and galena (light grey) replace and fill cellular mass in mid-portion of photo; some sphalerite partially extends into the galena-filled cleats. Scale bar is 0.5 mm (GSC 204077-K).

Hydrocarbon alteration

A special aspect of Yava deposit geology is the widespread presence of coaly fragments, notably in the grey sandstone member (Fig. 23). Earlier studies of reflectance (Ro) values in this coaly material, relative to proximity to the ore, had revealed higher Ro values close to the ore zones (Scott, 1980; Vaillancourt and Sangster, 1986). Ro values for regionally-dispersed material in Salmon River Basin ranged between 0.6 and 1.3 (median = 0.85) whereas material collected in the Yava mine area ranged from 0.7 to 1.4 (median = 1.15; Vaillancourt and Sangster, 1986). Similar observations had led previous researchers to conclude the higher reflectance values were due to an ore-related thermal event (Scott, 1980; Bonham, 1982). To further test the thermal history of the Yava deposit, the thermal alteration of kerogen extracted from shales interlayered with mineralized sandstone was analyzed to determine the extent of alteration in the surrounding rocks. The results from shale are in conflict with those from coal in adjacent sandstone. Thermal alteration indices for kerogen in shales were generally low, with values between -2 and + 2, corresponding to reflectance values between 0.47 and 0.9, significantly lower than those recorded for coaly material at the same locations. This difference in reflectance values suggested to Vaillancourt and Sangster (1986) that a thermal event was probably not responsible for the apparent high coal rank at Yava. If high temperature had affected the coal, it should also have affected adjacent interlayered shale. To explain the disparity in reflectance values, both within the Yava deposit and between Yava and the regional samples, Vaillancourt and Sangster (1986) proposed that a chemical, rather than thermal, event related to ore deposition was responsible for the anomalous results. Because mineralization is much more abundant in the sandstone relative to that in shale, ore-bearing fluids were thought to have travelled through the sandstone aquifer in preference to the shale aquiclude. Unknown chemical factors associated with the passage of these ore fluids were considered to have brought about the aberrant Ro values in coaly material close to the Yava deposit (Vaillancourt and Sangster, 1986).

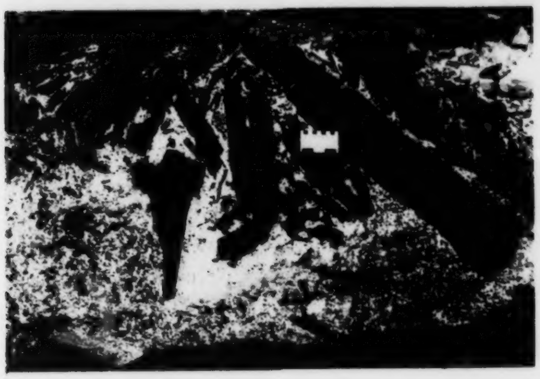

Figure 23. Bedding-plane view of randomly-oriented coalified woody material, Yava dump. White scale card is 9 cm long (GSC 205002-A).

A much more detailed study of organic matter in the Yava deposit area (Héroux et al ., 1989) revealed that oxidation-reduction conditions in the vicinity of the deposit had, indeed, resulted in alteration of the organic matter. Specifically, the effect of sulphur and sulphides seems to cancel, in much the same manner as thermal coalification, the effects of oxygenation discernible under the microscope. The study concluded that the principal changes in organic matter correlatable with proximity to metalliferous zones are:

1) replacement of organic matter by sulphides;

2) loss of spore fluorescence accompanied by increase in sphalerite fluorescence;

3) appearance of abnormally high anisotropy in collinite accompanied by enhancement of plant textures on telecollinite;

4) formation of fractures and vesicles on pseudovitrinite and corpocollinite;

5) formation of alteration rims on organic matter; and

6) an abnormal evolution of reflectance gradients up to 10 percent Ro/km within the Yava deposit and, in some cases, a decrease in thermal alteration index (T.A.I.) and Ro with depth toward the mineralized zones.

Paragenesis

Textural studies to date suggest that a paragenetic sequence began with early diagenetic pyrite in coaly material and other locally reduced areas in the sandstone. Near coal, carbonate also appears to have precipitated early. Sphalerite in coaly debris and sandstone formed in association with the pyrite as inclusions and, in places, as groundmass.

Silica overgrowths on quartz grains followed the early pyrite and sphalerite and marked the beginning of the major mineralizing event. Galena shortly postdated the secondary overgrowths, occurring in the available pore space and in reaction with earlier sulphide stages. Barite, where present, occurred contemporaneously with galena. As a final phase, carbonate cement filled some unoccupied pore spaces and a late sphalerite phase replaced earlier galena.

Lead isotopes

To identify likely source(s) of lead in Yava and other deposits, lead isotopic determinations were carried out on galenas from several deposits in the Salmon River and Loch Lomond basins (Table 5). Samples from the Salmon River porphyry and the Chisholm Brook-Irish Cove granodiorite were analyzed for Pb, U, and Th concentrations and isotopic ratios (Table 6). All determinations were carried out by Geospec Consultants Ltd., Edmonton, Alberta under contract to the Geological Survey of Canada (see Appendix B).

On a standard ^{207}Pb/^{204}Pb versus ^{206}Pb/^{204}Pb diagram, lead from deposits in the Salmon River and Loch Lomond basins falls into two distinct groups (Fig. 24). One group of three, with ^{206}Pb/^{204}Pb ratios less than 18.2, represent occurrences in the Rock Elm district at the eastern end of the Salmon River Basin. Data from

Table 5. Lead isotope ratios in galena, Salmon River and Loch Lomond basins.

Deposit	^{206}Pb/^{204}Pb	^{207}Pb/^{204}Pb	^{208}Pb/^{204}	Sample
Yava	18.337	15.626	38.213	SP-2359
	18.409	15.629	38.233	SP-2393
	18.399	15.626	38.279	SP-2373
	18.319	15.619	38.193	SP-2377
	18.369	15.632	38.294	SP-2379
	18.333	15.619	38.204	SP-2387
	18.417	15.627	38.304	LPC-S-YD34
	18.433	15.625	38.322	CO-S-YD22
	18.414	15.632	38.314	LPC-S-YD32
	18.446	15.638	38.353	SP-4503
	18.326	15.615	38.191	SP-4530
Big Glen	18.352	15.615	38.184	S-BG4-359
	18.408	15.633	38.291	S-BG4-569
	18.405	15.629	38.285	S-BG8-426
	18.411	15.624	38.282	BB74-2-545
	18.368	15.624	38.223	SV2-197
Terra Nova	18.511	15.649	38.447	TN74-1-177
	18.525	15.651	38.479	TN74-9-19
	18.518	15.648	38.451	S-TN74-9
Lake Enon	18.363	15.633	38.258	S-M-4
	18.357	15.628	38.220	S-M-1
	18.366	15.633	38.241	S-M-2
	18.366	15.634	38.231	TQ84-199
Pine Brook	18.487	15.653	38.428	PBD-1
	18.488	15.652	38.408	PBD-2
	18.479	15.645	38.401	KQ84-64
Rock Elm	18.159	15.612	38.109	SI1 1-467
	18.187	15.611	38.136	SI1-464
	18.085	15.616	38.127	SI1 2-693

Table 6. Lead, uranium, and thorium abundance and isotope ratios, Loch Lomond complex.

	Sample	Concentration (ppm)								
		U	Th	Pb	^{206}Pb/^{204}Pb	^{207}Pb/^{204}Pb	^{208}Pb/^{204}Pb	^{238}U/^{204}Pb	^{235}U/^{204}Pb	^{232}Th/^{204}Pb
Chisholm Brook granodiorite	LL-1	2.50	12.00	9.48	19.871	15.729	39.869	17.42	0.1263	86.48
	LL-6	2.34	13.00	8.21	19.889	15.725	40.040	18.88	0.1369	108.40
	LL-7	2.78	13.40	9.29	19.916	15.722	39.934	19.82	0.1437	98.73
	LL-8	2.42	11.60	9.94	19.667	15.717	39.799	16.02	0.1162	79.70
	LL-9	2.09	7.97	7.50	19.896	15.732	39.785	18.40	0.1334	72.55
	LL-31	2.24	11.40	11.00	19.372	15.698	39.278	13.26	0.09614	69.74
	*LL-38	3.11	13.60	11.80	19.610	15.709	39.586	17.27	0.1253	78.00
	*=Irish Cove									
Salmon River porphyry	LL-12	1.40	19.2	20.9	18.502	15.585	38.477	4.266	0.03094	60.46
	LL-18	2.77	-----	47.8	18.428	15.607	38.468	3.686	0.02673	-------
	LL-19	13.1	12.9	3200	18.379	15.623	38.243	0.2603	0.001888	0.2634
	LL-20	11.4	28.2	171	18.511	15.628	38.334	4.222	0.03062	10.79
	LL-21	1.86	28.9	43.6	18.535	15.587	38.405	2.714	0.01968	43.56
	LL-22	2.56	27.7	23.1	18.939	15.614	38.919	7.129	0.05170	79.85
	LL-25	6.27	32.5	31.6	18.991	15.629	39.007	12.79	0.09274	68.45
	LL-26	4.79	27.2	38.0	18.867	15.613	38.546	8.063	0.05848	47.23
	LL-39	7.84	28.3	58.7	18.612	15.597	38.296	8.481	0.06151	31.63

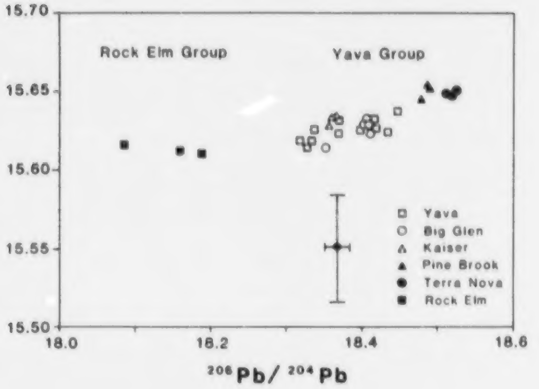

Figure 24. Lead isotope ratios in galena from deposits in the Salmon River and Loch Lomond basins. Bars represent 2-σ analytical uncertainty.

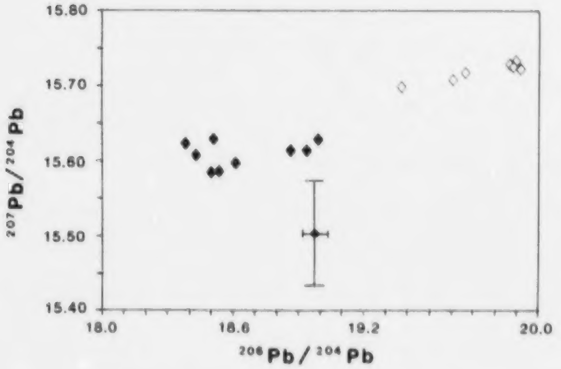

Figure 25. Present-day lead isotope ratios in Salmon River porphyry (closed diamonds) and Chisholm Brook-Irish Cove granodiorite (open diamonds). Bars represent 2-σ analytical uncertainty.

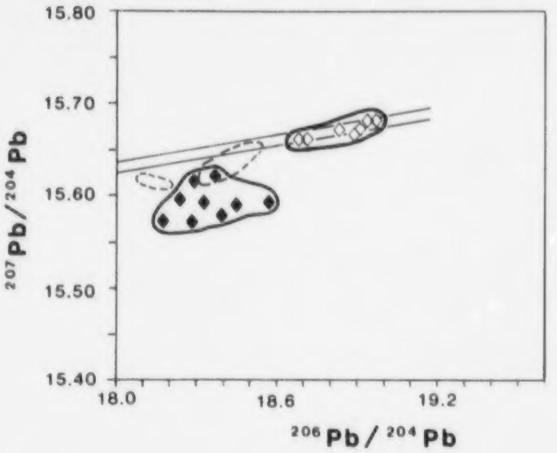

Figure 26. Lead isotope ratios in same rock suites as shown in Figure 25 but corrected to 325 Ma. Dashed lines show relative positions of "Yava group" and "Rock Elm group" galenas (see Fig. 24). Solid parallel lines are the projection of the granodiorite data; note they intersect the Yava group galena leads (see text for discussion).

Yava, Big Glen, Terra Nova, Pine Brook, and Lake Enon (Kaiser) deposits compose a second group ('Yava Group') with $^{206}Pb/^{204}Pb$ values greater than 18.3. Rock leads, plotted on the same type of diagram, fall into two groups — one of nine samples of Salmon River porphyry with $^{206}Pb/^{204}Pb$ ratios less than 19.1, and a second group of seven granodiorite samples with ratios greater than 19.3 (Fig. 25).

In view of the abundant evidence, discussed previously with respect to undeformed sulphide-filled wood cells, indicating mineralization occurred during early diagenesis of the Westphalian-age host rock sandstones, extraction and deposition of lead at that time would appear to be a reasonable option. Accordingly, lead isotopic compositions of both the porphyry and granodiorite were back-calculated to 325 Ma and the ratios so obtained are displayed in Figure 26. Dashed lines indicate fields occupied by the galena leads; solid lines enclose the recalculated rock lead isotopic values. The "Yava group" leads are distributed along a mixing line between the recalculated porphyry cluster and the projection of the granodiorite cluster at 325 Ma whereas the Rock Elm group falls outside the porphyry cluster.

To unequivocally indicate simple mixing between the porphyry and granodiorite, the "Yava group" plot should directly intersect the granodiorite cluster rather than simply its projection. In view of the fact that all granodiorite samples were taken from outcrop, together with the coarse grained nature of the rock, loss of uranium during Recent (or older) weathering is a distinct possibility. Leaching of uranium would result in a shift in the isotopic ratios to a calculated position more radiogenic than the granodiorites actually possessed at 325 Ma. Further calculations reveal that addition of an average 0.5 ppm U, or about 20 percent of their measured contents, to each of the samples would result in a shift of the granodiorite cluster, along its projected slope at 325 Ma, to a position centred about a $^{206}Pb/^{204}Pb$ ratio of about 18.6. At this position, the granodiorite cluster would intersect the "Yava group" leads and thereby be compatible with a dual source (porphyry and granodiorite) for the ore leads. To test the validity of the uranium loss possibility, the data were examined on a $^{208}Pb/^{204}Pb$ plot. Thorium is considered to be far less mobile than uranium and, consequently, should more accurately determine the original source compositions. The test revealed that the "Yava group" ore lead cluster intersects both the granodiorite and porphyry clusters at 325 Ma. Thus, the lead isotope data confirm that lead in the "Yava group" of deposits (i.e. Yava, Big Glen, Terra Nova, Pine Brook, and Lake Enon) was likely derived from both the Salmon River porphyry and the Chisholm Brook-Irish Cove granodiorite.

When the "Yava group" ore leads are examined in greater detail (Fig. 24) the association with local basement is even more evident. Deposits spatially associated with porphyry basement (Yava and Big Glen) have lead isotopic compositions similar to those of the porphyry; deposits underlain by the granodiorites (Pine Brook and Terra Nova) show isotopic compositions close to those of the granodiorites (Fig. 2). The exception to this are the three samples from the Lake Enon (Kaiser) celestite deposit (Fig. 2). These isotope ratios are closest to those of Yava in spite of the fact that the Lake Enon deposit is underlain by granodiorite (Boehner and Prime, 1985). All samples were taken from the MacRae pit which, of all the Lake Enon deposits, is the only one with significant sulphides present (Forgeron, 1977). The MacRae pit is cut off on the northeast by the post-Carboniferous Terra Nova Fault (Fig. 2). Sulphide mineralization is most abundant in the northern end of the pit, closest to the fault, and occurs as coarse grained discordant veins and clusters in the celestite. These observations suggest sulphide mineralization could be related to the late-stage faulting and, as such, could represent mobilization of lead from pre-existing galena in adjacent sandstone. Since sandstone north of the Terra Nova Fault lies on porphyry basement, this may explain why lead isotopes in sulphides from the MacRae pit are similar to the Big Glen and Yava deposits which lie on porphyry.

The "Rock Elm group" (Fig. 24) of galena leads is significantly less radiogenic than the "Yava group" and cannot have been derived from the same sources as the latter. The Rock Elm district lies approximately 7 km northeast of the East Zone of the Yava deposit, well beyond the Loch Lomond basement complex. Basement in the Rock Elm area is, instead, undivided deformed and metamorphosed Hadrynian to Ordovician volcanic and sedimentary rocks (Boehner and Prime, 1985). Rocks of this age and composition would be expected to have lead isotope compositions similar to those of Rock Elm galenas although, unfortunately, these basement rocks were not analyzed for their isotopic compositions.

Thus, lead isotopic studies in the Loch Lomond and Salmon River basins show that the deposits can be divided into three groups on the basis of their isotopic compositions: 1) Yava, Big Glen, Lake Enon (Kaiser); 2) Pine Brook, Terra Nova; and 3) Rock Elm. Comparison with isotopic compositions in basement rocks shows that the first group of leads is most likely derived from the Salmon River porphyry, whereas the second group is largely derived from the Chisholm Brook-Irish Cove granodiorite. A Hadrynian-Ordovician complex is the likely source of the Rock Elm leads.

Sulphur isotopes

Sulphur isotope determinations were performed at the Ottawa-Carleton Geoscience Centre Stable Isotope Lab in Ottawa. Isotope measurements were made on SO_2 gas and were normalized to Canyon Diablo troilite $\delta^{34}S$ = 0‰ and OGS-1 seawater sulphate $\delta^{34}S$ = +20.58‰). Sample and machine reproducibility averaged 0.1 to 0.2‰.

Two hundred mineral separates were measured for sulphur isotope abundance; a total of 177 samples were selected from Yava, Big Glen, Terra Nova, and Rock Elm in the Salmon River Basin and the Lake Enon celestite deposit and the Pine Brook barite deposit of the Loch Lomond Basin. Details of sample location and analytical procedures are presented in Appendix C.

Sulphide

Yava

Galena — Twenty-eight samples of galena obtained from sandstone in the Yava deposit display a range between -25.7 and +27.67‰, with the majority occurring in the 0 to +10‰ range (Fig. 27a). Galenas obtained from the green sandstone are heavier, whereas those from the coal-rich grey sandstone have the lightest values.

Thirty-seven samples of galena in coaly material at the base of the Yava sandstone sequence were also analyzed. Values range from -28.25 to +11.88‰, with the majority occurring in the -20 to -10‰ range (Fig. 27b). This range can be subdivided into two distinct groups, a group from 0 to -30‰ is associated with the grey sandstone, whereas another group from 0 to +20‰ is associated with the green sandstone.

Pyrite — Nineteen samples of pyrite were selected from the grey and green sandstone at Yava. Pyrite in the grey sandstone is usually associated with coal and galena whereas the pyrite in the green sandstone occurs as isolated, randomly disseminated grains and isolated blebs. Sulphur isotopes show a very wide range from -28.7 to +65.12‰ (Fig. 27c). Samples from the grey sandstone are the lightest, ranging from -28.7 to +13.26‰; all but one of the green sandstone samples range from +28.19 to +65.12‰.

The 47 pyrite samples obtained from coaly material at Yava are from both sandstone types. The pyrite exhibits a broad range, from -27.82 to +27.73‰ (Fig. 27d). As is the case for pyrite in sandstone at Yava, pyrite in coal shows distinct isotopic ranges for each of the grey and green sandstone types. Pyrite in coal in the grey sandstone shows a range from -27.82 to -2‰, with most values in the -25 to -20‰ range. Pyrite in coal in the green sandstone ranges from -0.46 to +27.73‰, with a majority of values in the +5 to +15‰ range.

Pyrite-galena pairs — Twenty-eight samples of coexisting pyrite and galena were selected from mineralized coal and sandstone in the Yava deposit (Appendix C). Because pyrite is more abundant in the coaly material than elsewhere, 25 of the 28 pyrite-galena pairs are from coaly material. Pyrite values, which average -16.48‰, are generally lighter than galena values which average -12.78‰, for the same samples.

In 23 of the 28 pairs, pyrite was isotopically lighter than galena. Differences ranged from 0.2 to 22.2‰. Elimination of the latter value reduced the range to 0.2 to 9.2‰. The isotopic difference in the remaining 22

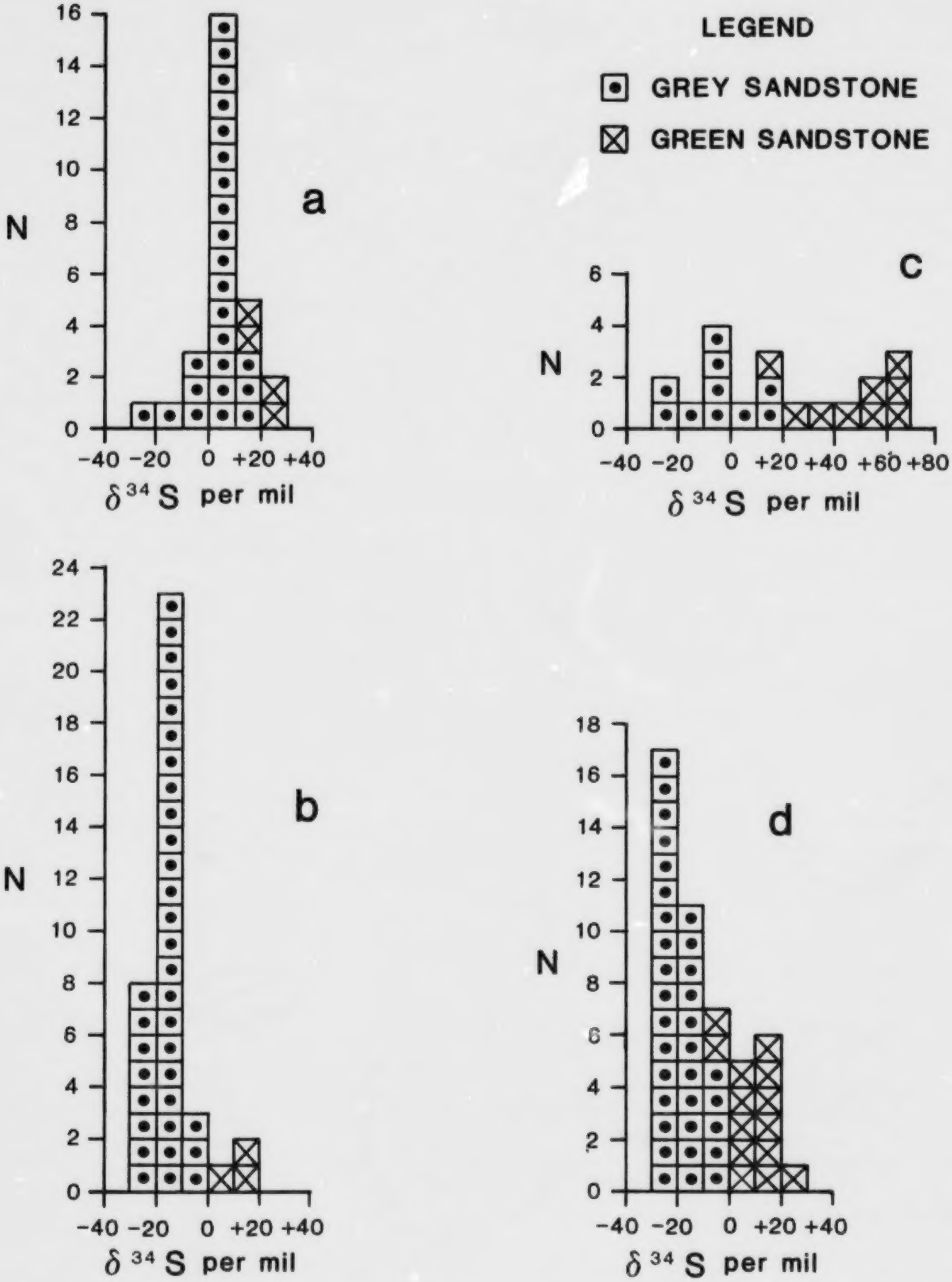

Figure 27. Sulphur isotopic compositions of Yava sulphides. a) Galena in sandstone. b) Galena in coal. c) Pyrite in sandstone. d) Pyrite in coal.

pyrite-galena pairs then averaged 3.9‰. Using the fractionation equation of Ohmoto and Rye (1979) this difference is equivalent to an isotopic equilibrium temperature of 511 ± 20°C. In view of the absence of thermal effects on organic matter in the Yava deposit (Héroux et al., 1989), this isotopic temperature is interpreted to be in error and attributed to isotopic inequilibrium between galena and pyrite.

Other areas

Thirteen pyrites from sandstone at Terra Nova (Fig. 28a) were selected and yielded values similar to pyrite in the green sandstone at Yava (Fig. 27c). Isotope values fall between +4.7 and +57.44‰, but of these, eleven are in the +20 to +50‰ range and five are in the +30 to +40‰ range. These isotope values are most similar to pyrite from the green sandstone at Yava.

Although the nature of the pyrite occurrence in the Rock Elm and Big Glen areas is similar to that in the sandstone at Terra Nova or in the green sandstone at Yava, thirteen isotope values, which range from -0.78 to +36.76‰ are inconclusive (Appendix C). Pyrite in the Lake Enon and Pine Brook deposits ranged from -12.17‰ to +48.93‰ (Appendix C). Too few samples were selected and the isotopic range is so broad that further sampling is needed to establish a diagnostic isotopic signature of pyrite in these areas (Fig. 28b).

Twelve galenas were analyzed from the Rock Elm, Big Glen, and Terra Nova occurrences in the Salmon River Basin and Pine Brook and Lake Enon (Kaiser) occurrences in Loch Lomond Basin (Fig. 28c). Isotope abundances range from -30 to +34.88‰, averaging -3.79‰, but do not appear to have any distinct population distributions. Further sampling is needed to establish isotope characteristics for these occurrences.

Sulphates

Barite

Five barites from Yava, within well mineralized sandstone, and two from the stratiform Pine Brook barite deposit (within Windsor Group redbeds) were selected for analysis. Barite at Pine Brook commonly contains very minor disseminated galena. All samples show a very uniform distribution, ranging from +8.99 to +19.02‰ and average +12.9‰ (Fig. 28d).

Gypsum

Seven samples were separated from gypsum modules in MacKeigan Lake Formation shale in the Big Glen, Rock Elm, and Yava areas. Gypsum usually occurs as thin intercalations in the shale and is not associated with any other mineral. Values range from +13.81 to +21.49‰ with an average of +17.2‰ (Fig. 28e)

Because seawater sulphur isotope values for Lower Carboniferous sulphates are not well established (Claypool et al., 1980), gypsum from the Windsor Group was collected from numerous quarries and roadcuts throughout Nova Scotia. Data from 16 of these localities, combined with 10 values from Gibling et al. (1989) are shown in Figure 28f and range from +14.5 to +16.3‰ with an average of +15.5‰. This average lies between that for barite from Pine Brook and Yava (avg. = +12.9‰) and gypsum from shales of MacKeigan Lake Formation (avg. = +17.2‰).

DISCUSSION

Prior to arriving at a genetic model for the Yava deposit, some discussion is necessary in order to focus on several significant features of the deposit and their interrelationship.

Timing of mineralization

Because of a lack of datable ore-stage minerals or postore events, determination of absolute age of mineralization has not been possible at Yava. Certain features of the deposit, however, render estimates of the relative timing of ore deposition possible.

That the ore is clearly epigenetic (i.e. postsedimentation) is evidenced by the habit of galena, as cement between detrital quartz grains, and its paragenetic position, which places it later than the siliceous overgrowths. Galena also replaces cell walls in the coaly material found throughout the deposit and is paragenetically later than sphalerite that fills cell interiors.

Rapid accumulation of Silver Mine Formation sandstone in a fluvial environment was probably responsible for the preservation of the organic material. By the same token, however, rapid accumulation of sediments would also result in compaction of the weak *Calamites* and *Lepidodendron* cellular material soon after deposition. The presence of sulphide-filled wood cells showing little or no evidence of compaction, however, points to a very early, probably diagenetic, stage of mineralization (Fig. 20).

Controls

Two of the more obvious physical controls to ore deposition are porosity and the fluvial channels of the sandstone aquifer. Galena clearly forms the cement-filling intragrain voids in the sandstone (Fig. 12 and 13). Moreover, direct measurements have shown that porosity of mineralized grey sandstone is significantly less than that of unmineralized grey sandstone (Table 2).

Although, unfortunately, the mine closed before detailed sedimentological studies could determine the nature and distribution of the fluvial channels in the sandstone, there is a clear correspondence between high lead contents and depressions in the basement quartz porphyry (Fig. 6). These depressions have been interpreted to be fluvial paleochannels which directed the northwestward flow of meteoric groundwaters off the topographically high Loch Lomond complex (Fig. 7).

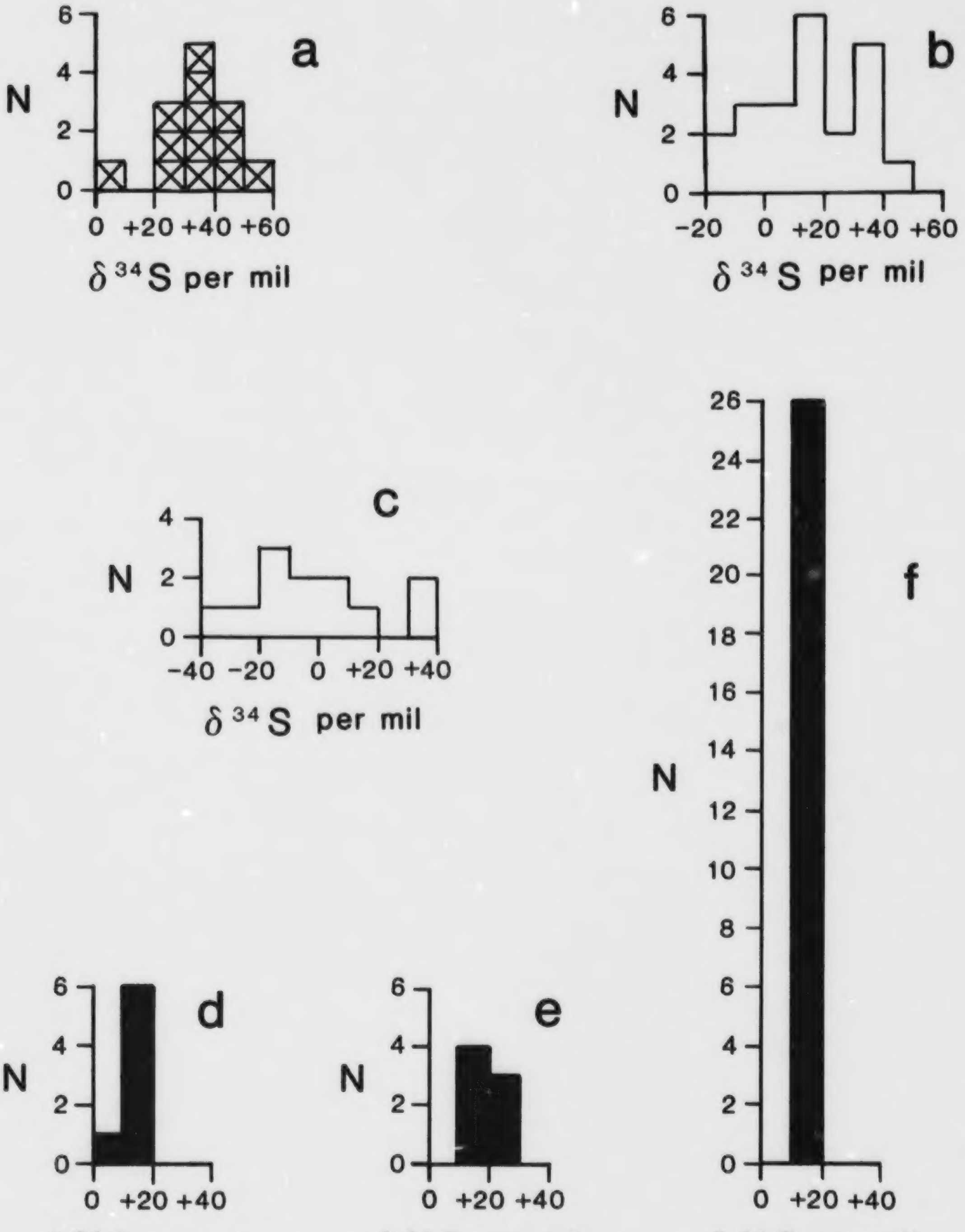

Figure 28. Sulphur isotopic compositions, Salmon River and Loch Lomond basins. a) Pyrite in sandstone, Terra Nova. b) Pyrite in Rock Elm, Big Glen, Pine Brook, and Lake Enon occurrences. c) Galena in Big Glen, Lake Enon, Pine Brook, Rock Elm, and Terra Nova occurrences. d) Barite at Pine Brook, Terra Nova, and Yava. e) Gypsum at Big Glen, Rock Elm, and Yava. f) Gypsum from gypsum quarries in Nova Scotia (includes values from Gibling et al., 1989).

Direction of flow of mineralizing fluids

Two lines of evidence may be used to estimate the direction of ore fluid flow: 1) the pattern of lead grade contours; and 2) mineral zoning. Lead grade contours in all three zones of the Yava deposit display clear northwest-southeast trends, perpendicular to the basin outcrop margin (Fig. 6), suggesting fluid flow either from southeast to northwest or the reverse. Lead grades in all zones decrease rapidly to the northwest, suggesting that ore fluids entered the sandstone from the southeast and flowed downdip to the northwest.

The basinward position of the zinc-rich zone relative to the lead zones (Fig. 9) also suggests a northwestern fluid flow direction inasmuch as, at any given pH, sphalerite requires much more reducing conditions to precipitate than does galena (Fig. 29a). If the original fluids entering the sandstone were meteoric groundwater, the waters would become more reducing the farther they travelled in the organic-rich sandstone (Fig. 29b). Fluids carrying both lead and zinc would therefore deposit galena first while zinc would be carried farther downdip, becoming more reduced as they travelled and were buffered by the reducing sediments, until the stability field of sphalerite was reached. The general decrease in Eh from meteoric water to shallow groundwater is shown in Figure 29b.

Temperature of ore deposition

Although the most direct method of determining depositional temperatures at Yava would be measurement of fluid inclusion homogenization temperatures in sphalerite, these studies have not yet been performed. In the absence of these data, maximum temperatures attained by the ore fluids can only be estimated.

Previous studies determined that the median vitrinite reflectance of Salmon River Basin organic material is 0.85 (Hacquebard and Donaldson, 1970) and this has been confirmed by more detailed study (Héroux et al., 1989). This level of organic maturation corresponds to a temperature of 100 to 160°C, depending on heating duration (Fig. 80 in Bustin et al., 1983). As detailed studies of organic material have shown that the Yava deposit does not constitute a thermal anomaly (Héroux et al., 1989), these temperatures must be regarded as a maximum for the ore solutions. Evidence was presented above that mineralization occurred during early diagenesis of the sandstone. If this is accepted, then the temperatures recorded by the vitrinite reflectance data would represent postore burial. Actual temperatures of ore deposition might therefore have been close to meteoric conditions, possibly close to 25°C.

Sources of sulphur and lead

In a continental, fluvial environment such as the Salmon River Basin, a source of the millions of tonnes of sulphur in the Yava deposit presents a problem because one cannot simply call upon sulphate in coeval seawater as is commonly done for stratabound sulphide deposits in marine sedimentary rocks.

In the case of sandstone-hosted deposits of the Salmon River Basin, a different source is required. The sulphur isotope data presented earlier (Fig. 27 and 28) revealed a very wide range of values for sulphides, and a relatively narrow range for gypsum and barite, from all Salmon River-Loch Lomond basin deposits. The similarity in compositions of Yava gypsum and barite with those of gypsum from MacKeigan Lake shales and Windsor evaporite (Fig. 28d,e,f), suggests the latter were the probable sources of sulphide sulphur in the deposits.

Reduction of sulphate with average $\delta^{34}S = +15‰$ (Fig. 28f) would produce reduced sulphur isotopically lighter than the starting composition. Thus all sulphides with compositions lighter than +15‰ are compatible with such a process (Fig. 27). In an environment of low sulphate content, such as meteoric groundwater percolating through sandstone, mass balance considerations require that, as the sulphate is being reduced to produce isotopically light sulphide, the remaining sulphate in solution will become progressively heavier. As the remaining sulphate, in turn, is reduced, it will generate sulphide isotopically heavier than that initially produced; as this process continues, heavier and heavier sulphide is generated. If this sulphide is immediately precipitated as pyrite and galena, their isotopic compositions will range from very light to very heavy, exactly as shown in data presented in Figures 27 and 28.

Comparison of lead isotope ratios in ore galenas and basement rocks strongly indicates a local source of lead for deposits in Salmon River Basin; lead in all deposits except Rock Elm appears to be derived from both the Chisholm Brook granodiorite and the Salmon River porphyry (Fig. 26). More specifically, however, Yava deposit lead seems to have been derived largely from the underlying porphyry whereas lead in Terra Nova deposit was sourced from the nearby granodiorite.

The concept of derivation of Pb and Zn from local basement rocks finds support in the geochemistry of the Chisholm Brook granodiorite compared with that of Salmon River porphyry (Table 1). The former contains an average 62 ppm Zn as compared with 31 ppm Zn in Salmon River porphyry. The granodiorite also contains approximately twice as much Fe as does the porphyry, supporting the concept of Zn substituting for Fe in the mafic constituents of the granodiorite. Conversely, the granodiorite is considerably lower in Pb (8 ppm) compared with the porphyry (30 ppm). Because Pb commonly substitutes for K in minerals such as microcline, the higher Pb content of the porphyry is paralleled by the higher K content of the porphyry as compared to the granodiorite (Table 1). With these metal ratios in mind, it is instructive to note that the Terra Nova deposit, with Chisholm Brook-Irish Cove granodiorite as its basement, is Zn-rich relative to the Yava deposit which is underlain by the Salmon River porphyry.

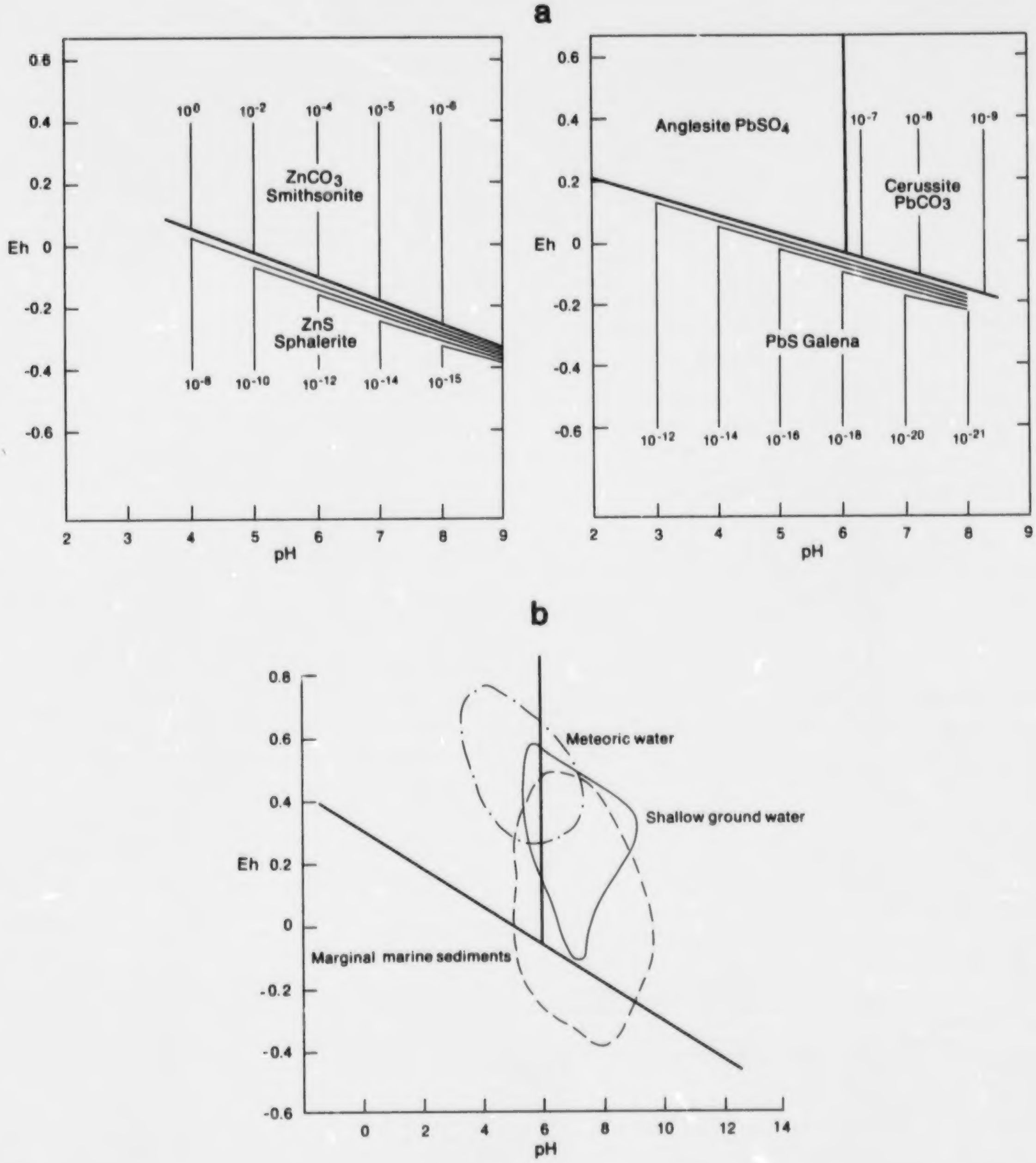

Figure 29. a) Stability fields of some zinc and lead compounds as functions of pH and Eh. Narrow vertical lines are contours of activity of Zn^{+2} and Pb^{+2}. b) Approximate areas of Eh and pH for some natural environments. Note the decrease in Eh of meteoric water as it transforms to groundwater. In the case of Yava, the Eh of groundwater in the grey sandstone member would be further decreased by the presence of abundant organic matter. Vertical and diagonal heavy straight lines are the Pb compound boundaries as shown in the stability field diagram above; PbS is stable below the diagonal line (from Bjørlykke and Sangster, 1981).

In considering the Salmon River porphyry as a potential source of lead for the Yava deposit, it is instructive to note that the porphyry intrusion likely extended much farther eastward than it does at the present. McMullin (1984) suggested the porphyry was intruded as a high-level laccolith with the present outcrop representing the intrusive axis. The porphyry extending to the west beneath the Carboniferous sedimentary rocks was interpreted by McMullin (1984) as the western side of the laccolith. Thus, the eastern side of the laccolith (i.e. that portion east of the present outcrop exposure of the porphyry; see Fig. 2) is now eroded. If this interpretation is correct, the original Salmon River porphyry was much larger than exposed at present and much of the now-missing eastern half of it could have been the source of Salmon River Basin clastics.

Although the lead isotope and geochemical data indicate the source of the metal, they provide little or no information on the processes that resulted in the transfer of lead from sialic source rocks to a sulphide deposit. The important concept here, however, is that the evidence seems to indicate both lead and sulphur are locally derived and appeals to distant sources are unnecessary.

Diagenetic processes in Silver Mine sandstone

Petrographic studies have shown that the average mineral abundances in grey sandstone host rock at Yava are: quartz grains — 70 to 85%, clay minerals — 1 to 15%, feldspar/muscovite/coal/calcite/heavy minerals/amorphous silica — 3%, porosity — 15 to 22%. Of these, amorphous silica and clay minerals formed after sedimentation but before mineralization. In view of the evidence for early mineralization, these authigenic minerals probably formed during very early diagenesis. Calcite, although largely occurring later than sulphides in the paragenetic sequence, appears to be the last in the diagenetic/mineralization sequence discussed below.

Inasmuch as sandstone of the Silver Mine Formation was deposited in a fluvial environment, the abundant coaly material may be safely assumed to have been continually exposed to oxidizing meteoric waters during early diagenesis. Oxidation of organic debris would result in production of CO_2 ($C + O_2 = CO_2$) which, in turn, would hydrolyze to carbonic acid as follows:

(1) $CO_2 + H_2O = H^+ + HCO_3^-$

The lowering of pH resulting from these processes was a major factor leading, ultimately, to the destruction of most of the detrital minerals in the original sandstones including microcline feldspar and muscovite. The former presence of these latter minerals, although virtually totally destroyed now, can be inferred from the rare examples of altered potassium feldspar and muscovite occasionally seen in thin section (Fig. 11). Acidic conditions, present during early diagenesis of what is inferred to have originally been feldspathic sandstone, would have altered potassium feldspar to kaolinite and silica as indicated according to the following processes:

(2) $$\underset{\text{Microcline}}{H_3O^+ + KAlSi_3O_8} = \underset{\text{Kaolinite}}{Al_2Si_2O_5(OH)_4} + \underset{\text{Silica}}{SiO_2.nH_2O} + K^+$$

Detrital muscovite could, on further diagenetic alteration, also produce kaolinite:

(3) $$H_3O^+ + \underset{\text{Muscovite}}{KAlSi_3O_{10}(OH)_2} = \underset{\text{Kaolinite}}{Al_2Si_2O_5(OH)_4} + K^+$$

The processes shown above resulted in the production of kaolinite, the most abundant clay mineral (Fig. 14), and secondary silica, the most abundant nonclay mineral, at Yava. The second most abundant clay mineral in Yava sandstone is illite. It is also considered to be authigenic and may represent a transitional mineral formed during the alteration of potassium feldspar to kaolinite:

(4) $$H_3O^+ + \underset{\text{Microcline}}{KAlSi_3O_8} = \underset{\text{Illite}}{KAl_3Si_3O_{10}(OH)_2} + \underset{\text{Silica}}{SiO_2 \cdot nH_2O} + K^+$$

(5) $$H_3O^+ + \underset{\text{Illite}}{KAl_3Si_3O_{10}(OH)_2} = \underset{\text{Kaolinite}}{Al_2Si_2O_5(OH)_4} + K^+$$

Processes (2) to (5) all involve consumption of hydrogen ions; as a result of these processes over time, pH gradually increases until, finally, calcite precipitates late in the paragenetic sequence through reaction between carbonic acid and calcium ions. The latter were probably released during albitization of plagioclase and/or the destruction of mafic minerals originally present in the sandstone and originating in the granodiorite.

Although chlorite is present throughout the entire sandstone sequence, it is most abundant in the green sandstone (Table 2). From its morphology and mode of occurrence in mudclasts, it appears to be mostly detrital. Minor authigenic chlorite in sandstone probably resulted from both recrystallization of detrital grains as well as the breakdown of original detrital mafic minerals. As the latter are lacking in the Salmon River porphyry, it is assumed that rocks such as the Chisholm Brook granodiorite that contain abundant mafic minerals were the source.

GENESIS

The absence of syn- or post-Westphalian igneous intrusions in the Yava area effectively renders improbable a magmatic-hydrothermal genetic model for the deposit. A detrital origin for the sandstone-hosted galena is also ruled out by the abundant textures indicating that the galena is a cement, interstitial to the silicate grains, rather than a clastic.

This process of elimination leaves only some form of sedimentary-hydrothermal process(es) as a viable genetic model for the Yava deposit. Based on the nature of the ore solutions envisaged, two such sedimentary-hydrothermal models for sandstone-lead deposits in general have been proposed (Bjørlykke and Sangster, 1981, p. 202): 1) a basin brine model; and 2) a groundwater or meteoric model.

The basin brine model, popularized by Rickard et al. (1979) for deposits in the Scandinavian Caledonides, embodies three basic tenets: 1) dewatering of sediments in a marine basin laterally equivalent to the ore-hosting sandstones. The migrating water would have a high salinity and metal content, the latter carried as chloride complexes; 2) the metal-bearing brines would then move outward and upward through permeable sandstones to the marginal parts of the basin; and 3) precipitation of metals as functions of decreasing temperature and pressure or by mixing with sulphide-bearing groundwater. Direct comparison with Mississippi Valley-type (MVT) ore fluids was made by both Rickard et al. (1979) and Lindblom and Doryphoros (1989). One of the main arguments in favour of the basin brine model is the similarity in the compositions of fluid inclusions in the Scandinavian deposits with those from MVT deposits and recent basin brines.

The groundwater model was described in detail by Samama (1969) based on his observations in the Largentière district, France. Samama (1976) later summarized five basic features of the groundwater model: 1) prolonged weathering of the basement; 2) progressive formation of a pediment by active mechanical sedimentation; 3) metal enrichment of saline groundwater percolating through the pediment; 4) precipitation of metals at the contact between groundwater and marine water at the edge of a shallow marine basin; and 5) diagenetic and epigenetic reorganization of the ore minerals.

Following a world review of the geology of sandstone-lead deposits, Bjørlykke and Sangster (1981) favoured a modified groundwater model and suggested the following parameters were necessary to form such deposits, although recognizing that the significance of each of these will vary from one deposit to the other: 1) a sialic basement having a high average lead content (>30 ppm); 2) stable tectonic conditions leading to thorough weathering of the basement and/or overlying siliciclastic detritus in order to release lead from potassium feldspar; 3) a sufficiently large drainage area with suitable topography to channel the groundwater flow; 4) evaporation to increase the salinity of the surface waters and, hence, the groundwater (and thereby increase the base metal content of the fluids) or, conversely, humid climate to simply provide considerably more fluid of lower metal content; 5) a permeable host rock containing sulphate and carbon to produce sufficient reduced sulphur; and 6) stability of the above conditions for a prolonged period of time.

In the case of Yava, a basin brine model is difficult to defend on the basis of the following: 1) no evidence of a Pennsylvanian marine basin has been reported anywhere in the entire Atlantic Canada region. Marine sequences of Visean age do exist in the region, however, and are thickest offshore between Nova Scotia and Newfoundland. To invoke compaction of these sediments as a source of saline brines which ultimately resulted in formation of the Yava deposit in overlying sediments would require upward cross-stratal movement of these fluids. As compaction processes normally result in outward dewatering through sedimentary aquifers, fluid movement by this process is lateral, rather than vertical; 2) the evidence, discussed previously, of the early diagenetic emplacement of sulphides and silica within the Pennsylvanian sandstones. If this evidence is accepted, then it is unlikely that sufficient sedimentation would have taken place during early Pennsylvanian time to effect significant compaction of the underlying marine strata; 3) lead isotope data indicate a very local source of lead for deposits in the Salmon River Basin, even to the point of identifying the Salmon River porphyry as the main source for Yava lead and the Chisholm Brook-Irish Cove granodiorite for Terra Nova lead. A similarly local source for lead in the Osen deposit, Norway was also reported by Bjørlykke and Thorpe (1983). In view of the very local sources indicated by these studies, long-distance migration of ore fluids, such as would be required by the basin brine model, appears unlikely.

In contrast, local geology and petrographic observations are compatible with a meteoric groundwater model for the formation of the Yava deposit. The authors suggest the entire mineralizing process took place, within a continental milieu, in three main steps: 1) mechanical weathering and erosion of basement to produce a feldspathic quartz sandstone — the Silver Mine Formation; 2) successive chemical degradation of mineral components in the sandstone through prolonged passage of meteoric groundwaters during early burial and diagenesis with resultant release of trace metals held in the silicate lattice; and 3) precipitation of sulphides by reaction with reduced sulphur produced by bacterial reduction of sulphate. These main steps are shown schematically in Figure 30 and are discussed below:

1) Mechanical weathering of the felsic igneous intrusions surrounding the Salmon River Basin produced feldspathic sandstones considered to be the original Silver Mine Formation lithology. The fluvial system in which these sediments were deposited sorted the clastics into the several fining upward cycles described by Bonham (1983). The limestone and shale flake conglomerates occurring at the base of these cycles were derived mainly from the underlying MacKeigan Lake Formation. In contrast, and taking into account the mineralogical composition of the main basement rocks in the area, the sandstone, when originally deposited, probably consisted of quartz and feldspar (from both the Salmon River porphyry and Chisholm Brook granodiorite), mafic minerals (chiefly hornblende and chlorite from Chisholm Brook granodiorite) in early stages of alteration, muscovite (from Kelvin Glen metasedimentary rocks), and coaly debris. Porosity immediately after sedimentation was probably close to 40 percent, average for fine sands.

2) The presence of paleochannels in basement rocks beneath all three Yava zones as well as the Terra Nova

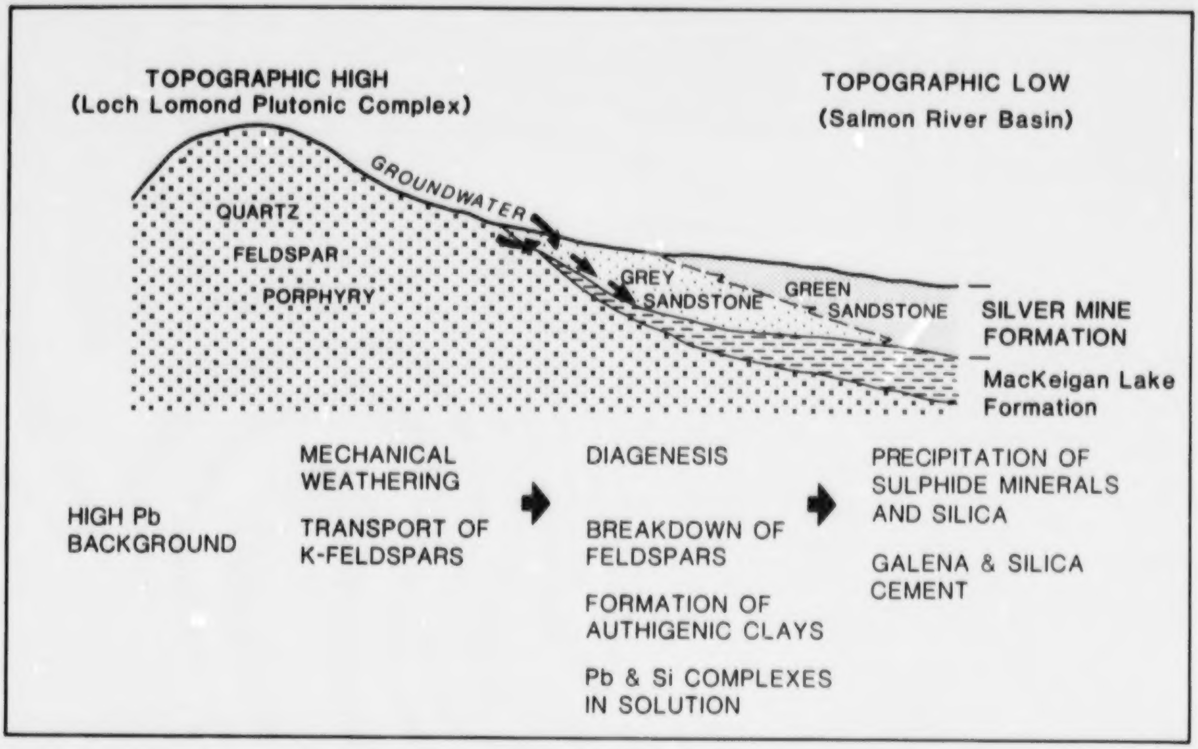
TOPOGRAPHIC HIGH
(Loch Lomond Plutonic Complex)
TOPOGRAPHIC LOW
(Salmon River Basin)
GROUNDWATER
QUARTZ
FELDSPAR
PORPHYRY
GREY SANDSTONE
GREEN SANDSTONE
SILVER MINE FORMATION
MacKeigan Lake Formation
HIGH Pb BACKGROUND
MECHANICAL WEATHERING
TRANSPORT OF K-FELDSPARS
DIAGENESIS
BREAKDOWN OF FELDSPARS
FORMATION OF AUTHIGENIC CLAYS
Pb & Si COMPLEXES IN SOLUTION
PRECIPITATION OF SULPHIDE MINERALS AND SILICA
GALENA & SILICA CEMENT

Figure 30. Schematic representation of genetic model for Yava deposit (from Vaillancourt and Sangster, 1986).

deposit, the fluvial nature of the sedimentary environment, and the orientation of ore zones subperpendicular to the presently-exposed sediment-basement contact, all indicate channelling of surface waters off the surrounding basement rocks into the Salmon River Basin.

The distribution and orientation of modern streams (solid lines in Fig. 31) draining into Salmon River Basin, as well as the position of the Yava paleochannels (Fig. 7), may be combined to present an approximation of the fluvial system that was present when Yava and other deposits formed. Note the prominent northerly orientation of streams on the southeastern flank of the basin and the southeast orientation of those on the northwestern flank (Fig. 31). It has been argued that the position and orientation of those streams on the southeastern flank are controlled by an exhumed Pennsylvanian drainage (Sangster and Vaillancourt, 1990). Based on this concept, extrapolation of these streams basinward (dashed lines in Fig. 31) suggests the former presence of a northeastward-flowing river (proto-Salmon River?) positioned near the middle of Salmon River Basin. These former streams on the southeastern flank would therefore have been tributaries to this main river. Based on paleocurrent directions measured in a small area in the West Zone of the Yava deposit, Bonham (1983) reported fluvial sediment transport from west to east. Because of the small area involved (350 x 200 m), Bonham (1983) concluded that this flow pattern was a local phenomenon only and was strongly influenced by the immediately underlying paleolandscape. Paleocurrent data on Silver Mines Formation sandstone derived from measurements on the southeastern flank of the basin indicate a general northward to north-northwestward flow direction (Prime and Boehner, 1984). The same authors reported data compatible with a northeastward flow direction for sandstone of the Glengarry Formation which is situated near the middle of the basin approximately in the position of the former "river". Thus the data presented for the Pennsylvanian drainage system results in a scenario of northward-draining tributaries on the southeastern flank feeding a larger river flowing northeastward down the middle of the Salmon River Basin, a drainage system virtually identical to that existing today.

The Lennox Passage Fault (Fig. 1), with neither sense nor magnitude of its movement known, effectively precludes a similar basinward extrapolation of the modern streams on the northwestward side of the basin. The general southeastward orientation of the modern streams, however, is compatible with the concept of them being tributaries to a northeastward-flowing proto-Salmon River.

A fluvial system such as envisaged in Figure 31 places each of the three Yava zones and the Terra Nova deposit on a tributary to the "proto-Salmon River". Consideration of the provenance of these tributaries (i.e. Salmon River porphyry for Yava and Chisholm Brook granodiorite for Terra Nova) supports the lead isotopic evidence relating to different sources of lead for each of these two deposits (Fig. 26). The north to north-northwestward flow

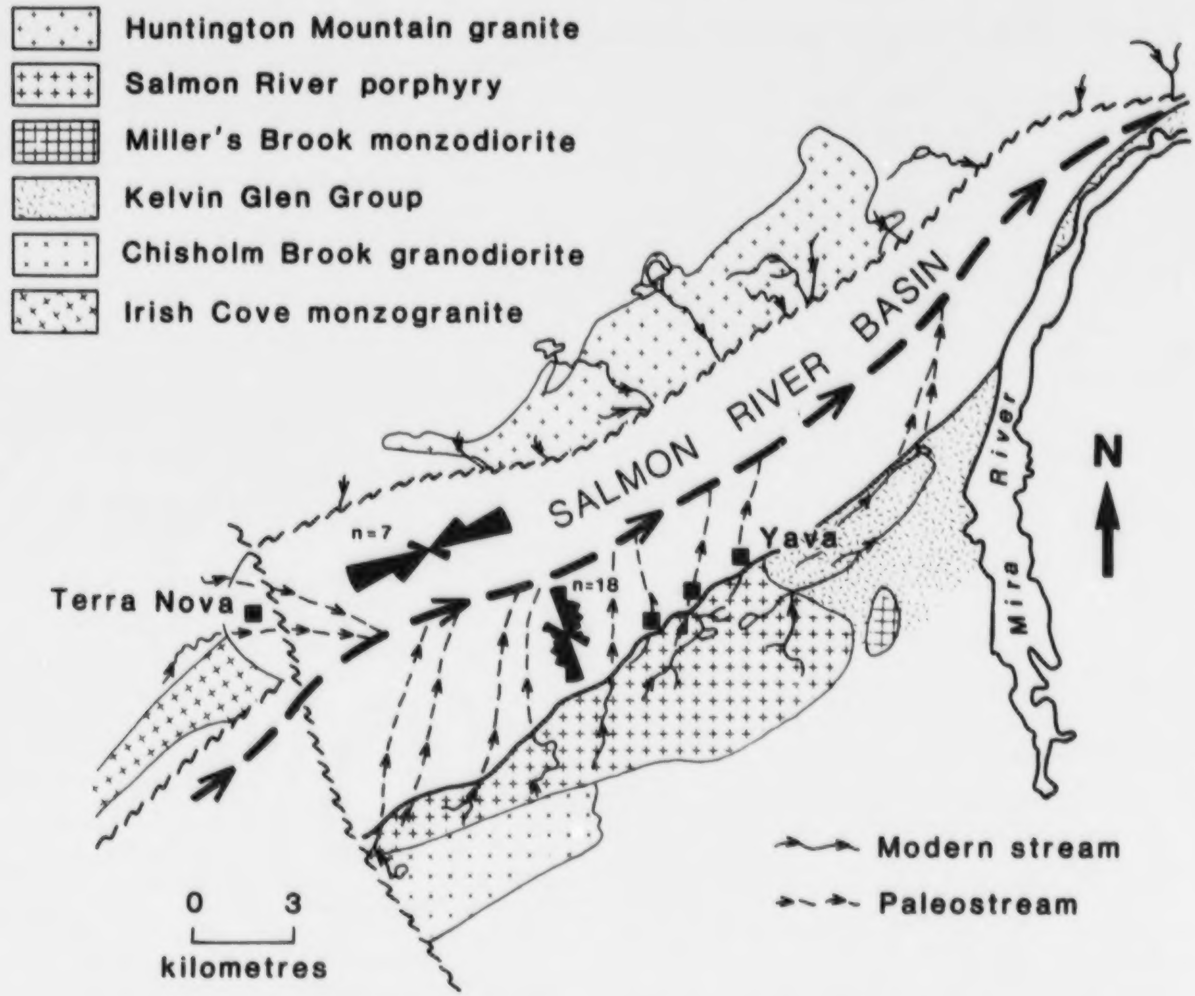

Figure 31. Schematic representation of possible fluviatile system, and compositions of basement provenance, existing during deposition of Silver Mine Formation sandstones. Position of paleostreams inferred from position of modern streams as discussed in text. Note that the three Yava zones and Terra Nova are all situated on tributaries to an inferred proto-Salmon River situated in the central portion of the Salmon River Basin. Rose diagrams (Prime and Boehner, 1984) refer to primary current lineations and trough intersections in sandstones of the Glengarry Valley Formation (centre of basin) and Silver Mine Formation (southeastern edge of basin).

direction for streams on the Yava side of the basin is also compatible with the northwestward flow direction of mineralizing fluids deduced from lead grade contours and mineral zoning as discussed previously.

Prolonged passage of meteoric water through the fluvial sediments resulted in alteration of woody material and silicate minerals in the sandstone. Exposure to meteoric water resulted in very early oxidation of wood trash and lowering of pH in the sandstone (see process (1)). The most unstable of the detrital silicate minerals, hornblende and chlorite from Chisholm Brook-Irish Cove granodiorite, altered first. This likely began during weathering and erosion and continued during early diagenesis. Degradation of hornblende to authigenic chlorite resulted in release of iron during the conversion process. Zinc, substituting for iron in the hornblende lattice because of similar ionic radii (Fe = 0.75Å; Zn = 0.74Å), was also released at the same time. The Chisholm Brook-Irish Cove complex, because of its higher mafic mineral content, contains higher iron and zinc contents than does the more felsic Salmon River porphyry (Table 1). This early release of iron and zinc corresponds with the position of pyrite and sphalerite early in the paragenetic sequence (see previous discussion).

Following destruction of mafic minerals, feldspar and muscovite, under the low pH conditions of early diagenesis (equation (1)) underwent alteration to a variety of clay minerals with concomitant release of silica (see equations (2) to (4)). Alteration of plagioclase released calcium which was later precipitated as calcite cement upon the return to less acidic conditions (see previous discussion).

Because of the similarity in ionic radii with potassium (K = 1.33Å), lead (Pb = 1.21Å) and barium (Ba = 1.35Å) would be released during conversion of microcline and muscovite to kaolinite:

$$(6)\quad H_3O^+ + \underset{\text{K-spar}}{(K,Pb,Ba)AlSi_3O_8} = \underset{\text{kaolinite}}{Al_2Si_2O_5(OH)_4} + (K,Pb,Ba)^+ + \underset{\text{silica}}{SiO_2 \cdot nH_2O}$$

$$(7)\quad H_3O^+ + \underset{\text{muscovite}}{(K,Pb,Ba)AlSi_3O_{10}(OH)_2} = \underset{\text{kaolinite}}{Al_2Si_2O_5(OH)_4} + (K,Pb,Ba)^+$$

3) The abundant limestone and shale flake conglomerate found in the Silver Mine Formation attest to the rapid erosion of underlying lithologies. As MacKeigan Lake shales can contain up to 50 percent gypsum (Bonham, 1983, p. 34), sulphate, occurring either as detrital gypsum or dissolved in fluvial waters, could have been readily supplied to the fluvial sandstones. During the initial oxygenated stages of diagenesis, this sulphate would combine with barium released from microcline or muscovite (equations (6) and (7)) to produce barite with essentially the same sulphur isotopic composition as the original gypsum (Fig. 28d,e,f). As dissolved oxygen became progressively depleted in the interstitial waters due to oxidation of coaly material, the resultant decrease in Eh favoured bacterial reduction of sulphate to sulphide. The reduced sulphur then combined with iron, zinc, and lead to precipitate pyrite, sphalerite, and galena as cement in any available openings, mainly pore spaces between detrital quartz grains and within wood cells.

Oxidation of the woody material by passage of meteoric waters initially resulted in a lowering of reflectance values in the sandstone aquifers. Adjacent shales, acting as aquacludes, in contrast, were not affected and organic material in these units retained their initial reflectance properties. The eventual production of reduced sulphur by bacterial action, however, resulted in a reversal of the oxidation effects such that reflectance of organic matter in sandstone increased, at least in part, toward the mineralized zones (Héroux et al., 1989).

SUMMARY AND CONCLUSIONS

The main points arising from this study of the Yava deposit are:

1) Host rocks to the deposit are coal-bearing fluviatile sandstones of Westphalian age;
2) Mineralization occurs exclusively in grey sandstone of the lower unit of the Silver Mine Formation;
3) Quartz and clay are the main mineral constituents of the grey sandstone with kaolinite the most abundant clay mineral;
4) Highest grade mineralization in each of the three zones at Yava are situated immediately above paleochannels in underlying porphyry basement;
5) The alignment of modern streams with the paleochannels suggests the presence of an exhumed Pennsylvanian topography;
6) Sulphide minerals, principally galena but with minor sphalerite and pyrite, occur mainly as cement between detrital quartz grains. Lesser amounts are found as cell fillings and replacement of woody material;
7) Organic matter close to sulphide mineralization has undergone chemical alteration which has resulted in apparent thermal maturation of the organics;
8) In over 130 sulphur isotope determinations in galena and pyrite, values range from -28 to +65‰; those in green sandstone are consistently lighter than those in grey sandstone. Sulphur isotopes in accessory barite and gypsum in the Yava deposit average within about 2‰ of that of Lower Carboniferous gypsum, suggesting that the source of sulphur at Yava was gypsum from the underlying MacKeigan Lake Formation.
9) Lead isotope determinations of basement rocks and ore-stage galena show that lead was derived from both Chisholm Brook granodiorite and Salmon River porphyry. The data are consistent with a derivation of lead at about 325 Ma (i.e. early Late Carboniferous).
10) Textural relations and mineral abundances indicate detrital potash feldspar and muscovite, originally eroded from basement rocks surrounding Salmon River Basin, were diagenetically altered to produce kaolinite and secondary silica, both of which are presently abundant in the host grey sandstone. Trace lead and barium in the feldspar lattice were released during this process and combined with sulphur to precipitate galena and barite. Similar alteration of mafic minerals during diagenesis is suggested as the source of the minor amounts of zinc and iron sulphides in the deposit.

ACKNOWLEDGMENTS

We are grateful to Dr. J.A. Garnett, former Assistant Deputy Minister, Mines and Minerals, Nova Scotia Department of Mines and Energy, for permission to carry out research on the Yava deposit, which was owned by the Nova Scotia government at the time. Numerous and stimulating discussions with R.C. Boehner, Nova Scotia Department of Mines and Energy, O.J.H. Bonham and J.M. Patterson, both formerly of Barymin Exploration Ltd., did much to clarify our understanding of the stratigraphy and geological history of Yava and the Salmon River Basin. The authors are particularly grateful to R.C. Boehner and B. Rust for critically reading the manuscript and offering many valuable suggestions which considerably improved the text. R.D. Knight, Kim Nguyen, G. Young, and R. Bretzlaff drafted the diagrams.

REFERENCES

Barr, S.M., Sangster, D.F., and Cormier, R.F.
1984: Petrology of Early Cambrian and Devono-Carboniferous intrusions in the Loch Lomond complex, southeastern Cape Breton Island, Nova Scotia; *in* Current Research, Part A, Geological Survey of Canada, Paper 84-1A, p. 203-211.

Belt, E.S.
1965: Stratigraphy and paleogeography of the Mabou Group and related Middle Carboniferous facies; Geological Society of America, Bulletin, v. 76, p. 777-802.
1968: Carboniferous continental sedimentation, Atlantic Provinces, Canada; *in* Geological Society of America, Special Paper 106, edited by G. De V. Kelvin, p. 127-176.

Bjørlykke, A. and Sangster, D.F.
1981: An overview of sandstone-lead deposits and their relation to red-bed copper and carbonate-hosted lead-zinc deposits; Economic Geology, Seventy-Fifth Anniversary Volume, p. 179-213.

Bjørlykke, A. and Thorpe, R.I.
1983: The source of lead in the Osen sandstone lead deposit on the Baltic Shield, Norway; Economic Geology, v. 76, p. 1205-1210.

Boehner, R.C.
1983: Loch Lomond Basin, Cape Breton Island, Windsor Group project — an update: *in* Mines and Mineral Branch, Report of Activities 1982, Nova Scotia Department of Mines and Energy, Report 83-1, p. 97-107.

Boehner, R.C. and Prime, G.
1985: Geology of the Loch Lomond Basin and Glengarry Half Graben; Nova Scotia Department of Mines and Energy, Map 85-2, scale 1:50 000.

Bonham, O.J.
1982: The Yava lead deposit, Salmon River, Cape Breton: exploration (1962-1981) and mining activities (1979-1981); Report prepared for the Nova Scotia Department of Mines and Energy, 55 p.
1983: Geology of the Yava sandstone-lead deposit, Cape Breton, Nova Scotia; M.Sc. thesis, Dalhousie University, Halifax, Nova Scotia, 181 p.

Bustin, R.M., Cameron, A.R., Grieve, D.A., and Kalkreuth, W.D.
1983: Coal petrology — its principles, methods, and applications; Geological Association of Canada, Short Course Notes, v. 3, 230 p.

Claypool, G.E., Holser, W.T., Kaplan, I.R., Sakai, H., and Zak, I.
1980: The age curves of sulphur and oxygen isotopes in marine sulphate and their mutual interpretation; Chemical Geology, v. 28, p. 199-260.

Forgeron, S.
1977: The Kaiser celestite mining operation and mineral potential of the Loch Lomond Basin, Cape Breton, Nova Scotia; Nova Scotia Department of Mines and Energy, Open File Report 328, 102 p.

Gibling, M.R., Zentilli, M., and McReady, R.G.L.
1989: Sulphur in Pennyslvanian coals of Atlantic Canada: geologic and isotopic evidence for a bedrock evaporite source; International Journal of Coal Geology, v. 11, p. 81-104.

Hacquebard, P.A. and Donaldson, J.R.
1970: Coal metamorphism and hydrocarbon potential in the Upper Paleozoic of the Atlantic Provinces, Canada; Canadian Journal of Earth Sciences, v. 7, p. 1139-1163.

Héroux, Y., Michoux, D., Desjardins, M., and Sangster, D.F.
1989: Pétrographie et géochimie des matières organiques des séquences plombo-zincifères d'âge Carbonifère, Bassin Salmon River, Nouvelle-Écosse, Canada; Organic Geochemistry, v. 14, p. 253-268.

Keppie, D.
1982: Tectonic Map of the Province of Nova Scotia; Nova Scotia Department of Mines and Energy, scale 1:500 000.

Lindblom, S. and Doryphoros, C.
1989: Fluid inclusion studies on sandstone environments related to lead-zinc ore deposition; 28th International Geological Congress, Washington, U.S.A., Abstracts, v. 2, p. 302-303.

McCabe, P.J. and Schenk, P.E.
1982: From sabkha to coal swamp — the Carboniferous sediments of Nova Scotia and New Brunswick; Field Excursion Guidebook, Excursion 4A, International Association of Sedimentologists, 11th International Congress on Sedimentology, McMaster University, Hamilton, Ontario.

McMullin, D.W.
1984: Geology and geochemistry of the granitoid rocks of the Loch Lomond Irish Cove area, Cape Breton Island; M.Sc. thesis, Acadia University, Wolfville, Nova Scotia, 239 p.

Ohmoto, H. and Rye, R.O.
1979: Isotopes of sulfur and carbon; *in* Geochemistry of Hydrothermal Ore Deposits, 2nd edition, edited by H.L. Barnes, John Wiley and Sons, New York, p. 509-567.

Patterson, J.M.
1979: Salmon River lead deposit of Yava Mines, Nova Scotia; Canadian Mining Journal, v. 100, p. 56-57.
1987: Zinc enrichment and exploration possibilities at Yava mine, Salmon River, Cape Breton County; Report of Activities 1986, Part A, Nova Scotia Department of Mines and Energy, Report 87-5, p. 83-84.

Poole, W.H.
1967: Tectonic evolution of the Appalachian region, Canada; *in* Collected Papers on Geology of the Atlantic Region, edited by E.R.W. Neale and H. Williams, Geological Association of Canada, Special Paper 4, p. 9-51.

Prime, G. and Boehner, R.C.
1984: Preliminary report on the geology of the Glengarry Half-Graben and vicinity, Cape Breton Island, Nova Scotia; *in* Mines and Minerals Branch, Report of Activities, 1983, Nova Scotia Department of Mines and Energy, Report 84-1, p. 61-69.

Rickard, D.T., Willden, M.Y., Marinder, N.E., and Donnelly, T.H.
1979: Studies on the genesis of the Laisvall sandstone lead-zinc deposit, Sweden; Econmic Geology, v. 74, p. 1255-1285.

Samama, J.C.
1969: Contribution à l'étude des gisements de type Red-Beds; Ph.D. thesis, Université de Nancy, Nancy, France, 276 p.
1976: Comparative review of the genesis of the copper-lead sandstone-type deposits; *in* Handbook of Strata-Bound and Stratiform Ore Deposits, v. 6, edited by K.H. Wolf, Elsevier Publishing Company, Amsterdam, p. 1-20.

Sangster, D.F. and Vaillancourt, P.D.
1990: Geomorphology in the exploration for undiscovered sandstone-lead deposits, Salmon River Basin, Nova Scotia; Canadian Institute of Mining and Metallurgy Bulletin, v. 83, p. 62-68.

Scott, P.
1980: Geochemistry and petrography of the Salmon River lead deposit, Cape Breton Island, Nova Scotia; M.Sc. thesis, Acadia University, Wolfville, Nova Scotia, 111 p.

Vaillancourt, P.D.
1985: Sandstone lithology in the Silver Mine Formation and its relation to galena occurrence in the Yava deposit, Cape Breton Island, Nova Scotia; *in* Current Research, Part A, Geological Survey of Canada, Paper 85-1A, p. 743-751.

Vaillancourt, P.D. and Sangster, D.F.
1984: Petrography of mineralization at the Yava sandstone-lead deposit, Nova Scotia; *in* Current Research, Part A, Geological Survey of Canada, Paper 84-1A, p. 345-352.
1986: Isotope and hydrocarbon studies of the Yava sandstone-lead deposit, Cape Breton Island, Nova Scotia: a progress report; *in* Current Research, Part A, Geological Survey of Canada, Paper 86-1A, p. 133-140.

Williams, H.
1979: Appalachian Orogen in Canada; Canadian Journal of Earth Sciences, v. 16, p. 792-807.

Williams, H., Kennedy, M.J., and Neale, E.R.W.
1972: The Appalachian structural province; *in* Variations in Tectonic Styles in Canada, edited by R.A. Price and R.J.W. Douglas, Geological Association of Canada, Special Paper 11, p. 181-261.

APPENDIXES

Appendix A

Clay mineral determinations

Specimens were cut and crushed to minus 200 mesh and separated into a <2 μm size fraction. By using the grain size fraction <2 μm, the effect of well crystallized detrital white mica on illite crystallinity determinations is reduced. Twenty gram samples of the fine fraction were bottled and used for the clay determinations. The procedure outlined below is the standard method used for clay mineral determinations by the Sedimentology Section at the Geological Survey of Canada in Ottawa. For this study, a 1 to 2 g sample from each of the 20 g vials was placed in a modified milkshake mixer with replaceable nalgene blades. Each sample was washed three times in the mixer with approximately 600 mL of Sodium Hexametaphosphate solution. After each washing, the suspension was allowed to settle for about five seconds and then decanted into a 1000 mL nalgene centrifuge bottle. The bottles were then centrifuged for three minutes at 750 r/min. This left particles <2 μm (ESD) still in suspension while the silt fraction was brought down. The supernatant portion (<2 μm) was decanted into a second series of centrifuge bottles and spun at 2800 r/min for 14 minutes. Although some fines remained in suspension after this run, further centrifuging did not appreciably alter the amount of clay brought down. Using this method, the clay particles removed range from 0.2 to 2.0 μm ESD. Throughout the procedure, observations were noted with respect to distinctive colour bands or inclusions. Fine particles remaining in suspension after the 14 minute run were discarded and a long-handled stainless steel spatula used to scrape the clay into nalgene cups with distilled water added to facilitate scraping. Small amounts of the pasty residue from the 14 minute run were extracted by pipette, smeared on glass slides, and dried at room temperature. The smear-on-glass technique was adopted because it yielded satisfactory precision and accuracy.

X-ray determination and interpretation

Methods

X-ray charts were obtained with a Philips PW 1710 X-ray diffractometer using copper radiation at 40 kV and 20 mA, and a scan rate of 2 degrees 2 theta per minute for the 2 theta range 3 to 40 degrees. For each of the samples studied, X-ray diffraction charts were obtained from an air dried mount. Area measurements were done on the 7 Å (12.5 degrees, (001) kaolinite reflections and (002) chlorite reflections) kaolinite and chlorite peak and the 10 Å (8.8 degrees, (001) reflections) illite peak. Intensity measurements were done on the 3 Å (24.9 degrees) kaolinite peak and the 3 Å (25.2 degrees) chlorite peak. Because the scan speed of the diffractometer was 40 mm/1 degree, adjustments in calculations were made for determinations of illite crystallinity. Measurements taken from the charts were divided by 4 to be standardized to 10 mm/1 degree and subsequently by 10 to establish the value in terms of degrees delta 2-theta.

Based on these measurements, semiquantitative abundances of kaolinite, chlorite, and illite were determined. To determine kaolinite abundance in each sample, the 7 Å kaolinite and chlorite area measurement is multiplied by the fraction of the kaolinite intensity over the combined chlorite and kaolinite intensities. Similarly, for the chlorite abundance in each sample, the 7 Å kaolinite and chlorite area measurement is multiplied by the fraction of the chlorite intensity over the combined chlorite and kaolinite intensities. The illite abundance was determined by calculating the ratio of the area occupied by the illite peak to the other measurements made on kaolinite and chlorite. On the charts obtained from these clay samples, chlorite was over-represented and, as a result, a weight factor of 0.5 was applied to the calculated chlorite abundance, while illite and kaolinite were assigned weight factors of 1.

Appendix B

Lead isotope determinations

Sampling

Rock samples from the Salmon River porphyry and Chisholm Brook-Irish Cove granodiorite were taken from outcrop locations shown in Barr et al. (1984). Weathered surfaces were removed by either cobbing or sawing and the sample then reduced to powder. One split of the powder was used for chemical analyses and age dating (Barr et al., 1984) and another used for U-Th-Pb isotopic analyses.

Analytical procedures

All isotopic analyses were performed by Geospec Consultants Ltd., Edmonton. For galena, small grains were picked under the microscope, dissolved in 8 mL of 2N HCl overnight, and then evaporated to dryness. The dried sample was taken up in HBr-HCl and passed through an anion exchange column. The resulting Pb solution was dried and approximately 1 μg loaded on a single Re filament using the silica gel-phosphoric acid technique.

Comparison with the standard indicates a precision of better than 0.1% per mass unit (95% C.L.). At the time of analysis (1984) the 2-σ error on isotope ratios were:

$^{206}Pb/^{204}Pb \pm 0.96‰$
$^{207}Pb/^{204}Pb \pm 1.07‰$
$^{208}Pb/^{204}Pb \pm 1.58‰$

as determined from repeated analyses of NBS SRM-981 common lead standard.

Rock powders were first dissolved in HF-HNO_3 and Pb was purified using HBr-HCl ion exchange columns. Analytical error at the time of measurement (1984) at the 2-σ level was similar to that for galena as determined from repeated analyses of NBS SRM-981 common lead standard.

Appendix C

Sulphur isotope determinations

Samples for sulphur isotope analysis were selected from drill core and the Yava mine dump to obtain a representative suite of rock types in and beyond the Yava mine area. These areas include all occurrences of galena within the Salmon River and Loch Lomond basins. Within Yava, particular attention was paid to obtaining representative proportions of pyrite and galena in the grey and green sandstone as well as in wood fragments or coal.

Sulphur isotope determinations were performed at the Ottawa-Carleton Geoscience Centre Stable Isotope Lab in Ottawa. Isotope measurements were made on SO_2 gas and were normalized to Canon Diablo troilite ($\delta^{34}S$ = 0‰) and OGS-1 seawater sulphate ($\delta^{34}S$ = +20.58‰). Sample and machine reproducibility averaged 0.1-0.2‰.

Data

PYRITE IN SANDSTONE AT YAVA

DDH#	FOOTAGE	VALUE	DDH#	FOOTAGE	VALUE
030	170	13.05	312	94	65.12
080	280	-8	320	90	46.33
105	146	9.69	322	95	13.26
159	271	28.19	328	160	11.84
164	609	53.06			
185	82	-28.7			
233	256A	-2.98			
233	256B	-0.53			
250	56	35.17			
253	112	59.4			
273	192	-20.55			
273	199.5	-16.03			
275	89	61.51			
297	140	63			
305	79.5	-2.15			

PYRITE IN COAL AT YAVA

DDH#	FOOTAGE	SAMPLE	VALUE
		SP2422	14.93
		SP4074	-18.3
		SP4503	-18.4
		SP4512	-12.2
		SP4532	-27.7
		YD-12A	-23.9
		YD-12B	-21.8
		YD-15B	-12.7
		YD-22B	-24
		YD-23B	-23.9
		YD-27B	-12.9
		YD-29B	-18.4
		YD-29C	-17.6
		YD-30A	-20.29
		YD-30B	-19.1
		YD-31B	-14.3
		YD-35B	-25.4
055	156		-8.58
055	350		-8
061	406A		-22.9
061	406B		-22.8
068	131		-0.46
075	205		-7.22
105	193		7.09
138	320C		-22.5
150	542		-7.2
150	572		-10.9
185	33		-2
224	121		11.63
228	246		-23.52
250	58		27.73
251	178A		-21.41
251	178B		-21.9
255	203		8.78
273	127		15.31
294	66		-2.57
305	194		10.66
328	104		15.04
332	171		-22.3
341	110		11.8
341	115A		5.97
341	115B		7.9
341	361		-27.82
347	130		-22.4
347	427		-22.59
348	130		-15.7
352	203		
352	619		4.8

PYRITE IN SANDSTONE AT TERRA NOVA

DDH#	FOOTAGE	VALUE
TN74-07	178	42.54
TN74-07	187	57.44
TN74-10	68	49.9
TN74-11	36	25.63
TN74-12	60	32.68
TN74-14	129	33.09
TN74-14	207	35.69
TN74-17	107	26.99
TN74-18	50	39.93
TN74-7	55	42.81
TN74-7	182	4.7
TN77-23	23	38.96
TN78-36	42	20.12

PYRITE IN SANDSTONE AT ROCK ELM

DDH#	FOOTAGE	VALUE
SI1	53	29.58
SII1	50	32.57
SII1	72	25.75
SII1	155	30.88
SII2	115	2
SII2	263	16.6

PYRITE IN SANDSTONE AT BIG GLEN

DDH#	FOOTAGE	VALUE
BBG5	234	4.79
BBG5	747	16.23
BBG5	823	36.76
BBG74-4	626	-0.78
BBG74-4	680	36.09
BG14	264	15.5
BG14	339	33.33

PYRITE AT LAKE ENON AND PINE BROOK

DDH#	FOOTAGE	SAMPLE	VALUE
K436	30		16.25
K436	345		15.48
K436	358		-1.13
K436	586		-11.75
		M-1	-12.17
PBG6	117		48.93
PBG6	233		13.26
PBG6	244		-5.5
PBG6	250		8.87

GALENA IN SANDSTONE AT YAVA

DDH#	FOOTAGE	SAMPLE	VALUE
		YD-10	8.53
		YD-14	6.97
		YD-16	9.16
		YD-17	6.38
		YD-18	7.56
		YD-19	4.57
		YD-20	9.04
		YD-23A	6.39
		YD-24	8.04
		YD-36	10.14
		YD-37	10.32
		YD-38	9.43
018	180		21.84
018	190		27.67
033	122		12.22
127	351		11.91
130	208		-4.06
138	319		4.79
150	564		8.4
181	813		14.6
185	82		-25.7
185	85A		1.89
185	85B		2.77
233	260		9.15
251	180A		-5.15
251	180B		-2.15
273	192		4.7
349	439.63		-14.01

GALENA IN COAL AT YAVA

DDH#	FOOTAGE	SAMPLE	VALUE
		SP4074	-14.4
		SP4503	-15.6
		SP4512	-9.4
		SP4532	-27.5
		YD-12A	-18.8
		YD-12B	-18.9
		YD-15A	-10.55
		YD-15B	-14.8
		YD-21	-26.7
		YD-22A	-19.92
		YD-22B	-21.3
		YD-23B	-19.4
		YD-25	-20.23
		YD-27A	-11.5
		YD-27B	-3.7
		YD-29A	-20.87
		YD-29B	-15.9
		YD-29C	-15.2
		YD-30A	-15.25
		YD-30B	-12.9
		YD-31A	-16.14
		YD-31B	-12.4
		YD-33	-28.25
		YD-35A	-22.63
		YD-35B	-18.7
061	406B		-24
068	131		3.92
138	320A		-11.92
138	320B		-18.53
150	542		-10.8
150	572		-6.5
224	121		11.88
251	178B		-17.4
305	194		10.06
332	171		-15.4
347	130		-18.5
348	130		-15.9

GALENA IN MISCELLANEOUS OCCURRENCES, LOCH LOMOND AND SALMON RIVER BASINS

DDH#	FOOTAGE	SAMPLE	VALUE
BB74-2	545		-21.41
BG5	383		-27.11
K212-8	71		7.91
		M-3	-14.48
		M-1	-15.8
		M-2	-15.82
		PBD-1	-0.32
SII1	464		-30.32
SV2	112		-4.61
TN74-09	203		34.88
TN74-1	177		13.76
TN74-9	195		32.43

BARITE AT PINE BROOK, TERRA NOVA, AND YAVA

DDH#	FOOTAGE	SAMPLE	VALUE
PB83-1	56		12.18
		PBD-1	13.3
		PBD-2	14.82
TN74-17	77		11.39
		YD-19	10.58
		YD-24	19.02
		YD-16	8.99

GYPSUM AT BIG GLEN, ROCK ELM, AND YAVA

DDH#	FOOTAGE	VALUE
BBG1	316	13.81
BG4	282	14.02
BG5	300	13.78
SII1	418	20.78
SII2	585	21.15
068	270	15.61
134	290	21.49

PYRITE-GALENA PAIRS IN COAL AND SANDSTONE AT YAVA

DDH#	FOOTAGE	SAMPLE	GALENA	PYRITE
		SP4074	-14.4	-18.3
		SP4503	-15.6	-18.4
		SP4512	-9.4	-12.2
		SP4532	-27.5	-27.7
		YD-12A	-18.8	-23.9
		YD-12B	-18.9	-21.8
		YD-15B	-14.8	-12.7
		YD-22B	-21.3	-24
		YD-27B	-3.7	-12.9
		YD-29B	-15.9	-18.4
		YD-29C	-15.2	-17.6
		YD-30A	-15.2	-20.29
		YD-30B	-12.9	-19.1
		YD-31B	-12.4	-14.3
		YD-35B	-18.7	-25.4
		YD-23	-19.4	-23.9
061	406B		-24P	-22.8
068	131		3.9	-0.46
150	542		-10.8	-7.2
150	572		-6.5	-10.9
224	121		11.8	11.63
251	178B		-17.4	-21.9
305	194		10.0	10.66
332	171		-15.4	-22.3
347	130		-18.5	-22.4
348	130		-15.9	-15.7
185	82		-25.7	-28.7
273	192		4.7	-20.55

Strontium isotopic geochemistry of lead-zinc/barite deposits and host rocks of the Carboniferous Minas Sub-basin, Nova Scotia[1]

C.E. Ravenhurst[2*], P.H. Reynolds[2], M. Zentilli[2], H.W. Krueger[3], and J. Blenkinsop[4]

Ravenhurst, C.E., Reynolds, P.H., Zentilli, M., Krueger, H.W., and Blenkinsop, J., Strontium isotopic geochemistry of lead-zinc/barite deposits and host rocks of the Carboniferous Minas Sub-basin, Nova Scotia; in Mineral Deposit Studies in Nova Scotia, Volume 1, edited by A.L. Sangster, Geological Survey of Canada, Paper 90-8, p. 245-256, 1990.

Abstract

Lead-zinc and barite deposits in central Nova Scotia generally occur at the Tournaisian-Visean (Mississippian) clastic-carbonate/evaporite disconformity overlying Cambrian to Devonian metasedimentary and granitic rocks. The deposits are located at the southern margin of the >10 km deep Carboniferous Maritimes (Fundy/Magdalen) Basin. Strontium isotopic compositions of calcite and barite indicate that there is a genetic link among these deposits. The ore-stage minerals of the larger and/or higher grade deposits such as the Gays River lead-zinc deposit, have a relatively high $^{87}Sr/^{86}Sr$ ratio (= 0.712), suggesting a massive influx of mineralizing fluid considerably different from Carboniferous marine water as recorded in the host carbonates ($^{87}Sr/^{86}Sr$ = 0.708). No unique source for the radiogenic strontium can be determined, but the most likely is the Horton Group clastic rock which is in close proximity to all the deposits.

A mineralization age of ca. 300 Ma is suggested by rubidium-strontium data on illite from samples collected over a ten metre section of Tournaisian (Horton Group) sandstone at the disconformity with the overlying Visean (Windsor Group) carbonates and evaporites.

Résumé

Dans la partie centrale de la Nouvelle-Écosse, les gisements plombo-zincifères et de barytine se manifestent généralement à l'endroit de la discordance tournaisienne-viséenne (mississippienne) entre les roches détritiques et les roches carbonatées, d'une part, et les évaporites, d'autre part; cette discordance est sus-jacente à des roches granitiques et métasédimentaires datant du Cambrien au Dévonien. Les gisements sont situés à la bordure sud du bassin carbonifère des Maritimes (Fundy/Îles de la Madeleine), dont la profondeur dépasse 10 km. L'étude de la composition isotopique du strontium dans la calcite et la barytine indique qu'il existe un lien entre l'origine de ces deux genres de gisements. Le rapport $^{87}Sr/^{86}Sr$ des minéraux au stade de minerai dans les gisements plus vastes ou à plus forte teneur ou les deux, comme le gisement plombo-zincifère de Gays River, est relativement élevé (0,712) : ce phénomène pourrait indiquer l'apport possible d'une grande quantité de fluide minéralisateur considérablement différent de l'eau de mer du Carbonifère, ainsi qu'en témoignent les roches carbonatées hôtes dont le rapport $^{87}Sr/^{86}Sr$ est de 0,708. On n'a pu déterminer avec certitude d'où provient le strontium radiogénique mesuré; toutefois, les roches détritiques du groupe de Horton, qui se trouvent à proximité de tous les gisements, sont la source la plus vraisemblable de cet isotope.

Les auteurs ont estimé l'âge de la minéralisation à environ 300 millions d'années par datation Rb-Sr de l'illite extraite d'échantillons recueillis le long d'une coupe de dix mètres dans du grès tournaisien (groupe de Horton), à la discordance avec les évaporites et les roches carbonatées viséennes (groupe de Windsor) sus-jacentes.

---

[1] Contribution to the Canada - Nova Scotia Mineral Development Agreement, 1984-1989. Project carried by the Mineral Resources Division, Geological Survey of Canada, Project 860008.

[2] Department of Geology, Dalhousie University, Halifax, Nova Scotia, B3H 3J5.

[3] Geochron Laboratories, Krueger Enterprises, Inc., Cambridge, Massachusetts, 02139.

[4] Department of Earth Sciences, Carleton University, Ottawa, Ontario, K1S 5B6.

[*] Now at Geology Department, Smith College, Northampton, Massachusetts, 01063.

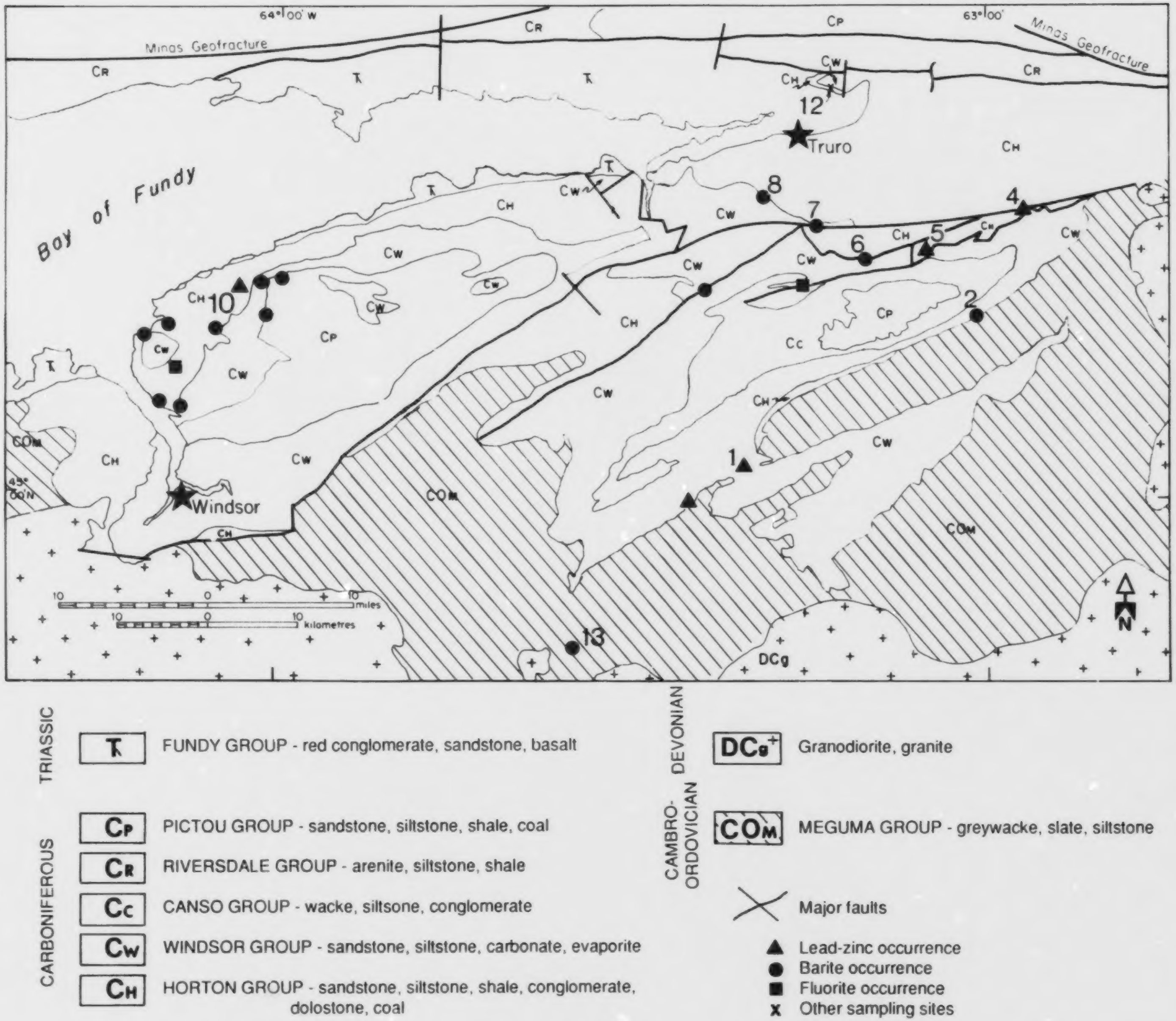
64°00' W
63°00'
Minas Geofracture
Minas Geofracture
Bay of Fundy
Truro
Windsor
45°00'N
1
2
4
5
6
7
8
10
12
13
CR
CP
T̶R
CH
CW
CC
COM
DCg
10 0 10 miles
10 0 10 kilometres
N
TRIASSIC
CARBONIFEROUS
DEVONIAN
CAMBRO-ORDOVICIAN
T̶R FUNDY GROUP - red conglomerate, sandstone, basalt
CP PICTOU GROUP - sandstone, siltstone, shale, coal
CR RIVERSDALE GROUP - arenite, siltstone, shale
CC CANSO GROUP - wacke, siltsone, conglomerate
CW WINDSOR GROUP - sandstone, siltstone, carbonate, evaporite
CH HORTON GROUP - sandstone, siltstone, shale, conglomerate, dolostone, coal
DCg+ Granodiorite, granite
COM MEGUMA GROUP - greywacke, slate, siltstone
Major faults
▲ Lead-zinc occurrence
● Barite occurrence
■ Fluorite occurrence
x Other sampling sites

Figure 1. Location map of mineral occurrences and sampling sites in the Minas Sub-basin. 1=Gays River, 2=Southvale, 4=Pembroke, 5=Smithfield, 6=Middle Stewiacke, 7=Brookfield, 8=Hilden, 10=Walton/Magnet Cove, 12=Upper Brookside (isochron site), 13=Lake Fletcher.

INTRODUCTION

The occurrence of lead-zinc and barite deposits along the margins of Carboniferous sedimentary basins in Nova Scotia suggests a genetic link between the deposits and hydrothermal fluids evolved from these basins. Previous work has shown that some of the Nova Scotian deposits have affinities with Mississippi Valley-type deposits (e.g. similar geological setting) and with Irish-type deposits (e.g. similar temperatures of formation) (Russell, 1976; Akande, 1982). The deposits studied are all located at the southern margin of the large ($\geq 250\ 000$ km^2) and deep (>10 km) Maritimes (Fundy/Magdalen) Basin and south of the Cobequid-Chedabucto Fault System, also known as the Minas Geofracture (Fig. 1). They range from the former Zn-Pb mine at Gays River and the presently producing barite quarry at Brookfield, to small barite vein occurrences at Hilden and Southvale (Fig. 1). The small Pb deposit at Pembroke was mined over 100 years ago, and the Smithfield Pb-Zn-Cu-Ba deposit was recently the focus of a diamond-drilling project. The large Walton/Magnet Cove Ba-Zn-Cu-Pb-Ag deposit was a former producer. Almost all the deposits occur near the base of the Mississippian Windsor Group and many are associated with faults (Boyle, 1972; Felderhof, 1978; Akande, 1982).

In Nova Scotia, the Carboniferous stratigraphy has been divided, in ascending order, into the Horton, Windsor, Canso/Riversdale, and Pictou groups (Bell, 1929). Many of these units are time-transgressive (Hacquebard et al., 1960; Belt, 1964; Hacquebard, 1972; Howie and Barss, 1975), and are better referred to as stages as defined on the basis of spores from reference sections (Belt, 1964). However, the geological time scale of Harland et al. (1982) was adopted here for the approximate time equivalents of each group.

Horton Group strata of Tournaisian age (360-350 Ma) were mainly deposited in fault-bounded continental basins and typically vary rapidly through fanglomerate, fluvial, and lacustrine facies, including nonmarine limestone and evaporite. A thickness of at least 3 to 4 km of Horton and related strata accumulated (Howie and Barss, 1975).

The Windsor Group of Visean age (348-336 Ma) is composed of a thick (>600 m), laterally extensive sequence of carbonates, evaporites, and siltstones unconformably overlying pre-Mississippian basement or Horton redbeds (Fig. 1). These strata represent the only major marine deposits in the Carboniferous sequence, and are preceded and followed by continental sedimentation. The basal carbonate stratum is either a black laminated Macumber dolostone/limestone or the fossiliferous Gays River Formation. Also occurring at this stratigraphic level is the Pembroke breccia, a chaotic unsorted mass of angular fragments or slabs, mainly of Macumber laminated limestone, but with scattered exotic pebbles of granite and other Horton Group clasts (Weeks, 1948). The fragments vary in size from a few millimetres to several metres, and the breccia unit itself varies in thickness from zero to thirty metres. The origin of the Pembroke breccia is controversial. It has been interpreted either as a near-synsedimentary karstic breccia (Schenk, 1984) or as a much later solution collapse breccia (Clifton, 1967). Its variable distribution, but occurrence near many of the mineral deposits studied, along with its angular fragmental nature suggests that it may have been formed by a hydrofracturing mechanism related to the mineralizing event. The basal carbonate units and breccia are overlain by 250 to 400 m of evaporites that would have formed an effective seal to fluid flow.

Up to 6 km of clastic sediments of the Canso/Riversdale (336-300 Ma) and Pictou (300-280 Ma) groups overlie the Windsor Group (Howie and Barss, 1975). The Late Carboniferous Westphalian B (305-300 Ma) was the time of peak evaporite tectonism (Boehner et al., 1986). During Westphalian C through Early Permian times a broad fluvial basin, inferred to be a flexural foredeep, occupied the Maritimes Basin area (Bradley, 1988).

The purpose of this study was to determine: 1) if a genetic link exists among the different deposits around the margin of the Minas Sub-basin; 2) if the mineralizing fluids may have derived at least part of their calcium and barium components from Horton Group clastic rocks; ascertaining an age for homogenization of strontium in the Horton strata and thus the age of what may have been a hydrothermal event would be an added bonus; and 3) if strontium isotopic analysis of ore-stage minerals is a useful exploration tool.

GEOLOGY OF THE DEPOSITS

All the Nova Scotian deposits studied show strong epigenetic characteristics and some have a well defined paragenetic sequence composed of pre-ore, ore, and post-ore stages. The results of isotopic and dating work on these deposits is documented in Ravenhurst et al. (1989). The following numbers refer to deposit locations on Figure 1.

1) The Gays River Zn-Pb deposit contains about 12 million tonnes of 7 percent combined lead and zinc hosted in a dolomitized carbonate bank of the Gays River Formation. Its mineralogy, paragenetic sequence, and fluid inclusion temperatures have been documented by MacEachern and Hannon (1974a,b) and Akande and Zentilli (1983, 1984).

2) The Southvale barite occurrence consists of a small bed of fine grained to cryptocrystalline barite showing replacement characteristics, and is underlain by the basal dolomitic limestone of the Windsor Group (Felderhof, 1978).

4) The Pembroke Pb deposit is made up of galena in calcite veins and with vug-filling calcite, in a limestone of the Windsor Group (Ponsford, 1983).

5) The Smithfield Pb-Zn-Cu-Ba deposit contains a half million tonnes of 6 percent combined lead and zinc and occurs in a brecciated basal Windsor limestone, disconformably overlying highly pyritized Horton clastic rocks (Felderhof, 1978; Walker, 1978). There is a distinct paragenetic sequence: pyrite (with calcite) layers in vug-filling barite, followed by sphalerite, calcite, galena, and more barite.

6) The Middle Stewiacke barite occurrence is structurally controlled. Barite is hosted in massive limestone and limestone breccia of the upper Windsor Group, where it is in fault contact with Horton clastic rocks (Felderhof, 1978).
7) The Brookfield barite deposit contains at least 56 000 tonnes of 50 percent barite and is a "replacement" deposit hosted entirely in fractured Horton clastic rocks (Felderhof, 1978), but directly overlain by Windsor limestone. Barite is intergrown with siderite. Secondary quartz is also present (Stevenson, 1951).
8) The Hilden barite occurrence is a vein in basal limestone and limestone breccia of the Windsor Group (Felderhof, 1978).
10) The Walton/Magnet Cove Ba-Zn-Cu-Pb-Ag deposit is made up of barite and sulphide orebodies in a limestone conglomerate (Pembroke breccia), fissile limestone, and anhydrite of the Windsor Group directly overlying the Horton clastics (Boyle, 1972; Boyle et al., 1976).
13) The Lake Fletcher barite occurrence is a vein in Meguma slates (Felderhof, 1978).

Genetic hypotheses that can be applied to these deposits include: penecontemporaneous sabkha-type deposition (MacLeod, 1975, 1984; Mossman and Brown, 1986); early diagenetic deposition from convecting hydrothermal fluids (Russell, 1976); formation from late diagenetic compaction-driven mineralizing fluids that migrated laterally from the adjacent sedimentary basins (Lydon, 1978), as suggested by Jackson and Beales (1967) for the Pine Point deposit; formation from gravity-driven fluids present after uplift of part of the basin, as suggested by Garven and Freeze (1984a,b) for the Pine Point deposit; or deposition from fluids from a "deep source", as suggested by Krebs and Macqueen (1984) for the Pine Point deposit.

The sabkha model has been ruled out by fluid inclusion temperatures (>200°C) measured in sphalerite by Akande (1982; Akande and Zentilli, 1984) and Ravenhurst (1987; Ravenhurst et al., 1989). The early diagenetic model of Russell (1976) is difficult to envisage in a sedimentary sequence with significant thicknesses of evaporites. Compaction-driven episodic expulsion of fluids under an evaporite seal is the mechanism we postulate was responsible for the mineralizing event by the transfer of hot overpressured brines from deep in the Magdalen Basin, to the basin margins (Ravenhurst and Zentilli, 1987; Ravenhurst et al., 1989).

SAMPLE PREPARATION AND ANALYTICAL METHODS

Samples of barite, calcite, and host rock carbonate were selected for strontium analysis from a number of mineral deposits around the margin of the Minas Sub-basin (Fig. 1). Sample selection was based on position in the paragenetic sequence, location in the deposit, and colour (Ravenhurst et al., 1986). A careful sample preparation procedure was followed. The calcite and host carbonate samples were broken up with a percussion mortar and sieved in plastic sieves. Approximately 2 g of sample of the +20 to -40 mesh (841-355 microns) fraction were handpicked. The samples were then washed repeatedly with super-clean ethyl alcohol in a sonic bath and crushed using an agate mortar and pestle. Relatively strontium-rich barite samples were prepared in a similar manner, but in a separate locality to avoid contamination. One portion of calcite sample RSB-32 (32a) was prepared with the barites and another portion (32b) with the calcites. A comparison of the two results gives a good indication of the cleanliness of the preparation system (Table 1). Sieves were cleaned with compressed air and super-clean ethyl alcohol between samples and the mortar and pestle were cleaned with quartz between samples.

The carbonate samples were first dissolved in 3N HCl and strontium was then isolated by conventional cation exchange techniques. Barite was first fused with $LiBO_2$ in a graphite crucible, then dissolved in dilute HCl. Isotopic analyses were performed at Geochron Laboratories, Cambridge, Massachusetts and at the Department of Earth Sciences, Carleton University, Ottawa. Analyses at Carleton University were done on a Finnigan-MAT 261 multi-collector mass spectrometer. Inclusion fluids from two Gays River galena samples were analyzed at Geochron Laboratories.

For rubidium-strontium dating, samples of 2 to 4 kg of grey Horton sandstone were selected at regular stratigraphic intervals (over 10 m) at location 12 (Fig. 1). The site is remote from any large mineral occurrence but the area is structurally complex. Steeply dipping (75°NE) Windsor strata occur just north of the sample site, and flat-lying overturned strata occur at the sample site itself. Because no glauconite could be found, clays were separated by a procedure similar to that of Halliday (1978). The samples were crushed to -18 mesh (<1 mm) and dry sieved in a sieve shaker for 20 minutes. About 100 to 600 g of the -230 mesh (<63 microns) fraction of each sample were stirred into 1 or 2 L of distilled water in beakers. After 48 hours the water was siphoned off and the samples were let dry until sticky/wet. Using weighing paper (which adhered to the surface), about 1 mm of the clays was skimmed off the top. Semi-oriented smears of the samples were run on the X-ray diffractometer for a qualitative determination of the relative amount of illite in each. At this point about half of the original samples were rejected. The remaining illite-rich samples are tabulated in Table 2. All samples contained some quartz and albite in addition to illite, muscovite, and chlorite. No detailed mineralogical study was done.

The clay samples were dissolved in hydrochloric and perchloric acids. Strontium isotopic compositions were measured on the multi-collector mass spectrometer at Carleton University. Rubidium and strontium concentrations in clays were determined by X-ray fluorescence techniques to a precision of ca. ± 5 percent.

DATA AND INTERPRETATION

Strontium isotopes

Strontium isotopes are useful for tracing the calcium and barium components of minerals such as calcite, barite, and fluorite. Because these minerals usually contain

Table 1. Results of strontium isotopic analyses. Uncertainties are ± 0.00008 (2 standard deviations) or better, unless otherwise noted.

Location	Sample number	Composition	Description	$^{87}Sr/^{86}Sr$
1. Gays River	AGR-137	Pre-ore dolomite	Recrystallized micrite host rock	0.70825
1. Gays River	AGR-139	Pre-ore dolomite	Recrystallized micrite host rock	0.70847
1. Gays River	SPA-119-2	Ore-stage calcite	Vein calcite intergrown with sphalerite	0.71200
1. Gays River	AGR-119-2	Post-ore calcite	Vug-filling calcite overgrowths on galena	0.7083
1. Gays River	AGR-201-2	Post-ore calcite	Vug-filling calcite in fracture-related cavity	0.71050
1. Gays River	NE-105-1	Post-ore calcite	Scalenohedral calcite in vugs	0.70868
1. Gays River	AGR-131	Post-ore calcite	Recrystallized secondary limestone (dedolomite)	0.70890
1. Gays River	AGR-133a	Post-ore calcite	Recrystallized limestone breccia	0.70895
1. Gays River	AGR-139 (Geochron)	Pre-ore dolomite	Recrystallized micrite	0.7082 ±.0003
1. Gays River	DW4-360	Pre-ore anhydrite	Stratigaphically higher evaporite	0.7090 ±.0002
1. Gays River	AGR-07	Ore-stage calcite	Vein calcite	0.7118 ±.0003
1. Gays River	AGR-91	Ore-stage calcite	Vein calcite	0.7114 ±.0002
1. Gays River	AGRF-1	Post-ore fluorite		0.7097 ±.0003
1. Gays River	AGRB-1	Post-ore barite		0.7088 ±.0001
1. Gays River	DW4-405	Post-ore gypsum	Vug-filling	0.7085 ±.0001
2. Southvale	RSB-47	Barite	White barite in basal Windsor carbonate	0.71018
4. Pembroke	FHd	Pre-ore dolomite	Skeletal grainstone host rock	0.70851
4. Pembroke	P13-VN	Mineralized calcite	Vein calcite with galena	0.71193
4. Pembroke	RSB-46	Mineralized calcite	Vein calcite with galena	0.70837
4. Pembroke	P9-VN	Unmineralized calcite	Vein calcite	0.70833
5. Smithfield	RSB-31	Pre-ore calcite	Carbonaceous limestone host rock	0.70775
5. Smithfield	RSB-34b	Pre-ore calcite	Limestone host from quarry 800 m west	0.70816
5. Smithfield	RSB-27	Barite	Pink crystalline barite	0.70978
5. Smithfield	RSB-28a	Barite	Reddish crystalline barite	0.70875
5. Smithfield	RSB-28b	Barite	White crystalline barite	0.70990
5. Smithfield	RSB-29a	Barite	White crystalline barite	0.71002

Table 1. Continued

Location	Sample number	Composition	Description	$^{87}Sr/^{86}Sr$
5. Smithfield	RSB-30	Mineralized calcite	Vein calcite	0.70828
5. Smithfield	RSB-32	Post-ore calcite	Vein calcite a) prep with barites b) prep with calcites	 0.70867 0.70864
6. Middle Stewiacke	RSB-51	Pre-ore calcite	Limestone host rock	0.70812
6. Middle Stewiacke	RSB-49	Barite	Red vein barite	0.70958
6. Middle Stewiacke	RSB-50	Barite	Pink to white vein barite	0.70977
6. Middle Stewiacke	RSB-54	Barite	Vein barite that cuts calcite veins	0.70912
7. Brookfield	RSB-40	Pre-ore calcite	Porous crystalline Windsor limestone	0.70808
7. Brookfield	RSB-35	Barite	Pink massive barite from quarry centre	0.71175
7. Brookfield	RSB-36	Barite	Red massive barite from quarry centre	0.71171
7. Brookfield	RSB-37	Barite	Pink massive barite from SW quarry wall	0.71145
7. Brookfield	RSB-38	Barite	White massive barite from SW quarry wall	0.71144
7. Brookfield	RSB-39	Barite	Pink massive barite from quarry centre	0.71127
8. Hilden	RSB-67	Barite	Pink vein barite	0.70877
8. Hilden	RSB-68	Barite	Pink massive barite associated with siderite	0.70904
10. Walton	RSB-69	Barite	Crystalline barite with sulphides	0.71055
10. Walton 650' level	EC-788	Unmineralized calcite	Crystalline calcite	0.70894
10. Walton 850' level	EC-785	Pre-ore limestone	Dark laminated Macumber limestone	0.70845
10. Walton 850' level	EC-761	Barite	Massive, white, fine grained	0.71058
10. Walton 850' level	EC-752	Barite	Laminated, pink-white	0.71049
10. Walton 850' level	EC-789	Barite	Crystalline, pink-white	0.71064
13. Lake Fletcher	RSB-62	Barite	White vein barite in Meguma slate	0.71230
13. Lake Fletcher	RSB-63	Barite	White vein barite in Meguma slate	0.71228

negligible quantities of rubidium, their strontium isotope ratios are a measure of the isotopic composition of the strontium in the mineralizing fluids. The strontium isotope ratios in gangue minerals from Mississippi Valley-type deposits indicate that where mineralization is sparse, the minerals precipitated from fluids that were in local isotopic equilibrium with the host carbonates. Conversely, in districts with major deposits, the ratios are anomalous and increase as mineralization progresses. In these districts, the process appears to be one of mixing of fluids containing strontium derived from silicate minerals in the sedimentary succession with locally derived strontium-bearing fluids (Kessen et al., 1981). Thus within a given basin, prospects in which calcite, barite, or fluorite have relatively high $^{87}Sr/^{86}Sr$ ratios may represent good exploration targets.

$^{87}Sr/^{86}Sr$ ratios of minerals from the deposits tabulated in Table 1 are plotted in Figure 2. The paths with arrows in Figure 2 indicate the paragenetic sequence at each mineral occurrence. Observed $^{87}Sr/^{86}Sr$ ratios of the host dolomite (0.70825 to 0.70851) and host limestone (0.70775 to 0.70845) for all deposits are in the range of expected values for Mississippian seawater (Burke et al.,

Table 2. Rubidium-strontium isotopic compositions of clay samples taken from location 12, Upper Brookfield (see Fig. 1).

Sample number	Description	Mineral components	^{87}Rb/^{86}Sr (±1.5%)	^{87}Sr/^{86}Sr (±0.004%)
RSB-98	Unweathered upper Horton sandstone with hematite	chlorite muscovite illite	1.05	0.71407
RSB-101	Horton sandstone 1.5 m "below" Windsor; weathered outcrop	muscovite illite chlorite	8.13 (omitted from isochron)	0.74636
RSB-102	Horton sandstone 3.0 m "below" Windsor; weathered outcrop	illite muscovite chlorite	failed	failed
RSB-103	Horton sandstone 4.5 m "below" Windsor; unweathered	illite muscovite chlorite	5.89	0.73506
RSB-104	Horton sandstone 6.0 m "below" Windsor; some weathering	muscovite illite chlorite	4.93	0.73048
RSB-105	Horton sandstone 8.0 m "below" Windsor; some weathering	illite muscovite chlorite	6.21	0.73631
RSB-106	Horton sandstone 10 m "below" Windsor; some weathering	illite muscovite chlorite	3.19	0.72293
RSB-100a	First calcite in breccia Horton/ Windsor contact	calcite		0.70867 ±.00005
RSB-100b	Later brown calcite	calcite		0.70918 ±.00007

1982). The single anhydrite sample has a somewhat higher ratio (0.7090). Mineralized calcite at Gays River, one mineralized calcite sample at Pembroke, and barite at Brookfield all have strontium isotope ratios (0.71127 to 0.7120) substantially higher than that of the host carbonate. This result is similar to that seen in the major Mississippi Valley districts by Kessen et al. (1981). Post-ore calcite at Gays River indicates a return to lower strontium ratios after the main mineralizing event (Fig. 2 and 3). Strontium ratios in barite at Gays River, Southvale, Smithfield, Middle Stewiacke, Hilden, and Walton are intermediate between the host rock and the highly anomalous values. Also intermediate are strontium ratios of inclusion fluids in two galena samples from Gays River (0.70940 and 0.70950; Ravenhurst, 1987) which may indicate mixing of early primary inclusion fluids with later secondary fluids when the samples were crushed in vacuum. The highest strontium ratios were found in barite within Meguma Group slates at Lake Fletcher.

The ^{87}Sr/^{86}Sr ratios (at 300 Ma) for the Meguma Group metasedimentary rocks (0.7124-0.7244) and for granodiorites from the South Mountain Batholith (0.7104-0.7127) (calculated from data in Lambert et al. (1984) and Clarke and Halliday (1980)) indicate that either could have been a source of relatively radiogenic strontium (Ravenhurst et al., 1987)(Fig. 3). However, the Horton Group rock, a direct clastic derivative of the Meguma metasedimentary rocks and granodiorites, was the likely immediate source. This conclusion is also suggested by lead isotopic data (Ravenhurst et al., 1989), although more analyses of the Horton rocks are needed. The barite vein in Meguma slates at Lake Fletcher (0.71229) was probably precipitated from a fluid that had penetrated along fractures down into the Meguma where it picked up slightly more radiogenic strontium.

Rubidium-strontium dating of clays

The rubidium-strontium method applied to glauconite or 2M-illite has been shown, in some cases, to result in well defined isochrons which are characteristically much younger than stratigraphic ages (Clauer, 1982; Posey et al., 1983; Stein and Kish, 1985). These isochrons are generally interpreted to represent significant strontium-homogenizing events in the sediments, possibly related to major fluid flow.

The clay samples separated from Horton rocks at Upper Brookside (Fig. 1) all contained illite, albite, and quartz, but some also had substantial amounts of muscovite and chlorite (Table 2). Five of these six samples define an isochron with a mean square of weighted deviates (MSWD) of 1.0 (Fig. 4). The calculated age is 300 ± 6 Ma with an initial ratio of 0.7096 ± 0.0002 (2 sigma errors quoted) (Ravenhurst et al., 1986; Ravenhurst and Zentilli, 1987). The sample with the highest Rb/Sr ratio plots significantly off the isochron. The reason for this is unclear. The isochron may represent a significant strontium homogenizing event possibly related to basinal brine flow in the Horton rocks of the Minas Subbasin. This event would have likely been associated with the Hercynian Maritime Disturbance of Poole (1967) and may also be related to mineralization.

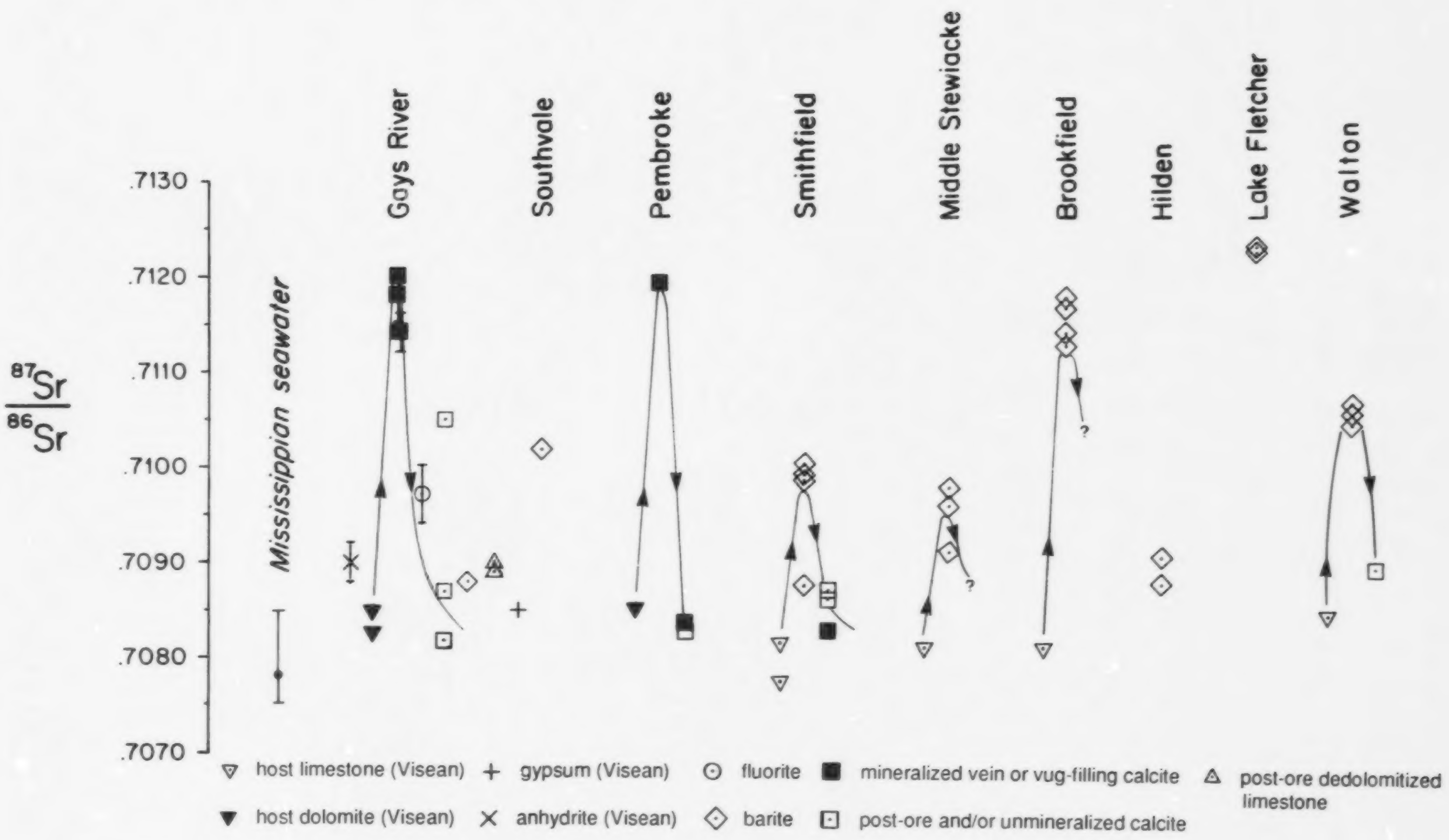

Figure 2. Strontium isotopic compositions at the mineral deposits studied. Analytical errors fall within the symbols. Mississippian seawater data from Burke et al. (1982). Arrows indicate probable paragenetic sequence at each deposit.

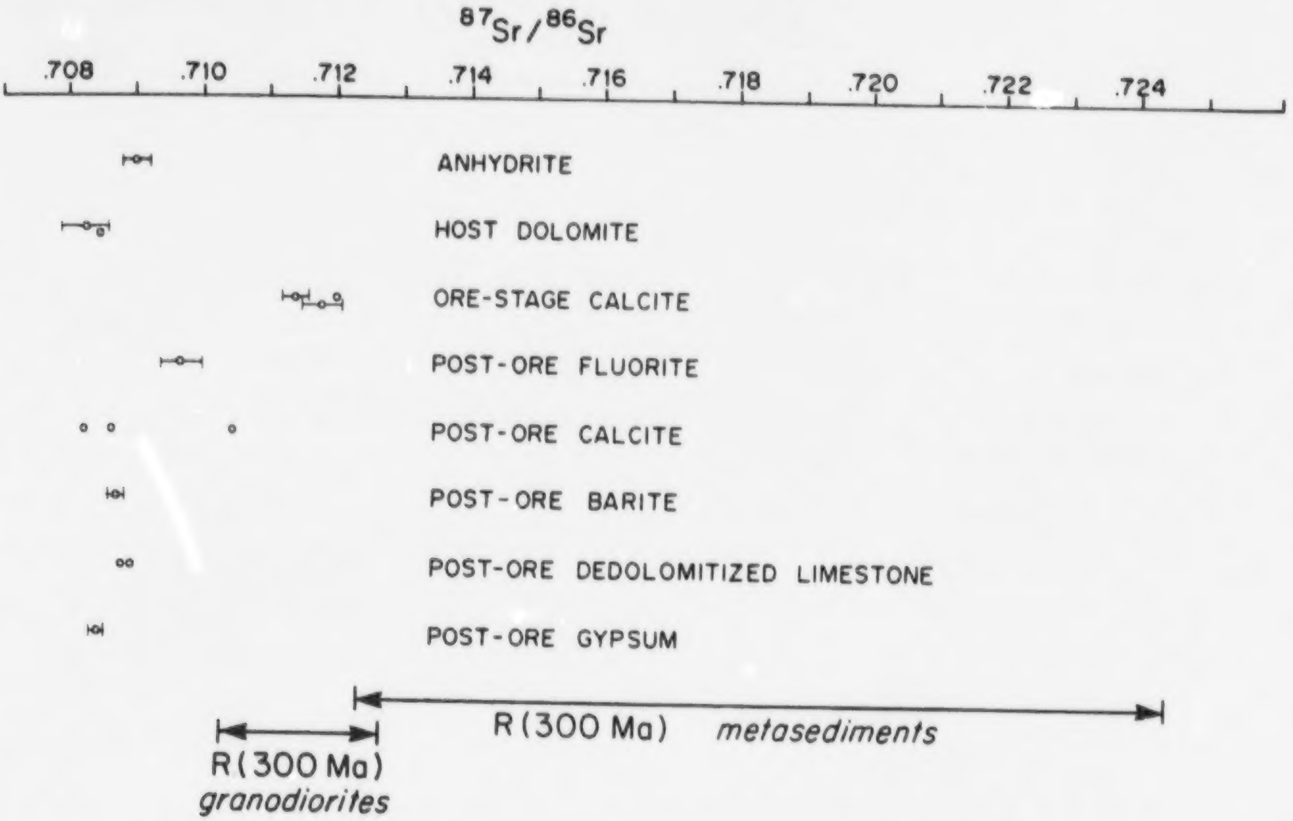

Figure 3. Strontium isotopic compositions of the mineralization at Gays River replotted. Minerals are arranged in the paragenetic sequence. Error bars represent the 2 sigma uncertainties. In some cases uncertainties are smaller than the plotted symbol. Also shown are the calculated ranges in $^{87}Sr/^{86}Sr$ ratio (R) at 300 Ma for Meguma Group metasedimentary rocks and South Mountain Batholith granodiorites.

Calcite cementing brecciated Horton strata at the nearby Horton/Windsor contact has $^{87}Sr/^{86}Sr$ ratios of 0.70918 and 0.70867 (Table 2), values which are close to the initial ratio of the isochron (0.7096). The breccia therefore may have been a conduit for the fluids in this part of the Horton, but because the initial Sr ratio is not as high as that of ore-stage calcite and barite at some of the deposits, the Horton rocks at this location could not have been the sole source or conduit for the mineralizing fluids. Other parts of the Horton strata may have been homogenized at a higher initial $^{87}Sr/^{86}Sr$ ratio.

DISCUSSION

The strontium isotope data indicate that marine carbonates cannot be the predominant source of strontium preserved in the mineral deposits. A source of more radiogenic strontium is needed to explain the data. High $^{87}Sr/^{86}Sr$ values in subsurface fluids can be generated by: 1) albitization or dissolution of potassium feldspar in either granitic basement rocks or detrital clastic component of sedimentary rocks; or 2) cation exchange with clay minerals (Banner et al., 1989). During attempts to date any thermal events in the Horton clastic rocks we found that very little feldspar other than albite exists, probably due to extensive albitization of these detrital derivatives of the Devonian granodiorites and Meguma metasedimentary rocks. This suggests that the Horton Group was the source of the radiogenic strontium, although no nearby deep sedimentary basin existed as a fluid source at the probable time of mineralization (300-330 Ma)(Ravenhurst et al., 1989). We postulate that the mineralizing fluids originated in Horton strata under the Windsor Group evaporites in the Magdalen Basin >100 km away (Ravenhurst and Zentilli, 1987; Ravenhurst et al., 1989).

CONCLUSIONS

Strontium isotope data for calcite and barite indicate that at least part of the strontium (and presumably therefore part of the calcium and barium) in the mineralizing fluids originated from a source much more radiogenic than Carboniferous carbonates or evaporites. The Horton clastic sediments of the Magdalen (Maritimes) sedimentary basin are a likely source for this radiogenic component.

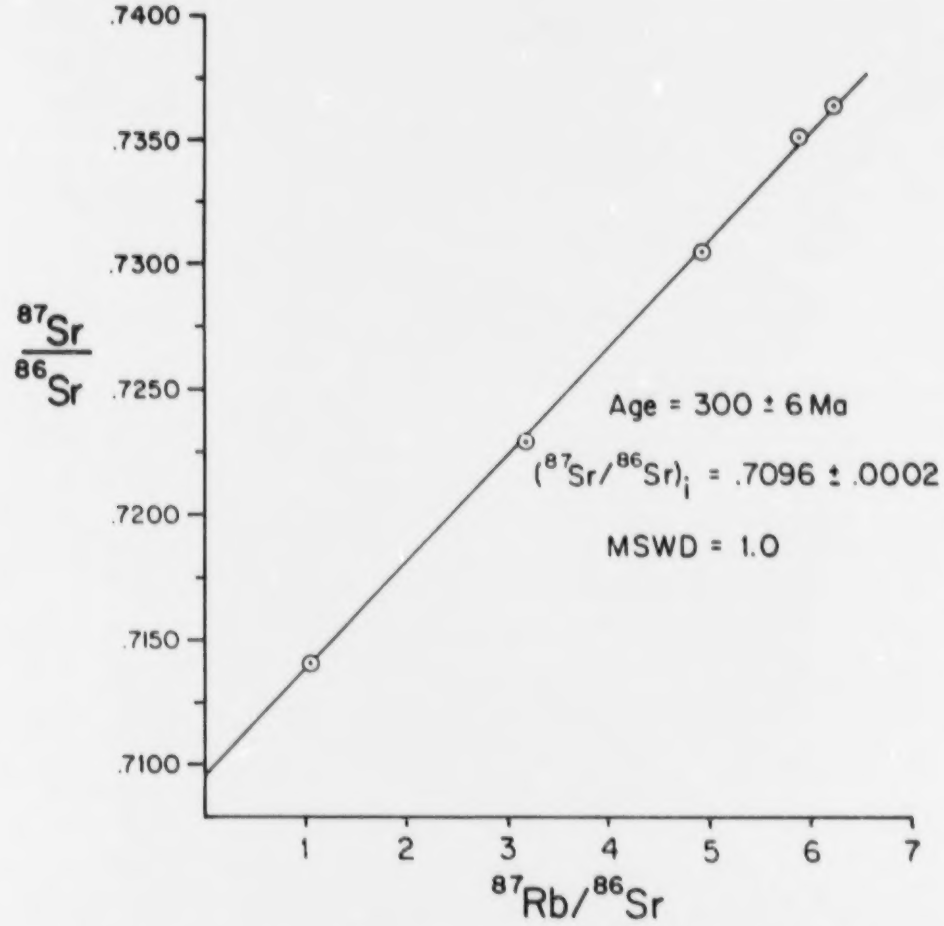

Figure 4. Rubidium-strontium isochron. Isochron formed from Rb/Sr and $^{87}Sr/^{86}Sr$ analyses of five clay separates from Horton sandstone collected over a 10 m stratigraphic interval. Sampling site was 7 km northeast of Truro, Nova Scotia (site 12, Fig. 1).

There does appear to be a genetic link among the mineral occurrences around the Minas Sub-basin and the strontium data have potential applications in mineral exploration within a sedimentary basin. The ore minerals of the larger and/or higher grade deposits have relatively high $^{87}Sr/^{86}Sr$ ratios (ca. 0.712), suggesting a large influx of mineralizing fluid considerably different in isotopic composition from Carboniferous seawater as recorded in the host carbonates ($^{87}Sr/^{86}Sr = 0.708$). Smaller, lower grade deposits have strontium isotopic compositions that are probably mixtures of mineralizing fluids with locally derived fluids.

The Rb-Sr isotopic data suggest an anomalous temperature or fluid-flow event sufficient to locally homogenize strontium in the Horton rocks at about 300 Ma, during the Hercynian Maritime Disturbance of Poole (1967). This is the first good age determination of an event which affected Horton clastic rocks in the Pennsylvanian and may have been related to the mineralization in the Minas Sub-basin.

ACKNOWLEDGMENTS

The Ph.D. thesis of Samuel Akande and the B.Sc. thesis of Mark Ponsford contributed to this study. A.M. Grist did much of the handpicking. Financial contributions to this research were made through operating grants to M.Z. and P.H.R. from the Natural Sciences and Engineering Research Council of Canada (NSERC), and graduate scholarships to C.E.R. from NSERC and Petro-Canada Limited. Most of the strontium isotope work was funded by the Geological Survey of Canada Economic Geology Division (contract #OST85-00052) under the Canada-Nova Scotia Mineral Development Agreement.

REFERENCES

Akande, S.O.
1982: Genesis of the lead and zinc mineralization at Gays River, Nova Scotia, Canada: a geologic, fluid inclusion and stable isotopic study; Ph.D. thesis, Dalhousie University, Halifax, Nova Scotia, 349 p.

Akande, S.O. and Zentilli, M.
1983: Genesis of the lead-zinc mineralization at Gays River, Nova Scotia, Canada; *in* International Conference on Mississippi Valley Type Lead-Zinc Deposits, Proceedings Volume, edited by G. Kisvarsanyi, S.K. Grant, W.P. Pratt, and J.W. Koenig, University of Missouri-Rolla, Rolla, Missouri, p. 546-557.
1984: Geologic, fluid inclusion and stable isotope studies of the Gays River lead-zinc deposit, Nova Scotia, Canada; Economic Geology, v. 79, p. 1187-1211.

Banner, J.L., Wasserburg, G.J., Dobson, P.F., Carpenter, A.B., and Moore, C.H.
1989: Isotopic and trace element constraints on the origin and evolution of saline groundwaters from central Missouri; Geochimica et Cosmochimica Acta, v. 53, p. 383-398.

Bell, W.A.
1929: Horton-Windsor district, Nova Scotia; Geological Survey of Canada, Memoir 155, 268 p.

Belt, E.S.
1964: Revision of Nova Scotia Middle Carboniferous units; American Journal of Science, v. 262, p. 653-673.

Boehner, R.C., Calder, J.H., Carter, D.C., Donohoe, H.V., Jr., Ferguson, L., Pickerill, R.K., and Ryan, R.J.
1986: Carboniferous-Jurassic sedimentation and tectonics: Minas, Cumberland and Moncton basins, Nova Scotia and New Brunswick; Atlantic Geoscience Society, Special Publication 4, 122 p.

Boyle, R.W.
1972: The geology, geochemistry, and origin of the barite, manganese, and lead-zinc-copper-silver deposits of the Walton-Cheverie area, Nova Scotia; Geological Survey of Canada, Bulletin 166, 181 p.

Boyle, R.W., Wanless, R.K., and Stevens, R.D.
1976: Sulfur isotope investigation of the barite, manganese, and lead-zinc-copper-silver deposits of the Walton-Cheverie area, Nova Scotia, Canada; Economic Geology, v. 71, p. 749-762.

Bradley, D.C.
1988: Carboniferous strike slip and foreland tectonics of the Canadian Appalachians, and implications for the evolution of coastal New England; Geological Society of America, Abstracts with Program, v. 20, p. 9.

Burke, W.H., Denison, R.E., Heatherington, E.A., Koepick, R.B., Nelson, H.F., and Otto, J.B.
1982: Variation of seawater $^{87}Sr/^{86}Sr$ throughout Phanerozoic time; Geology, v. 10, p. 516-519.

Clarke, D.B. and Halliday, A.N.
1980: Strontium isotope geology of the South Mountain batholith, Nova Scotia; Geochimica et Cosmochimica Acta, v. 44, p. 1045-1058.

Clauer, N.
1982: The rubidium-strontium method applied to sediments — certitudes and uncertainties, *in* Numerical Dating in Stratigraphy, edited by G.S. Odin, Wiley, New York, p. 245-276.

Clifton, H.E.
1967: Solution-collapse and cavity filling in the Windsor Group, Nova Scotia, Canada; Geological Society of America Bulletin, v. 78, p. 819-832.

Felderhof, G.W.
1978: Barite, celestite and fluorite in Nova Scotia; Nova Scotia Department of Mines and Energy, Bulletin 4, 463 p.

Garven, G. and Freeze, R.A.
1984a: Theoretical analysis of the role of groundwater flow in the genesis of stratabound ore deposits. 1. Mathematical and numerical model; American Journal of Science, v. 284, p. 1085-1124.
1984b: Theoretical analysis of the role of groundwater flow in the genesis of stratabound ore deposits. 2. Quantitative results; American Journal of Science, v. 284, p. 1125-1174.

Hacquebard, P.A.
1972: The Carboniferous of eastern Canada; *in* Septieme Congres International de Stratigraphie et de Geologie du Carbonifere, republished in Benchmark Papers in Geology, 1984, edited by C.A. Ross and J.R.P. Ross, v. 77, p. 45-66.

Hacquebard, P.A., Barss, M.S., and Donaldson, J.R.
1960: Distribution and stratigraphic significance of small spore genera in the Upper Carboniferous of the Maritime Provinces of Canada; 4th International Congress of Stratigraphy and Carboniferous Geology, Heerlen, 1958, Compte Rendu, v. 1, p. 237-245.

Halliday, A.N.
1978: $^{40}Ar/^{39}Ar$ stepheating studies of clay concentrates from Irish orebodies; Geochimica et Cosmochimica Acta, v. 42, p. 1851-1858.

Harland, W.B., Cox, A., Llewellyn, P.G., Pickton, C.A.G., Smith, A.G., and Walters, R.
1982: A geologic time scale; Cambridge, Cambridge University Press, 131 p.

Howie, R.D. and Barss, M.S.
1975: Upper Paleozoic rocks of the Atlantic Provinces, Gulf of St. Lawrence, and adjacent continental shelf; Geological Survey of Canada, Paper 74-30, p. 35-50.

Jackson, S.A. and Beales, F.W.
1967: An aspect of sedimentary basin evolution; the concentration of Mississippi Valley type ores during late stages of diagenesis; Canadian Society of Petroleum Geologists Bulletin, v. 15, p. 383-433.

Kessen, K.M., Woodruff, M.S., and Grant, N.K.
1981: Gangue mineral $^{87}Sr/^{86}Sr$ ratios and the origin of Mississippi Valley-type mineralization; Economic Geology, v. 76, p. 913-920.

Krebs, W. and Macqueen, R.
1984: Sequence of diagenetic and mineralization events, Pine Point lead-zinc property, N.W.T.; Canadian Society of Petroleum Geologists Bulletin, v. 32, p. 434-464.

Lambert, R.St.J., Chamberlain, V.E., and Muecke, G.K.
1984: Rb-Sr age and geochemistry of the Halifax Formation, Meguma Group, Nova Scotia; Geological Association of Canada-Mineralogical Association of Canada, Program with Abstracts, v. 9, p. 81.

Lydon, J.W.
1978: Observations on some lead-zinc deposits of Nova Scotia; Geological Survey of Canada, Paper 78-1A, p. 293-298.

MacEachern, S.B. and Hannon, P.
1974a: The Gays River discovery — a Mississippi Valley-type lead-zinc deposit in Nova Scotia; Canadian Mining and Metallurgical Bulletin, v. 67, p. 61-66.
1974b: The Gays River discovery; Canadian Mining Journal, v. 95, p. 77-79.

MacLeod, J.
1975: Diagenesis and sulfide mineralization at Gays River, Nova Scotia; B.Sc. thesis, Dalhousie University, Halifax, Nova Scotia, 132 p.

MacLeod, J.L.
1984: Diagenesis and its effects on base metal mineralization within a Mississippian carbonate complex, Gays River, Nova Scotia, Canada; 9th International Congress, Stratigraphy and Geology of the Carboniferous, 1979, Compte Rendu, v. 3, p. 193-204.

Mossman, D.J. and Brown, M.J.
1986: Stratiform barite in sabkha sediments, Walton-Cheverie, Nova Scotia; Economic Geology, v. 81, p. 2016-2021.

Ponsford, M.A.P.
1983: Geologic, fluid inclusion and stable isotope study of a carbonate-hosted lead deposit at Pembroke (Glenbervie), Colchester County, Nova Scotia; B.Sc. thesis, Dalhousie University, Halifax, Nova Scotia, 65 p.

Poole, W.H.
1967: Tectonic evolution of Appalachian region of Canada; Geological Association of Canada, Special Paper 4, p. 9-51.

Posey, H.H., Stein, H.J., Fullager, P.D., and Kish, S.A.

1983: Rb-Sr isotopic analysis of the Upper Cambrian glauconites, southern Missouri; implications for movement of Mississippi Valley-type ore fluids in the Ozark region; *in* International Conference on Mississippi Valley Type Lead-Zinc Deposits, Proceedings Volume, edited by G. Kisvarsanyi, G. Grant, S.K. Pratt, and J.W. Koenig, University of Missouri-Rolla, Rolla, Missouri, p. 166-173.

Ravenhurst, C.E.

1987: An isotopically and thermochronologically constrained model for lead-zinc and barium mineralization related to Carboniferous basin evolution in Nova Scotia, Canada; Ph.D. thesis, Dalhousie University, Halifax, Nova Scotia, 251 p.

Ravenhurst, C.E. and Zentilli, M.

1987: A model for the evolution of hot (>200°C) overpressured brines under an evaporite seal; the Fundy/Magdalen Basin of Atlantic Canada and its Pb-Zn-Ba deposits; *in* Sedimentary Basins and Basin-Forming Mechanisms, edited by A.J. Tankard and C. Beaumont, Canadian Society of Petroleum Geologists, Memoir 12, p. 335-349.

Ravenhurst, C.E., Reynolds, P.H., and Zentilli, M.

1986: Strontium isotopic studies of rock and mineral samples in the Shubenacadie Basin, Nova Scotia; *in* Current Research, Part B, Geological Survey of Canada, Paper 86-1B, p. 547-555.

Ravenhurst, C.E., Reynolds, P.H., Zentilli, M., and Akande, S.O.

1987: Isotopic constraints on the genesis of Pb-Zn mineralization at Gays River, Nova Scotia, Canada; Economic Geology, v. 82, p. 1294-1308.

Ravenhurst, C.E., Reynolds, P.H., Zentilli, M., Krueger, H.W., and Blenkinsop, J.

1989: Formation of Pb-Zn and barite mineralization from basin-derived fluids, Nova Scotia, Canada; Economic Geology, v. 84, p. 1471-1488.

Russell, M.J.

1976: Incipient plate separation and possible related mineralization in lands bordering the north Atlantic; *in* Metallogeny and Plate Tectonics, edited by D.F. Strong, Geological Association of Canada, Special Paper 14, p. 339-349.

Schenk, P.E.

1984: Carbonate-sulfate relations in the Windsor Group — central Nova Scotia, Canada; 9th International Congress of Carboniferous Stratigraphy and Geology, 1979, Compte Rendu, v. 3, p. 143-162.

Stein, H.J. and Kish, S.A.

1985: The timing of ore formation in southwestern Missouri; rubidium-strontium glauconite dating at the Magmont Mine, Viburnum Trend; Economic Geology, v. 80, p. 739-753.

Stevenson, I.M.

1951: Structure and petrology of the barite deposit at Brookfield, Colchester County, Nova Scotia; M.Sc. thesis, McGill University, Montreal, Quebec, 50 p.

Walker, S.D.

1978: Geological and mineralogical studies at the Smithfield lead-zinc prospect, Colchester County, Nova Scotia; B.Sc. thesis, Dalhousie University, Halifax, Nova Scotia, 93 p.

Weeks, L.J.

1948: Londonderry and Bass River map areas, Cochester and Hants counties, Nova Scotia; Geological Survey of Canada, Memoir 245, 86 p.

Trace elements in bituminous coals, roof clays, and underclays of the Sydney Basin, Nova Scotia: ash chemistry, element sites, and mineralogy[1]

D. Birk[2] and J.C. White[3]

Birk, D. and White, J.C., Trace elements in bituminous coals, roof clays, and underclays of the Sydney Basin, Nova Scotia: ash chemistry, element sites, and mineralogy; in Mineral Deposit Studies in Nova Scotia, Volume 1, edited by A.L. Sangster, Geological Survey of Canada, Paper 90-8, p. 257-281, 1990.

Abstract

A multielement geochemical survey was conducted on 11 bituminous coal seams in the Sydney Coalfield, Nova Scotia, to characterize the distribution of trace elements within the seams and associated strata, including partitioning between organic and mineral phases. Some 66 elements were measured in coal ash of which majors, 33 trace elements, and total rare earths are discussed in this report. Bulk geochemical analyses by neutron activation, X-ray fluorescence, and inductively coupled plasma mass spectrometry, were supplemented by scanning electron microscopy (SEM) and energy dispersive X-ray spectrometry (EDX) on polished coal grain mounts, to identify element abundances, sites, and associations.

The SEM-EDX surveys measure trace elements resident in accessory minerals, located in carbargillite or as inclusions in macerals. Trace elements were also identified as dispersed or adsorbed phases of major sedimentary minerals and coal macerals.

Element pairs yield different correlation coefficients for coal ash and underclays which suggest partitioning between clay minerals, sulphides, and macerals. Some positive linear correlations in the claystones contrast with poor correlations in the coal ashes because of alternate organic/mineral sites. Organic affinity is shown by nonlinear negative correlations with ash or sulphur content. Elements found in the macerals include B, Be, Br, Ga, Ge, I, Mo, Se, and W. Elements resident in both minerals and macerals include Cl, Cu, Sn, Sr, V, and Zn. The majority of trace elements reside in clays, sulphides, and accessory heavy minerals. Sulphides contain As, Co, Cu, Ni, Pb, Sb, Tl, and Zn.

Sydney underclays and roof rocks carry trace element levels similar to the North American Shale Composite. The adjacent coals are enriched in most metals and contain high levels of As, Pb, and Zn. Transition zones of shaly coal (>30 percent ash) carry ash with higher K, Rb, Th, and lesser sulphides than seam ash. Anomalous metal enrichments that occur past the transition zones at seam margins are attributable to organic adsorption from waters at the lignite stage or sulphate reduction from hydrothermal fluids similar to the Mississippi Valley-type Zn-Pb mineralization.

Résumé

Pour caractériser la distribution des éléments en traces dans les couches et strates associées, y compris le cloisonnement des phases organiques et minérales, on a réalisé un levé géochimique de plusieurs éléments dans onze couches de charbon bitumineux dans le champ houiller de Sydney. Quelque 66 éléments ont été mesurés dans la cendre de charbon dont les éléments majeurs, 33 éléments en traces et les terres rares totales sont traités dans le présent document, Pour déterminer

---

[1] Contribution to the Canada – Nova Scotia Mineral Development Agreement, 1984-1989. Project carried by the Mineral Resources Division, Geological Survey of Canada, Project 860008.

[2] Geofuel Research Inc., 2704 Ashridge Place, Oakville, Ontario, L6J 1K3.

[3] Department of Geology, Dalhousie University, Halifax, Nova Scotia, B3H 3J5

les quantités de ces éléments, leurs sites et les associations, on a eu recours à des analyses géochimiques par activation neutronique, fluorescence et spectrométrie de masse par plasma à couplage inductif complétées par des analyses par microscopie électronique à balayage (SEM) et par spectrométrie des rayons X à dispersion d'énergie (EDX) de plaques polies de grain de charbon.

Les levés par SEM-EDX permettent de mesurer les éléments en traces contenus dans les minéraux accessoires du schiste bitumineux ou présents sous forme d'inclusions dans les macéraux. Les éléments en traces sont aussi identifiés en phases dispersées ou adsorbées de principaux minéraux sédimentaires et macéraux de charbon.

Les paires d'éléments donnent des coefficients de corrélation différents selon qu'il s'agit de la cendre de charbon ou des murs argileux laissant supposer un cloisonnement des minéraux argileux, des sulfures et des macéraux. Certaines corrélations linéaires positives dans les argilites contrastent avec les faibles corrélations observées dans les cendres de charbon en raison d'une alternance des sites organiques et minéraux. L'affinité organique est indiquée par des corrélations négatives non linéaires avec la teneur en cendre ou en soufre. Les éléments trouvés dans les macéraux sont notamment B, Be, Br, Ga, Ge, I, Mo, Se et W. Les éléments résidant à la fois dans les minéraux et les macéraux sont, entre autres, Cl, Cu, Sn, Sr, V et Zn. La majorité des éléments en traces résident dans des argiles, des sulfures et des minéraux lourds accessoires. Les sulfures contiennent les éléments As, Co, Cu, Ni, Pb, Sb, Tl et Zn.

Les murs argileux et les roches de toit de Sydney ont des teneurs en éléments en traces semblables au schiste argileux composite de l'Amérique du Nord. Les charbons adjacents sont enrichis de la plupart des métaux et leurs teneurs en As, Pb et Zn sont élevées. Les zones de transition de charbon schisteux (30 pour cent de cendre) contiennent de la cendre dont la teneur en K, Rb et Th est plus élevée que celle de la cendre en couche mais la teneur en sulfures l'est moins. Des enrichissements anormaux de métaux au-delà des zones de transition, en bordure des couches de charbon, sont attribuables à une adsorption organique due à la présence d'eau à l'étape du lignite ou à la réduction de sulphate due à des fluides hydrothermaux semblables à ceux qui sont associés à la minéralisation en Zn-Pb de type vallée du Mississippi.

INTRODUCTION

Bituminous coal contains most of the elements of the Periodic Table in minor to trace amounts (<0.01 percent in coal or <0.1 percent in ash). The distribution of trace elements reflects the unique geochemical environment provided by coal — an oxygen-depleted organic matrix and a complex history of coalification. Krejci-Graf (1983) and Valkovic (1983) have reviewed the coal literature for trace element distributions. Nicholls (1968), Bouska (1981), and Swaine (1983) have discussed their geological significance.

Multielement studies are turning to statistical methods to define organic/inorganic affinities and to characterize coal seams. Coefficients of correlation between trace elements, major elements, and ash have been used by Chatterjee and Pooley (1977), Sandeman (1979), Harris et al. (1981), Asuen (1987, 1988), Mukherjee et al. (1988), and others. Glick and Davis (1984) summarized multivariate statistics for 335 U.S. coal seams.

Finkelman (1978, 1988) emphasized the value of scanning electron microscopy and energy-dispersive X-ray spectrometry (SEM-EDX) for the identification of trace element sites in accessory minerals. Harvey et al. (1983) used this technology to find trace Cl, Cr, Mn, Cu, and Pb in macerals. Palmer and Filby (1984) conducted a multielement analysis of low-temperature ash, separated into size and gravity fractions, to reveal mineral associations. Gluskoter et al. (1977) and Harvey et al. (1983) used an "organic affinity index" based on washability data.

Local enrichments of certain trace elements in coals have stimulated interest in their distribution and potential for economic recovery. Swaine (1961) reported up to 1000 ppm Ni resident as millerite in Australian coal. In Illinois high sulphur coals, Zn was deposited as sphalerite cleat-fill by hydrothermal fluids similar to those responsible for Mississippi Valley-type Zn-Pb mineralization (Whelan et al., 1988). Sydney coals represent a similar metallogenetic province, being high sulphur and adjacent to Mississippian evaporites and Pb-Zn deposits (Akande and Zentilli, 1984).

PREVIOUS WORK

The Sydney Basin contains 2 km thickness of Carboniferous coal-bearing terrestrial strata of the Morien Group, lying unconformably on marine Windsor sediments (Boehner and Giles, 1986; Rust et al., 1987). Sixteen major bituminous seams are present (Table 1), which were deposited under fluviolacustrine conditions in a floodplain environment (Hacquebard and Donaldson, 1969). Rust et al. (1987) postulated that peat swamps developed in large flood basins between unconfined channels of large meandering rivers. Northeast-trending paleoriver channels have been mapped in the submarine mine workings (Forgeron et al., 1986). Zodrow (1983) described the geochemistry of seam roof rocks (between channels), which consist mainly of claystones and siltstones, and postulated a common sedimentary source and diagenesis.

The earliest analyses of Sydney coals included elements such as Cl (Brown, 1871, p. 79) but comprehensive trace element geochemistry dates from the classic papers of Hawley (1955a,b). Hawley (1955b) attempted seam correlation with 25 trace elements in nine Sydney coal seams and found enrichment in Mn, As, Pb, and possibly Sr and Ba. Nicholls (1968) reworked Hawley's (1955b) trace element data to determine organic affinities versus mineral sites. Tupper and Loring (1961) reported on Rb and Sr in ash, showing an Rb/Sr ratio too low for geochronological work. Low U contents in coal (0.03 to 4.2 ppm) were reported by Zodrow and Zentilli (1979) and Zodrow et al. (1987).

Sandeman (1979) and Birk and Pilgrim (1985) used neutron activation analysis to measure a larger suite of elements in run-of-mine Sydney whole coals. Enrichments were shown for Cl, As, Se, Br, S, Mn, Mo, Sb, and Zn. Zodrow (1986, 1987) published mean ash values (calculated to whole coal) for 42 elements in channel samples from nine Sydney seams. Zodrow's work confirmed Hawley's (1955a,b) reports of top and bottom enrichments or depletions for select elements and also showed cyclical trends within seams.

Birk (1989, 1990) used SEM-EDX technology with computer image analysis to define trace element sites in minerals and macerals for 28 elements (Table 2) and quantify the weight and size distribution of major minerals. Changes in mineral facies vertically and laterally for the Harbour seam were reported.

ANALYTICAL PROCEDURES

Samples were collected in mines and open pits as seam sections in columnar benches representing 11 accessible seams (Fig. 1; Tables 1 and 3) of which 7 were from the Sydney Mines Formation (upper Morien) and 4 from the South Bar Formation (lower Morien). Columnar benches were individually analyzed to reveal the vertical diversity in geochemical facies within seams. Ten pairs of roof and floor rocks were included. Representative coal splits were pulverized (-60 mesh) and ashed at 500°C in a muffle furnace. Trace elements were analyzed as part of a comprehensive multielement geochemical survey (Tables 4a,b,c) using instrumental neutron activation analysis (INAA), X-ray fluorescence (XRF), direct current plasma spectrometry (DCP), and inductively coupled-plasma mass spectrometry (ICPMS).

The bituminous coal standard NBS-SRM2685 (from National Bureau of Standards) and two other coals were analyzed as whole coals by INAA and as ash (500°C and 750°C) during the multielement survey to test the loss of elements during muffle furnace ashing. Subsequently, the lower ashing temperature was used to reduce inorganic material loss. Roof and floor rocks were analyzed after identical ashing procedures (Tables 5a,b).

The study spanned 1985 to 1988 during which time analytical procedures evolved from INAA on both whole coal and ash, to multiple standard methods (XRF, DCP), and finally to ICPMS on coal ash. Nuclear Activation

Table 1. Sydney Coalfield: stratigraphic column.

STRATA	LITHOLOGY	COAL SEAMS	THICKNESS
MORIEN GROUP			1500 m*
Sydney Mines Formation	mudstone, shale, algal limestone, sandstone, major coal seams	Murphy	1.5 + 1.5
		Point Aconi (PA)	1.1
		Lloyd Cove (LC)	2.0
		Hub (Hu)	2.3
		Harbour (Ha)	1.8
		Bouthillier	0.9
		Indian Cove (IC)	1.2
		Phalen (Ph)	2.0
		Emery (Em)	1.1
		/Spencer? (Sp)	
		McRury?	0.38
		Gardiner (Ga)	1.2
Waddens Cove Formation	siltstone, mudstone, sandstone		
South Bar Formation	sandstone, conglomerate, thin coals	Mullins (Mu)	1.8
		Coalbrook?	0.3
		Tracy (Tr)	1.5
		Shoemaker (Sh)	0.15
		McAulay (Mc)	0.46
REGIONAL UNCONFORMITY			
CANSO GROUP	calcareous siltstone, sandstone, limestone		
WINDSOR GROUP	siltstone, sandstone, conglomerate, marine limestone, gypsum, anhydrite		

Modified after Boehner and Giles (1986). Bracketed symbols are seams in this study. ? = seam in dispute — Spencer seam is a local name for a coal seam at the same stratigraphic horizon as the Emery seam. Equivalent names in Gibling et al. (1989) and Zodrow (1987): Lloyd Cove = Bonar; Hub = Stubbart; Harbour = Sydney Main; Indian Cove = Backpit. * industry average thickness or well borehole thickness in metres.

Services Ltd. (McMaster University, Hamilton, Ontario) conducted INAA as described by Abel and Rancitelli (1975) and Hoffman and Ernst (1982). X-Ray Assay Laboratories Ltd. (Don Mills, Ontario) supplied the XRF, DCP, and ICPMS data. Reproducibility of ICPMS in rocks is reported to be better than 3 percent even at <1 ppm concentrations with limits of detection even lower than achieved by INAA (Jarvis, 1988). Results from this study for reference standards NBS-SRM2685 (ashed bituminous coal) and NBS-SRM1633a (fly ash) are given in Tables 4a,b.

Correlation matrices were developed using commercial software (CSS: Complete Statistical System, from Statsoft Inc., Tulsa, Oklahoma). Pearson product moment correlations were calculated based on covariances, using pairwise deletion of missing data and reducing "less than" values by 50 percent.

Element sites were investigated by scanning electron microscopy, using polished coal grain mounts and SEM-EDX techniques described by Birk (1989). Minerals were differentiated from macerals as brighter grains in backscattered electron images (BEI). Video signal strength was proportional to the average atomic number. Elemental composition of minerals and macerals was recorded as EDX spectra (Fig. 2 and 3).

Some coal samples were cleaned prior to SEM-EDX, by flotation in heavy organic liquids (Certigrav and Varisol), to isolate maceral mineralogy. These samples revealed bromine in the EDX spectra, attributed to contamination from the flotation media (e.g. washed Hub coal, Fig. 3).

ANALYTICAL RESULTS

Mineral and maceral sites

Birk (1989) published EDX spectra for Sydney coal minerals including trace elements. Additional spectra are presented here for heavy minerals and coal macerals to illustrate trace element sites (Fig. 2 and 3). A comprehensive list of minerals and recorded element sites for eight seams are given in Table 2.

All coal macerals or mineral inclusions larger than 1 micron diameter yield reproducible element spectra, unless the polished grain surface shows relief that influences X-ray geometry. Submicron grains or thin films of soluble minerals (halite, gypsum) usually include interference peaks from surroundings.

Macerals yield lower count rates and larger Bremsstrahlung backgrounds than minerals. Spectral profiles for macerals differ within seams as much as between

Table 2. Sydney Coalfield: coal minerals and element sites.

MINERALS:	EDX ELEMENT	SITES:	SEAMS:							
	MAJOR	TRACE	PA	LC	Hu	Ha	Ph	Em	Ga	Mu
MAJOR MINERALS:										
quartz	Si		m	m	m	m	M*	m	m	m
pyrite	Fe,S	As,Cu	M*	M*	M*	M*	M*	M*	M*	M*
illite	Si,Al,K,Fe,Ti		m	M	m	M	m	m	m	m
kaolinite	Al,Si	Fe	M	M	M	M	M	M	M	M
chlorite	Si,Fe,Al,Mg	Mn,Ti,Cu	—	—	t	M	t	t	—	—
mixed clay	Si,Al,Fe,K	Na,Ti	m	m	m	m	m	m	m	m
montmorillonite	Si,Al,K,Fe,Na		—	—	—	—	t	—	—	—
calcite	Ca	Fe,Mg,Mn	—	—	*	m	M*	—	—	—
dolomite	Ca,Mg	Fe,Mn,Cl	—	—	—	m	t	—	—	—
ankerite	Ca,Fe	Mn,Mg,Cl	—	—	t	M*	—	—	—	—
siderite	Fe	Ca,Mn	—	—	*	M*	t	—	t	—
ACCESSORY MINERALS:										
biotite	Si,Fe,K,Al	Ti,Mn,Mg	—	—	—	t	—	—	t	—
zircon	Si,Zr	Ti,Ce	t	—	—	t	—	t	t	t
rutile	Ti		t	t	t	t	t	t	t	t
ilmenite	Fe,Ti	Cu	—	—	—	—	—	—	t	—
apatite	Ca,P	Cl,Yb	—	—	—	m	t	—	—	—
monazite	Ce,P,Th,Si	La,Ca	t	—	t	t	t	t	t	t
florencite?	P,Al,Ce,Sr,Ca,Ba	Fe,K	t	—	t	—	t	—	—	t
xenotime	P,Y	Gd,Yb,Er?	—	—	—	t	t	t	—	—
gypsum	S,Ca	Cl	—	—	*	*	t*	—	—	—
halite	Cl,Na		—	t	—	—	t*	—	t	—
barite	Ba,S		t	—	—	—	t	t	t	—
chalcopyrite	S,Fe,Cu		t*	—	—	t*	—	t	t	—
arsenopyrite	Fe,S,As		—	—	—	—	—	—	m	—
sphalerite	S,Zn	Cu	t	—	—	—	t	t	—	t
galena	S,Pb		*	t*	—	t	—	—	t	t
millerite	Ni,S		—	—	—	t	—	—	—	—
cassiterite	Sn		—	—	—	t	—	—	—	—
tennantite?	S,Fe,Cu,Zn		—	—	—	—	—	t	—	—
almandite?	Fe,Si,Al	Cu	—	—	t	t	—	—	—	—
gibbsite?	Al		—	t	—	t	—	—	—	—
SECONDARY MINERALS:										
Sulphur	S		—	—	—	—	—	t	—	t
goethite	Fe		*	*	—	t	—	*	t*	—
copiapite?	S,Fe	Al,Mg,K	*	t	—	t	—	t	—	—
COAL MACERALS:	S,Fe,Si,Al		M	M	M	M	M	M	M	M
		Ti	—	t	—	t	—	t	t	t
		K	—	—	—	t	—	—	t	t
		Ca	m	t	t	m	m	m	m	m
		Cl	m	m	m	m	M	m	m	m
		Br	—	t	t	—	—	—	—	—
		Cu	—	t	t	t	t	—	—	t

Identification by EDX element: M=major, m=minor, t=trace. Elements below atomic no. 11 (C,H,N,O,F,B,Be,Li) not monitored. Artifacts from SEM contribute Cu,Fe,Al,Si. Not detected: — *=reported visually (megascopic). ?=identity undertain. Seams: Point Aconi; Lloyd Cove; Hub; Harbour; Phalen; Emery; Gardiner; Mullins (in descending stratigraphic order).

seams but correlation to microlithotypes is difficult with SEM imaging. Fusinite yields a spectrum similar to a pure carbon SEM stub except for a strong sulphur peak (Fig. 3).

The only "trace" elements detected in Sydney macerals were Cl, Br (as laboratory heavy liquid contaminant), and Cu (possible instrument artifact). This contrasts with reports of Cr and Pb in the inertinite spectra of Harvey et al. (1983). Other trace elements present must therefore be highly dispersed, and thus hidden in the Bremsstrahlung background, unless they reach minor element concentrations.

Detection of trace elements by EDX is hampered by severe peak interference and overlap. For example, Ce L lines (at 4.84, 5.26, and 5.61 keV) overlap with Ba L series (at 4.47, 4.82, and 5.25) and hide weak L lines for

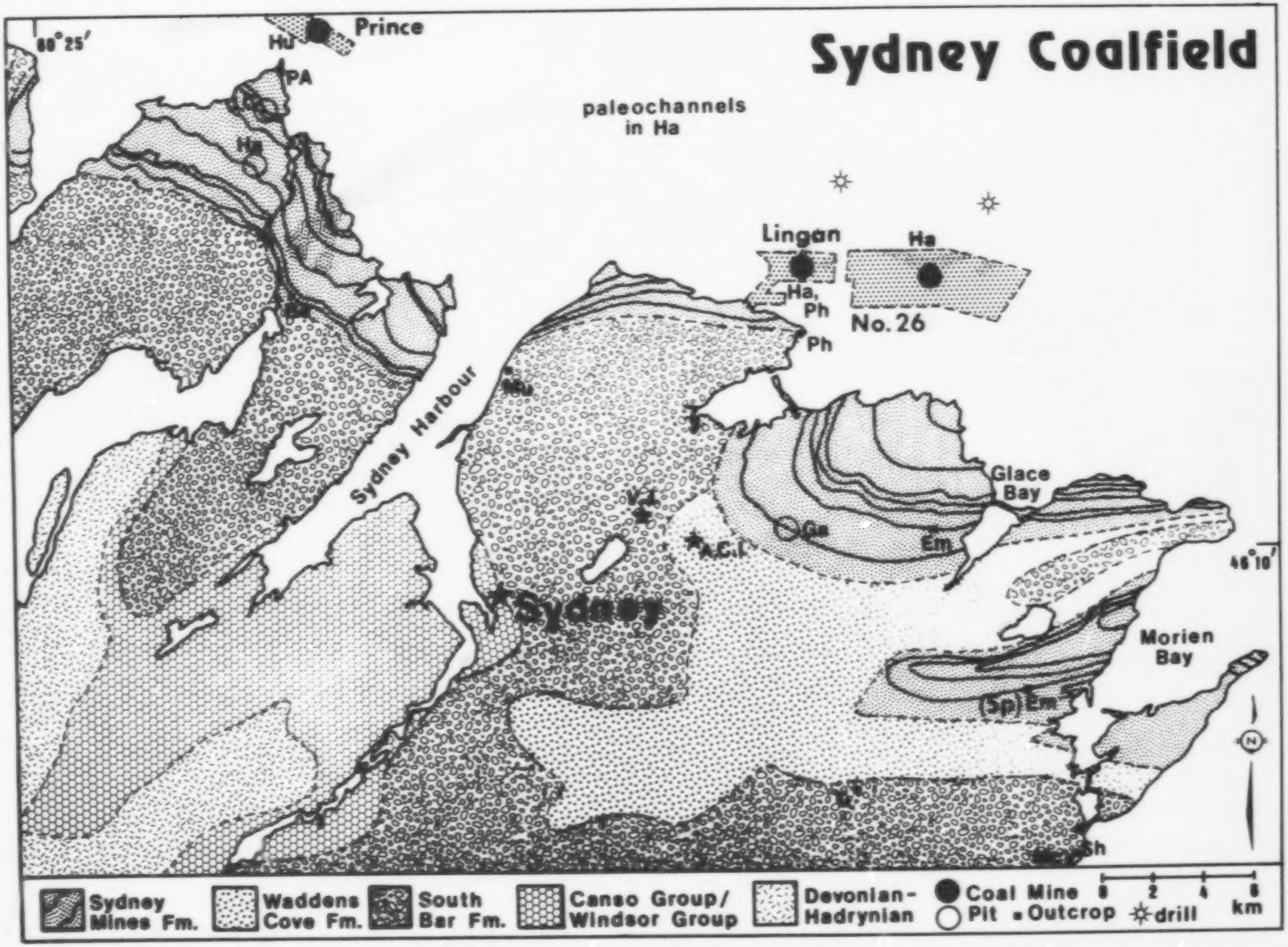
Sydney Coalfield
60°25′
Prince
Hu
PA
Ha
paleochannels in Ha
Lingan
Ha, Ph
Ha
No. 26
Ph
Mu
Sydney Harbour
VJ
A.C.I.
Ga
Em
Glace Bay
46°10′
Morien Bay
(Sp) Em
Sh
Sydney
Sydney Mines Fm.
Waddens Cove Fm.
South Bar Fm.
Canso Group/ Windsor Group
Devonian-Hadrynian
● Coal Mine
○ Pit
▪ Outcrop
☼ drill
0 2 4 8 km
N

Figure 1. Sydney Coalfield (modified after Boehner and Giles, 1986, Forgeron et al., 1986). ACI = Atlantic Coal Institute. VJ = Victoria Junction coal wash plant. Seam sampling sites: Ba = Backpit; Em = Emery; Ga = Gardiner; Ha = Harbour; Hu = Hub; Mc = McAuley; Mu = Mullins; PA = Point Aconi; Ph = Phalen; Sh = Shoemaker. Donkin tunnel (not shown) runs northeast under Morien Bay

Table 3. Sydney Coalfield seam bench samples (38) analyzed for trace elements.

Seam Name	Mine Site	Sample Number	Seam Part	Bench Site	Field Notes	Coal % ash	Coal % S	Coal ppm Cl	Ash % Al	Ash % Fe	Ash % K	Ash % Ca	Ash ppm P	Ash* TREE	LREE/ HREE
Point Aconi	PA	PA332	.00 .07	top	TR: Ox	34.6	4.1	---	11.49	8.1	1.5	0.20	611	402	10.3
	PA	PA333	.07 - .15	top	C:Sul	7.5	5.3	---	9.32	34.1	0.5	0.60	480	170	4.8
	PA	PA334	.50 - .65	mid	C:br,sbr	3.4	3.4	---	8.73	31.2	1.7	1.00	349	89	7.7
	PA	PA335	.85 - 1.00	base	C:dull,Py	20.0	15.9	---	1.74	61.7	0.3	0.20	218	72	2.4
u.Lloyd Cove	B	LC2H	.33 - .48	mid	C:br,Py	3.4	2.9	640	2.62	53.1	0.1	1.30	530	107	4.4
l.Lloyd Cove	B	LC3J	.46 - .61	mid	C:sbr,dr,Py	14.6	9.8	540	4.87	51.8	0.1	<.4	160	88	2.9
Hub	Pr	HP8G	.90 - 1.05	mid	C:br,Py,Gy	2.1	1.0	4050	14.20	12.6	0.8	2.60	290	437	7.2
Harbour	N	HN1H	.32 - .47	mid	C:br,cl,Py	13.9	8.0	1340	7.82	47.0	0.1	0.60	2500	429	6.5
	N	HN1N	.92 - 1.07	mid	C:br+dull	7.0	4.7	1330	4.51	48.3	0.3	0.80	450	320	6.9
	L	HL6H	1.05 - 1.2	mid	C:br	3.2	0.8	2420	11.50	19.8	0.7	1.90	780	376	7.3
Indian Cove	SM17	IC10G	.90 - 1.15	mid	C:	13.3	6.7	2020	3.98	41.8	0.9	1.90	200	158	3.0
	SM18	IC11C	.00 - .17	top	TR:	40.3	2.4	---	10.85	15.2	2.1	1.40	1353	288	16.3
	SM18	IC11I	1.38 - 1.46	base	C:	16.9	7.6	---	2.69	40.3	0.4	8.90	230	82	3.5
Phalen	P	PP7A	.00 - .15	top	C:br, Py	4.9	2.6	---	5.65	35.3	0.7	4.00	290	285	1.7
	P	PP7C	.30 - .45	mid	C:br,Py	6.8	1.8	---	10.00	16.6	1.3	3.90	240	265	6.8
	P	PP7F	.75 - .90	mid	C:br,fs,Ca	4.8	1.3	4620	5.10	16.7	0.3	12.00	410	194	4.8
	P	PP7H	1.05 - 1.2	mid	C:br,Ca	6.4	4.5	---	2.83	48.1	0.2	3.00	160	87	5.1
	P	PP7J	1.35 - 1.5	mid	C:br,Ca	3.9	2.1	---	6.41	26.4	0.6	4.20	940	159	6.3
	P	PP7L	1.65 - 1.83	base	C:br,Py,Ca	10.1	6.0	---	3.50	40.7	0.5	4.00	6100	218	3.1
Emery	SH	E4K	0.93 - 1.08	mid	C:bone, Fe	9.6	0.8	2010	14.70	3.5	0.2	0.20	780	417	8.1
Spencer	PM45	S12D	.00 - .30	top	C:	7.7	2.3	---	11.06	24.8	1.5	1.70	262	327	5.8
	PM45	S12H	1.2 - 1.3	base	TR:	30.6	5.9	---	13.61	15.5	2.6	0.30	306	293	6.3
	PM48	S13E	.30 - .60	mid	C:	6.5	2.7	---	11.00	24.7	1.7	0.90	240	282	6.7
Gardiner	N	G321	.00 - .15	top	C:br,Fe,Cy	5.0	1.0	---	13.02	11.3	2.0	1.70	698	405	7.2
	N	G326	.65 - .80	mid	C:Cy	7.5	3.4	---	8.73	30.9	1.7	1.30	349	291	9.7
	N	G3210	1.09 - 1.23	base	TR:dull,Cy	38.1	5.4	---	14.03	12.5	3.4	0.20	306	312	12.5
Mullins	NW13	M14D	.00 - .20	top	C:	18.8	9.0	---	6.93	37.5	1.9	0.30	160	154	6.6
	NW13	M14E	.20 - .45	mid	C:	10.4	4.9	---	8.67	32.3	2.1	0.80	410	287	7.1
	NW13	M14F	.45 - .70	mid	C:	20.2	11.0	---	5.44	44.7	0.9	0.30	160	161	5.4
	NW13	M14G	.70 - .95	mid	C:	8.9	5.7	2020	5.25	46.8	0.5	0.90	160	247	7.8
	NW13	M14H	.95 - 1.20	mid	C:	6.8	5.2	---	3.19	54.4	0.3	1.20	160	117	7.2
	NW13	M14I	1.20 - 1.45	mid	C:	5.8	3.8	---	5.79	44.2	0.9	1.00	200	170	6.9
	NW13	M14J	1.45 - 1.75	base	C:	8.5	6.4	---	3.89	50.1	0.5	0.90	160	156	4.7
	NW16	M15E	.00 - .25	top	C:	23.6	11.8	---	4.32	45.3	1.1	0.30	40	112	5.8
	NW16	M15H	.75 - 1.0	mid	C:	9.6	5.8	---	5.61	45.7	0.6	0.90	300	147	8.2
	NW16	M15L	1.75 - 1.95	base	C:	18.4	9.9	---	4.55	45.1	1.2	0.40	20	143	6.1
Tracy	PM65	T16G	.81 - 1.07	mid	C:	11.7	4.7	2370	6.30	17.8	0.7	14.00	3000	170	6.9
McAulay	RI	MC9G	.25 - .33	base	C:cleats,Ca	11.7	7.8	1160	2.21	46.0	0.1	5.40	240	216	2.7
					Average:	12.53	5.22	2043	7.27	33.7	0.97	2.25	638	227	6.38

LOCATION: B= Brogan pit; L=Lingan Mine; P= Phalen Mine; PA= Point Aconi cliff; Pr= Prince Mine; N= Novaco pit; RI= Round Island; SH= Steel's Hill; others refer to drill core sites.
FIELD NOTES: C= coal; TR= shaly transition zone; Cy= clay; br= bright; sbr= semibright; cl= clarain; dr= durain; fs= fusain; Ca= calcite, Fe= iron oxide, Gy= gypsum, Ox= oxidi
ANALYSES: ASTM ash, %S by Leco, Elements by INAA, XRF, and ICPMS. * Y not included in rare earths (REE). Light/heavy REE ratio (LREE/HREE) abreviated elsewhere to LH. Seam Part= metres from roof.

Table 4a. Trace elements in coal ash from the Sydney Coalfield, Nova Scotia.

		As	B	Ba	Be	Br	Co	Cr	Cs	Cu	Ga	Ge	Hf	Mo	Nb
SEAM	TEST:	INAA	DCP	DCP	DCP	INAA	INAA	INAA	INAA	DCP	RNAA	XRF	INAA	INAA	DCP
	DETECT*:	1	10	10	1	0.5	0.1	0.5	0.2	0.5	2	10	0.2	2	10
	SAMPLE #	ppm	ppm	ppm	ppm	ppm	ppm	ppm	ppm	ppm	ppm	ppm	ppm	ppm	ppm
NBS coal	2685	70	560	660	10	2	23	120	7.6	63	30	..	4.5	8	30
NBS fly ash	1633a	150	40	1300	14	3	44	190	11.1	100	62	..	6.9	22	40
UPPER MORIEN COALS:															
Point Aconi	PA332	120	70	604	12	0.5	7.1	150	6.4	62	20	<10	10.0	15	42
	PA333	420	150	315	35	1.1	32	53	1.6	130	37	280	2.0	24	27
	PA334	2700	390	453	44	1.1	22	62	2	360	14	200	<.2	48	30
	PA335	3000	10	282	25	<.5	31	58	1	320	13	260	<.2	58	35
u.Lloyd Cove	LC2H	4900	330	330	38	3.3	50	49	1.1	290	23	19	1.2	120	30
l.Lloyd Cove	LC3J	1200	80	240	20	0.8	78	74	0.7	52	17	<10	0.9	75	50
Hub	PH8G	230	420	350	14	11	42	150	7.8	150	38	22	4.7	45	30
Harbour	HN1H	870	110	370	27	2.6	140	91	<0.5	100	25	160	0.2	29	50
	HN1H	700	170	250	19	2.4	26	70	1.4	260	16	20	3.2	44	30
	HL6H	90	210	900	12	17	23	140	5.7	220	45	31	4.4	56	30
Indian Cove	IC10G	340	110	310	14	4.9	19	64	4.2	120	44	..	1.2	110	40
	IC11C	180	80	863	9	..	10	100	11	61	31	50	2.0	60	12
	IC11I	1300	30	131	13	..	35	34	3	210	17	90	<1	131	4
Phalen	PP7A	180	160	540	46	14	27	110	2.3	99	130	..	2.2	57	50
	PP7C	62	140	410	8	13	15	100	9.7	90	34	10	4.6	23	50
	PP7F	37	250	240	3	23	18	52	1.3	92	12	<10	1.7	56	20
	PP7H	1900	100	310	7	7.0	11	43	1.4	66	12	<10	1.1	120	30
	PP7J	660	150	560	15	7.6	16	86	4.1	150	25	<10	3.1	210	40
	PP7L	2100	70	370	22	8.1	30	75	2.1	160	34	230	1.3	180	30
LOWER MORIEN COALS:															
Emery	E4K	35	100	540	5	3.9	19	150	22.7	87	37	10	7.8	37	40
Spencer	S12D	1500	140	..	36	..	90	96	13	120	40	120	3.0	127	13
	S12H	1100	80	..	14	..	87	98	15	130	40	50	3.0	82	18
	S13E	500	170	570	15	6.3	76	150	13.3	150	22	10	3.8	57	30
Gardiner	G321	1000	100	540	95	12	37	140	11.4	120	65	430	7.3	60	33
	G326	1400	60	462	16	6.9	81	100	7.6	180	18	<10	3.7	61	26
	G3210	610	60	628	11	2	54	140	11.9	120	34	<10	5.6	12	19
Mullins	M14D	920	50	400	11	3.4	86	86	8.2	180	17	<10	2.3	82	40
	M14E	490	70	360	14	3.8	32	100	12.2	130	31	..	3.1	97	40
	M14F	950	40	300	13	3.6	92	74	5.9	150	15	<10	2.0	130	50
	M14G	560	70	320	19	4.3	21	72	6.8	110	17	..	2.1	120	40
	M14H	790	80	340	16	3.8	43	47	2.9	120	15	..	1.5	130	20
	M14I	460	90	420	12	5.9	56	83	7.5	130	12	..	3.0	90	40
	M14J	1100	60	370	23	5.9	71	74	4.9	160	17	30	2.2	120	40
	M15E	1900	<10	390	18	..	142	48	7	280	12	<10	2.0	62	5
	M15H	770	30	..	15	..	34	..	6	180	12	<10	1.0	127	9
	M15L	1900	<10	376	22	..	71	42	7	200	12	20	2.0	66	5
Tracy	T16G	170	110	230	8	6.1	10	57	6.6	61	<14	..	3.0	41	40
McAulay	MC9G	1100	100	170	3	6.3	46	33	0.9	150	49	60	0.3	100	50
	Average:	1006	117	407	20	6.2	47	85	6.3	151	28	70	2.7	81	31

* detection or better. For statistics, < values set to half.

Nd (5.23) and Sm (5.64). The Y L line (1.92) lies between K lines for Si (1.74), P (2.01), and Zr (2.04), therefore weak signals are "lost" in these major peak tails. The detection of trace elements by EDX requires high local concentrations (>0.5 percent) and the absence of interference peaks from host coal or instrument.

Major element inorganic chemistry

The channel bench samples show a wide range in ash and sulphur (S) composition within each seam (Table 3) which reflects lithotype banding and changes in mineral suites. High ash and S values are recorded for coal benches at the top and base of seams and adjacent to stone partings, but transition zones of shaly coal, where ash content exceeds 30 percent, do not have proportionately high S (Fig. 4). This shows that optimum conditions for bacterial sulphate reduction occurred at the coal interface, not in the shaly transition. The ash from transition zones is also marked by higher K content, likely from detrital feldspars or illite.

The cleaner coals (ash <4 percent) carry low S values (as low as 0.8 percent) and generally yield a high aluminum and silica ash derived from clay minerals. The lowest Al content (1.7 percent) correlates to extremely high S (15.9 percent) and high Fe (62 percent), reflecting pyritic mineral matter. To assist in identifying trace element sites and associations in Sydney coal and associated strata, Tables 3 and 5a include elements usually identified with clay phases (Al,K), sulphides (Fe,S), and marine influence (Ca,Cl) respectively.

Roof and floor rocks show uniform chemistry with low Fe and Ca, and high Al content (Table 5a, 5b) except for the high carbonate roof of Indian Cove (Ca = 21 percent). This data set cannot differentiate between the roof and floor rocks, except by colour (underclays are lighter grey).

Table 4b. Trace elements in coal ash from the Sydney Coalfield, Nova Scotia.

SEAM	TEST: DETECT*: SAMPLE #	Ni DCP 1 ppm	Pb DCP 2 ppm	Rb INAA 5 ppm	Sb INAA 0.1 ppm	Sc INAA 0.01 ppm	Se INAA 0.5 ppm	Sr DCP 1 ppm	Th INAA 0.2 ppm	U INAA 0.1 ppm	V DCP 2 ppm	W INAA 1 ppm	Y DCP 10 ppm	Zn DCP 0.5 ppm	Zr DCP 10 ppm
NBS coal	2685	55	46	110	2.1	21.6	1.3	510	14	5.7	180	6	20	120	200
NBS fly ash	1633a	100	94	160	7.2	43.6	8.1	850	24	10.7	290	12	90	220	280
UPPER MORIEN COALS:															
Point Aconi	PA332	40	190	83	5.1	27.5	<.5	444	26	7.7	150	6	68	260	305
	PA333	100	280	<10	41	14.4	<.5	141	6.4	2.3	66	11	<10	3400	55
	PA334	64	2200	<10	42	12.1	<.5	351	6.4	2.3	56	37	<10	7000	85
	PA335	110	640	<10	58	11.3	<.5	<.5	4.2	3.2	170	<1	<10	1500	<10
u.Lloyd Cove	LC2H	160	360	<10	63	6.0	2.7	150	4.0	1.8	42	88	10	310	<10
l.Lloyd Cove	LC3J	170	500	<10	16	10.2	8.6	40	4.4	2.6	280	4	<10	170	<10
Hub	PH8G	100	270	30	4.1	23.5	3.6	580	19	5.3	170	12	50	520	200
Harbour	HN1H	90	1200	<10	9.2	7.1	<0.5	1200	2.2	1.0	100	9	10	2600	<10
	HN1H	93	560	<10	8.7	12.2	<1.0	140	10	3.2	83	16	<10	220	90
	HL6H	55	50	51	4.6	21.4	3.7	570	14	3.9	130	4	50	96	180
Indian Cove	IC10G	58	62	71	7.6	15.1	<0.7	150	7.0	3.4	120	<3	10	220	20
	IC11C	33	290	108	5.8	20.0	<.5	833	14.8	3.3	200	4	21	66	140
	IC11I	110	230	26	18	22.0	<.5	133	3.8	2.9	52	3	35	200	18
Phalen	PP7A	160	190	<10	25	59.5	2.2	480	8.6	4.7	140	16	100	320	40
	PP7C	62	62	120	2.3	19.6	<0.5	590	14	3.8	130	4	40	120	180
	PP7F	35	38	<10	1.1	7.5	4.8	1000	5.1	1.7	57	2	30	180	30
	PP7H	30	88	<10	2.6	5.2	<0.7	280	3.4	1.3	74	<2	<10	160	<10
	PP7J	36	700	<10	3.0	12.2	<0.5	780	10	3.4	87	7	30	400	100
	PP7L	70	600	30	71	18.6	4.5	320	5.0	18.1	220	<3	10	240	40
LOWER MORIEN COALS:															
Emery	E4K	48	100	190	4.1	31.9	<0.5	940	24	6.9	240	<1	60	110	330
Spencer	S12D	170	90	128	34	51.0	<0.5	..	17.3	4.2	250	7	87	140	..
	S12H	200	160	184	20	59.0	<0.5	..	20	8.3	510	2	62	130	..
	S13E	260	130	90	10	22.1	<0.7	270	17	3.8	190	<6	20	330	170
Gardiner	G321	100	190	129	56	26.5	<0.5	985	18	5.4	180	6	93	330	194
	G326	140	160	160	9	17.0	<0.5	349	11	2.5	150	2	<10	160	102
	G3210	180	180	223	34	30.4	<0.5	204	18	5.3	210	<1	18	1100	126
Mullins	M14D	190	260	130	21	13.6	<0.7	130	8.7	3.4	170	<3	<10	100	80
	M14E	100	420	140	9.1	18.0	<0.5	330	11	4.2	140	5	10	150	120
	M14F	210	..	50	11	11.2	<1.0	110	8.0	2.4	140	<4	<10	82	70
	M14G	100	520	42	6.2	10.3	1.4	300	7.2	2.9	81	<3	<10	140	30
	M14H	140	680	<10	6.4	5.2	0.8	390	3.9	1.3	48	<4	<10	160	<10
	M14I	190	480	90	5.1	10.8	1.1	470	8.1	2.3	82	<5	<10	220	90
	M14J	160	6	<10	24	10.0	<1.0	300	6.1	2.4	140	7	<10	170	80
	M15E	360	560	60	58	30.0	<0.5	74	6.8	2.3	120	2	26	96	87
	M15H	120	840	36	4.2	29.0	<0.5	..	7.4	2.4	90	2	24	150	..
	M15L	360	840	48	98	263	<0.5	104	9.9	3.4	160	5	34	69	57
Tracy	T16G	26	6	70	2.6	10.5	3.0	360	8.4	2.2	69	<4	20	80	100
McAulay	MC9G	52	460	<10	35	3.2	<0.5	210	1.4	1.0	30	19	30	120	<10
	Average:	123	394	62	21.9	25.7	1.2	392	10.0	3.7	140	7	27	574	90

* see table 4a.

Table 4c. Trace elements coal ash (limited sampling) from the Sydney coalfield, Nova Scotia.

test: detect: SAMPLE #	Bi ICPMS 0.1 ppm	Li AA 1 ppm	Sn XRF 2 ppm	Tl ICPMS 0.1 ppm
COAL ASH:				
PA332	1.4	170	17	1.6
PA333	0.4	130	56	4.0
PA334	0.3	29	94	15.6
PA335	0.2	10	35	14.3
IC11C	1.0	68	10	4.8
IC11I	0.3	24	109	11.8
S12D	1.3	48	72	15.6
S12H	0.7	100	13	8.3
COAL ASH continued:				
G321	0.7	74	48	4.7
G326	0.5	43	74	16.1
G3210	0.6	88	14	4.1
M15E	0.5	48	22	10.8
M15H	0.7	60	51	8.1
M15L	0.7	20	17	17.2
Averages:	0.7	65	45	9.8

Table 5a. Ash, major elements, and trace elements in roof clays and underclays from the Sydney Coalfield, Nova Scotia.

SEAM *	#	test: Colour	Ash ASTM %	Al XRF %	K XRF %	Fe XRF %	Ca XRF %	P XRF %	S LECO %	TREE INAA ppm	ratio LREE/ HREE	As INAA ppm	B DCP ppm	Ba XRF ppm	Be DCP ppm	Bi DCP ppm	Br INAA ppm	Co INAA ppm	Cr XRF ppm
ROOF CLAYS:		**								***	***								
u.Lloyd Cove(B)	LC2A	gy bn	90.5	12.6	2.4	1.6	0.45	0.29	1.13	97	5.3	97	80	1300	7	1.5	3.4	11	103
Hub (Pr)	HP8P	dk gy	90.0	15.5	3.4	2.6	0.14	0.05	0.20	304	8.3	11	70	890	6	0.6	3.1	18	96
Harbour (L)	HL60	dk gy	93.6	11.4	2.9	3.6	0.11	0.04	0.68	206	7.4	2.7	80	630	4	0.3	2.5	17	82
Indian (SM17)	IC10B	gy	73.2	4.7	1.2	5.0	20.7	0.23		97	5.3	97	10	450	3	0.2	3.4	11	34
Phalen (P)	PP7N	dy gy	88.3	14.8	3.3	2.3	0.11	0.03	0.73	280	11.8	8.0	70	790	4	0.5	6.0	14	89
Emery (SH)	E4R	gy Fe	84.3	13.8	3.4	2.7	0.04	0.03	0.72	280	8.8	21	70	650	5	0.7	7.0	27	96
Spencer (PM48)	S13C	gy	91.8	12.2	3.1	3.5	0.09	0.03		271	10.6	34	90	720	5	0.4	1.0	17	82
Mullins (NW13)	M14C	gy	94.2	12.7	4.3	3.5	0.05	0.02		166	8.7	12	70	820	4	0.3	2.8	10	89
Tracy (PM65)	T16C	gy	80.8	11.7	3.7	2.3	0.21	0.14		456	11.6	34	110	1100	4	0.5	5.8	10	89
McAulay (RI)	MC9D	dk gy	89.6	13.6	4.6	4.8	0.21	0.03	2.07	241	16.7	54	80	640	5	0.5	1.9	24	89
	Average:		87.6	12.3	3.2	3.2	2.2	0.09	0.9	240	9.4	37	73	799	5	0.6	3.7	16	85
UNDERCLAYS:																			
l.Lloyd Cove(B)	LC3O	gy	89.7	7.4	2.2	3.9	0.42	0.12	2.62	223	5.9	190	70	430	4	0.3	2.2	26	62
Hub (Pr)	HP80	lt gy	94.4	8.8	1.9	1.9	0.04	0.02	0.39	196	8.3	6.7	70	550	2	0.3	2.5	11	55
Harbour (L)	HL6N	lt gy	89.8	13.8	3.8	2.8	0.08	0.03	1.36	259	12.1	14	80	830	5	0.5	4.1	26	96
Indian (SM17)	IC10K	gy	81.8	10.8	2.9	6.0	0.34	0.14		323	15.6	230	70	980	4	0.5	2.2	16	82
Phalen (P)	PP7M	lt gy	91.1	12.2	3.5	3.7	0.22	0.07	0.79	255	9.8	27	80	610	6	0.4	6.0	33	89
Emery (SH)	E4A	bk gy	81.2	12.9	4.1	4.8	0.02	0.03	3.04	233	14.6	37	70	740	5	0.6	6.1	27	96
Spencer (PM48)	S13H	gy	85.4	14.6	3.5	2.5	0.19	0.04		331	15.1	44	100	880	5	0.5	1.5	35	89
Mullins (NW13)	M14K	gy	94.7	9.2	2.7	2.3	0.05	0.03		239	8.5	4.8	70	560	3	0.3	1.3	10	68
Tracy (PM65)	T161	gy	91.2	12.7	3.5	3.1	0.13	0.03		254	11.6	6.8	70	730	4	0.5	1.6	21	75
McAulay (RI)	MC9H	gy	93.8	10.9	3.0	4.0	0.25	0.03	0.22	251	9.0	8.2	80	560	4	0.4	1.3	24	75
	Average:		89.3	11.3	3.1	3.5	0.17	0.05	1.4	256	11.0	57	76	687	4	0.4	2.9	23	79

* Channel sections and mine sites correspond to Tables 2, 3 and Figure 1.

** Colours in field: grey (gy), black (bk), brown (bn), light (lt), dark (dk), Fe (iron oxide).

*** Y not included in REE.

Table 5b. Ash, major elements, and trace elements in roof clays and underclays from the Sydney Coalfield, Nova Scotia.

SEAM	test: #	Cs INAA ppm	Cu DCP ppm	Hf INAA ppm	Li XRF ppm	Mo INAA ppm	Nb XRF ppm	Ni DCP ppm	Pb DCP ppm	Rb INAA ppm	Sb INAA ppm	Sc INAA ppm	Se INAA ppm	Sr XRF ppm	Th INAA ppm	U INAA ppm	V RNAA ppm	Y XRF ppm	Zn DCP ppm	Zr XRF ppm
ROOF CLAYS:																				
u.Lloyd Cove(B)	LC2A	4.5	230	1.3	110	15	30	42	46	150	1.4	10.1	3.4	6500	5.5	1.30	180	70	85	190
Hub (Pr)	HP8P	14.4	36	4.5	260	2.5	20	<1	36	240	1.2	26.9	3.5	<10	21	4.43	160	30	160	150
Harbour (L)	HL60	6.2	43	4.7	78	1.3	40	<40	20	160	0.5	20.9	5.3	180	12	3.17	130	30	170	170
Indian (SM17)	IC10B	4.5	41	1.3	22	15	20	42	46	78	1.4	10.1	3.5	800	5.5	1.30	58	<10	52	10
Phalen (P)	PP7N	14.3	47	4.2	210	2.2	10	90	26	240	1.3	25.3	1.8	280	18	4.44	170	30	130	130
Emery (SH)	E4R	12.0	79	4.5	140	3.3	20	<50	26	230	1.3	24.2	4.7	250	19	4.50	160	40	120	180
Spencer (PM48)	S13C	10.2	38	5.7	94	16	20	60	28	210	2.2	23.2	1.4	170	15	4.12	170	40	180	220
Mullins (NW13)	M14C	10.2	16	4.5	53	<0.4	10	70	10	260	0.9	24.0	<0.9	110	14	4.13	170	30	140	180
Tracy (PM65)	T16C	13.0	84	4.3	59	2.3	20	110	36	230	2.3	24.9	4.7	850	16	7.88	150	30	150	150
McAulay (RI)	MC9D	16.8	34	3.1	120	4.2	20	80	30	290	2.6	22.7	<0.5	190	16	5.82	160	10	180	80
	Average:	10.6	65	3.8	115	6.2	21	54	30	209	1.5	21.2	2.8	933	14	4.1	151	31	137	146
UNDERCLAYS:																				
l.Lloyd Cove(B)	LC3Q	6.5	40	9.3	27	3.0	30	90	76	130	8.0	15.0	<1.3	130	12	4.63	90	30	320	410
Hub (Pr)	HP80	6.8	24	9.7	69	0.4	40	67	16	130	1.6	15.7	<0.5	<10	12	4.01	98	40	94	380
Harbour (L)	HL6N	18.0	49	3.7	95	1.4	20	60	30	250	2.4	24.9	0.9	300	16	4.16	160	20	210	120
Indian (SM17)	IC10K	11.7	100	3.7	54	44	10	100	150	190	8.8	20.2	2.7	2500	18	4.79	140	10	220	70
Phalen (P)	PP7M	11.6	45	4.8	60	7.7	30	140	26	250	2.6	23.4	<1.0	<10	15	6.85	150	40	200	190
Emery (SH)	E4A	18.2	74	3.0	110	8.8	20	120	52	240	5.5	22.6	2.4	230	17	7.58	200	20	100	90
Spencer (PM48)	S13H	14.5	81	3.6	110	6.3	40	80	76	260	2.2	25.8	<0.5	280	16	5.73	180	20	160	120
Mullins (NW13)	M14K	---	28	9.3	92	1.7	20	<40	8	180	0.7	18.8	<0.9	<80	14	3.82	100	50	120	360
Tracy (PM65)	T161	12.6	47	5.1	59	0.8	20	80	22	240	1.6	25.9	<0.5	120	16	4.09	130	50	170	170
McAulay (RI)	MC9H	14.9	47	6.4	130	0.5	20	90	14	250	0.9	22.2	1.0	40	14	4.13	150	40	180	240
	Average:	12.8	54	5.9	81	7.5	25	85	47	212	3.4	21.45	0.93	365	15	4.97	140	32	177	215

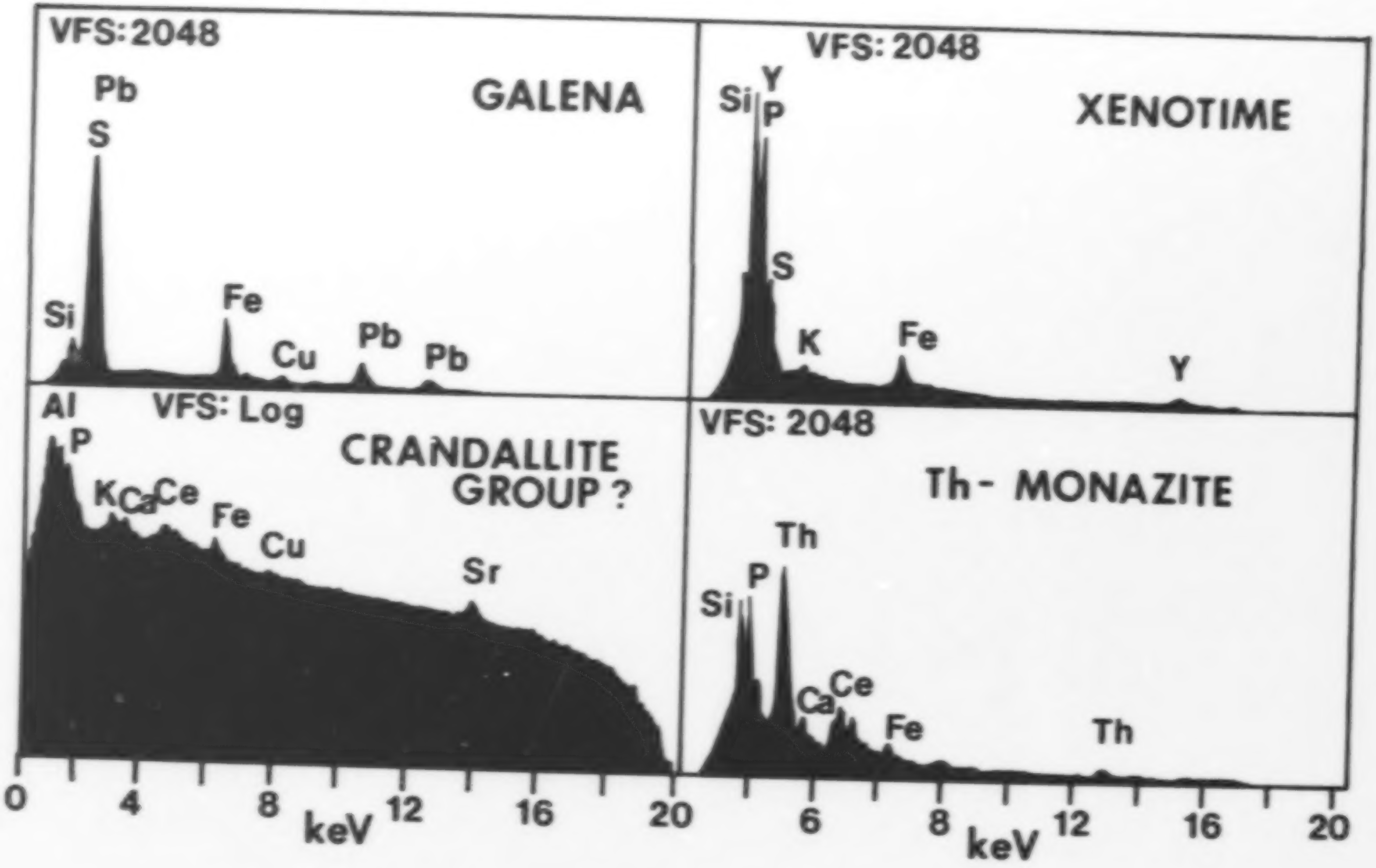

Figure 2. Trace elements in accessory minerals of bituminous coal (Sydney Coalfield). Energy dispersive X-ray (EDX) spectra were collected in spot mode for 50 seconds at 20 keV. The vertical full scales (VFS) varied with signal strength, i.e. X-ray counts for main channels. The crandallite group spectrum is shown at log scale to enhance the Sr peak. The monazite is enriched in Th. Some matrix interference or instrument artifact peaks are also present (e.g. Fe, Si).

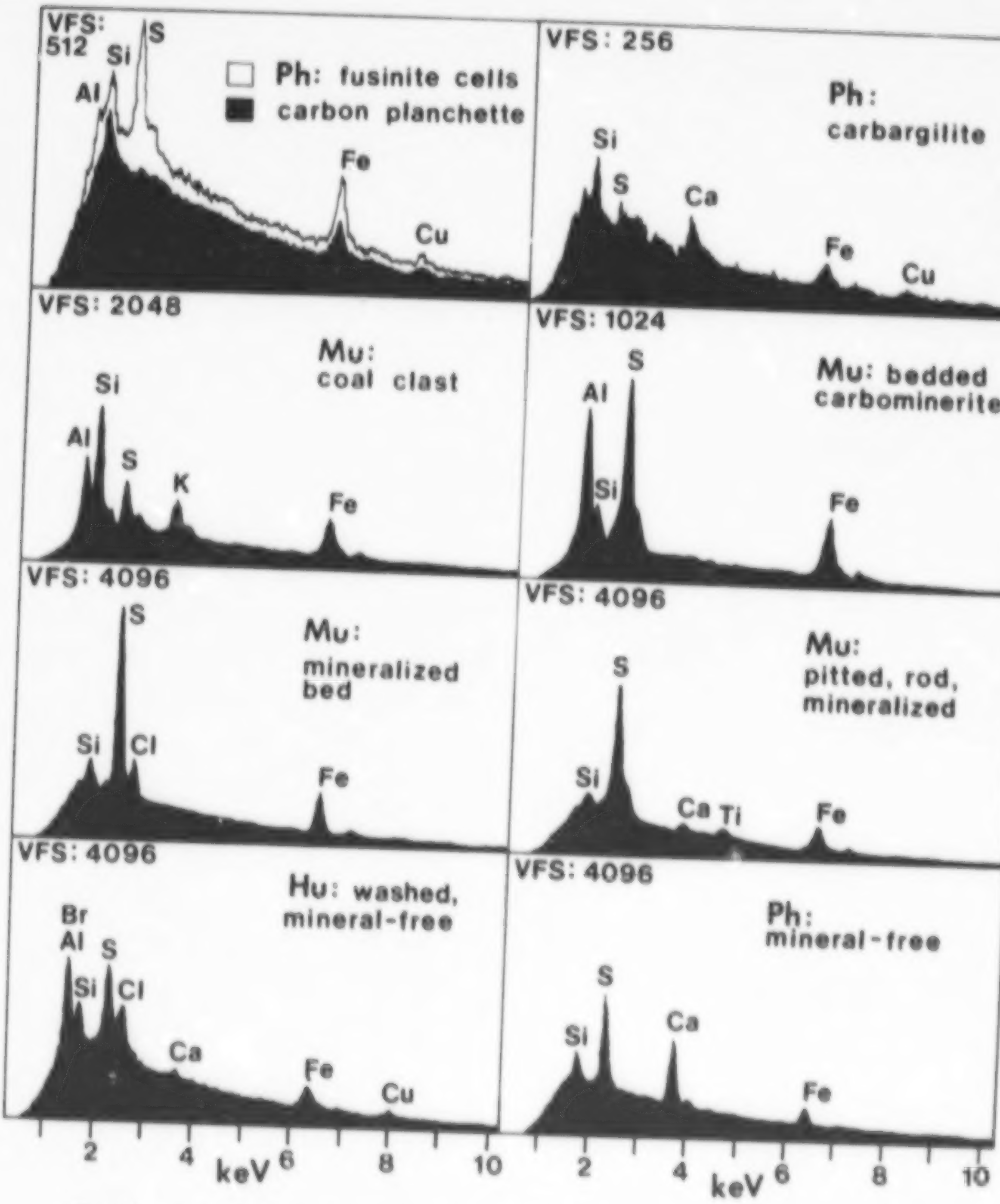

Figure 3. Elements in macerals of Sydney bituminous coal. Seam names abbreviated as in Figure 1. EDX spectra are characterized by a large Bremsstrahlung background. Major peaks are Si, S, Fe, and Al. Compare vertical full scale (VFS) to that in Figure 2. Some of the Si and Fe are instrument artifacts at such low count rates, as shown by the spectum from a carbon planchette. The only "trace" elements are Cl and Br at minor element levels, but Br is a contaminant from laboratory heavy liquids.

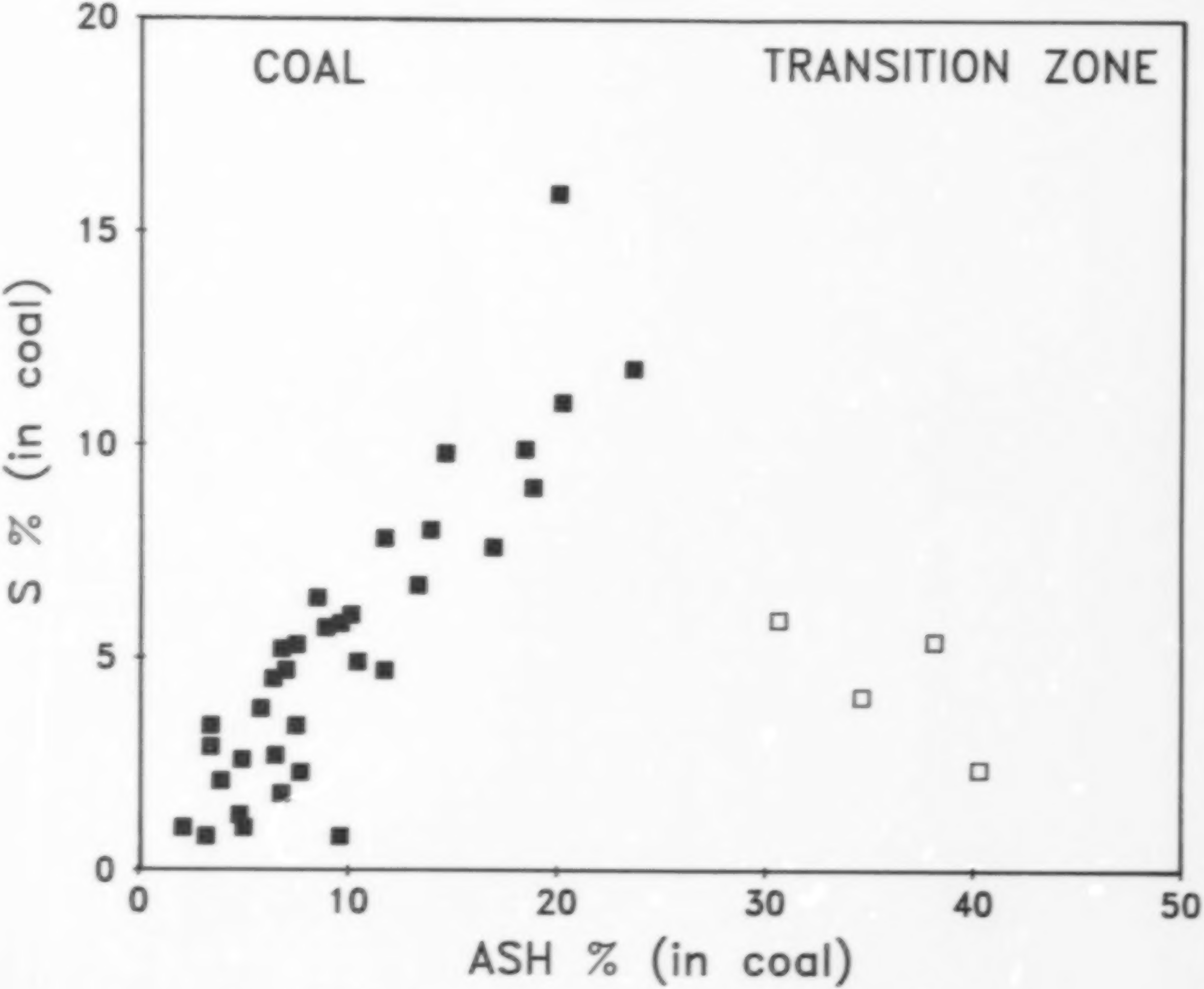

Figure 4. Correlation of sulphur to ash in whole coal and shaly coal (transition zone). Pyritization peaked

Trace element chemistry

Sixty-six elements were analyzed in ash and 44 elements in whole coal for the total survey and compiled in Birk et al. (1986) and White (1988). Elements partially lost during the ashing procedure included Au, Br, Cl, F, Hg, I, S, and Se. No significant difference was noted for samples ashed at 750°C or 500°C. The 14 rare earth lanthanides were analyzed individually but are only summarized in Tables 3 and 5a as total rare earth elements (TREE) and the ratio of light to heavy rare earth elements (LREE/HREE). A detailed discussion of the lanthanides is given by Birk and White (in press).

Some elements were measured in a limited number of samples (Table 4c). Elements that were monitored in coal ash but found near or below detection limits include Ag (<0.5 ppm), Au (<40 ppb), Cd (<1 ppm except Point Aconi at 1 to 30 ppm), Hg (<70 ppb), I (<5 ppm), In (<0.5 ppm), Ir (<5 ppm), and Ta (<2 ppm).

Tables 5a and 5b compile major and trace elements for roof rocks and seat earths. Elements measured at low concentrations and not shown include Ag (<2.4 ppm), Au (<9 ppb), Cd (<0.4 ppm), Ge (<10 ppm), Ta (<4 ppm), and W (<3 ppm).

The following discussion focuses on the trace elements, 32 in coal ash and 27 in host rocks, of which 2 have suffered material loss (Br, Se). Whole coal analyses were omitted except for Cl and S (Table 3) because many of the elements were below detection limits. Classical methods (ASTM, 1983) on five samples yielded a range of whole coal values from 110 to 260 ppb for Hg and 40 to 150 ppm for F.

A chemical comparison of the coal ash versus claystones reveals that elements are either present in similar concentrations or are enriched in the coal ash (i.e. B, Be, Br, Co, Cu, Ge, Mo, Ni, Pb, Sb, Sc, W, As). Some elements (Sc, Zn, W, V) are at relatively uniform low concentrations in roof rock and seat earths but show highly variable distribution in coal ash. The ash in transition zones (>30 percent ash) shows enrichment in K, Rb, Th, and possibly U relative to adjacent coal ash. This may reflect original sedimentation, i.e. elements derived from clastic micas and feldspar. Enrichments in the coal ash indicate organic uptake by peat, or epigenetic mineralization after burial.

Stratigraphic differences in element distributions are evident. The lower Morien coal ashes are enriched in Ni and Rb while upper Morien ashes show higher Zn, Sr, and B. Contributing factors are not apparent. Clastic or floral source material may have changed with basin deposition or elements may have been remobilized by groundwaters controlled by stratigraphy. Evidence for the former comes from associated strata. Carbonate-rich roof rock at the Indian Cove seam is depleted in Al, TREE, B, Zr, Zn, Y, Sc, Rb, Li, Cs, and Hf relative to aluminosilicate claystones.

This should not be confused with the trends reported by Zodrow (1987) on a whole coal basis. He suggested that higher Pb, Zn, Ni, and Cu occurred in younger seams and showed that thin seams have higher element levels than thick seams. His data reflect relative ash content of coal rather than changes in ash composition.

Iodine shows a subtle bimodal stratigraphic distribution in whole coal data (White, 1988). Lower Morien coals average 4 ppm I whereas upper Morien coals (above the Phalen seam) average 2 ppm I. Iodine correlates to other halogens in the whole coal (Sandeman, 1979) and may have been remobilized by pore waters. Such volatiles were lost on ashing, and are not investigated further.

The concentration ranges and means for most trace elements in coal ash are similar to those reported by Hawley (1955b) and Zodrow (1986) except for lower Se (48 ppm, Zodrow, 1986) and higher Sn and Zn (4 to 18 ppm Sn, 115 to 550 ppm Zn, Hawley, 1955b). Selenium was partially lost during ashing, while higher Sn values may reflect improvements in analytical techniques. The enrichment of As and Pb in Sydney coals, as reported by Hawley (1955b) was confirmed. Anomalous Zn was also measured.

The As, Co, Cu, Cr, Ni, Pb, Th, U, V, and Zn contents of roof and floor rocks are the same order of magnitude as those reported by Zodrow (1983). Averages for 15 elements do not differ appreciably from the NASC ("North American Shale Composite" of Gromet et al., 1984) except for higher Sr, Br, and Cr, and lower Al and Ca. Likewise the coal ashes differ from NASC by slightly higher Sr, Sb, Ni, and Br, and much greater As. Claystones that are anomalously high in Sr also show enriched Cu and Ba which may identify local sulphate mineralization.

Correlation coefficients

Tables 6 and 7 show correlation coefficients (r) for element pairs in coal ash and claystones respectively. The ash percent, S percent, and Cl ppm in Table 6 pertain to whole coal, while all other elements represent constituents of the ash. Only linear correlation was tested, but binary plots were used to reveal nonlinear relationships. Nicholls (1968) pointed out the possibility for nonlinear correlations related to whole coal.

Interpretation must consider inherent correlations due to closure ("constant sum problem" of Skala, 1979) and spurious correlations due to analytical outliers. Binary plots have been reviewed for each element pair to discover such anomalous correlations. For example, one sample from the Mullin seam shows anomalously high Sc that may be an analytical outlier.

An example of closure is given by the stronger negative coefficient for Al and Fe in coal ash ($r = -.86$) compared to associated strata ($r = -.32$). As major constituents, Fe and Al are interdependent in such percentage data. The much higher Fe in coal ash compared to claystones results in greater correlation with Al due to closure.

Spurious correlations occur when anomalous values control the slope of the linear regression. For example,

Table 6. Linear correlation coefficients (r) for elements and coal ash from the Sydney Coalfield, Nova Scotia. The correlation coefficients, based on data from Tables 3, 4a, and 4b, were calculated with CSS software (Pearson product moment correlations). Ash, percent S, and Cl are based on whole coal — other elements are based on 500°C ash. LH refers to ratio of LREE/HREE (light and heavy rare earth elements).

	Li	Mo	Nb	Ni	Pb	Rb	Sb	Sc	Se	Sn	Sr	Th	Tl	U	V	W	Y	Zn	Zr
Li	1.00																		
Mo	-.51	1.00																	
Nb	.44	-.07	1.00																
Ni	-.32	-.01	-.35	1.00															
Pb	-.40	.07	-.05	.06	1.00														
Rb	.27	-.30	-.13	.15	-.38	1.00													
Sb	-.41	.05	-.31	.49	.28	-.10	1.00												
Sc	-.24	-.10	-.29	.54	.09	.12	.54	1.00											
Se	--	.03	.19	-.11	-.11	-.31	-.03	-.12	1.00										
Sn	-.39	.47	-.02	-.31	.29	-.37	-.15	-.30	--	1.00									
Sr	.28	-.17	.14	-.46	-.01	.15	-.36	-.13	-.00	-.11	1.00								
Th	.67	-.40	-.08	-.01	-.36	.71	-.18	.19	-.19	-.50	.33	1.00							
Tl	-.83	.44	-.29	.41	.42	-.25	.40	.38	--	.45	-.46	-.51	1.00						
U	.61	.13	-.03	-.08	-.11	.29	.26	.11	.19	-.49	.07	.40	-.47	1.00					
V	.21	-.11	-.10	.27	-.24	.59	.09	.24	.10	-.50	.04	.57	-.09	.53	1.00				
W	-.08	.05	.06	-.01	.27	-.31	.32	-.08	.09	.46	-.11	-.20	.22	-.17	-.29	1.00			
Y	.30	-.18	-.07	-.02	-.32	.29	.06	.29	-.04	-.11	.45	.61	-.21	.29	.36	-.05	1.00		
Zn	-.07	-.28	.04	-.15	.73	-.23	.20	-.11	-.15	.41	.03	-.18	.15	-.13	-.20	.30	-.21	1.00	
Zr	.74	-.44	.06	-.15	-.27	.62	-.25	.05	-.18	-.40	.39	.95	-.65	.34	.63	-.18	.54	-.11	1.00

	Ash	S	Cl	Al	Fe	K	Ca	P	TREE	LH	As	B	Ba	Be	Bi	Br	Co	Cr	Cs	Cu	Ga	Ge	Hf
Ash	1.00																						
S%	.40	1.00																					
Cl	-.51	-.64	1.00																				
Al	.20	-.55	.44	1.00																			
Fe	-.18	.67	-.74	-.86	1.00																		
K	.52	-.15	.52	.63	-.53	1.00																	
Ca	-.22	-.22	.52	-.24	-.20	-.27	1.00																
P	-.00	-.06	-.03	-.04	-.09	-.13	.30	1.00															
TREE	.06	-.53	.31	.77	-.66	.30	-.16	.15	1.00														
LH	.47	-.37	.32	.59	-.53	.59	-.23	-.02	.42	1.00													
As	-.07	.36	-.56	-.44	.53	-.15	-.19	.04	-.50	-.31	1.00												
B	-.51	-.58	.48	.25	-.27	-.11	.16	-.03	.19	-.03	.12	1.00											
Ba	.26	-.47	.11	.66	-.56	.52	-.33	.04	.51	.65	-.28	.07	1.00										
Be	-.26	-.12	-.54	.12	.01	.12	-.20	.02	.12	-.15	.31	.18	.09	1.00									
Bi	.33	-.50	--	.52	-.61	.31	-.22	.38	.73	.46	-.56	-.08	.70	-.08	1.00								
Br	-.48	-.57	.82	.12	-.40	-.07	.57	.05	.25	-.14	-.34	.31	.23	.01	.06	1.00							
Co	.18	.46	-.41	-.01	.29	.13	-.37	-.10	.00	-.11	.23	-.25	-.14	.08	-.06	-.26	1.00						
Cr	.11	-.52	.31	.85	-.72	.48	-.30	.01	.82	.48	-.46	.17	.70	.12	.61	.17	-.06	1.00					
Cs	.25	-.34	.21	.74	-.66	.59	-.24	-.12	.51	.50	-.34	-.16	.48	-.07	.58	.02	.07	.64	1.00				
Cu	-.16	.32	-.23	-.29	.39	-.06	-.22	-.14	-.35	-.20	.66	.22	-.10	.21	-.73	-.21	.17	-.29	-.27	1.00			
Ga	-.12	-.34	-.03	.27	-.27	.12	-.01	.02	.42	-.21	-.24	.16	.31	.43	.29	.37	-.14	.37	.11	-.22	1.00		
Ge	-.16	.06	-.24	.05	.04	.01	-.04	.34	.06	-.21	.22	.02	-.06	.79	-.30	-.09	-.09	-.05	-.15	.17	.45	1.00	
Hf	.16	-.50	.34	.73	-.75	.40	-.15	-.06	.69	.47	-.44	.02	.51	.08	.63	.11	-.21	.80	.63	-.34	.19	-.07	1.00
Li	.36	-.41	--	.64	-.67	.29	-.31	.38	.62	.34	-.77	.04	.41	-.05	.52	-.15	-.26	.60	.23	-.69	.38	-.05	.71
Mo	-.25	.11	-.34	-.51	.43	-.29	.08	.18	-.44	-.34	.29	-.17	-.24	-.05	.02	.00	-.02	-.40	-.21	.07	-.12	-.05	-.41
Nb	-.25	-.01	-.65	-.04	.06	-.25	-.02	.10	.17	-.28	-.21	.11	-.10	.01	.06	-.14	-.11	.18	-.15	-.30	.26	.03	.11
Ni	.20	.44	-.54	-.08	.29	.26	-.41	-.32	-.22	-.11	.27	-.30	-.06	.11	-.12	-.25	.73	-.08	.17	.29	-.09	-.19	-.11
Pb	-.10	.26	-.48	-.20	.36	-.09	-.25	.09	-.26	.02	.38	.20	-.10	.22	-.39	-.39	.14	-.29	-.35	.52	-.24	.26	-.43
Rb	.43	-.23	.11	.70	-.62	.78	-.22	-.07	.47	.54	-.28	-.27	.45	-.08	.38	-.05	.12	.58	.87	-.27	.10	-.11	.60
Sb	.10	.39	-.58	-.22	.28	.07	-.20	.16	-.26	-.29	.67	-.10	-.12	.49	-.31	-.21	.26	-.29	-.15	.50	.08	.47	-.20
Sc	.17	.14	.32	.06	-.03	.20	-.14	-.12	.01	.01	.08	-.21	.09	.09	.14	.25	.15	-.04	.20	.07	.08	-.08	.06
Se	-.23	-.07	.13	-.13	.03	-.35	.30	.30	-.08	-.30	.01	.30	-.13	-.05	--	.32	-.08	-.02	-.31	-.18	.03	-.10	-.13
Sn	-.74	-.21	--	-.29	.25	-.42	.66	-.21	-.34	-.40	.31	.46	-.59	.25	-.37	.19	-.12	-.37	-.45	.39	-.11	.29	-.38
Sr	-.16	-.61	.50	.49	-.57	.00	.20	.25	.62	.35	-.42	.25	.41	.15	.52	.52	-.14	.44	.28	-.41	.24	.15	.34
Th	.30	-.49	.38	.88	-.83	.59	-.25	-.10	.72	.55	-.41	.08	.63	.03	.80	.08	-.12	.85	.80	-.28	.23	-.12	.88
Tl	-.48	.34	--	-.54	.61	-.30	.14	-.58	-.52	-.45	.81	.11	-.51	-.03	-.33	-.02	.41	-.60	-.22	.66	-.46	-.09	-.60
U	.18	-.13	.28	.29	-.33	.23	-.07	.65	.33	-.00	-.02	-.07	.23	.07	.54	.07	-.15	.38	.28	-.10	.25	.23	.34
V	.44	.04	-.08	.53	-.37	.50	-.34	.07	.34	.13	-.08	-.20	.40	.03	.33	-.10	.29	.46	.58	-.22	.20	-.01	.29
W	-.27	-.18	-.40	-.17	.20	-.18	-.06	-.05	-.15	-.15	.66	.60	-.09	.32	-.18	-.14	-.04	-.19	-.30	.46	.08	.03	-.19
Y	.01	-.44	.52	.51	-.59	.22	.11	-.08	.56	.00	-.26	.11	.39	.38	.67	.50	-.09	.51	.41	-.25	.68	.17	.54
Zn	-.12	.03	-.13	.11	.04	.07	-.15	.03	-.13	.03	.25	.43	-.00	.33	-.44	-.32	-.02	-.11	-.27	.42	-.06	.46	-.25
Zr	.15	-.52	.34	.84	-.82	.41	-.17	-.03	.59	.55	-.45	.12	.59	-.03	.88	.10	-.23	.82	.77	-.21	.12	-.12	.91

Table 7. Linear correlation coefficients (r from CSS software) for data on roof clays and underclays, Sydney Coalfield, Nova Scotia. Data from Tables 5a, 5b.

	Ni	Pb	Rb	Sb	Sc	Se	Sr	Th	U	V	Y	Zn	Zr
Ni	1.00												
Pb	.28	1.00											
Rb	.32	-.17	1.00										
Sb	.49	.83	-.13	1.00									
Sc	.18	-.17	.87	-.14	1.00								
Se	-.37	.11	-.28	-.09	-.11	1.00							
Sr	-.09	.36	-.31	.12	-.55	.30	1.00						
Th	.14	.09	.73	.15	.88	-.05	-.49	1.00					
U	.67	.12	.61	.33	.62	-.13	-.41	.64	1.00				
V	.23	.00	.75	-.05	.58	.04	.18	.48	.42	1.00			
Y	-.20	-.44	-.08	-.39	-.14	-.04	.37	-.22	-.27	.11	1.00		
Zn	.31	.35	.20	.58	.26	-.29	-.23	.31	.30	-.03	-.15	1.00	
Zr	-.11	-.28	-.29	.00	-.23	-.35	-.15	-.14	-.08	-.35	.57	.28	1.00

	Ash	Al	K	Fe	Ca	P	S	TREE	LH	As	B	Ba	Be	Bi	Br	Co	Cr	Cs	Cu	Hf	Li	Mo	Nb
Ash	1.00																						
Al	.23	1.00																					
K	.16	.78	1.00																				
Fe	-.41	-.32	.05	1.00																			
Ca	-.63	-.64	-.57	.35	1.00																		
P	-.48	-.43	-.54	.07	.51	1.00																	
S	-.59	-.20	.30	.58	.16	.12	1.00																
TREE	-.15	.42	.45	-.09	-.45	-.33	-.16	1.00															
LH	-.19	.50	.67	.33	-.35	-.40	.41	.56	1.00														
As	-.42	-.42	-.36	.53	.21	.60	.62	-.06	.04	1.00													
B	.37	.58	.54	-.39	-.81	-.30	-.13	.65	.41	-.21	1.00												
Ba	-.12	.53	.28	-.32	-.31	.40	-.11	.27	.22	.10	.47	1.00											
Be	.02	.63	.40	-.12	-.29	.22	.10	.04	.10	.02	.34	.54	1.00										
Bi	-.03	.42	.07	-.36	-.24	.49	.02	-.14	-.05	.11	.24	.74	.71	1.00									
Br	-.42	.26	.23	-.14	.01	.08	.09	.19	.02	-.15	-.02	.18	.26	.23	1.00								
Co	-.03	.35	.37	.19	-.24	-.34	.38	.24	.40	.01	.26	-.21	.42	-.02	.14	1.00							
Cr	.18	.90	.74	-.26	-.68	-.18	.04	.36	.40	-.22	.65	.67	.76	.60	.37	.30	1.00						
Cs	-.03	.67	.78	.10	-.41	-.59	.20	.57	.77	-.32	.38	.12	.24	-.04	.21	.50	.54	1.00					
Cu	-.23	.16	-.14	-.21	-.08	.70	.07	-.12	-.07	.35	.20	.74	.56	.91	.19	-.06	.42	-.22	1.00				
Hf	.57	-.33	-.25	-.24	-.36	-.44	-.12	.11	-.24	-.10	.15	-.52	-.54	-.47	-.34	-.07	-.38	-.16	-.50	1.00			
Li	.16	.69	.31	-.35	-.31	-.30	-.40	.23	.13	-.40	.16	.24	.41	.32	.20	.09	.52	.46	.04	-.13	1.00		
Mo	-.45	-.18	-.23	.56	.20	.48	.35	.01	.25	.75	-.17	.31	.12	.19	-.10	-.10	-.03	-.17	.41	-.35	-.23	1.00	
Nb	.23	-.16	-.33	-.33	-.07	.05	-.11	-.16	-.25	-.10	.22	-.15	.01	.03	-.18	.28	-.15	-.39	.12	.24	-.19	-.26	1.00
Ni	-.19	.01	.29	.34	-.17	-.03	.45	.31	.49	.23	.28	.03	.02	-.12	.26	.36	.08	.34	.01	-.04	-.34	.18	-.11
Pb	-.51	-.12	.16	.50	.07	.41	.76	.22	.36	.87	-.03	.28	.10	.13	-.08	.17	-.00	-.03	.37	-.23	-.20	.82	-.08
Rb	.21	.82	.93	-.03	-.57	-.59	.01	.52	.67	-.42	.56	.25	.41	.07	.16	.47	.71	.86	-.15	-.19	.44	-.25	-.33
Sb	-.34	-.22	-.04	.58	-.10	.20	.85	.19	.33	.84	-.00	.01	.01	-.04	.00	.26	-.04	.06	.13	.07	-.33	.61	-.13
Sc	.17	.77	.80	-.09	-.54	-.73	-.19	.71	.59	-.48	.53	.14	.20	-.18	.18	.40	.57	.78	-.37	-.02	.45	-.28	-.28
Se	-.46	.02	-.16	-.01	.22	.41	-.24	.11	-.27	.07	-.07	.32	.17	.29	.45	-.27	.17	-.26	.38	-.42	.16	.18	-.01
Sr	-.14	-.01	-.27	-.13	.04	.80	.01	-.32	-.20	.44	.02	.70	.44	.84	.02	-.31	.25	-.40	.93	-.45	-.06	.50	.03
Th	.06	.68	.67	.02	-.56	-.67	-.08	.75	.62	-.22	.41	.09	.15	-.14	.24	.37	.52	.77	-.32	.10	.54	-.06	-.37
U	-.14	.37	.65	.12	-.46	-.41	.46	.73	.65	-.10	.56	.07	.12	-.18	.38	.46	.39	.65	-.20	.08	.05	-.10	-.07
V	.10	.87	.74	-.15	-.59	-.25	.13	.30	.51	-.26	.60	.61	.69	.53	.29	.33	.91	.62	.36	-.44	.50	.01	-.19
Y	.58	.11	-.16	-.67	-.40	.09	-.42	-.19	-.48	-.31	.28	.23	.23	.50	-.05	-.20	.21	-.32	.39	.31	.10	-.27	.22
Zn	.27	.05	.19	.26	-.41	-.19	.29	.35	.18	.41	.36	-.15	.12	-.25	-.25	.45	.10	.16	-.22	.35	-.16	.07	.02
Zr	.65	-.31	-.33	-.43	-.39	-.20	-.09	-.09	-.46	-.06	.19	-.35	-.31	-.16	-.29	-.11	-.26	-.37	-.19	.91	-.15	-.38	.37

the one high calcium roof rock (IC10B; Table 5a) causes spurious correlation between Ca and ash as well as the following elements: Al, B, Cr, Th, and V. Correlation coefficients are attenuated between Al and Th, and between Al and V because of the one aluminum-deficient sample.

Correlation coefficients are also dependent on the number of samples, sample treatment, and element concentration. Limited sampling (e.g. Cl, Bi, Li, Sn, Tl; Tables 3 and 4c) or volatilization of elements during ashing (Se, Br) yield statistically less significant values, as do concentrations close to the detection limits. Niobium for example, has a high detection limit (10 ppm) and uniformly low concentrations in both coal ash and claystones (4 to 50 ppm) which lead to weak correlations.

Chemical properties

Certain chemical associations are expected from the geochemical behaviour of elements. The element pairs K:Rb, Rb:Cs, Zr:Hf, Al:Cr, Th:TREE, and Cs:Th show a high degree of correlation in both coal ash and claystones (coefficient $r > .70$ in Tables 6 and 7; see also Fig. 5). The alkali metals K, Rb, and Cs are in Group IA of the Periodic Table, characterized by large atomic size. Zr and Hf belong to Group IVA and have near identical atomic radii. These elements substitute in crystal lattice sites of clays and resistate minerals in both coals and claystones.

Scandium, yttrium, and rare earths (TREE) are Group IIIA transition metals. If the Sc outlier in Table 4b (263 ppm in the Mullins seam) is omitted, Sc correlates better to Y ($r = +.77$ compared to $r = +.29$ in Table 6) as expected. However, Y correlates poorly to TREE ($r = +.56$ coal ash; -.19 rock) or the ratio LREE/HREE ($r = .00$ coal ash; $r = -.48$ rock). Yttrium may have been fractionated from the lanthanides by ion exchange with clays or crystallization of the resistate mineral xenotime.

Mineral sites

Illite, chlorite, biotite, and minor kaolinite, found in three samples of floor rock studied by SEM-EDX, are the major aluminosilicates. Coal minerals are dominated by the presence of kaolinite (Table 2) but illite, chlorite, and mixed clays are common.

Strong positive correlations between Al and the elements K, Cr, Li, and V are present in the roof and floor rock suggesting a clay or mica association. In coals, Li correlates better with Al than K, suggesting substitution of Li for Al in chlorites rather than illite or biotite.

Coal ash Th shows a high positive correlation with Zr as well as Al, Hf, Cr, Cs, and Bi ($r = +.95$ to $+.80$), and weaker correlation to TREE ($r = +.72$) and a strong negative association with Fe ($r = -.83$). Thorium has been found in the coal mineral monazite (see Fig. 7a,b; Fig. 2) and may also be coresident with Zr in zircons. The other element associations suggest at least partial cohabitation of Zr and Th in clay minerals.

Thorium in claystone correlates best with Sc, TREE, Cs, and Rb ($r = +.88$ to $+.73$) and less with Al ($r = +.68$). Ion exchange between claystones and waters may have depleted available Th or else the element was removed from the claystone by leaching. In floor rocks alone, Th shows a strong linear negative correlation with Zr suggesting element substitution and the influence of leaching on all but the resistate mineral zircon.

Chromium in claystone shows a strong correlation with Al, K, and V (Fig. 5) and Rb with Al, K, Sc, and Cs, indicating element substitution within illite or biotite. V correlates poorly to Cr in the coal ash ($r = +.46$) where it resides partially in the organic matter.

Coal ash P does not correlate well with Ca ($r = +.30$) despite the association with detrital apatite defined by SEM-EDX. The high correlation of P with U is spurious but enrichments may identify U scavenging by fish-bone apatite (i.e. sample PP7L, Tables 3 and 4b — P = 6100 ppm, U = 18 ppm) as has been reported for REE (Birk and White, in press).

Elements with organic affinities

Coals with low mineral matter yield ashes enriched with inorganic elements derived from macerals. When correlated with the ash content, elements with organic affinities yield weak negative coefficients. For Sydney coals, these include B, Be, Br, Ga, Se, and W. Binary plots (Fig. 6) are curvilinear, with a significant enrichment of the element at low ash levels, as predicted by Nicholls (1968).

Because the S content in coal correlates positively to ash content (Fig. 4), curvilinear plots can also be generated between percent S (in coal) and these elements. Strontium shows a negative curvilinear relationship to coal ash but erratic high concentrations in transition zone ash and claystones. This relationship suggests that the combined influence of maceral affinity in low ash coals and mineral concentration as detrital celestite may be important in understanding Sr distribution.

Similar organic affinity in claystones is evident for volatile elements Se and Br, which still show weak negative correlation, despite loss on ashing.

Element pairs that correlate positively in coal ash but poorly in claystones include Al:Zr, Al:Hf, Zr:Cs, Cr:Hf, Zr:Bi, and Th:Bi. In this case, both elements are resident in macerals or their association is sedimentological.

Elements with sedimentological associations

Some correlations are sedimentological and not indicative of element cohabitation. Detrital clays and resistate minerals of fine particle size travelled together as washload in the paleorivers. Elsewhere heavy minerals (barite, REE phosphates, galena, etc.) may have been selectively concentrated by specific gravity. This could explain the good correlation of element pairs Ba:Bi ($r = +.74$), Cu:Sr ($r = +.93$), and Ba:Cu ($r = +.74$) in roof rocks, which are not normally found together. Correlation of

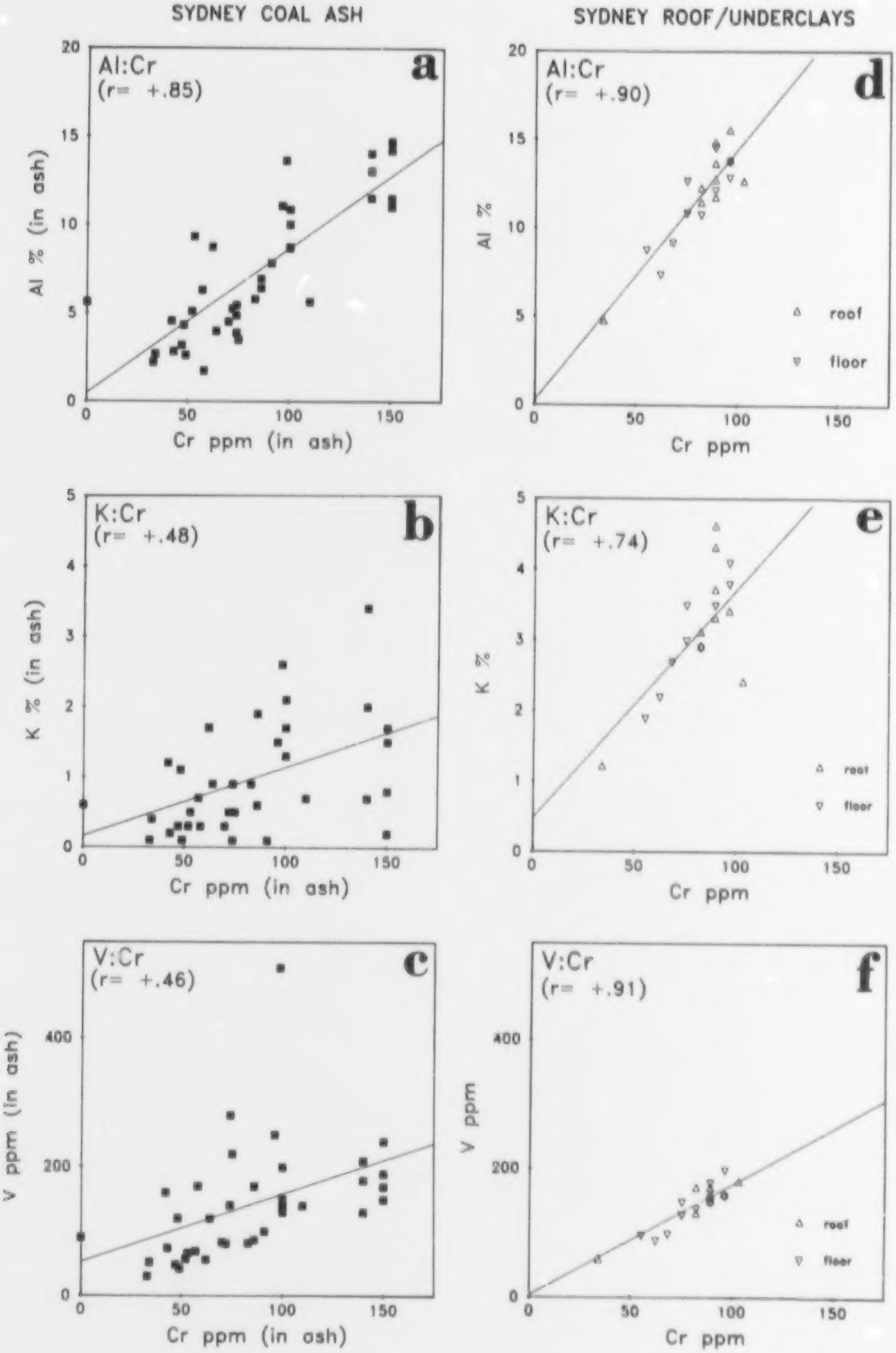

Figure 5a to 5f. Correlation of Cr to Al, K, and V in coal ashes and claystones. Note the higher gradient of regression lines in claystones and the greater data scatter for coal. The scatter may be due to partitioning of Cr and V between illites and macerals in coals versus claystone biotite and its alteration product, chlorite.

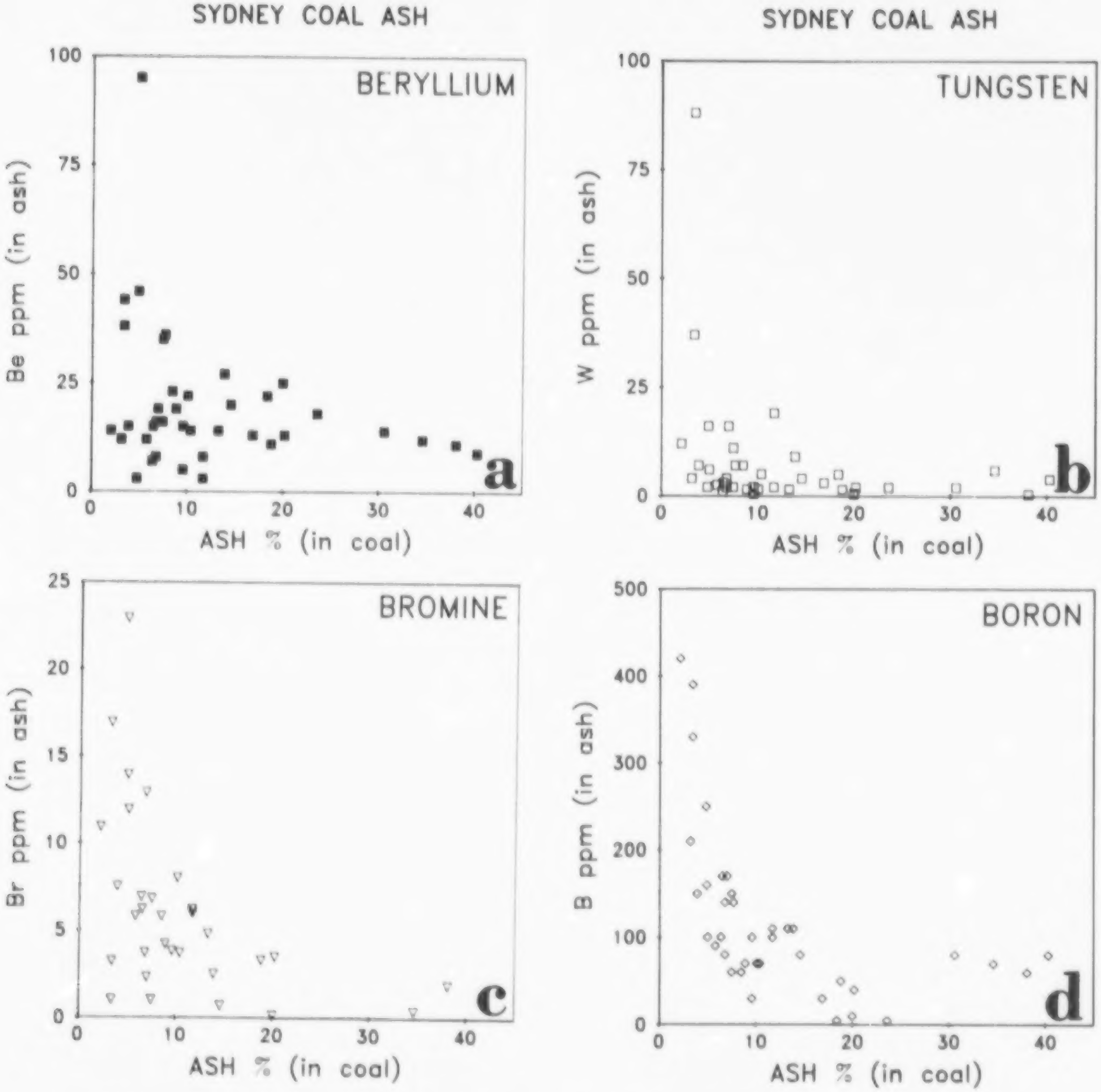

Figures 6a to 6d. Trace elements with organic affinity: Be, W, Br, and B concentrations (in coal ash) show a nonlinear relationship to percent ash in coal.

coal ash Bi to other heavy elements Ba (r = +.70), Th (r = +.80), TREE (r = +.73), and Zr (r = +.88) may reflect deposition of resistates in carbominerite.

Increased abundance of Al in claystones reflects increased aluminosilicate clays with less input of other detritus such as quartz or resistates (e.g. zircon). In carbonates, both Al and Zr are low. Correlation of Zr to Al content is therefore negative. In coal ash, the same increase in Al indicates derivation from carbominerite phides and therefore yields a positive correlation with elements in clastic sedimentary rocks (e.g. Zr).

The Fe content of coal ash shows a strong negative correlation with elements derived from detrital resistates or clays (Al, Cr, Th, Hf, Zr: r = -.72 to -.86). This reflects the domination of syngenetic and epigenetic pyrite in Sydney coal ash at the expense of clastic clays and heavy minerals. Iron in ash shows a weak correlation with clastics (clays, resistates) at the expense of syngenetic sul- sulphur levels in coal (r = +.67) indicating either that Fe was introduced during sulphate reduction or S was preferentially fixed in iron-rich coal bands.

Maceral/mineral partitioning of elements

The elements As, Cu, Mo, Pb, and Zn are enriched in coal ash relative to rock strata suggesting organic affinity, but correlation to ash is poor and binary plots are broad. The presence of sulphates in the swamp waters of the Sydney Coalfield should have favoured sulphide formation over organic fixation for chalcophile metals but both sulphide mineralogy and organic affinity are evident. Authigenic crystals of chalcopyrite occur in the Harbour seam (Fig. 7c) but Cu is present in maceral EDX spectra (Table 2, Fig. 3). Copper correlates positively to Sr and Bi in claystone but negatively to coal ash. This suggests that element partitioning between minerals and macerals is controlled by concentration, as discussed by Nicholls (1968).

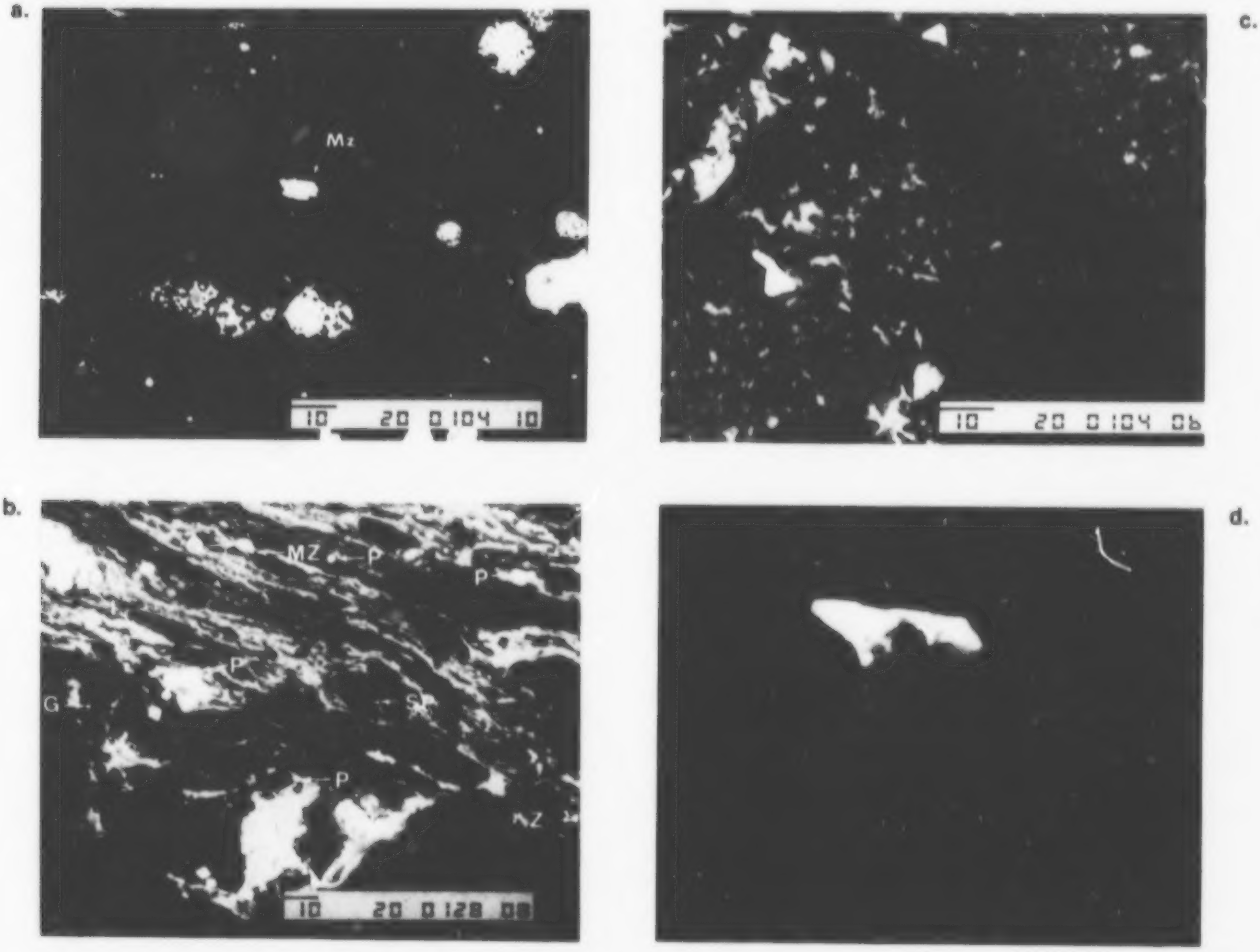

Figure 7. a) Pyrite framboids (white) and illite clay (dark grey) in bedding plane of Hub seam coal. One bright monazite grain (Mz) lies concordant. Note that this sample was a 1.4 specific gravity coal float: such heavy liquid separation does not remove fine accessory minerals. Legend window shows bar scale (10 microns), accelerating voltage (20 keV), and photomicrograph identification. Backscattered electron image (BEI) at magnification of 1000x (GSC 205074-C). b) Carbominerite from the Mullins seam showing pyrite (P), quartz (Q), illite (I), and accessories. Micron-size detrital heavy minerals carry REE, Th (MZ = monazite), and Zr (Z = zircon). Within maceral breccia, authigenic (?) sphalerite (SP) and galena (G) are present, contributing Zn and Pb respectively. 750x, BEI, 20 keV (GSC 205074-B). c) Rare chalcopyrite crystals (white, tetrahedral) in grey, mottled chlorite (chamosite) filling cell lumen, Harbour seam. The mineral assemblage includes siderite and only minor pyrite. In sulphide-rich portions of the seam, Cu is likely dispersed in pyrite. 1000x, BEI, 20 keV (GSC 205074-A). d) Galena (white) intergrowth with pyrite (grey) in Harbour seam. This may explain some positive correlation coefficients with Pb. 3500x, BEI, 20 keV (GSC 205074).

Strong As correlations with claystone Sb, Pb, and Mo and weak As correlations with coal ash Cu and Fe suggest a chalcophile character, confirmed by the SEM-EDX report of arsenopyrite in the Gardiner seam (Table 2). Limited sampling for coal ash Tl correlates negatively to Al, Li, and ash but positively to As, implying affiliation with As in arsenopyrite.

In the roof and floor rocks, low levels of Pb correlate with claystone S (r = +.76), As (r = +.87), and Sb (r = +.83) but correlation with moderate levels of Zn (r = +.35) is poor. In coal ash, Pb and Zn show positive correlation (r = +.73) and erratic enrichment. Microscopic examinations have revealed sphalerite and galena adjacent to kerogen in claystone and as inclusions or cell fill in coal macerals (Fig. 7b). Enrichments represent epigenetic mineralization of sulphides at organic sites thus masking element affinity in bulk geochemical data.

Our limited data for Sn suggests a strong negative correlation with coal ash (r = -.74, Table 6) and thus organic association, but the SEM-EDX survey reported detrital cassiterite. Thus Sn, likewise, is resident in both macerals and minerals. Correlation of Sn to Ca (r = +.66) is spurious.

Chlorine shows a negative correlation with S (r = -.64) and Fe (r = -.74) indicating no association with sulphide mineralization. A high positive correlation is evident with Br (r = +.82) but correlations between these halogens and the organophile elements Be and Ge are poor. Therefore the halogens are likely not complexed with the organics but may be present as pore-filling halides. The submarine position of Sydney coals today suggests contamination from saline ground waters.

DISCUSSION

Trace element source

River waters carry suspended loads and dissolved loads with element enrichment dependent on solubility. Trace elements in the dissolved loads occur as fine colloids, free ions, complexes of $(OH)^-$, $(SO_4)^{2-}$, $(CO_3)^{2-}$, and organic complexes, dependent on the pH conditions and available constituents. Acidic rivers (e.g. Amazon at pH = 6) carry free ions whereas alkaline rivers (e.g. Mississippi at pH = 8) carry complexes (Goldstein and Jacobsen, 1988). Elements transported as dissolved species may accumulate in alkaline clay sediments by surface ion exchange but are readily leached by humic acids or acidic river water.

The Sydney Coalfield is associated with alluvial sedimentary rocks and freshwater biota but a high sulphur content. In other coal provinces, high sulphur is associated with marine roof rocks but in the Sydney Coalfield, sulphur has been attributed to fluvial dissolution of bedrock gypsum in the Windsor Group (Rust et al., 1987; Gibling et al., 1989). We can therefore expect that the geochemical character of fluvial sediments in the Sydney Coalfield has been partially overprinted by contributions from marine bedrock. Sulphates in the river waters would have formed metallic complexes from the dissolved load precipitated in the acidic swamp.

The bulk of detrital clays washed into the Sydney coal swamps carried adsorbed elements inherited from granitoid weathering and were accompanied by resistate minerals (rutile, apatite, REE-phosphates, zircon). Illites from the Sydney Coalfield are mainly detrital (Birk, 1990) as shown by bedded textures (Fig. 7a). Thus illite-rich coals in transition zones are dominated by a terrestrial shale trace element pattern characterized by high K, Rb, and Th. The main coals with mineral facies dominated by syngenetic pyrite, kaolinite, and chlorite carry a mixed marine/terrestrial element signature derived partially from dissolved Windsor evaporites.

Some trace elements were leached from the underclays by acidic swamp water which resulted in their "bleached" appearance. A continued influx of dissolved ions and complexes occurred at coal seam margins after burial through the sandstone paleoriver channels.

The local accumulation of metals in coal did not require high concentrations in the natural waters. At peat and lignite stages of coalification the adsorptive capacity of the organic matter is 120 times that of bituminous coal (Ong and Swanson, 1966). Therefore prolonged flushing with low metal (ppb level) waters could have created enrichments. This process was likely not operative after metamorphism since it is not evident with present-day groundwaters (Drever et al., 1977).

Element sites

Hawley (1955b) was the first to address the problem of element sites in the Sydney Coalfield using heavy liquid separations. His results were ambiguous but he suggested an association of Co and Ni with pyrite and possible organic affinity for B, Ba, Cr, Ge, Sr, Ti, Y, and Zn. Nicholls (1968) reinterpreted Hawley's (1955b) data using binary plots and suggested that Ge was adsorbed on clays in the Lloyd Cove seam but bound to organics in the Mullins seam. Zodrow et al. (1987) considered low levels of uranium distribution to reflect clay sedimentology and ruled out organic enrichment. Zodrow (1986) suggested sulphide affinities for some 12 trace elements and clay sites for Cr, Th, and U.

In discrete minerals, trace elements may form part of the unit cell or affiliate as an exchange cation or adsorbate. With macerals, element association may be as replacement cations or as porphyrin complexes. Metallo-organic complexes are known to form from elements Co, Cr, Cu, Fe, Ga, Mn, Ni, Sn, V, and Y (Bonnett and Czechowski, 1981; Mukherjee et al., 1988). On the other hand, most metals that occur as cations in solutions are adsorbed by organic matter (Ong and Swanson, 1966).

The geochemical behaviour of the trace elements can be attributed to differences in ionic size and the valence state in response to changing redox environments. Nicholls (1968) suggested that the mode of occurrence of trace elements was dependent on pH, element concentration, and the abundance of clay adsorbent. Ong and

Swanson (1966) postulated interaction during coalification whereby fixed metals were exchanged with cations of higher ionic potential or reduced by H_2S to metal sulphides. A simple classification of elements as to their organic/inorganic affinity is therefore likely not appropriate over the whole coalfield (Chatterjee and Pooley, 1977).

Finkelman (1978, 1988) and Finkelman and Stanton (1978) have suggested that many trace elements in the Waynesburg coal can be accounted for in the accessory minerals of carbominerite bands. Their calculated element concentrations from grain counts were similar to bulk chemistry. Our SEM-EDX survey for Sydney coals (Birk, 1990) likewise detected trace elements mainly as discrete heavy minerals (Fig. 7a to d) and only rarely as minor constituents of major minerals or macerals. The North American Shale Composite "standard" shows REE heterogeneity attributed to uneven distribution of resistate minerals (Gromet et al., 1984).

This study suggests however, that peak interference and concentrations below detection have biased the identification of element sites by SEM-EDX. Element sites as minor constituents in common rock-forming minerals or ion exchange sites in clays and organic complexes are well demonstrated for the Sydney Coalfield by the bulk geochemical evidence.

Most authors assign an inorganic nature to the elements As, Ba, and Pb. Results from SEM-EDX and statistical correlation allow assignment of the following elements in the Sydney Coalfield to minerals: As, Co, Cu, Ni, Pb, Sb, Tl, Zn (sulphides); Cr, Cs, Rb, Sc, TREE, V (illite, biotite); Cr, Hf, Li, Sc, Th, Zr (chlorite, mixed clays); and Ba, Cl, Cr, Hf, Sc, Sn, Sr, Th, TREE, Y, Zr (accessory minerals). The nature of ion exchange with clay minerals appears to differ between coal and associated strata because of differences in concentration or mineral facies.

Previous publications have attributed an organic affinity to Br, Ge, I, and W. The following elements are organically affiliated in the Sydney Coalfield: B, Be, Br, Ga, Ge, I, Mo, Se, and W. Many elements have multiple sites and have been variously assigned to mineral phases, macerals or both (Chatterjee and Pooley, 1977; Harvey et al., 1983; Asuen 1987, 1988; Finkelman 1988; Mukherjee et al., 1988). Partitioning between minerals and macerals in the Sydney coal seams varied with geochemical environment in coal, shaly coal, and associated claystone. Associations are better defined (higher coefficients) in the claystones and are more diffuse in the coals. Elements found in both minerals and macerals include Cl, Cu, Sn, Sr, V, and Zn.

Seam correlation

Several authors have attempted stratigraphic correlation based on trace element content. Simplistic attempts used bulk character samples (Newmarch, 1950; Nichols and D'Auria, 1981). Bouska (1981) reviewed the theoretical criteria for seam correlation and identification. A trace element is diagnostic if a vertical seam profile shows an element to be unique or enriched in one seam or else uniform throughout. Swaine (1983) used vertical "trend curves" to correlate two Australian coal regions.

Newmarch (1950) found the elements Na, Ba, Si, V, and Mg to be most useful for coal ash correlation, while Swaine (1983) used Cu, Ga, V, and Y. Hawley (1955b) tried to solve seam ambiguities for the Sydney Coalfield using histograms of 13 elements to correlate seams, but his conclusions do not match present geological consensus.

Chatternee and Pooley (1977) and Hart and Leahy (1983) suggested the use of correlation coefficients. They found patterns of element association to be unique in some seams. The present study suggests that element affinities are altered in response to changes in concentration and the geochemical environment of coal and associated strata. Changes in mineral suites, vertically and laterally within a seam control element distributions and affect ion exchange with macerals and pore waters. Especially erratic are the distributions of chalcophile elements (As, Co, Cu, Ni, Pb, Sb, Zn) and fossil bone elements (P, REE) at seam margins.

Environmental significance

Zodrow (1982) drew attention to the environmental impact of trace elements released from combustion of Sydney coals at the Lingan Power Station. The obvious hazards relate to high As and Pb levels, characteristic of these coals. Reduction of toxic trace elements by physical washing of the coal at the Victoria Junction Plant (Fig. 1) is limited by particle size and the organic/mineral affinities revealed in our study. Elements such as As, if affiliated with pyrite, can be substantially removed by current beneficiation procedures.

ACKNOWLEDGMENTS

This study formed part of contract research by the Atlantic Coal Institute, funded by the Geological Survey of Canada (Energy Mines and Resources, Ottawa) under the Canada-Nova Scotia Mineral Development Agreement. Dr. T.C. Birkett acted as Scientific Authority for the duration of contracts and Dr. A.L. Sangster provided funding for this paper. Contributing Institute staff include Donna McMahon, Robert O'Donnell, Alex Dove, and Helen Costello. Employees of the Cape Breton Development Corporation (Steve Forgeron, Kevin MacPherson, and Brendon Mackenzie) assisted in underground sampling. Don MacNeil and Jim Langille of the Nova Scotia Department of Mines and Energy helped retrieve archived drill core. We thank X-Ray Laboratories Ltd. (Don Mills, Ontario) for XRF and ICPMS and Nuclear Activation Services Ltd. (McMaster University, Hamilton, Ontario) for INAA.

REFERENCES

Abel, K.H. and Rancitelli, L.A.
1975: Major, minor and trace element composition of coal and fly ash, as determined by instrumental neutron activation analysis; *in* Trace Elements in Fuel, Advances in Chemistry Series 141, edited by S.P. Babu, American Chemical Society, Washington, D.C., p. 118-138.

Akande, S. and Zentilli, M.
1984: Geologic, fluid inclusion, and stable isotope studies of the Gays River lead-zinc deposit, Nova Scotia, Canada; Economic Geology, v. 79, p. 1187-1211.

ASTM
1983: Annual Book of ASTM Standards, Section 5: Petroleum Products, Lubricants and Fossil Fuels; Gaseous Fuels, Coal and Coke, v. 05.05, American Society for Testing and Materials, 1916 Race Street, Philadelphia, Pennsylvania, 19103.

Asuen, G.O.
1987: Assessment of major and minor elements in the Northumberland Coalfield, England; International Journal of Coal Geology, v. 9, p. 171-186.
1988: Elemental concentrations and their relationship in Howick Coal Group, England; Chemie der Erde, v. 48, p. 321-332.

Birk, D.
1989: Coal minerals: quantitative and descriptive SEM-EDX analysis; Journal of Coal Quality, v. 8, no. 2, p. 55-62.
1990: Quantitative coal mineralogy by SEM-EDX-AIA: Sydney Coalfield, Nova Scotia, Canada; Canadian Journal of Earth Science, v. 27, p. 163-179.

Birk, D. and Pilgrim, J.
1985: Development of the beneficiation potential for Eastern Canadian coals: analysis of chosen r.o.m. coals; CANMET, Energy Mines and Resources Canada, unpublished contract report, 3 volumes.

Birk, D. and White, J.C.
in press: Rare earth element distribution in bituminous coals of the Sydney Basin, Nova Scotia, Canada; International Journal of Coal Geology.

Birk, D., Pilgrim, J., and Zodrow, E.
1986: Trace element content of coals and associated rocks of the Sydney Basin, Nova Scotia; Geological Survey of Canada, Open File 2090, 52 p. and appendices.

Boehner, R.C. and Giles, P.S.
1986: Geological map of the Sydney Basin, Cape Breton Island, Nova Scotia; Nova Scotia Department of Mines and Energy, Map 86-1, scale 1:50 000.

Bonnett, R. and Czechowski, F.
1981: Metals and metal complexes in coal; Philosophical Transactions of the Royal Society of London, A, v. 300, p. 51-63.

Bouska, V.
1981: Geochemistry of Coal; Coal Science and Technology Series, v. 1, Elsevier, New York, 284 p.

Brown, R.
1871: The Coal Fields and Coal Trade of the Island of Cape Breton; Low and Searle, London, 166 p.

Chatterjee, P.K and Pooley, F.D.
1977: An examination of some trace elements in South Wales coals; Proceedings, Australasian Institute of Mining and Metallurgy, no. 263, p. 19-30.

Drever, J.I., Murphy, J.K., and Surdam, R.C.
1977: The distribution of As, Be, Cd, Cu, Hg, Mo, Pb, and U associated with the Wyodak coal seam, Powder River Basin, Wyoming; Contributions to Geology, University of Wyoming, v. 15, no. 2, p. 93-101.

Finkelman, R.B.
1978: Determination of trace element sites in the Waynesburg coal by SEM analysis of accessory minerals; Scanning Electron Microscopy, v. 1, p. 143-148.
1988: The inorganic geochemistry of coal: a scanning electron microscopy view; Scanning Microscopy, v. 2, no. 1, p. 97-105.

Finkelman, R.B. and Stanton, R.W.
1978: Identification and significance of accessory minerals from a bituminous coal; Fuel, v. 57, p. 763-768.

Forgeron, S., MacKenzie, B., and MacPherson, K.
1986: The effects of geological features on coal mining, Sydney Coalfield, Nova Scotia; Canadian Institute of Mining and Metallurgy, Bulletin, v. 79, no. 891, p. 79-87.

Gibling, M.R., Zentilli, M., and McCready, R.G.L.
1989: Sulphur in Pennsylvanian coals of Atlantic Canada: geologic and isotopic evidence for a bedrock evaporite source; International Journal of Coal Geology, v. 11, p. 81-104.

Glick, D.C. and Davis, A.
1984: Variability in the inorganic content of United States coals — a multivariate statistical study; DOE/PC/30013-F10, The Pennsylvania State University, 404 p. Available from: U.S. Department of Commerce, Springfield, Virginia, 22161.

Gluskoter, H.J., Ruch, R.R., Miller, W.G., Cahill, R.A., Dreher, G.B., and Kuhn, J.K.
1977: Trace elements in coal: occurrence and distribution; Illinois State Geological Survey, Circular 499, 154 p.

Goldstein, S.J. and Jacobsen, S.B.
1988: Rare earth elements in river waters; Earth and Planetary Science Letters, v. 89, p. 35-47.

Gromet, L.P., Dymek, R.F., Haskin, L.A., and Korotev, R.L.
1984: The "North American shale composite": its compilation, major and trace element characteristics; Geochimica et Cosmochimica Acta, v. 48, p. 2469-2482.

Hacquebard, P.A. and Donaldson, J.R.
1969: Carboniferous coal deposition associated with flood-plain and limnic environments in Nova Scotia; *in* Environment of Coal Deposition, edited by E.C. Dapples and M.E. Hopkins, Geological Society of America, Special Paper 114, p. 141-191.

Harris, L.A., Barrett, H.E., and Kopp, O.C.
1981: Elemental concentrations and their distribution in two bituminous coals of different paleoenvironments; International Journal of Coal Geology, v. 1, p. 175-193.

Hart, R.J. and Leahy, R.M.
1983: The geochemical characterization of coal seams from Witbank Basin; Geological Society of South Africa, Special Publication, v. 7, p. 169-174.

Harvey, R.D., Cahill, R.A., Chou, C.L., and Steele, J.D.
1983: Mineral matter and trace elements in the Herrin and Springfield coals, Illinois Basin coal field; Illinois State Geological Survey, ISGS Contract 1983-4, 161 p.

Hawley, J.E.
1955a: Germanium content of some Nova Scotia coals; Economic Geology, v. 50, p. 517-532.
1955b: Spectrographic study of some Nova Scotia coals; Canadian Mining and Metallurgical Bulletin, v. 48, p. 712-726.

Hoffman, E.L. and Ernst, P.C.
1982: Analytical geochemistry advanced by neutron activation; Journal of Radioanalytical Chemistry, v. 71, no. 1-2, p. 447-462.

Jarvis, K.E.
1988: Inductively coupled plasma mass spectrometry: a new technique for the rapid or ultratrace level determination of the rare-earth elements in geological materials; Chemical Geology, v. 68, p. 31-39.

Krejci-Graf, K.
1983: Minor elements in coals; *in* The Significance of Trace Elements in Solving Petrogenetic Problems and Controversies, edited by S.S. Augustithis, Theophrastus Publications S.A., Athens, Greece, p. 533-597.

Mukherjee, K.N., Dutta, N.R., Chandra, D., Pandalai, H.S., and Singh, M.P.
1988: A statistical approach to the study of the distribution of trace elements and their organic/inorganic affinity in Lower Gondwana coals of India; International Journal of Coal Geology, v. 10, p. 99-108.

Newmarch, C.B.
1950: The correlation of Kootenay coal seams; Canadian Mining and Metallurgical Bulletin, v. 43, p. 141-148.

Nicholls, G.D.
1968: The geochemistry of coal-bearing strata; *in* Coal and Coal Bearing Strata, edited by D. Murchison and T.S. Westoll, American Elsevier, New York, p. 269-307.

Nichols, C.L. and D'Auria, J.M.
1981: Seam location differentiation of coal specimens using trace element concentrations; Analyst, v. 106, p. 874-882.

Ong, H.L. and Swanson, V.E.
1966: Adsorption of copper by peat, lignite and bituminous coal; Economic Geology, v. 61, p. 1214-1231.

Palmer, C.A. and Filby, R.H.
1984: Distribution of trace elements in coal from the Powhatan No.6 mine, Ohio; Fuel, v. 63, p. 318-328.

Rust, B.R., Gibling, M.R., Best, M.A., Dilles, S.L., and Masson, A.G.
1987: A sedimentological overview of the coal-bearing Morien Group (Pennsylvanian), Sydney Basin, Nova Scotia, Canada; Canadian Journal of Earth Science, v. 24, p. 1869-1885.

Sandeman, R.M.
1979: Thermal and epithermal neutron activation analysis of Nova Scotian raw and washed coals; M.Sc. thesis, Dalhousie University, Halifax, Nova Scotia, 122 p.

Skala, W.
1979: Some effects of the constant sum problem in geochemistry; Chemical Geology, v. 27, p. 1-9.

Swaine, D.J.
1961: Occurrence of nickel in coal and dirt samples from the Coal Cliff colliery (Bulli seam); The Australian Journal of Science, March, p. 301-302.
1983: Geological aspects of trace elements in coal; *in* The Significance of Trace Elements in Solving Petrogenetic Problems and Controversies, edited by S.S. Augustithis, Theophrastus Publications S.A., Athens, Greece, p. 521-532.

Tupper, W.M. and Loring, D.H.
1961: A short note on the relative abundance of rubidium and strontium in vitrain ashes from coals in Nova Scotia; Geochimica et Cosmochimica Acta, v. 24, p. 314-316.

Valkovic, V.
1983: Trace Elements in Coal; CRC Press Inc., Boca Raton, Florida, v. 1, 210 p., v. 2, 281 p.

Whelan, J.F., Cobb, J.C., and Rye, R.O.
1988: Stable isotope geochemistry of sphalerite and other mineral matter in coal beds of Illinois and Forest City basins; Economic Geology, v. 83, p. 990-1007.

White, J.C.
1988: Gallium and germanium potential of Sydney Basin coals, Nova Scotia; Geological Survey of Canada, unpublished contract report, 27 p. and appendices.

Zodrow, E.L.
1982: Tentative identification of chemical elements likely to escape in the atmosphere at the Lingan coal-fired power plant, Lingan, Nova Scotia; Canadian Institute of Mining and Metallurgy, Bulletin, v. 75, no. 845, p. 138-140.
1983: Some geochemical aspects of sedimentary rocks in proximity of coals, Sydney Coalfield (Upper Carboniferous), Cape Breton Island, Nova Scotia, Canada; International Journal of Coal Geology, v. 2, p. 299-320.
1986: Coal-stratigraphic geochemistry: trends in coal samples from Sydney Coalfield, Upper Carboniferous, Nova Scotia; Canadian Institute of Mining and Metallurgy, Bulletin, v. 79, no. 893, p. 83-85.
1987: Geochemical trends in whole-seam coal channel samples from the Sydney Coalfield (Upper Carboniferous), Nova Scotia, Canada; Maritime Sediments and Atlantic Geology, v. 23, p. 141-150.

Zodrow, E.L. and Zentilli, M.
1979: Uranium content of rocks, coal and associated minerals from the Sydney Coalfields, Cape Breton Island, Nova Scotia; *in* Current Research, Part C, Geological Survey of Canada, Paper 79-1C, p. 31-36.

Zodrow, E.L., Banerjee, S.K., and Jessome, D.R.
1987: Uranium content and distribution in whole-coal samples, Sydney Coalfield (Upper Carboniferous), Nova Scotia, Canada; International Journal of Coal Geology, v. 8, p. 299-303.